TECHNISCHE UNIVERSITÄT WIEN

Dissertation

NOVEL STRATEGIES FOR EXTRACTION AND SYNTHESIS VIA COMBINATION OF SUPERCRITICAL CARBON DIOXIDE AND IONIC LIQUIDS

Ausgeführt zum Zwecke der Erlangung des akademischen Grades eines Doktors der technischen Wissenschaften am Institut für Angewandte Synthesechemie unter der Leitung von

Univ. Prof. Dipl.-Ing. Dr. techn. Katharina Schröder

Eingereicht an der Technischen Universität Wien
Chemische Fakultät

von

Aitor Sainz Martinez, MSc

Wien, im August 23

Table of Contents

Acknowledgements

Completing this thesis is a major milestone in my life. This achievement could have never been realized without the opportunity given to me by Univ.Prof.in Dipl.-Ing.in Dr.in techn. Katharina Schröder to work at her research group. I feel deeply indebted to her, not only for her academic supervision, but also for her invaluable guidance and time invested in me. From the beginning of the project to its completion, her unwavering enthusiasm for chemistry kept me constantly engaged with my research. She has always supported me and inspired me throughout my several years of research, without which this work would have never been possible.

I would like to also acknowledge the inestimable assistance of Associate Prof. Dipl.-Ing. Dr.techn. Michael Schnürch for his co-supervision during my last years of my PhD. He was always eager to discuss, to give me feedback and to share his expertise with me.

I am very thankful to Associate Prof. Dipl.-Ing.in Dr.in techn. Heidrum Halbwirth, for her assistance, feedback and great energy during our joint projects as well as to her PhD student, Christoph Kornpointner, who was my partner in crime working on some of these projects.

My sincere gratitude also goes to Univ.Prof. Dipl.-Chem. Dr.rer.nat. DDr.h.c. Thomas Rosenau for the thorough reading and evaluation of my thesis.

I would like to express my gratitude to my current and previous lab colleagues: Ádám Márk Pálvölgyi, Alice Cognigni, Apurba Ranjan Sahoo, Blete Hulaj, Christian Hauzenberger, Fabian Scharinger, Jakob Smith, Kristóf Stágel, Lisa Eisele, Olga "Alina" Lanaridi and Philipp Miksovsky for the great atmosphere, teamwork, support, and friendliness during my stay. With special mention to Apurba Ranjan Sahoo, I noticed his professionalism, his great personality, readiness to help, his focus, enthusiasm, mental fortitude, and positivity that inspired me to carry on with the challenges a PhD had to offer. He not only guided me splendidly during his stay, but also became one of my main pillars during my PhD and a life-long friend. Speaking about life-long friends, Alina has a special mention here. Her advice, extreme pickiness for the English language, overwhelming energy, positivity, and happiness also helped me during my PhD.

Special thanks go to Ao.Univ.Prof. Dipl.-Ing. Dr.techn. Helmuth Hoffmann and Dr. Zita Csendes, for their valuable input in solid material analysis. I would like to acknowledge all the non-scientific staff of the institute who assisted me during my PhD work.

To conclude, I am extremely thankful to my parents for their love, caring and sacrifices for educating and preparing me for my future.

Abstract

The growing concern surrounding conventional solvents in recent years has greatly influenced the field of sustainable chemistry. The need to replace toxic, flammable, or environmentally damaging solvents is one of the major challenges that we are currently facing. Consequently, considerable research effort has been invested in the search for an alternative technology that can circumvent the use of environmentally undesirable solvents. In this regard, alternative solvents such as supercritical carbon dioxide ($scCO_2$) have attracted attention.

This thesis is based on the employment of alternative solvents for the extraction of bioactive compounds from biomass and for catalysis. In total, three different topics were addressed during the course of this work.

(1) The first topic is centered on the application of supercritical carbon dioxide for the extraction of three different bioactive compounds from haskap berries (*Lonicera caerulea* L.). The parameter optimization of the dynamic streamlined process with different volumetric percentages of ethanol led to the initial removal of lipids, partial separation of iridoids and simultaneous extraction of iridoids and anthocyanins. Furthermore, the dynamic streamlined process developed is a promising approach with broad applicability.

(2) The second topic focuses on the employment of ionic liquid technologies in combination with supercritical carbon dioxide, with the aim of extracting cannabinoids from hemp (*Cannabis sativa* L.). The optimization of this novel alternative process resulted in high extraction efficiencies of cannabinoids comparable to conventional extraction approaches. Additionally, the developed process has the potential to be applied on an industrial level for the extraction of secondary metabolites from different natural resources.

(3) The last topic concentrates on cycloaddition reaction of propylene oxide with the aid of supercritical carbon dioxide and supported ionic liquid materials, aiming for the continuous production of propylene carbonate. Significant differences in catalytic activity were observed when using ionic liquids in batch mode (homogeneous fashion) and supported ionic liquid materials in continuous flow (heterogeneous fashion). By combining silica support material with ionic liquids, a synergistic effect was noticed. On the one hand, supported ionic liquid phases prepared *via* physisorption exhibited higher catalytic activity, however, they were not convenient in the longer run as a significantly fast decrease in their yield was observed. On the other hand, supported ionic liquid catalysts obtained *via* chemisorption displayed lower yields, but a greater long-term stability: a balance between activity and stability is paramount here.

Kurzfassung

Die wachsende Besorgnis über herkömmliche Lösungsmittel hat in den letzten Jahren einen erheblichen Einfluss auf das Gebiet der nachhaltigen Chemie gehabt. Der Ersatz von giftigen, brennbaren oder umweltschädlichen Lösungsmitteln ist eine der größten Herausforderungen, mit der wir aktuell konfrontiert sind. Infolgedessen wurde ein erheblicher Forschungsaufwand in die Suche nach neuen Technologien investiert, wodurch alternative Lösungsmittel wie etwa superkritisches Kohlendioxid (scCO$_2$) zunehmende Aufmerksamkeit erhalten.

Diese Arbeit basiert auf dem Einsatz alternativer Lösungsmittel zur Extraktion bioaktiver Komponenten aus Biomasse und zur Katalyse. Insgesamt wurden drei verschiedene Projekte abgeschlossen.

(1) Der erste Teil befasst sich mit der Anwendung von überkritischem Kohlendioxid zur Extraktion von drei verschiedenen bioaktiven Komponenten aus Haskap-Beeren (*Lonicera caerulea* L.). Die Parameteroptimierung des dynamischen optimierten mit unterschiedlichen Volumenprozentsätzen in überkritisches Kohlendioxid führte zur anfänglichen Entfernung von Lipiden, zur teilweisen Trennung von Iridoiden und zur gleichzeitigen Extraktion von Iridoiden und Anthocyanen.

(2) Das zweite Projekt konzentriert sich auf die Anwendung ionischer Flüssigkeitstechnologien in Kombination mit überkritischem Kohlendioxid mit dem Ziel, Cannabinoide aus Hanf (Cannabis sativa L.) zu extrahieren. Die Optimierung dieses neuartigen alternativen Verfahrens führte zu einer hohen Extraktionseffizienz von Cannabinoiden, die mit der traditionellen Extraktion vergleichbar ist. Darüber hinaus kann das entwickelte Verfahren eine neue potenzielle industrielle Anwendung finden, um Sekundärmetaboliten aus verschiedenen natürlichen Ressourcen zu extrahieren.

(3) Das letzte Projekt widmet sich der Cycloadditionsreaktion von Propylenoxid unter Verwendung von überkritischem Kohlendioxid mit geträgerten ionischen Flüssigkeitsmaterialien zur kontinuierlichen Herstellung von Propylencarbonat. Signifikante Unterschiede in der katalytischen Aktivität wurden beobachtet, wenn ionische Flüssigkeiten im homogenen Batch-Modus oder heterogen als geträgerte ionische Flüssigkeitsmaterialien verwendet wurden. Durch die Kombination von Kieselgel als Trägermaterial mit ionischen Flüssigkeiten wurde ein synergistischer Effekt festgestellt. Einerseits zeigten durch Physisorption hergestellte geträgerte ionische Flüssigphasen eine höhere katalytische Aktivität, aber auch eine starke Abnahme der Reaktivität. Auf der anderen Seite zeigten Katalysatoren, die durch Chemisorption erhalten wurden, geringere Ausbeuten, aber eine größere Langzeitstabilität, was darauf hindeutet, dass ein Gleichgewicht zwischen Aktivität und Stabilität nötig ist.

List of Figures

List of Schemes

List of Tables

List of Abbreviations

AC	Activated carbon
AcAcH	β-Diketone
AcO⁻/⁻OAc	Acetate anion
AGE	Allyl glycidyl ether
$AlCl_3$	Aluminium chloride
Aliquat 336	*N*-Methyl-*N,N,N*-trioctylammonium chloride
[Amim]⁺	1-Allyl-3-methylimidazolium cation
[Amim]Cl	1-Allyl-3-methylimidazolium chloride
[Amim][HCOO]	1-Allyl-3-methyl imidazole formate
BASIL	Biphasic Acid Scavenging utilizing Ionic Liquids
BASF	Badische Anilin- und Soda Fabrik (Baden Aniline and Soda Factory)
BDTACl	Benzyldimethyl(tetradecyl)ammonium chloride
$[BF_4]^-$	Tetrafluoroborate anion
Br⁻	Bromide anion
Bu	Butyl
[Bzmim][OTf]	1-Benzyl-3-methylimidazolium trifluoromethanesulfonate
[Bzmim][Tosyl]	1-Benzyl-3-methylimidazolium tosylate
[Bzmim]Cl	1-Benzyl-3-methylimidazolium chloride
CBD	Cannabidiol
CBDA	Cannabidiolic acid
CBG	Cannabigerol
CBGA	Cannabigerolic acid
CCU	Carbon capture and utilization
CCS	Carbon capture and storage
CFCs	Chlorofluorocarbons
$[CF_3SO_3]^-/[OTf]^-$	Triflate anion
$CF_3(CF_2)_6COOH$	Pentadecafluoro-*n*-octanoic acid
CH_3^-	Methide anion
CH_4	Methane
C_2H_4	Ethylene
CH_3COOH	Acetic acid
[Chol]Cl	Choline chloride
CILs	Carboxyl-possessing imidazolium ILs

Cl^-	Chloride anion
$[ClO_4]^-$	Perchlorate anion
$[C_1mim][MeSO_4]$	1,3-Dimethylimidazolium methyl sulfate
$[C_2mim]^+/C_2mim$	1-Ethyl-3-methylimidazolium cation
$[C_2mim][BF_4]$	1-Ethyl-3-methylimidazolium tetrafluoroborate
$[C_2mim]Cl$	1-Ethyl-3-methylimidazolium chloride
$[C_2mim][EtSO_4]$	1-Ethyl-3-methylimidazolium ethyl sulfate
$[C_2mim]F$	1-Ethyl-3-methylimidazolium fluoride
$[C_2mim][NTf_2]/[Emim][NTf_2]$	1-Ethyl-3-methylimidazolium bis(trifluoromethylsulfonyl)imide
$[C_2mim][OAc]$	1-Ethyl-3-methylimidazolium acetate
$[C_2mim][OTf]$	1-Ethyl-3-methylimidazolium trifluoromethane sulfonate
$[C_2mim][PF_6]$	1-Ethyl-3-methylimidazolium hexafluorophosphate
$[C_2OHmim]Cl$	1-(2-Hydroxyethyl)-3-methylimidazolium chloride
$[C_4DMDDAm]Br$	Benzyldodecyldimethylammonium bromide
$[C_4mim]^+ / [C_4mim]$	1-Butyl-3-methylimidazolium cation
$[C_4mim][BF_4]$	1-Butyl-3-methylimidazolium tetrafluoroborate
$[C_4mim][Br]$	1-Butyl-3-methylimidazolium bromide
$[C_4mim][CF_3SO_3]$	1-Butyl-3-methylimidazolium triflate
$[C_4mim]Cl$	1-Butyl-3-methylimidazolium chloride
$[C_4mim]DCA$	1-Butyl-3-methylimidazolium dicyanamide
$[C_4mim][MeSO_4]$	1-Butyl-3-methylimidazolium methyl sulfate
$[C_4mim][methide]$	1-Butyl-3-methylimidazolium methide
$[C_4mim][NO_3]$	1-Butyl-3-methylimidazolium nitrate
$[C_4mim][NTf_2]/[C_4mim][Tf_2N]$	1-Butyl-3-methylimidazolium bis(trifluoromethylsulfonyl)imide
$[C_4mim][PF_6]$	1-Butyl-3-methylimidazolium hexafluorophosphate
$[C_4mim][OTf]/[C_4mim][TfO]$	1-Butyl-3-methylimidazolium trifluoromethanesulfonate
$[C_4mim][Tosyl]$	1-Butyl-3-methylimidazolium tosylate
$[C_6mim][Tf_2N]$	1-Butyl-3-methylimidazolium bis(trifluoromethylsulfonyl)imide
$[C_4mmim]^+$	1-*n*-Butyl-2,3-dimethylimidazolium cation
$[C_4mpy]Cl$	1-Butyl-3-methylpyridinium chloride
$[C_4py]Cl$	1-Butylpyridinium chloride
$[C_8mim]^+$	1-Octyl-3-methylimidazolium cation
$[C_8mim][BF_4]$	1-Octyl-3-methylimidazolium tetrafluoroborate
$[C_8mim][NTf_2]$	1-Octyl-3-methylimidazolium bis(trifluoromethanesulfonamide)

$[C_n mim][BF_4]$	1-Alkyl-3-methylimidazolium tetrafluoroborate
CO	Carbon monoxide
CO_2	Carbon dioxide
-COOH	Carboxyl group
CPMO	Octyl(phenyl)-*N,N*-diisobutylcarbamoylmethyl phosphine oxide
CuCl	Copper (I) chloride
Cyanex 302	Diisooctyl-thiophospinic acid
Cyanex 923	Trialkyl phosphine oxide
[DBNH][AcO]	1,5-Diazabicyclo[4.3.0]non-5-ene acetate
[DCA]	Dicyanamide
$[DCA]^-$	Dicyanamide anion
DC18C6	Dicyclohexano-18-crown-6
DDC	Diethyldithiocarbamate
D_2EHPA	Bis(2-ethylhexyl)phosphoric acid
D_2EHTPA	Bis(2-ethylhexyl)monothiophosphoric acid
DES	Deep eutectic solvent
DMA	Dimethylarsenic acid
DSSCs	Dye sensitised solar cells
Ee	Enantiomeric excess
EO	Ethylene oxide
Et	Ethyl
$[EtNH_3][NO_3]$	Ethylammonium nitrate
$[EtOSO_3]^-$	Ethyl sulfate anion
Et_2SO_4	Diethyl sulfate
FDDC	Bis(trifluoroethyl) dithiocarbamate
GC	Gas chromatography
GRAS	Generally recognized as safe
Gt	Gigaton
H_2	Hydrogen
HBr	Hydrobromic acid
$HC_n im^+$	1-Alkylimidazolium cation
$[HC_1 im]Br$	1-Methylimidazolium bromide
$[HC_1 im]Cl$	1-Methylimidazolium chloride
HCl	Hydrochloric acid

[HC$_2$mim]Br	3-Hydroxyethyl-1-methylimidazolium bromide
HCO$_3^-$	Hydrogen carbonate anion
HCOO$^-$	Formate anion
Hex	Hexyl
HF	Hydrofluoric acid
HFA	Hexafluoroacetylacetone
HFCs	Hydrofluorocarbons
HNO$_3$	Nitric acid
H$_2$O	Water
H$_2$SO$_4$	Sulfuric acid
HPLC	High-performance liquid chromatoraphy
Htta	Thenoyltrifluoroacetone
I$^-$	Iodide anion
IFP	Institute Français du Pétrole
IFPEN	Institute Français du Pétrole Energy Nouvelles
IL	Ionic liquid
ILTEC	Ionic liquid cooling technology
IMIS	Commercial silica surface
Li$^+$	Lithium cation
LiCl	Lithium chloride
Li[NTf$_2$]	Lithium bis(trifluoromethanesulfonyl)imide
[MBPy][Tf$_2$N]	4-Methyl-*N*-butyl-pyridinum bis(trifluoromethylsulfonyl)imide
Me	Methyl
[MeOCO$_2$]$^-$	Methyl carbonate anion
[(MeO)$_2$PO$_2$]$^-$	Dimethyl phosphate anion
[MeOSO$_3$]$^-$ / [MeSO$_4$]$^-$	Methyl sulfate anion
[MeSO$_3$]$^-$	Methanesulfonate anion
[Methide]$^-$	Methide anion
MMA	Monomethylarsenic acid
MPD	Melting point depression
[MTOA]Br	Methyltrioctylammonium bromide
N$_2$	Nitrogen
NaDDC	Sodium diethyldithiocarbamate
[NBu$_4$]Br	Tetrabutylammonium bromide

[NBu$_4$][TfePF$_3$]	Tetrabutylammonium trifluoro[tris(perfluoroethyl)]phosphate
[NBu$_4$][Tosyl]	Tetrabutylammonium tosylate
[N(CN)$_2$]$^-$	Dicyanamide anion
NEt$_4$Br/TEABr	Tetraethylammonium bromide
NEt(HE)$_3$Br	*N*-Ethyl-2-hydroxy-*N*,*N*-bis(2-hydroxyethyl)ethanammonium bromide
NEt$_2$(HE)$_2$Br	*N*,*N*-Diethyl-2-hydroxy-*N*-(2-hydroxyethyl)ethanammonium bromide
NEt$_3$(HE)Br	*N*,*N*,*N*-triethyl-2-hydroxyethanammonium bromide
-NH$_2$	Amine group
N(HE)$_4$Br	Tetrakis(2-hydroxyethyl)ammonium bromide
[NHex$_4$]Br	Tetrahexylammonium bromide
[NHep$_4$]Br	Tetraheptylammonium bromide
[NO$_3$]$^-$	Nitrate anion
[NOct$_4$]Br	Tetraoctylammonium bromide
[NPr$_4$]Br	Tetrapropylammonium bromide
[NTf$_2$]$^-$	Bis(trifluoromethanesulfonyl)imide anion
Nu	Nucleophile
O$_2$	Oxygen
[OCOCF$_3$]$^-$	Trifluoroacetate anion
-OH	Hydroxyl group
[OSO$_2$CF$_3$]$^-$	Trifluoromethanesulfonate anion
[PBu$_3$EtOH]I	(2-Hydroxyethyl)triphenylphosphonium iodide
[PBu$_4$]Br/PBu$_4$Br	Tetrabutylphosphonium bromide
PBu$_4$OH	Tetrabutylphosphonium hydroxide
PC	Propylene carbonate
P$_C$	Critical pressure
PET	Polyethylene terephthalate
PETRONAS	Petroliam Nasional Berhad
[PF$_6$]$^-$	Hexafluorophosphate anion
Ph	Phenyl
PH$_3$	Phosphine
PhCl	Chlorobenzene
PhCO$_2^-$	Benzoate anion
PMO	2-Phenoxymethyloxirane
PO	Propylene oxide

[POct$_3$][MeOCO$_2$]	Trioctylphosphonium methyl carbonate
PPh$_3$BuBr	Triphenylbutylphosphonium bromide
PPh$_3$BuI	Triphenylbutylphosphonium iodide
PPh$_3$MeI	Triphenylmethylphosphonium iodide
Pu(NO$_3$)$_4$	Plutonium(IV) nitrate
PUREX	Plutonium uranium reduction extraction
QUILL	Queen´s University Ionic Liquid Laboratories
[Rh(acac)(CO)$_2$]	Dicarbonyl(acetylacetonato)rhodium(I)
[Rmim][NTf$_2$]	1-Alkyl-3-methylimidazolium bis(trifluoromethanesulfonyl)imide
[RSO$_4$]$^-$	Alkyl sulphates
RTIL	Room temperature ionic liquid
Ru(O$_2$CMe)$_2$(*R*-tolBINAP)	Diacetato[(S)-(-)-2,2'-bis(di-*p*-tolylphosphino)-1,1'-binaphthyl] ruthenium(II)
[SbF$_6$]$^-$	Hexafluoroantimonate anion
SC	Styrene carbonate
scCO$_2$	Supercritical carbon dioxide
SCF	Supercritical fluid
[SCN]$^-$	Thiocyanate anion
SEM	Scanning electron microscopy
SF-CO$_2$	Supercritical fluid - carbon dioxide
SFE	Supercritical fluid extraction
SILC	Supported ionic liquid catalyst
SILP	Supported ionic liquid phase
SiO$_2$	Silica dioxide
SO	Styrene oxide
SO$_2$	Sulfur dioxide
STY	Space-time yield
TBABr	Tetrabutylammonium bromide
TBACl	Tetrabutylammonium chloride
TBAI	Tetrabutylammonium iodide
TBP	Tri-*n*-butylphosphate
T$_C$	Critical temperature
TEABr	Tetraethylammonium bromide
THACl	Tetrahexylammonium chloride

THC	Tetrahydrocannabinol
THCA	Tetrahydrocannabinolic acid
TiO_2	Titanium dioxide
TOACl	Tetraoctylammonium chloride
TPPO	Triphenylphosphine oxide
TSIL	Task-specific ionic liquid
tta	Thenoyltrifluoroacetylacetonate
TOF	Turnover frequency
TON	Turnover number
UO_2	Uranium dioxide
$UO_2(NO_3)_2$	Uranium nitrate oxide
UO_3	Uranium trioxide
VOC	Volatile organic solvent
w.t.	Weight percent
$2\text{-}NH_2C_6H_4CO_2^-$	2-Aminobenzoate anion
$4\text{-}CH_3C_6H_4CO_2^-$	4-Methylbenzoate anion
$4\text{-}CH_3C_6H_4SO_3^-$	4-Methylbenzenesulfonate anion
$4\text{-}NO_2C_6H_4CO_2^-$	4-Nitrobenzoate anion
$[4\text{-}MBP][NTf_2]$	4-Methyl-1-butylpyridinium bis(trifluoromethylsulfonyl)imide

1. Introduction

In recent years, there has been a shift in the world of chemistry towards a more sustainable and environmentally benign direction. With the birth of Green Chemistry not so long ago, one of the major problematic issues that came to light was the employment of traditional volatile organic compounds (VOCs) as solvents for reactions, extractions, and chemical processes. Scientists recognized the numerous drawbacks associated with the use of VOCs, such as environmental damage, toxicity, and health hazards in their handling. As a consequence, researchers worldwide have invested considerable efforts in the search for a new technology that led to the use of alternative solvents.[1] Currently, we are facing a major challenge, which is the replacement of VOCs employed in laboratories and industries with the objective of developing more environmentally benign processes. Despite the challenges of this endeavor, a great opportunity for this innovation is presented, as there is scarcity of large-scale applications that employ alternative solvents. Countless possible new processes may be developed in laboratories in the future contributing to the welfare of the environment.[1] In the present work, different strategies were considered, for example (i) inorganic systems, such as water (H_2O) and supercritical carbon dioxide ($scCO_2$), (ii) nonvolatile systems, e.g., ionic liquids (ILs) and (iii) easily recyclable systems (fluorous solvents) as well as solvent-free processes.[1] The base of this thesis was the development of new environmentally benign processes using alternative solvents, mainly $scCO_2$ and/or $scCO_2$ in combination with ionic liquid (IL) technologies for extraction of bioactive compounds and catalysis.

1.1 Supercritical fluid extraction

1.1.1 Historical background

Baron Charles Cagniard de la Tour discovered the supercritical phase in 1822, while he was studying the behaviour of solvents at a certain temperature and pressure.[2],[3] Afterward, Thomas Andrews carried out experiments in 1869 with partly liquefied carbonic acid to study the influence of pressure and temperature in a closed glass vessel. He noticed the disappearance of two phases at a certain temperature and pressure which he named critical temperatures (T_C) and critical pressure (P_C), respectively.[2],[4] One century later, in 1960, the basis for the supercritical fluid extraction (SFE) technology and its application using carbon dioxide (CO_2) as a supercritical fluid was developed by Hannay and Hogarth.[5] One of the first industrial applications was developed in Germany: green coffee beans were treated with supercritical fluids (SCFs) for their decaffeination.[6] Later, in Australia, oil from hops was extracted using liquid CO_2.[7] In the eighties, both extraction approaches found new applications and expanded.[5] At the present, this technology is employed world-wide, and it is used to generate high value-added products.

1.1.2 Fundamentals

Supercritical fluid extraction is a technique where SCFs are employed for the separation of a target compound from a matrix. This technique can be utilized for solid as well as for liquid matrixes.[8] Any stable substance that above its critical temperature and critical pressure achieves the supercritical state is regarded as supercritical fluid.[9] Moreover, each stable compound contains a triple and a critical point. The highest temperature at which a substance can exist as a liquid is regarded as the critical temperature (T_C). Above the mentioned critical temperature, the molecules cannot remain attached to each other, because the overwhelmingly high kinetic energy overcomes the intermolecular attraction. Consequently, a single supercritical fluid phase is formed. The critical pressure (P_C) is defined as the pressure above which liquid and gas cannot coexist at any temperature. The point defined by the coordinates P_c and T_c is regarded as the critical point of the fluid.[10] Moreover, each stable compound has a triple point. Several solvents that are commonly used as supercritical fluids and their respective critical parameters are presented below (Table 1).

Die approbierte gedruckte Originalversion dieser Dissertation ist an der TU Wien Bibliothek verfügbar.
The approved original version of this doctoral thesis is available in print at TU Wien Bibliothek.

TU Bibliothek Your knowledge hub
WIEN

Table 1. Critical parameters of solvents commonly employed in their supercritical state.[11]

Solvent	Molecular formula	Critical pressure (MPa)	Critical temperature (°C)	Critical density (g/cm³)
Water	H_2O	22.06	373.99	0.322
Carbon dioxide	CO_2	7.38	31.10	0.469
Methane	CH_4	4.60	- 82.59	0.162
Ethane	C_2H_6	4.87	32.17	0.203
Propane	C_3H_8	4.25	96.68	0.217
Ethylene	C_2H_4	5.04	9.19	0.215
Propylene	C_3H_6	4.60	91.75	0.232
Methanol	CH_3OH	8.10	239.49	0.272
Ethanol	C_2H_5OH	6.15	240.77	0.276
Acetone	C_3H_6O	4.70	234.95	0.278

As can be seen in Table 1, non-polar compounds have more accessible critical conditions than polar ones. Compounds that reach critical state at mild conditions are ideal for SFE, thus, polar compounds are disregarded. Additionally, several other parameters need to be considered in the selection process of a compound for SFE, for instance, its purity, cost, non-toxicity, and inertness. The solvent that possesses the majority of the desired properties is CO_2, as it is non-toxic, non-flammable, relatively unreactive, inexpensive and easily available.[12] Supercritical carbon dioxide reaches its supercritical state at 31.3 °C (304.45 K) and 7.4 MPa or 74 bars, as depicted in the phase diagram (Figure 1).[12]
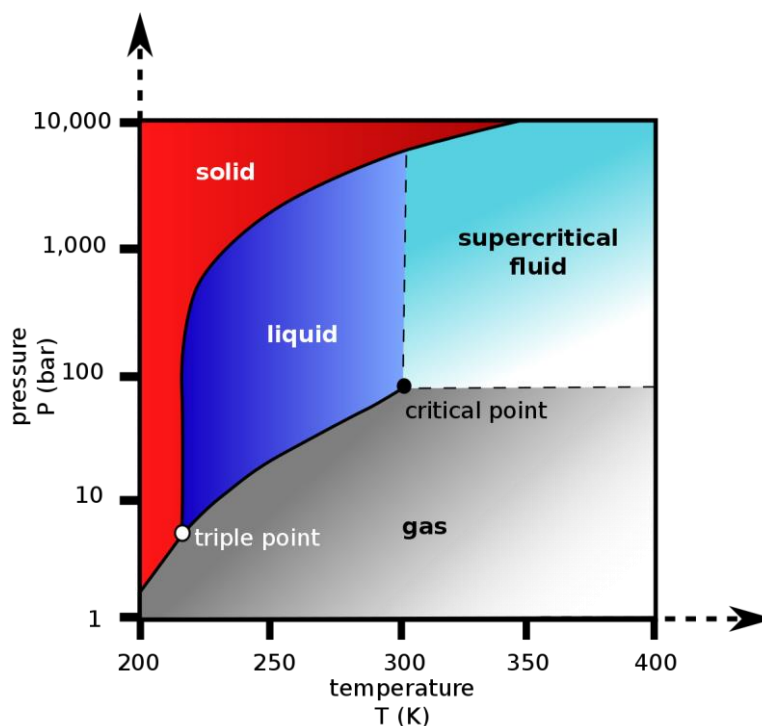
Figure 1. CO_2 phase diagram (P=f(T)).[13] Open access, CC0 1.0

In the supercritical state, the distinction between the gas phase and the liquid phase does not exist.[9],[12] Below the critical parameters, two different phases are distinguished. As the temperature rises, the liquid starts expanding. Then, the separation between both phases becomes less clear. At the end, there is no longer any separation between the phases, but only the supercritical phase (Figure 2, stages 1-4).
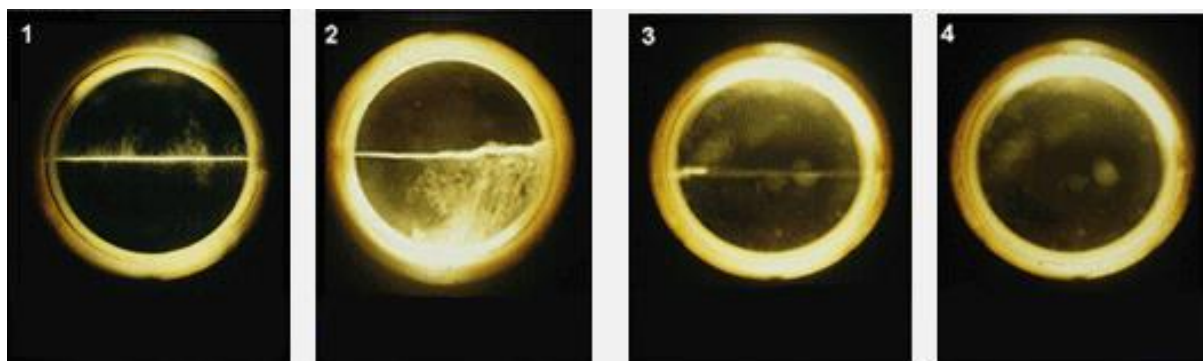
Figure 2. The stepwise formation of the supercritical phase (stages 1 to 4).[14]

The physicochemical properties related to the SCFs are of remarkable interest, as they possess intermediate properties between gas and liquid (Table 2). The considerable penetrating power of the SCF is due to its relatively high density and its relatively low viscosity.[12] In addition, the properties of the fluid can be fine-tuned by modifying the pressure and temperature to approximate either liquid-like or gas-like behavior. Compared to a liquid, a supercritical fluid exhibits an increase in solute mass transfer. The merit of SFE lies in the tunability of its solvating power, which is dependent not only on its density, but also on the temperature and pressure near its critical point.[12] Modification of the pressure and temperature near the critical state, results in a significant change of the density and viscosity. The solvating strength of $scCO_2$ can be modified to allow the selective extraction, purification, and fractionation of products. It is a rapid and efficient extraction as $scCO_2$ is able to rapidly penetrate and exit solid matrices.[15]

Table 2. Physical properties of typical gases, supercritical fluids, and liquids near the critical region.[16]

State	Density (kg/m³)	Dynamic viscosity (mPa s)	Kinematic viscosity (10^6 m²/s)	Diffusion coefficient (10^6 m²/s)
Gases	$0.6 - 2$	$0.01 - 0.3$	$5 - 500$	$10 - 40$
SCFs	$200 - 500$	$0.01 - 0.03$	$0.02 - 0.1$	0.07
Liquids	$600 - 1600$	$0.2 - 3$	$0.1 - 5$	$0.0002 - 0.002$

Combining the attributes of gases and liquids, supercritical fluids possess several unique properties; namely, they exhibit intermediate behavior of gases and liquids, they enable reactions that are not feasible in conventional solvents, and they have solvent power equivalent to light hydrocarbons for most of the solutes. In addition, finely divided solids can be precipitated by rapid expansion of the supercritical fluids. SCFs are miscible with permanent gases, such as H_2 or N_2, thus, enabling higher concentrations of dissolved gases than those achievable with conventional solvents.[8]

Apart from that, the selectivity of the supercritical fluids can be tuned by modification of the physical conditions (temperature, pressure) and they offer the possibility of employing multi-step extraction, thereby targeting different bioactive compounds. In comparison with traditional solvent extraction, it is regarded as more environmentally benign. Furthermore, SFE instruments can normally be equipped with automatic samplers, leading to a high level of automatization, and, therefore, minimum risk of sample contamination. On a related note, product fractionation is feasible by process tuning, resulting in higher product purity.[17]

1.1.3 Influential parameters of supercritical carbon dioxide extraction

In the SFE process for the extraction of bioactive compounds several experimental aspects need to be separately optimized, e.g., extraction temperature, pressure, nature of the solvent, volumetric percentage of co-solvent and sample size, among other parameters.[18-20]

Three concepts must be discussed regarding the most important factors of the SFE process: (i) maximization of diffusion, (ii) maximization of solubility and (iii) optimization of the flow rate. Diffusion can be maximized in three different ways: firstly, by increasing the temperature, secondly, by swelling of the solid matrix, or, lastly, by reducing the particle size of the solid sample. An increase in temperature or the addition of a co-solvent can positively contribute to the swelling of the matrix. To maximize the solubility, the pressure can often be increased. However, near the critical point, an increase of the temperature leads to a decrease in density and, therefore, also in dissolving power. When the critical pressure is sufficiently exceeded, by increasing the temperature the solubility increases too. Alternatively, solubility can be maximized when the target compounds are polar, by employing limited amounts of polar co-solvents, which can also positively influence the solubility. The rate of extraction can be significantly enhanced by an increase in the flow rate; however, the downside of this approach is a substantial increase in the solvent consumption. Therefore, a balance between solvent consumption and rate of extraction needs to be found. Additional factors that need to be considered are process duration and financial aspects related to operational costs. Most importantly, the flow rate should be selected to optimize the solubility and diffusion.[8]

Among these three concepts, the dependence of the solubility on the SFE parameters is a topic that necessitates further discussion, considering that the solubility of the target compounds is a decisive factor in their extraction. Solubility is defined as the equilibrium of intermolecular forces reached by solvent and solute, accompanied by a modification in the entropy of the solute, hence, solubility is regulated by pressure, temperature, and system polarity.[21]

Solubility increases with increasing density of the fluid, when a constant temperature is maintained. The density of the fluid rises according to the augmentation of pressure, which leads to higher probability of interactions between the solute and solvent (Figure 3). The effect of temperature is more complex. When the density is constant, an increase in temperature leads to a concomitant rise. Nonetheless, on the edge of the critical state, the density can drastically decrease as a response to a small increment on the temperature, leading to a possible decrease in the solubility. Subsequently, the solubility increases again together with the vapor pressure of the solute.[22]
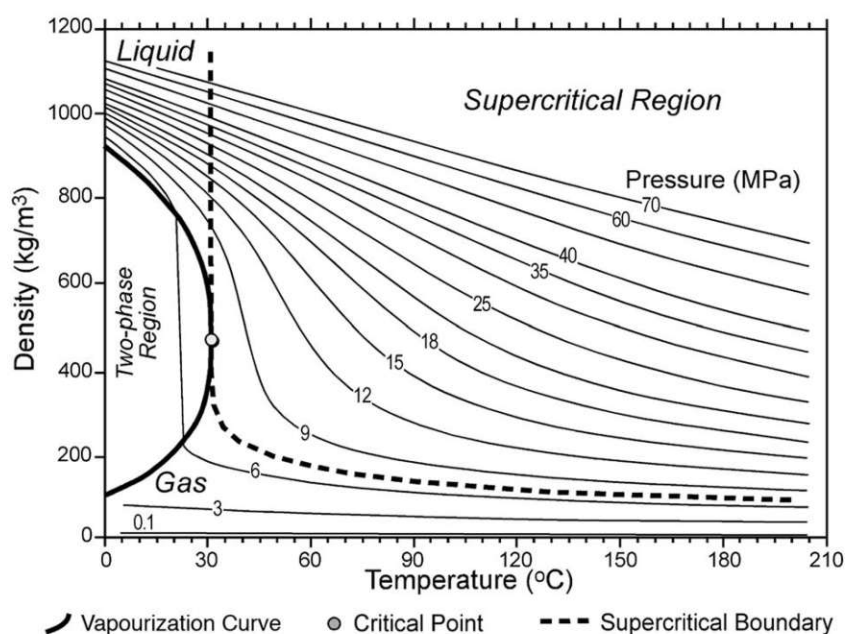
Figure 3. Variation of CO_2 density with temperature.[23]

The isotherms in the pressure-solubility diagram intersect at a point called the crossover point, which represents the pressure at which the operating temperature increases (Figure 4).[24] Below the crossover pressure, the reduction in the $scCO_2$ density is so significant that even a slight increase in the temperature leads to a drop in the solubility. However, above the crossover pressure, by increasing the temperature, the solute vapor pressure dominates, causing an increase in the solubility.[25]
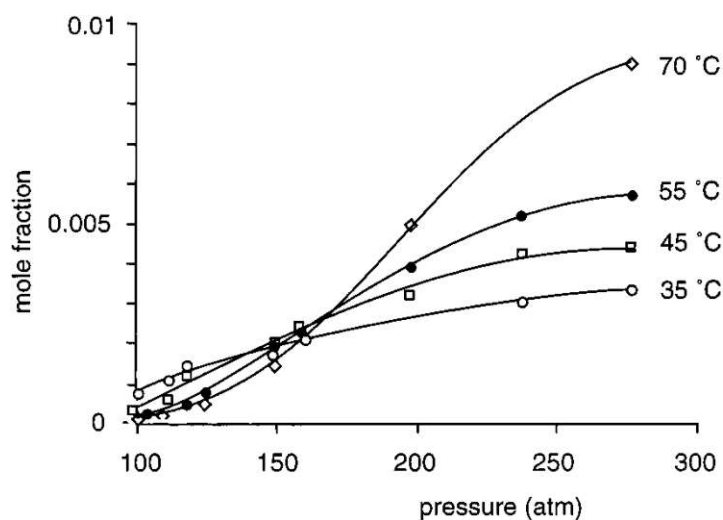
Figure 4. Mole fraction solubility of benzoic acid in scCO$_2$ as a function of pressure and temperature. The crossover pressure is approximately 160 atm.[25]

The solubility of target compounds in scCO$_2$ depends not only on their own characteristics, such as their vapor pressure, polarity, and molecular weight, but also on the solute-solvent and solute-solute interactions, such as hydrogen bonding. Among compounds of comparable molecular weights, the non-polar ones exhibit higher solubility than the polar ones in the non-polar scCO$_2$, while an increase in the molecular weight of the solutes exerts a negative impact on the observed solubility. Relatively low-density conditions, favor the solubilization of non-polar constituents of high vapor pressure and low molecular weight in scCO$_2$. On the other hand, accessing less volatile, larger and slightly polar constituents requires higher density conditions. Apparently, a wide range of compounds can be targeted with scCO$_2$ since its selectivity can be tuned by simple modifications in temperature and pressure. This selectivity is one of the main advantages that SFE technology has to offer. Nonetheless, scCO$_2$ has a limited solvating power and low polarity; therefore, in order to expand its use to more polar target molecules, polar co-solvents or modifiers in small quantities are employed. In the field of food processing, ethanol is commonly the co-solvent of choice, due to its environmental friendliness and its GRAS (generally recognized as safe) status.

The interactions between solute and co-solvent, for instance hydrogen bonding, charge transfer complex formation, and dipole-dipole coupling increase the density of the solvent mixture, thereby resulting in an increase in solubility.[22] The most commonly employed concentration of ethanol related to the CO$_2$ flow is 10 %.[3],[26] However, depending on the sample, target compounds and final objectives this concentration may vary. Additionally, the introduction of the co-solvent not only affects the extraction yield but also the quality of the extracts, which are enriched in polar valuable compounds, such as phenolic, antioxidant and anti-inflammatory compounds.[27-29] The downside of employing high quantities of co-solvent is a decrease of selectivity with altered critical parameters of the solution.[28]

7

In addition, some practical aspects regarding SFE need to be considered. When high extraction pressures are employed, lower quantities of solvents are required;[30] however, the quality of the extractant can be negatively affected, as excessively increasing the pressure could affect the antioxidant activity and also reduce the diffusivity of the SCF, thereby lowering the solute dissolution.[31] Furthermore, depending on the sample´s nature, the inserted material could be compressed under high pressure conditions in a way that negatively affects the extraction yield.[32] Increasing the temperature at a constant pressure leads to two opposite effects. Firstly, by increasing the temperature, the solvent density is decreased, hence, the solvating power of the fluid is also reduced and as a result the solubility of the target compounds along with the extraction yield are reduced. Secondly, the target constituents are affected positively, since their vapor pressure increases and, consequently, also their solubility and extraction efficiencies are raised.[30],[31],[33] The latest publications suggest that the extraction temperature and pressure must be carefully considered, in order to avoid degradation of thermally sensitive compounds;[3] precisely, temperatures between 35 to 60 °C and pressures of about 400 bar are recommended.[20] Several characteristics of the raw materials, namely their nature, moisture content, particle size, shape, surface area, and porosity can have a decisive impact on the extractability of the target compounds. These parameters affect the solubility and the mass transfer during the SFE.[34] In the majority of cases, the sample is dried prior to extraction to decrease its moisture content, because the water can interact with the solute, thereby negatively affecting the extraction yields, as it may interfere with the extracting solvent. However, in some cases the water is not removed, as it may interact positively with the extracting solvent, for instance in the extraction of caffeine from coffee beans. The appropriate range of moisture content lies between 4 – 14 %.[35] Particle size and porosity have a direct impact on the mass-transfer rate. The extraction efficiency is augmented by decreasing the particle size; with smaller particles, the contact surface area is larger, and the diffusion pathway of the extracting solvent is shorter. Consequently, the SFE extraction rate is accelerated. However, the particle size of the samples should not be excessively small, as it may promote resistance of the internal mass transfer, decreasing the efficiency and yield.[3],[20],[32],[35] Based on available literature data, the particle size of natural products extracted by SFE usually ranges from 0.25 to 2.0 mm[3],[35] Concerning the impact of the extraction time, employing short extraction times may lead to incomplete extraction of the target constituents. On the other hand, long extraction times may not be appropriate, due to increased solvent consumption, prolonged process duration and possible degradation of bioactive constituents.[32] On a related note, flow rate plays a key role in this matter; it has been demonstrated that employing high flow rate, leads to short extraction time, but as previously mentioned, also results in higher solvent consumption. In order to maximize the extraction yields, the optimum extraction time and flow rate must be employed.[27]

1.1.4 Supercritical fluid extraction - requirements and flow scheme.

In order to perform a SFE and to reach the supercritical state, specific equipment is required (Figure 5): a CO_2 supply source, a pump for the CO_2, a cooler that cools the CO_2 before it enters the pump, a pressure vessel or extraction cell to contain the sample, an oven with a thermostated pre-heating coil wherein the extraction vessel will be placed, a pressure-maintenance system, a gas-liquid separator and a sample collector compartment. Additionally, after being used, the CO_2 could be released into the atmosphere, or it could be cooled and compressed for reuse. The employed fluid is pumped into the system and then it is heated and pressurized to reach its supercritical state. When the SCF reaches the extraction cell and comes in contact with the sample, it diffuses through it, dissolving the sample material and extracting sample constituents.[8]
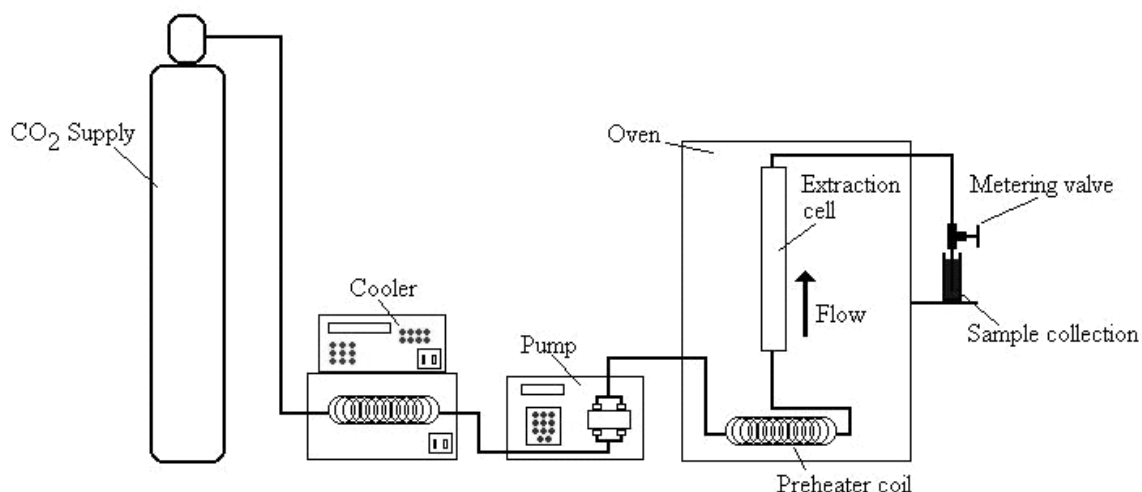
Figure 5. Flow scheme of the SFE equipment.[8]

Different pumps can be employed depending on the scale of the extraction. For laboratory-scale extractions, syringe or reciprocating pumps are employed. For industrial-scale extractions, diaphragm pumps are commonly utilized. The extraction vessels must resist high pressures and temperatures. The vessel is heated by different heat sources, i.e., oven, oil or electrically heated jacket, depending on its size.[8] These extraction cells are normally HPLC columns in which the sample is placed during the SFE process. Prior to its placement in the extraction cell, the sample is normally pre-treated, for instance it is dried or milled. Diffusion of the $scCO_2$ through the matrix, yields extractions of the soluble compounds and transports them through diffusion to the separator where the pressure is reduced and/or the temperature increased, in order to separate the solvent from the extract. At the end of the process, the target compounds are collected in the sample collector, whereas the solvent has already been removed in the previous step.[7],[35],[36] The system pressure can be regulated by a simple

restrictor, capillary tube adjusted to length, needle valve or a back pressure regulator. Apart from that, the adiabatic expansion of the CO_2 leads to considerable cooling; therefore, heating must be provided. Prior to its pumping in the system, CO_2 is cooled down to below 5 °C and turns into liquid and once it enters the system, it is pressurized, and heated.[8]

Whenever a co-solvent is employed, it can be inserted into the system either as a mixed fluid through the pumping system or by direct addition into the sample prior to extraction. Alternatively, a cylinder tank of pre-modified CO_2 can be used for the co-solvent introduction but it is generally not preferred due to its high cost.[32]

The SFE can be performed in static mode or in dynamic mode. In the static mode, the SCF is absorbed by the sample and it remains in the extraction vessel during the extraction process, while in the dynamic mode the SCF constantly flows through the sample.[37]

The extraction of bioactive compounds employing traditional techniques, typically results in the co-extraction of non-desired products and, therefore, in lower quality of extracts. Nonetheless, SFE is a sophisticated technique, that allows the fractionation of the extracts, hence, enhancing the selectivity and affording extracts of high quality.[38] In order to target specific compounds, a multi-step process can be designed by attaching separators consecutively and setting up individual conditions, i.e., pressure and temperature, according to the equilibrium solubility of each target compound.[39]

1.1.5 Supercritical fluid extraction - supercritical carbon dioxide applications in plant matter extraction

In former times, conventional extraction techniques were mostly employed for the extraction of bioactive constituents from plant matter, e.g., maceration, Soxhlet extraction and hydrodistillation. These processes rely on the extracting power of the organic or inorganic solvents employed and on the polarity of the compound of interest.[40] Conventional extraction techniques are still used as reference, mostly Soxhlet extraction. However, they have several drawbacks, such as low selectivity and high organic solvent consumption which leads to considerable environmental contamination. As a consequence, newer and more sophisticated techniques were developed that are less environmentally harmful.[41] To this end, SFE rose in popularity, as it is considered an environmentally benign and sustainable alternative for the recovery of natural products, particularly in the food, pharmaceutical and cosmetic industries. Supercritical carbon dioxide has been employed to a considerable degree and great developments have been achieved in those fields. In addition, its low toxicity does not affect the consumers' well-being.[42] In addition, compared with conventional extraction, the extracted bioactive constituents by the $scCO_2$ extraction have lower loss or denaturing of flavor or fragrance, leading to a better reproducibility and results. Apart from that, thermolabile

compounds are not significantly affected by scCO$_2$ extraction, since it can be performed at lower temperatures which diminish the probability of thermal decomposition. The lack of oxygen and light during scCO$_2$ extraction is beneficial as oxidation is minimized. Lastly, the extracts collected by scCO$_2$ *via* high-pressure gradient pressure release, contain neither living microorganisms nor their spores, thus they have longer shelf-life.[43]

Traditionally, plants have been a supply of chemical components employed in natural remedies against diseases. The plants produce secondary metabolites which are organic compounds that have a significant role in plants´ self-defence. Not only do they increase their chances of survival against predators and microbes, but they also aid communication with other organisms; hence, they are necessary for their growth and evolution.[44] These secondary metabolites are present in plant-related products, such as fruits, vegetables, herbs, spices, aromas and even in plant residues. They also have a wide array of medicinal effects on human health and, currently, the constituents present in plants are employed for functional foods (e.g., colorants, flavorants, additives, fragrances and so on), natural pesticides and development of new drugs.[40],[42]

SFE has been utilized for the extraction of bioactive compounds from more than 300 plant species.[45] It has already been employed in a vast variety of natural resources, such as thyme (*thymus praecox polytrichus*),[46] sage (sage *officinalis*),[47] hops (*humulus lupulus*)[48] and sweet wormwood (*artemisia annua* L.)[49], with the purpose of extracting their medicinally active compounds, which exhibit a wide array of health beneficial effects, for instance antibacterial, anti-inflammatory, antioxidant, anti-cancer and antimalarial, among many others.[46-49]

Plants produce their natural bioactive compounds through four primary pathways: shikimic acid pathway, the malonic acid pathway, the mevalonic acid pathway and the methylerythritol pathway.[40],[50] The bioactive compounds obtained from these pathways can be classified into three main groups: alkaloids, terpenoids/terpenes and phenolics.[50-52] They are present in different parts of the plants, namely leaves, flowers, buds, stems, roots, fruits, seeds, and tubers.[53]

Alkaloids defend the plant against herbivores and pathogens, and they also contain medicinally active compounds. They are employed as narcotics, poisons, stimulants or pharmaceuticals. The most popular alkaloids are caffeine, nicotine, cocaine, morphine, and codeine.[50],[54] Particularly, caffeine is present in many different natural plants and is used in soft beverages and drinks for its stimulant properties. Nonetheless, it also has several side-effects on humans, for example insomnia, nervousness, anxiety, hostility and potentially other health issues.[55] Hence, the interest of consumers shifted toward decaffeinated products, and the removal of caffeine from coffee beans with modern techniques gained attention. In the 1960s, Dr. Kurt Zosel´s innovative scCO$_2$-assisted decaffeination process set the ground for the current large-scale caffeine extraction process (Figure 6).[6] Currently, not only coffee, but also tea and several other products have already been decaffeinated with scCO$_2$.[56]

In addition, scCO₂ has been employed to remove other alkaloids (i.e., olchicine, vinblastine, vincristine) from plants, such as leaves of pepper elder (*piper amalago*), seeds of wild plants of autumn crocus (*colchicum autumnale* L.) and periwinkle (*catharanthus roseus*), among many others.[57-59]
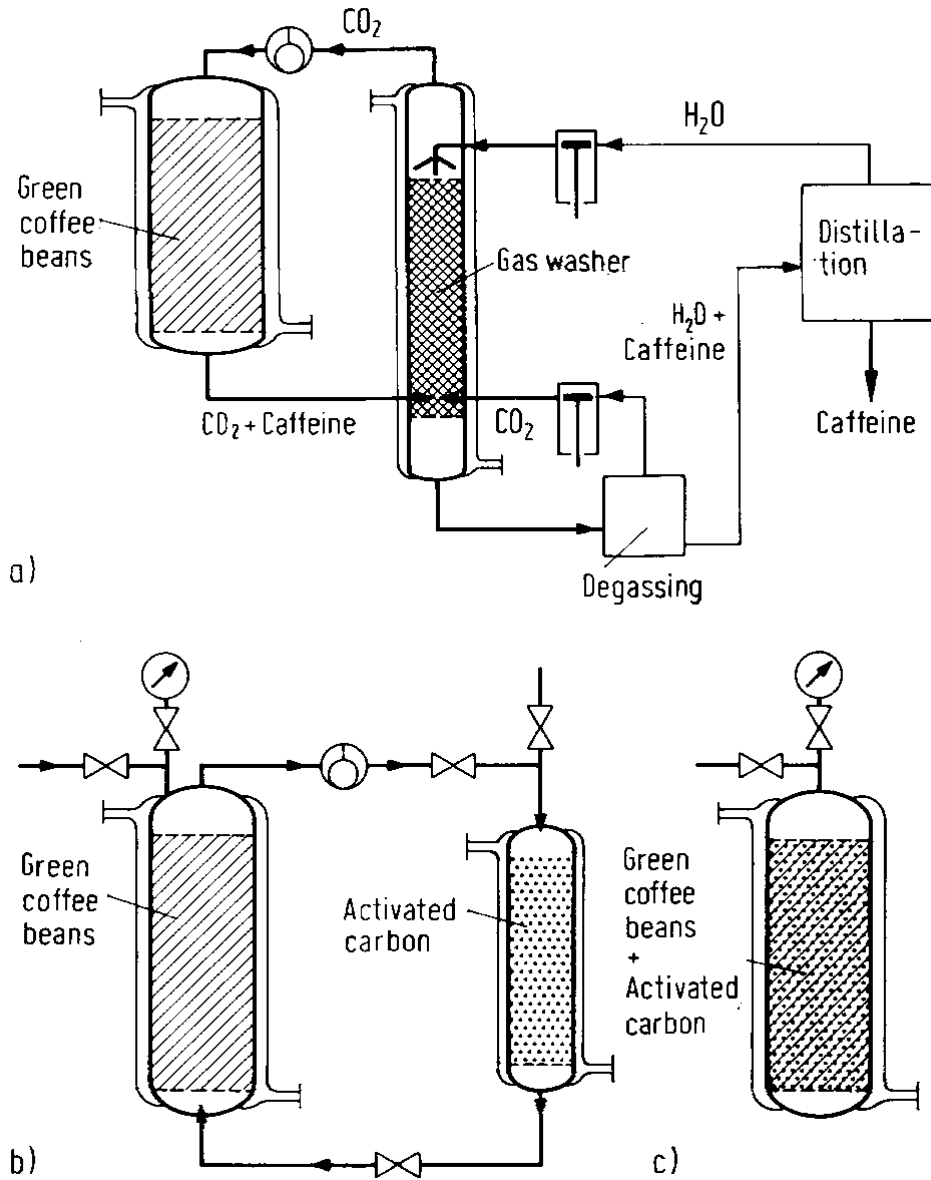
Figure 6. Decaffeination of green coffee beans with supercritical CO_2 by K. Zosel.[6] a) Caffeine is removed from the CO_2 by washing with water. b) Caffeine is removed from the CO_2 by adsorption on activated charcoal. c) The caffeine is removed from the CO_2, without recycling, by adsorption on activated charcoal admixed with the coffee beans.

Terpenes or terpenoids are essential for the physiological activity of the plant, including its defence, growth and reproduction. Monoterpenes and sesquiterpenes present in plants are utilized as fragrance agents, flavorants and food additives. They are found in food products, beverages, perfumes and soaps.[60] Moreover, carotenoids, which are tetraterpene plant pigments can be found in pumpkins, tomatoes, and carrots. Additionally, they have health benefits, for instance pro-vitamin A activity, anti-cancer activity and antioxidant capacity. Carotenoids from different vegetable matters (i.e., mango peels, Nantes carrots peels, tomato) have also been successfully extracted by scCO$_2$.[61-64]

The essential oils of several species of herbs and aromatic plants contain terpenes and terpenoids. They are employed in medicine, herbicides, food additives, cosmetics, insecticides, and more.[65] They possess several health benefitting properties, involving antioxidant, antibacterial, anti-inflammatory and antifungal activity.[66] Due to their biological activity, they have gained attention from academia and the pharmaceutical industry. Supercritical carbon dioxide has been utilized to extract the essential oil from different plant matrixes, such as green coffee beans,[67] apple seed,[68] spearmint leaves,[69] and rosemary (*rosmarinus officinalis*).[70]

Different types of phenolic compounds are known, such as flavonoids, stilbenes, lignans and gallic acids (Figure 7).[52] They are important secondary plant metabolites that regulate the growth, pigmentation and reproduction of the plants and offer protection against pests.[71] They also possess medicinal properties, such as antioxidant capacity, free radical scavenging properties, control of metabolism and weight, among others. For example, the antioxidant activity of polyphenols is exploited in many food products, because it prolongs their shelf life.[50],[71]

Flavones **Flavonols** **Flavonones** **Dihydroflavonol** **Isoflavones**

Stilbene backbone **Lignan backbone** **Gallic acid**
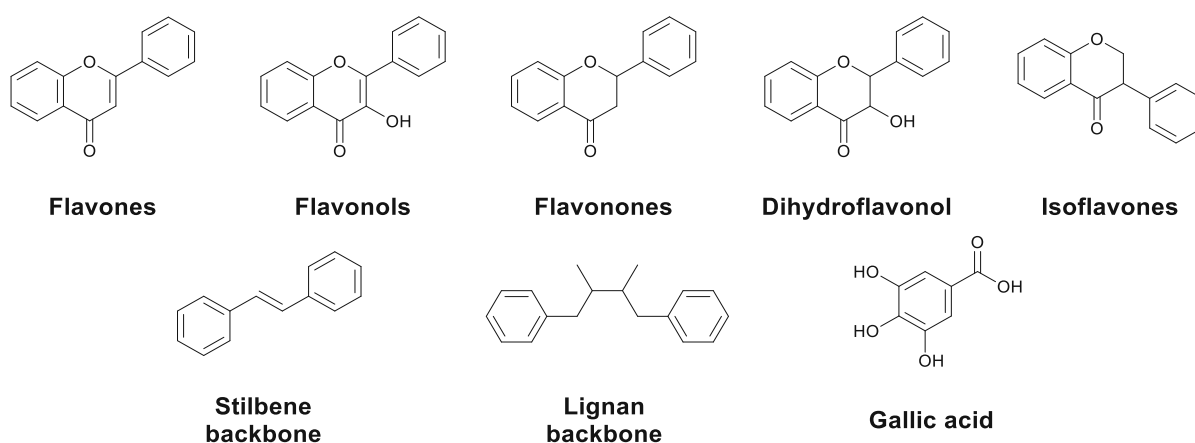
Figure 7. Chemical structures of different types of phenolic compounds.

Flavonoids contribute to the plant pigmentation and protection against pathogens. They are encountered in fruits, seeds, leaves, bark and flowers.[72],[73] In addition, they prevent cancer, cardiovascular disease, and chronic inflammatory conditions.[73] Not surprisingly, several phenolic compounds (i.e., flavonoids, total phenols, tocotrienols, tocopherol) were extracted from different plant material, such as pecah kaca leaves (*strobilanthes crispus*),[72] strawberry (*arbutus unedo* L.),[74] annatto seed (*bixa orellana* L.)[75] and quinoa (*chenopodium quinoa* willd.).[76]

In the field of food chemistry, scCO$_2$ has been employed for the extraction of bioactive compounds from food waste. A wide array of food sources ranging from mango peels,[61] egg yolk,[77] meat products,[78] coffee,[39] fish[79] and many more have been subjected to scCO$_2$-based extraction, aiming for the extraction of natural antioxidants,[61] lipids and cholesterol,[79] caffeine,[39] natural glycosides[80] and free amino acids.[81]

In the pharmaceutical sector, SCFs are employed for the isolation of the desired compound(s) from a mixture and for the extraction of medicinally active constituents for subsequent use in drugs. For instance, artemisin and its derivatives, which have antimalarial activity, have been extracted from *artemisia annua* L. for medicinal purposes.[49] In addition, alkaloids have also been extracted from periwinkle (*catharanthus roseus*)[59] and *melocactus zehntneri*[82] for application in drug preparations.

Natural products are also commonly employed in cosmetic formulations. Antioxidants are one of the most commonly utilized ingredients, as they increase the self-life of the products, protect human cells and prevent skin-cancer.[83] Antioxidant and parabens were isolated by scCO$_2$ from different cosmetic products. In addition, several different natural sources, i.e., mint leaves, strawberry seeds, blackcurrant seeds and hop cones, have been subjected to scCO$_2$-based extraction, and their extracts were proven to be employable as ingredients for shower gels.[84]

1.1.6 Supercritical fluid extraction - supercritical carbon dioxide applications in metal extraction

The use of scCO$_2$ as extractant is not limited to natural products; heavy metals, such as Pb, Cd, Cr, Fe, Cu, Zn, Ni, W, are inorganic pollutants that possess high toxicity and are, thus, detrimental to the environment if not handled properly. Some of these heavy metals are essential trace elements, for instance Cu, Fe and Zn, while Ni and Cr exhibit relatively low toxicity.[85-88]

Heavy metal elements can severely contaminate the environment through soil, air, water as well as biomes.[89],[90] Particularly, plants and soil absorb heavy metals, that later enter the food chain, resulting in terrible damage to human health.[91],[92]

Heavy metal pollution is regarded as persistent, easily accumulative, highly toxic, long-lasting and has irreversible impact. Thus, heavy metal pollution management has drawn the attention of the

agricultural, ecological, and environmental science fields world-wide.[93],[94] For the extraction of heavy metals, several techniques have been developed, such as chemical precipitation, barrier separation,[95] adsorption[96] and ion-exchange[97],[98] among other technologies. Over the last few years, SFE technology has rapidly progressed in extracting active components from natural plants, and it was found to be effective (see section 1.1.5). Therefore, researchers also thought of employing SFE in the field of environmental science to extract organic pollutants, for instance polycyclic aromatic hydrocarbons, polychlorinated biphenyls, organic phosphorus, chlorinated pesticides.[99-102] Special components can be extracted by modifying the pressure and temperature and considering the size, boiling point, polarity and molecular weight. The extraction efficiency depends on the solvent strength of the SCF which is strictly related to the temperature and pressure. In addition, when required by manipulating pressure and temperature the SCF becomes a normal gas, it can be directly recycled and the extracted metals are separated and collected for further purification.[103] Thus, SFE is considered an environmentally benign alternative to extract heavy metal ions, because of its high diffusivity and low viscosity, compared to traditional solvent extraction for heavy metals from polluted samples.[104-106]

In order to efficiently extract heavy metals, some important parameters need to be considered and optimized, such as extraction pressure, extraction temperature, extraction time, use of complexing agents, use of modifying agents, pH, heavy metal species and matrix and use of surfactants.[107]

It is worth mentioning that heavy metal ions possess strong polarity and CO_2 is non-polar. Therefore, the extraction of heavy metal ions from polar substances becomes a very challenging task. The main reason is the minimal interaction between the SCF and the metal ions. In order to make the extraction process possible and to maximize the extraction efficiencies, positively and negatively charged complexing agents are introduced to coordinate heavy metal ions.[107] The following complexing agents are traditionally employed: dithiocarbamic acid ligands, organophosphorus salts, acetylacetone (AcAcH), amines, crown ethers and porphyrins among others.[108-110] The structure of several complexing agents is depicted in Figure 8.[111]
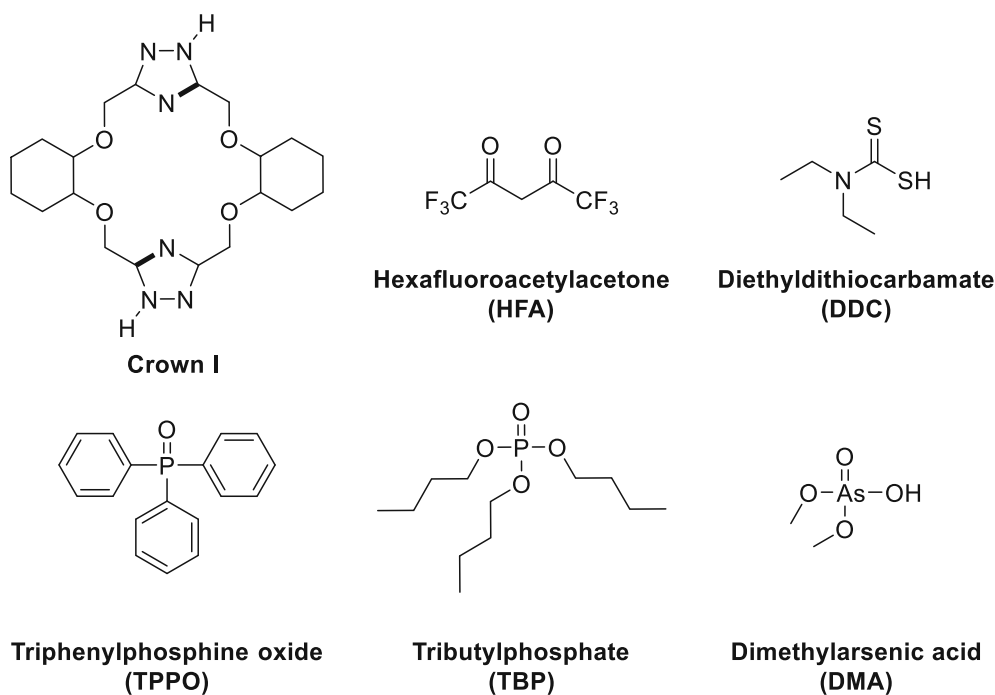
Figure 8. Structures of selected complexing agents.[107],[111]

Particularly, Cyanex 302, Aliquat 336, D$_2$EHPA, D$_2$EHTPA are habitually used. Depending on their nature the ligands can be classified into four categories[112]:

1. Acid ligands (e.g., Cyanex 302, D$_2$EHPA)

2. Acid chelating ligands (e.g., NaDDC[113], DMA and MMA[114])

3. Anion exchangers (e.g., Aliquat 336)

4. Solvating ligands. (e.g., Cyanex 923)

On a related note, SFE technology has also been considered for the treatment of nuclear waste, namely for the separation of actinides, lanthanides and fission products, which are important for the nuclear waste management and spent fuel reprocessing.[115]

In the early 1990s, Laintz et al.[116] published the first scCO$_2$-based process for dissolution and extraction of metal species. In their first publication, their objective was to investigate methods to dissolve metal ions in scCO$_2$. By utilizing a fluorinated dithiocarbamate chelating agent, i.e., bis(trifluoroethyl) dithiocarbamate (FDDC), complexes were formed that possessed high solubilities compared to their non-fluorinated analogues.[116] In their subsequent publication, it was reported that copper ions (Cu^{2+}) in aqueous solutions were successfully extracted by utilizing FDDC as complexing agent.[117] Nowadays, fluorine-containing compounds are regarded as "CO$_2$"-philic.

Numerous publications reported the successful extraction of trivalent lanthanide ions and uranyl ions, dissolved in water or spiked in solid materials, employing fluorinated β-diketonates as complexing agents.[118-120]

Later on, fluorinated β-diketonates for the extraction of uranium oxides directly in $scCO_2$ were further investigated by Wai and Waller.[121] Thenoyltrifluoroacetone (Htta) achieved the direct dissolution of solid UO_3 (uranium trioxide) in $scCO_2$. In addition, by adding tri-*n*-butylphosphate (TBP) the dissolution of solid UO_3 is obtained with a higher efficiency. The stronger Lewis base TBP could replace water in $UO_2(tta)_2$ H_2O to generate $UO_2(tta)_2$ TBP, which is a more soluble adduct complex.[121]

Further publications reported the extraction of actinides in $scCO_2$ using fluorinated β-diketonates and organophosphorus reagents.[122],[123] Plutonium and americium in soil were effectively removed with $scCO_2$ with the aid of Htta and TBP.[122] In addition, Murzin et al. investigated the solubilities in $scCO_2$ of uranium, plutonium, neptunium, and americium β-diketonates and their adducts with organophosphorus reagents.[123]

Relevant progress was made in the field of uranium extraction when Lin et al.[124] published the SFE of uranyl ions in nitric acid solutions utilizing TBP as extractant in the traditional PUREX (Plutonium uranium reduction extraction) process. In other related publications, Meguro et al.[125],[126] published uranium extractions using $scCO_2$ and TBP.

Smart et al.[127] suggested a supercritical fluid-PUREX process for reprocessing spent nuclear fuel. In that process depicted in Figure 9, conventional organic solvents are replaced with $scCO_2$, achieving possibly higher mass transport properties, faster extraction rates, and tuneable distribution coefficients of uranium and other actinides. On the negative side of this process, acidic liquid waste would be generated. After Smart´s proposed application, the research in this field focused heavily on a dry process for the dissolution of UO_2 (uranium dioxide) in $scCO_2$.[128]
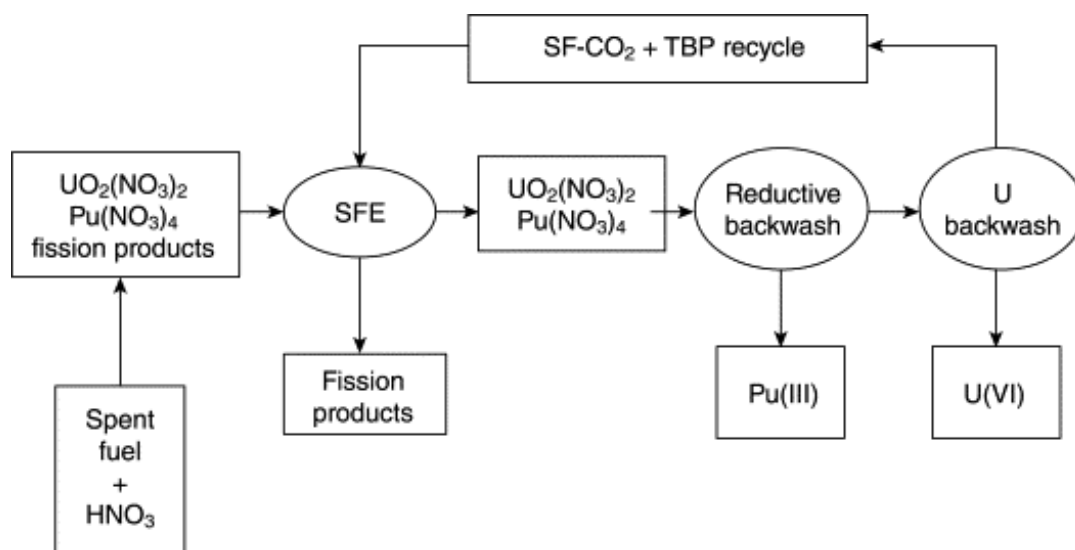
Figure 9. Schematic diagram of the supercritical fluid-PUREX process proposed by Smart et al. 1998.[127]

Afterwards, Wai et al.[129] proposed in 2002 a theoretical illustration (Figure 10) of a dry-scCO$_2$ dissolution for reprocessing spent nuclear fuel. TBP-HNO$_3$ complex would be utilized for the dissolution in scCO$_2$ phase of lanthanides, uranium and transuranic elements, while fission products, such as Sr and Cs, would remain in the residues. Furthermore, in the hypothetical ligand regeneration step, UO$_2$(NO$_3$)$_2$(TBP)$_2$ would be transformed into UO$_2$ and TBP-HNO$_3$ would be recovered. Even though considerable research efforts would need to be invested to make this process feasible, this is the direction in which the research is pointing, namely into a more environmentally benign process.[130]
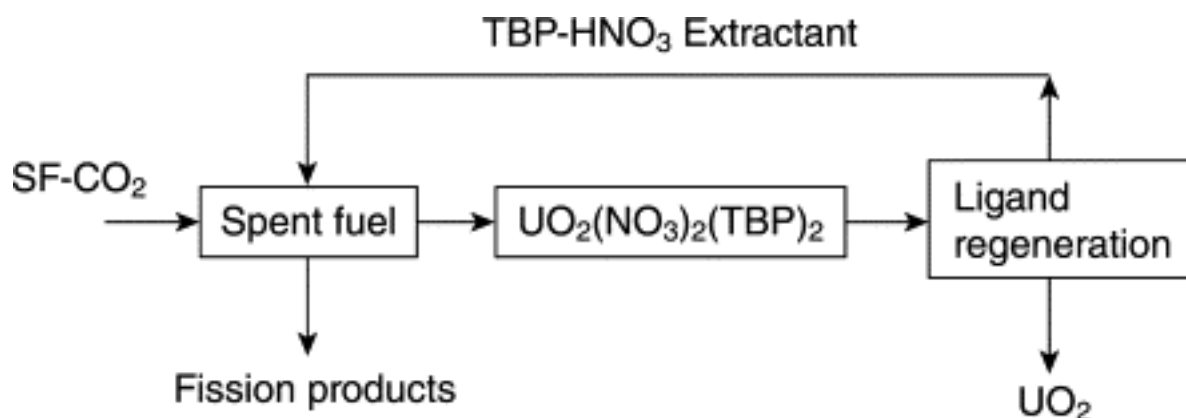
Figure 10. A conceptual illustration of reprocessing spent nuclear fuel in scCO$_2$ using a TBP-HNO$_3$ Lewis acid-base complex.[129]

Wai et al. reported the extraction of fission products (^{90}Sr and ^{137}Cs) *via* scCO$_2$ utilizing crown ethers as selective ligands.[131],[132] The scCO$_2$ extractions were performed in water employing the ligand dicyclohexano-18-crown-6 (DC18C6). This ligand has been proven to be CO$_2$ soluble and selective towards Sr^{2+} in traditional solvent extractions. However, results pointed to the direction that the produced Sr-DC18C6 complex does not dissolve in the scCO$_2$ phase. In order to make the scCO$_2$ extraction feasible, Wai et al.[131] thought of using fluorinated counter anions that would neutralize the charge of the complex, leading to an ion-pair soluble in CO$_2$ phase. For the extraction of Sr^{2+} and Cs$^+$ using crown ether ligands in scCO$_2$, the following fluorinated counter ions have proven to be effective: ammonium or potassium salts of pentadecafluoro-*n*-octanoic acid and perfluoro-1-octane sulfonic acid. Selective extraction of Sr^{2+} in water by scCO$_2$ was achieved utilizing DC18C6 and pentadecafluoro-*n*-octanoic acid (CF$_3$(CF$_2$)$_6$COOH). In another publication by Wai et al.,[132] Cs$^+$ was extracted selectively *via* scCO$_2$ using dicyclohexano-21-crown-7 and perfluoro-1-octanesulfonate.

1.2 Ionic Liquids

1.2.1 Historical background

In 1888, Gabriel published the discovery of the compound ethanolammonium nitrate, that appears to be the earliest synthesized organic salt with a melting point below 100 °C, specifically 52-55 °C.[133] Paul Walden discovered in 1914 that [EtNH$_3$][NO$_3$] (ethylammonium nitrate) has a melting point below room temperature at 12 °C.[134] He was interested in researching the relationship between the molecular size and the conductivity of these molten salts. However, the importance of this finding did not draw attention at that time.

In 1975, Bob Osteryoung´s group was studying the electrochemistry of two iron (II) diamine complexes, ferrocene and hexamethylbenzene, at room temperature employing the same system and same molar ratio employed by Hurley and Weir.[135] They noticed that this system was liquid at room temperature only at a particular molar ratio. Therefore, they invested their efforts into discovering new systems that would be liquid in a much broader range of compositions, and the [C$_4$py]Cl:AlCl$_3$ system was investigated specifically.[136]

During the 1980s, scientists showed a spark of interest in ILs, leading to an expansion of IL-based research and their application beyond the field of electrochemistry. Wilkes synthesized for the first time ILs based on 1,3-dialkylimidazolium cations, specifically 1-alkyl-3-methylimidazolium chloride-aluminium chloride, which demonstrated high transport properties.[137] The fields of inorganic and coordination chemistry of transition metal species had considerable interest in finding other solutes in room temperature haloaluminate ILs.[138]

Ionic liquids achieved another level of progress owing to another publication of Wilkes regarding air and water stable 1-ethyl-3-methylimidazolium based,[139] as this publication became the spark that boosted subsequent discoveries, leading to an expansion in the quantity and range of ILs regarding their cations and anions.[140],[141]

Toward the end of the 20th century, ILs got the attention of a broader scientific public, while the numerous possible combinations of building cations and anions rendered them a "designer solvent" status.[142] It was the perceived number of potential applications that increasingly attracted researchers to the field of ILs, as this is reflected by the steadily growing rate of relevant publications in the following years (Figure 11).
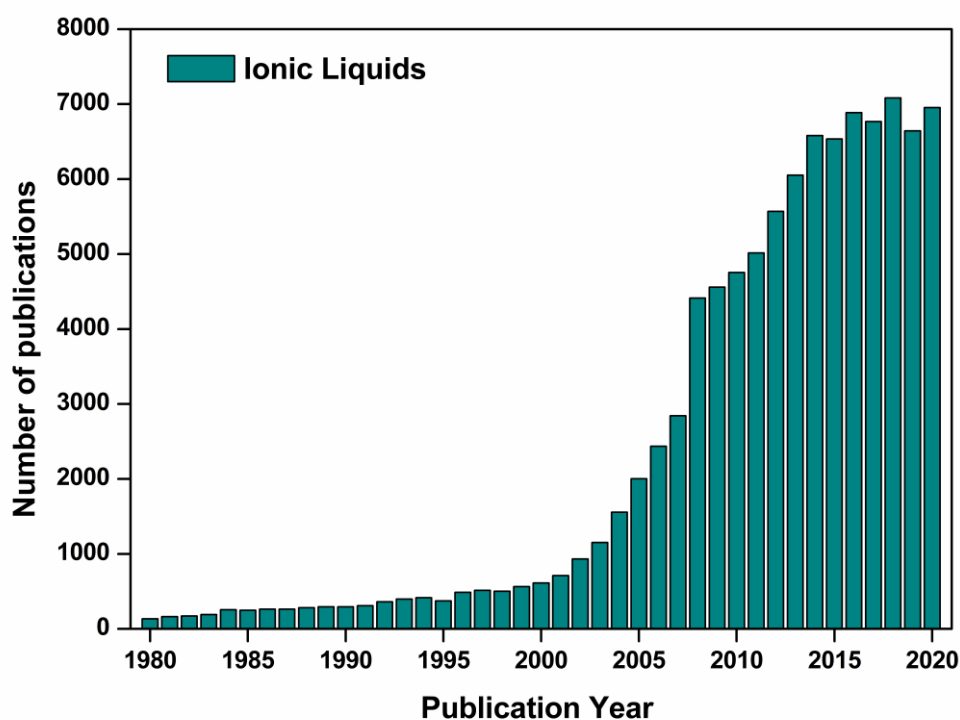
Figure 11. Number of publications related to ILs provided by SCOPUS (search term: ionic liquids, date of search: 26.05.2021).

In 2002, Swatlosky et al.[143] reported that some ILs can dissolve and regenerate cellulose. As a consequence, the interest in the potential application of ILs, not only in cellulose processing but also in biomass processing, rose drastically and it developed into a highly active research field. Ionic liquids also were used to dissolve whole wood[144] and to selectively extract lignin from biomass.[145] In addition, biomass polymers in ILs have been used to generate biomass-derived products.[146]

Several ILs have also been used in energy generation and storage[147],[148] due to their non-volatility and non-flammability.[149] Besides, they also possess many other advantages over traditional solvents, such as wide electrochemical window, stability to different electrode materials and optimum discharge and cycle capability.[150] Furthermore, ILs have proven to be useful in the separation and extraction of bioactive compounds.[151]

As mentioned in the previous sections, ILs are quite versatile, because of their two constituents, namely cation and anion. Scientists can exploit that characteristic and tailor the function and properties of ILs, as their use in variety of applications indicates (Figure 12). The enormous number of possible combination of cations and anions together with their extensive array of properties can potentially lead to new undiscovered horizons in terms of applications.
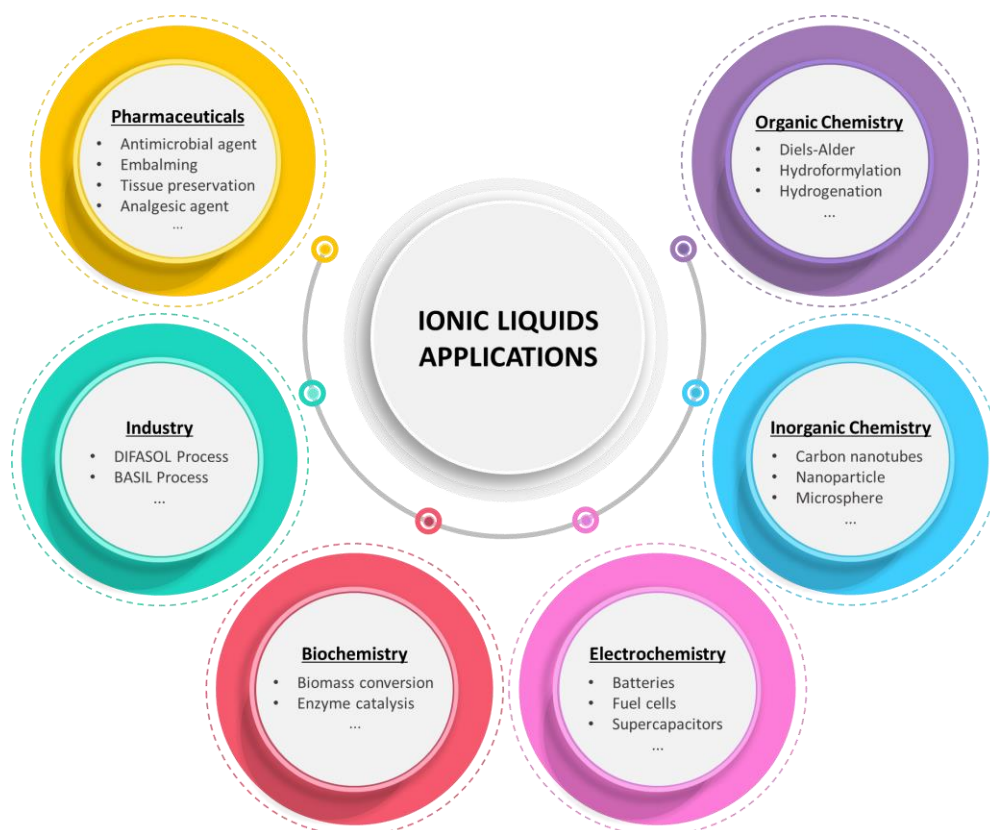
Figure 12. Some of the most important applications of ILs.

Apart from that, the rising environmental concern related to traditional chemistry, involving toxic, hazardous, and non-environmentally benign processes, have placed ILs at a favorable position. Researchers have considered ILs as a more environmentally benign alternative to develop new processes, as an eco-friendly, sustainable, and less-toxic alternative. Currently, ILs have been broadly employed in several different fields, due to their benefitting characteristics, to name a few, high chemical, physical, biological, and thermal stability.[152]

1.2.2 Fundamentals

Per definition, ILs are liquids entirely composed of ions, which have melting points below 100 °C.[153] Particularly, ILs that have a melting point near room temperature are classified as "room-temperature ionic liquids" (RTILs).[154] Their liquid state is favored, because of the large size and conformational flexibility of their ions, resulting in small lattice enthalpies and large entropy changes.[155-157] The comparison between a typical symmetric inorganic salt and typical IL is depicted in Figure 13.
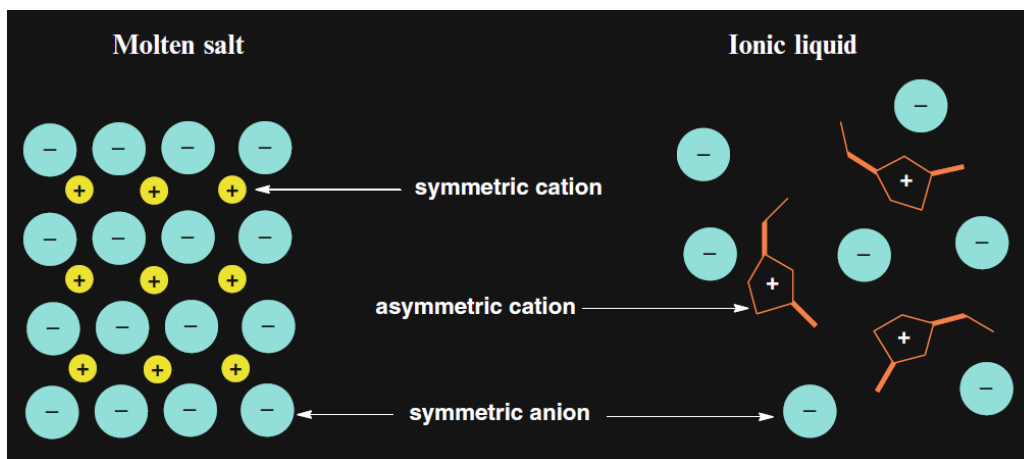
Figure 13. Comparison between a typical symmetric inorganic salt and a typical IL.[158]

Contrary to traditional organic solvents, ILs possess negligible vapor pressure, are non-flammable and many of them withstand higher temperatures without losing thermal stability. Ionic liquids have also broader liquid ranges compared to traditional organic solvents[159] and possess wide electrochemical windows and high ionic conductivity.[160] Broader solubility and miscibility ranges can be accessed with ILs, since they can be designed to be more hydrophobic or hydrophilic.[161] They can be employed in a broad array of chemical transformations as solvents or catalysts and can also be utilized for separation of chemicals from aqueous and conventional organic solvents. After ILs are used as catalysts and/or solvents, they could also be recycled.[162]

Ionic liquids display high tuneability of their properties (i.e., chemical, physical and biological), due to the fact that their anions and cations (dual functionality) can be varied, particular functionalities can be introduced into their cations and/or anions.[163]

The most frequently used cations are depicted in Figure 14.[164] Imidazolium ILs containing 1-alkyl-3-methylimidazolium cations have been the most extensively researched.
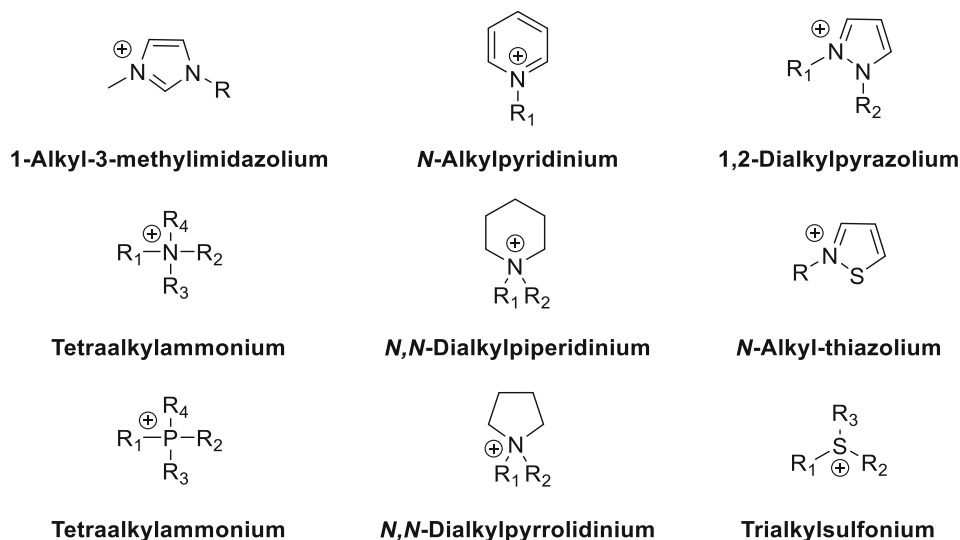
Figure 14. Traditional cations employed in ILs, where R, R_1, R_2, R_3, and R_4 refer to alkyl groups.

Some of the most commonly employed anions[164] are illustrated in Figure 15 in their corresponding increasing order of hydrophobicity.[160]

Additionally, other anions can also be employed, i.e., nitrates, chloroaluminates, *p*-toluenesulfonates, trifluoromethylsulfonates, bis(perfluoroethylsulfonyl)amides, dicyanamides, tris(pentafluoroethyl)trifluorophosphates, metal complexes between many others.
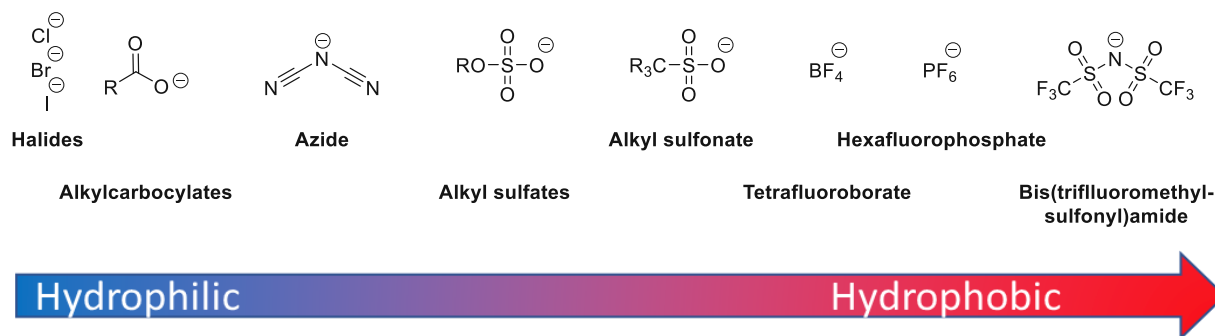
Figure 15. Examples of most employed anions in ILs, where R and R_3 are alkyl groups, in increasing order of hydrophobicity.

The structure and molecular packing of the ions are the key factors that contribute to the low melting points of ILs, which can be achieved by increasing the size, anisotropy, and internal flexibility of the ions. Additionally, the melting point is influenced by the length and symmetry of the alkyl chain of the cations. Besides, the melting point is habitually elevated by the high molecular symmetry and short *N*-alkyl chains.[165]

Compared to conventional solvents, RTILs are between ten and thousand times more viscous,[166] with the anion having a significant impact on their final viscosity.[140],[167],[168] For instance, ILs bearing a

bis(trifluoromethanesulfonyl)imide anion ($[NTf_2]^-$) exhibit lower viscosity, as well as ILs containing a hexafluorophosphate anion ($[PF_6]^-$), because their anions have non-planar symmetry. Interestingly, viscosity is significantly affected by the relative basicity of anions and their capability to create hydrogen bonds or to permit Van der Waals interactions. Additionally, higher viscosities are obtained by increasing the alkyl chain length of the cations.[161],[169]

Contrary to traditional solvents, ILs contain strong ionic interactions, which lead to higher enthalpies of vaporization. The vaporization is affected by the symmetry of the anions. Specifically, ILs that contain more symmetric anions (i.e., Cl^-, $[BF_4]^-$) have higher vaporization enthalpy compared to $[NTf_2]^-$-containing salts. However, there are ILs that can degrade in the gas phase, for instance $[C_2mim]Cl$ (1-ethyl-3-methylimidazolium chloride).[170-172]

Certain IL properties, such as viscosity, polarity, conductivity and in some cases even solubility, are significantly affected by the presence of water. Depending on the selection of the anion, a hydrophobic or hydrophilic IL can be synthesized. On one hand, anions such as $[PF_6]^-$, $[SbF_6]^-$ (hexafluoroantimonate anion), $[OSO_2CF_3]^-$ (trifluoromethanesulfonate anion) and $[OCOCF_3]^-$ (trifluoroacetate anion) are hydrophobic; on the other hand, anions such as halide, pseudo-halide, $[BF_4]^-$, methyl sulfate, NO_3^- and ClO_4^- are hydrophilic.[161] The solubility of the IL in water depends predominantly on the anion; the strength of the hydrogen bonds depends on the interaction with the anion, which directly influences the solubility of the IL in water.[173]

1.2.3 Synthesis methods

The number of available ILs has increased along with the variety of their developed synthesis methods. The most traditional methods of synthesizing different ILs are going to be discussed in this section.

The alkylation reaction is the first step to the preparation of ILs; a nucleophile in the presence of an alkylating agent (i.e., haloalkane or a dialkyl sulfate) produces the IL. The reaction temperature depends on the employed haloalkane, and the reaction time can vary between 24 h to 72 h. In addition, the reactivity rate follows increasing size and nucleophilicity: Cl < Br < I.[139],[140],[174],[175] The reactions can be performed in a solvent-free fashion or in the presence of organic solvents. The reaction mixture should be kept away from moisture, as synthesized products are frequently significantly hygroscopic, thus, reactions are carried out in inert atmosphere (N_2). Generally, halide salts are denser that the solvent, which allows the removal of the solvent by decantation. After synthesis, re-crystallization might be necessary for the purification of the obtained IL.[176]

The production of these ILs in large scale is performed in solvent-free fashion while an ultrasound unit,[177] microwave unit,[178] or a continuous-flow set-up can be employed.[179]

In order to access a wider array of ILs, after the alkylation (or quaternization), the anion exchange is commonly employed as second step. The anion exchange comprises two categories: 1) the synthesis of ILs *via* anion metathesis and 2) combination of halide salts with Lewis acids.[180] The anion exchange step allows the exchange of the halide anion and it can be performed in two different routes, which rely on the water solubility of the target ILs, metathesis *via* free acids or group I metals/ammonium salts, or silver salt metathesis.[181]

For instance, the syntheses of [C$_2$mim]Cl and [C$_4$mim]Cl (1-butyl-3-methylimidazolium chloride) *via* alkylation are illustrated in Scheme 1A.[182] By reacting the previously illustrated ILs with stoichiometric ratio of lithium bis[(trifluoromethyl)sulfonyl]amide the metathetic reaction takes place (see Scheme 1B).[140],[183] On the negative side, in the anion-exchange step, formation of 1 equivalent waste LiCl occurs, which requires extensive washing to remove Li$^+$ and Cl$^-$ and extensive drying to remove remaining water traces.

A)

1-methylimidazole + chloroethane →(90 °C, 96 h, neat) [C$_2$mim]Cl

1-methylimidazole + chlorobutane →(90 °C, 96 h, neat) [C$_4$mim]Cl

B)

[C$_2$mim]Cl + Li[NTf$_2$] →(1) r.t., 1h, Ar; 2) reflux, 2h, Ar) [C$_2$mim]NTf$_2$ + LiCl
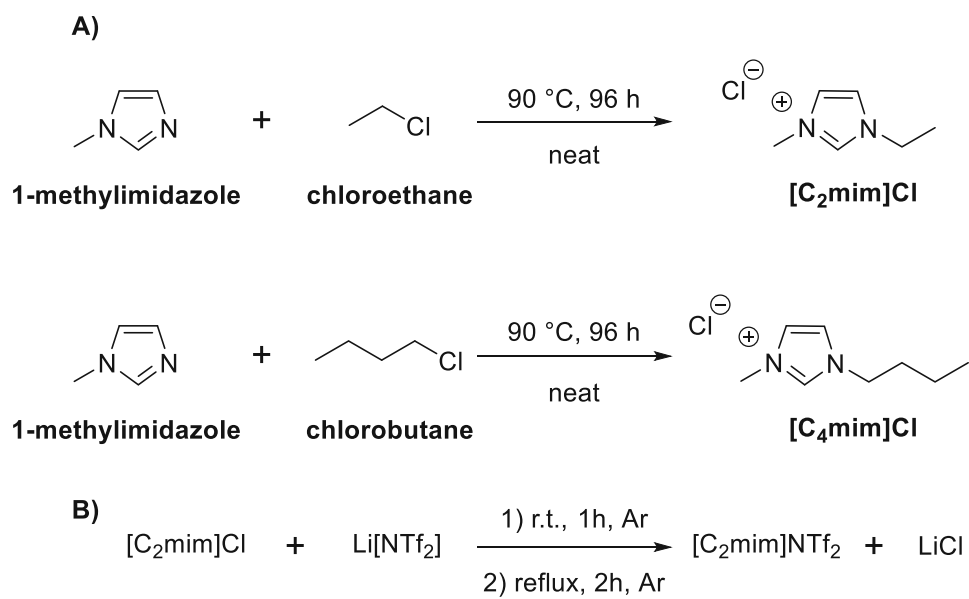
Scheme 1. IL synthesis: A) alkylation step[182] and B) anion exchange.[140],[184],[185]

1.2.4 Applications

The rising environmental concern related to traditional chemistry, involving toxic, hazardous, and not environmentally benign processes, have placed ILs in a favorable position. Researchers have considered ILs as a more environmentally benign alternative to develop new processes, that could potentially serve the objective of sustainability. Currently, ILs have been broadly employed in several different fields, due to their beneficial characteristics, to name a few, high chemical, physical, biological, and thermal stability.[152]

The industrial field has also developed applications utilizing ILs both in commercial and pilot scale. The first IL-based industrial application was developed in 1996 by Eastman Chemical Company and, in the following decades, a remarkable rise in the IL-based industrial applications was observed (Figure 16).[186]
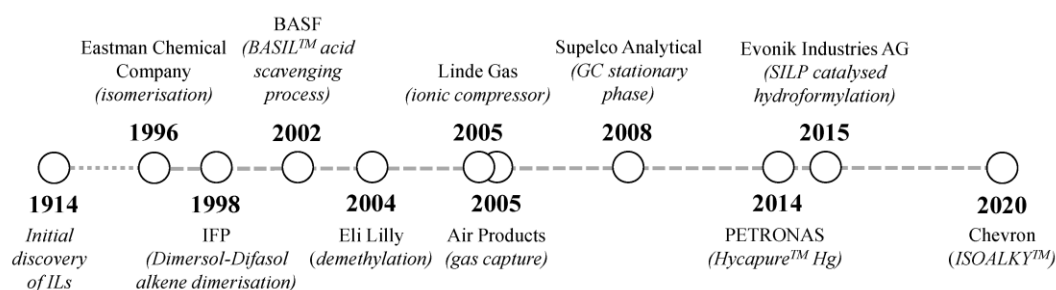
Figure 16. Commercialized IL-based processes ordered chronologically.[186]

1.2.4.1 Commercial scale processes

In 1996, Eastman Chemical Company developed the isomerisation of 3,4-epoxybut-1-ene to 2,5-dihydrofuran, which is an intermediate of tetrahydrofurane.[187] The process was carried out in a continuously fed reactor, employing a Lewis acid catalyst and tetraalkylphosphonium iodide as Lewis base IL, generating around 1400 tons each year until 2004.[188],[189]

In 2002, BASF (Badische Anilin- und Sodafabrik) became one of the first companies that commercialized an IL-based application, known as Biphasic Acid Scavenging utilizing Ionic Liquid (BASIL) process.[190],[191] The developed BASIL process produced alkoxyphenylphosphines, which are key raw materials for photoinitiators. Initially, BASF synthesized diethoxyphenylphoshine by employing tertiary amines to scavenge the HCl that was produced as a by-product. Scavenging the HCl (hydrochloric acid) with tertiary amines in a non-aqueous media led to a thick nearly non-stirrable slurry, and consequently, to a suboptimal mixing, inefficient heat transfer and low yields.

To circumvent this issue, BASF designed the BASIL process,[190],[191] which employed an 1-methylimidazole as an acid scavenger (Scheme 2), resulting in the formation of the IL 1-methyl-imidazolium chloride ([HC$_1$im]Cl). This by-product was liquid at the reaction temperature and

lead to the generation of two clear liquid phases. The lower phase contained the pure IL and the upper phase was composed of the pure product.
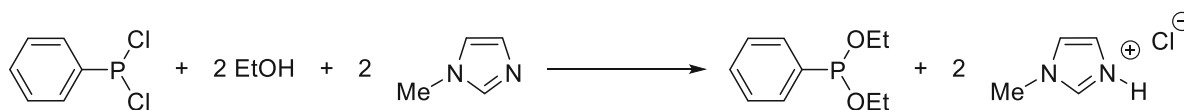
Scheme 2. BASF´s BASIL process for the synthesis of diethoxyphenylphosphine.[190]

The BASIL process had several advantages, such as easy separation of the product and the opportunity to recycle and purify the IL by simple protonation and deprotonation. Additionally, a new smaller reactor was designed and the productivity increased outstandingly from 8 kg m^{-3} h^{-1} to 690000 kg m^{-3} h^{-1} (a factor of 8 x10^4).[190],[191]

1.2.4.1.1 Alkylation

Ionic liquids have demonstrated to be a suitable and safer alternative to the corrosive acids (H$_2$SO$_4$ and HF) utilized during the alkylation process.[192] The ISOALKY^{TM} technology was investigated by Chevron in cooperation with QUILL (Queen´s University Ionic Liquid Laboratories). This process employs a chloroaluminate-based IL in conjunction with an organic chloride co-catalyst, achieving a mixture that possesses a remarkably high acidity and high hydrophilicity. The reactants need to be dried to H$_2$O content < 1 ppm, in order to avoid possible hydrolysis. After completion of the reaction, the IL can be separated from the product stream *via* proprietary coalescing technology, feeding the product stream to a distillation column and leaving behind the IL catalyst. In 2020, Chevron had the ISOALKY^{TM} technology unit fully operational. The process utilized lower amount of catalyst, because the catalyst has higher activity and achieved a substantial increase in the product yield and quality, meanwhile, the construction and operational costs were maintained.[193-195]

The Ionikylation process was developed by China University of Petroleum-Beijing and licensed through Well Resources. The Ionikylation process is an isobutene alkylation process that utilizes a liquid composite catalyst compressing a chloroaluminate IL with CuCl (high concentration of AlCl$_4$-CuCl$^-$). Isobutene alkylation is a common refinery process in the production of high-quality gasoline.[196-198] Conventionally, H$_2$SO$_4$ or anhydrous HF is used as a catalyst for the process. However, handling large quantities of those chemicals raises significant safety and environmental concerns. Although the operating conditions are similar to conventional commercial processes, there is an improvement in the C$_8$ yield and the selectivity for trimethyl pentane. Trimethylpentanes are the desirable components of alkylate gasoline, due to their high-octane numbers (> 100). This technology was transferred to six units, which are in operation, and together generate 1200 kton/year of alkylate.[199],[200]

Die approbierte gedruckte Originalversion dieser Dissertation ist an der TU Wien Bibliothek verfügbar.
The approved original version of this doctoral thesis is available in print at TU Wien Bibliothek.

1.2.4.1.2 Analytical uses

In 2008, Supelco^{TM} Analytical (part of Sigma-Aldrich) developed a range of GC columns with IL stationary phases.[201] The first GC column introduced to the market by the company was 1,9-Di(3-vinylimidazolium)nonane bis(trifluorosulfonyl)imide (SLB-IL100), which was employed for the analysis of both neutral and polarizable analytes.[201]

Hitachi High-Tech Corporation has developed an IL (HILEM® IL 1000) which allows the visualization of biological samples under high vacuum using SEM.[202],[203]

1.2.4.1.3 Gas capture

Traditionally, gases are physically absorbed to a solid absorbent (activated carbon or zeolites) in a cylinder at sub-atmospheric pressures. Currently, ILs can be modified to have a similar reactivity to different gases *via* ion-pair adjustment, and compared with porous solids, ILs can be pumped and have an enhanced heat-transfer rate. Lewis basic ILs are able to reversibly complex with Lewis acidic gases, for example, BF_3 and AsH_3, meanwhile, Lewis acidic ILs can reversibly complex with Lewis basic gases (PH_3) with a 2:1 mol ratio (IL:PH_3).[204] Air Products (now Versum Materials, Inc.) tested in laboratory scale dialkylimidazolium tetrafluoroborate salts ($[C_nmim][BF_4]$) for the reversible complexation with BF_3; results exhibited excellent gas evolution rates, long-term gas/liquid stability and after repeated cycles, there was negligible loss in capacity. Consequently, this technology was transferred to commercial scale development.[205]

Conventionally, mercury vapor is removed through chemically modified activated carbon, however, chemically modified activated carbon exhibits lower efficiency and three times shorter lifetime than ILs. A new method to separate mercury from natural gas stream was developed by PETRONAS together with QUILL.[206-210] The HycaPure^{TM} Hg technology utilizes the benefits of heterogeneous and homogeneous systems, to be more precise, supported ionic liquid phase (SILP) with a high surface area is impregnated with a chlorocuprate (II) IL. In that process, oxidative dissolution takes place, copper oxidizes mercury to create an anionic mercury complex. Subsequently, this complex is incorporated into the IL to generate a copper chloride as residue.[206] The HycaPure^{TM} Hg process was installed in a commercial natural gas plant in Malaysia.

1.2.4.1.4 Dissolution

In the "Natural Fibre Welding®" process, $[C_2mim][OAc]$ (1-ethyl-3-methylimidazolium acetate) has been employed to process natural fibers (e.g., cellulose, hemicellulose, silk), in order to create a congealed network which retains the native polymer structure.[211] This novel technology was used to

generate new high-performance textiles for a wide range of applications through recycling existing natural materials.[212]

Polyethylene terephthalate (PET), a plastic used in food packaging, has been recycled using ILs. Chemical recycling is used to break down the polymer to its monomeric units for reprocessing. Those monomers obtained can be utilized as feedstock to then generate higher quality materials. This is a clear advantage compared to mechanical recycling which decreases the quality of the product.[213],[214] Currently, Ioniqa patented a process utilizing ionic media, which creates virgin quality plastic from waste PET in a scale of 10000 tonne per year.[215],[216]

1.2.4.1.5 Electrochemical applications

Scionix reported a chromium electroplating process utilizing a system based on choline chloride and chromium (III) chloride to create a deep eutectic solvent (DES), substituting toxic chromium (IV) salts and avoiding embrittlement of the coating.[187],[217-220] Ionic liquids provided higher efficiencies (> 90%) and crack-free, corrosion-resistant coatings. Two commercial-scale processes (>1 tonne) have been reported by Scionix and seven pilot-scale processes (50-250 Kg) for a range of different metals.[221] NOHMs Technologies commercialised Li-ion batteries employing ILs as electrolytes (NanoLyte) achieving 400% more cycle-lifetime[222],[223] and NantEnergy used ILs in Zinc-air batteries.[224-227] Furthermore, Novasina and Iolitec commercialized ILs in electrochemical gas sensors and Panasonic in supercapacitors.[228]

1.2.4.1.6 Operating fluids

Ionic liquids have been employed as operating fluids, as heat transfer materials or lubricants.[229],[230] Mettop GmbH together with Proionic developed a new cooling technology (ILTEC), in which water was exchanged with an equivalent viscosity IL (IL-B2001). IL-B2001 consisted of $[C_2mim][BF_4]$ (97%), $[C_2mim]F$ (1.5%), water (0.5%) and unknown compounds (1%). With this exchange, the cooling system provided chemical inertness, a high operating temperature up to 250 °C and more efficient heat recovery.[231],[232]

Lately, with the increased usage of electric motors in rolling bearings, increased levels of electric erosion have been observed, leading to premature failure of the bearing. Klüber Lubrication utilized ILs to increase the electrical conductivity of lubricants and to dissipate the generated electric current, reducing considerably the damage created by it.[233]

Linde gas utilized ILs as a liquid piston in an "ionic compressor" instead of the traditional metal piston compressors.[234] The IL possessed low compressibility and low miscibility with the compressed gas, leading to saving energy, reducing material costs and reducing servicing intervals by a factor of 10.[235]

Currently, this technology has been applied to a wide array of gases and it has been utilized in more than 90 H_2 refuelling stations worldwide.[236],[237]

1.2.4.1.7 Performance additives

The advantageous properties of ILs allowed them to be utilized as performance additives. The company 3M developed ILs as antistatic additives in a range of 1 – 5 w.t.%, with the objective of decreasing particles and dust and improving safety by reducing electrostatic discharge events.[238] Quaternary ammonium salts with bis(triflluorosulfonyl)imide anions were utilized to create their product 3M™ Ionic Liquid Antistat FC-4400. Alternatively, an alcohol group can be introduced into the cation core to obtain polymer compatibility, such as urethanes. Several ILs were commercialised for the same purposes by BASF, Evonik and KOEI Chemical Co., Ltd.[239-241]

Evonik investigated the use of ILs as secondary dispersant additive to homogeneously stabilize water-based pigments in water- and solvent-based paints and prevent sedimentation.[242],[243] Evonik´s Tego® brand utilized ammonium- and quaternary heterocyclic-based ILs to improve color strength and brightness.

1.2.4.2 Pilot scale processes

1.2.4.2.1 Chlorination

Conventionally, the chlorination of hydrocarbons is performed using phosgene which is a hazardous and highly toxic reagent. In 1990, BASF utilized on a pilot scale low melting Vilsmeier salts (ILs) to activate HCl for the chlorination of diols.[205],[244],[245] The generated chlorinated product was not miscible with the IL, leading to a simple separation and catalyst recycling.

1.2.4.2.2 Demethylation

An IL-assisted process involving the demethylation of 4-methoxyphenylbutyric acid to achieve the synthesis of a valuable pharmaceutical intermediate was published by Eli Lilly and Company.[246] Previously, the reaction was performed by refluxing HBr in acetic acid, leading to harsh conditions. In their developed method, a protic pyridinium hydrochloride IL was utilized, which allowed scaling up of the pilot plant up to 190 litres.

1.2.4.2.3 Dimerization

In 1997, IFP commercialized the Dimersol process (Figure 17), which consists of the dimerization of alkenes, typically propene (Dimersol-G) and butenes (Dimersol-X), to render high value added branched hexenes and octenes. Traditionally, the reaction is carried out without solvent and the catalyst is a cationic nickel complex [LNiCH$_2$R'][AlCl$_4$] (PR$_3$). The catalyst was dissolved in a hydrocarbon and injected into a cascade reactor system with the alkene feed.[244],[247],[248] The difficulty of this reaction was the catalyst separation from the reaction mixture. The catalyst was removed *via* washing, however, as a consequence, the reaction yield was low, and the cost increased. This process was installed on numerous of their plants across the globe, generating a total of 3500000 tonnes of product *per* year. Later, Yves Chauvin (Nobel laureate) and Hélène Olivier-Bourbigou developed the biphasic Difasol process (Figure 17), which utilizes chloroaluminate (III) ILs as a solvent for the nickel-catalysed dimerization.[247],[249],[250] The range of the employed temperature is between 5 °C and 215 °C and two phases are formed: the IL phase (lower) and the product phase (upper). In the IL phase, the catalyst selectively remains, meanwhile in the upper phase the products are generated. Interestingly, compared with the monomeric reactants, the dimerized products formed exhibited lower solubility enhancing their separation into the polar IL phase, leading to higher yields, selectivity, smaller reactor size and the catalyst could be recycled. Apart from the many advantages of the Difasol process, this process can be retrofitted into existing Dimersol plants. Until now, this technology has only been operating on a pilot plant scale.[247],[248]
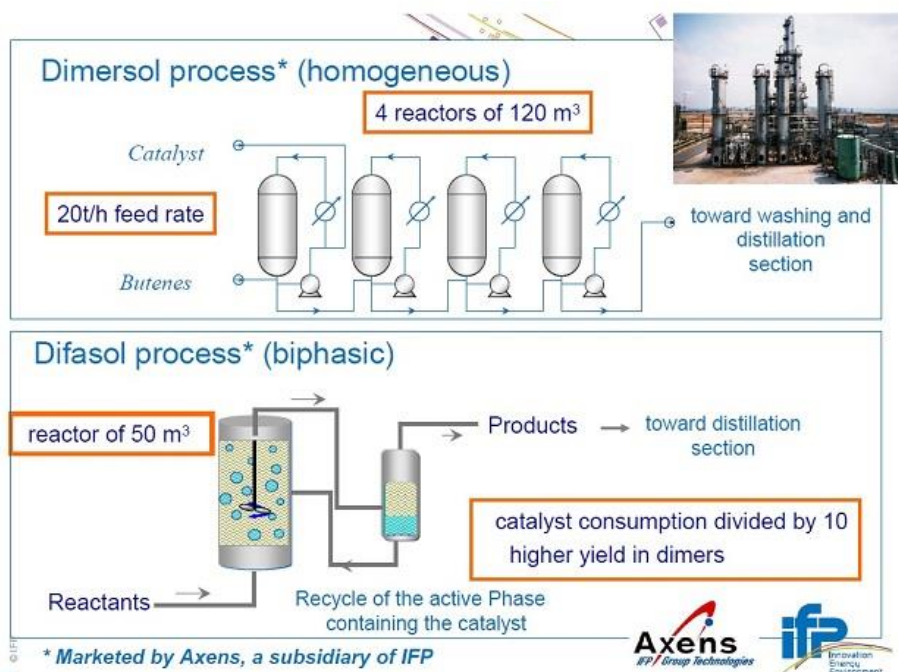
Figure 17. Dimersol process (homogeneous) and Difasol process (biphasic) scheme.[251]

1.2.4.2.4 Dissolution

Aalto University in Finland developed an alternative Lyocell-type process (entitled Ioncell® process) focusing on the dissolution of wood pulp, textiles and newspapers, using ILs to obtain highly oriented cellulose fibers with high tenacity and a feasible solvent recovery step.[252] The optimum performance was obtained by superbase ILs, for example, 1,5-diazabicyclo[4.3.0]non-5-ene acetate ([DBNH][AcO]), which induced cellulose degradation.[253] The developed process by Aalto University led to the construction of a pilot plant able to produce 10 kg of fibre per day.[192]

In 2018, more than 100 million tonnes of textile fibers were generated. The production of textile fibers is not regarded as sustainable, because they are commonly produced *via* oil refining or viscose method. Metsä Spring utilized ILs and closed-loop manufacturing system for cellulose-based textile fabrics, leading to a new and more environmentally friendly process. Their method focuses on using an IL-based wood pulp dissolution process. Currently, Metsä Spring is building a test plant, which would be able to produce 40 kg of fibre per hour.[254],[255]

The Imperial College of London developed a process focusing on the pre-treatment of lignocellulosic biomass to separate cellulose from hemicellulose and lignin, named the IonoSolv process. In that process, a heated aqueous IL solution is utilized to dissolve lignin and hemicellulose, leading to the selective extraction of cellulose.[256-258]

Chitin is the most abundant polymer in the marine environment and is present in the hard shells of crustaceans.[259] Chitin is completely insoluble in water and in the majority of organic solvents, due to

its vast network of hydrogen bonds. Traditionally, chitin is generated in three steps; firstly, the crushed shells undergo acid washing (demineralization) and secondly the removal of proteins *via* alkali washing and lastly the decolorization step. Rogers et al. found out that the selective dissolution of chitin was possible utilizing [C$_2$mim][OAc] combined with microwave heating, which improved the dissolution efficiency. Water was utilized to precipitate the chitin and after drying, a 94 % recovery was obtained with high purity and molecular weight, achieving better results than commercial processes.[260],[261]

1.2.4.2.5 Electrochemical applications

In the application of aluminum plating, BASF utilized 1-ethyl-3-methylimidazolium chloride on a pilot scale. In the same application and scale, C-Tech Innovation, IoLiTec and Xtalic have also developed aluminum plating using diverse ILs.[228],[262-266] In lithium batteries, ILs have also been utilized by Pionics Co. Ltd.[267] Another electrochemical application involving ILs are dye sensitized solar cells (DSSCs). Regarding this application, ILs were piloted in DSSCs by Iolitec and H. Glass. Additionally, Iolitec utilized ILs for electrochromic windows and as solvents/additives in redox flow electrolytes for Zn-Br batteries and ZapGo for supercapacitors.[228],[268]

1.2.4.2.6 Extraction

Rare earth elements are utilized in various catalytic, electric, magnetic and optical applications. They are extremely difficult to separate from one another, because of their analogous chemical structure. Industrial processes focus on extraction with solvents which possess the potential to be recycled and upscaled. They utilize organophosphorus derivatives generating huge quantities of acidic waste and additionally require a considerable number of stages.[269] In the latest years, the recycling of used devices to recover these rare elements has drawn considerable attention, due to their supply risk. Not long ago, Queens University Belfast and Seren Technologies filed numerous patents focusing on the task-specific IL utilization to extract and separate neodymium and dysprosium present in permanent magnets from an acidic aqueous solution.[270-272] The metals present in the IL phase can be selectively separated *via* precipitation or electrodeposition. In 2018, a pre-commercial magnet recycling plant was opened by Seren Technologies in England. The highly selective process performed in this recycling plant is able to receive multi-ton shipments of magnets and is searching for commercialization.[273-275]

1.2.4.2.7 Hydroformylation

In 2015, a homogeneous IL catalyst in a hydroformylation reaction was utilized by Evonik Industries.[276] In biphasic aqueous systems, such as industrial Ruhrchemie/Rhône-Poulenc oxo process aldehydes are produced using the hydroformylation reaction of alkenes with CO/H$_2$ and a metal catalyst either of

cobalt or rhodium.[277] Other companies such as IFP Energy Nouvelles (IFPEN) utilized IL media to produce aldehydes.[249],[278],[279] Evonik utilized SILP catalyst for the same purpose, achieving approximately 800 h of constant output with high selectivity, however, further optimization was required to make it feasible on a pilot scale.[276] Finally, long-term stability (2000 h) was achieved *via* a rhodium complex with ligands containing a polycyclic anthracene triol motif, dissolved in an IL consisting of an imidazolium cation and a binary amine anion. As a consequence, a SILP system for the first time had potential for commercialization.

1.2.4.2.8 Hydrosilylation

Commonly, the hydrosilylation reaction is used for the synthesis of polyethersiloxanes which are utilized in a wide range of applications. The polyethersiloxanes are synthesized through a condensation reaction of alcohols with Si-Cl functional groups. On the negative side of this reaction, HCl is also created as a by-product. Thus, metal catalyzed reaction of alkenes with Si-H species is preferred.[280] Due to the minimal amount of the homogeneous Pt catalyst used to catalyze the reaction (few ppm), the recovery of the metal is seldom. Additionally, the recovery of the metal is avoided, because of the high cost of the process and because the final product´s purity would decrease.[280],[281] Degussa developed a biphasic reaction, in which the catalyst was dissolved in the IL-phase. Different imidazolium- and pyridinium-based ILs with different anions, i.e., $[BF_4]^-/[RSO_4]^-/[NTf_2]^-$, were used with the objective of recovering the catalyst and increasing its purity.[280] Owing to the better phase separation, the catalyst remained in the IL-phase, the pure product could be decanted, and a conversion of >99% was obtained on a pilot scale.[282]

1.2.4.2.9 Fluorination

In the past, chlorofluorocarbons (CFCs) were mainly utilized as refrigerants, however, their use has exerted a negative impact on global warming.[283] Currently, hydrofluorocarbons (HFCs) are used as their substitutes, which possess a lower ozone depletion potential. HFCs are products of the reaction between chlorohydrocarbons with HF. Traditionally, antimony pentachloride catalyst suffered from deactivation and in order to re-oxidize the metal an excess of chlorine gas was necessary.[284] The company Arkema utilized an IL containing chloro- or fluoro-antimony-based anion to catalyze the fluorination reaction. In this reaction, the catalyst deactivation was avoided by employing the IL and, additionally, it was proven that the reaction could be performed on a micropilot scale for >1000 h and a selectivity surpassing 99.5%.[284],[285]

1.3 Ionic liquids and supercritical carbon dioxide: a unique combination

1.3.1 Biphasic ionic liquids/Carbon dioxide system

If a number of phases, such as supercritical, gaseous and liquid are employed in catalytic systems, the solubility phenomena is an important factor to take into consideration. One of the most representative examples would be the IL/CO_2 biphasic system. In this system, the catalyst-containing phase (catalytic phase) is a stationary phase, and the CO_2 acts as a carrier and/or extracting agent. However, for the system to be functioning smoothly, some pre-requisites need to be fulfilled. Firstly, the solubility of CO_2 in ILs must be high, and lastly the solubility of IL in CO_2 needs to be specifically low. When these pre-requisites are met, cross-contamination or catalyst loss is circumvented, particularly in continuous-flow fashion.[286] Besides solubility phenomena, the swelling phenomena also play an important role. This phenomenon takes place, when CO_2 is dissolved in traditional liquid phases, resulting in a significant hindrance of the reaction rate in numerous catalytic reactions, because of complications in dilution.[286]

Over the last years, carbon dioxide´s solubility in a variety of ILs has been investigated employing both low- and high-pressure conditions. Initially, the solubility of CO_2 in several ILs was tested by Brennecke´s research team.[287],[288] In this research pipeline, different parameters, such as pressure, temperature, the anion, the cation and the impurities of the ILs were the focus of the investigation. [286-289] Most importantly, Brennecke´s group investigated the influence of different anions in the [C_4mim]$^+$ family, manipulating the pressure range from 0 to 160 bar and keeping the temperature constant at 3 individual values, specifically 25 °C, 40 °C and 60 °C. The obtained results for the experiments at 40 °C are depicted in Figure 18. The addition of CO_2 is easier at lower pressures (60 – 80 bars), where the concentration of CO_2 remarkably rises, because the interaction of CO_2 and IL anion do not affect significantly the conformational arrangement of the IL. However, above 100 bar the liquid phase is saturated and, therefore, a modification of the structural disposition of the IL would be necessary, hampering the further addition of CO_2.[290-293] The highest CO_2 solubility was obtained by ILs containing fluoroalkyl groups in the anion, such as [CH_3]$^-$ (methide) and [NTf_2]$^-$, meanwhile the non-fluorinated inorganic anions exhibited the lowest, for instance [NO_3]$^-$ and [DCA] (dicyanamide). It was also demonstrated that by increasing the alkyl chain length of the alkyl groups on the cation, the CO_2 solubility was positively affected in a smaller scale.[288]
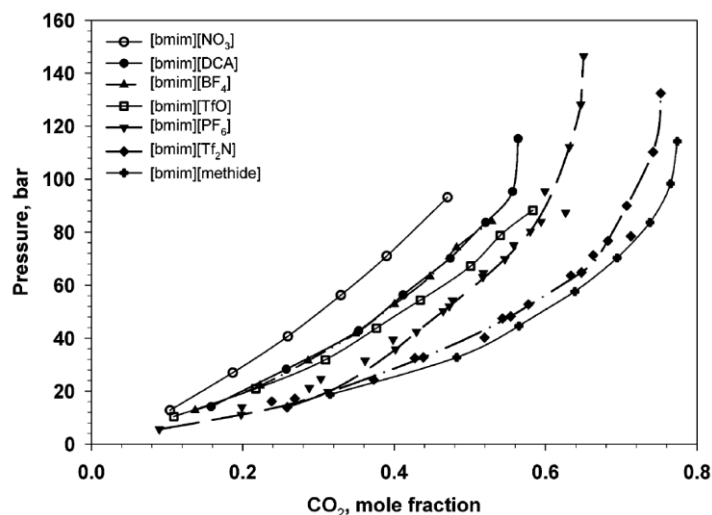
Figure 18. Effect of anion and pressure on the solubility of CO_2 in [C_4mim]-based ILs at 40 °C.[288]

Principally, by augmenting the pressure, the solubility of CO_2 in ILs rises; nonetheless, increasing the temperature has a negative influence on the solubility. Yokozeki and Shifflett who published on this topic, calculated the influence of temperature on [C_6mim][Tf_2N] and compared it with empirical data. As depicted in Figure 19, it was demonstrated that by increasing the temperature, the solubility of CO_2 in the IL decreased, but most importantly, CO_2 exhibited high solubility in the IL.[294]
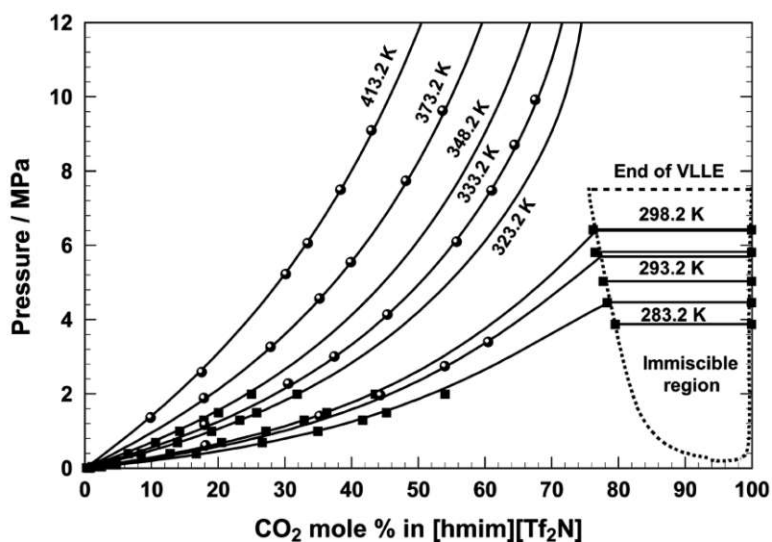
Figure 19. Solubility of CO_2 in [C_6mim][Tf_2N] at different temperatures (EoS calculations illustrated with lines and empirical values depicted with symbols).[294]

It is important to mention, that the solubility of CO_2 is expressed in mol % and even though it may be high, the related mass % solubility is typically lower. Consequently, the molecular weight of the IL plays a role in it, meaning that the higher the molecular weight, the higher the CO_2 solubility from a molar fraction basis perspective.[295]

Several investigations have been published regarding the influence of the anion and cation. It was demonstrated that the selection of the anion had a significant influence on the CO_2 solubility in the IL. Anions containing fluoroalkyl groups, such as $[CF_3]^-$, $[NTf_2]^-$ and $[OTf]^-$ (triflate anion) exhibited high solubility, meanwhile, anions lacking fluorinated anions, for example $[NO_3]^-$ and $[DCA]^-$ (dicyanamide anion), displayed low solubility. The influence of the cations was also investigated, by testing ILs with various anions (for example $[NTf_2]^-$, $[PF_6]^-$ and $[BF_4]^-$) and imidazolium as cationic structure with slight modifications of the alkyl groups present in the cation motif. However, results showed that the cation has a less remarkable effect on solubility, because the modifications of the alkyl group slightly impacted the solubility of CO_2 with all the anions that were mentioned. It was demonstrated that the introduction of a methyl substituent in the C_2 carbon of the $[C_4mim]^+$ cation core to produce $[C_4mmim]^+$ (1-*n*-butyl-2,3-dimethylimidazolium cation) did not significantly influence the solubility.[288],[289] Interestingly, the combination of fluoroalkyl group containing anions with partially fluorinated alkyl chains on the imidazolium-based structures, resulted in a rise of the CO_2 solubility.[296]

Another important factor which plays a vital role in biphasic systems is the solubility of CO_2 in ILs. At pressures above 100 bar, the solubility is governed by the molecular interactions and organization of CO_2 around the anions.[290-293] However, at low pressures, Henry´s law constant of gases is utilized in order to compare the solubility of gases. Compared to other gases, CO_2 in mol % displays higher solubility in ILs than many other traditionally-employed gases (Table 3). Carbon dioxide and water exhibit high solubility, due to the large dipole moments and quadrupole moments, however, non-polar gases with low polarizability exhibit lower solubilities.[297]

Table 3. Henry´s Law constant (bar) for gases in $[C_4mim][PF_6]$.[287]

Gas	T = 25 °C	T = 50 °C
CO_2	53.4 ± 0.3	81.3 ± 0.5
C_2H_4	173 ± 17	221 ± 22
CH_4	1690 ± 180	1310 ± 290
O_2	8000 ± 5400	1550 ± 170
H_2	Undetected (>1500)	Undetected (>1500)

Regarding the IL solubility in CO_2, ILs do not dissolve in CO_2, thus, a solute dissolved in the IL phase can be extracted *via* $scCO_2$ without cross contamination. There are two main reasons for this; the extremely low vapor pressure of the IL and that CO_2 is not able to solvate ions in the gaseous phase. However, there could be a mixture of other compounds present in the $scCO_2$ phase, which also play a role in the dissolving capability of $scCO_2$. For instance, reactants and products could behave as cosolvents and drastically improve the ability of $scCO_2$ to dissolve ILs.[298]

With regard to swelling, CO_2 addition to the majority of the traditional solvents results in a volume expansion. Nonetheless, when utilizing ILs there is a minimum volume expansion of around 10 mol %.[289] This phenomenon takes place, because CO_2 molecules are predominantly placed in larger sized cavities of the ILs, meaning that in the process of dissolving the CO_2, the volume expansion is minimized.[299] At a certain point, the CO_2 cannot be any longer dissolved in the IL, because no more unoccupied spaces are left. It has been demonstrated that even by employing high pressures no significant amount of CO_2 can be further dissolved in the IL.[300]

Concerning the melting point of ILs, the ones that are liquid at room temperature are employed as solvents. However, not all ILs are in liquid state at room temperature. In order to expand the pool of ILs that can serve as solvents at room temperature, high CO_2 pressure could be employed to induce a melting point depression of the ILs. A wide array of ILs has been tested under high pressure CO_2 conditions to investigate their melting point depression (Table 4).[301],[302]

Table 4. Melting point depression (MPD) observed under CO_2 pressure for various ILs.[301],[302]

compound	T_m (°C)	$_pCO_2$ (bar)	MPD (°C)
[PBu$_4$]Br	103.5	150	42.4
[NBu$_4$]Br	102 – 105	150	23.3
[NBu$_4$][Tosyl]	71.5	150	33.8
[NBu$_4$][BF$_4$]	156	150	119.8
[NBu$_4$][TfePF$_3$]	54	34.8	36.7
[NPr$_4$]Br	100 – 101	150	18.8
[NHex$_4$]Br	99	150	71.2
[NHep$_4$]Br	90	150	40.2
[NOct$_4$]Br	97.5	150	37.6
[MTOA]Br	57.2	40	38.2
[C$_4$DMDDAm]Br	48 - 52	50	23
[C$_2$mim][PF$_6$]	60	147	35
[C$_4$mim]Cl	69	150	10.2
[C$_4$mim][OTf]	64	150	34
[C$_4$mim][Tosyl]	67	150	25.8
[Bzmim][Tosyl]	105	160	13
[Bzmim][OTf]	73	170	20

The values given for MPD are expressed as the difference of the melting point
under ambient conditions (T_m) from the respective melting point
at a given CO_2 pressure (pCO$_2$).

Most precisely, tetrabutylammonium-, imidazolium- and phosphonium-based ILs, and quaternary ammonium bromides have been investigated. It was demonstrated that ILs containing quaternary ammonium and phosphonium cations exhibited a remarkable decrease in their melting point, namely around 80 °C. However, imidazolium- and pyridinium-based ILs had only 20 °C of decrease.[301-303] It was concluded that the dissolution of CO_2 in the lattice of the crystal structure was most likely the main reason for the depression of the melting point, because this dissolution generates the disruption of the crystal structure. Additionally, the melting-point is significantly influenced by the interaction between CO_2 molecules and the anion of the IL, however, the cation may inhibit or enable the interaction.

With respect to the viscosity of ILs, many of them are regarded as remarkably viscous. In IL-based biphasic catalytic systems, the viscosity is also a factor that has a significant importance. Therefore, the influence of CO_2 in the mass transport properties was investigated.[161] Several [Rmim][NTf$_2$] (1-alkyl-3-methylimidazolium bis(trifluoromethanesulfonyl)imide) based ILs with different alkyl chains, such as ethyl, *n*-hexyl and *n*-decyl were tested at different temperatures (25, 50 and 70 °C) and at pressures up until 287 bar.[304] As depicted in Figure 20, temperature and pressure had a minor influence at pressures above 50 bar for [C$_2$mim][NTf$_2$]. Additionally, it was concluded that by increasing the chain length of the alkyl substituent of the imidazolium-based IL below 50 bar, the viscosity also increased.
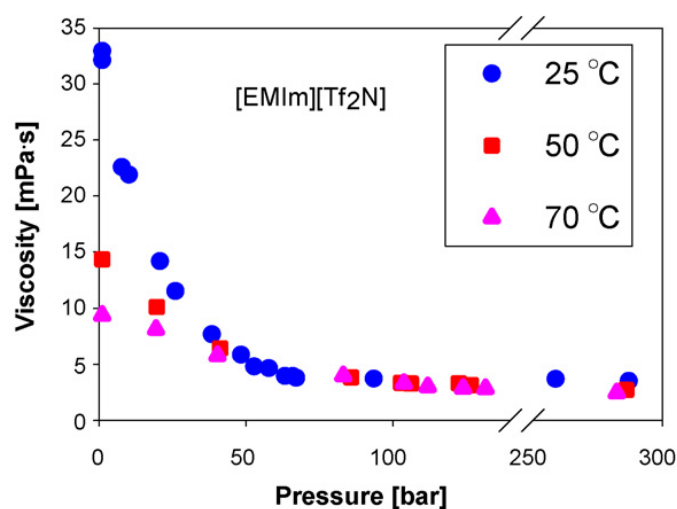
Figure 20. Viscosity of [C$_2$mim][NTf$_2$] with CO_2 pressure at 25, 50 and 75 °C.[304]

Another important characteristic that needs to be taken into consideration would be the diffusion coefficient, which is a constant that reflects the mass transport properties of the ILs. Several publications reported that the investigated ILs exhibited, at low pressure, diffusion coefficients one or two orders of magnitude smaller compared to traditional organic solvents. In those publications, different gases, among them CO_2, and several ILs, such as [C$_2$mim][NTf$_2$], [C$_4$mim][PF$_6$], [C$_2$mim][OTf], were tested. Thus, this could be a restraining factor affecting many potential applications of ILs because molecules would have difficulties diffusing through the IL phase.[305],[306] It was also demonstrated that whenever the viscosity decreased, the diffusion of CO_2 in IL increased. In the same topic, another investigation was also published related to phosphonium-based ILs. Results showed that the gas diffusivity was inversely proportional to the viscosity. In addition, it showed that the relationship between diffusivity and viscosity was distinct depending on different ILs classes. For instance, phosphonium-based ILs exhibited significantly higher gas diffusivity than imidazolium-based ILs with similar viscosity.[307]

The application of moderate to high pressure CO_2 unquestionably reduces the viscosity and, therefore, enhances the diffusion of molecules inside ILs, thereby positively impacting many catalytic applications. However, it also has repercussions, which may not be advantageous for some reactions, for example in the partitioning behavior of a solute between two phases.

Apart from that, ILs have a broad range of structures that interact in many diverse ways with CO_2 on a molecular level, to name a few, hydrogen bonds and Coulomb interactions. Weingärtner et al.[165] published in this regard a very detailed review. For example, ILs containing fluorinated anions or CO_2-philic groups interact relatively strongly with CO_2.

1.3.2 Ternary (ionic liquids + supercritical fluid) systems

The number of possible ternary systems is vast compared to binary systems. Nonetheless, the ternary (IL + supercritical fluid) systems that have been studied are rather small. The majority of the investigated ternary (IL + supercritical fluid) systems are composed of an IL, supercritical CO_2 and an organic compound, for instance alkane, alcohol, ketone, ester.[308-318] In certain cases, water has also been employed.[319-321]

The common phase behavior of ternary (IL (liquid) + CO_2 (vapor) + organic (liquid)) mixtures is illustrated in Figure 21.[322]
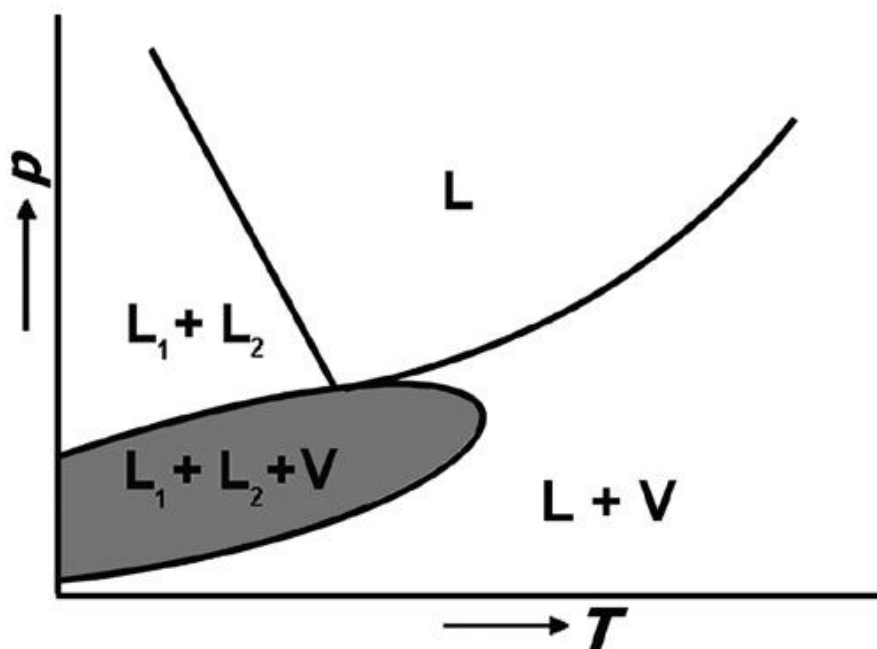
Figure 21. Phase behavior of ternary (IL + scCO$_2$ + organic) systems.[322]

If the organic compound and the IL are miscible at ambient conditions (liquid + vapor), a second liquid phase can be potentially generated by increasing the CO_2 pressure in the mixture (liquid (1) + liquid (2) + vapor).[308-317] The three phases consist of a liquid IL-rich phase (+ organic + CO_2), a liquid organic-rich phase (+ IL + CO_2) and vapor CO_2-rich phase (+ organic). By further increasing the CO_2 pressure, the liquid organic-rich phase is going to enlarge and at some point, the vapor CO_2-rich phase combines with the liquid organic-rich phase.[309-317] After merging, the small quantity of IL, that was present in the liquid organic-rich phase, is forced out to the IL-rich phase (+ organic + CO_2), leading to a liquid CO_2 + organic phase. Ultimately, by continuing to increase the CO_2 pressure, one homogeneous liquid phase (IL + organic + CO_2) is obtained.[314],[315]

As a matter of interest, by rising the CO_2 pressure, it is possible to cause the system to transition in the following manner: two-phase to three-phase to two-phase to one-phase.[314] This described scCO$_2$ induced phase transition behavior in ternary systems is depicted in Figure 22. Most importantly, this phenomenon was already known for ternary CO_2 systems in the absence of an IL, however, it was demonstrated that it also takes place in ternary CO_2 systems with an IL.[308]
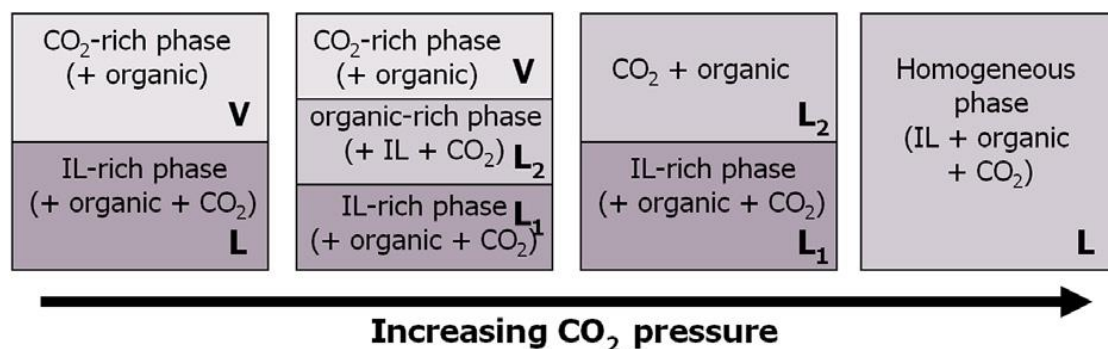
Figure 22. Supercritical CO_2-induced "two-phase"–"three-phase"–"two-phase"–"one-phase" transition in ternary (IL + CO_2 + organics) systems.[322]

The ternary (IL + CO_2 + water) systems behave in a similar manner to ternary (IL + CO_2 + organic). In these cases, increasing the CO_2 pressure can lead to liquid-liquid separation in hydrophilic (IL + water) mixtures.[319-321]

1.3.3 Applications related to the combination of ILs with scCO$_2$

1.3.3.1 Solute extractions from ILs using CO$_2$

Ionic liquids face similar obstacles to traditional solvents in chemical reactions with relation to the product recovery. For example, when extractions are carried out using water, the IL must not be soluble in water, so that the hydrophilic products can be extracted without any cross contamination. However, ILs could be partially soluble in water, leading to an impure extracted product. One of the most commonly used techniques for solute extraction is distillation, which requires high energy, and it is only appropriate for products that are thermally stable and volatile. These obstacles and limitations can be overcome with scCO$_2$, because it can extract efficiently a wide range of compounds from ILs with significantly low cross-contamination. Additionally, the majority of the ILs are practically not soluble in CO$_2$.[286]

With the objective of extracting a solute from the IL phase, the affinity of the solute needs to be considered. For example, the solute, which is highly volatile and low in polarity, exhibits affinity for CO$_2$. However, a solute that is characterized by high polarity and aromaticity is going to exhibit strong affinity for the IL-phase. Thus, to easier extract the solute from the IL mixture, compounds of interest must have high affinity for CO$_2$. In addition, employing scCO$_2$ is an appropriate alternative to extract thermally sensible or non-volatile solutes.[298]

Initially, Blanchard et al.[323] presented a process for extraction of valuable compounds out of the IL phase. Naphthalene was extracted from [C$_4$mim][PF$_6$] in nearly quantitative yields using CO$_2$ at 40 °C and 38 bar and after the extraction and depressurization the IL was recovered in pure form. At a later time, Blanchard and Brennecke investigated numerous aromatic and aliphatic solutes that were extracted in batchwise mode from [C$_4$mim][PF$_6$] with scCO$_2$, obtaining high recovery rates (≥ 95 %).[324] Additionally, the basics behind the phase behavior of biphasic IL/scCO$_2$ systems were established.[300]

The first catalytic implementation of scCO$_2$ for the extraction of valuable products was carried out by Brown et al.,[325] more precisely, for the asymmetric hydrogenation of tiglic acid in [C$_4$mim][PF$_6$]/H$_2$O. At room temperature and by employing the catalyst Ru(O$_2$CMe)$_2$(R-tolBINAP) (diacetato[(S)-(-)-2,2'-bis(di-p-tolylphosphino)-1,1'-binaphthyl] ruthenium(II)) high conversion and enantioselectivity were obtained, i.e., >97% and >85%, respectively. The catalyst remained in the IL phase and the catalytic system could be reutilized up to four times without a considerable effect on its activity and selectivity.

Roth et al.[326] published an extensive review focusing on the extraction applications in reactions performed in ILs.

1.3.3.2 Biphasic system (IL/CO$_2$) for heavy metal extraction

The 1-alkyl-3-methylimidazolium cation in combination with different anions is one of the most used RTILs for the extraction of metal ions. By selecting a fluorinated anion, a C$_4$mim-based IL of hydrophobic nature is obtained. Particularly, one of the most appropriate anions to extract metal ions would be bis(trifluoromethylsulfonyl)imide anion, because of its water stability, relative low viscosity, high conductivity, good electrochemical and thermal stability.[327] In order to render aqueous metal ions soluble in this type of IL, hydrophobic ligands or chelating agents are employed.

In 2007, Binnemans reported the extraction of uranyl ions, trivalent lanthanides and actinides from nitric acid solutions into ILs. A wide array of ligands were utilized, for instance, TBP, octyl(phenyl)-*N,N*-diisobutylcarbamoylmethyl phosphine oxide (CPMO), β-diketone, and acidic dialkylorganophosphorus.[328]

Mekki et al.,[327],[329] reported the extraction of Cu^{2+} ions and trivalent lanthanides (La^{3+} and Eu^{3+}) from aqueous solutions, utilizing [C$_4$mim]-based ILs with $^-$NTf$_2$ as counter ion and β-diketones as extractants. By means of scCO$_2$ at 50 °C and 150 atm, the metal-β-diketonates were extracted from the IL phase. Using these parameters, the extraction efficiency of lanthanide-β-diketonates is higher than 98%.[327],[329] It is noteworthy, that volatile organic solvents were traditionally utilized for the dissolution and separation of radioactive elements (i.e., nuclear waste).[115]

Supercritical CO$_2$ could serve as an ideal medium for the stripping step of metal species dissolved in ILs, because it would not transfer IL residues into the CO$_2$ phase. Thus, an alternative process was proposed for the extraction of radioactive materials from aqueous solution. The alternative process included 3 phases (water, IL and scCO$_2$) and consisted of two steps. Additionally, the proposed process possessed three major advantages: firstly, the transfer of radionuclides from aqueous waste can be performed under ambient temperature and the nucleotides can be concentrated in the IL phase; secondly, the selectivity of the back-extraction of radionuclides from the IL phase to the scCO$_2$ can be achieved by modifying the solvating strength of scCO$_2$ and ultimately, residues of organic solvents and loss of IL in the back-extraction are avoided. After the last step, by decreasing the CO$_2$ pressure, the solutes are precipitated and the CO$_2$ can be recovered and re-used, and the IL can also be reutilized.[115] Wang et al.[330] reported the transfer of uranyl ions (UO$_2$)$^{2+}$ from aqueous nitric acid solutions to [C$_4$mim][NTf$_2$] by means of a complexing agent (TBP) and subsequent stripping of the uranyl complex from the IL phase to the supercritical fluid phase (Figure 23).
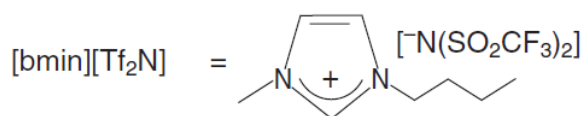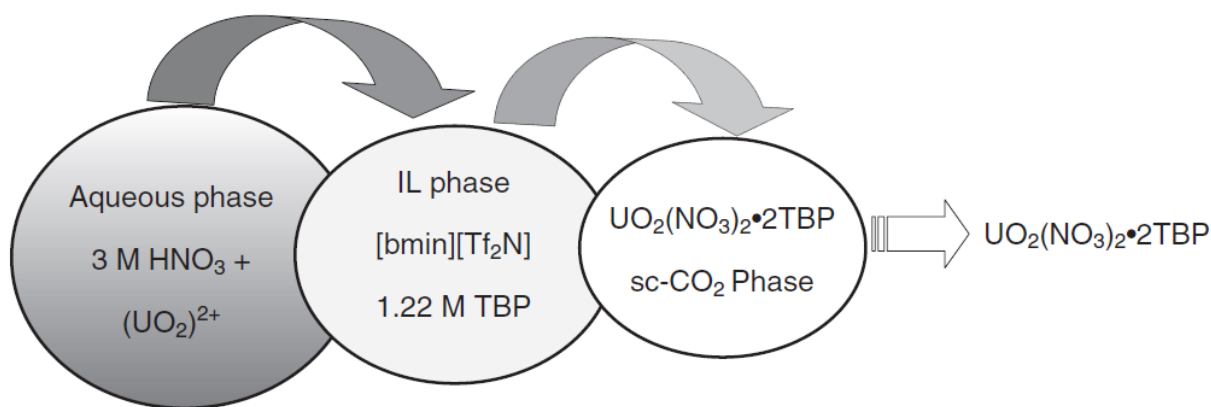
Figure 23. Extraction of uranium from nitric acid solution using IL and scCO$_2$ in conjunction – a two-loop extraction system involving three phases.[115],[330]

1.3.3.3 Biphasic system (IL/CO$_2$) in catalysis in batch mode

In homogeneous catalysis, biphasic solvent systems commonly contain two phases, the lower phase and the upper phase. In the lower phase, the solvent dissolves the catalyst, meanwhile in the upper phase, the solvent brings the substrate where the reaction takes place and then gets the product out. Ideally, the lower phase can dissolve the homogeneous catalyst and the substrate, while the upper solvent is able to dissolve the substrate and the products. Additionally, the upper solvent, due to its insignificant extraction capabilities, does not interact with the lower phase and catalyst, however, the products can be easily extracted in the upper phase.[325] Among other examples, the biphasic systems can be 1) aqueous/organic, 2) fluorous/organic, 3) H$_2$O/scCO$_2$, and 4) IL/scCO$_2$. Several possible drawbacks have been linked to the first three biphasic systems mentioned, such as low environmental compatibility and partial solubility of the catalyst in the organic phase.[331-334]

In 1994, Jessop et al.[335] developed a biphasic IL/CO$_2$ batch system to obtain dimethyl formamide using scCO$_2$. Meanwhile the dimethyl formamide was produced and directly extracted from the IL phase into the scCO$_2$ phase, while the catalyst remained in the IL phase.

Afterwards, the biphasic IL/scCO$_2$ systems were employed in numerous metal-catalyzed organic reactions (Scheme 3).[336],[337]
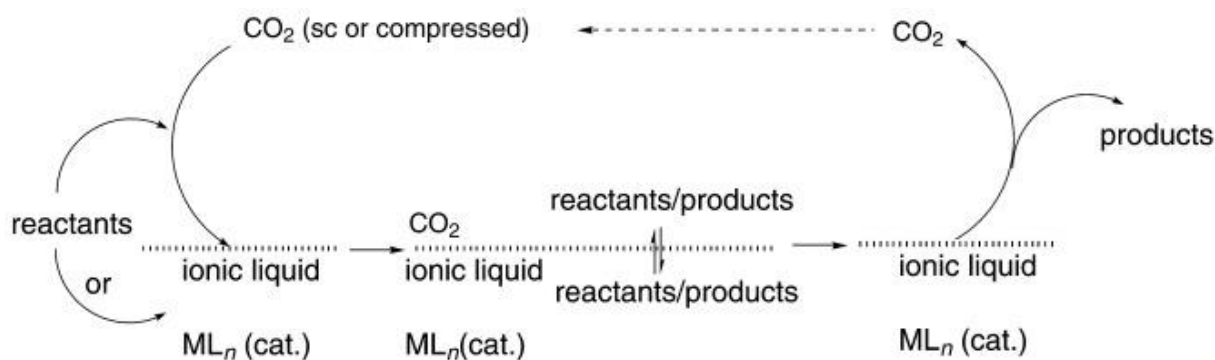
Scheme 3. Metal-catalysed organic reactions conducted in an IL and supercritical or compressed CO_2.[337]

Liu et al.[338] effectively utilized [C$_4$mim][PF$_6$] for two purposes: firstly, for the hydrogenation of alkenes at 50 °C and, secondly, for the production of formamides by reacting amines in IL/scCO$_2$. It is worth mentioning that the latter reaction obtained a conversion of 100 % and a selectivity of 99%. With these two examples, Liu et al.[338] introduced the biphasic IL/CO$_2$ system (Scheme 4).

* **R** = reactant, **P** = product, **I** = polar intermediate
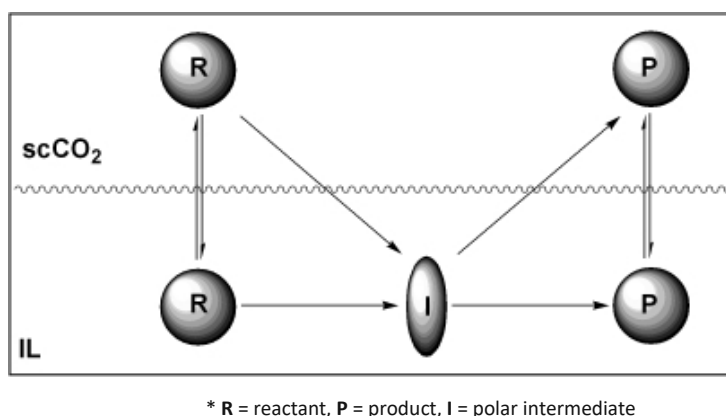
Scheme 4. Schematic representation of scCO$_2$/IL biphasic system.[338]

As depicted in Scheme 4, both reactants and products are present in the IL phase and in the scCO$_2$ phase. By manipulating the CO$_2$ pressure, their individual solubility, meaning their partitioning behavior, can be affected. Usually, by increasing the pressure, the solubility in the CO$_2$ phase rises. In the best case, the reaction takes place in the IL phase and the product remains in it. It can be subsequently forced to the CO$_2$ phase by extraction or continuous streaming, thereby leaving the catalytic system behind.[338] This concept has been employed for several different reactions specified in Table 5.

Table 5. Summary of catalyzed reactions in biphasic IL/scCO$_2$ systems.

Catalyzed Reactions	
Dimerization[339]	Hydrogenation[340]
Electro-oxidation[341]	Hydrovinylation[342]
Enantioselective hydrogenation[340]	Polymerization[343]
Hydroformylation[344]	Wacker oxidation[345]

After many studies utilizing the scCO$_2$/IL biphasic system, the key parameters were determined to be temperature, pressure, reaction time, effect of cosolvent or antisolvent in the CO$_2$ phase, choice of IL (anion and cation), degradation of the catalyst, solubility, viscosity, diffusion, mass transfer and molecular interactions.[286]

Even though the biphasic reaction system (either in batch or continuous mode) has remarkable advantages for the ideal cases, these are not applicable to all reactions. In some cases, if the reactant is more soluble in the CO$_2$ phase than in the IL phase, it can lead to separation of reactant and catalyst, thus interfering with the reaction. In some cases, it can be applicable to other reactions, in order to extract the products after the reaction is finalized. Nevertheless, in an industrial-scale operation, the repeated pressurization and depressurization steps should be avoided to be able to design a process that is more energy- and time-efficient. For this purpose, continuous reactions are preferred, which are stationary, with constant pressure and temperature parameters.[286]

1.3.3.4 Biphasic system (IL/CO$_2$) for continuous catalytic processes

Sellin et al.[346] published the hydroformylation of alkenes in a biphasic IL/CO$_2$ continuous catalytic fashion without employing a solid support. Their assumption was that scCO$_2$ should aid the diffusion of reactants into the ILs and act as the carrier for a flow system. The biphasic IL/scCO$_2$ system in combination with rhodium complexes for the hydroformylation of hex-1-ene exhibited an enhanced aldehyde selectivity. When performing the reaction with batch reactors, the scCO$_2$ was used to extract the reactants. The same catalyst remained in the IL phase, thereby affording the possibility to repeat the reaction. After 23 recycling steps, the activity and selectivity diminished due to the reaction of the [PF$_6$]$^-$ anion to release HF (hydrofluoric acid). In continuous flow, the hydroformylation of oct-1-ene was carried out for 30 h, employing a rhodium catalyst at 100 °C. Afterwards, the same group continued investigating the hydroformylation of alkenes and provided an illustration of their flow scheme (Figure 24).[347]
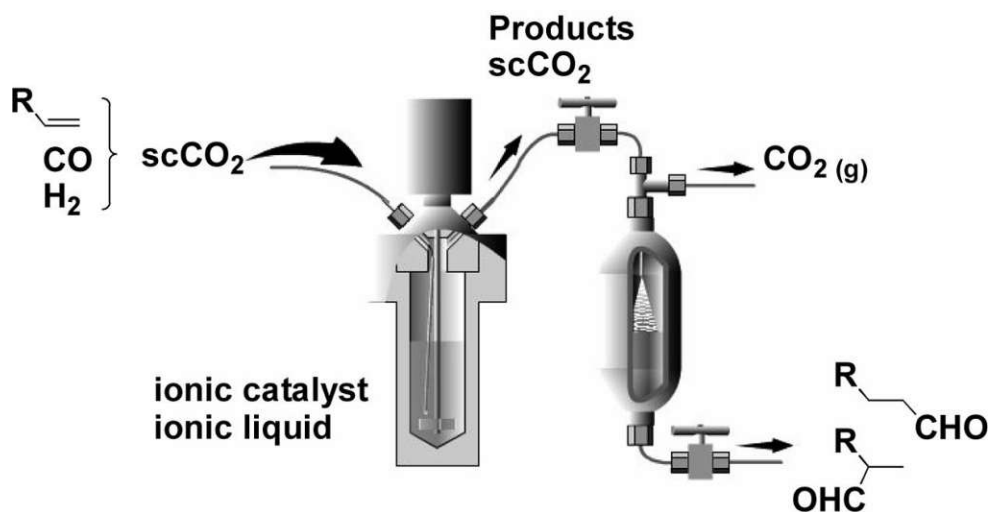
Figure 24. Continuous flow hydroformylation of alkenes in supercritical fluid-IL biphasic systems.[347]

In another publication by Zayed et al.,[348] the IL/scCO$_2$ biphasic catalyst system was employed for the continuous Friedel-Crafts acylation (Scheme 5), in which a wide variety of catalytically active metal salts was used at 60 °C at 300 bar.
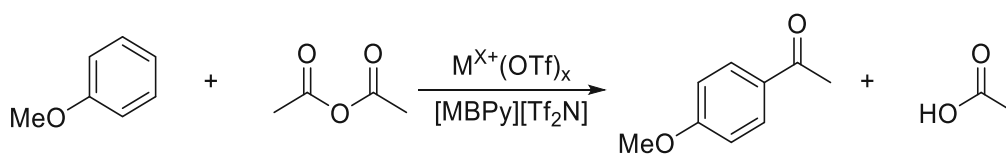
Scheme 5. Friedel-Crafts acylation in ILs.[348]

Biphasic continuous reaction systems have exhibited highly favorable results, however, the slow diffusion of reactants inside the IL phase, particularly in reactions with relatively little amount of catalyst, is one of the obstacles that is commonly encountered. Moreover, if these systems would be transferred into industrial scale, the required high quantities of IL would be a major economical hurdle, significantly limiting their applicability. Therefore, the main objective would be decreasing the quantity of IL needed. Particularly, a very thin IL layer seems to be a very appropriate stationary phase in continuous-flow fashion, due to its extremely low solubility in CO$_2$. To obtain a homogeneous thin layer of IL in a continuous reaction system which is not prone to agglomeration, especially in the continuous reaction systems, is rather challenging, thus, an alternative strategy was designed to avoid these issues, namely the development of SILP (supported ionic liquid phase) catalysts.[286]

1.3.3.5 Biphasic systems (IL/CO$_2$) for heterogeneous catalysis

To design an industrial scale-process, the substitution of homogeneous systems with heterogeneous systems is required to achieve an economically feasible process. To obtain high yields, the process relies on efficient catalyst separation and product isolation, employing batch or continuous flow operations.[349] In this matter, supported ILs have attracted remarkable attention in heterogeneous catalysis.[350-361] Heterogeneous catalytic systems, which are based on a SILP, have several significant advantages compared to the analogous homogeneous catalytic systems, for instance the possibility of utilization in fixed reactors, recyclability and the simple separation from the reaction medium.[362] The implementation of a material to support the catalyst gives a chance to fine-tune the properties of the catalyst and even to increase the catalytic activity. However, there are also some variables that may have a negative influence and must be carefully controlled, such as, catalyst deactivation, loss of catalyst activity and leaching of the catalyst.[363-365]

SILPs can be obtained *via* immobilization of ILs as thin layers on porous materials *via* physisorption or chemical binding to the solid support.[366] To be more precise, ILs can be immobilized through different strategies, for instance simple impregnation, grafting, polymerization, sol-gel method, encapsulation or pore trapping.[367-372] One of the simplest techniques consists of impregnation of the support material utilizing an IL that was diluted with a molecular solvent, for example acetone, followed by the evaporation of the co-solvent, yielding a uniform and thin IL layer on the pore structure of the support material. In this case, it is important to consider that for liquid-phase processes, a bulk solvent must be selected which is not miscible with the IL. In addition, together with the IL, transition metal ions or complexes and other modifier compounds could be dissolved.[373] Some of the most representative examples of synthesis of different silica-supported ILs are depicted in Scheme 6.

1. n-Bu₄NBr + SiO₂ →(Methanol / Co-dispersion)→ n-Bu₄NBr / SiO₂

2. [C₄mim]⁺[X]⁻ + SiO₂ →(Acetone / Co-dispersion)→ [C₄mim]⁺[X]⁻ / SiO₂

3. SiO₂-C₃H₆-Cl + P(n-Bu)₃ →(Toluene, 110°C, 7 days)→ SiO₂-C₃H₆-P⁺(Bu)(Bu)(Bu) Cl⁻

4. Imidazole + Cl–C₃H₆–Si(OEt)₃ →(Toluene, 110°C, 3 h)→ N-substituted imidazole–C₃H₆–Si(OEt)₃

R-X, Toluene, reflux; R = -methyl, ethyl; X = Cl⁻, Br⁻, I⁻

→ quaternized imidazolium–C₃H₆–Si(OEt)₃ →(Silica)→ silica-supported imidazolium IL

5. SiO₂(Si–OH)(Si–OH) + (MeO)₃Si–C₃H₆–I →(Reflux, toluene)→ SiO₂(Si–O)(Si–O)Si(OMe)–C₃H₆–I

→(Toluene, reflux; 4-(pyrrolidin-1-yl)pyridine)→ SiO₂(Si–O)(Si–O)Si(OMe)–C₃H₆–N⁺-pyridinium-pyrrolidine I⁻

Scheme 6. Synthesis of different silica-supported ILs.[374],[375-378]

Several different support materials can be used for the SILP preparation, such as TiO₂,[379] SiO₂[380-383] or activated carbon (AC)[366],[384] among others.[385] The SILP materials, depending on their pore diameter, can be grouped into three categories: microporous (d < 2.0 nm), mesoporous (2.0 < d < 50 nm) and macroporous (d > 50 nm).[386] Ionic liquids can be spread on the inner surface of the porous structure, so that a large specific surface area is maintained together with the mechanical properties of the support material, thereby, overcoming the mass transportation limitations and the necessary high amounts of ILs. This material is regarded as SILP.[380],[381]

When utilizing the SILP technology, in contrast to the traditional two-phase system containing an IL phase, the IL usage is remarkably efficient, due to its relatively short diffusion distance for reactants. Furthermore, ILs possess negligible vapor pressure, a large liquid range and high thermal stability, meaning that even at high temperatures, the IL immobilized on the solid support remains in its fluid state. As a consequence, SILP is extremely desirable in continuous-flow processes.[387]

There are two main applications for SILP systems, in separation processes[380],[382],[384],[388-392] and in catalysis.[355],[366],[373],[385],[393-396] In separation applications, the SILP has been employed as an alternative to traditional separation and purification processes, for example in desulfurization (SO_2 emissions removal)[380],[384] SILP materials with high absorption capacity and selectivity can absorb SO_2 (sulfur dioxide) in an efficient manner.[397] It has also been reported that several ILs have SO_2 sorption capacity.[398] Similarly, CO_2 separation and purification have also been considerably published.[399],[400] SILP materials containing a broad range of imidazolium-based ILs were prepared with different IL loadings, ranging from 5 – 60% (w/w).[380],[384],[399],[400]

Initially, there were two major contributions related to the use of silica-supported ILs in catalytic processes. In 2002, Mehnert et al. reported supported ILs synthesized *via* covalent bonding to the silica surface.[361] In parallel, Wasserscheid reported supported IL-phases synthesized *via* physisorption in 2003.[401]

Supported ionic liquid phase catalysts have drawn remarkable attention in the field of catalysis. The volatility of the solvent is the most evident limitation that conventional catalysis exhibits, in the case of an aqueous phase or traditional organic solvents. By combining a designed catalyst complex, non-volatile ILs and porous solid support, numerous advantages lead to the substantial progress of highly selective heterogenized homogeneous catalysts.[370]

The SILP contains a very fine layer of IL covering a solid support; in the meantime, it still acts as a "liquid" IL phase in which the catalyst is located (Figure 25). This solid behaves like a free-flowing powder that can be utilized in fixed-bed flow reactors. By employing SILPs instead of the ILs, the IL thin layer present in the SILP contains catalytically active species which are immobilized, allowing a reduction of the diffusion barrier. In addition, by contrasting SILP catalysts to ILs, the handling of the material is also drastically facilitated.[385]
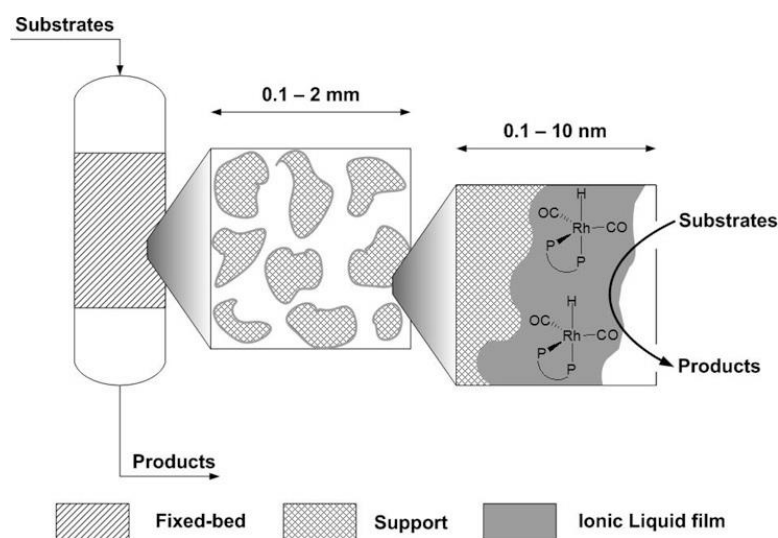
Figure 25. Schematic illustration of SILP catalysts for fixed-bed reactor technology.[385]

Many investigations have devoted effort to the development of new SILP materials and their application on several reaction types, for example hydroformylations, hydrogenations and CC-coupling reactions, among others. Up until now, by employing SILP catalysts in batch and in continuous flow fashion, various reactions have been improved, particularly hydroformylation, hydrogenation and oxidation. The applications of SILPs in the field of catalysis were reviewed by Riisager et al.[385]

For the first time, Ciriminna and co-workers combined SILP catalysis with scCO$_2$ for aerobic alcohol oxidation.[402] Sol-gel entrapped perruthenate catalysts were employed in order to synthesize silica-IL-supported species. In another publication by Xie et al.,[403] a similar reaction system was employed for the aerobic oxidation of benzyl alcohol utilizing SILP catalysts.

Hintermair et al.[359],[404] reported the hydroformylation of 1-octene in continuous reaction fashion *via* a fixed-bed SILP catalyst in combination with scCO$_2$. The SILP catalyst contained [Rh(acac)(CO)$_2$] (dicarbonyl(acetylacetonato)rhodium(I)) complex dissolved in [C$_8$mim][NTf$_2$] (1-octyl-3-methylimidazolium bis(trifluoromethanesulfonamide)) supported on silica by adsorption (Figure 26). It was previously reported that by performing this reaction in batch fashion over nine cycles, the product selectivity, in terms of linear to branched, decreased from 3.7 to 2.5, possibly due to the oxidation of the ligand, resulting in higher solubility of the catalyst complex in the scCO$_2$ phase and, thus, exhibiting leaching.[346] In order to avoid the aforementioned obstacles, by performing the reaction in continuous fashion, there was no deactivation during at least 40 h, achieving a constant product ratio of 3.1 (linear/branched) and a minimal leaching of less than 1 ppm.
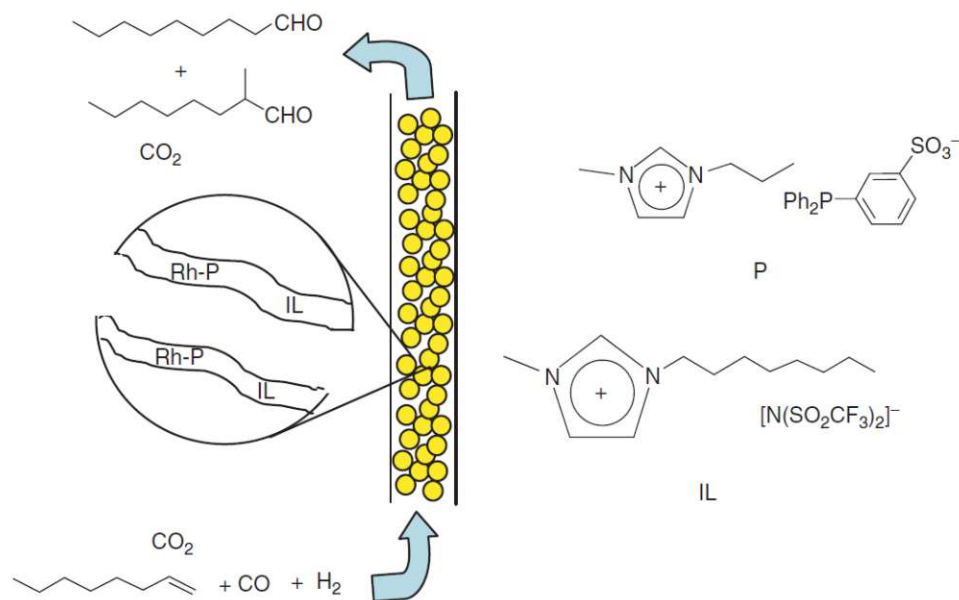
Figure 26. Continuous-flow 1-octene hydroformylation in a SILP system with CO$_2$ flow.[405]

In another publication by Hintermair et al.[406] it was demonstrated that SILP catalysis in continuous fashion can be employed for enantioselective reactions, namely enantioselective hydrogenation of dimethyl itaconate using a scCO$_2$ flow system. The chiral QUINAPHOS-Rh catalyst contained a Rh(I) complex bearing a chiral phosphine-based ligand immobilized in imidazolium-based ILs on dehydroxylated silica. Several different ILs were investigated in short experimental runs (up to 350 h). The optimum IL was found to be [C$_2$mim][NTf$_2$] (Figure 27).
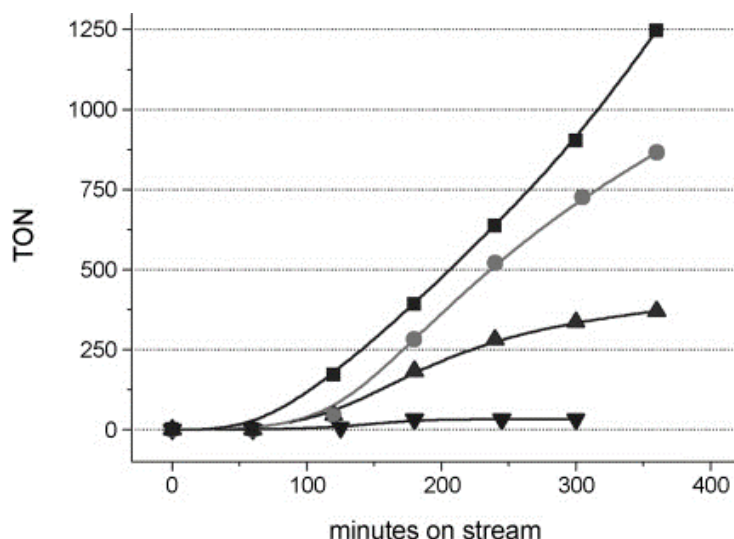
Figure 27. Cumulative turnover numbers (TONs) of silica-based SILP catalysts with different ILs over time. ■ [C$_2$mim][NTf$_2$] (>99 % ee); ● [4-MBP][NTf$_2$] (>99 % ee); ▲ [C$_4$mim][BF$_4$]; ▼ [C$_6$mim][OTf].[406]

Based on the IL results, the QUINAPHOS-Rh catalyst was combined with [C$_2$mim][NTf$_2$] in a dehydroxylated silica for the long-term experiments (up to 65 h). At the beginning, full conversion with >99% ee was achieved together with >2000 h^{-1} turnover frequency (TOF) and 0.3 kg L^{-1} h^{-1} space-time yield (STY). Nevertheless, over time until 65 h the enantiomeric excess dropped up to 70-75 % (Figure 28). In a later publication by Hintermair et al., it was determined that the main reason for the enantiomeric excess reduction was the deactivation of the catalyst by water.[407]
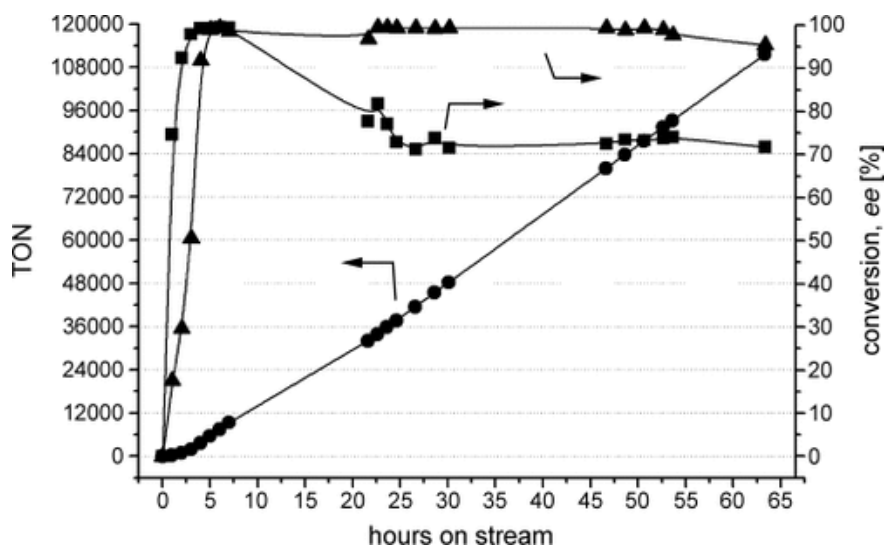
Figure 28. Conversion (▲), enantioselectivity (▪), and cumulative TONs (•) of QUINAPHOS-Rh catalyst in [C_2mim][NTf_2] on silica (α = 0.35, m = 1560 mg) over time [T = 40 °C, *p* = 120 bar, V(dimethyl itaconate) = 0.01 mL min^{-1}, V (CO_2) = 85 mL min^{-1}, V (H_2) = 10 mL min^{-1}].[406]

Hintermair et al.[407] also reported a continuous-flow process relying on a chiral transition-metal complex in a SILP with scCO_2 as the mobile phase for the asymmetric catalytic transformation of low-volatility organic substrates at mild reaction temperatures (Figure 29).
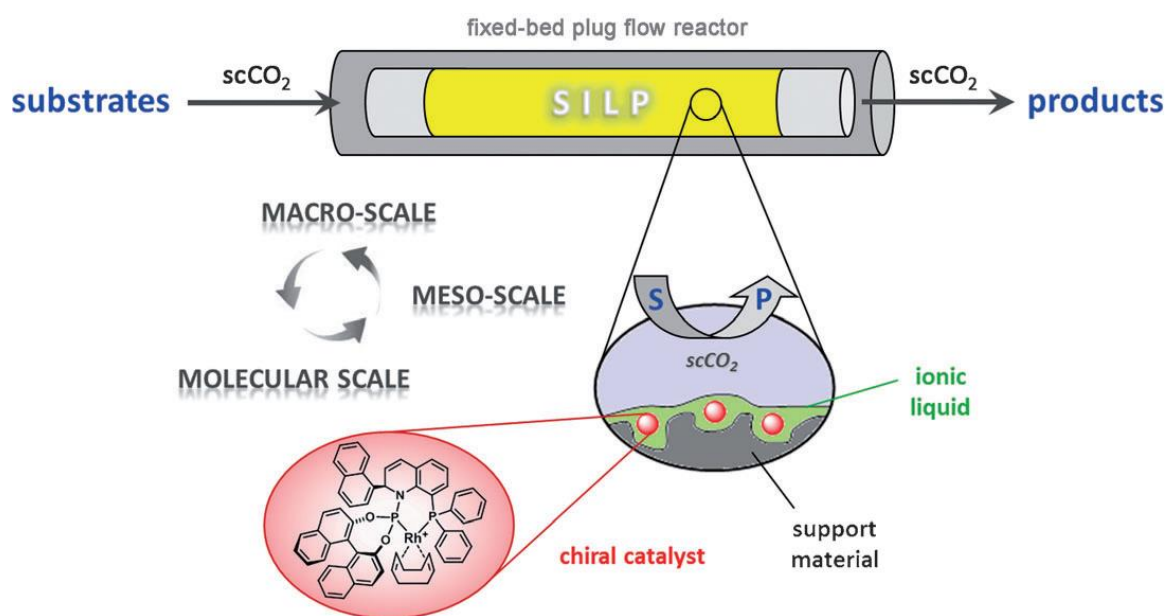
Figure 29. Concept of continuous-flow supported ionic liquid phase catalysis with scCO_2.[407]

The chiral QUINAPHOS-rhodium complex allowed quantitative conversion and an enantioselectivity of >99% ee in the hydrogenation of dimethylitaconate (Scheme 7), achieving turnover number (TON) over 100000 up to 30h.[407]
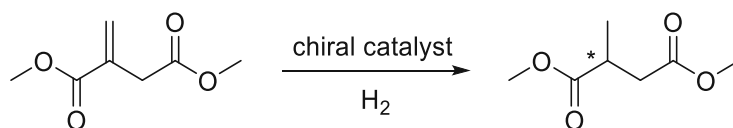
Scheme 7. Enantioselective hydrogenation of dimethylitaconate to dimethyl-2-methylsuccinate.[407]

The optimized system attained stable selectivities and productivities equal to 0.7 kg L^{-1} h^{-1} STY and a minimum of 100 kg product per gram rhodium or 14 kg per gram of ligand. The catalyst deactivation caused by water poisoning was circumvented by utilizing hydrophobic support surface obtained by fluorination together with a more hydrophobic IL or by introducing water scavengers inside the processing unit (Figure 30).[407]
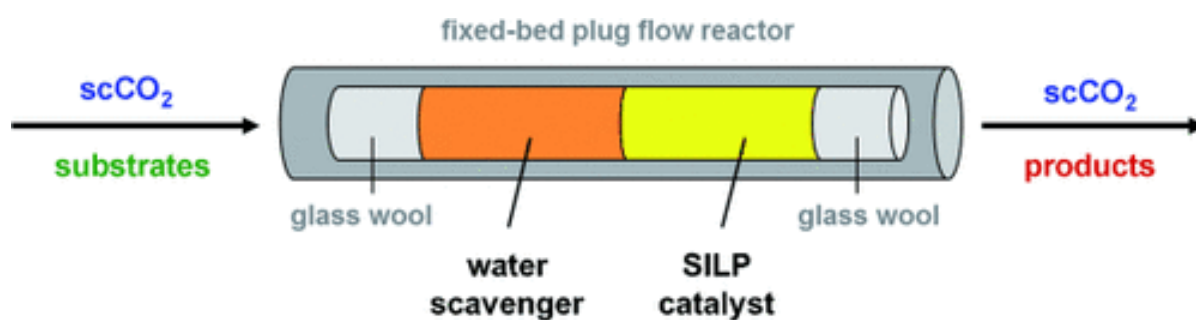
Figure 30. Schematic representation of the reactor setup using a water scavenger.[407]

2. Aim of the thesis

As a result of the increasing awareness for the necessity to switch towards sustainable chemistry, the search in chemical reactions and processes for solvents with a greener life cycle and reduced environmental impact has become a key issue. Several solvents with a diverse set of advantages and disadvantages have been identified as alternatives to commonly employed solvents, to be more precise ILs, supercritical fluids and their combination.

The interesting and complementary properties of ILs and scCO$_2$ have offered several potential applications for separation and catalysis and provided the basis for this PhD thesis. More specifically, three main research pipelines were investigated.

In the first research pipeline (Figure 31), the main objective was investigating the behavior of the secondary metabolites from plant matter. A new green and sustainable streamlined extraction process utilizing scCO$_2$ and ethanol as a co-solvent for the extraction of several bioactive compounds present in haskap berries (*Lonicera caerulea* L.) was developed. Various scCO$_2$ and ethanol ratios were used and the results obtained were compared to solvent extraction with conventionally employed solvents. The desirable outcome would be the development of a process that would lead to differentiation of secondary metabolites at different ethanolic levels and that could serve as a base concept for the extraction of high value-added bioactive compounds from other source materials.

Figure 31. Graphical summary of the first research pipeline.

In the second line of investigation (Figure 32), the primary aim was to extract valuable natural products with scCO$_2$ from biomass following IL pre-treatment. A novel combined IL- and scCO$_2$-based extraction (IL-SFE) of cannabinoids from *Cannabis sativa* L. was developed, consisting of three steps: 1) biomass pre-treatment with IL, 2) dilution with H$_2$O and 3) supercritical fluid extraction of target cannabinoids. Several process parameters were optimized, such as time and pressure during IL pre-treatment, dilution with water and, lastly, pressure and temperature during SFE. Additionally, with the developed combined IL-SFE process different ILs were also evaluated. The preferable outcome would be a synergistic effect between IL and scCO$_2$ which would lead to high extraction yields of the target cannabinoids, offer the possibility to recycle the ILs without the aid of any organic solvents and, additionally, lead to a cost reduction in conjunction with the simplification of the subsequent processing steps.
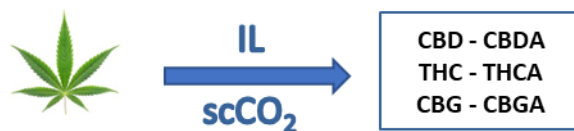
Figure 32. Graphical summary of the second line of investigation.

In the third and last research pipeline (Figure 33), the major objective was to produce propylene carbonate (PC) in continuous flow using scCO$_2$ in combination with supported IL technologies. A continuous flow reaction was developed using silica-supported ILs as catalyst, starting from propylene oxide and utilizing scCO$_2$ as solvent and reagent. The reaction was investigated in two different modes, i.e., homogeneous catalysis in batch mode and heterogeneous catalysis in continuous flow. Several ILs were tested in batch mode and the continuous reaction conditions were optimized. Additionally, different solid supported catalysts, which were synthesized *via* physisorption and chemisorption, were utilized in continuous flow mode. The desirable outcome would be to simultaneously achieve highest catalytic activity and long-term stability in heterogeneous fashion utilizing optimum reaction conditions and solid support catalyst.
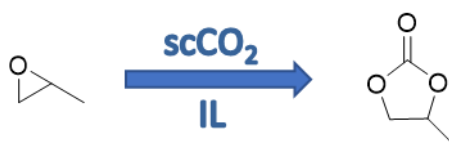
Figure 33. Graphical summary of the third research pipeline.

3. Extraction of bioactive compounds from plant matter utilizing supercritical fluid extraction.

3.1 Overview

Bioactive compounds of plant origin have always attracted scientific interest, due to their wide range of health-benefitting properties for humans and animals. Those bioactive compounds are regarded as secondary metabolites that are present in different parts of the plant, such as leaves, stem, roots, seeds, flowers and fruits. Typically, those bioactive compounds have been extracted with conventional techniques, such as steam distillation, solvent-based extraction (closed-vessel and Soxhlet), mechanical pressing, and hydrodistillation. However, those techniques have major disadvantages, for example, time-consumption, usage of large amounts of organic solvents, loss of volatile compounds, degradation of thermolabile compounds, toxic solvent residuals in the final extract, low yield and low extraction efficiency.[40],[42]

In the past years, the scientific field is leaning towards more environmentally sustainable techniques with the objective of reserving energy, replacing traditional solvents, reducing solvent consumption, decreasing extraction time. With this in mind, modern extraction techniques were developed for the recovery of bioactive compounds of plant origin, such as ultrasound-assisted extraction, pressurized liquid extraction, microwave-assisted extraction and supercritical-fluid extraction.[40],[42]

In this chapter, the supercritical-fluid extraction of haskap berries with an initial separation of lipids, followed by the simultaneous extraction of iridoids and anthocyanins will be presented.

The main objective of the first project was to develop a process that would extract the bioactive compounds from the berries of *Lonicera caerulea* L., namely iridoids (i.e., loganin and loganic acid) and anthocyanins (i.e., cyanidin, peonidin and pelargonidin) while, simultaneously, getting an insight into the behavior of the aforementioned secondary metabolites, with the final purpose of achieving a separation of those secondary metabolites during the extraction. A dynamic streamlined extraction which employs different $scCO_2$ and ethanol ratios was developed. Eventually, our developed dynamic streamlined fractionated $scCO_2$ extraction with different concentrations of ethanol would be compared to traditional ethanolic extraction.

The following manuscript will be presented in this chapter:

❖ Sainz Martinez, A.; Kornpointner, C.; Haselmair-Gosch, C.; Mikulic-Petkovsek, M.; Schröder, K.; Halbwirth, H. Dynamic streamlined extraction of iridoids, anthocyanins and lipids from haskap berries. *LWT* **2021**, *138*, 110633.

The first author equally contributed to this manuscript with the second author, in terms of planning, designing, performing the experimental work as well as drafting the manuscript.

3.2 Haskap berries (Lonicera caerulea L.)

The fruits produced by *Lonicera caerulea* L. also commonly known as haskap berries (Figure 34), have received increased attention over the last few years, due to their interesting and rich phytochemical content. Among many other berries commonly known for their health-beneficial properties, because of their higher ascorbic acid and anthocyanin content.[408] Recently, the European commission officially authorized haskap berries as novel foods.[93]

Figure 34. Haskap berries.[409] Open access, CC BY-SA 3.0.

Haskap is native to North-Eastern Russia, China, Japan and Canada. Its habitat is in wetlands by the side of marshes, rivers and in forests. It is regarded as a fresh fruit, which is suitable for human nutrition and useful as a base material for preparation of juices, purees, jellies, snacks, wine, dry fruits, tea, jams, gelatine, candies, food supplements and medicinal products.[410-412]

In East Asia, Blue Honeysuckle berries are not only used as comestibles but have also constituted an element of traditional medicine for centuries.[413],[414] The fruits are known for their health properties, which can be attributed to their variable bioactive ingredients, such as anthocyanins, iridoids, polyphenolics, lipids and several organic acids.[410],[415-417]

The bioactive compounds, namely lipids, iridoids and anthocyanins, are the focus of the following section of the thesis.

3.2.1 Lipids, iridoids and anthocyanins

Several lipids are contained in fruits and their juice. One major group are fatty acids, which represent 0.89% of the total weight of the berries, mainly palmitic (38.2%), oleic (27.6%), stearic (14.7%) and myristic acid (9.2%) have been identified (Figure 35).[418] Highly unsaturated acids have a positive effect in reducing the risk of inflammatory and cardiovascular diseases.[419]

Palmitic acid

oleic acid

Myristic acid

stearic acid
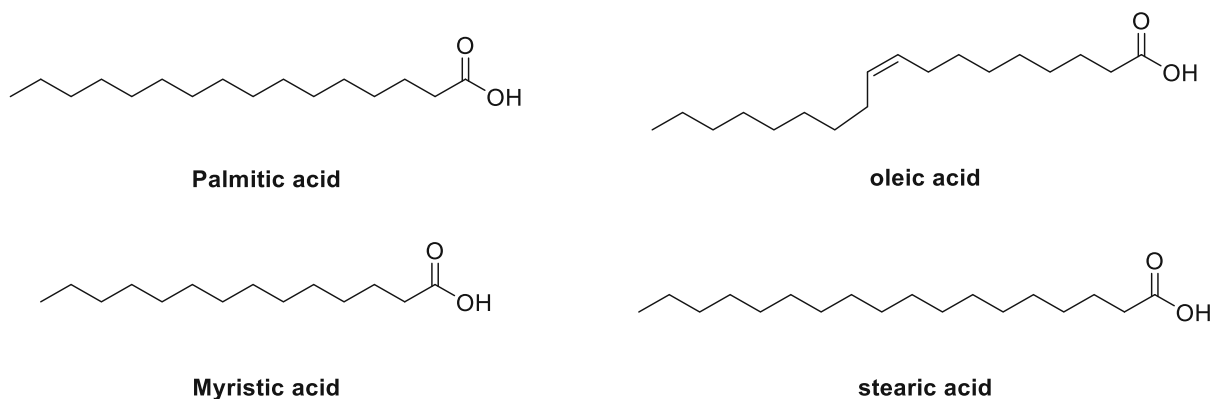
Figure 35. Main fatty acids identified in haskap berries.

Iridoids are secondary metabolites that are present in animal and plant species. They are structurally associated with a type of monoterpenoid with a cyclopentanopyran moiety and they are most commonly encountered in the glycosylated form.[410] Several iridoids have been identified in Blue Honeysuckle berries, for example loganic acid, loganin, sweroside, secologanin and secoxyloganin (Figure 36).[411] Iridoids possess a broad range of bioactive properties, such as antioxidant, antiviral, antimicrobial, anti-inflammatory, antispasmodic and antitumor.[420]

Loganic acid   **Loganin**   **Sweroside**   **Secologanin**   **Secoxyloganin**
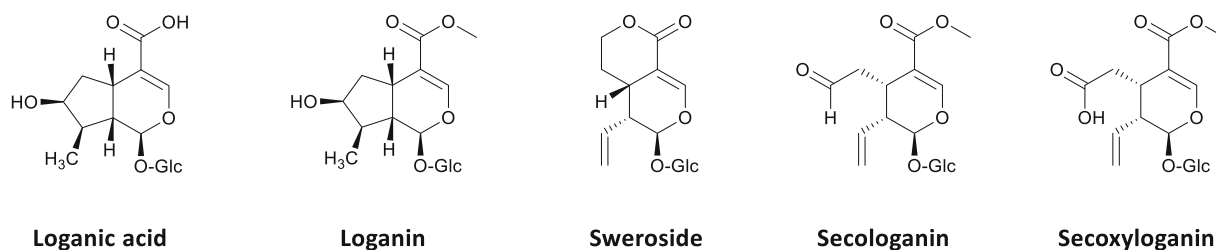
Figure 36. Examples of iridoids identified in haskap berries.

Apart from iridoids, another group of secondary metabolites is present in haskap, namely anthocyanins. They contain a flavylium ion as their base structure and are commonly found as glycosides in nature.[421] They are composed of glycosides of polymethoxy- and polyhydroxy- derived flavylium salts or 2-phenylbenzopyrylium.[422] Cyanidin, pelargonidin and peonidin derivatives have been determined as the major components of the anthocyanin family present in the berries (Figure 37).[423] Anthocyanins are known to exhibit antioxidant, anti-inflammatory, antimicrobial and antiviral properties, among other pharmacological benefits.[410],[424]

Cyanidin **Peonidin** **Pelargonidin**
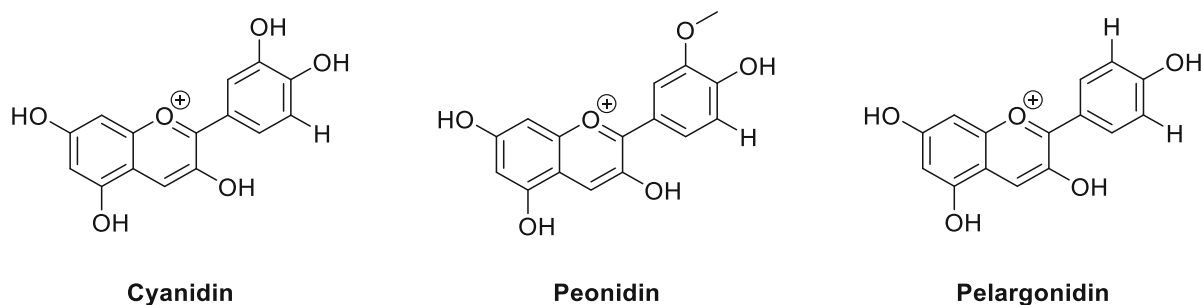
Figure 37. Major anthocyanins compounds present in haskap berries.

The most commonly employed technique to extract fatty acids, iridoids and anthocyanins is solvent-based extraction. Fatty acids require apolar solvents, such as hexane,[425],[426] whereas iridoids and anthocyanins are extracted with polar solvents, such as methanol or ethanol.[427],[428] In addition, anthocyanins are also traditionally extracted with acetone, acidified methanol and acidified water.[429] Even though anthocyanins exhibit greater solubility in methanol, ethanol is more appropriate as it regarded as fit for human consumption and food products.[430]

Supercritical fluid extraction has also been employed for the extraction of lipids, iridoids and anthocyanins. In previous sections, the basics, properties, influential parameters, and applications have already been discussed. However, it is important to mention that the main advantages of SFE employing scCO$_2$ are the low surface tension, lower viscosity and high diffusivity, resulting in enhanced mass-transfer during the process and the increased extraction efficiency of target bioactive compounds from plant matter.[431],[432] In addition, the possibility of applying mild process conditions coupled with the absence of light and oxygen enhances the chances of preservation of the extracted bioactive compounds.[43]

The nonpolar nature of scCO$_2$ allows the extraction of lipids; nonetheless, for the extraction of iridoids and anthocyanins, which are more polar compounds, the addition of polar modifiers is required. The most common polar modifier employed for the extraction of bioactive compounds from plant matter is ethanol.[433]

No extraction of fatty acids from haskap berries using scCO$_2$ has been thus far reported in literature, however, the extraction of fatty acids from other plant matters has already been reported, for instance rice bran (*oryza sativa*)[425] and penny bun (*boletus edulis).*[426] Similarly, no extraction of iridoids from haskap berries employing scCO$_2$ has been reported up until now; nonetheless, four different plant materials (i.e. *plantago asiatica,*[434] *picrorhiza kurroa*[435] and *valeriana glechomifolia*[431] and *lippia citriodora*[436]) have been extracted with the purpose of extracting their iridoids, such as geniposidic acid, picroside I, picroside II and iridoids valepotriates.

Anthocyanins have been extracted utilizing scCO$_2$ from various types of plant matter, like corn cob (*zea mays*),[437] crajiru (*arrabidaea chica* Verlot),[438] juçara (*euterpe edulis* Mart.),[439] roselle (*hibiscus sabdariffa* L.),[440] portuguese myrtle (*myrtus communis* L.),[441] açai (*euterpe oleracea*),[442] eggplant (*solanum melongena* L.),[443] saffron crocus (*crocus sativus*).[444] However, regarding the berries of *Lonicera caerulea* L., only one publication has reported, that cyanidin-, peonidin- and pelargonidin-based glycosides were obtained, giving a total of 5 different anthocyanins.[445]

Dynamic streamlined extraction of iridoids, anthocyanins and lipids from haskap berries

Aitor Sainz Martinez [a,1], Christoph Kornpointner [b,1], Christian Haselmair-Gosch [b], Maja Mikulic-Petkovsek [c], Katharina Schröder [a,**], Heidi Halbwirth [b,*]

[a] Institute of Applied Synthetic Chemistry, Technische Universität Wien, Getreidemarkt 9/163, 1060, Vienna, Austria
[b] Institute of Chemical, Environmental and Bioscience Engineering, Technische Universität Wien, Getreidemarkt 9/166, 1060, Vienna, Austria
[c] Department of Agronomy, Biotechnical Faculty, University of Ljubljana, Ljubljana, Slovenia

ABSTRACT

The European Commission recently authorized the placing of haskap (*Lonicera caerulea* L.) berries as a novel food on the EU market. It has been suggested that these berries have several health beneficial properties, due to their considerable content of highly valuable secondary metabolites, such as anthocyanins, phenolic acids, iridoids and fatty acids. Herein, we report a dynamic streamlined extraction process for iridoids and anthocyanins with supercritical carbon dioxide and ethanol as modifier. In particular, we have focused on the iridoids loganic acid and loganin, as well as on different hydroxylation patterns of the anthocyanins. The developed multiple step extraction process leads to initial separation of lipids at low ethanolic concentrations (1 vol%), followed by partial extraction of iridoids at 10 vol% ethanol and ultimately to combined extraction of iridoids and anthocyanins at higher ethanol amounts (>10 vol%). The sequential extraction can be performed in a closed system by automated variation of two innocuous solvents, but uses higher solvent amounts. In comparison to conventional ethanolic extraction, the dynamic streamlined yielded 97% of iridoids and about 7% more anthocyanins.

1. Introduction

The haskap berry (*Lonicera caerulea*; also named e.g. Blue Honeysuckle or Honeyberry), commonly grows circumpolar in North-Eastern Russia, China, Japan and Canada (Celli et al., 2014; Kucharska and Fecka, 2016; Kucharska et al., 2017; Oszmiański et al., 2016). In December 2018, it was officially authorized as a novel food by the European Commission (Commission et al., 2018).

Haskap are of interest for growers because of their very short vegetation period. On the one hand, this results in robust plants, which are not affected by late spring frosts and withstand hot and dry summers. On the other hand, fruits are harvested early in the season even before all the other berries, which is a significant commercial benefit. However, their main attractiveness comes from their rich spectrum of bioactive phytocompounds e.g. anthocyanins, iridoids, polyphenols, lipids and several organic acids which are known to possess a broad scope of bioactive and health related properties (Finley & Shahidi, 2001; Gołba et al., 2020; Jurikova et al., 2011; Jurikova et al., 2012; Kucharska et al., 2016; Palíková et al., 2008; Senica et al., 2018; Svarcova et al., 2007; Tundis et al., 2008).

Among these, an exceptionally high anthocyanin concentration, which is strongly correlated with high antioxidative capacity, is reported. In addition, the presence of rare iridoids, which possess strong anti-inflammatory activity has to be highlighted (Gołba et al., 2020). In Eastern Asia, haskap berries have been used for centuries, not only as food but also as part of traditional medicines (Kaczmarska et al., 2015).

At least 15 iridoids have been identified in haskap berries, but the spectrum varies significantly (Golba et al., 2020; Kurcharska et al., 2017). Several glycosides variations of cyanidin, pelargonidin and peonidin have been reported in haskap berries with cyanidin 3-*O*-glucoside as the most abundant anthocyanin comprising 79–88% of the total anthocyanin content (Chaovanalikit et al., 2004).

Apart from consumption as fresh fruits, processing of haskap to food products and creation of functional products is of high interest. In

---

Table 1

Conventional solvent extraction of iridoids and anthocyanins using EtOH, water and acidified EtOH. Anthocyanins were analyzed as anthocyanidins after acidic hydrolysis. (n = 3 ± SD).

Solvent (°C)	Loganic acid /[mg/g]	Loganin /[mg/g]	Cyanidin /[mg/g]	Peonidin /[mg/g]	Pelargonidin /[mg/g]
Vostorg (Batch 1)					
ac. EtOH (50)	5.13 ± 0.17c	2.533 ± 0.019d	9.3 ± 0.3 ab	0.631 ± 0.021a	0.165 ± 0.003a
ac. EtOH (80)	4.68 ± 0.12a	3.10 ± 0.08c	2.9 ± 0.3c	0.192 ± 0.019d,e	0.094 ± 0.008bc
EtOH (80)	4.35 ± 0.09a	2.120 ± 0.015a	9.9 ± 0.5a	0.664 ± 0.029a	0.115 ± 0.005b
H₂O (80)	5.44 ± 0.15b,c	2.94 ± 0.04b	6.5 ± 0.4e	0.447 ± 0.029b	0.083 ± 0.006cd
Aurora (Batch 2)					
ac. EtOH (50)	5.57 ± 0.05b	1.163 ± 0.009f	7.91 ± 0.36d	0.502 ± 0.051b,c	0.153 ± 0.015a
ac. EtOH (80)	5.73 ± 0.07b	1.55 ± 0.04e	2.91 ± 0.07c	0.186 ± 0.006e	0.0674 ± 0.0010d
EtOH (50)	5.47 ± 0.16b,c	1.11 ± 0.05e	8.25 ± 0.23bd	0.553 ± 0.021c,d	0.169 ± 0.005a

ac. acidified.

Quantification range (0.01–100 μg/mL).

Mean values with different letters (a, b, c, etc.) within the same column are statistically different (p < 0.05).
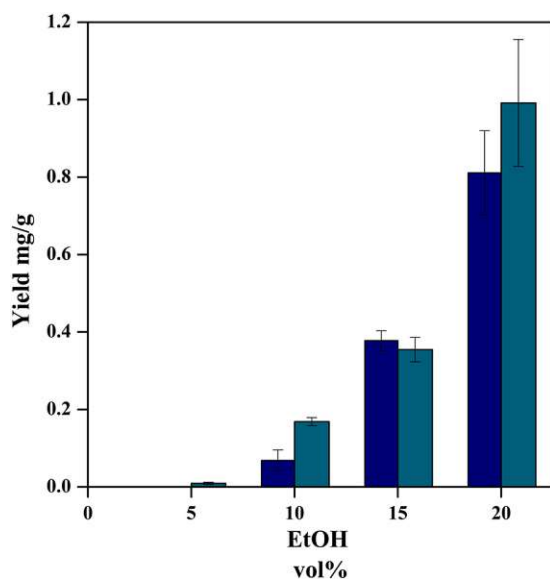
Fig. 1. Partial supercritical carbon dioxide extraction of loganic acid (navy blue) and loganin (dark cyan) from haskap berries. (n = 3 ± SD). (For interpretation of the references to colour in this figure legend, the reader is referred to the Web version of this article.)

addition, haskap berry pulp, or residues of the production of haskap juice and wines could be an interesting approach to create value added products for a diet rich in bioactive phytocompounds. Main targets could be the anthocyanins, which provide the intense and stable colour of haskap juice, and could be therefore used as natural food colorants and the rarely occurring iridoids (Celli et al., 2014; Kucharska et al.,

Table 2

SFE of loganic acid and loganin with ethanol as modifier (0–20 vol%) at 80 °C, 30 MPa from dried haskap berries. (n = 3 ± SD).

EtOH /[vol%]	Loganic acid /[mg/g]	Loganin /[mg/g]
0	–	–
1	–	–
5	–	0.009 ± 0.003
10	0.069 ± 0.027	0.169 ± 0.010
15	0.377 ± 0.025	0.35 ± 0.03
20	0.81 ± 0.11	0.99 ± 0.16

Quantification range (0.01–100 μg/mL).

2016; Kucharska et al., 2017; Oszmiański et al., 2016).

Traditionally, iridoids and anthocyanins are extracted with volatile organic solvents in multiple steps. In the case of iridoids, methanol and ethanol are the most commonly employed solvents, since both are affordable and dissolve iridoids efficiently (Suomi et al., 2000). The most prevalent solvents used for the extraction of anthocyanins are water acidified with hydrochloric acid or methanol, sometimes in combination with acetone (Kerbstadt et al., 2015). Although the solubility of anthocyanins in methanol is higher than in ethanol, ethanol is preferred because of its compatibility with products intended for human consumption (Kazan et al., 2016). On the contrary, fatty acids are extracted with non-polar solvents, usually *n*-hexane (Garcia et al., 1996).

Supercritical fluid extraction (SFE) relies on the utilization of supercritical fluids as extracting solvents, aiming for the separation of one or several compounds of interest from the matrix. While a number of different solvents exist for supercritical fluid extraction, it is most commonly performed with carbon dioxide as supercritical fluid due to its low critical pressure (7.4 MPa) and temperature (32 °C). (Hamid et al., 2018; Udin et al., 2015). Furthermore, it is easily accessible in high purity at a low cost, is non-toxic, non-flammable and easily removable from the extract. When the supercritical state is reached, the solvent exhibits low surface tension, lower viscosity and higher diffusivity, thus promoting mass-transfer. As a result, several studies showed that the extraction efficiency of valuable compounds from different plant materials can be increased compared to conventional solvent extraction (Kerbstadt et al., 2015; Müller et al., 2012; Woźniak et al., 2016). Currently, extracts from over 300 plant species have been isolated with supercritical carbon dioxide (Woźniak et al., 2016). However, pure supercritical carbon dioxide (scCO2) is considered to be a relatively apolar solvent and in order to extract polar compounds, such as iridoids and anthocyanins, a polar co-solvent is necessary. For the supercritical extraction from plant-based materials, typically ethanol or methanol is used as a modifier (Kerbstadt et al., 2015).

Regarding the SFE of iridoids, there are only a few reported studies available. So far, the SFE extraction of iridoids was reported for three different plant sources: *Valeriana glechomifolia*, *Picrorhiza kurroa* and *Plantago asiatica*. The iridoids valepotriates, picroside I, picroside II and geniposidic acid (iridoid glucoside) have been extracted from these plants (Müller et al., 2012; Patil et al., 2012; Wang et al., 2014). Currently, there is no information available in the literature concerning the supercritical fluid extraction of iridoids from haskap berries. Numerous supercritical fluid extraction processes of anthocyanins from various plant materials have been reported, such as black plum (*Syzygium cumini*), sour cherry (*Prunus cerasus*), elder berry (*Sambucus nigra*) and blueberry (*Vaccinium myrtillus*) (Kerbstadt et al., 2015; Maran et al., 2014; Vatai et al., 2009; Woźniak et al., 2016). There is one study available on the SFE of anthocyanins from the berries of *L. caerulea*, in

Fig. 2. All 18 fractions of the dynamic streamlined extraction. Fractions 1–2 (1 vol% EtOH), Fractions 3–6 (10 vol% EtOH), Fractions 7–10 (20 vol% EtOH), Fractions 11–14 (50 vol% EtOH) and Fractions 15–18 (acidified EtOH).
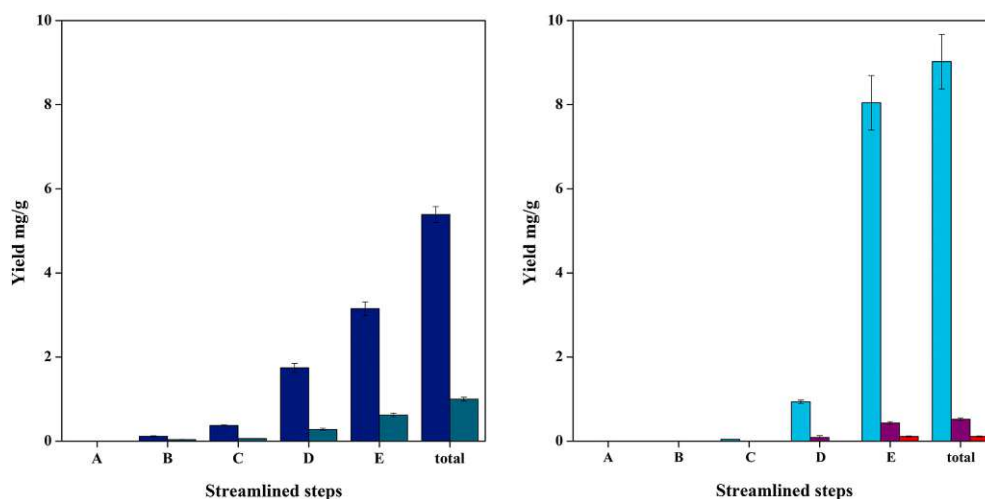
Fig. 3. Distribution of extraction of iridoids (left, loganic acid: navy blue, loganin: dark cyan) and anthocyanins (right, cyanidin: cyan blue, peonidin: purple and pelargonidin: red) during the dynamic streamlined extraction at 50 °C and 30 MPa. A-D is vol % EtOH (A = 1, B = 10, C = 20, D = 50) and E is acidified EtOH. (n = 3 ± SD). (For interpretation of the references to colour in this figure legend, the reader is referred to the Web version of this article.)

which case five anthocyanins were obtained, namely cyanidin 3-*O*-glucoside, cyanidin 3,5-*O*-diglucoside, cyanidin 3-*O*-rutinoside, pelargonidin 3-*O*-glucoside and peonidin 3-*O*-glucoside (Jiao & Kermanshahi pour, 2018). Successful SFE of fatty acids with pure $scCO_2$ has been reported in the literature (Garcia et al., 1996). However, no data regarding the supercritical extraction of fatty acids from haskap berries has been published up to date. Moreover, studies typically focus on the extraction and analysis of individual valuable ingredients with limited information of co-extracted secondary metabolites. Streamlined extraction processes addressing the simultaneous extraction of different secondary metabolites, such as a combined process for iridoid and anthocyanin extractions are rare.

In this work, initially, iridoids (loganin and loganic acid) and anthocyanins (cyanidin, peonidin, pelargonidin) were targeted with conventional solvent extraction approaches. Additionally, the first SFE of loganin and loganic acid was performed. Based on that, our objective was to further study the behaviour of these secondary metabolites in haskap by doing dynamic streamlined extraction with relation to the $scCO_2$ and ethanol ratio on a laboratory scale. Therefore, we aimed to obtain the optimum process conditions which led to a differentiation of secondary metabolites, specifically focusing on the initial extraction of fatty acids for the first time from haskap berries with $scCO_2$ and the simultaneous extraction of iridoids and anthocyanins. Thus, we report on the development of a dynamic streamlined fractionated supercritical carbon dioxide extraction for the initial separation of lipids with low concentrations of EtOH, the subsequent partial extraction of iridoids, followed by simultaneous extraction of iridoids and anthocyanins at higher ethanolic levels.

2. Material and methods

2.1. Plant material

Haskap berries were collected from commercial orchards in St. Ulrich in Greith, Austria (batch 1, cv. 'Vostorg') and Litija, Slovenia (batch 2, cv. 'Aurora') at physiologically ripe stages. The berries were frozen with liquid nitrogen, grounded with a Fritsch Universal Pulverisette 19 mill (Fritsch, Oberstein, Germany) and lyophilized until constant weight. Samples were stored in the dark until analysis.

2.2. Supercritical and conventional extractions

All supercritical fluid extractions were performed with a $scCO_2$ device manufactured by Jasco (Jasco Corporation, Tokyo, Japan). Liquid CO_2 (>99.995% purity; with ascension pipe; Messer GmbH, Vienna, Austria) was pressurized by two CO_2-pumps (PU-2086, Jasco Corporation, Tokyo, Japan) with cooled heads (CF40, JULABO GmbH, Seelbach, Germany). An HPLC pump (PU-2089, Jasco Corporation, Tokyo, Japan) supplied solvents. A heating coil and one HPLC-cartridge (L 127 mm, ID 10 mm) filled with haskap berry powder were placed in an oven (CO-2060, Jasco Corporation, Tokyo, Japan) and thermostated to the desired temperature. A back-pressure regulator (BP-2080, Jasco Corporation, Tokyo, Japan), a gas/liquid separator (HC-2086-01, Jasco Corporation, Tokyo, Japan), and a product collector (SCF-Vch-Bp, Jasco Corporation, Tokyo, Japan) were used to obtain the extracts (ESI Fig. S2).

The optimization of the supercritical carbon dioxide extraction of iridoids started from literature data (Patil et al., 2012; Wang et al., 2014) for similar structures as our target compounds and the SFE parameters

Table 3

Extracted amounts of iridoids and anthocyanins during the dynamic streamlined extraction at 50 °C and 30 MPa. The fractions were taken every 30 min under different ethanolic concentrations. Anthocyanins were analyzed as anthocyanidins after acidic hydrolysis. (n = 3 ± SD).

Fraction	Loganic acid /[mg/g]	Loganin /[mg/g]	Cyanidin /[mg/g]	Peonidin /[mg/g]	Pelargonidin /[mg/g]
F01	–	–	–	–	–
F02	–	–	–	–	–
1 vol% EtOH	–	–	–	–	–
F03	0.0169 ± 0.0027	0.014 ± 0.003	–	–	–
F04	0.043 ± 0.003	0.0113 ± 0.0018	–	–	–
F05	0.032 ± 0.008	0.0068 ± 0.0021	–	–	–
F06	0.023 ± 0.008	0.0046 ± 0.0015	–	–	–
10 vol% EtOH	0.115 ± 0.013*	0.037 ± 0.004*	–	–	–
F07	0.085 ± 0.007	0.0137 ± 0.0017	0.0059 ± 0.009	–	–
F08	0.104 ± 0.006	0.0170 ± 0.0021	0.0121 ± 0.0012	–	–
F09	0.097 ± 0.007	0.0159 ± 0.0020	0.0130 ± 0.0005	–	–
F10	0.090 ± 0.005	0.0149 ± 0.0020	0.0136 ± 0.0006	–	–
20 vol% EtOH	0.375 ± 0.012*	0.061 ± 0.004*	0.0446 ± 0.0016*	–	–
F11	0.47 ± 0.07	0.075 ± 0.017	0.195 ± 0.021	0.0198 ± 0.0024	–
F12	0.52 ± 0.06	0.084 ± 0.015	0.264 ± 0.017	0.0260 ± 0.0026	–
F13	0.42 ± 0.04	0.067 ± 0.010	0.249 ± 0.014	0.0231 ± 0.0016	–
F14	0.339 ± 0.029	0.053 ± 0.006	0.227 ± 0.028	0.0200 ± 0.0016	–
50 vol% EtOH	1.74 ± 0.10*	0.278 ± 0.026*	0.935 ± 0.041*	0.0889 ± 0.004*	–
F15	2.54 ± 0.16	0.51 ± 0.04	6.2 ± 0.6	0.35 ± 0.03	0.111 ± 0.012
F16	0.370 ± 0.024	0.072 ± 0.017	1.13 ± 0.18	0.056 ± 0.009	–
F17	0.152 ± 0.016	0.027 ± 0.004	0.446 ± 0.021	0.0224 ± 0.0024	–
F18	0.086 ± 0.007	0.0136 ± 0.0011	0.27 ± 0.04	–	–
ac EtOH	3.15 ± 0.16*	0.62 ± 0.04*	8.0 ± 0.6*	0.43 ± 0.03*	0.111 ± 0.012
Total	**5.39 ± 0.19***	**0.99 ± 0.05***	**9.0 ± 0.6***	**0.52 ± 0.03***	**0.111 ± 0.012**

ac. acidified.

*Standard deviation calculated with error propagation.

Quantification range (0.01–100 μg/mL).

were adapted for this purpose. The CO_2 flow rate was set at 2.0 mL/min, the oven temperature at 80 °C and the back pressure was regulated to 30 MPa. Cumulatively, the berries were extracted for 2 h; 1 h in static mode and 1 h in dynamic mode. In total, 0.5 g of ground haskap berries (batch 1) were used. Ethanol was used as a modifier from 0 to 20 vol% adjusted in relation to the overall CO_2 flow.

The following parameters were employed in the streamlined supercritical carbon dioxide extraction; 1 h static and 9 h dynamic extraction, overall CO_2 flow rate 2.0 mL/min at 30 MPa. Multiple extraction steps with increasing amounts of EtOH as modifier were performed. The haskap berries (batch 2) were extracted for 1 h with 1 vol% EtOH, 2 h each with 10, 20 and 50 vol% EtOH and in the final step, 2 h with acidified EtOH (3 vol% formic acid) under subcritical conditions (ESI Fig. S3). A fraction was collected every 30 min (ESI Table S2) and subjected to HPLC analysis. For the extractions, 1.0 g of milled haskap berries were placed into the extraction vessel.

For comparison, conventional solvent extractions were performed in 30 mL Teflon screw cap vials. The quantity used in each extraction was 0.2 g of milled berries (batch 1 and 2). The sample was extracted for 2 h with 10 mL solvent under magnetic stirring at 100 rpm. Different subcritical extraction conditions were evaluated; 2 h extraction with ethanol, acidified ethanol (3 vol% formic acid) and water at various temperatures (50 °C and 80 °C).

2.3. Characterization

A Dionex UltiMate© RSLC System with DAD-3000RS Photodiode Array Detector (Thermo Scientific, Germering, Germany) was used for HPLC analysis in combination with a Dionex Acclaim™ RSLC 120 C18 (2.2 μm, 120 Å, 2.1 × 150 mm, Bonded Silica Products: No. 01425071) column. The flow rate was set to 0.2 mL/min and the temperature of the oven was set at 25 °C (Lima et al., 2017). All employed chemicals were of analytical grade (ESI Table S1) unless otherwise specified.

Prior to the quantification of loganic acid and loganin, the HPLC was calibrated with reference compounds purchased from Extrasynthese (Genay, France). The mobile phase consisted of a combination of water

(0.1 vol% formic acid) (A) and acetonitrile (0.1 vol% formic acid) (B). The following gradient program was applied: 10 min at 2 vol% (B), 10 min to 99 vol% (B), 2 min at 99 vol% (B), 0.5 min to 2 vol% (B), 7.5 min at 2 vol% (B). The detection wavelength was set at 245 nm.

Anthocyanins were quantified as anthocyanidins after removal of their respective sugar moieties by acidic hydrolysis as described previously (Lima et al., 2017). Commercial standard substances (Extrasynthese, Genay, France) of cyanidin, pelargonidin and peonidin were used for the construction of the external calibration curve. For acidic hydrolysis, the samples were kept in 4 N HCl at 95 °C for 1 h. The elution solvents were water (0.1 vol% formic acid) (A) and water (22.5 vol% acetonitrile, 22.5 vol% methanol, 10 vol% formic acid) (B). An elution gradient of 10 min at 9 vol% (B), 30 min to 90 vol% (B), 10 min at 90 vol% (B) was chosen for the separation. The detection wavelength was set at 520 nm.

Fatty acids were transformed into fatty acid methyl esters, according to an established derivatization process (Liu et al., 2010). They were identified by using a FOCUS GC Chromatographic Unit (Thermo Fisher Scientific S. p. A., Milan, Italy) coupled to an ISQ LT Single quadrupole MS (Thermo Fisher Scientific, Austin, USA). FAME separation was performed on a Rxi-5Sil MS cross-bond 1,4-bis(dimethylsiloxy)phenylene dimethyl polysiloxane capillary column (L 30 m, ID 0.25 mm, 0.25 μm film thickness).

2.4. Statistical data analysis

OriginPro 8.1 was used in order to perform the statistical data analysis. For multiple groups, one-way ANOVA followed by Tukey honestly significant difference (HSD) post hoc test at the 0.05 significance level were employed.

3. Results and discussion

We aimed to establish a dynamic streamlined extraction process using supercritical carbon dioxide for iridoids and anthocyanins with initial separation of lipids. As the spectrum of iridoids is variable

between varieties and growing conditions, we focused on loganic acid and loganin as lead compounds, which are abundantly present in haskap berries (Kucharska et al., 2017). Concerning anthocyanins, the cultivar Vostorg, which was used in the first batch, contains 87% cyanidin 3-*O*-glucoside, 6% other cyanidin glycosides, 4% peonidin 3-*O*-glycosides and only traces of pelargonidin 3-*O*-glucoside (Kucharska et al., 2017), whereas we previously observed a relatively low content of only 51% cyanidin 3-*O*-glucoside and a much higher peonidin glycoside concentration (30%) in the cultivar Aurora used in the second batch. In this study, we evaluated the extraction efficiency by analysing anthocyanins after removal of sugar moieties and distinguishing between the anthocyanin classes only.

Conventional solvent extractions of haskap berries cv. Vostorg, performed with EtOH at 80 °C, exhibited high extraction efficiency for cyanidins (9.9 mg/g DW) contrary to the lower extracted amounts of peonidins (0.664 mg/g DW) and pelargonidins (0.115 mg/g DW). The overall amount of anthocyanidins was 10.7 mg/g DW (Table 1). In corresponding literature, anthocyanins in fresh haskap berries ranged from 65.12 to 112.37 mg/100 g fresh weight (Senica et al., 2018). Caprioli et al. (2016) extracted 12.317 mg/g of total anthocyanins from dried haskap berries by using a mixture of acidified ethanol and water, which is consistent with the data reported herein. Conventional extractions with H_2O as well as acidified EtOH at 80 °C resulted in a significant reduction of the cyanidin yield. The same was observed for peonidin and pelargonidin; however, the lowest yields for pelargonidin were obtained with water instead of acidic alcohol. A decrease in temperature from 80 °C to 50 °C in combination with acidified EtOH as solvent lead to an increase in the extraction efficiency of anthocyanins in agreement with Kazan et al. (2016). Specifically, for pelargonidin based anthocyanins, the highest yield was obtained under these extraction conditions (Table 1). We observed no significant difference ($p < 0.05$) between extractions performed with EtOH at 50 °C and acidified EtOH at 50 °C for anthocyanins and loganic acid.

3.1. Supercritical carbon dioxide extraction of iridoids

We first investigated the various extraction conditions of iridoids. To estimate the amounts of loganic acid and loganin, conventional solvent extractions of haskap berries were performed at 80 °C in EtOH. The extractions yielded 4.35 mg/g DW loganic acid and 2.12 mg/g DW loganin. The highest yield of loganic acid (5.13 mg/g DW) was obtained with H_2O and of loganin (3.10 mg/g DW) with acidified EtOH, both at 80 °C. By using acidic ethanol and adjusting the temperature to 50 °C, an increase in the yield of loganin and a decrease in the yield of loganic acid was observed (Table 1). Other scientific studies reported 35.22–182.28 mg/100 g FW for loganic acid when extracted with acidified methanol, from various cultivars of Honeysuckle berries (Kucharska et al., 2017). Thus, the haskap samples accumulated high amounts of iridoids.

So far, only few studies on SFEs of iridoids have been published. Wang et al. (2014) reported the scCO$_2$ extraction of geniposidic acid from plantain seeds, where the highest yield was obtained at 80 °C, 20 MPa and 8 vol% of EtOH. Furthermore, picroside I from *Picrorhiza kurroa* was extracted at 40 °C, 30 MPa and 10 vol% MeOH (Patil et al., 2012). These two studies indicate that the combination of high pressure and temperature with moderate amounts of polar modifier leads to high extraction efficiency of iridoids.

Several experiments were carried out to evaluate the selective extraction of loganic acid and loganin from haskap berry powder. First, all scCO$_2$ parameters were kept constant and the ethanol concentration was varied in a range from 0 to 20 vol% at 80 °C and at a pressure of 30 MPa (Fig. 1).

We observed that the highest yields of loganin (0.99 mg/g DW) and loganic acid (0.81 mg/g DW) during SFE were obtained with 20 vol% of ethanol without the extraction of the target anthocyanins (Table 2), showing that scCO$_2$, especially in the absence of modifiers, is capable of extracting only a small portion of the target iridoids. Hence, the increase

of alcoholic modifier content led to higher concentrations of extracted iridoids (see section 3.2). Up to a modifier concentration of 1 vol% neither loganic acid nor loganin were detected, and at 5 vol% of ethanol a total amount of 9 μg/g DW loganin was extracted.

3.2. Dynamic streamlined extraction of iridoids, anthocyanins and lipids

The focus of these studies was to develop a dynamic streamlined extraction process with supercritical CO$_2$ on laboratory scale, combined with ethanol in pure as well as acidified form. The extraction was performed at 50 °C and 30 MPa. In order to get an insight into the extraction behaviour of the target compounds, fractions were collected every 30 min throughout the entire process and subsequently analyzed by HPLC. The collected fractions are depicted in Fig. 2.

Iridoids and anthocyanins were not present in the fractions obtained from the haskap berry powder with scCO$_2$ and 1 vol% EtOH. Lipids were, however, extracted under these conditions. Herein, the first supercritical CO$_2$ extraction of fatty acids from the fruits of *Lonicera caerulea* L. was performed. Apart from that, the extraction of fatty acids under supercritical conditions from rice bran was established (Garcia et al., 1996). The presence of fatty acids in the berries of haskap, in particular palmitic acid, oleic acid, stearic acid and palmitoleic acid was reported (Svarcova et al., 2007). Our GC-MS results confirm these findings as we detected these acids after derivatization in form of their methyl esters (FAME). The FAMEs of palmitic acid as well as the unsaturated palmitoleic acid, oleic acid and linoleic acid were detected by GC-MS in our research (ESI Table S5, ESI Figs. S9-S12). A 30 min extraction process with 1 vol% of ethanol was sufficient for the extraction of the respective fatty acids. This initial and selective separation step for lipophilic compounds provides a considerable advantage for the purity of the successively extracted secondary metabolites, if they are intended as food additives; in fact, tedious separation steps of lipophilic compounds, such as waxes, via freezing can thus be omitted.

There is an apparent correlation between the concentration of the co-solvent and the extracted amount of the iridoids (Fig. 3). The yield of loganic acid increased from 0.115 to 0.375 mg/g DW and of loganin from 0.037 to 0.061 mg/g DW, as the vol% of EtOH increased from 10 to 20%. The extraction with lower amounts of EtOH resulted in only iridoids (Table 3), as was visually indicated by the yellowish colour of the extracts (Fig. 2). Simultaneous extraction of the target iridoids and anthocyanins was feasible with 20 vol% EtOH at 50 °C, as 44.6 μg/g DW cyanidin after acidic hydrolysis were observed. However, no pelargonidin or peonidin were detected under the same conditions. A decrease of the temperature from 80 °C to 50 °C led to an increase in the extraction yield of anthocyanins with 20 vol% of EtOH (Table 1). The highest yield, during the supercritical extraction, for both iridoids (loganic acid and loganin) and anthocyanins (cyanidin and peonidin type) was obtained at a modifier concentration of 50 vol% (Table 3). Overall, the amount of pelargonidin-based anthocyanidins was below the limit of quantification during the dynamic streamlined SFE. A higher amount of iridoids than anthocyanins was extracted with 50 vol% EtOH. However, according to the conventional extractions at 50 °C in EtOH and acidic EtOH for the cultivar Aurora higher contents of the investigated anthocyanins compared to the iridoids were observed (Table 1).

Eventually, in the concluding step of the streamlined process (4 fractions), conventional extraction with acidified EtOH was performed. The overall highest yield of iridoids and anthocyanins was detected in the first fraction (F15), which is also visually indicated by the dark reddish colour of the collected extract, mainly attributed to its enrichment in anthocyanin glycosides (Fig. 2). This fraction contained 47% of loganic acid, 51% of loganin, 69% of cyanidin, 67% of peonidin and 100% of pelargonidin of the overall dynamic streamlined extraction yield. This implies that acidified EtOH assists the fast extraction of those compounds. This assumption is additionally supported by the observed gradual decrease of anthocyanins during the concluding step of the extraction. Unlike the supercritical portion of the extraction process,

where the amounts of secondary metabolites are virtually equally distributed in the collected fractions. Thus, it is assumed that $scCO_2$ significantly inhibits the extraction force for iridoids and anthocyanins from haskap berries.

The presented dynamic streamlined extraction process consumes altogether 314 mL of ethanol for 1 g haskap berry powder which is considerably higher than the 50 mL/g used in the conventional process for the extraction of anthocyanins and iridoids. However, it offers the advantage of a simple and fully automatable process in a closed system, in which only two solvents are required that are both innocuous and widely used in the food industry. Furthermore, automated fractioning by increasing polarity is possible by varying the ratio of the two, without the use of undesired organic solvents. In haskap, this enables the separation of the lipid fraction and provides two extracts, one containing only iridoids and a mixed anthocyanin/iridoid extract, which can be both exploited as secondary products. Despite the higher general ethanol consumption, the extracts are not as diluted as one would expect, because the majority of the compounds are concentrated in a few fractions. In higher diluted fractions, the ethanol can be easily evaporated (Souza et al., 2020). Overall, 5.39 mg/g loganic acid, 0.99 mg/g loganin, 9.0 mg/g cyanidin, 0.52 mg/g peonidin and 0.111 mg/g pelargonidin were obtained from the dynamic streamlined extraction of the dried berries (Table 3). Thus, the yields of loganin, loganic acid, cyanidin and peonidin are not significantly different ($p < 0.05$) compared to the conventional extraction with EtOH at 50 °C.

4. Conclusions

In the presented study, a dynamic streamlined extraction process using supercritical carbon dioxide for iridoids and anthocyanins with initial separation of lipids was developed. Furthermore, we report the first SFE of iridoids and fatty acids from haskap berries. Loganin and loganic acid were for the first time extracted under supercritical conditions. Partial extraction of loganin and loganic acid was achieved and subsequently, simultaneous extraction of the target anthocyanins (cyanidin, peonidin and pelargonidin based types), by adjusting the concentration of the modifier solvent (10–50 vol%). Additionally, several fatty acid methyl esters were separated at low concentrations of alcoholic modifier (1 vol% EtOH) prior to the extraction of the secondary metabolites. This process provides an important contribution to the fractional extraction of different substance classes from haskap berries. In comparison to the conventional extraction the suggested streamlined process provided comparable yields.

The streamlined extraction process can be considered as a base concept for the partial extraction of high valuable secondary metabolites and can be adapted for other source materials, e.g. agricultural waste or by-products in the food industry. Hence, the presented developed process can be considered for a range of products, which have reached the end of their life cycle and therefore, it supports the idea of end-of-life product biocascading. Ultimately, a promising and environmentally benign approach for obtaining different high-value natural product classes with a broad applicability (e.g. food colourants) has been developed.

Author contribution statement

HH, CHG and KS conceived the research. ASM, CK, KS and HH designed the experiments. CHG and MMP provided plant material. ASM and CK performed the experiments. ASM and CK drafted the manuscript. All authors analysed the data and approved the manuscript.

Declaration of competing interest

The authors declare that they have no known competing financial interests or personal relationships that could have appeared to influence the work reported in this paper.

Appendix A. Supplementary data

Supplementary data to this article can be found online at https://doi.org/10.1016/j.lwt.2020.110633.

References

Caprioli, G., Iannarelli, R., Innocenti, M., Bellumori, M., Fiorini, D., Sagratini, G., & Bramucci, M. (2016). Blue honeysuckle fruit (*Lonicera caerulea* L.) from eastern Russia: Phenolic composition, nutritional value and biological activities of its polar extracts. *Food and Function, 7*(4), 1892–1903.

Celli, G. B., Ghanem, A., & Brooks, M. S. (2014). Haskap berries (*Lonicera caerulea* L.)-A critical review of antioxidant capacity and health-related studies for potential value-added products. *Food and Bioprocess Technology, 7*, 1541–1554.

Chaovanalikit, A., Thompson, M. M., & Wrolstad, R. E. (2004). Characterization and quantification of anthocyanins and polyphenolics in blue honeysuckle (*Lonicera caerulea* L.). *Journal of Agricultural and Food Chemistry, 52*(4), 848–852.

Commission, E. (2018). Commission implementing regulation (EU) 2018/1991 of 13 december 2018 authorising the placing on the market of berries of *Lonicera caerulea* L. As a traditional food from a third country under regulation (EU) 2015/2283 of the European parliament and of the council and amending commission implementing regulation (EU) 2017/2470 (text with EEA relevance.). *OJ L320, 61*, 22–24. http://data.europa.eu/eli/reg_impl/2018/1991/oj.

Finley, J. W., & Shahidi, F. (2001). *The chemistry, processing, and health benefits of highly unsaturated fatty acids: An overview. ACS publications*.

Garcia, A., De Lucas, A., Rincón, J., Alvarez, A., Gracia, I., & García, M. (1996). Supercritical carbon dioxide extraction of fatty and waxy material from rice bran. *Journal of the American Oil Chemists' Society, 73*(9), 1127–1131.

Gołba, M., Sokół-Łętowska, A., & Kucharska, A. Z. (2020). Health properties and composition of honeysuckle berry *Lonicera caerulea* L. An update on recent studies. *Molecules, 25*(3), 749.

Hamid, I. A. A., Ismail, N., & Rahman, N. A. (2018). Supercritical carbon dioxide extraction of selected herbal leaves: An overview. *Materials Science and Engineering, 358*, 0102037.

Jiao, G., & Kermanshahi pour, A. (2018). Extraction of anthocyanins from haskap berry pulp using supercritical carbon dioxide: Influence of co-solvent composition and pretreatment. *LWT-Food Science and Technology, 98*, 237–244.

Jurikova, T., Rop, O., Mlcek, J., Sochor, J., Balla, S., Szekeres, L., & Kizek, R. (2011). Phenolic profile of edible honeysuckle berries (genus lonicera) and their biological effects. *Molecules, 17*(1), 61–79.

Jurikova, T., Sochor, J., Rop, O., Mlček, J., Balla, Š., Szekeres, L., & Kizek, R. (2012). Evaluation of polyphenolic profile and nutritional value of non-traditional fruit species in the Czech Republic—a comparative study. *Molecules, 17*(8), 8968–8981.

Kaczmarska, E., Gawroński, J., Dyduch-Sieminska, M., Najda, A., Marecki, W., & Żebrowska, J. (2015). Genetic diversity and chemical characterization of selected Polish and Russian cultivars and clones of blue honeysuckle (*Lonicera caerulea*). *Turkish Journal of Agriculture and Forestry, 39*, 394–402.

Kazan, A., Sevimli-Gur, C., Yesil-Celiktas, O., & Dunford, N. T. (2016). Investigating anthocyanin contents and in vitro tumor suppression properties of blueberry extracts prepared by various processes. *European Food Research and Technology, 242*(5), 693–701.

Kerbstadt, S., Eliasson, L., Mustafa, A., & Ahrné, L. (2015). Effect of novel drying techniques on the extraction of anthocyanins from bilberry press cake using supercritical carbon dioxide. *Innovative Food Science & Emerging Technologies, 29*, 209–214.

Kucharska, A. Z., & Fecka, I. (2016). Identification of iridoids in edible honeysuckle berries (*Lonicera caerulea* L. *Var. kamtschatica* sevast.) by UPLC-ESI-qTOF-MS/MS. *Molecules, 21*(9).

Kucharska, A. Z., Sokol-Letowska, A., Oszmianski, J., Piorecki, N., & Fecka, I. (2017). Iridoids, phenolic compounds and antioxidant activity of edible honeysuckle berries (*Lonicera caerulea var. kamtschatica* sevast.). *Molecules, 22*(3).

Lima, Á. S., Soares, C. M. F., Paltram, R., Halbwirth, H., & Bica, K. (2017). Extraction and consecutive purification of anthocyanins from grape pomace using ionic liquid solutions. *Fluid Phase Equilibria, 451*, 68–78.

Liu, L., Li, Y., Feng, R., & Sun, C. (2010). Direct ultrasound-assisted methylation of fatty acids in serum for free fatty acid determinations. *Canadian Journal of Chemistry, 88*(9), 898–905.

Maran, J. P., Priya, B., & Manikandan, S. (2014). Modeling and optimization of supercritical fluid extraction of anthocyanin and phenolic compounds from Syzygium cumini fruit pulp. *Journal of Food Science & Technology, 51*(9), 1938–1946.

Müller, L. G., de Andrade Salles, L., Sakamoto, S., Stein, A. C., Cargnin, S. T., Cassel, E., & von Posera, G. L. (2012). Effect of Storage time and conditions on the diene valepotriates content of the extract of *Valeriana glechomifolia* obtained by supercritical carbon dioxide. *Phytochemical Analysis*, 222–227.

Oszmiański, J., Wojdyło, A., & Lachowicz, S. (2016). Effect of dried powder preparation process on polyphenolic content and antioxidant activity of blue honeysuckle berries (*Lonicera caerulea* L. *var. kamtschatica*). *LWT-Food Science and Technology, 67,* 214–222.

Palíková, I., Heinrich, J., Bednář, P., Marhol, P., Kren, V., Cvak, L., & Kolář, M. (2008). Constituents and antimicrobial properties of blue honeysuckle: A novel source for phenolic antioxidants. *Journal of Agricultural and Food Chemistry, 56*(24), 11883–11889.

Patil, A. A., Sachin, B. S., Shinde, D. B., & Wakte, P. S. (2012). Supercritical CO_2 assisted extraction and LC–MS identification of picroside I and picroside II from Picrorhiza kurroa. Phytochemical analysis. *24,* 97–104.

Senica, M., Bavec, M., Stampar, F., & Mikulic-Petkovsek, M. (2018). Blue honeysuckle (*Lonicera caerulea* subsp. *edulis* (Turcz. ex Herder) Hulten.) berries and changes in their ingredients across different locations. *Journal of the Science of Food and Agriculture, 98*(9), 3333–3342.

Souza, M. C., Santos, P. M., Sumere, B. R., Silva, L. C., Cunha, D. T., Martínez, J., Barbero, G. F., & Rostagno, M. A. (2020). Isolation of gallic acid, caffeine and flavonols from black tea by on-line coupling of pressurized liquid extraction with an adsorbent for the production of functional bakery products. *LWT-Food Science and Technology, 117,* 108661.

Suomi, J., Sirén, H., Hartonen, K., & Riekkola, M. (2000). Extraction of iridoid glycosides and their determination by micellar electrokinetic capillary chromatography. *Journal of Chromatography A, 868*(1), 73–83.

Svarcova, I., Heinrich, J., & Valentovaa, K. (2007). Berry fruits as a source of biologically active compounds: The case of *Lonicera caerulea*. *biomedical Papers of the medical Faculty of palacky University in olomouc. 151*(2).

Tundis, R., Loizzo, M. R., Menichini, F., Statti, G. A., & Menichini, F. (2008). Biological and pharmacological activities of iridoids: Recent developments. *Mini Reviews in Medicinal Chemistry, 8*(4), 399–420.

Udin, M. S., Sarker, M. Z. I., Ferdorsh, S., Akanda, M. J. H., Easmin, M. S., Shamsudin, S. H. B., & Yunus, K. B. (2015). Phytosterols and their extraction from variousplant matrices using supercritical carbon dioxide: A review. *Journal of the Science of Food and Agriculture, 95,* 1385–1394.

Vatai, T., Škerget, M., & Knez, Ž. (2009). Extraction of phenolic compounds from elder berry and different grape marc varieties using organic solvents and/or supercritical carbon dioxide. *Journal of Food Engineering, 90*(2), 246–254.

Wang, J. D., Liu, B., & Chang, Y. L. (2014). Optimization of supercritical fluid extraction of geniposidic acid from plantain seeds using response surface methodology. *Green Chemistry Letters and Reviews, 7*(3), 309–316.

Woźniak, Ł., Marszałek, K., & Skąpska, S. (2016). Extraction of phenolic compounds from sour cherry pomace with supercritical carbon dioxide: Impact of process parameters on the composition and antioxidant properties of extracts. *Separation Science and Technology, 51*(9), 1472–1479.

4. Extraction of cannabinoids *via* a combined IL-scCO$_2$ technology.

4.1 Overview

During the last years, ILs have attracted remarkable attention as alternative media for the extraction of biomass, due to their high dissolution properties related to lignocellulosic biomass, high thermal stability, broad liquid range, among others.[446]

In order to overcome the limitations of the already existing extraction techniques for cannabinoids, volatile apolar scCO$_2$ and non-volatile polar ILs could be combined. It is noteworthy mentioning that scCO$_2$ is highly soluble in ILs, but ILs cannot dissolve in scCO$_2$, resulting in the facile penetration of scCO$_2$ in ILs and the subsequent extraction of cannabinoids. Additionally, as cannabinoids are soluble in scCO$_2$, they can be easily recovered from the extract in their solid, pure and solventless form.[300]

In the present chapter, a first-time and newly developed process will be presented which comprises an IL -based pre-treatment and subsequent scCO$_2$-based extraction with the objective of extracting six main cannabinoids from *Cannabis sativa* L. and of avoiding drawbacks which are typical of traditional solvent-extraction techniques (Figure 38), for instance filtration of the raw material, evaporation of solvents and post-processing of the recovered extract, to name a few. After fine-tuning of the parameters related to the IL-assisted pre-treatment and the SFE, along with the investigation of several ILs, the optimized final process was obtained.
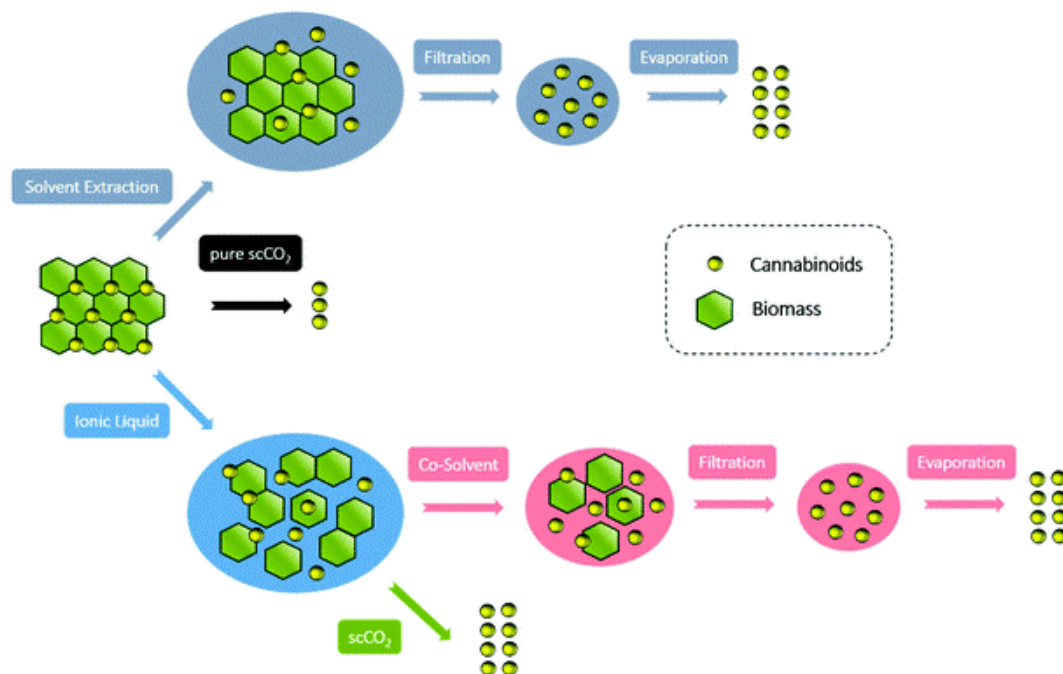
Figure 38. Comparison of cannabinoid extraction techniques, involving work up steps and cannabinoid yields.[447]

The following manuscripts will be presented in this chapter:

- ❖ Sainz Martinez, A.; Lanaridi, O.; Stagel, K.; Halbwirth, H.; Schnürch, M.; Bica-Schröder, K. Extraction techniques for bioactive compounds of cannabis. *Nat. Prod. Rep.,* **2023**, *40*, 676-717.

The first and second authors equally contributed to the manuscript in terms of writing the original draft, editing and reviewing the manuscript.

- ❖ Kornpointner, C.; Sainz Martinez, A.; Schnürch, M.; Halbwirth, H.; Bica-Schröder, K. Combined ionic liquid and supercritical carbon dioxide based dynamic extraction of six cannabinoids from *Cannabis sativa* L. *Green Chem.*, **2021**, *23*, 10079-10089.

The first and second authors equally contributed to the manuscript in terms of research conception, planning, designing and performing the experimental work and also by writing the original draft, editing and reviewing the manuscript.

4.2 Ionic liquids for biomass processing

Biomass is organic matter, i.e., wood, crops, seaweed, animal waste, that can be used for the production of energy.[448] It is a renewable energy source that has drawn considerable attention in recent years.[449] Therefore, there have been efforts invested in the investigation of different types of biomass with the objective of transforming them to valuable outputs (chemicals or energy). The major biomass constituents are quite diverse, depending on the biomass source. Agarose, cellulose, chitin, dextrin, hemicellulose, lignin, pectin, silk fibroin, starch and wool keratin are the major constituents of the different natural biomass.

Dry plant matter is classified as lignocellulosic biomass, which consists of cellulose, hemicellulose (carbohydrate polymers) and lignin (aromatic polymer). The lignocellulosic structure of a plant cell is depicted in Figure 39, followed by the structure of the three fundamental constituents in Figure 40.[450]
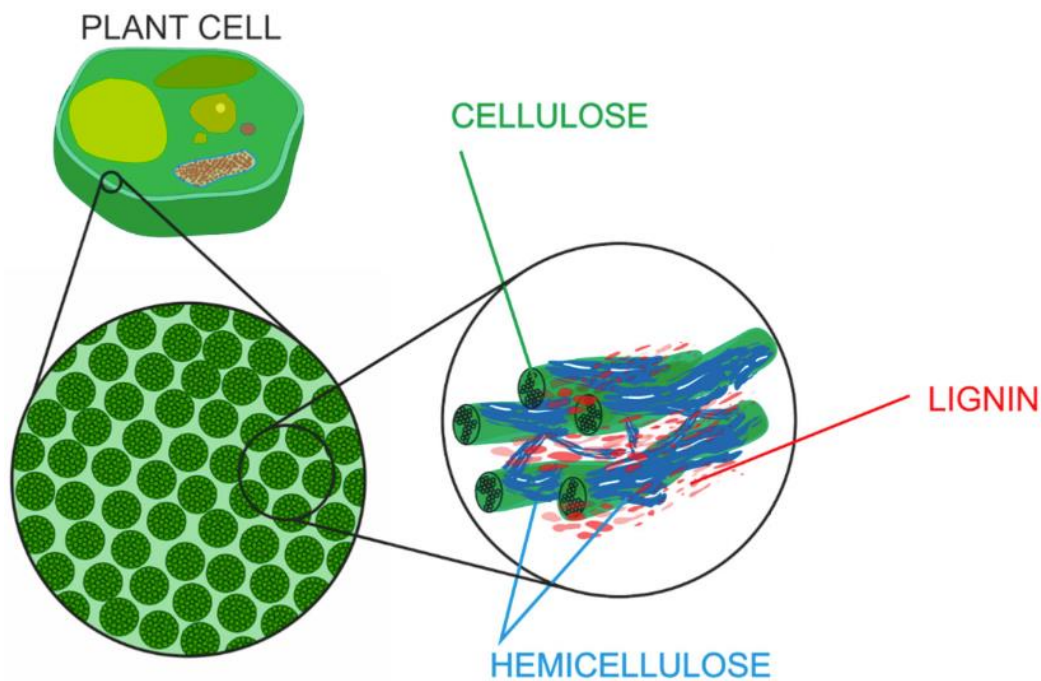
Figure 39. Structure of lignocellulosic biomass.[451]
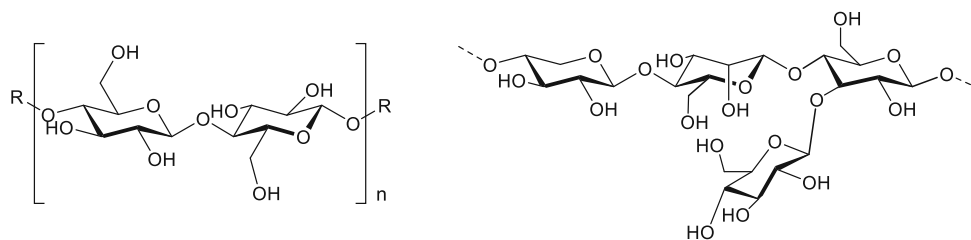
Cellulose

Hemicellulose
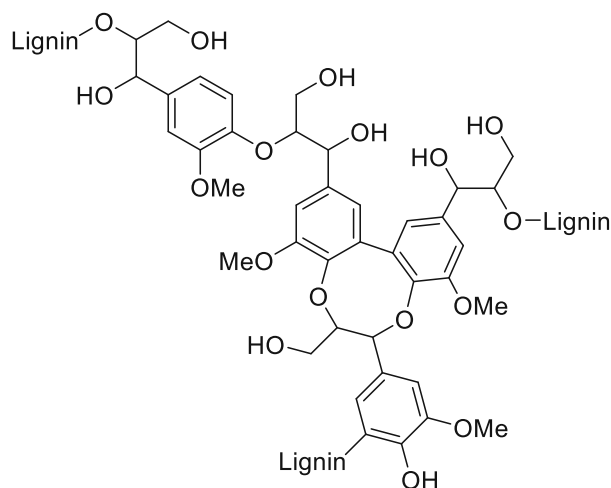
Lignin

Figure 40. The fundamental constituents of lignocellulosic biomass.

In order to facilitate the extraction of those bioactive compounds, ILs were considered as optimal candidates, due to their physicochemical and biomass dissolution properties. Initially, imidazolium-based ILs have been employed for biomass dissolution, specifically the dissolution of pure cellulose.[143] Over time, this field has progressed and currently a wide variety of ILs were able to dissolve cellulose.[452-455] In addition, ILs can also dissolve hemicellulose[456], lignin[457] and raw lignocellulosic biomass[144],[458]. ILs serve as a novel, versatile alternatives to process biomass compared to volatile organic solvents, because they do not produce emission and the degradation of the regenerated biopolymers is insignificant.[260, 459, 460]

Traditional organic solvents and water have difficulties in dissolving cellulose, due to the stiff molecules and close chain packing via several intermolecular and intramolecular hydrogen bonds. Several solvent systems have been employed to dissolve cellulose; however, they are toxic, expensive, require harsh conditions and are hard to recover.[461],[462]

Several dialkylimidazolium ILs have been investigated in the dissolution of cellulose. The IL [C$_4$mim]Cl was able to dissolve cellulose. By increasing the alkyl chain of the dialkylimidazolium ILs, the solubility of the cellulose decreased. Regarding the anion selection, Cl$^-$, Br$^-$ (bromide anion) and [SCN]$^-$

(thiocyanate anion) could efficiently dissolve cellulose. Nonetheless, [BF$_4$]$^-$ or [PF$_6$]$^-$, which are non-coordinating anions, were not efficient.[143] Additionally, the ILs [C$_4$mpy]Cl (1-butyl-3-methylpyridinium chloride), [amim]Cl (1-allyl-3-methylimidazolium chloride), and BDTACl (benzyldimethyl(tetradecyl)ammonium chloride) was also found to be useful for cellulose as non-derivatizing solvent.[452],[463] An IL containing an hydroxyl group, namely [C$_2$OHmim]Cl (1-(2-hydroxyethyl)-3-methylimidazolium chloride), was proven to be achieve the dissolution of cellulose. It is possible that the presence of the hydroxyl group in the side chain of the cation, allow the formation of hydrogen bonds with cellulose, affecting positively the dissolution process.[464] An acetate based-IL, [C$_2$mim][OAc], which is a less toxic and corrosive IL, achieved higher dissolution of cellulose.[454],[465] An IL containing formate as anion, [amim][HCOO] (1-llyl-3-methyl imidazole formate), displayed outstanding solubility for cellulose. Compared to chloride salts, this IL has stronger hydrogen bond basicity, which allows the dissolution of cellulose at lower temperatures.[466] A number of ILs bearing an alkylimidazolium core with anions, such as [MeSO$_3$]$^-$ (methanesulfonate anion), [MeOSO$_3$]$^-$ (methyl sulfate anion), [EtOSO$_3$]$^-$ (ethyl sulfate anion) and [(MeO)$_2$PO$_2$]$^-$ (dimethyl phosphate anion) could also dissolve cellulose under mild conditions.[455] A series of ammonium based ILs containing formate and acetate were also capable of dissolving cellulose.[467],[468] Several ILs which dissolve cellulose are illustrated in Figure 41.

X = OAc, MeSO$_3$, MeSO$_4$, EtSO$_4$, (MeO)$_2$PO$_2$ X = Cl

X = Cl   X = Cl

X = OAc, Cl, Br, SCN   X = HCOO, OAc

X = Cl, HCOO   X = OAc
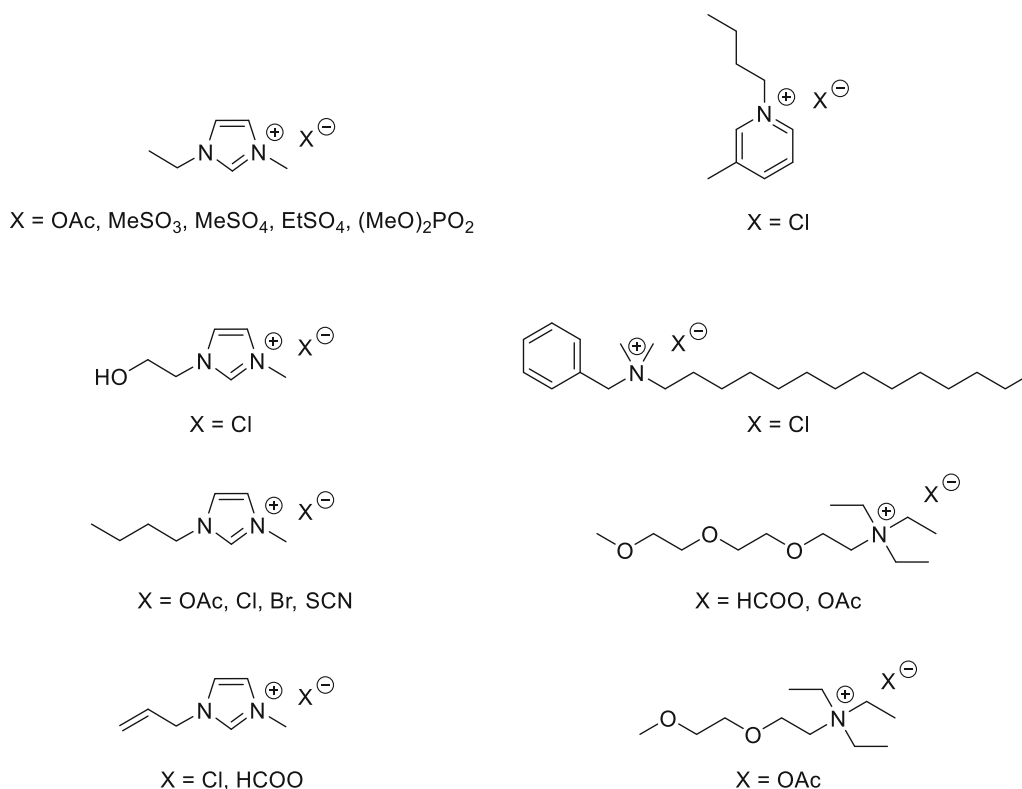
Figure 41. Ionic liquids capable of dissolving cellulose.

In summary, both the cation and the anion may have an influence in the dissolution of cellulose. Overall, the anions influence seems to be more predominant and better comprehended than the cations effect. The key factor for the dissolution of cellulose is the hydrogen bond accepting ability of the anions. It was observed that by increasing the hydrogen bond acceptability of the anion the solubility also increases almost linearly. The hydrogens of the hydroxyl groups present in cellulose interact with the anion (e.g. Cl^-, OAc^- and $[HCOO]^-$).[143],[463] Between these anions, the higher basicity of acetate and formate promotes the disruption process of inter- and intramolecular hydrogen bonding present in the cellulose.[454],[466] With regard to the cations of the ILs, by increasing the alkyl chain length on imidazolium based ILs, and thereby increasing the size of the cation, the solubility of cellulose decreases.[143] In addition, it was found that $[amim]^+$ (1-allyl-3-methylimidazolium cation) has higher dissolution than $[C_4mim]^+$, because of its allylic nature and smaller size.[463]

Lignin is one of the main constituents of the lignocellulosic structure and it is an amorphous polymer that comprises methoxylated phenylpropane structures and aromatic groups. It plays a vital role in the lignocellulosic structure, because functions as a resin that holds the whole structure together. It is found in between the cellulose and hemicellulose and it fills the spaces by forming a covalent bond with hemicellulose.[469] Several imidazolium-based ILs have been able to dissolve lignin and Kraft lignin (Indulin AT) (Figure 42).[457],[470],[471]

X = MeSO$_4$

X = BF$_4$

X = Cl, OAc, CH$_3$COOH

X = Cl

X = Cl, Br, MeSO$_4$, CF$_3$SO$_3$

X = Cl
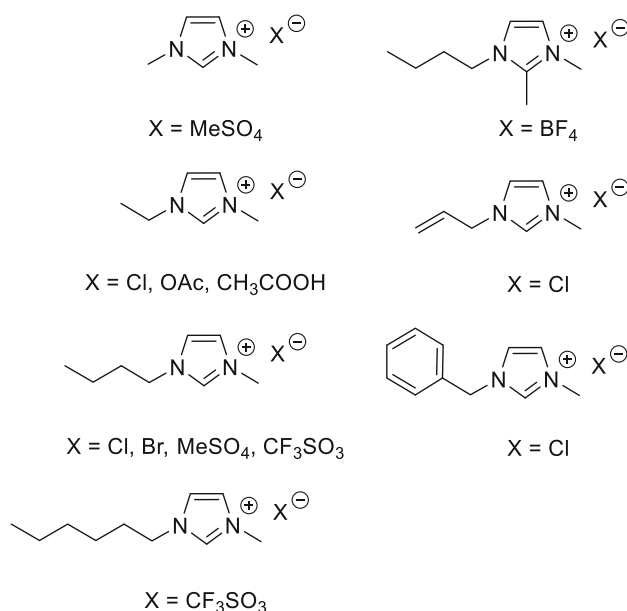
X = CF$_3$SO$_3$

Figure 42. Ionic liquids capable of dissolving lignin.

Between these ILs $[C_1mim][MeSO_4]$ (1,3-dimethylimidazolium methyl sulfate) and $[C_4mim][CF_3SO_3]$ (1-butyl-3-methylimidazolium triflate) were the ones that achieved the highest dissolution.[470] Ionic liquids with slightly lower dissolution capabilities were $[C_4mim][MeSO_4]$ (1-butyl-3-methylimidazolium

methyl sulfate), [C$_2$mim][OAc], and [amim]Cl.[457],[471] The ILs [bzmim]Cl (1-benzyl-3-methylimidazolium chloride) and [C$_4$mim]Cl had lowest solubility.[470] Between the [C$_4$mim]$^+$ (1-butyl-3-methylimidazolium cation) containing ILs, the anion dissolution efficiency related to lignin was as follows: [CF$_3$SO$_3$]$^-$ > [MeSO$_4$]$^-$ >Cl$^-$ ≈ Br$^-$. The anions that exhibited lowest dissolution capability or no dissolution at all were [BF$_4$]$^-$ and [PF$_6$]$^-$.[457],[470]

Hemicellulose is a natural polysaccharide which is also present in the lignocellulosic structure. It contains different sugar moieties, such as glucose, xylose, mannose and galactose among others.[472] Hemicellulose has not been as extensively investigated as cellulose and its dissolution mechanism is unknown. However, some imidazolium-based ILs, such as [C$_2$mim]OAc, [C$_2$mim]Cl and [C$_4$mim]Cl are able to dissolve xylan, which is the major component of hemicellulose.[456],[471],[473]

REVIEW

Check for updates

Extraction techniques for bioactive compounds of cannabis

Aitor Sainz Martinez, [ID] †[a] Olga Lanaridi, [ID] †[a] Kristof Stagel,[a] Heidi Halbwirth, [ID] [b] Michael Schnürch [ID] [a] and Katharina Bica-Schröder [ID] *[a]

Historically, cannabis has always constituted a component of the civilized world; archaeological discoveries indicate that it is one of the oldest crops, while, up until the 19th century, cannabis fibers were extensively used in a variety of applications, and its seeds comprised a part of human and livestock nutrition. Additional evidence supports its exploitation for medicinal purposes in the ancient world. The cultivation of cannabis gradually declined as hemp fibers gave way to synthetic fibers, while the intoxicating ability of THC eventually overshadowed the extensive potential of cannabis. Nevertheless, the proven value of certain non-intoxicating cannabinoids, such as CBD and CBN, has recently given rise to an entire market which promotes cannabis-based products. An increase in the research for recovery and exploitation of beneficial cannabinoids has also been observed, with more than 10 000 peer-reviewed research articles published annually. In the present review, a brief overview of the history of cannabis is given. A look into the classification approaches of cannabis plants/species as well as the associated nomenclature is provided, followed by a description of their chemical characteristics and their medically valuable components. The application areas could not be absent from the present review. Still, the main focus of the review is the discussion of work conducted in the field of extraction of valuable bioactive compounds from cannabis. We conclude with a summary of the current status and outlook on the topics that future research should address.

[a]Institute of Applied Synthetic Chemistry, TU Wien, Getreidemarkt 9/163, Vienna, Austria. E-mail: katharina.schroeder@tuwien.ac.at

[b]Institute of Chemical, Environmental and Bioscience Engineering, TU Wien, Getreidemarkt 9/166, Vienna, Austria

† Both authors have contributed equally to the manuscript.

1. Introduction

1.1. History of cannabis

Cannabis sativa is an annual herbaceous flowering plant native to eastern Asia; nevertheless, its sophisticated uses and wide range of applications lead to its global distribution.[1] Humans across different eras have cultivated it for a variety of applications, such as nutrition, recreation, generation of seed oil and fiber for industrial purposes, religious and spiritual practices and medicine.

Cannabis sativa existed prior to the development of agriculture, which began about 13 000 years ago, therefore, it is assumed to have been one of the most critical crops for the development of civilization.[2] Hemp strands discovered in clay pots from tombs dating back to 10 000 BC constitute the earliest archaeological proof of human use of the plant, thus, indicating that *Cannabis sativa* is one of the oldest crops on earth.[3,4] Outlining the ancient history of *Cannabis sativa* in its entirety is almost impossible since its utilization and cultivation dates before the time of the earliest discovered written texts.

Cannabis sativa was predominantly valuable as a fiber source for the most part of the documented history. It was considered to be one of the most important crops up until the 19th century, because of its useful properties, precisely its rot-resistance capabilities, strength and durability[5] and it was utilized for several applications, such as production of coarse fabrics and paper and manufacturing of components used in the maritime sector. It is noteworthy that traditional planting, harvesting, and processing of hemp for fiber were exhausting processes, mostly performed by sentenced criminals and slaves. Principally, the abolition of slavery and, additionally, the industrial revolution, the manufacturing of synthetic fibers and its prohibition due to its intoxicating potency lead to the downfall of the hemp fiber. Eventually, hemp cultivation was forbidden in various parts of the world; however, in the majority of the Soviet Union, in most of Eastern Europe, and in Asia, specifically in China, it was authorized.[6]

In the 1990s, Western countries, specifically Europe and the British Commonwealth, started developing an increasing interest in the re-launch of the hemp sector driven by purely economic motives. Nowadays, around 36 countries produce

Aitor Sainz Martinez received his Bachelor's degree in chemistry in 2014 and his Master's degree in synthetic and industrial chemistry in 2015 at the University of the Basque Country, Spain. Then, he was a PhD student under the supervision of Prof. Katharina Schröder in the Laboratory of Sustainable Organic Synthesis and Catalysis at TU Wien. He is about to finalize his PhD degree; meanwhile he is working as a Product and Validation Specialist at Intervet GesmbH (MSD) in the animal health field.

Olga Lanaridi received her BSc and MSc degrees in Chemistry from the National and Kapodistrian University of Athens, Greece. After her studies, she was employed as a chemist in Austria. In 2021 she received her PhD in the research group of Prof. Schröder at TU Wien. Her research focused on alternative approaches for the recovery of precious metals from secondary raw materials with the aid of ionic liquids and deep eutectic solvents. She is currently employed as a Post-doc student at the University of Vienna.

Kristof Stagel finished his BSc studies at the University of Pannonia, Veszprem, Hungary, in 2017. Thereafter, he studied as a pharmaceutical engineer at the Budapest University of Technology. He joined the Schröder research group as a PhD candidate in January 2020. His research mainly focuses on the continuous synthesis of hydrophobic ionic liquids and their catalytic application, and on continuous carbon dioxide valorization.

Heidi Halbwirth obtained her diploma and PhD degree at TU Wien in Biochemistry and Food Chemistry. After a postdoctoral stay in the group of Prof. Forkmann at TU München, she returned to TU Wien and started her independent scientific career in Phytochemistry and Plant Biochemistry. In 2016, she was appointed as Assistant Professor at the Institute of Chemical, Environmental and Bioscience Engineering, TU Wien where she became Associate Professor in 2018. Her main research interests are secondary metabolism in plants, structure–function relationships of enzymes, and the valorization of bioactive compounds from natural resources.

remarkable amounts of hemp, while China still holds its place as the largest producer of hemp on a global scale.[6]

The discovery of cannabis seeds in Chinese tombs dates back to over 4500 years.[7] They have been used for human consumption as nourishment and for livestock for at least three millennia.[8] Even though there is not much evidence from ancient times in Europe, traditional European recipes, including hempseeds as ingredients, support the assumption that these seeds, at least to a lesser degree, were utilized in human nutrition for centuries[9] and were generally consumed by the underprivileged. Hempseed oil was also used as lighting oil up until the commencement of the 19th century, due to its lower cost compared to whale oil.[6]

The 19th and the beginning of the 20th century were the golden ages of hemp cultivation; nevertheless, the economic importance of hemp seeds was minor for the major part of history and by the mid-20th century it became insignificant. During the second half of the 20th century, hemp seeds were usually used as animal foodstuff and only occasionally for human consumption.[6]

Regarding the intoxicating properties of cannabis, evidence has been found that it was used for shamanistic rituals in ancient China prior to the Han Dynasty, during which its medicinal properties were first documented in a written format.[10–12] Cannabis remains (leaves and bracts, which have the highest THC content) along with utensils discovered in the 2500 years-old Yanghai tombs, located in China, suggest that the intoxicating effects of cannabis may have been known.[13] In southern Asia, cannabis usage was established for medicinal purposes and religious events.[14,15] In other major countries of the ancient world, such as Rome, the Islamic empire, Greece, India, Egypt and Assyria, cannabis was utilized as medicine.[16–18] However, access to cannabis for medicinal purposes was extremely limited during the first millennium A.D. and it seems that in Europe the species were mainly cultivated for hemp fiber.

By the late 19th century, recreational marijuana use reached Mexico and in the southern US cannabis tinctures were first listed in the American pharmacopoeia in 1850.[14,19] Between the
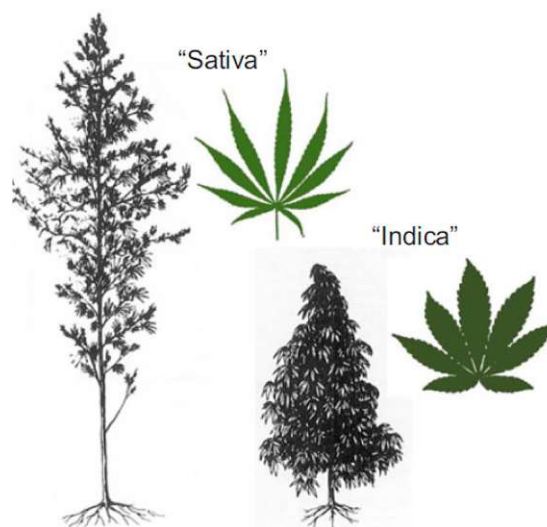
Fig. 1 Cannabis vernacular taxonomy.[6] Public domain. The Biodiversity Heritage Library considers that this work is no longer under copyright protection.[30]

mid-19th century and World War II, cannabis was largely employed in the West for its medical value, whereas its recreational use was strictly associated with low-class and underprivileged people of rural areas. In the second half of the 20th century, cannabis became highly popular as a recreational intoxicant among cultured people residing in urban areas. Eventually, the rise of hedonism and psychedelia in the late 60s and their globally perceived inextricable link with marijuana brought about an extensive global illegal market. Cannabis developed into the world's leading illicit entertainment drug during the last century.[6]

1.2. Cannabis classification and nomenclature

The naming of *Cannabis sativa* species follows the binomial nomenclature, which is a formal system of naming living organisms by assigning to them a two-part Latin name. The first part of the name establishes the genus and the second part

Michael Schnürch received his PhD degree in 2005 under the supervision of Prof. Peter Stanetty. He completed his habilitation in 2013 and in 2016 he was promoted to the position he still holds, Associate Professor for Organometallic Chemistry at TU Wien. His research interests lie in the field of synthesis of heterocyclic compounds for the manipulation of cell differentiation and GABAA receptors, C–H activation and sp³ centers, green chemistry and energy storage via organic molecules.

Katharina Schröder (born K. Bica) received her PhD 2006 from TU Wien and later joined the Queen's University Belfast/UK for a post-doctoral stay. Her research interests lie in sustainable organic chemistry, with a special focus on novel catalytic processes for asymmetric synthesis, carbon capture and utilization and waste valorization. In 2019, she received the ERC consolidator grant. Since 2021, she was appointed Full Professor in Sustainable Chemistry at TU Wien.

Table 1 Vernacular taxonomy, botanical taxonomy and characteristics of cannabis species[32]

Vernacular taxonomy	Description	Formal botanical name
"Indica"	Broad leaflets, compact habits, early maturation	*Cannabis afghanica*
"Sativa"	Narrow leaflets, slender and tall habit, late growth	*Cannabis indica*
"Ruderalis"	Varied leaflets, shorter stature, small size and wild-looking	*Cannabis sativa*

identifies the species within the genus.[20] Sativa comes from the Latin botany-related adjective *sativa* (f), *sativus* (m) and *sativum* (n), which means cultivated, and it is assigned to seed-grown domestic crops which are beneficial for human health.

The species of *Cannabis sativa* L. belong to the family of Cannabaceae with which the former family of *Celtidaceae* was recently merged.[21] The conventional botanical taxonomy of cannabis acknowledges two subspecies: *Cannabis sativa* subspecies *sativa*, and *Cannabis sativa* subspecies *indica* (Fig. 1),[22] which are regarded as disparate species by some botanists.[23,24] The terms "Sativa" and "Indica" are typically used by aficionados and medicinal users of cannabis and this vernacular taxonomy of drug-type cannabis has rapidly spread worldwide. However, we should draw attention to the fact that the terms *Cannabis sativa* and *Cannabis indica* (in italics) have no relation to the terms "Sativa" and "Indica" (in quotations marks). This difference has developed into a source of confusion in proper labelling.[25]

Cannabis species were initially classified in 1753, by the Swedish botanist Carl Linnaeus.[26,27] The initial description of the appearance of the *Cannabis sativa* flower by Linnaeus is utilized for all the plants of the cannabis genus.[27,28] The formal botanical name, *Cannabis indica*, was introduced by Lamarck and was assigned to the plants of Indian origin and to their South African and Southeast Asian descendants.[29] *Cannabis indica* has noticeable morphological differences from *Cannabis sativa*, in the flowers, leaflets, branching habitus and stalks. Additionally, *Cannabis indica* produces a strong distinctive scent which can induce intoxication when smoked.[6]

The vernacular categorization defines three terms: "Indica" as *Cannabis afghanica*, "Sativa" as *Cannabis indica*, and "Ruderalis" as *Cannabis sativa*, which is quite misleading (Table 1). The botanists McPartland and Guy suggested to align the formal botanical name with the vernacular nomenclature by matching the names *Cannabis indica* and *Cannabis sativa* with "Indica" and "Sativa", respectively, for the sake of consistency.[31,32] Nevertheless, only some researchers have taken this classification into consideration.[32–34]

The lack of a universally accepted classification system for cannabis varieties has, unfortunately, enabled the development of the vernacular classification. Consequently, the classification used by consumers of commercial cannabis can be distinct from the one assigned by botanical taxonomy.[35]

1.3. Valuable compounds present in cannabis and their medicinal merit

1.3.1. Cannabinoids. Cannabinoids are an atypical category of terpenophenolic secondary metabolites present in cannabis plants.[23,36] They are a distinctive characteristic of cannabis plants and the most valuable cannabinoids, in terms of biological activity, present in *Cannabis sativa*. Currently, more than 500 constituents in cannabis have been reported. Among them, 125 cannabinoids, 42 phenolics, 34 flavonoids, 120 terpenes and 2 alkaloids have been identified.[37]

Cannabinoids in their neutral form have a skeleton comprising 21 carbon atoms. The structures of the principal cannabinoids are depicted in Fig. 2. They have been classified in 10 different sub-categories, namely, (i) cannabidiol (CBD), (ii) cannabigerol (CBG), (iii) cannabichromene (CBC), (iv) cannabicyclol (CBL), (v) cannabielsoin (CBE), (vi) cannabinol (CBN) and cannabinodiol (CBND), (vii) cannabitriol (CBT), (viii) Δ^8-tetrahydrocannabinol (Δ^8-THC), (ix) Δ^9-tetrahydrocannabinol (Δ^9-THC) and (x) miscellaneous.[38]

Cannabinoids are mainly encountered in their carboxylated form in the living plant. Decarboxylation naturally occurs in the plant (Fig. 3); however, the storage conditions after harvesting can accelerate this process (refer to section 1.6 for details). Their production primarily takes place in the glandular hairs.[39]

Cannabinoid nomenclature is based on 2 different numbering systems, meaning that the same compound can
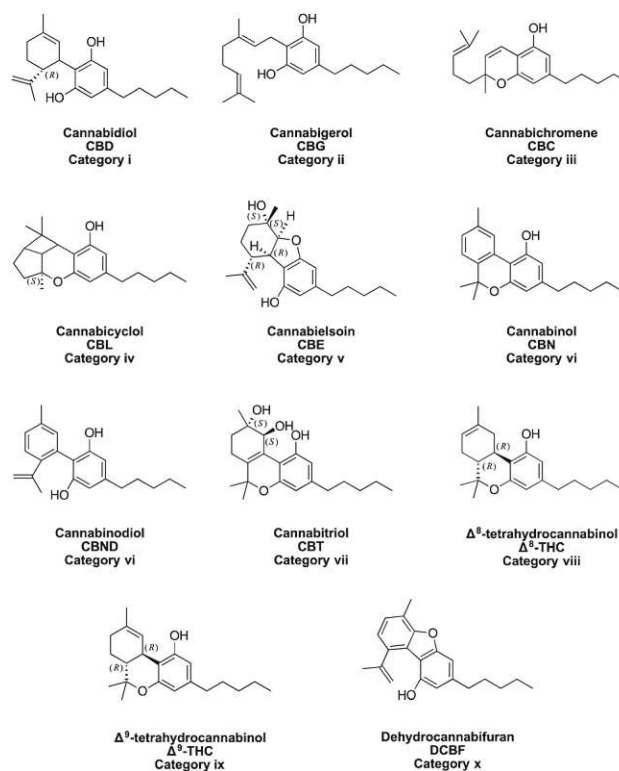
Fig. 2 Structures of principal cannabinoids.

This journal is © The Royal Society of Chemistry 2023

84

Nat. Prod. Rep., 2023, **40**, 676–717 | **679**
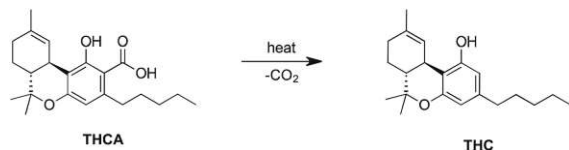
Fig. 3 Decarboxylation of tetrahydrocannabinolic acid (THCA) to tetrahydrocannabinol (THC).
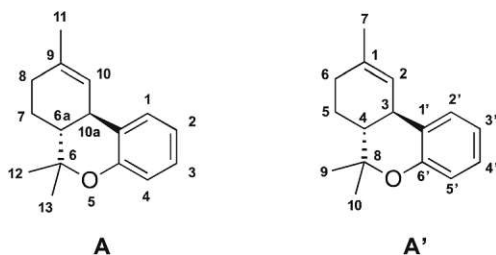
Fig. 4 (A) Dibenzopyran numbering, (A′) monoterpenoid numbering.

have 2 different names; numbering can start either at the dibenzopyran ring (used for pyran-type compounds, preferred in North America) or at the monoterpenoid ring/unit (refers to cannabinoids as substituted monoterpenoids, preferred in Europe). The classification according to the dibenzopyran nomenclature of Δ^9-THC, indicates the existence of a carbon–carbon double bond between C-9 and C-10 carbon atoms[40] and it is equivalent to Δ^1-THC in the monoterpenoid nomenclature (Fig. 4A and A′, respectively).

Typically, drug-type plants (*e.g.*, medicinal marihuana) contain THCA and THC as the most abundant cannabinoids, whereas fibre-type plants (*e.g.*, hemp) have CBDA and CBGA, followed by their decarboxylated analogues, CBD and CBG. Cannabinoid acids are not regarded as intoxicants, however, when they are exposed to heat, their decarboxylation naturally occurs, generating the corresponding cannabinoids, namely THC and CBD. Like THC, CBD is also one of the most abundant constituents in the plant; however, it is non-intoxicating, and it has tremendous medical potential.[41–44] THC was characterized and synthesized for the first time in the middle of the 1960s.[36,45] It affects the central nervous and cardiovascular systems, and it has been reported that it produces pleasant effects, such as euphoria; however, it may produce hallucinations and tachycardia if large quantities are consumed.[46,47] The intoxicant capability of *Cannabis sativa* can be mainly attributed to the decarboxylated form of THC. Although this intoxicating effect is modified by the presence of other cannabinoids and possibly terpenes, THC remains the chief intoxicating component. It also possesses properties that can be medically exploited; however, CBD, which is also present in considerable amounts, demonstrates higher medical potential than THC.[6]

CBD has received significant consideration in the course of recent years, because of its numerous beneficial properties, both medicinal and pharmacological.[48–50] Due to its relatively low toxicity, it is suitable for medical applications and it can be used alone or combined with several cannabinoids. It has

proven to have antiinflammatory properties and can be useful in the treatment of neuroinflammatory disorders, including various central nervous system and peripheral disorders, for instance, Alzheimer and it can function as an antimicrobial, anticonvulsive and antiepileptic,[49,50] analgesic, antibacterial, antiemetic, antipsychotic, and antispasmodic.[14,51] It has been proven that it can also reduce or prevent the anxiogenic effect of THC.[47] CBD is the main cannabinoid encountered in the seeds, while no THC is present.[52] Nonetheless, the seeds can be contaminated with THC either *via* contact with the plant resin or ineffective sieving. Depending on the country of origin, hemp seed products can contain THC in the range of 0.005 to 10 ppm.[53]

Overall, cannabinoids have exhibited outstanding therapeutic potential, as they can alleviate the effects of nausea and emesis in patients undergoing chemotherapy, can stimulate the appetite of HIV-positive patients, and can reduce spasticity in adults suffering with multiple sclerosis.[51] They have also shown potential in controlling Tourette's syndrome and chronic pain.[54,55] Moreover, they have demonstrated a beneficial effect as antitumor or anticancer agents and in the treatment of diseases, such as epilepsy, glaucoma and schizophrenia.[56,57]

Over the last decades, considerable steps have been made in the direction of interpreting the interaction of cannabis with the human physiology. Furthermore, new medicinal products and technologies are being developed, tested or, in certain cases, already accepted as beneficial and the volume of the available literature data has significantly increased; however, there is still no unanimous agreement on the merit of medical marijuana. In various jurisdictions, medical marijuana has become commercially available to a great extent owing to the spread of medical dispensaries.[14]

Currently, many different medicines are prepared using the bulk material of *Cannabis sativa* to treat chronic diseases, epilepsy, neuropathic pain and multiple sclerosis.[58–60] As a matter of fact, the first phytocannabinoid medicine was authorized in the UK in 2011 to treat multiple sclerosis muscle spasms.[61,62] In 2018, a CBD-containing anticonvulsant drug was approved in the USA.[63]

Many researchers use the term "medical marijuana" which particularly refers to the herbal material, while others take additionally into account the extracts and the natural and synthetic cannabinoids. Others suggest the term "medical cannabis" for non-herbal material, as it has less negative connotation.[6]

On the one hand, the plants that do not produce or produce limited amounts of THC, but generate high quantities of CBD, are designated for fiber and oilseed production, and are classified in *Cannabis sativa* subspecies *sativa*. On the other hand, plants that produce high content of the intoxicating THC are classified in *Cannabis sativa* subspecies *indica*. The inflorescence, typically the female one, contains the majority of THC and it is used for drug preparations.[6]

1.3.2. Chemovars classification; the solution for medicinal cannabis consumers? In a recent study, the chemical composition of 500 different cannabis flower samples was determined. The most consumed plant product, as established by Leafly

680 | *Nat. Prod. Rep.*, 2023, **40**, 676–717

85

This journal is © The Royal Society of Chemistry 2023

database (largest cannabis-related online site in the world), did not exhibit comparable results in THC strength and in some cases even the product appearance was different.[64]

It becomes, thus, apparent, that appropriate labelling of cannabis products enables their proper categorization and allows end users/consumers to select the product that best suits their needs. The chemical content of each commercially available product should be provided. This is especially important for users of medicinal cannabis, who face the major challenge of obtaining a product that is appropriate for their respective treatments, since the chemical profile of the product must precisely fit their medical needs. A wide variety of legally accessible, high-quality, consistent, and safe cannabis products must be guaranteed.[65] Medical consumers and their physicians could benefit from an overview of chemical content in commercially available cannabis to effectively shift from a beneficial illegally acquired product to a high-quality equivalent accessed through a legal route. Creating a new classification method based on chemical profiling ("chemovars") might be complex, but the main benefit is that the chemical content description is detailed and the composition reproducible.[65]

Varieties of cannabis that contain 0.3% or less THC by dry weight are characterized as hemp, whereas varieties that contain more than 0.3% THC by dry weight are classified as marijuana.[14] According to their cannabinoid content, cannabis varieties can be further classified as follows: type I – THC-abundant > 0.3% and CBD < 0.5%; type II – a mixture of THC and CBD with different moderate concentrations, which is virtually CBD dominant, and type III – CBD-dominant with low THC content.

Type I varieties can have intoxicating effects, with THC reaching >30%, and they are suitable for medicinal and therapeutic use. Type II CBD-rich varieties can help attenuate the intoxicating effect of THC, thereby increasing the chance of patients strictly adhering to their daily recommended dosage and, at the same time, increasing the therapeutic effect of CBD on the receptors. Type III refers to cannabis that contains mainly CBD in concentrations higher than THC, while the THC content is less than 0.3%. This range has been randomly assigned for legal hemp production. Type III cannabis is considered for fiber or drug-production, and if it is both rich in cannabinoids and terpenes, for industrial goods, such as cellulose plastics, paper, and fabric.[66]

1.3.3. Other valuable biologically active compounds present in cannabis. In conventional eastern medicine, hempseed has been used for alleviating diverse illnesses.[67] Hemp seeds, as historical records demonstrate, were utilized as an analgesic, for jaundice, skin diseases, cough, sores, and colic. Currently, an alternative treatment approach for constipation and blood problems is based on hempseed pills derived from Chinese medical practices.[68,69]

Hemp seeds contain many components, which can have a beneficial effect on health, such as polyunsaturated fatty acids (PUFAs), digestible proteins and trace amounts of terpenes and cannabinoids.[70] The fatty acid composition of the seeds determines the quality of the oil, specifically, the higher the amount of PUFAs the better the nutritional value. Hempseed oil has

PUFAs in abundance (normally over 80%), among them, necessary fatty acids, such as γ-linolenic acid (GLA, 18 : 3, ω-6, 1–6%) and stearidonic acid (SDA, 18 : 4, ω-3, 0–3%), and two essential fatty acids (EFAs), principally linoleic acid (50–60%) and α-linolenic acid (20–30%). Besides, hempseed oil also contains a monosaturated fatty acid (MUFA), namely oleic acid (18 : 1, 10–16%).[14] The aforementioned PUFAs have a positive influence on the cell membrane functions, stimulate cell immunology and have demonstrated their potential in alleviating atopic dermatitis and psoriasis,[71] while the omega fatty acids can promote cardiovascular health.[72]

Hempseed oil is rich in natural essential fatty acids and, additionally, it is the most balanced among commonly consumed plant oils for human nutrition; the ω-6 and ω-3 EFAs ratio (2 : 1–3 : 1) is the most favorable for human digestion.[73–75] The dietary EFAs, which are easily absorbed by skin tissues, contribute to the formation and regeneration of cell membranes and function as precursors in the synthetic route of several biochemicals that regulate the body's metabolic pathways.[76,77]

Several tocopherols, such as α-, β-, γ- and δ-tocopherols, are present in low amounts (0.1%) in hemp seeds.[75,78] Tocopherols, which have antioxidant properties, are part of the vitamin E group and are vital for human nourishment. In comparison to other available dietary oils, hempseed contains higher relative quantities of vitamin E, typically 100 to 150 mg g^{-1} of oil.[79–81] Moreover, hempseed contains around 0.7% of phytosterols, in particular campesterol and β-sitosterol. They also provide many health-beneficial effects, such as reduction of the total blood cholesterol and low-density lipoprotein (LDL) cholesterol levels in human serum, thus, treating atherosclerosis. Hemp seeds, additionally, consist of 25–30% proteins, which include the eight essential amino acids.[82,83]

High content of phenols and polyphenols can be found in hempseeds. Positive health effects are attributed to phenolic compounds since they are considered to be effective antioxidants and frequently exhibit antiinflammatory and cardioprotective properties.[84] Apart from that, hemp seeds also contain carbohydrates (20–30%), oil (25–35%), dietary fiber (10–15%) and minerals (4–6%), namely zinc, sulfur, potassium, phosphorus, magnesium, iron and calcium.[14,73]

Table 2 Medicinal properties of common terpenes of cannabis[92]

Terpene/terpenoid	Properties
α-Pinene	Antiinflammatory, antibacterial, bronchodilatory
β-Caryophyllene	Antiinflammatory, protects lining of digestive tract, antimalarial
β-Myrcene	Analgactesic, antiinflammatory, sedative, muscle relaxant
Caryophyllene oxide	Antifungal, decreases platelet aggregation, treats nail infections
Limonene	Antidepressant, immunostimulant, antibacterial
Linalool	Antianxiety, sedative, local anesthetic, anticonvulsant
Nerolidol	Antimalarial, sedative
Phytol	Sedative, prevents certain congenital malformations

Cannabis plants give out a characteristic scent, provided by the essential oil. Essential oils are a complex mixture of volatile secondary metabolites that consist of terpenes (monoterpenes, sesquiterpenes and other terpene-like compounds) and non-terpene hydrocarbons and their oxygenated derivatives, such as alcohols, ethers, ketone, aldehydes, esters, phenols, phenol ethers and lactones.[85,86]

Generally, terpenes are the major component of essential oils and many of them are responsible for the intense scent, since they can be detected by the sense of smell even at low concentrations. Currently, around 140 terpenes and terpenoids have been identified in *Cannabis sativa* and their medicinal properties are widely acknowledged (Table 2).[86] In the case of cannabis plants, monoterpenes normally represent most of the essential oil and its particular aroma is produced by pinene and limonene, which comprise more than 75% of the volatile components.[87–89] The essential oil composition varies significantly among different strains and cultivars of *Cannabis sativa*.[90,91] It is worth mentioning, that the interaction between natural terpenes and cannabinoids may have a therapeutic effect.[92,93]

An overview of the valuable compounds encountered in the cannabis plant along with their location in the respective plant parts is presented in Fig. 5.

1.4. Non-medical applications of cannabis

Cannabis sativa can be grouped into 2 main categories; the one is the cannabis cultivated for the production of financially significant materials, *i.e.*, fiber, seed oil and psychotropic drugs, whereas, the other category comprises "wild" (weedy) plants which are not subject to the applied cultivation practices. Hemp fibers are used for the manufacturing of ropes and textiles, and seed oil is employed in the production of industrial oils and dietary supplements, while it can be additionally utilized as livestock feed, human food and occasionally as biofuel.

1.4.1. Fiber. In principle, the level of THC in fiber plants is significantly less than 1%, which makes them unsuitable for pharmaceutical or medical exploitation. China has been the dominant hemp fiber producer for several millennia, principally in the textile industry. Nowadays, the importance of hemp fibers in the textile sector has significantly diminished due to the introduction of synthetic and natural fibers in the market.[6,97,98]

Even though certain hemp applications, such as clothing and paper, are currently obsolete, a diversity of novel applications has emerged and revived the hemp industry, to name a few, horticultural planting media, biodegradable mulch, cordage products, pressed and molded fiber products, building construction products, animal bedding based on hurds, compressed cellulose plastics, plastic biocomposites and as insulation material in the automotive industry.[14,99,100]

1.4.2. Seeds and oil. Three different types of oil can be derived from *Cannabis sativa*; (i) vegetable (fixed) oil, which can be extracted from the plant seeds and mainly comprises triglycerides, (ii) essential oil, which is produced in the flowering part of the plant and can be obtained *via* distillation and (iii) hashish oil, which is a THC-rich solvent extract (highly concentrated marijuana) intended for recreational purposes. Vegetable oils, aside from their comestible value, can be used for fuel, medication, and personal care products. Essential oils are complex organic mixtures containing various volatile compounds which are responsible for the distinctive scent of the cannabis plant. Despite their medicinal properties and their potential as flavorants and odorants, their low yield and high price has not resulted in their widespread market exploitation and their use still remains rather limited.[6]

Often the terms "hemp oil" and "hempseed oil" are erroneously used interchangeably; however, they do not refer to the same type of oil. "Hemp oil" may refer either to the vegetable oil or to the essential oil, thus, the oilseed industry has assigned the term "hempseed oil" to the edible vegetable oil to avoid ambiguity. The term "cannabis oil" is even more vague since it can be used to refer to either of the 3 oils derived from the cannabis plant.[6]

Recently, the seeds have proven to be an important source of edible oil and suitable for the production of pharmaceuticals, nutraceuticals and functional foods. Europe and Canada have recently cultivated varieties of cannabis that focus on oilseed production. It is foreseen that the oilseed crops of cannabis will create a more profitable market than the fiber crops, at least in industrially advanced countries. Importing hemp seed from China, which is currently the leading country in hempseed production, is not at the best interest of other countries due to various reasons; required sterilization of the seeds prior to import signifies delay in the import process, increased costs and a decrease in the quality of the seeds. Additionally, sterilized seeds go stale rather fast, which is an undesirable property of seeds intended for human consumption. Domestic-seed production is, therefore, preferable. The EU, which was heavily focused on fiber crops, has only recently realized the promising future of the oilseed. In contrast, Canada, which has always exploited the oilseed crops, has emerged as the global provider of hempseed products used in the manufacturing of natural foods, nutraceuticals and cosmetics. The USA is
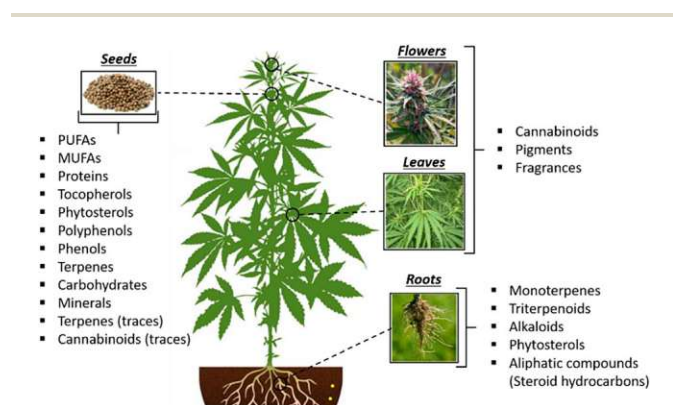
Fig. 5 Valuable compounds present in the cannabis plant. PUFA: polyunsaturated fatty acids; MUFA: monosaturated fatty acid.[94–96] Open access, CC BY 4.0, https://creativecommons.org/licenses/by/4.0/.

682 | *Nat. Prod. Rep.*, 2023, **40**, 676–717

87

This journal is © The Royal Society of Chemistry 2023

expected to follow suit ensuing the local legalization of industrial hemp.[6]

Nowadays, many food preparations, such as breads, yogurts, and salad dressings, contain hemp seeds and/or hemp seed oil. Additionally, hemp essential oil is used as a flavorant for alcoholic beverages. Hemp seeds have been typically used complementary to poultry feed.[101] The seed cake, obtained from extracting the oil from the seeds, has proven to be an exceptional nutrition source for sheep, lambs and cattle.[102,103] Since the late 20th century, hempseed oil has been used in a different array of cosmetic products, such as soaps, shampoos, and lip balms. It is also present in industrial products, such as printing inks, lubricants for machinery, sealants, varnishes and oil paints.[104] In addition, it has been transformed into biodiesel and has been used as a green alternative to non-renewable fuel sources.[105]

The essential oil of *Cannabis sativa* is costly (approximately 1100 € per liter) since the obtained yields are quite low (around 1.3 liter per ton fresh weight – 10 liter per hectare).[90,106]

1.6. Cannabis storage and impact on composition

Ensuring the integrity of sample characteristics from the time of collection until the time of analysis implies that the transportation and storage conditions should be carefully monitored in order to minimize its degradation and/or contamination.

A crucial factor that can affect the overall quality, medical efficacy and value of cannabis products is the humidity level upon storage of the harvested and cured flower. According to the American Society of Testing and Materials (ASTM) International, the optimal humidity level for cannabis storage is in the range of 55–65%. Exceeding the recommended values exposes the harvested flower to possible growth of mold and fungus, while failing to reach the minimum value can lead to extensive dryness, thus, substantial loss of critical components, such as cannabinoids and volatile constituents, such as terpenes.[107]

Sample processing prior to analysis or extraction is another important consideration that will largely determine the sample homogeneity and associated reliability of the analytical outcome. Despite the advantageous effects of sample grinding, *i.e.*, increased homogeneity and surface area and decreased particle size, all of which benefit extraction efficiency, at the same time, grinding also impacts the sample in an undesirable manner; increased contamination risk, introduction of humidity, possible losses of volatile compounds and alteration of labile ones. Cryogenic grinding is an alternative that can largely circumvent the unwanted outcomes mentioned above.[108]

Studies have demonstrated that THC, both in herbal and resin cannabis preparations (marijuana and hashish), progressively decomposes over time to CBN,[109] which is believed to be a mere chemical degradation product rather than a naturally/biochemically occurring component.[110] Decomposition of Δ^9-THC, when exposed to light and air, to CBN, proceeds through an oxidation reaction.

Although this gradual conversion of THC to CBN is an inevitable process, storage conditions can significantly delay or accelerate it. Taking into consideration that there might be either a considerable time lapse between sample reception and analysis or the need for re-evaluation of an old sample or even both, it is crucial to be able to accurately determine the effect of time and storage conditions on the sample composition.

It has been known since 1969 that the THC content of marijuana stored at RT is decreasing at a rate of 3–5% per month.[111] Three independent 4 year long stability studies, demonstrated that light and temperature have a dramatic effect on the decomposition of THC to CBN, while they mediate different aspects of the process; light impacts the stoichiometry of the conversion of THC to CBN, whereas temperature accelerates the conversion.[109,112,113] In any case, samples stored at RT in direct contact with the atmospheric air, either in light or darkness, suffered the most pronounced losses in THC, ranging from 65% to almost 100%, depending on the sample origin and initial composition. Since many of the substances in cannabinoids can undergo oxidation, sealing the samples in plastic bags can reduce the losses to 25–42%. It should be mentioned that the increase in the total amount of CBN does not correspond with the total decrease of THC, an observation which implies that THC degrades to other products apart from CBN. Negligible impact on the initial concentrations of cannabinoids is observed when samples are stored in the freezer at −20 °C. In contrast, storage conditions have no significant impact on the CBD content.[112]

Short-term stability studies (15–30 days) of cannabinoids (THC, CBN, CBD) extracted in organic solvents (methanol, chloroform, light petroleum, methanol : chloroform 9 : 1) indicate that the form of cannabinoids and storage temperature, rather than the nature of the extractant, are crucial parameters affecting their stability in solution. Specifically, neutral cannabinoids are stable for up to 15 (at 20 °C) to 30 days (at −18 °C and 4 °C) stored in the dark,[114] while exposure to daylight leads to their dramatic decomposition.[115] In the case of acidic cannabinoids, decomposition occurs both in dark and light with the rate increasing with temperature.[114]

In addition to the discussed parameters, the material of the containers in which cannabinoid extracts are stored can also have a significant effect on the cannabinoid content determined in solution. The loss of acidic THC on container walls is a function of both solvent type and container material since they both appear to compete to bind with it. Generally, the loss determined in organic diluents is significantly lower than in the case water is used as the cannabinoid diluent, owing to the higher solubility of cannabinoids in organic solvents. As far as material is concerned, the losses are far less pronounced in the case of polar materials (contact angle < 70°), such as glass and acrylic, than in non-polar materials (contact angle > 70°), such as HDPE. Additional losses are observed with increasing surface tension and decreasing pH and conductivity. Large volumes of stored solution are preferrable because losses attributable to both pipetting and exposed surface area are minimized.[116]

1.7. Inconsistencies and misconceptions in result reporting in literature

When one reviews the developed and reported extraction processes, it is quite apparent that an accurate and meaningful

This journal is © The Royal Society of Chemistry 2023

88

Nat. Prod. Rep., 2023, **40**, 676–717 | **683**

comparison of their performance is a rather challenging task. The inherent differences of the various cultivars extracted cannot be overcome; however, it is rather the inconsistent reporting that constitutes a major obstacle in the evaluation of the reported results.

As far as the input sample is concerned, only a handful of manuscripts report the composition of the input sample material (either relying on Soxhlet as a reference method or on data provided by the raw-material supplier, while in some cases no specification is given),[42,117–123] whereas most researchers only focus on the extracted amount of valuable compounds. Undoubtedly, the amount extracted is highly valuable information; nevertheless, the recovery of the target compounds, which is largely absent, is indicative of the performance of the developed method and, thus, a crucial factor for the evaluation of its potential economic and ecological merit in comparison to state-of-the-art approaches. Additionally, information regarding the input sample moisture[78,121,122,124–130] or the particle size[131–137] or both[42,118,138–148] is often omitted, thereby rendering result interpretation further complicated; water content affects both the extraction outcome/extracted amount of the valuable compounds and the accuracy of the reported concentrations, when those are calculated with reference to the input sample.

With respect to extraction conditions with supercritical solvents, namely supercritical carbon dioxide ($scCO_2$), variable pressure (bar, MPa) and CO_2 flow rate units (g min^{-1}, kg h^{-1}, mL min^{-1}) are reported,[119,124,125,133,138,149] whereas, in certain cases, $scCO_2$ density is provided *in lieu* of pressure[150] or flow rate;[117] furthermore, the value of the density is reported in different units (g mL^{-1},[150] kg m^{-3},[117]) which sometimes can be attributed to differences in journal requirements. Lamentably, in certain cases, failure to report the overall extraction time of the process[117,119,120,125,133] or even the process conditions altogether,[118,126,132,151–154] as well as ambiguity in the reported conditions,[78,130,144,147] does not allow fair and complete assessment of the presented results.

As we previously discussed, the storage conditions of the samples are crucial for the outcome of the quantification procedures. Review of the available literature reveals that the employed storage conditions can significantly vary between experiments conducted by different researchers. Milling and grinding prior to storage can have a considerable impact on the outcome, since these processes can not only contaminate the sample but also modify its composition, thus storage and analysis after milling/grinding[117,124,155,156] means that information on the composition of the original plant material has been lost. Drying of the plant material prior to storage and analysis is often reported; however, when drying is performed at elevated temperature[157–160] it leads to decarboxylation, thereby modifying the original composition of the material. It is not uncommon though that the drying is simply performed at RT.[120,124,151] As a far as storage is concerned, storage conditions of RT,[117,149,156] 4 °C,[124,126] <18 °C/refrigerator[155,161] and even −20 °C[157] have been reported. Even more unfortunate than the variation of storage conditions though is the unclear and/or incomplete storage and/or pre-treatment information of the sample material,[118–120,125,131–133,151–154,158–160,162–164] while even in the cases

that this information is complete the duration of the storage is not discussed at all. It is also quite important to point out that no information on the storage containers has been provided, which is rather important considering the impact the material of the containers can have, as we saw earlier.

Aside from the evidently inconsistent information provided on the input material and the process conditions, the reported results are a source of additional confusion. Unfortunately, % recovery data is rarely reported,[149,153] even when the input-material composition has been determined with the aid of a reference extraction method. On the other hand, the yield from hemp flowers and residues (overall or per extracted valuable compound or both) is most commonly reported; however, the yield is not calculated consistently. It has been calculated with reference to the input sample material,[42,78,123,124,127–129,133–135,139,143–148,153,165–167] to the recovered extract[117–119,121,122,136,138,140–142,162,168,169] and to the overall cannabinoid extract process,[117,125] while in some cases it is not clearly specified,[122,131,163,170] thereby, causing confusion and only leading to assumptions and misunderstandings on the part of the reader. Providing the equation on which the calculations are based, as certain publications do,[78,134,144,145,153,158,159,163,167] could effectively eliminate this problem. In contrast, the fatty acid yield from hemp seeds is invariably referenced to the extracted hempseed oil.[126,131,149,151–153] Additionally, cannabinoid yields have been reported either as % (w/w),[119,122,124,125,134,138,148] as µg g^{-1},[141,143] as mg g^{-1},[117,118,140,162] as mg mL^{-1},[142,168] as percentage %[136] and as cumulative yield,[141] while the input sample amount is not always provided.[117,118,124,139,147] Regarding the oil yield, it has been reported in % w/w,[78,144–146,165,167] in g[144] and in percentage %.[127,130,147]

Certain authors make a distinction between THC and total THC,[125] however, in the majority of cases THC is reported without clarification as to whether this refers to pure THC or total THC (THC + THCA). Unfortunately, error values (procedural, measurement or both) of the reported results are frequently excluded;[117,122–124,127,138,139,142,150,153,163,170] this information is quite significant, not only because in certain cases it can be considerable, which is not unexpected when working with naturally derived samples[133] but also because its absence renders the comparison of different experimental outcomes problematic.

Concerning the statistical aspect of the reported procedures, it seems that performed extraction repetitions are not enough, in some cases, to confidently accept the reliability of the reported results. We consider that this might not be feasible in certain techniques, *e.g.*, $scCO_2$; however, at least triplicate extractions would be necessary to exclude/eliminate any erroneous conclusions. Nevertheless, the majority of the publications report triplicates,[128–130,134–137,140,141,143–145,147,149,152,158,163,164,166–168,171] while some report duplicates.[42,120,121,125,138,146,148,150,162,165] Unfortunately, sometimes, this crucial information is entirely omitted.[117–119,123,124,126,127,131–133,139,140,142,151,153–155,159–161,163,166,170,172]

It becomes thus apparent, that it is, currently, an impossible challenge to compare different publications on this topic, due to the lack of consensus between researchers on specifying in

684 | *Nat. Prod. Rep.*, 2023, **40**, 676–717

89

This journal is © The Royal Society of Chemistry 2023

a standardized manner the experimental parameters and the obtained results. Arriving at an agreement of consistent data reporting would be an extremely valuable contribution to the field, which cannot be tackled by an individual researcher but would need to be an effort with broad support of the community.

With regard to misconceptions, a critical point that needs to be addressed, which appears not only in the referenced reviews (except Lazarjani et al.)[173] but also in the majority of the publications reported herein, is the seemingly existing confusion between intoxicating and psychotropic/psychoactive properties. Intoxication is associated with a state of euphoria and mild cognitive impairment, i.e., in layman's terms "getting high", and according to the Cambridge dictionary an intoxicating substance is "able to make you lose some control of your actions or behaviour". However, a psychoactive substance does not simply "get one high" but rather affects mental processes, e.g., perception, consciousness, cognition or mood and emotions.[174] Psychotropic substances have effects on psychological function.[175] According to the Anatomical Therapeutic Chemical classification system the five classes of psychotropic drugs are antipsychotics, antidepressants, anxiolytics, hypnotics and mood stabilizers. Based on this nomenclature, it is clearly wrong to assign CBD as non-psychoactive/non-psychotropic;[176] it clearly falls into the psychoactive/psychotropic classification by definition due to its anxiolytic capacity.

An apparent term misuse in the reported literature concerns the terms "terpenes" and "terpenoids". They have been used in an interchangeable manner in several publications reported herein. Nevertheless, there is a distinct difference between the two; terpenes are hydrocarbons that arise from the head-to-tail joining of five-carbon isoprene units, while terpenoids are oxygenated forms of terpenes.[177] Some authors collectively refer to terpenes and terpenoids as "terpenoids"[118,134] while others collectively refer to terpenes and terpenoids as "terpenes".[120,121,148,164]

1.8. Recent reviews on cannabis extraction

It should be mentioned here that a number of reviews on the topic of cannabinoid and bioactive compound extraction from cannabis has been published. Specifically, Lazarjani et al.,[173] Pattnaik et al.,[178] Al Ubeed et al.,[179] and Qamar et al.[180] have published most recently on this topic.

There is, currently, no review that provides an exhaustive overview of all available extraction methods, conventional and more recently developed, from all different parts of the cannabis plant but there is rather a focus on certain compound groups (i.e., cannabinoids) or certain extraction methods (e.g., supercritical CO_2). Additionally, in our review other groups of known value (e.g., polyphenols) have been addressed, in addition to cannabinoids. The review does not only focus on the medicinal value of the plant but also on the sometimes overlooked industrial (nutrition, cosmetics) value of the plant, while a historical overview allows a clear understanding of the longstanding value of the cannabis plant for the human civilization. Unlike other reviews, we have decided to address several inconsistencies that appear in experimental procedures and reported results which obscure their value and practicality.

2. Extraction techniques for cannabinoids and other valuable bioactive cannabis compounds

In the present section of the review, the techniques that have been employed for the extraction of valuable compounds from the cannabis plant will be discussed in detail. An overview of the employed techniques as well as the respective plant parts to which they have been applied along with the distribution of each technique is presented in Fig. 6 and 7.

2.1. Supercritical fluid-based extraction

The contemporary quest towards sustainable processes has placed supercritical CO_2 (scCO$_2$) in the forefront of alternative solvents which are under investigation as promising candidates
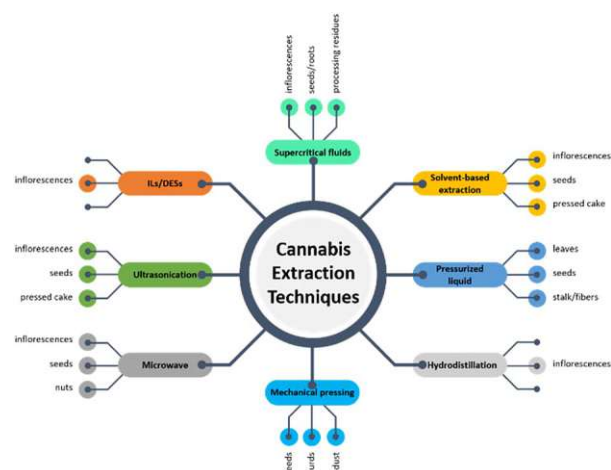
Fig. 6 Reported techniques for the extraction of valuable compounds from various parts of the cannabis plant.
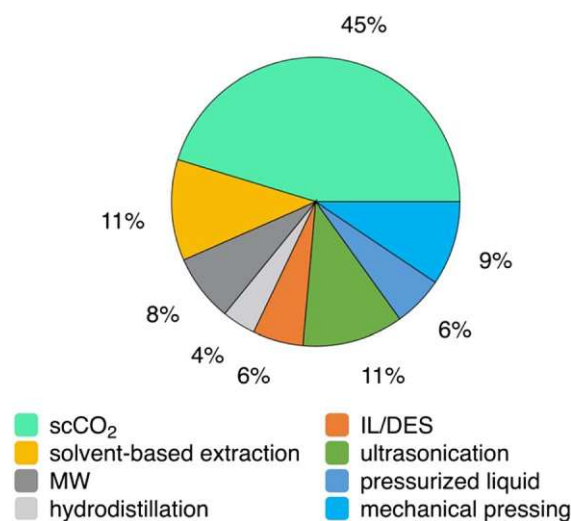
Fig. 7 Distribution of the reported extraction techniques. scCO$_2$: supercritical CO_2, IL: ionic liquid; DES: deep eutectic solvent, MW: microwave.

Table 3 Summary of scCO$_2$ extraction conditions and respective results pertaining to flowers of the cannabis plant[a]

Entry no.	Input sample	Particle size (mm)	Conditions	Extracted compounds	Ref. no.
1	*Cannabis sativa* L., strain: hash berry (Sativa 50%, Indica 50%), leaves & buds (ground), 500 g	1.2	55 °C, 340 bar, 200 g min^{-1} (12 kg h^{-1})	[b]THC: 25.78 ± 1.82, THCA: 49.75 ± 2.54, total THC: 69.41 ± 2.87, CBDA: 1.09 ± 0.93, extraction efficiency: 90	125
2	*Cannabis sativa* L., strain: sour alien OG (Sativa 40%, Indica 60%), leaves & buds (ground), 500 g	1.2	55 °C, 340 bar, 200 g min^{-1} (12 kg h^{-1})	[b]THC: 20.55, THCA: 46.37, total THC: 61.21, CBDA: 1.66, extraction efficiency: 89	125
3	*Cannabis sativa* L., strain: white widow (Sativa 60%, Indica 40%), leaves & buds (ground), 500 g	1.2	55 °C, 340 bar, 200 g min^{-1} (12 kg h^{-1})	[b]THC: 23.07, THCA: 39.68, total THC: 57.86, CBDA: 0.97, extraction efficiency: 90	125
4	*Cannabis sativa* L., strain: abusive OG (*indica*), leaves & buds (ground), 500 g	1.2	55 °C, 340 bar, 200 g min^{-1} (12 kg h^{-1})	[b]THC: 27.69, THCA: 39.68, total THC: 56.06, CBDA: 0.01, extraction efficiency: 92	125
5	Mixed plant material (dried, ground), 500 g	n.a.	60 °C, 320 bar, 150 g min^{-1}, 600 min	[b]THC: 28, CBD: 17	138
6	Ripe cannabis inflorescences (dried, milled)	<0.5	60 °C, 330 bar, 0.55 kg h^{-1}, 240 min, 2% wt EtOH	[d]THC: 6.06, total THC: 37.85, overall yield: 16	124
7	Marijuana (air-dried, ground), 0.5 g	0.063 < *d* < 0.125	40 °C, density 0.9 g mL^{-1}, 1.5 mL min^{-1}, 130 min	THC: complete removal	150
8	Girl scout cookies (hybrid: 60% Sativa, 40% Indica), flowers (milled), 6 g	0.24	50 °C, 165 bar, 2.5 mL min^{-1}, 6% (v/v) EtOH	[c]THC: 87.91 ± 1.10, CBD: 5.08 ± 1.01, CBN: 0.53 ± 0.59, overall yield: 30, α-pinene: 4.79 ± 0.45, β-pinene: 2.20 ± 0.08, myrcene: 15.35 ± 2.38, (*R*)-limonene: 0.81 ± 0.13, caryophyllene: 31.67 ± 0.28, α-humulene: 11.09 ± 0.63, β-panasinsene: 12.62 ± 1.57, selina-3,7(11)-diene: 16.49 ± 2.10	119
9	Durga mata II (10% Sativa, 90% Indica), flowers (milled), 6 g	0.32	50 °C, 240 bar, 2.5 mL min^{-1}, 6% (v/v) EtOH	[c]THC: 27.96 ± 0.57, CBD: 33.81 ± 0.43, CBN: 0.23 ± 0.13, overall yield: 27, α-pinene: 17.99 ± 1.32, β-pinene: 6.08 ± 0.86, myrcene: 12.34 ± 0.50, (*R*)-limonene: 7.45 ± 0.44, caryophyllene: 20.97 ± 1.78, α-humulene: 8.75 ± 0.26, β-panasinsene: 9.15 ± 1.96, selina-3,7(11)-diene: 11.17 ± 2.15	119
10	*Cannabis sativa* L., cultivar: a (undisclosed), flowers buds, leaves, trimmings (milled)	2	Near-critical propane	[c]THC: 18.1, THCA: 1.18, CBD: 315, CBDA: 86.6, CBG: 5.76, CBGA:0.71, CBN: 0.36	117
11	*Cannabis sativa* L., cultivar: B1 (Ferimon 12), flowers buds, leaves, trimmings (milled)	2	Pressurized dimethylether	[c]THC: 18.0, THCA: 0.03, CBD: 229, CBDA: 5.03, CBG: 6.94, CBGA: 0.17, CBN: 0.82	117
12	*Cannabis sativa* L., cultivar: B2 (Ferimon 12), flowers buds, leaves, trimmings (milled)	2	40 °C, 100 bar, density 628.6 kg m^{-3}	[b]CBD: 97.8	117

686 | *Nat. Prod. Rep.*, 2023, **40**, 676–717

91

This journal is © The Royal Society of Chemistry 2023

Table 3 (*Contd.*)

Entry no.	Input sample	Particle size (mm)	Conditions	Extracted compounds	Ref. no.
13	*Cannabis sativa* L., cultivar Felina, inflorescences (dried), 150 g	0.2–0.6	40 °C, 100 bar, density < 600 kg m^{-3}	n.r.	120
14	*Cannabis sativa* L., chemovar: cherry kush, flowers	n. r.	n. r.	^{a}THC: 7.75 ± 0.19, THCA: 69.4 ± 5.2, CBD: 0.53 ± 0.06, CBDA: 9.12 ± 0.21, CBG: not detected, CBN: 0.15 ± 0.01, α-pinene: 0.48 ± 0.11, β-pinene: 0.48 ± 0.08, β-myrcene: 0.13 ± 0.03, (*R*)-limonene: 1.19 ± 0.33, β-caryophyllene: 20.60 ± 2.40, α-humulene: 5.69 ± 0.55, linalool: 3.14 ± 0.66, fenchyl alcohol: 4.04 ± 0.47, α-terpineol: 5.06 ± 0.46, α-bisabolol: 4.53 ± 1.25	118
15	*Cannabis sativa* L., chemovar: blackberry kush, flowers	n. r.	n. r.	^{a}THC: 10.6 ± 0.23, THCA: 74.9 ± 8.4, CBD: 0.09 ± 0.06, CBDA: 0.70 ± 0.05, CBG: 0.79 ± 0.06, CBN: 1.1 ± 0.1, α-pinene: 0.31 ± 0.05, β-pinene: 0.39 ± 0.08, β-myrcene: 0.14 ± 0.02, (*R*)-limonene: 1.09 ± 0.20, β-caryophyllene: 2.10 ± 0.65, α-humulene: 1.65 ± 1.43, linalool: 0.93 ± 0.17, fenchyl alcohol: 4.01 ± 0.45, α-terpineol: 4.65 ± 0.36, α-bisabolol: not detected	118
16	*Cannabis sativa* L., chemovar: pineapple kush, flowers	n. r.	n. r.	^{a}THC: 17.4 ± 0.38, THCA: 65.1 ± 4.5, CBD: 0.19 ± 0.05, CBDA: 0.33 ± 0.06, CBG: 0.11 ± 0.02, CBN: 0.1 ± 0.02, α-pinene: 0.44 ± 0.60, β-pinene: 0.32 ± 0.05, β-myrcene: 1.30 ± 0.21, (*R*)-limonene: 1.40 ± 0.19, β-caryophyllene: 10.38 ± 0.24, α-humulene: 3.23 ± 0.12, linalool: 4.00 ± 0.56, fenchyl alcohol: 2.68 ± 0.17, α-terpineol: 3.35 ± 0.18, α-bisabolol: 4.96 ± 0.54	118
17	*Cannabis sativa* L., chemovar: purple sour diesel, flowers	n. r.	n. r.	^{a}THC: 0.998 ± 0.27, THCA: 67.5 ± 4.4, CBD: not detected, CBDA: 2.03 ± 0.60, CBG: 2.05 ± 0.09, CBN: 1.5 ± 0.007, α-pinene: 1.30 ± 0.14, β-pinene: 0.57 ± 0.01, β-myrcene: 5.46 ± 0.40, (*R*)-limonene: 1.06 ± 0.21, β-caryophyllene: 14.55 ± 0.46, α-humulene: 4.10 ± 0.09, linalool: 4.72 ± 0.28, fenchyl alcohol: 2.05 ± 0.33, α-terpineol: 2.60 ± 0.38, α-bisabolol: 2.05 ± 0.90	118

This journal is © The Royal Society of Chemistry 2023

92

Nat. Prod. Rep., 2023, **40**, 676–717 | **687**

Table 3 (*Contd.*)

Entry no.	Input sample	Particle size (mm)	Conditions	Extracted compounds	Ref. no.
18	*Cannabis sativa* L., chemovar: ripped Bubba, flowers	n. r.	n. r.	[c]THC: 0.97 ± 0.21, THCA: 71.5 ± 5.3, CBD: not detected, CBDA: 0.31 ± 0.02, CBG: 1.14 ± 0.08, CBN: 0.16 ± 0.07, α-pinene: 0.17 ± 0.01, β-pinene: 0.210 ± 0.003, β-myrcene: 0.55 ± 0.05, (R)-limonene: 0.60 ± 0.01, β-caryophyllene: 7.59 ± 0.96, α-humulene: 2.06 ± 0.22, linalool: 3.64 ± 0.16, fenchyl alcohol: 2.84 ± 0.16, α-terpineol: 3.63 ± 5.3, α-bisabolol: not detected	118
19	*Cannabis sativa* L., chemovar: harlequin, flowers	n. r.	n. r.	[c]THC: 5.5 ± 0.2, THCA: 33.3 ± 2.6, CBD: 1.74 ± 0.09, CBDA: 44.5 ± 0.37, CBG: not detected, CBN: not detected, α-pinene: 1.51 ± 0.26, β-pinene: 0.65 ± 0.26, β-myrcene: 1.78 ± 0.40, (R)-limonene: 1.27 ± 0.24, β-caryophyllene: 8.40 ± 0.96, α-humulene: 2.48 ± 0.27, linalool: 3.58 ± 0.71, fenchyl alcohol: 2.53 ± 0.28, α-terpineol: 3.94 ± 0.31, α-bisabolol: not detected	118
20	*Cannabis sativa* L., chemovar: Futura 75, flowers, leaves and stems	2	70 °C, 200 bar, 5.0 mL min^{-1} [C$_2$mim][OAc]	[d,e]THC: 0.542 ± 0.016 CBD: 15.6 ± 0.7 CBG: 0.335 ± 0.016	157
21	*Cannabis sativa* L., chemovar: Futura 75, flowers, leaves and stems	2	70 °C, 200 bar, 5.0 mL min^{-1} [Ch][OAc]	[d,e]THC: 0.535 ± 0.010 CBD: 15.4 ± 0.5 CBG: 0.401 ± 0.024	157
22	*Cannabis sativa* L., chemovar: Futura 75, flowers, leaves and stems	2	70 °C, 200 bar, 5.0 mL min^{-1} [C$_2$mim][DMP]	[d,e]THC: 0.449 ± 0.025 CBD: 11.8 ± 0.9, CBG: 0.292 ± 0.028	157

[a] All concentrations of extracted compounds within the table are reported as %, regardless of the units in which they were originally reported by the authors, in order to facilitate their comparison. [b] Reported as % of the cannabinoid extract. [c] Reported as % of the total extract. [d] Reported as % of the input sample. [e] Pretreatment at 70 °C for 15 min with IL : H$_2$O 1 : 3. (n. r. = not reported), [C$_2$mim][OAc] = 1-ethyl-3-methylimidazolium acetate, [Ch][OAc] = choline acetate, [C$_2$mim][DMP] = 1-ethyl-3-methylimidazolium dimethyl phosphate.

688 | *Nat. Prod. Rep.*, 2023, **40**, 676–717

93

This journal is © The Royal Society of Chemistry 2023

that can promote this goal. Supercritical CO_2 possesses a range of unique properties that are superior to the commonly used organic solvents. Namely, its non-toxic and non-flammable nature, its tunability by simple variation of the process parameters, its recyclability, as well as its low price and easy separation from the extracted products, render it a highly versatile alternative solvent. Additionally, the supercritical state can be reached at relatively mild pressure (73.8 bar) and temperature (31.0 °C) conditions. Although the non-polar nature of $scCO_2$ renders it ideal for the solvation of non-polar and weakly polar compounds, addition of polar co-solvents can expand its solvation range. It should be pointed out here that the properties of non-toxicity and the recovery of products without any solvent residues make the $scCO_2$ extraction technology particularly attractive to the pharmaceutical and food industries.[181,182]

2.1.1. Flowers. The $scCO_2$ extraction conditions and the respective results that are discussed in this section pertaining to cannabis flowers are summarized in Table 3.

Cannabinoids (THC, THCA, CBDA) from ground plant material (leaves, buds) were extracted with $scCO_2$ via one-step and multi-step approaches (Table 3, entries 1–4).[125] While a three-step cascade extraction with sequential increase in applied pressure (sequential pressure increase 170 → 240 → 340 bar yields (82.99 ± 1.87) g cannabinoid extract) offers the possibility for selectivity tuning of extraction speed and overall yield at different steps, it is not as effective as a one-step extraction at higher pressures ((92.57 ± 2.14) g cannabinoid extract); high pressure implies increased solvating power, faster extraction rate and, consequently, lower solvent consumption (a solvent/feed ratio >70 is required at 240 bar to obtain the same extraction efficiency as with solvent/feed = 40 at 340 bar). Nevertheless, the extraction behavior seems to be dependent on the plant material used, specifically, the lower the cannabinoid concentration in the plant material the lower the extraction yield and the slower the extraction rate. Regardless of the selected $scCO_2$ extraction approach, partial decarboxylation of THCA occurs during the process as a result of the exposure of the plant material to increased temperatures.

The effect of co-solvent on the one-step $scCO_2$ extraction was evaluated with two different modes of addition; ethanol was supplied either at a constant flow rate or in a pulse mode (Fig. 8). As expected, the addition of a polar co-solvent increases the solvating power of $scCO_2$ towards polar molecules, thus, favors the overall extraction yield of cannabinoids and the extraction rate. The pulse-mode experiments were designed so that the same amount of ethanol as in the constant-flow experiments was supplied, i.e., higher % EtOH was supplied at three shorter intervals. Although the overall extraction yield between the two approaches was comparable, the pulse mode delivered the maximum extraction yield already after the first pulse was applied, which means that a lower amount of ethanol than expected was consumed to achieve the same extraction yield as in the constant-flow experiments at significantly shorter time.[125] It would have been very interesting if the authors had also considered running the extraction experiments with
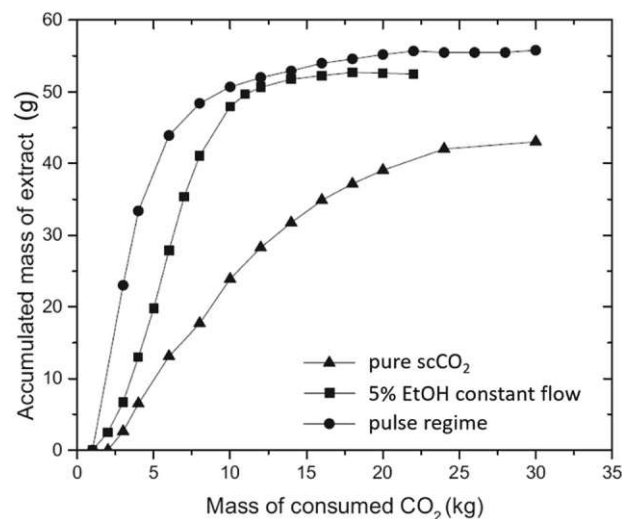
Fig. 8 Comparison of pure $scCO_2$, constant EtOH flow rate and pulse regime on the extraction (white widow).[125] Reprinted with permission from Elsevier.

a higher EtOH concentration but for a shorter duration to assess whether the outcome would be the same.

Highly efficient extraction of medicinally valuable cannabinoids, namely CBD and THC, from cannabis buds was performed with $scCO_2$ without the aid of a co-solvent (Table 3, entry 5).[138] The impact of critical input parameters, i.e., CO_2 flow rate, time and pressure, with a fixed temperature of 60 °C, on the obtained yields was established; extraction of CBD is clearly favored with increasing flow rate, while both higher flow rate and longer time positively impact THC yield. Interestingly, the ratio of the output CBD to THC can be tuned by adjusting the flow rate; however, increasing the ratio to recover higher amounts of the desirable CBD is detrimental to the overall extraction yield. Complete cannabinoid recoveries and overall extraction yield were obtained at increased flow rates, high pressure (320 bar) and long extraction time (60 °C, 320 bar, 150 g min^{-1}: 101.1% CBD, 98.6% THC, yield 7.1% vs. 60 °C, 320 bar, 40 g min^{-1}: 78.1% CBD, 73.6% THC, yield 5.6%).[138]

THC of high purity (90.1%) could be obtained from dried cannabis plant material (inflorescences) with the aid of supercritical fluid extraction (SFE) combined with solid phase extraction (SPE) (Table 3, entry 6).[124] Models were constructed to determine the optimum SFE parameters for the enrichment of the extracts in THC. While an increase in pressure, temperature and amount of co-solvent (EtOH) increases the overall extraction yield, at the same time, it decreases the amount of extracted THC, which can be attributed to the variation of the solvent selectivity with the modification of these extraction parameters (40 °C, 150 bar: yield 4.83%, THC 32.25%; 80 °C, 150 bar, yield 6.32%, THC 31.08%; 80 °C, 330 bar: yield 10.41%, THC 24.73%; 80 °C, 330 bar, 5% wt. EtOH: yield 26.36%, THC 15.52%). Addition of ethanol as a co-solvent has proven to be necessary to boost the extraction yields and THC amounts since it has the capacity to extract highly polar compounds; however, it should be kept within a certain range to maximize its extracting ability.

Subsequent isolation and recovery of the extracted THC was achieved *via* SPE, yielding a highly pure product, as NMR and GC-FID analysis demonstrated. For the SPE, the extract was dissolved (0.05% trifluoroacetic acid in water) and injected into an SPE column packed with octadecyl-modified silica gel. A linear solvent gradient (0.05% trifluoroacetic acid in acetonitrile) from 0% to 100%, at a constant flow rate of 1.0 mL min^{-1}, was employed.[124]

The particle size of ground marijuana plants has a noticeable effect on the extracted amount of THC *via* scCO$_2$ (Table 3, entry 7).[150] Various particle sizes in the range of 0.800 mm < d < 0.063 mm (where d is the particle diameter) were evaluated. Even though complete removal of THC was observed in all samples, the highest amount of THC was recovered from the fractions with particle sizes of 0.063 mm < d < 0.125 mm, since the THC concentration varies with particle size (Fig. 9). Microscopic observation elucidated the observed differences; smaller particle sizes contain resinous parts rich in THC, whereas bigger particle sizes mainly consist of leaves and plant parts poor in THC.[150]

The effect of decarboxylation prior to scCO$_2$ extraction and consequent winterization on the enrichment of cannabinoids extracted from cannabis flowers *via* scCO$_2$, has been reported (Table 3, entries 8 and 9).[119] Decarboxylation serves the conversion of the acids of THC and CBD present in the flowers to their respective neutral compounds and is simply performed by exposing the flowers to increased temperature for a set amount of time. Winterization involves the suspension of the scCO$_2$ extracts to an organic solvent for the removal, *via* decanting, of the extracted flower waxes. Two varieties of cannabis with different cannabinoid composition were evaluated. Highest extraction yields were obtained with conventional organic solvent-based extraction (girl scout cookie: 37%, durga mata II: 31%), followed by scCO$_2$ extraction with the aid of a co-solvent (girl scout cookie: 32%, durga mata II: 26%) and, lastly, extraction with pure scCO$_2$ on samples decarboxylated prior to the extraction (girl scout cookie: 18%, durga mata II: 17%). In any case, scCO$_2$-based extractions exhibit higher selectivity towards the target cannabinoids compared to conventional extraction. Additionally, decarboxylation enriches the extracts

in THC and CBD (28% and 34% with decarboxylation *vs.* 9% and 6% without, respectively, for durga mata II), while winterization only has a negligible impact on the cannabinoid content of the recovered extracts. Concerning the essential oils extracted by scCO$_2$, it is observed that higher pressures favor their recovery.[119]

Efficient cannabinoid extraction from hemp material (buds, leaves, trimmings) can be obtained with the aid of scCO$_2$ and near-critical propane (Table 3, entries 10–12).[117] Although the solubility of cannabinoids follows an upward trend with increasing extraction pressure, the overall yield achieved in the case of raw (non-decarboxylated) material is higher than in the decarboxylated one (approx. 4% difference), which can be probably attributed to (i) the water present in the raw material, which acts as a polar co-solvent that favors the extraction of the more polar sample components and (ii) the presence of volatile compounds in the raw material that are extractable by scCO$_2$. Despite the lower overall yield obtained from decarboxylated samples, the selectivity towards cannabinoids as well as their respective recovery is higher (THC: 23 mg g^{-1}, CBD: 342 mg g^{-1} *vs.* THC: 5.49 mg g^{-1}, CBD: 24.7 mg g^{-1}) due to the much lower amount of the cannabinoid acidic forms present in the decarboxylated samples. An increase in pressure positively affects the extraction of cannabinoids, while addition of ethanol as co-solvent has a positive impact mainly on the acidic cannabinoids, specifically CBDA and THCA (for non-decarboxylated sample; with EtOH-CBDA: 442 mg g^{-1}, THCA: 24.0 mg g^{-1} *vs.* without EtOH-CBDA: 278 mg g^{-1}, THCA: 11.4 mg g^{-1}). Propane seems to be more efficient and faster than CO$_2$ in the recovery of the acidic cannabinoids from raw material and the recovered extracts are significantly richer (approx. 20%) in the desirable CBD.[117]

Tuning of the scCO$_2$ parameters for extraction of volatile compounds (monoterpenes, sesquiterpenes) from inflorescences of *Cannabis sativa* L. allows the recovery of fractions of different chemical profiles (Table 3, entry 13).[120] Additionally, the low temperatures employed, as opposed to conventional hydrodistillation processes, result in an aromatic extract of high quality since thermo labile components are spared degradation, while less energy is consumed in the process. The results are verified by their comparison and overlap with the output values of head space solid-phase microextraction.[120]

A study performed on six cannabis chemovars demonstrated that the chemical profile of extracts obtained *via* scCO$_2$ is not representative of the original flower (Table 3, entries 14–19).[118] Specifically, the scCO$_2$-derived concentrates are characterized by higher THC and CBD potency than the flower (THC: 75%, CBD: 41% *vs.* THC: 28%, CBD: 11%), while the observed decrease of monoterpene content and the increase in terpene alcohols and sesquiterpenes fail to reproduce the organoleptic characteristics (flavor, fragrance) of the flower (Fig. 10).[118] In this interesting study, the authors failed to point out that differences in terpene and terpenoid concentration between flowers and extracts are to be expected, if we consider that the volatility of these compounds differs in these two cases.

Recently, the combination of scCO$_2$ with ionic liquids (ILs) for the extraction of cannabinoids from industrial hemp has
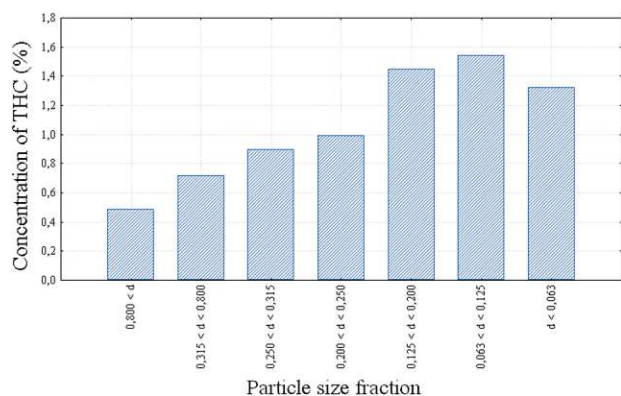
Fig. 9 THC concentration of different sieve fractions of marijuana.[150] Reprinted with permission.

690 | *Nat. Prod. Rep.*, 2023, **40**, 676–717

95

This journal is © The Royal Society of Chemistry 2023
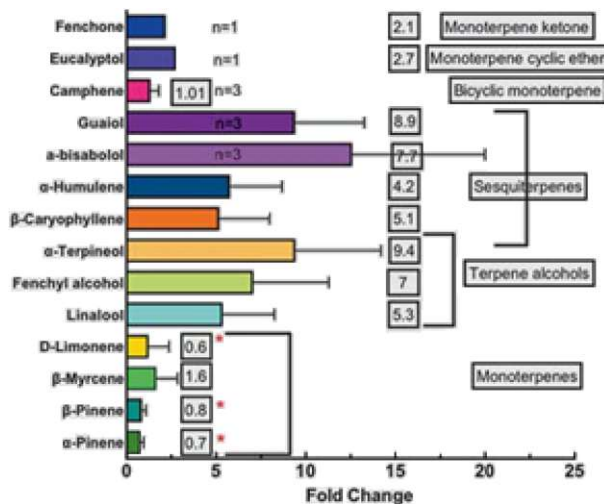
Fig. 10 Changes in the extraction efficiency of 14 terpenes/terpenoids across 6 cannabis chemotypes. Bars are the average fold change between flower and concentrate across all samples and error bars are the standard deviations (*n* is labelled when <6 samples contained this terpene or terpenoid).[118] Reprinted with permission, ©Georg Thieme Verlag KG.

Fig. 11 Conceptualization for the comparison of work up steps and yields of cannabinoid extraction techniques.[157] Used with permission of the Royal Society of Chemistry, permission conveyed through Copyright Clearance Center, Inc.

been reported (Table 3, entries 20–22).[157] The ability of ILs for partial dissolution of the hemp material prior to scCO$_2$ extraction was exploited; a relatively short time (15 min) at 70 °C, is enough to maximize the cannabinoid yield (THC, CBD, CBG) during the IL-based pretreatment step. Subsequent dilution before the scCO$_2$ extraction with H$_2$O is deemed necessary to reduce viscosity and optimize the mass transport, thereby allowing better scCO$_2$ penetration and higher extraction yields. Yields obtained with pure IL verify this hypothesis while results obtained with pretreatment based on pure H$_2$O indicate that ILs have the capacity to preserve the neutral forms of the target cannabinoids. The authors further demonstrated that the extraction yield and the IL cation are inextricably connected with acetate-based ILs exhibiting higher extraction efficiency than phosphate-based ones. Although the scCO$_2$-based approach had only slightly higher yield than the reference solvent-based approach, scCO$_2$ has the major advantage of enabling recovery of the target compounds in pure (non-contaminated with solvents) form, while the ratio of carboxylated to decarboxylated cannabinoids in the extract can be adjusted by simple tuning of the extraction parameters. Additionally, the IL used in the process can be recovered and reused for subsequent extraction cycles. An overview of the process developed by the authors is presented in Fig. 11.[157]

2.1.2. Seeds. The scCO$_2$ extraction conditions and the respective results that are discussed in this section pertaining to cannabis seeds are summarized in Table 4.

The quality characteristics of oil extracted from ground hemp seeds with scCO$_2$ under varying conditions of temperature and pressure were investigated by Da Porto *et al.* (Table 4, entry 23).[151] With constant scCO$_2$ flow rate and hemp seed particle size, it was determined that there was no significant difference in the yield of fatty acids extracted with various scCO$_2$
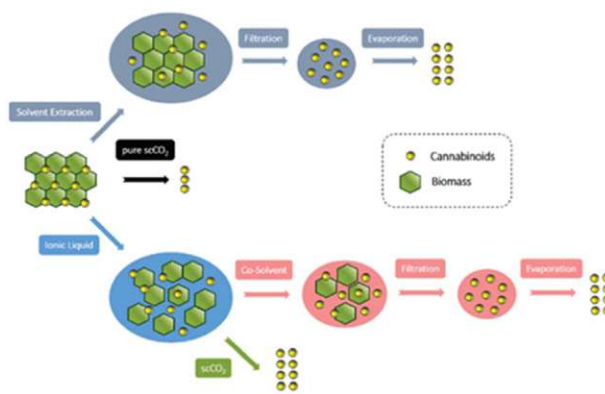
conditions of temperature (40, 60, 80 °C) and pressure (300, 400 bar) and Soxhlet extraction performed with *n*-hexane. The highest total oil recovery was obtained at two different sets of scCO$_2$ conditions (40 °C, 300 bar: 72.2% and 80 °C, 400 bar: 72.1%); nevertheless, it was still lower than the 100% yield obtained *via* Soxhlet extraction. On the other hand, the high selectivity of scCO$_2$ towards tocopherols results in a tremendously increased oxidation stability of the oil (2.18 *vs.* 0.17 mM eq. Vit E) compared to Soxhlet extraction, however, at the expense of total oil recovery.[151]

After experimentally setting the preliminary scCO$_2$ extraction parameters, the research group focused on determining, *via* response surface methodology (RSM), the effect of temperature, pressure and particle size on the total oil yield and its respective quality (expressed as oxidation stability) (Table 4, entry 24).[126] At a fixed flow rate and temperature of 50 °C, an increase in pressure (250 to 350 bar) significantly impacts the total oil yield in a positive manner, while a decrease in particle size further assists the observed positive impact. An increase in pressure implies increased scCO$_2$ density, thus, higher oil solubility, while smaller particle size, which results from seed grinding, means release of the oil from the broken seed cells as well as increased contact surface between solvent and seed. When the particle size is kept constant, maximum total oil yield is obtained at 40 and 60 °C, provided the pressure is over 300 bar, whereas, at values below 300 bar increasing temperature has a negative impact on the total yield. This behavior clearly implies the dominant effect of increased oil vapor pressure on the extraction at high pressures, while at lower pressures the density drop of scCO$_2$ is the dominant extraction factor. As far as oxidative stability is concerned, pressure and temperature are the factors with the highest influence, when a constant particle size is used; highest stability is favored at low pressures, regardless of the employed temperature, while higher pressures need to be combined with high temperatures to maximize the oxidative stability. When the temperature is kept constant at 50 °C, maximum yield stability is observed at the lowest pressure combined with the largest particle size. At constant

Table 4 Summary of scCO$_2$ extraction conditions and respective results pertaining to seeds of the cannabis plant[a]

Entry no.	Input sample	Particle size (mm)	scCO$_2$ conditions	Oil characteristics	Ref. no.
23	*Cannabis sativa* L., cultivar: Felina, seeds (ground), 300 g	1.50	80 °C, 300 bar, 10 kg h^{-1}, 30 kg CO$_2$ per kg feed	[c]Yield: 16.8 ± 0.7, [d]oxidation stability: 2.18 ± 0.04	151
24	*Cannabis sativa* L., cultivar: Felina, seeds (ground), 15 g	0.71	40 °C, 300 bar, 8 × 10^{-5} kg s^{-1}	[c]Yield: 21.5, [e]oxidation stability: 1.87 ± 5.6, [f]palmitic acid: 5.85 ± 0.06, stearic acid: 1.45 ± 0.04, oleic acid: 10.67 ± 0.14, linoleic acid: 59.21 ± 0.70, γ-linolenic acid: 3.40 ± 0.09, α-linolenic acid: 18.47 ± 0.63, eicosenoic acid: 0.12 ± 0.06, behenic acid: 0.84 ± 0.01	126
25	*Cannabis sativa* L., cultivar: Felina, seeds (ground),[b] 15 g	0.83 ± 0.05	40 °C, 300 bar, 8 × 10^{-5} kg s^{-1}, 4 h	[c]Yield: 24.50 ± 0.06, [e]oxidation stability: 0.80 ± 0.4, [f]palmitic acid: 5.70 ± 0.21, stearic acid: 1.91 ± 0.09, oleic acid: 11.10 ± 0.21, linoleic acid: 58.86 ± 0.01, γ-linolenic acid: 3.32 ± 0.02, α-linolenic acid: 18.14 ± 0.15, eicosenoic acid: 0.17 ± 0.04, behenic acid: 0.79 ± 0.01	152
26	*Cannabis sativa* L., seeds (dried, ground), 4 g	0.70	80 °C, 400 bar, 3 mL min^{-1}	[c]Yield: 0.442	153
27	*Cannabis sativa* L., genotype: Fedora 17, seeds (ground), 100 g	0.38 ± 0.15	40 °C, 400 bar, 1.94 kg h^{-1}	[c]Oil content: 33.34 ± 0.23, [f]palmitic acid: 6.36 ± 0.05, oleic acid: 12.67 ± 0.03, linoleic acid: 57.04 ± 0.02, γ-linolenic acid: 2.99 ± 0.03, α-linolenic acid: 15.68 ± 0.04, stearic acid: 2.68 ± 0.02, lignoceric acid: 0.19 ± 0.02, behenic acid: 0.44 ± 0.02, arachidic acid: 0.98 ± 0.01, β-citosterol: 85.83 ± 0.54, campesterol: 9.69 ± 0.08, stigmasterol: 4.00 ± 0.06	154
28	*Cannabis sativa* L., seeds (ground), 50 g	0.43	76 °C, 300 bar, 13 g min^{-1}, EtOH 8% of scCO$_2$ flow rate, 4 h	n. r.	155
29	*Cannabis sativa* L., cultivar: USO31, seeds (milled), 18 g	$d \leqq 1$	40 °C, 300 bar, 10 mL min^{-1}, 195 min	[c]Yield: 30.98 ± 1.02, [g]peroxide value: 5.50 ± 1.0, [f]palmitic acid: 6.36 ± 0.05, oleic acid: 12.67 ± 0.03, linoleic acid: 57.04 ± 0.02, γ-linolenic acid: 2.99 ± 0.03, α-linolenic acid: 15.68 ± 0.04, stearic acid: 2.68 ± 0.02, lignoceric acid: 0.19 ± 0.02, behenic acid: 0.44 ± 0.02, arachidic acid: 0.98 ± 0.01, β-citosterol: 85.83 ± 0.54, campesterol: 9.69 ± 0.08, stigmasterol: 4.00 ± 0.06, chlorophyll α: (107.23 ± 2.80) × 10^{-4}, chlorophyll β: (23.29 ± 3.99) × 10^{-4}, carotenoids: (61.00 ± 1.04) × 10^{-4}, α-tocopherol: (39.57 ± 0.72) × 10^{-4}, γ-tocopherol: (770.08 ± 10.75) × 10^{-4}, [h]polyphenols: 51.42 ± 0.31, [f]hexanal: (39.57 ± 0.71) × 10^{-4},	149

692 | *Nat. Prod. Rep.*, 2023, **40**, 676–717

97

This journal is © The Royal Society of Chemistry 2023

Table 4 (*Contd.*)

Entry no.	Input sample	Particle size (mm)	scCO$_2$ conditions	Oil characteristics	Ref. no.
				octadienal: $(10.29 \pm 3.18) \times 10^{-4}$, heptadienal: $(9.38 \pm 1.41) \times 10^{-4}$, nonanal: $(8.34 \pm 1.28) \times 10^{-4}$, nonenal: $(8.77 \pm 1.27) \times 10^{-4}$, hexanol: $(30.66 \pm 0.95) \times 10^{-4}$	
30	*Cannabis sativa* L., dehulled seeds (milled), 4 g	n. r.	40 °C, 400 bar, 1.15 mL min^{-1} scCO$_2$, 4 h	[i]Acidity index: 5.21 ± 0.08, [f]palmitic acid: 6.14 ± 0.08, oleic acid: 12.64 ± 0.03, linoleic acid: 57.97 ± 0.10, α-linolenic acid: 18.43 ± 0.04, stearic acid: 2.61 ± 0.03, eicosenoic acid: 0.31 ± 0.01, palmitoleic acid: 0.09 ± 0.00, erucic acid: 0.02 ± 0.01	131
31	*Cannabis sativa* L., dehulled seeds (milled), 4 g	n. r.	40 °C, 60 bar, 2.45 mL min^{-1} *n*-propane, 30 min	[i]acidity index: 4.95 ± 0.01, [f]palmitic acid: 6.09 ± 0.01, oleic acid: 13.16 ± 0.05, linoleic acid: 57.11 ± 0.05, α-linolenic acid: 18.53 ± 0.03, stearic acid: 2.83 ± 0.03, eicosenoic acid: 0.35 ± 0.02, palmitoleic acid: 0.11 ± 0.02, erucic acid: 0.21 ± 0.01	131
32	*Cannabis sativa* L., pressed-seed cake (ground)	0.38 ± 0.15	45 °C, 250 bar, 1.2 kg h^{-1}, 3.5 h	[c]Oil content: 9.97, [j]peroxide value: 2.98, [f]chlorophyll α: 19.35×10^{-3}, chlorophyll β: 3.54×10^{-3}, carotene: 12.54×10^{-3}	163
33	*Cannabis sativa* L., genotype: Fedora 17, pressed-seed cake (ground)	n. r.	60 °C, 300 bar, 2.80 kg h^{-1}, 1.75 h	[c]Yield: 14.97, [f]chlorophyll α: 27.27×10^{-3}, chlorophyll β: 9.79×10^{-3}, carotene: 9.18×10^{-3}	132

[a] All concentrations of extracted compounds within the table are reported as %, regardless of the units in which they were originally reported by the authors, in order to facilitate their comparison. [b] Ultrasonication prior to scCO$_2$ extraction (20 KHz, 10 min). [c] Reported in g oil per 100 g seeds. [d] Reported in mM eq. Vit E. [e] Reported in eq. a-tocopherol per mL oil. [f] Reported in % of the extracted hempseed oil. [g] Reported in meq. O$_2$ per kg oil. [h] Reported in mg of gallic acid eq. per kg of oil. [i] Reported in mg KOH per mg oil. [j] Reported in mmol O$_2$ per kg oil. (n. r. = not reported).

pressure of 300 bar, highest temperature applied at the smallest particle sizes maximizes the oxidative stability of the extracted oil. The oil derived by scCO$_2$ is of higher quality than the oil extracted *via* solvent extraction with Soxhlet (1.87 ± 5.6 *vs.* 0.84 ± 1.2 Eq α-toc/mL oil), however, the overall oil yield is lower (30% *vs.* 21.5%). It could be argued, considering the significantly large error margin in the oxidation stability of the oil, that the argument for higher quality of scCO$_2$-extracted oil based on this parameter alone can be easily questioned. However, the major factor which contributes to oil quality derived by scCO$_2$ is its higher selectivity; lack of selectivity in Soxhlet extraction implies removal of pigments and waxes, along with the oil, which are contaminated with solvent residues. In this case, refining of the oil is required which decreases its health value. As far as fatty acids are concerned, there is no significant difference in the obtained yields between scCO$_2$ and Soxhlet approach. Optimized scCO$_2$ conditions that would simultaneously maximize the total oil yield and the oxidative stability of the oil could not be determined.[126]

The research group further investigated the effect of ultrasonication on the scCO$_2$ extraction capacity of hempseed oil and fatty acids from intact hemp seeds (Table 4, entry 25).[152] Ultrasonication of the hemp seeds, in the absence of solvent, for 10 min, exerted a minor positive effect on the extraction yield (3.3% increase), compared to scCO$_2$ extraction without prior ultrasonication, most probably due to the enhanced mass transfer brought about by the augmented penetration rate of scCO$_2$. An increase, however, in the ultrasonication time had a reverse effect on the extraction yield, which can be attributed to ensuing degradation reactions occurring following the temperature increase generated by the effect of sonic cavitation during the ultrasonication process. Differences in fatty acid extraction yields obtained by *n*-hexane, scCO$_2$ and scCO$_2$ with prior ultrasound pre-treatment were only negligible (30%, 21% and 25%, respectively). Slightly higher primary oxidation of the oil was observed when ultrasonication was employed prior to scCO$_2$ extraction; however, it was still approximately half of the oxidation levels obtained by Soxhlet extraction. Concerning antiradical capacity (expressed in equivalents of tocopherol per mL of oil), the highest levels were obtained *via* scCO$_2$ due to its high selectivity towards tocopherols, while a significant decrease was observed *via* ultrasonication and Soxhlet extraction (1.87 *vs.* 0.80, 0.84).[152]

The impact of varying the parameters of temperature (40–80 °C) and pressure (200–400 bar) on the scCO$_2$-based recovery of oil from hemp seeds has been evaluated by Tomita *et al.* (Table 4, entry 26).[153] At low pressure, a reverse significant dependency of the yield on the extraction temperature was established (at 200 bar; 40 °C: 39%, 60 °C: 18%, 80 °C: 6%). In contrast, when high pressure was employed the correlation of the extraction efficiency on the employed temperature was negligible (at 400 bar; 40 °C: 39%, 60 °C: 41%, 80 °C: 44%), while the obtained yield was comparable to that achieved by Soxhlet extraction with *n*-hexane (42%). This is in contrast to the observation that Da Porto *et al.* made,[151] where scCO$_2$ could not reach a total extraction yield comparable to Soxhlet, however, in that case a lower flow rate was employed. As temperature rises, the positive impact of increasing temperature on the overall oil recovery becomes quite notable. In any case, concurrently employing high temperatures and pressures favors the overall extraction yield. It should be noted that even though the nutritionally desirable ratio of ω-6 to ω-3 fatty acids (~3 : 1) is similar when scCO$_2$, Soxhlet or cold-press extractions are employed, unsaturated fatty acid, linoleic acid and linolenic acid are selectively extracted by scCO$_2$.[153]

The effect of variable scCO$_2$ conditions on the extraction of tocopherols, fatty acids and pigments from hempseed oil has been studied and compared to traditional extraction approaches, namely, Soxhlet and cold pressing (Table 4, entry 27).[154] Temperature, pressure and time were varied, while hemp particle size and solvent flow rate were kept constant throughout the experiments. Fatty acid extraction (α- and γ-linolenic, oleic and linoleic acid) showed no dependency on the process temperature, in contrast to tocopherols (α- and γ-) which were reduced to almost half by an increase in temperature by 20 °C (40 to 60 °C). In a similar fashion, no effect of pressure was exhibited on fatty acid extraction efficiency, while an increase in pressure by 100 bar (300 to 400 bar) exerted a dramatically negative impact on tocopherol extraction, which was more pronounced for the α-form (α-form: 110 to 31 mg g^{-1}, γ-form: 182 to 164 mg g^{-1}). These observations regarding the dependency of fatty acid yield on the employed extraction conditions so far agree with what has been previously reported by Tomita *et al.*[153]

Pigment extraction can widely vary depending on the scCO$_2$ extraction parameters; however, extraction time appears to have the most marked impact (Table 4, entry 27). With regard to overall hempseed oil yield, it was affected to a negligible degree by a 20 °C increase in temperature and it was favored by higher pressure. In terms of the amount of accessed tocopherols, scCO$_2$ extraction had superior performance to the other approaches, while all 3 approaches performed equally in fatty acid extraction. The lowest total pigment recovery is obtained with scCO$_2$, whereas the mechanical force applied in cold pressing results in the highest pigment recovery.[154]

A statistical model (central composite design of response surface methodology) was developed and experimentally verified to obtain the optimum scCO$_2$-based extraction of ω-6 linoleic and ω-3 α-linolenic fatty acids from hemp seed oil (Table 4, entry 28).[155] The output response of several input parameters, namely temperature, pressure, CO$_2$ flow rate, hemp seed particle size and co-solvent flow rate, was evaluated for the process optimization, while all input parameters were found to be statistically significant. Experimental results demonstrate that, in practice, variations in temperature do not affect the extraction profile of the fatty acids; although mass transfer is favored by an increase in temperature, at the same time, the impact it has on solvent density, *i.e.*, by reducing it, implies reduced solubility of the target compound, therefore, these 2 concurrent phenomena balance out each other's effect on extraction efficiency. Reducing the particle size of the hemp seed only has a positive effect on the extraction efficiency (27% to 34%). Pressure also has a positive effect, with a 150 bar increase (200 bar to 350 bar) leading to an approx. 10% higher

694 | *Nat. Prod. Rep.*, 2023, **40**, 676–717

99

This journal is © The Royal Society of Chemistry 2023

overall extraction efficiency (24% to 36%), which can be explained by the pressure-induced increase of the $scCO_2$ density, thus, increased solubility in the solvent. Higher flow rates, both for $scCO_2$ and co-solvent, have a considerable impact on the overall extraction ($scCO_2$: 5 g min^{-1}-22%, 10 g min^{-1}-34% and co-solvent: 0% of CO_2: 20%, 10% of CO_2: 35%), due to increased solute–solvent interaction and hydrogen bonding formation between –OH groups of the co-solvent and the charged polar groups of the fatty acids, respectively.[155]

The advantageous properties of CO_2, either in super- or subcritical state, in contrast to conventional liquid extraction of hemp seed oils has been demonstrated (Table 4, entry 29).[149] Aside of its environmental compatibility, CO_2 has the ability to enhance either the yield or selectivity towards valuable compounds.

Although the recoveries obtained with CO_2-based approaches were lower (93% for supercritical, 68% for subcritical) compared with the liquid extraction relying on n-hexane (100%), the oxidation of the recovered hemp seed oil was lower. The effect of fluctuating temperature, air and light in the opened-system conventional extraction is partly accountable for the observed difference. An additional factor, which explains the significantly lower oxidation in the case of subcritical CO_2, is the substantially smaller amount of extracted chlorophyll (27 mg kg^{-1} oil vs. 143 mg kg^{-1} oil), which acts as a photosensitizer that accelerates the oil oxidation.

Total polyphenol extraction between CO_2 and n-hexane does not have a statistically significant difference, however CO_2 is marked by higher selectivity towards these compounds. Even though higher tocopherol yields are obtained with the conventional extraction, subsequent refinement leads to substantial content reduction, thus, the yield of the food grade product obtained with all 3 approaches is ultimately comparable.

Non-intoxicating cannabinoids, cannabidiol (CBD) and cannabinol (CBN), are selectively assessed by subcritical CO_2 which also enhances the obtained yields by approx. a factor of 2 compared to n-hexane and $scCO_2$-based approaches (subcritical CO_2; CBD: 72 mg kg^{-1} oil, CBN: 114 mg kg^{-1} oil vs. n-hexane; CBD: 41 mg kg^{-1}, CBN: 47 mg kg^{-1} and $scCO_2$; CBD: 69 mg kg^{-1}, CBN: 77 mg kg^{-1}, respectively). The extraction method had no significant effect on the yields of fatty acids, triglycerides and phytosterols. Volatile organic compounds, namely aldehydes (hexanal, octadienal, heptadienal, nonanal, nonenal), characterized by pleasant odor are dominantly extracted with CO_2.[149]

The merit of pressurized n-propane as an alternative to $scCO_2$ for the extraction of oil from dehulled hemp seeds has been reported (Table 4, entries 30 and 31).[131] Reduction in operational costs can be achieved due to the ability of propane to access the same amount of oil as $scCO_2$ at lower pressures (approx. 37–40% at 42.5 bar instead of 73.8 bar for $scCO_2$) and with significantly lower solvent consumption (flow rates: 1.15 mL min^{-1} for propane, 2.45 mL min^{-1} for $scCO_2$). Additionally, it was demonstrated that the use of dehulled hemp seeds favored the extraction yield with the same $scCO_2$ conditions described in the literature. Product of high nutritional value, as

Table 5 Summary of $scCO_2$ extraction conditions and respective results pertaining to processing residues of the cannabis plant[a]

Entry no.	Input sample	Particle size (mm)	$scCO_2$ conditions	Extracted compounds	Ref. no.
34	*Cannabis sativa* L., variety: Santhica, hemp dust residues	n. r.	50 °C, 350 bar, 35 g min^{-1}, 4 h	[b]CBD: 0.12 ± 0.04, [c]fatty acids: 2000 ± 100, n-policosanols: 790 ± 20, fatty aldehydes: 990 ± 10, n-alkanes: 1250 ± 20, wax esters: 1350 ± 30, sterols: 1600 ± 10	160
35	*Cannabis sativa* L., cultivar: Beniko, threshing residues (dried, ground), 10 g	0.2	70 °C, 465 bar, 2–3 standard L min^{-1}, density 0.0018 g mL^{-1}, 2 h	[d]CBD: 2.47 ± 0.03, CBDA: 26.1 ± 0.22	162
36	*Cannabis sativa* L., cultivar: Felina 32, threshing residues, 500 g	n. r.	45 °C, 450 bar, 7 kg h^{-1}	[e]THC: 5.7, d^8-THC: 1.6, THCA: 0.9, CBD: 509, CBDA: 109, CBC: 27.3, CBG: 9.1, CBN: 6.1	133
37	*Cannabis sativa* L., cultivar: Kompolti (2014), threshing residues, 500 g	n. r.	45 °C, 450 bar, 7 kg h^{-1}	[e]THC: 18.6, d^8-THC: 3.6, THCA: 0.5, CBD: 791, CBDA: 118, CBC: 36.4, CBG: 18.2, CBN: 7.9	133
38	*Cannabis sativa* L., cultivar: Kompolti (2016), threshing residues, 500 g	n. r.	45 °C, 350 bar, 7 kg h^{-1}	[e]THC: $(10 \pm 4.3) \times 10^{-3}$, d^8-THC: $(2.6 \pm 0.4) \times 10^{-3}$, THCA: $(46.1 \pm 3) \times 10^{-3}$, CBD: $(160.7 \pm 71.4) \times 10^{-3}$, CBDA: $(1660.7 \pm 53.6) \times 10^{-3}$, CBC: $(17.9 \pm 1.8) \times 10^{-3}$, CBG: not detected, CBN: $(1.3 \pm 0.3) \times 10^{-3}$	133
39	*Cannabis sativa* L., cultivar: Kompolti, threshing residues (ground), 500 g	0.44 ± 0.01	45 °C, 450 bar, 7 kg h^{-1}, 10% (w/w) EtOH	n. r.	161

[a] All concentrations of extracted compounds within the table are reported as %, regardless of the units in which they were originally reported by the authors, in order to facilitate their comparison. [b] n. r. [c] Reported in μg g^{-1} of hemp dust. [d] Reported as % of the total extract. [e] Reported as % of the input sample. (n. r. = not reported).

This journal is © The Royal Society of Chemistry 2023

100

Nat. Prod. Rep., 2023, **40**, 676–717 | **695**

this is expressed in ω-3 to ω-6 fatty acid ratio (2.5–5.0), is obtained by employing a propane-based extraction, as well as of lower acidity and humidity values. Furthermore, the total tocopherol yield is higher and, unlike $scCO_2$ where higher temperatures favor tocopherol extraction, independent of the employed extraction temperature, thus, yielding an oil of superior antioxidant value with lower energy consumption.[131]

Aladić *et al.*[163] demonstrated the residual oil from hemp pressed cake can be fully removed with the aid of $scCO_2$ (Table 4, entry 32). The residual oil obtained with this approach is richer in pigments (chlorophyll α & β, carotene) than the cold press-based extracted oil (chlorophyll α: 194 μg g^{-1} oil, chlorophyll β: 35 μg g^{-1} oil & carotene: 125 μg g^{-1} oil *vs.* chlorophyll α: 59 μg g^{-1}, chlorophyll β: 39 μg g^{-1} & carotene: 31 μg g^{-1}, respectively).[163]

In a subsequent study, the same research group performed additional studies on the recovery of residual oil from hemp pressed cake with the aid of $scCO_2$ (Table 4, entry 33).[132] An RSM experimental design was utilized to optimize the extraction parameters; the effect of the variation in pressure, solvent flow rate and temperature on the output responses of extraction yield, pigment content (chlorophyll α & β, carotene) in the recovered oil and extraction time was evaluated. An increase in pressure and solvent flow rate shortens the duration of the extraction process (from 7.5 h to 1.5 h), while temperature does not appear to have any statistically significant effect. The oil solubility is favored at higher pressures, thus, the overall yield is favored at high pressure, whereas concurrent increase in temperature enhances the positive impact. The most decisive factor in the extraction of pigments is pressure; an increase has a dramatically positive effect on the extraction yield, which is statistically independent from the variations in temperature and solvent flow rate.

Extraction *via* $scCO_2$ was successful in the complete removal of residual oil from pressed hemp cake, which has been in the prior step subjected to cold-pressing for oil recovery. Following the cold-pressing process, the defatted hemp cake is enriched in proteins and fibers suitable for other food-related applications, meaning that a zero-waste process has been developed.[132]

2.1.3. Processing residues. The $scCO_2$ extraction conditions and the respective results that are discussed in this section pertaining to cannabis processing residues are summarized in Table 5.

The feasibility of recovery and exploitation of valuable compounds from waste dust generated during processing of hemp for fiber extraction was demonstrated, while two extraction approaches relying on Soxhlet and $scCO_2$ were evaluated and compared (Table 5, entry 34).[160] The chemical composition of fractions collected from different steps of the fiber extraction process indicates that the machinery used in each step leads to the generation of residues with specific profiles; specifically, fractionation of the lipophilic components (unsaturated fatty acids, long-chain alcohols, fatty aldehydes and long-chain hydrocarbons, wax esters) was observed. It should be noted, that the highly desirable CBD was accumulated in one step of the mechanical process. Although the overall extraction yield of crude wax with $scCO_2$ is favored at high temperatures and

pressures (65 °C, 400 bar), the majority of the lipophilic compounds, with the exception of long-chain fatty acids, reaches the highest extraction yields at milder conditions (50 °C, 350 bar). Contrary to conventional extraction approaches, $scCO_2$ offers the possibility of simple separation of CBD from intoxicating and lipophilic compounds, by simple tuning of the temperature; CBD exhibits higher solubility at lower temperatures.[160]

Quantitative removal (90–99%) of the bioactive components present in *Cannabis sativa* threshing residues was successfully obtained with a combination of three extraction processes performed in a consecutive order; $scCO_2$, pressurized liquid (PLE) and enzyme-assisted extractions (EAE) (Table 5, entry 35).[162] The majority of the lipophilic cannabinoid fraction, which contains the bioactive CBD and CBDA, was recovered by applying the optimized $scCO_2$ parameters, which were generated *via* an RSM approach. Although all 3 parameters considered during RSM (pressure, temperature and extraction time) are significant in terms of the final yield, an increase in pressure seems to have the most dramatic impact on increasing the extraction of cannabinoids. It was observed, however, that during the extraction process decarboxylation of CBDA most probably took place, as demonstrated by the changing ratios of CBD and CBDA in the extract compared with their ratios in the threshing residue. For the recovery of the polar constituents with antioxidant properties, the residue of the $scCO_2$ extraction was subjected to PLE, which serves as a faster alternative to conventional extraction approaches, at elevated temperature and pressure. A two-step PLE with the aid of acetone and subsequently a mixture of $EtOH/H_2O$ results in the removal of the polar phenolic and flavonoid constituents. Additionally, in the final step, hydrophilic mono- and disaccharide fractions (glucuronic, malic, citric and succinic acid) can be accessed with EAE, resulting in a 94% recovery of sugars.[162]

The feasibility of a pilot plant scale $scCO_2$ set-up for the recovery of cannabinoids from different industrial hemp threshing residues was demonstrated (Table 5, entries 36–38).[133] The solvent flow rate and extraction temperature were kept constant, while the effect of pressure and fractionation on the cannabinoid yield were evaluated. Although an increase in pressure generally increases the solubility of solutes in $scCO_2$, thus, favoring the yield, it was concluded, in contrast to other reported studies, that mild pressures are sufficient to maximize the yield and any further increase in pressure does not exert any additional impact (Fig. 12). Fractionation of the extracted compounds was obtained by using two separators set at different pressure levels; the cannabinoids were recovered in the separator set at higher pressure and in the other fraction the fragrant compounds of the hemp residues were collected. Additionally, the dependency of the extracted cannabinoid amount on the quality of the threshing residue was demonstrated as well as the dependency of the nature of the extracted cannabinoids on storage time; freshly collected residues had higher amounts of the acidic form of the cannabinoids compared to older samples, in which cannabinoid decarboxylation naturally occurs over time.[133]
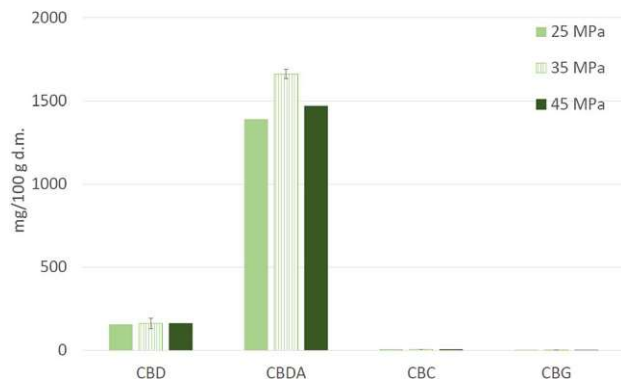
696 | *Nat. Prod. Rep.*, 2023, **40**, 676–717

101

This journal is © The Royal Society of Chemistry 2023

Fig. 12 Effect of extraction pressure on the non-intoxicating cannabinoids (d. m. = dry matter).[133] Open access, CC BY 3.0, https://creativecommons.org/licenses/by/3.0/.
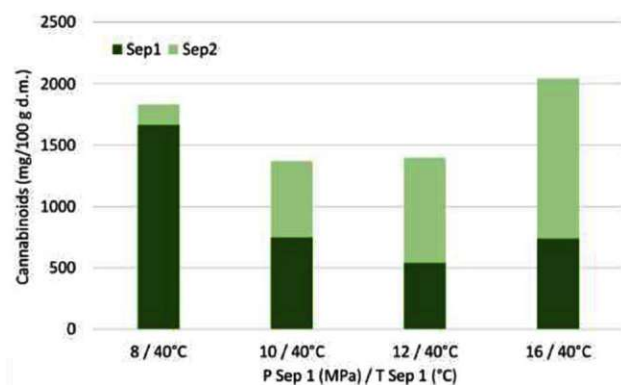

Fig. 13 Effect of separator pressure on the yield of cannabinoids in the extract from 1st and 2nd separator by scCO$_2$ extraction.[161] Open access, CC BY-NC-ND 4.0, https://creativecommons.org/licenses/by-nc-nd/4.0/.

The research group subsequently employed the pilot plant to investigate the effect of super- and sub-critical CO$_2$ on the recovery of valuable cannabinoids from six different industrial hemp threshing residues (Table 5, entry 39).[161] Comparison of the CO$_2$-based extractions with Soxhlet extraction revealed that conventional extraction leads to higher overall yield (1.8–2.3% *vs.* 21% with Soxhlet employing EtOH); however, higher

selectivity towards the target cannabinoids (THC, CBD, CBN, CBG, CBC) can be achieved with CO$_2$ extractions. Low pressure and moderate temperature favor the cannabinoid extraction, while neutral cannabinoids are extracted at the beginning of the process followed by their acidic equivalents. Fractionation of the cannabinoids was also performed by using two separators set at different pressures (Fig. 13). The majority of the cannabinoids was recovered in the separator operating at lower pressure, while their efficient separation from the hemp fragrant compounds was obtained. Addition of a co-solvent in the scCO$_2$ extraction significantly increases both the overall and cannabinoid yield (by 30% each). The subcritical CO$_2$ extraction operates at milder conditions and requires lower solvent consumption resulting in highly concentrated extracts.[161]

2.1.4. Roots. The scCO$_2$ extraction conditions and the respective results that are discussed in this section pertaining to cannabis roots are summarized in Table 6.

The impact of a scCO$_2$-based extraction on a largely neglected part of the hemp plant, namely its roots, has been recently reported (Table 6, entries 40–42).[156] From a chemical perspective, the profile of the roots differs significantly from the rest of the plant, since it is characterized by an abundance in triterpenes and phytosterols. As the authors demonstrated, both harvesting period and sample drying conditions seem to have an impact on the amount of the accessed triterpenoids, with harvesting after the summer months and increased drying temperatures exerting a negative impact. Comparison of the scCO$_2$ approach with conventional solvent-based extraction proves that conventional extraction has the advantage of higher extraction efficiencies with lower solvent consumption (Fig. 14); for the conventional extraction (*n*-hexane or EtOH) 8 mL of solvent are required, while for the scCO$_2$ approach, where EtOH is used as a modifier, 180 mL of CO$_2$ are consumed and 18 mL EtOH (3 mL min^{-1} CO$_2$, 10% EtOH, 60 min). Nevertheless, this is one of the first studies where extraction of triterpenoids, namely epifriedelinol and friedelin, with scCO$_2$ has been reported in the literature. Additionally, the study identified some previously unidentified metabolites, *i.e.*, two triterpenoids, four phytosterols and one aliphatic compound.[156]

It is evident thus far that employing scCO$_2$ in the recovery of valuable compounds from various cannabis sources (flowers, seeds, processing residues) is quite promising; apart from

Table 6 Summary of scCO$_2$ extraction conditions and respective results pertaining to roots of the cannabis plant[a]

Entry no.	Input sample	Particle size (mm)	scCO$_2$ conditions	Extracted compounds	Ref. no.
40	*Cannabis sativa* L., cultivar: Futura 75 (dried, milled), Jul. 2019, 0.5 g	1	60 °C, 200 bar, 3 mL min^{-1}, 10% (v/v) EtOH, 2 h (1 h static/1 h dynamic)	[b]Friedelin: 0.0373 ± 0.0012	156
41	*Cannabis sativa* L., cultivar: Futura 75 (dried, milled), Aug. 2019, 0.5 g	1	60 °C, 200 bar, 3 mL min^{-1}, 10% (v/v) EtOH, 2 h (1 h static/1 h dynamic)	[b]Friedelin: 0.0434 ± 0.0038	156
42	*Cannabis sativa* L., cultivar: Futura 75 (dried at 45 °C for 30 h, milled), Oct. 2019, 0.5 g	1	60 °C, 200 bar, 3 mL min^{-1}, 10% (v/v) EtOH, 2 h (1 h static/1 h dynamic)	[b]Friedelin: 0.0100 ± 0.0005	156

[a] All concentrations of extracted compounds within the table are reported as %, regardless of the units in which they were originally reported by the authors, in order to facilitate their comparison. [b] Reported as % in dried hemp root.
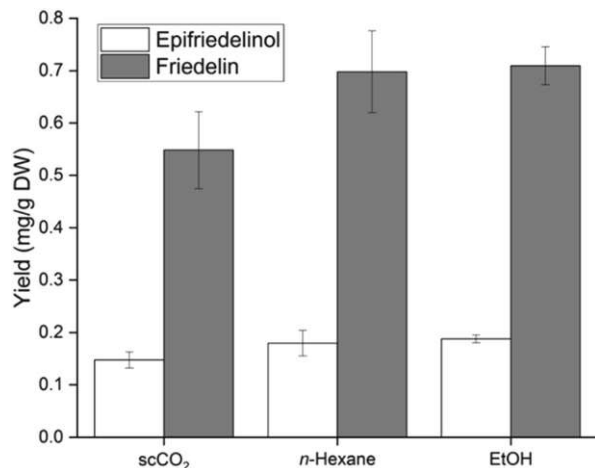
Fig. 14 Yield of epifriedelinol and friedelin in mg g^{-1} dry weight by different extraction approaches.[156] Open access, CC BY 4.0, https://creativecommons.org/licenses/by/4.0/.

Fig. 15 Schematic of pretreatment on lignocellulosic material.[187] Reprinted with permission from Elsevier.

having certain ecological advances, it offers the additional advantages of easy product separation from the extraction solvent by simple depressurization, which is a very attractive feature for food and pharmaceutical applications since there is no contamination of the product by solvent residues, increased extraction speed and selectivity, tunability of the extract composition by variation in pressure and temperature conditions, as well as fractionation of the recovered constituents.

Despite the extensive commercialization of scCO$_2$ in the cannabis industry, on a research level it is still at a nascent stage. There is still room to further understand and subsequently exploit the possibilities that scCO$_2$ has to offer; however, the basis that will eventually lead to this desirable direction has already been set.

2.2. Ionic liquids and deep eutectic solvents

Ionic liquids (ILs) are liquids that consist exclusively of ions and have melting points below 100 °C.[183] The distinctive and unique properties that characterize ILs, such as negligible vapor pressure, wide solubility range, non-flammability and tunable nature, by simple variation of their building anions and cations, has rendered them suitable for a wide range of extractions and separations. They are considered to be viable candidates for more sustainable extraction approaches, since they can replace the usually toxic and flammable organic solvents, reduce chemical waste and improve the safety of chemical processes and products.[183,184]

Ionic liquids are of particular interest for biomass extraction; the strong hydrogen bonding between the lignocellulose polymers poses a challenge for conventional solvents, while ILs have the ability to break these bonds, thus, allowing higher access to the active target compounds (Fig. 15). Apart from the higher extraction yield for active ingredients that can be obtained by employing ILs, they also significantly shorten the extraction time since they can be combined with microwave or ultrasound irradiation techniques.[185] The selection of the IL anion clearly
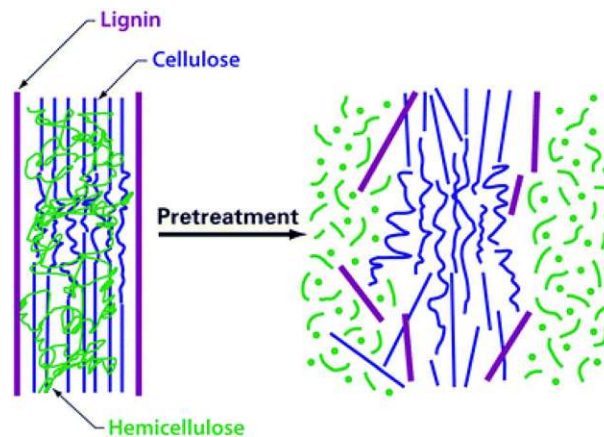
has an impact on the extraction efficiency of the IL with an increase in anion basicity being in line with extraction capacity. There does not seem to be a trend regarding the cation; however, the aromatic-based pyridinium and imidazolium ILs exhibit better extraction capacity than their phosphonium and ammonium counterparts.[186]

Deep eutectic solvents (DESs) are eutectic mixtures formed by the combination of two or more components; specifically, Lewis or Brønsted acids and bases comprising a variety of anionic and/or cationic species. They are considered to be IL analogues,[188] and are ideal candidates to replace commonly employed organic solvents due to their low toxicity and low vapor pressure, while, at the same time, they offer the advantage of tunability of their properties by simple variation of the mixing components and/or their respective ratios. Additionally, their comparably low price and biodegradable nature make them both financially desirable and environmentally compatible.[189]

The extraction conditions with ionic liquids/deep eutectic solvents and the respective results that are discussed in this section are summarized in Table 7.

Deep eutectic solvents were investigated for the extraction of CBD from powdered leaves of industrial hemp as a low cost and environmentally friendly approach with possibility for upscaling (Table 7, entry 43).[158] The evaluated DESs were based on choline chloride and betaine combined with various hydrogen bond donors. A preliminary screening at set conditions (DES concentration, solid : liquid ratio, temperature, time) revealed choline chloride/(+)-diethyl L-tartrate as the most efficient extractant for CBD with comparable performance to the less environmentally friendly methanol, which was used as a control sample. The highest polarity (experimentally determined) which is exhibited by this DES, compared to its counterparts, is a key indicator of its superior dissolving capacity towards the polar CBD. Nevertheless, calculations of the hydrogen bond ability of the evaluated DESs indicate that polarity alone is not the decisive factor of the DES's extracting capacity.

The impact of the individual extraction parameters on the process performance were individually evaluated. In order to

698 | Nat. Prod. Rep., 2023, 40, 676–717

103

This journal is © The Royal Society of Chemistry 2023

Table 7 Summary of extraction conditions with ionic liquids/deep eutectic solvents and respective results pertaining to the cannabis plant[a]

Entry no.	Input sample	Particle size (mm)	Conditions	Extracted compounds	Ref. no.
43	*Cannabis sativa* L., leaves (dried, powdered), 0.2 g	0.25	68% DES (choline chloride/(+)-diethyl-L-tartrate) in water, solid : liquid 1 : 24, 48 °C, 55 min (with the aid of ultrasonication)	[b]CBD: 1.2	158
44	*Cannabis sativa* L., inflorescences (ground), 0.02 g	n. r.	0.8 mL DES (L-menthol/acetic acid), 30 °C, 10 min (with the aid of ultrasonication)	[b]THC: 6.32 ± 0.72, THCA: 7.92 ± 1.44, CBD: 0.40 ± 0.08, CBDA: 1.68 ± 0.32	164
45	*Cannabis sativa* L., leaves (dried, powdered)	0.25	Pure IL [C_6mim][NTf_2], solid : liquid 1 : 25, 60 °C, 50 min	[b]CBD: 0.72	159

[a] All concentrations of extracted compounds within the table are reported as %, regardless of the units in which they were originally reported by the authors, in order to facilitate their comparison. [b] Reported as % of the input sample. (n. r. = not reported).

maximize the hydrogen bond capacity of the DES, while maintaining the viscosity at manageable levels, 70% of DES in water is deemed the optimum option; too much water (exceeding 50%) eliminates the desirable hydrogen bond interaction between the DES and the solute, whereas too little water (less than 30%) complicates the separation due to the high viscosity of the mixture. Similarly, driven by viscosity considerations, the solid : liquid ratio for the separation was set at 1 : 25. An increase in temperature favors the extraction (no CBD is detected at samples in RT) by enabling the mass transfer and diffusion processes, while it has the beneficial effect of reducing the system viscosity. However, it should be carefully adjusted to avoid the degradation of heat sensitive natural compounds. Prolonging the extraction process benefits the extraction up to a certain time point beyond which no further effect is observed. Mildly acidic pH, in which the extraction system itself results, is necessary to maximize the CBD yield (Fig. 16). An RSM approach, verified that the selected conditions were indeed the optimum to maximize CBD extraction.

Recovery of the CBD from the crude extract is feasible with the aid of macroporous resins. The highest recovery is reported with the microporous absorbent resin DM-130 (81%), resulting in a dried sample of 29% purity.[158]

An environmentally benign approach relying on hydrophobic DESs was developed for the recovery of cannabinoids (THC, CBD, THCA, CBDA) from ground cannabis inflorescences (Table 7, entry 44).[164] Menthol and carboxylic acids were the evaluated hydrogen-bond acceptor and hydrogen-bond donor, respectively. The extraction process was performed near RT (30 °C) with the aid of ultrasonication. The highest yields for all target cannabinoids were obtained with the DES comprising menthol and acetic acid, except for THC for which menthol combined with formic acid generated slightly higher yields. Additionally, replacing menthol with other terpenes, established menthol as the optimum hydrogen-bond donor to maximize extraction yields. Comparison of the developed DES extractant with commonly used organic solvents demonstrated the superior performance, in terms of extraction, of the DES (Fig. 17).[164]

Imidazolium-based ILs were evaluated as alternative solvents for CBD extraction from powdered industrial hemp leaves (Table 7, entry 45).[159] Decarboxylation of CBDA provides the desirable CBD. The rate of this conversion in the evaluated imidazolium IL extractants is much higher than in methanol

Fig. 16 Single factor effect on the extraction of CBD using choline chloride/(+)-diethyl L-tartrate; (a) solid : liquid 1 : 20, 40 °C, 60 min, pH not adjusted, (b) 70% DES, 40 °C, 60 min, pH not adjusted, (c) 70% DES, solid : liquid 1 : 25, 60 min, pH not adjusted, (d) 70% DES, solid : liquid 1 : 25, 50 °C, pH not adjusted, (e) 70% DES, solid : liquid 1 : 25, 50 °C, 60 min.[158] Reprinted with permission from Elsevier.

Fig. 17 Comparison of the extraction yields (mg g^{-1}) of target cannabinoids obtained with different organic solvents and the menthol : acetic acid (M : AA) hydrophobic DES.[164] Reprinted with permission from Elsevier.

This journal is © The Royal Society of Chemistry 2023

104

Nat. Prod. Rep., 2023, **40**, 676–717 | **699**

Table 8 Summary of solvent-based extraction conditions and respective results pertaining to the cannabis plant[a]

Entry no.	Input sample	Solvent	Conditions	Extracted compounds	Ref. no.
46	Cannabis, variety: Bedrocan, female flower tops (air dried, ground), 5 g	Naphtha, petroleum ether, ethanol, olive oil –water, olive oil	98 °C, 20–120 min, 4–20 mL solvent per g cannabis	[b]THC: 5–33, THCA: 67–95, [c]β-pinene: 7.5, myrcene: 23.1, β-phellandrene: 8.4, cis-ocimene: 12.1, terpinolene: 43.8, terpineol: 5.2, [d]β-caryophyllene: 25.8, humulene: 14.8, δ-guaiene: 14.4, γ-cadinene: 12.4, eudesma-3,7-(11)-diene: 13.1, elemene: 19.5	121
47	*Cannabis sativa* L., seeds (ground), 5 g	*n*-hexane	20–70 °C, 5–15 min, 3–10 mL solvent per g cannabis	[e]Hempseed oil: 26.6–30.4	165
48	*Cannabis sativa* L., seeds (ground), 5 g	*n*-hexane	20–70 °C, 10 min, 3–10 mL solvent per g cannabis	[e]Hempseed oil: 25.6–30.0	146
49	*Cannabis sativa* L., female inflorescences (ground), 5 g	Olive oil	35–145 °C, 40–120 min, 10 mL solvent per g cannabis	[f]THC: 0.3–15, THCA: 0.01–15.5	122
50	*Cannabis sativa* L., aerial parts of young and mature hemp (ground), 5 g	H_2O, EtOH (30–90%)	RT, 24 h, 20 mL solvent per g cannabis	[g]Phenols: 6.2–17.1, [h]flavonoids: 1.8–11.2	127
51	*Cannabis sativa* L., hemp press cake	200 mM NaCl, pH 12	RT, 30 min, pH adjusted with NaOH or HCl, 10% (w/w) press cake suspension, RT, 12 h (after pH adjustment)	[i]Total phenolic content: 81	172

[a] All concentrations of extracted compounds within the table are reported as %, regardless of the units in which they were originally reported by the authors, in order to facilitate their comparison. [b] Reported as % of the total extracted THC + THCA content. [c] Reported as % of total monoterpene content. [d] Reported as % of total sesquiterpene content. [e] Reported as % extracted oil from he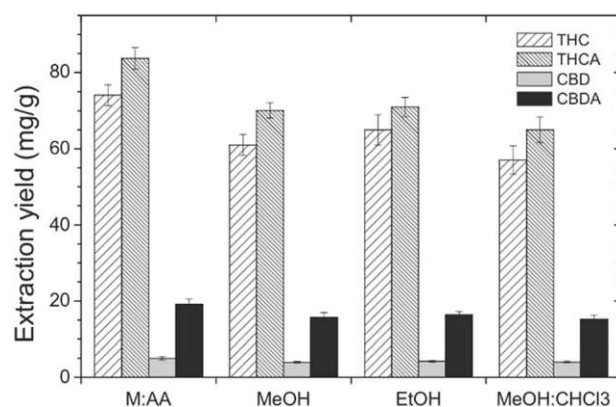mp seed. [f] Reported as % in olive oil extracts. [g] Reported as mg of gallic acid equivalent per g dry weight hemp. [h] Reported as mg of catechin equivalent per g dry weight hemp. [i] Reported as mg gallic acid equivalent per 100 g extract.

due to the lower polarity of these ILs compared to methanol. The solvation effect provided by ILs lowers the energy barrier required for the conversion reaction. Additionally, ILs enhance the stability of the extracted CBD *via* formation of hydrogen bonding with the photooxidation site of CBD. Increasing of the IL lipophilicity enhances the extraction of the lipophilic CBD; the IL with the longest cation chain and a hydrophobic anion, [C₆mim][NTf₂], was the optimum extractant with yields exceeding 80%, under optimized conditions of temperature, time and solid-to-liquid ratio. The majority of the extracted CBD can be recovered by back-extraction with a mixture of organic solvents or an $AgNO_3$ solution (>90% recovered in both cases), thus, enabling the recycling of the IL.[159]

2.3. Solvent-based extraction

The solvent-based extraction conditions and the respective results that are discussed in this section are summarized in Table 8.

Romano *et al.*[121] evaluated different organic solvents for cannabis oil extraction with the aim of obtaining an extract rich in health beneficial compounds (cannabinoids, terpenes) (Table 8, entry 46). Although sample pre-treatment *via* heating (oven or water bath) lead to the decarboxylation of the target cannabinoids, at the same time, it significantly reduced the terpene content, thus, sample heating prior to extraction was disregarded. Although all the solvents tested (naptha, petroleum ether, ethanol, olive oil) extracted only small amounts of THC, due to the relatively low extraction temperatures, olive oil exhibited the capacity for maximum terpene extraction.[121]

The *n*-hexane extraction of hempseed oil has been optimized by adjusting the parameters of extraction temperature, solvent-to-seed ratio and extraction time (Table 8, entry 47).[165] Outcomes of RSM indicate that increasing solvent-to-seed ratio (up to 10 : 1), at fixed temperature (20 °C), favors the hempseed oil yield regardless of the extraction time, an effect which is more noticeable at high solvent-to-seed ratios. The impact of time is dependent on the solvent-to-seed ratio; although negligible at low ratios, it becomes more pronounced as the ratio increases by increasing the oil yield. At high temperatures (45 °C; 70 °C), the hempseed oil yield increases up to a maximum point (30.4%) beyond which it decreases when increasing both

700 | *Nat. Prod. Rep.*, 2023, **40**, 676–717

105

This journal is © The Royal Society of Chemistry 2023

extraction time and solvent-to-seed ratio. At the highest extraction temperature (70 °C), the influence of solvent-to-seed ratio and extraction time are less appreciable since temperature becomes the main influencing factor. Increased temperatures promote the oil solubility and diffusion rate, thus, an increase in the oil yield is observed. Additionally, a multivariate data analysis approach was used to determine the optimum extraction parameters; although the parameters do not differ considerably from the RSM ones, the multivariate data analysis approach was found to be a more accurate prediction model than RSM, since the relative standard deviation between theoretical and experimentally obtained values was smaller.[165]

Kostić *et al.*[146] published an investigation on the kinetic and thermodynamic behavior of hempseed oil extraction *via* *n*-hexane (Table 8, entry 48). Elevated temperatures (45 °C; 70 °C) favor the oil yield, due to its increased solubility, while, from a kinetic perspective, the yield initially increases dramatically and progressively decelerates. The calculated temperature extraction coefficient indicates an increase factor of approx. 1 for every increase of 10 °C. Additionally, lower seed-to-solvent ratios (3 : 1; 6.5 : 1) promote oil extraction, since increasing amounts of solvent improve its dissolution capacity. Thermodynamic data support the endothermic nature of the reaction.[146]

The growing demand for oil extracts of cannabis for medicinal purposes prompted Casiraghi *et al.* (Table 8, entry 49).[122] to investigate the extraction of valuable constituents with the aid of olive oil. Prior to extraction, the impact of varying temperatures (70–110 °C) on cannabinoid decarboxylation was evaluated. A standardized medicinal sample comprising cannabis inflorescences was used for the experiments. Pre-heating promotes the conversion of THCA to THC, thus, the corresponding oil extracts are rich in THC, which is the pharmacologically valuable constituent. In contrast, no heat pretreatment of the sample allows the recovery of oil-based extracts with higher THCA content than the other approaches. Careful selection of pre-treatment temperature can afford high quality and quantity THC extracts. The extraction of THCA along with THC observed at temperatures up to 100 °C can be almost completely eliminated by further increase of the temperature. Combination of high temperature (130 °C) and prolonged heating time (40 min) elevates the THC amounts (up to 15%); however, prolonged time leads to formation of degradation products. Therefore, a compromise in the combination of temperature and time can lead to the recovery of THC-rich extracts of high quality.

Stability experiments indicated that the oil preparation is stable for at least 3 weeks, if stored in the fridge.[122]

The potential for recovery of valuable compounds from aerial parts of young and mature hemp *via* solvent extraction was investigated by Drinić *et al.* (Table 8, entry 50).[127] The study focused on the extraction yield, total phenolic (TP) content, total flavonoid (TF) content, antioxidant activity, and reductive capacity (Fig. 18). Solvent polarity has a positive impact on the overall extraction efficiency; therefore, water was more effective than aqueous ethanolic solutions of variable concentrations (30–90%), since it can solubilize more efficiently the target
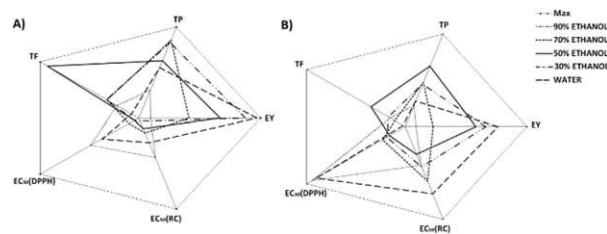
Fig. 18 Radar chart for all investigated parameters in obtained extracts of aerial parts of (A) young hemp and (B) mature hemp; EY – extraction yield, TP – total phenols content, TF – total flavonoids content, EC_{50} (DPPH) – effective concentration obtained by DPPH assay and EC_{50} (RC) effective concentration obtained by reducing power assay.[127] Open access, CC BY 4.0, https://creativecommons.org/licenses/by/4.0/.

compounds. The obtained yields (yield ranges) of young and mature hemp were comparable. Nevertheless, TP and TF values for young hemp were twice those of the mature one. Additionally, an aqueous ethanolic solution (50%) afforded the highest TP (17.1 mg g^{-1}) and TF (11.2 mg g^{-1}) contents, as well as the highest antioxidant capacity.[127]

The effect of varying a number of parameters on the extraction efficiency of proteins from undelipidated hemp press-cakes was evaluated (Table 8, entry 51).[172] Hemp proteins are recovered as aqueous extracts by simple suspension of the cake in distilled water and concurrent stirring, followed by continuous pH adjustment (to the desired level) and centrifugation. A decisive factor in the protein extraction efficiency is the pH level; a significant increase in the yield is observed as the pH exceeds 9 (8.4% at pH 8, 67.1% at pH 12), which is in line with the previously reported increase in the yield of the major hemp protein fraction, the globulins, at alkaline pH values.[83,190] In contrast, the minor hemp protein fraction, the albumins, are preferentially extracted at pH below 6. Concerning the appearance of the extractants, moving towards alkaline conditions leads to increasing brown coloration and turbidity, which can be attributed to progressive solubilization and/or modification of phenolic compounds. In principle, the modification of the ionic strength of the solution should impact the protein extraction yield (either by salting-in effect at low concentrations or salting-out effect at high concentrations), however, this effect is very much dependent on the pH and the surface properties of the proteins. Adjustment of the ionic strength by NaCl addition at the studied pH range of 9–12 did not have any significant impact on the protein extraction yield, while low ratios of press-cake to water (5–10 w/w %) are favorable. Even though alkaline pH maximizes the protein extraction efficiency, at the same time, this happens to the detriment of the nutritional and organoleptic characteristics of the extracts due to the oxidation of their phenolic compounds at these pH levels.[172]

2.4. Ultrasonication-assisted extraction

Ultrasound is regarded as mechanical waves of higher frequency than the human-audible frequency (>20 kHz). It is used to enhance the extraction of compounds of interest from plant matter. Ultrasonication-assisted extraction (UAE)

This journal is © The Royal Society of Chemistry 2023

106

Nat. Prod. Rep., 2023, **40**, 676–717 | **701**

Table 9   Summary of ultrasonication-assisted extraction conditions and respective results pertaining to the cannabis plant seeds and seedcakes[a]

Entry no.	Input sample	Solvent	Conditions	Extracted compounds	Ref. no.
52	*Cannabis sativa* L., seeds (ground), 5 g	*n*-Hexane	25 °C, 100–300 W, 15–40 min, 1–15 mL solvent per g cannabis	[b]Hempseed oil: 21.4–26.4	130
53	*Cannabis sativa* L., seeds (ground), 10 g	*n*-Hexane	25 °C, 20–100 W, 10–30 min	[c]Hempseed oil: 31.9–36.1	78
54	*Cannabis sativa* L., seed cakes (ground), 5 g	Methanol : acetone : water (7 : 7 : 6 v/v/v)	20–70 °C, 200 W, 20–40 min, 8–20 mL solvent per g cannabis	[d]Flavonoids: 5.6–38.3, [e]phenols: 475.4–2563.5	128
55	*Cannabis sativa* L., seed cake (ground), 5 g	Methanol : acetone : water (7 : 7 : 6 v/v/v)	70 °C, 200 W, 20 min	[d]Flavonoids: 6.4–19.2, [e]phenols: 467.5–1328.9	129
56	*Cannabis sativa* L., cold-pressed seed cake (ground), 1 g	Methanol (70%), acetone (80%), methanol : acetone (1 : 1 v/v)	1 min, 3 × 9 mL solvent per g cannabis	[f]4 main phenols: 2.2–2.8	135
57	*Cannabis sativa* L., flowers, leaves and husks (dried)	80% methanol	130 W, 15 min	[g]Total phenolic content: 312.452, [h]total flavonoids: 28.173, [i]ferric reducing antioxidant power: 18.79, [j]yield: 11	166

[a] All concentrations of extracted compounds within the table are reported as %, regardless of the units in which they were originally reported by the authors, in order to facilitate their comparison. [b] Reported as percentage of the amount extracted by the Soxhlet method. [c] Reported as % extracted oil from hemp seed. [d] Reported in mg of gallic acid equivalent per 100 g fresh hemp. [e] Reported in mg of luteolin equivalent per 100 g fresh hemp. [f] Reported as mg of catechin equivalents per g dry matter, extracted compounds: *N-trans*-caffeoyltryamine, cannabisin B (or isomers) and 2 unknown compounds. [g] Reported in mg of gallic acid equivalent per g of dry weight. [h] Reported in quercetin equivalents per g of dry weight. [i] Reported in ascorbic acid equivalents per g of dry weight. [j] Reported as % of plant dry weight.

consumes small amount of energy and it has a low investment cost; however, large solvent volumes might be required, a filtration step is necessary and it might deteriorate target compounds. The ultrasonic waves spread due to rarefaction and compression and as a result negative pressure is generated. Consequently, when the tensile strength of the solvent is smaller than the generated pressure, vapor bubbles are created that implode (cavitation), generating macroturbulences and perturbation. This cavitation near to the liquid–solid interface leads a fast-moving stream of liquid through the cavity at the surface. The impact of these microjets on the surface, generate erosion, particle breakdown and surface peeling, promoting the liberation of compounds of interest from the plant matter, hence, higher extraction efficiencies are obtained owing to the augmentation of mass transfer. Therefore, cell disruption and effective mass transfer are cited as major factors enhancing extraction with ultrasonic power. Ultrasound permits changes in processing conditions, as compared to other techniques lower pressures and temperatures are employed, allowing the extraction of thermolabile compounds.[191]

Regarding the most important parameters of ultrasound, frequency, wavelength, amplitude, power and the shape of the reactor play an important role in the extraction efficiency.[192]

The ultrasonication-assisted extraction conditions and the respective results that are discussed in this section are summarized in Table 9.

Lin *et al.*[130] first reported the effect of UAE on hempseed oil yield (Table 9, entry 52). The influence of the extraction time, the solid-to-solvent ratio, the acting on–off ratio and the ultrasonic power were evaluated using single-factor experiments (Fig. 19).

Extraction duration of 30 min was sufficient to obtain the maximum yield (86.5%), whereas any further increase in time is detrimental to the yield, considering that longer extraction times may promote the oxidation of unsaturated fatty acids (UFAs) and their decomposition. An increase of solvent-to-solid ratio initially leads to a significant increase in the extraction yield, but eventually the increase gets progressively less significant as the ratio further increases. With regard to the effect of acting on–off, a ratio of 20 : 20 s s^{-1} afforded the highest yield (88.20%). Either increase or decrease of the acting off ratio generates lower yields; an increase implies inadequate use of
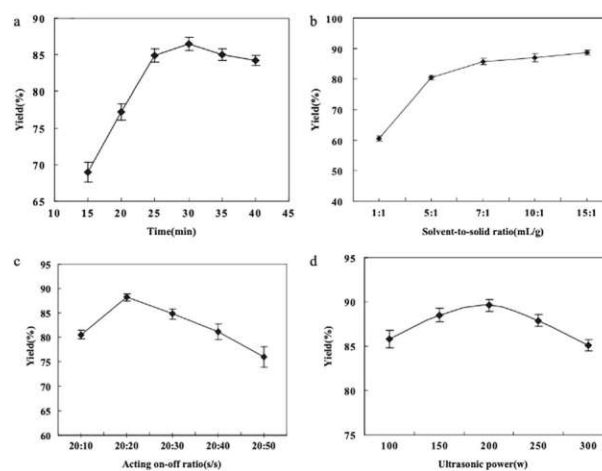

Fig. 19 Relationship between yield and various parameters: (a) extraction time, (b) solvent-to-solid ratio, (c) acting on–off ratio and (d) ultrasonic power.[130] Used with permission, John Wiley and Sons, ©2011 Wiley Periodicals, Inc.

ultrasonic waves, while a decrease leads to degradation of UFAs as a result of hot spots generated by the cavitation bubbles. The positive influence of ultrasonic power reaches a maximum value at 200 W and any further increase leads to progressive decrease of the yield. The optimum experimental conditions that maximize the obtained yield were determined using a three-variable, four-level orthogonal design $(L^9(3^4))$.[193] In terms of yield, the UAE outperformed the solvent-based extraction, however, no significant difference in the quality of the obtained oil was observed, which implies that the UAE has no influence on the fatty-acid content. Additionally, the antioxidant activity of the UAE-recovered oil was much higher.[130]

The impact of UAE on the recovered hempseed oil quality and its antioxidant activity has also been reported, focusing on the extraction of PUFAs and tocopherols, which are representative of the oil quality and its antioxidant activity, respectively, with the aid of *n*-hexane (Table 9, entry 53).[78] The effect of different variables, namely, extraction time (10–30 min) and ultrasound power level (20–100 W), was evaluated, while the parameters of duty cycle (percentage of the total process time during which the ultrasound signal is "on") and temperature were maintained constant. Increasing the ultrasound power and time favors the oil extraction efficiency, due to the affinity of hempseed oil for hexane and the advantageous effect of cavitation on its diffusion. Nevertheless, the combined effect of high ultrasound power, high temperature and long extraction times, lead to a reduction in the oxidation stability of the oil, since, under these conditions, thermal decomposition of long chain fatty acids occurs. With respect to antioxidant scavenging activity, longer extraction times and high ultrasound power, lead to higher quantities of tocopherol and phenolic compounds. By rising the ultrasound power from 20 W to 100 W the extraction of antioxidants was incremented. A compromise between ultrasound power and time needs to be found, so that energy is reserved and oil quality is maintained; this objective is achieved at the optimized conditions of 91 W and 10 min. Although Soxhlet-based extraction with *n*-hexane slightly favors the extraction yield (approx. by 4%), higher quality oil, characterized by stability and antioxidant activity (higher tocopherol content), can be derived *via* UAE.[78]

Ultrasonic assisted extraction (UAE) was applied for the extraction of TP and TF compounds from defatted hemp seed cake and other plant sources (Table 9, entry 54).[128] The impact of solvent volume, ultrasonication time (20–40 min) and temperature (20–70 °C) was evaluated. The TP and TF yields obtained from seed cakes with ultrasonication are dramatically higher than the respective conventional extraction-based yields. Additionally, UAE is more favorable than conventional solvent-based extraction in terms of antioxidant capacity of the recovered oil. Interestingly, the double amount of solvent (100 mL) than the one used for maximum TP extraction (50 mL) is required in order to obtain the maximum TF value. The ideal UAE time proved to be 20 min; exceeding this time leads to reduced recovery of polyphenols and lowers the antioxidant activity of the oil, which could be attributed to the degradation of polyphenols occurring at longer ultrasonication times. Increased polyphenol yield is in line with rising temperature;

highest TP and antioxidant activity are achieved at 70 °C, while lower temperatures are ideal to acquire the maximum TF yield.[128]

The effect of different pre-treatment approaches, namely, microwave (MW) and pulsed electric field (PEF), on the ultrasonic-based extraction of polyphenolic compounds from defatted hemp seed cake has been reported (Table 9, entry 55).[129] The optimization of the MW and PEF processes was performed with the aid of RSM. In the MW pre-treatment, the influence of MW power (440–1100 W), time (1–5 min) and liquid-to-solid ratio (4 : 1–6 : 1) on the total phenolic and total flavonoid extraction was investigated. An increase of the liquid-to-solid ratio and the processing time favors the extraction yield for both phenolics and flavonoids, whereas the positive impact of increased MW power reaches a maximum value beyond which it has a detrimental effect on the yields, possibly due to the thermal degradation of the target compounds. In the PEF pre-treatment, the influence of frequency, voltage, ethanol concentration and electroporation time on the extraction yields was investigated. Short processing times and low voltage values maximize the extraction of total flavonoids, while additional voltage increase further promotes the extraction of total phenolics. The low frequency and the use of ethanol as a solvent are advantageous for the yield, however, voltage is the factor that exerts the most decisive influence. The positive impact of ethanol can be attributed to its polarity, which (i) enhances cell permeability, thus, accelerating the extraction of polyphenols and (ii) implies increased conductivity of the solvent, thereby accelerating heat transfer to the cells.[129]

Liang *et al.*[135] reported a study on the UAE of phenolic compounds from cold-pressed hemp seed cake, particularly focusing on the effect of solvent, preheating temperature, and ultrasonication time (Table 9, entry 56). The developed process was divided into two steps; preheating treatment followed by UAE. Comparison of preheated hemp seed cakes with an unheated control sample demonstrated the positive effect of preheating on the TP yield in all the aqueous organic solvents that were evaluated. Regardless of the employed preheating conditions (temperature and exposure time), the highest TP (4.29 mg of gallic acid equivalent per g of dry matter) yield was obtained with an aqueous (80%) solution of acetone, which was higher by 30% and 40% compared to aqueous methanol and the mix of the 2 solvents, respectively. While the TP yield is significantly affected by the employed solvent and the preheating temperature, the preheating duration only has a negligible effect.[135]

Ultrasonication-based extraction for the recovery of bioactive compounds from cannabis inflorescence proved to be an approach of considerable merit, compared to conventional extraction, in terms of associated time, energy and costs (Table 9, entry 57).[166] Response surface methodology was used to evaluate the effect of the input extraction parameters, namely, time, input power and methanol concentration, on the output responses, *i.e.*, TP, TF, ferric reducing ability of plasma (FRAP) and total yield. The optimum parameters were experimentally verified and the respective outputs were compared to a control extraction process, which relied on mixing of the sample with

This journal is © The Royal Society of Chemistry 2023

108

Nat. Prod. Rep., 2023, **40**, 676–717 | **703**

50% MeOH while elevated temperature and constant stirring were applied.

Concerning TP extraction, the individual and combined effects of time and solvent composition have a pronounced positive effect; long sonication times favor the penetration of the solvent in the material, while higher content of methanol allows an increase in the solvent permeability. On the other hand, sonication power, either alone or in combination with solvent composition, has a negligible effect on TP extraction.

The most pronounced effect on TF extraction is brought about the solvent; in contrast to THC extraction, lower methanol content favors TF extraction. This observation can be attributed to the dual effect of water on the extraction; (i) expansion of the matrix resulting in an increase in the contact area of solvent and matrix and (ii) generation of hydroxyl radicals that further assist the extraction. Power and time, either separate or combined, exert a moderately positive effect on the TF extraction.

The ferric reducing ability of plasma seemed to be independent of the input experimental parameters. The overall yield is favored by lowering the methanol content due to the higher diffusivity of water as opposed to methanol, while it increases as a function of time. High power, however, can lead to degradation of heat sensitive compounds, thus, resulting in lower overall extraction, while its combined effect with either solvent or time is dependent on the nature of the compounds present in the sample.

Overall, the optimized output value of all evaluated responses was significantly higher than that of the control extraction (Fig. 20), thus, proving the undeniable value of the ultrasonication approach.[166]

2.5. Microwave-assisted extraction

Microwave-assisted extraction (MAE) is related to the generation of a non-ionizing electromagnetic radiation with a frequency of 300 MHz to 300 GHz. The microwave effect relies on the conversion of electromagnetic energy into heat by the direct influence of dipole polarization and ionic conduction. The molecules that possess a dipole moment align with the electric field, generating molecular friction, collisions and the release of heat energy into the medium, causing fast dielectric heating. The ionic conduction is also an important interaction that takes place. The ionic conduction generates higher temperatures and faster heating in solutions consisting of ions than the ones without. The influence of the electromagnetic waves can be determined by the dielectric properties of the solvent. The spreading of the heat all over the sample/matrix is promoted by solvents that have high dielectric constant and high dissipation factor, leading to higher extraction yields, however, non-polar solvents remain unaffected by the microwaves.[194]

Microwave-assisted extraction is characterized by shorter extraction time, higher extraction yield, higher selectivity and better quality of the extracts. On the negative side, chemical reactions could be enhanced and, depending on the extraction conditions, chemical structures could be modified, negatively affecting the yield. In addition, this technique is ineffective when non-polar compounds are the target and when non-polar solvents are employed. Moreover, it is not suitable for thermally unstable compounds. Regarding this technique, several factors play a main role, such as power and frequency of microwave, duration of the microwave irradiation, extraction temperature and pressure, moisture content and particle size of the plant material, the nature and concentration of solvent and ratio of solid to liquid.[195]

The microwave-assisted extraction conditions and the respective results that are discussed in this section are summarized in Table 10.

A MAE process for the efficient recovery of cannabinoids from hemp nuts was developed by Chang et al. (Table 10, entry 58).[143] and subsequently compared to other available extraction methods, namely, heat reflux extraction (HRE), Soxhlet extraction (SE), SFE and UAE. An RSM was employed in order to obtain the optimum MAE conditions, using as input parameters the solvent (methanol, ethanol, acetonitrile, isopropanol, ethyl acetate), the microwave power, the temperature and the extraction time (Fig. 21).

Of all the organic solvents tested, methanol afforded the highest yield. In contrast, water performed quite poorly due to its low solvating power towards cannabinoids and its large dielectric constant which leads to sample damage after exposure to high-temperature. Therefore, methanol was selected for further RSM optimization of the MAE process.

An increase in temperature favors the overall yield, however, temperatures beyond 100 °C are not considered since they lead to the degradation of cannabinoids. Specifically, THCA and CBDA progressively decarboxylate into THC and CBD, while THC can further convert to CBN, thus, affecting the yields of the carboxylated analogues by increasing the content of THC, CBD and CBN. Additionally, terpenes are sensitive to high temperatures.

Microwave power exerts a minor effect on the cannabinoid yield. While prolonging the extraction time (10–30 min) has
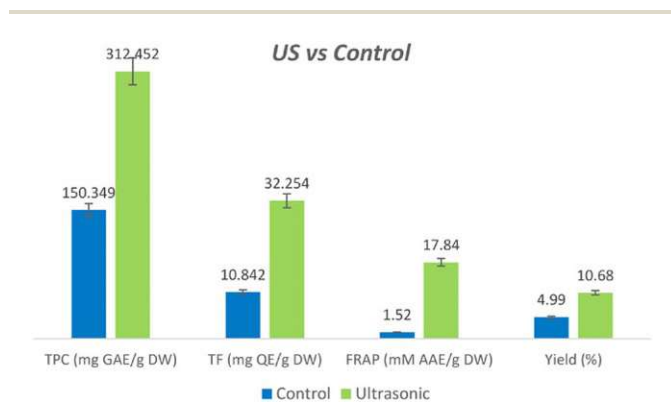
Fig. 20 Extraction yields obtained through ultrasonication (green) and control (blue) extractions (TPC = total phenolic content, GAE = gallic acid equivalents, DW = dry weight, TF = total flavonoids, QE = quercetin equivalents, FRAP = ferric reducing antioxidant power, AAE = ascorbic acid equivalents). The error bars indicate percentage error.[166] Used with permission, John Wiley and Sons, ©2018 Institute of Food Technologists®.

704 | Nat. Prod. Rep., 2023, 40, 676–717

109

This journal is © The Royal Society of Chemistry 2023

Table 10 Summary of microwave-assisted extraction conditions and respective results pertaining to the cannabis plant[a]

Entry no.	Input sample	Solvent	Conditions	Extracted compounds	Ref. No
58	*Cannabis sativa* L., nuts, 1 g	Methanol, ethanol, acetonitrile, isopropanol, ethyl acetate	40–160 °C, 100–1300 W, 5–35 min, 12 mL solvent per g cannabis	[b]THC: $(1.4–2.7) \times 10^{-4}$, CBD: $(1.5–2.6) \times 10^{-4}$, CBN: $(0.8–1) \times 10^{-4}$	143
59	*Cannabis sativa* L., inflorescences (crushed), 500 g	Distilled water	400–600 W, 46–100 min	[c]Essential oil: 0.15, [d]CBD: 9.3	134
60	*Cannabis sativa* L., cultivar: helena, leaves, blossoms, inflorescences and bracts (ground)	Ethanol	10–30 min, 0.07–0.2 mL, solvent per g cannabis	[e]Phenols: 0.9–2.7, [f]flavonoids: 0.5–1.4, [g]THC: 0.03–0.06, [g]CBD: 0.2–1.8	168
61	*Cannabis sativa* L., seeds (ground), 15 g	*n*-Hexane	300–600 W, 5–15 min, 10 mL solvent per g cannabis	[h]Hempseed oil: 25.7–36.0	167

[a] All concentrations of extracted compounds within the table are reported as %, regardless of the units in which they were originally reported by the authors, in order to facilitate their comparison. [b] Reported as % in hemp nut. [c] Reported as % in dried inflorescences. [d] Reported as % in the hemp essential oil. [e] Reported in mg gallic acid equivalent/mL extract. [f] Reported in mg catechin equivalent/mL extract. [g] Reported in mg mL^{-1} extract. [h] Reported as % in hemp seeds.

a positive impact on the extraction yield, exceeding the 30 min mark seems to negatively affect it.

The optimized RSM output parameters were subsequently experimentally verified and used in the ensuing comparative study. Microwave-assisted extraction demonstrated superior performance to the other methods in terms of obtained yield (up to 0.00027% THC), extraction time, solvent consumption, and simplicity of operation.[143]

An RSM-based approach for the optimization of the MAE of valuable compounds from cannabis inflorescences was evaluated (Table 10, entry 59).[134] The MAE approach was compared with hydrodistillation (HD), in terms of quality of the obtained essential oil. Concerning the MW experiments, microwave irradiation power (400–600 W), extraction time (46–100 min) and water added after moistening were evaluated. The RSM

Fig. 21 Effect of (A) extraction solvent, (B) microwave power, (C) temperature and (D) extraction time on the yields of cannabinoids. Different letters (a, b, c, d, e) indicate a significant difference (one-way ANOVA, *p* < 0.05).[143] Open access, CC BY 4.0, https://creativecommons.org/licenses/by/4.0/.

output values indicated that higher microwave power and longer extraction times augmented the essential oil yield and the CBD content. However, an increase in water content, decreased both. These theoretical predictions were experimentally verified. Both MAE and HD extracted similar amounts of oil, which were also similar with respect to their chemical make-up. Higher amounts of CBD were obtained with MAE (9%), while longer extraction time (almost double) was necessary in HD.

Overall, MAE is advantageous over HD due to its higher selectivity, shorter extraction time and reduced consumption of water and energy.[134]

A microwave-assisted process was reported as a simple, fast and environmentally benign approach for the extraction of polyphenols and cannabinoids from ground *Cannabis sativa* L. (leaves, blossoms, inflorescence, bracts) (Table 10, entry 60).[168] Evaluation of the influence of different extraction parameters, namely ethanol concentration, extraction time and solid-to-liquid ratio, on several output variables (extraction yield, total phenol and flavonoid content, antioxidant activity IC$_{50}$, reductive capacity EC$_{50}$, CBD and THC content) was based on a statistical model. The constructed response surfaces provide a comprehensive overview of the effect that variations in the combined extraction parameters exert on the individual output variables.

An increase in ethanol concentration has a negative impact on total yield and total phenol content, it positively influences total flavonoid content, while it maximizes CBD extraction up to a certain point (1.8 mg mL^{-1}) beyond which it negatively impacts it. Overall, increased solid-to-liquid ratios favor most parameters, whereas total yield and CBD are positively influenced after a certain point.[168]

Rezvankhah *et al.*[167] published a study on the recovery of hempseed oil *via* MAE (Table 10, entry 61). The fatty acid composition, antioxidant activity, as well as the physiochemical and thermal properties of the oil extracted from *Cannabis sativa*
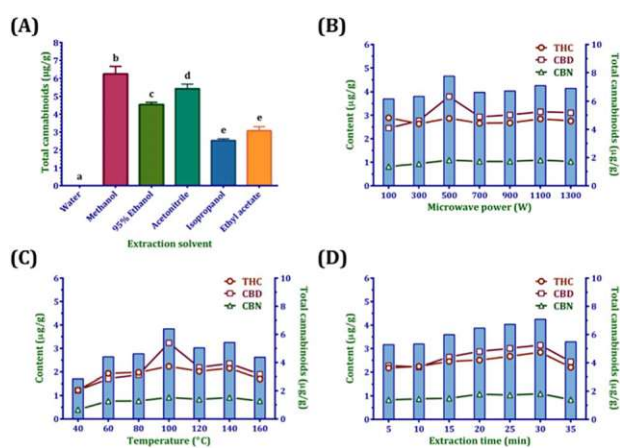
were evaluated. An RSM approach was employed for the optimization of the MAE extraction parameters. The MAE study focused on the quantity and quality of the extracted oil; higher MW power (450–600 W) and higher extraction time (15 min) promotes the oil yield (up to 36%). However, time seems to have a more significant impact than MW power; increasing time beyond a certain point, regardless of the employed MW power, can lead to thermal decomposition of the oil. Higher oil yield characterized by lower oxidation stability is obtained with SE; thus, MAE affords oil of higher quality.

Similar amounts of PUFAs and MUFAs were obtained, regardless of the employed extraction method, however, MAE is the more efficient approach since shorter extraction times are required. Additionally, MAE accesses a higher amount of total tocopherols (930 *vs.* 833 mg kg^{-1}).[167]

2.6. Pressurized-liquid extraction

Pressurized-liquid extraction (PLE) or accelerated-solvent extraction is based on the use of high temperature (50–200 °C) and pressure (35–200 bar) for the extraction of targeted chemicals in solid or semi-solid samples. On the one hand, high pressure positively influences mass transfer by promoting cell permeability. On the other hand, high temperatures enhance diffusion of the solvent into the sample, as the viscosity of the solvent is reduced. Moreover, it also increments the extraction rate by augmenting the solubility of the targeted compound and mass transfer. This technique is simple, provides a safe and fast extraction, has low solvent consumption, shorter extraction time, high reproducibility and accuracy. In addition, parameters can be modified and automatization is possible. However, it is expensive, high temperatures may result in the degradation of thermally labile compounds, the selectivity is governed by the solvent, meaning exhaustive and nonselective extractions and periodical cleaning of the equipment is necessary. With regard to the extraction yields and rate, the main key parameters are the temperature, pressure, type of solvent and number of cycles.[191]

The pressurized-liquid extraction conditions and the respective results that are discussed in this section are summarized in Table 11.

The recovery of valuable compounds from hemp with the aid of pressurized hot water extraction (PHWE) has been reported.[139] Specifically, the chemical make-up of untreated samples and steam-treated at different temperatures (100–160 °C) was evaluated. Fresh hemp stalk yielded the highest cellulose content (49%), while decorticated fibers attained the highest lignin content (27%). Similar amounts of proteins are contained in all plant parts. Higher amounts of cellulose and lignin were detected in dried and fresh hemp stalk and decorticated fibers, however, similar hemicellulose content was obtained regardless of the extracted plant part. By adjusting the temperature of PHWE, different compounds can be accessed; higher temperatures are ideal for hemicellulose extraction, while glucose and pectins can be recovered at lower temperatures. The phenolic compounds and fatty acids commonly found in industrial hemp bast fibers, were detected in the majority of the extracts.[139]

Nuapia *et al.*[136] published a study on the selective extraction of cannabinoids from *Cannabis sativa* L. seeds *via* PHWE, aiming for higher extraction of CBD and lower extraction of THC and CBN (Table 11, entry 62).[136] The study focused on 5 cannabinoids: THC, CBN, CBD, CBC and CBG. Response surface methodology (RSM) was used in order to get insight into the influence of the evaluated parameters, precisely, extraction time, extraction temperature and collector vessel temperature. The results showed that all 3 parameters have an impact on the THC and CBN extraction. Specifically, an increase in both temperatures favors solubility, thus, the yields of CBD, CBC and CBG increase. On the other hand, yields of THC and CBN diminish, due to their probable vaporization at elevated temperatures, as proven by their capture in methanol in the trapping system. Consequently, the final product has a high

Table 11 Summary of pressurized-liquid extraction conditions and respective results pertaining to the cannabis plant[a]

Entry no.	Input sample	Solvent	Conditions	Extracted compounds	Ref. no.
62	*Cannabis sativa* L., seeds (crushed), 5 g	Water	50–200 °C, 5–60 min	[b]THC: 0.02–3.2, CBD: 0.1–9.9, CBN: 2×10^{-3} to 0.7, CBG: 0.03–4.5, CBC: 0.03–6.7	136
63	*Cannabis sativa* L., buds, leaves and stems, 0.2 g	Isopropanol	500 mL solvent per g cannabis	[c]THC: 1.6–9.5 (buds), 0.087–0.72% (leaves, stems), CBD: 0.015–0.024 (buds), $<7.6 \times 10^{-3}$ (leaves, stems), CBN: 0.43–2.1% (buds), 0.09–0.97% (leaves, stems)	140
64	*Cannabis sativa* KC Virtus, flowers, leaves, stems 7.5–43.2 g	Ethanol	25–100 °C, 1–150 bar, 10–1000 min, 0.045–0.1 g hemp per g solvent	[d]THC: 4.9–10.7, CBD: 0.1–0.37	196
65	*Cannabis sativa* Finola, flowers, leaves, stems 7.5–43.2 g	Ethanol	25–100 °C, 1–150 bar, 10–1000 min, 0.045–0.1 g hemp per g solvent	[d]THC: 8.2–19.8, CBD: 1.5–2.6	196

[a] All concentrations of extracted compounds within the table are reported as %, regardless of the units in which they were originally reported by the authors, in order to facilitate their comparison. [b] Reported as % relative GC-peak area. [c] Reported as % in total extract. [d] Reported as mg g^{-1} of dry sample.

706 | *Nat. Prod. Rep.*, 2023, **40**, 676–717

111

This journal is © The Royal Society of Chemistry 2023

content of CBD, CBC and CBG and lower amounts of THC and CBN.[136]

A cannabinoid extraction approach relying on a hard-cap espresso machine, using 2-propanol, was developed as a rapid, simple and cheap alternative for their recovery from *Cannabis sativa* leaves, buds and stems (Table 11, entry 63).[140] Following the verification of cannabinoid stability under extraction conditions with the aid of standards, it was demonstrated that the developed approach could quantitatively extract all target cannabinoids (THC, CBD, CBN) within 40 s. The addition of a filter on the sample-containing capsule allows the simultaneous extraction and filtration of the cannabinoids from the plant sample, thus, circumventing additional filtration or centrifugation steps normally required for the recovery of the cannabinoid extract from the solid plant material.[140]

In 2020, a PLE-based extraction method was reported for the extraction of CBD and THC from two different varieties of *C. sativa* (KC Virtus and Finola), using ethanol as solvent (Table 11, entries 64 and 65).[196] The research examined the influence of different parameters, such as temperature, extraction time, and pressure on the extraction efficiency. Their results showed that relatively low pressures and 100 °C were sufficient to extract the cannabinoids with good yields. Approximately, 19.8 mg of CBD per gram of dry hemp has been extracted from the leaves of variety Finola.

2.7. Hydrodistillation

Hydrodistillation is a commonly used method for the extraction of bioactive compounds from plants. The key difference between steam distillation and hydrodistillation is that steam distillation uses steam, whereas hydrodistillation uses water, steam or the combination of both for the extraction. Since no organic solvents are involved in this process, this can be considered as an environmentally benign extraction method. On the other hand, because of the relatively high temperature needed in this method, volatile and thermo-labile compounds may be lost during the process.[197] The hydrodistillation conditions and the respective results that are discussed in this section are summarized in Table 12.

Fiorini *et al.*[148] reported a strategy for the enrichment of hempseed oil, derived by distillation of industrial fresh and dry hemp inflorescences, in cannabidiol (Table 12, entry 66). In order to maximize the enrichment efficiency, 5 different sample pre-treatment methods were evaluated; (i) no prior pre-treatment of fresh sample, (ii) drying for 1 month, (iii) grinding, (iv) chopping and heating at 120 °C and (v) cutting into small pieces and MW at 450 W (1 min) and 900 W (3 min).

Drying negatively impacts the extraction yield, since higher yield was obtained from fresh inflorescences; specifically, drying promotes the loss of monoterpenes.

While there was no significant difference in the overall oil yield between grinding and grinding combined with conventional or MW heating, the maximum extraction of CBD (9.1% in the extracted oil) was obtained with the aid of MW pre-treatment. Concerning the terpene content of the extracted oil, all pre-treatment approaches negatively impacted the monoterpene extraction, however, favored the extraction of sesquiterpenes.[148]

It has been demonstrated that microwave-assisted hydro-distillation has a considerable impact on the speed and yield of the extraction process (half time, triple yield) (Table 12, entry 67). Application of microwaves has the added advantage of inducing extensive carboxylation of the cannabinoids, which mostly remain in the residual biomass, thereby, providing more active forms of these compounds, while the reduced extraction time means that loss of volatile compounds and secondary metabolite degradation can be circumvented. The terpenoid fraction of MW-assisted hydrodistillation has a richer profile in terms of variety. Prolongation of the extraction time enriches the monoterpene content but, at the same time, the sesquiterpene content is decreased.[198]

2.8. Mechanical pressing

Mechanical pressing is regarded as a solid–liquid separation process utilized for the extraction of oils from oilseeds. It is preferentially used when the oil content is below 20%. This technique uses mechanical pressure and there are 2 classifications: whenever high temperature is applied (over 49 °C) it is defined as hot-pressing and if temperature is equal or below

Table 12 Summary of hydrodistillation conditions and respective results pertaining to the cannabis plant[a]

Entry no.	Input sample	Solvent	Conditions	Extracted compounds	Ref. no.
66	*Cannabis sativa* L., inflorescences, (i. ground, ii. fresh matter, iii. powdered), 100 g	Water	240 min, 35 mL water per g cannabis	[b]CBD: 4.6–9.1, α-pinene: 0.5–8.1, myrcene: 1–11.5, terpinolene: 0.5–3.2, (*E*)-caryophyllene: 25–52, α-humulene: 3.5–6.6, caryophyllene oxide: 10–22.5	148
67	*Cannabis sativa* L., cultivar: Monoica, inflorescences, leaves, stalks	Water	240 min, 1–5 kg plant per L solvent	[c]CBD: 23.83, α-pinene: 10.78, β-ocimene: 7.02, β-myrcene: 6.74, α-terpinolene: 2.55, δ-3-carene: 3.55, limonene: 1.82, camphene: 1.65	198

[a] All concentrations of extracted compounds within the table are reported as %, regardless of the units in which they were originally reported by the authors, in order to facilitate their comparison. [b] Reported as % in the extracted hemp essential oil. [c] Reported as % CBD in the resulting volatile fraction, based on GC-MS relative areas.

49 °C it is called cold-pressing. The pressing machine contains one inlet for seeds and two outlets, one for the attained oil (also known as oil-cake) and the other for the non-oiled cake. Expellers, expanders and twin-cold systems fall into the category of cold presses. Mechanical pressing is a simple, automatic, low cost, environmentally friendly process, as no solvents are used, and can be applied for a wide variety of applications. However, the main drawbacks are its low yield and low reproducibility of the obtained-product quality. Concerning the oil yield, the most influential factors are the parameters related to the process, to name a few, nozzle size, screw rotational speed and temperature. In addition, the pretreatment of the seeds is also a key parameter, including peeling, drying, solvent or enzymatic treatment.[199]

The mechanical pressing conditions and the respective results that are discussed in this section are summarized in Table 13.

The impact of cold pressing on the quality and extraction efficiency of hempseed oil has been reported (Table 13, entry 68).[123] Specifically, the pressing rate efficiency appears to be influenced not only by the diameter of the press nozzle but the hemp seed characteristics as well. Smaller nozzle diameters (4 mm) yield higher oil quantities, while hemp seeds that contain lower volatile matter promote the rate efficiency. Based on standard of quality, it was determined, by connecting the acidity and peroxide value, that exclusively the oil processed from the seeds with lower total volatile content meets the quality requirements for alimentary and therapeutic purposes.[123]

Apart from the cold pressing parameters, the fertilization techniques also appear to have an effect on the phenolic and polyphenolic content of hempseed oil extracted with cold-pressing (Table 13, entry 68).[169] The impact of various parameters, such as plant density, soil fertilization, foliar fertilization, extraction temperature (40–70 °C) and nozzle diameter (8–12 mm), was evaluated by Faugno et al.[169] It was demonstrated that foliar fertilization increased the extraction efficiency of phenolic compounds.

Extracts derived from non-fertilized plants of different densities, clearly show the impact of density on extraction efficiency (Table 13, entry 69); higher abundance of metabolites with a flavonoid skeleton were present in the higher density plants. High temperatures diminish the extraction of these metabolites, however, when larger nozzle sizes are employed, the effect of the temperature is less significant. Soil fertilization positively impacts the quality of the recovered hempseed oil which is abundant in phenolic and polyphenolic constituents. An overview of the mechanical screw press set-up used in the experiments is depicted in Fig. 22.[169]

The effect of several parameters of mechanical screw pressing on the yield of hempseed oil has also been reported (Table 13, entry 70).[137] The nozzle size was not considered (kept constant), however, the press temperature, the screw speed and the sample pre-treatment (heating vs. no heating) were varied. The most influential parameters on the oil yield were the screw rotational speed, followed by the extraction temperature and seed preheating. Regarding the extraction temperature, high temperatures lead to higher yields (up to 23%). In preheated and non-preheated samples, high rotational screw speed had a significant negative influence on the yield. Higher extraction of oil was obtained by combining lowest screw rotational speed, with preheated seeds at high temperatures.[137]

An RSM approach was used by Aladić et al.[163] in order to determine the input parameter values of cold pressing that maximize the extraction of high-quality oil; the input parameters of nozzle size, temperature and frequency were employed. Additional parameters, such as cold-press oil volume, oil after centrifugation, oil temperature, free fatty acid (FFA), insoluble impurities (II) and amount of residual oil in the press cake, were also considered.

Table 13 Summary of mechanical pressing conditions and respective results pertaining to the cannabis plant[a]

Entry no.	Input sample	Conditions	Extracted compounds	Ref. no.
68	Cannabis sativa L., seeds	Press nozzle diameter: 4–10 mm	[b]Hempseed oil: 24–30	123
69	Cannabis sativa L., seeds, 1000 g	40–70 °C, press nozzle diameter: 8–12 mm	[b]Hempseed oil: 26, relative content; phenols: 10–50, non-phenolic compounds: 10–78, flavonoids: 5–75	169
70	Cannabis sativa L., seeds, 1000 g	50–70 °C, press nozzle diameter: 8 mm, screw speed: 22–32 rpm	[b]Hempseed oil: 17–23	137
71	Cannabis sativa L., seeds (ground)	20 min, 294–410 bar	[b]Hempseed oil: 28–33	147
72	Cannabis sativa L., hurds (dried)	50 °C, 60% EtOH, 13% NaOH, feed rate: 2.2–2.5 kg h^{-1}, screw speed: 200 rpm	[c]Ferulic acid: 99, p-coumaric acid: 1814, [d]polyphenols: 5.8	171
73	Cannabis sativa L., dust (dried)	50 °C, 60% EtOH, 21% NaOH, feed rate: 2.2–2.5 kg h^{-1}, screw speed: 200 rpm	[c]Ferulic acid: 95, p-coumaric acid: 1150, [d]polyphenols: 9.0	171

[a] All concentrations of extracted compounds within the table are reported as %, regardless of the units in which they were originally reported by the authors, in order to facilitate their comparison. [b] Reported as % in hemp seeds. [c] Reported in mg kg^{-1} of raw organic material. [d] Reported in g of gallic acid eq. per kg of raw organic material.
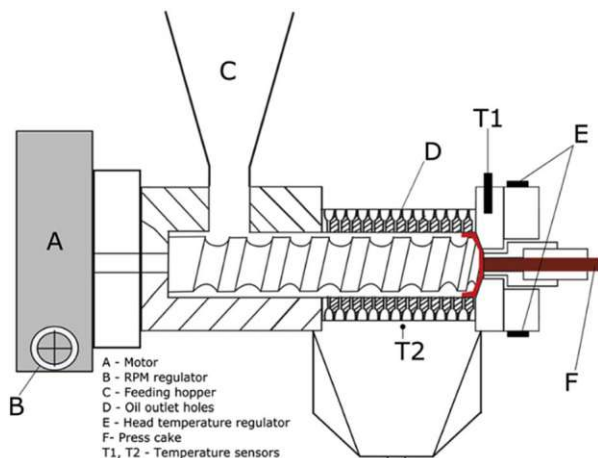
Fig. 22 Mechanical screw press for tobacco oil extraction used by Faugno *et al.* and Crimaldi and co-workers.[137,169] Reprinted with permission from Elsevier.

Larger nozzle sizes lead to a notable decrease of the amount of obtained oil. The FFA amount is an indicator of oil quality; lower amounts are correlated with high quality and long shelf life. Low temperatures, high frequencies and bigger nozzle sizes help maintain the FFA content at the desirable low levels. A satisfactory quality can be attributed to the recovered oil, due to the low co-extraction of impurities (0.33–0.49%).

With regard to the optimization of screw pressing of hemp seed oil, several parameters were studied using RSM with the aim to maximize the oil quality properties and the oil recovery. Among all the natural antioxidants tested, oregano provides the oil with the highest resistance towards oxidative degradation.[163]

An alternative cold-pressing approach, *i.e.*, enzyme-assisted cold-pressing extraction, for recovery of hempseed oil has been reported (Table 13, entry 71).[147] Enzyme-treated hemp seeds deliver significantly higher oil yields than untreated ones. Additionally, it was demonstrated that different enzymes favor the extraction yields of different fatty acids and tocopherol forms. In any case, the addition of an enzyme adjuvant is essential to maximize the yield of γ-tocopherol. The enzyme treated hempseed oil contains higher amounts of pigments, whereas its oxidation stability does not differ from the control sample.[147]

A twin-screw extrusion was evaluated for its potential to recover pharmaceutically valuable compounds from hemp by-products. Specifically, ferulic acid (FA) and *p*-coumaric acid (*p*-CA) in hemp hurds and dust were targeted (Table 13, entries 72 and 73).[171] Hurds proved to be a richer source of the target compounds since they contain 3 times the amount found in dust.

The extrusion process comprises the steps of (i) mixing the solid sample with the liquid solvent, (ii) extracting and (iii) separating the solid and liquid fractions, which are performed in a continuous mode. An aqueous ethanolic solvent is used for the solubilization of the target compounds, while the addition of NaOH in the solvent favors their extraction yields. Both target compounds are not primarily encountered in their free form, therefore, addition of a mildly basic NaOH solution is essential to access the etherified FA and the both etherified and esterified *p*-CA. Under these conditions, the polyphenol yield is also significantly increased, since NaOH breaks the intermolecular hydrogen bonds, thereby releasing the phenolic compounds. An additional advantage of NaOH is its ability to reduce the viscosity of the mixture inside the extruder. Increasing the temperature (from 50 °C to 100 °C) does not seem to have an effect on the extraction yield, therefore, mild temperatures are selected.

A fraction of the extracted compounds is retained in the solid residue; however, they can be recovered by a second extraction step with a polar solvent. While a single pass from the extruder (15 min) can recover half of the amount of polyphenols that can be recovered by alkaline batch extraction in 24 h, the respective yields for FA and p-CA are 2–4 times lower. Nevertheless, this trade-off is more than counterbalanced by the significantly lower amounts of NaOH (45 times less) used in the extrusion process and the low solid-to-liquid ratio, both of which signify economic and environmentally advantageous solvent consumption. Additionally, compared to conventional approaches, twin-screw extrusion is less time consuming and less energy demanding.[171]

2.9. Comparative studies

A comparative study on essential oil extraction from *Cannabis sativa* leaves using three different techniques, precisely, supercritical fluid extraction (SFE), steam distillation (SD) and hydrodistillation (HD), was reported by Naz *et al.*[144] The effect of temperature on extraction efficiencies was evaluated, while in SFE pressure was additionally considered. In the case of HD, increased temperature implies elevated vapor pressure which results in increased transfer rates, thus, higher extraction yields. On the other hand, in the case of SD, extraction is favored at lower temperatures which limit the negative impact of hydro diffusion, hydrolysis and thermal degradation. Between the two, higher oil yields were obtained with SD; lower hydrolysis rate, resulting from smaller water amounts used, as opposed to HD, minimizes thermal decomposition, thus, providing higher essential oil yields.

Regarding SFE, increasing pressure has a positive impact on the extraction efficiency of the oil components; scCO$_2$ density increases, thus, its dissolving ability is favored at elevated pressures. The combination of high pressure and low temperature is ideal to obtain high essential oil yield, which is also the highest among the 3 techniques that were compared. The natural aroma of the oil was preserved better when scCO$_2$ was employed, due to the higher percentage of extracted sesquiterpenes. Supercritical fluid extraction proved to be superior with regard to extraction yields, isolation and recovery of target compounds and energy consumption.[144]

In a subsequent study, the research group further expanded their study to include *Cannabis indica*. Elevated temperatures in HD negatively impact the extraction yield of the essential oil due to possible thermal degradation occurring at higher
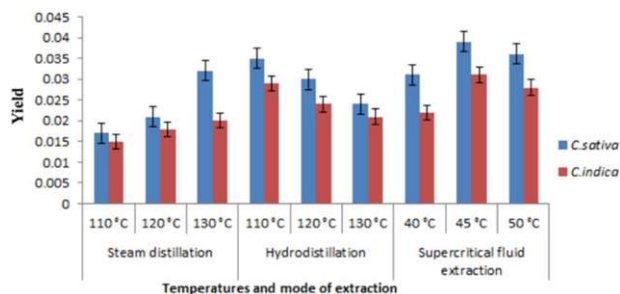
This journal is © The Royal Society of Chemistry 2023

114

Nat. Prod. Rep., 2023, **40**, 676–717 | **709**

Fig. 23 Extraction yields (%) obtained by various methods.[145] Reprinted by permission of Taylor & Francis Ltd.

temperature.[145] However, this observation is contradictory to what the authors previously reported; that high temperatures in HD lead to higher extraction yields.[144] In the case of SD, best yield was obtained at 130 °C, however, compared to the HD the yield was much lower.

This observed difference can be attributed to the lower penetration capacity of the steam in the plant material in the case of SD. While in HD the plant material is constantly submerged in boiling water, in SD the steam needs to vaporize and condense the water present in the plant material in order to access the target compounds; thus, longer extraction times are required, which can lead to thermal degradation of the target constituents.

In the case of $scCO_2$ extraction, an increase in temperature up to a certain point increases the yield, however, any additional increase beyond this point has no impact on the obtained yield. This can be attributed to the decrease of the $scCO_2$ density beyond this temperature point, since $scCO_2$ controls the increase of the solute vapor pressure at the corresponding pressure.

Regardless of the cannabis species, SFE afforded the highest oil yield of all 3 techniques compared. In any case, higher oil yield was obtained from *Cannabis sativa* than *Cannabis indica*, which is a result of different factors regarding the biotype and chemotype of the plant, geographical cultivation, climatic conditions and extraction process. An overview of the yields obtained by the compared methods is presented in Fig. 23.[145]

A comparative study of focused ultrasound extraction (FUSE) and SFE on the recovery of cannabinoids and sesquiterpenes from cannabis leaves and buds has been reported.

The sonication time, amplitude, sonication cycles and the extracting solvent composition were varied during the optimization of the FUSE. As factorial fractionated design indicates, the number of cycles has no significant effect, hence the value was set to the minimum. The highest value of amplitude is achieved at a ratio of 1 : 1 solvent mixture, which had a positive impact on the extraction of sesquiterpenes and cannabinoids. For both, the sonication time did not have a significant impact, therefore, it was set to the minimum (5 min).

The SFE was optimized with central composite design (CCD). Addition of co-solvent (EtOH) was deemed necessary to maximize the cannabinoid extraction, whereas lack of co-solvent and low temperature extractions are more favorable for terpene extraction. Cannabinoid extraction is not affected by changes in

temperature. Supercritical fluid extraction allowed the fractionation in 2 different extracts; one rich in terpenes and the other in cannabinoids.

While higher extraction yields are accessible with FUSE, SFE offers the advantage of fractionation, which enables the separation of cannabinoids and terpenes.[141]

De Vita *et al.*[142] published a comparative investigation of different methods, *i.e.*, UAE, MAE and an emulsion-based extraction for the recovery of main cannabinoids (THC, THCA, CBD, CBDA, and CBN) from commercially available hemp varieties and medical cannabis samples.

Regarding the UAE, the influence of solvent and extraction time was studied. Use of ethanol, combined with shorter extraction times, favors the cannabinoid extraction. Overall, for the commercially available hemp, conventional ethanol-assisted extraction was more favorable for CBDA, THCA and total CBD, while the optimized UAE extraction was more efficient for the other cannabinoids. In the case of the medical samples, ethanol-based extraction was more efficient than the optimized UAE for all target cannabinoids.

With regard to MAE, the effect of extraction time, extraction temperature, ramp time and solvent was evaluated. Prolonged extraction time and elevated temperature extracts an amount of CBD that is 4 times higher than the conventional extraction, while employing ethanol and short ramp time favors this outcome. Conversely, by increasing the time and temperature of extraction, a significant decrease in the CBDA yield is observed, which may be attributed to the transformation of CBDA into its decarboxylated analogue, *i.e.*, CBD, during the MAE process. Contrary to CBDA, an increase in temperature promotes THCA extraction. Overall, MAE obtained a higher amount of THC and THCA compared to the conventional extraction. Between MAE and UAE, higher extraction efficiency for CBD and THC is obtained with UAE.

Regarding the emulsion-aided extraction (Tween 20 in H_2O), the influence of the solvent, the extraction time and the extraction temperature were evaluated. Both THC and CBD yields were lower compared to the ones obtained with conventional extraction. Apart from that, total THC was comparable in all the emulsion-based extractions, regardless of the employed extraction parameters. Interestingly, higher CBD than CBDA quantities were present in the tween-based extract, even though in the conventional ethanolic extract CBDA was 5 times higher than CBD.[142]

Brighenti *et al.*[42] compared the efficiency of solvent extraction (SE), dynamic maceration (DM), ultrasound-assisted extraction (UAE), microwave-assisted extraction (MAE) and supercritical fluid extraction (SFE) on the recovery of cannabinoids from inflorescences.

Concerning the optimization of the extraction conditions, methanol and ethanol were the most appropriate solvents for the extraction of cannabinoids, followed by acetone, MeOH/$CHCl_3$ (9 : 1) and hexane. Each of the evaluated techniques were optimized in terms of extraction time and temperature. UAE and SFE had the poorest performance of all compared methods in terms of extracted amounts of CBDA, CBD and CBGA. While similar amounts of CBGA were obtained with both DM and
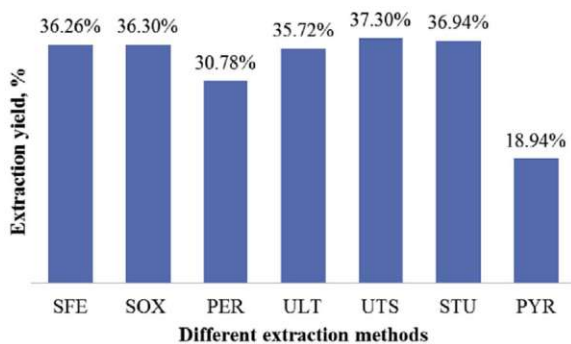
710 | *Nat. Prod. Rep.*, 2023, **40**, 676–717

115

This journal is © The Royal Society of Chemistry 2023

Fig. 24 Extraction yields obtained through different extraction processes.[170] Reprinted with permission from Elsevier.
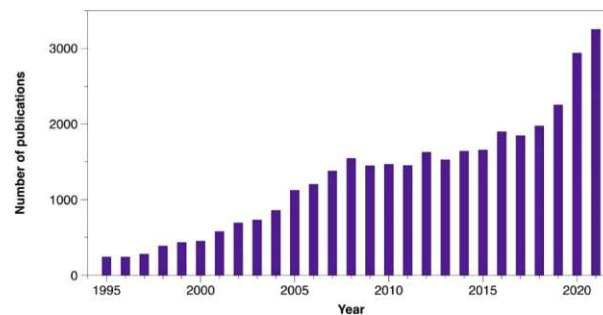

Fig. 25 Cannabinoids related publications based on the database of SciFinder[n] (search term: cannabinoids, 10.05.2022).

MAE, CBD yields were favored by MAE and CBDA by DM. Considering all the aforementioned, DM was selected as the best extraction method for non-intoxicating cannabinoids.[42]

A comparative study of different extraction approaches for hemp seed oil and their industrially-relevant financial assessment was performed. The following extraction techniques were evaluated; Soxhlet (SOX), percolation (PER), supercritical fluid extraction (SFE), ultrasonication (ULT), pyrolysis (PYR), ULT treated SOX (UTS) and SOX treated ULT (STU).

Maximum extraction efficiency is obtained *via* UTS (Fig. 24), however, SFE provides product of the highest purity. Aside from efficiency, the profile of the obtained fatty acids is significantly affected by the extraction method of choice. SFE and SOX are not only the most efficient in terms of extraction but they also provide the ideal ratio (3.22 and 2.40, respectively), from a dietary perspective, of ω-6 to ω-3 acids. In contrast, the high ratio obtained *via* UTS (9.24) renders it unsuitable for the extraction of fatty acids intended for nutritional purposes.

Concerning industrial upscaling, all the evaluated techniques are considered to be financially viable. Despite the high cost of SFE, the expected profit (high market value due to the high purity of the product), which exceeds 10-fold the profit of the other processes, more than counterbalances the high cost. The use of ultrasonication is the main reason that ULT and UTS exhibit the highest power consumption.[170]

3. Conclusion

In the last few years, there has been an increasing interest worldwide in cannabis-derived phytochemicals, mainly due to their medical potential, as well as their merit/role in the production of industrially valuable products (Fig. 25). Despite this dramatic boost, the extraction of high value-added products is still in its early stages, as new bioactive compounds are constantly discovered, and their identification and isolation remain challenging tasks. In this review, the extraction of phytochemicals present in cannabis plant with the aid of conventional techniques and more sophisticated ones has been discussed.

Evidently, the extraction of phytochemicals is a complex process and, up till now, progress in extraction of target compounds has been achieved with various levels of performance/effectiveness. It has been demonstrated that by substituting the conventional solvent extraction techniques with modern strategies has led to reduction of extraction time, decrease of solvent consumption, high extraction yields, increased selectivity, fractionation and stability of targeted compounds.

Nevertheless, there are still numerous questions that need to be addressed. The conducted research has mainly focused on valuable compounds, such as cannabinoids, essential oils and pigments, however, complete characterization of the extracts is notably absent. While high recovery of desirable compounds is the main objective, it is equally important to include data on the possible presence of contaminants, such as degradation products and/or residual pesticides and growth regulators, which apart from lowering the quality of the derived extracts, could also have a harmful effect if used in products intended for human consumption. Additionally, a concise interpretation of the obtained results could be useful; the impact of the extracted amount of each valuable compound on the extract quality, organoleptic features and stability should be clearly stated.

Regarding sample storage and preparation prior to extraction, both can drastically influence the chemical profile of the starting material and the yield and composition of the collected extract, as demonstrated in the research discussed in this review. Therefore, a reconciliation in the inconsistencies regarding storage conditions (fridge, freezer, RT, dark, light) and sample preparation (particle size, moisture content) is necessary in order to accurately evaluate the obtained results and compare the experimental outcomes of different research efforts. Furthermore, the merit of the developed extraction approaches could benefit from their further application to various cannabis sources (fibers, flowers, seeds, processing residues) and different cannabis varieties.

Reliable quantification of the extracts is of paramount importance and the development of a unified and validated analytical approach could mitigate quantification errors and deviations, which is especially important for extracts intended for medicinal applications. Additionally, a unified approach should be introduced regarding the input material characterization and the reported quantification results; we believe that this would significantly facilitate future research work and effectively simplify the comparison between different extraction approaches.

This journal is © The Royal Society of Chemistry 2023

116

Nat. Prod. Rep., 2023, **40**, 676–717 | **711**

Table 14 Summary of advantages and disadvantages for different extraction techniques

Extraction method	Principle	Advantages	Disadvantages
Supercritical fluid	Improved extraction efficiency due to low viscosity & high diffusivity	• Non-toxic & non-flammable • No solvent residues • Easy separation from product	• Limited to non-polar and weakly polar compounds • Energy-demanding • Special equipment required
Ionic liquids & deep eutectic solvents	Liquids with low vapour pressure, that consist of ions	• Tuneable properties • High extraction yields • Improved safety	• High cost • Viscosity issues
Solvent-based Soxhlett extraction	Organic solvents	• Low investment costs • High reproducibility	• Large solvent consumption • Use of persistent/flammable chemicals
Ultrasound-assisted	Local hotspots generated *via* cavitation	• Low energy consumption • Low investment costs	• Large solvent consumption Use of persistent/flammable chemicals
Microwave-assisted	Direct conversion of electromagnetic energy to heat	• Short extraction time • High extraction yields	• Ineffective for non-polar target compounds • Not suitable for thermally instable compounds
Pressurized liquid	High temperature (enhances solvent diffusion due to reduced viscosity) and pressure (promotes cell permeability) is applied	• Fast • Low solvent consumption • High reproducibility	• High cost • Degradation of thermo-labile compounds may occur
Hydrodistillation	Water and/or steam is applied for the extraction	• No organic solvent	• Volatile and thermo-labile compounds may be lost • Energy-intense
Mechanical pressing	Mechanical pressure	• Simple • Low cost • No solvent-free	• Low yields and reproducibility

We should point out, that there is no universal extraction technique, as each extraction technique has advantages and disadvantages (Table 14). Moreover, it is dependent on the part of the plant used and the nature of the target compound. Considerable attention needs to be paid to the aim of the investigation at hand and the target compounds when deciding on the pretreatment approach of the input material and the extraction technique. Scientists, motivated by the increased demand of extracting bioactive compounds present in plants, are in continuous search for suitable and more sophisticated extraction techniques. However, a combination of processes may be the beautiful and rewarding future of the extraction of cannabis-related bioactive compounds.

4. Abbreviations

AD	anno Domini
AgNO$_3$	Silver nitrate
ANOVA	Analysis of variance
BC	Before Christ
Cannabis sativa L.	*Cannabis sativa* Linnaeus
CBC	Cannabichromene
CBCA	Cannabichromenic acid
CBD	Cannabidiol
CBDA	Cannabidiolic acid
CBE	Cannabielsoin
CBG	Cannabigerol
CBGA	Cannabigerolic acid
CBL	Cannabicyclol
CBN	Cannabinodiol
CBT	Cannabitriol
CCD	Central composite design
CHCl$_3$	Chloroform
[C$_6$mim][NTf$_2$]	1-Hexyl-3-methylimidazolium bis(trifluoromethylsulfonyl)imide
DES	Deep eutectic solvent
DM	Dynamic maceration
EAE	Enzyme-assisted extraction
EFA	Essential fatty acids
EtOH	Ethanol
EU	European Union
FA	Ferulic acid
FFA	Free fatty acid
FRAP	Ferric reducing ability of plasma
FUSE	Focused ultrasound extraction
g	Grams

GC-FID	Gas chromatography-flame ionization detector
GLA	Gamma-linolenic acid
HD	Hydro distillation
HDPE	High-density polyethylene
H_2O	Water
II	Insoluble impurities
IL	Ionic liquid
LDL	Low-density lipoprotein
MAE	Microwave assisted extraction
MeOH	Methanol
mg	Milligrams
MUFA	Monounsaturated fatty acids
MW	Microwave
NMR	Nuclear magnetic resonance
RSC	Response surface methodology
p-CA	p-Coumaric acid
PCA	Principal component analysis
PEF	Pulsed electric field
PER	Percolation
PLE	Pressurized-liquid extraction
ppm	Part per millions
PUFA	Polyunsaturated fatty acid
PYR	Pyrolysis
RSM	Response surface methodology
$scCO_2$	Super critical carbon dioxide
SD	Steam distillation
SDA	Stearidonic acid
SE	Solvent extraction
SFE	Supercritical fluid extraction
SOX	Soxhlet
SPE	Solid phase extraction
STU	Soxhlet treated ultrasonication
TF	total flavonoids
THC	Δ^9-Tetrahydrocannabinol
THCA	Δ^9-Tetrahydrocannabinolic acid
TP	Total phenolics
Tween 20	polysorbate 20
UAE	Ultrasound assisted extraction
UFA	Unsaturated fatty acid
UK	United Kingdom
ULT	Ultrasonication
UN	United Nations
US(A)	United States of America
UTS	Ultrasonication treated Soxhlet

5. Author contributions

A. S. M. & O. L. conceived the review, analysed the data; wrote the original draft, O. L. edited and reviewed the draft. K. S. reviewed, edited and contributed to the manuscript content. K. B.-S.& H. H. conceived and supervised, edited and reviewed the draft. M. S. reviewed the draft.

6. Conflicts of interest

There are no conflicts of interest to declare.
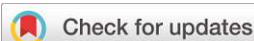
7. Acknowledgements

8. References

1 E. Small and A. Cronquist, *Taxon*, 1976, **25**, 405–435.
2 J. F. Hancock, *Plant evolution and the origin of crop species*, CABI, 2012.
3 C. T. Kung, *Archeology in China*, University of Toronto Press, Toronto, 1959, vol. 1, p. 131.
4 K.-C. Chang, *Science*, 1968, **162**, 519–526.
5 I. Bocsa and M. Karus, *The cultivation of hemp: botany, varieties, cultivation and harvesting*, Hemptech, 1998.
6 S. Chandra, H. Lata and M. A. ElSohly, *Cannabis sativa L.-botany and biotechnology*, Springer, 2017.
7 H.-E. Jiang, X. Li, Y.-X. Zhao, D. K. Ferguson, F. Hueber, S. Bera, Y.-F. Wang, L.-C. Zhao, C.-J. Liu and C.-S. Li, *J. Ethnopharmacol.*, 2006, **108**, 414–422.
8 R. E. Schultes, *Nat. Hist.*, 1973, **82**, 59.
9 G. Leson, in *Hemp: industrial production and uses*, ed. P. Bouloc, S. Allegret and L. Arnaud, CABI, 2013, ch. 16, pp. 229–238.
10 M. Touw, *J. Psychoact. Drugs*, 1981, **13**, 23–34.
11 H.-L. Li, *Econ. Bot.*, 1974, **28**, 437–448.
12 H.-L. Li, *J. Psychedelic Drugs*, 1978, **10**, 17–26.
13 A. Mukherjee, S. C. Roy, S. De Bera, H.-E. Jiang, X. Li, C.-S. Li and S. Bera, *Genet. Resour. Crop Evol.*, 2008, **55**, 481–485.
14 E. Small, *Cannabis: a complete guide*, CRC Press, 2016.
15 M. R. Aldrich, *J. Psychedelic Drugs*, 1977, **9**, 227–233.
16 R. Mechoulam and L. A. Parker, *Annu. Rev. Psychol.*, 2013, **64**, 21–47.
17 E. L. Abel, *Marihuana: the first twelve thousand years*, Springer Science & Business Media, 2013.
18 S. Wills, in *Cannabis: the genus cannabis*, CRC Press, 1st edn, 1998, pp. 1–27.
19 M. B. Bridgeman and D. T. Abazia, *Pharmacy and Therapeutics*, 2017, vol. 42, p. 180.
20 USDA, *Classification for Kingdom Plantae Down to Species Cannabis sativa L.*, **https://plants.usda.gov/java/ClassificationServlet?source=display&classid=CASA3**, accessed 27.10.2020.
21 J. M. McPartland, *Cannabis Cannabinoid Res.*, 2018, **3**, 203–212.
22 E. Small, P. Y. Jui and L. P. Lefkovitch, *Syst. Bot.*, 1976, **1**, 67–84.
23 K. W. Hillig and P. G. Mahlberg, *Am. J. Bot.*, 2004, **91**, 966–975.
24 R. C. Clarke and M. D. Merlin, *Cannabis: evolution and ethnobotany*, Univ of California Press, 2013.
25 J. M. McPartland and G. W. Guy, *Bot. Rev.*, 2017, **83**, 327–381.
26 G. Green, *The Cannabis Breeder's Bible: The Definitive Guide to Marijuana Genetics, Cannabis Botany and Creating Strains for the Seed Market*, Green Candy Press, New York, 2005.
27 C. Linnaeus, *Species Plantarum*, Laurentius Salvius, Stockholm, 1st edn, 1753.
28 C. Linnaeus, *Genera plantarum*, Laurentius Salvius, Stockholm, 5 edn, 1754.

This journal is © The Royal Society of Chemistry 2023

118

Nat. Prod. Rep., 2023, **40**, 676–717 | **713**

29 J. Lamarck, *Encyclopédique méthodique*, Botanique I, Paris, 1785.

30 L. C. Anderson, *Leaf Variation among Cannabis Species from a Controlled Garden*, **https://www.biodiversitylibrary.org/part/168641**, accessed November 2022.

31 J. M. McPartland and G. W. Guy, *The evolution of Cannabis and coevolution with the cannabinoid receptor - a hypothesis*, Royal Society of Pharmacists, London, 2004.

32 J. McPartland, O'Shaughnessy's (J Calif Cannabis Res Med Group), Autumn, 2014, 1.

33 P. Henry, *PeerJ PrePrints*, 2015, **3**, e1553.

34 R. Clarke and M. Merlin, *HerbalGram*, 2016, **110**, 44–49.

35 T. J. Sheehan, H. J. Hamnett, R. Beasley and P. S. Fitzmaurice, *Forensic Sci. Prog.*, 2019, **4**, 168–178.

36 R. Mechoulam, P. Braun and Y. Gaoni, *J. Am. Chem. Soc.*, 1967, **89**, 4552–4554.

37 M. M. Radwan, S. Chandra, S. Gul and M. A. ElSohly, *Molecules*, 2021, **26**, 2774.

38 R. Brenneisen, in *Marijuana and the Cannabinoids*, Humana Press, New Jersey, 2007, ch. 2, pp. 17–49.

39 I. J. Flores-Sanchez and R. Verpoorte, *Phytochem. Rev.*, 2008, **7**, 615–639.

40 D. M. Lambert and C. J. Fowler, *J. Med. Chem.*, 2005, **48**, 5059–5087.

41 G. Appendino, G. Chianese and O. Taglialatela-Scafati, *Curr. Med. Chem.*, 2011, **18**, 1085–1099.

42 V. Brighenti, F. Pellati, M. Steinbach, D. Maran and S. Benvenuti, *J. Pharm. Biomed. Anal.*, 2017, **143**, 228–236.

43 F. Pellati, V. Brighenti, J. Sperlea, L. Marchetti, D. Bertelli and S. Benvenuti, *Molecules*, 2018, **23**, 2639.

44 F. Pellati, V. Borgonetti, V. Brighenti, M. Biagi, S. Benvenuti and L. Corsi, *BioMed Res. Int.*, 2018, **2018**, 1691428.

45 Y. Gaoni and R. Mechoulam, *J. Am. Chem. Soc.*, 1964, **86**, 1646–1647.

46 N. M. Kogan and R. Mechoulam, *Dialogues Clin. Neurosci.*, 2007, **9**, 413.

47 S. Ameur, B. Haddou, Z. Derriche, J.-P. Canselier and C. Gourdon, *Anal. Bioanal. Chem.*, 2013, **405**, 3117–3123.

48 R. Mechoulam, L. A. Parker and R. Gallily, *J. Clin. Pharmacol.*, 2002, **42**, 11S–19S.

49 J. Fernández-Ruiz, O. Sagredo, M. R. Pazos, C. García, R. Pertwee, R. Mechoulam and J. Martínez-Orgado, *Br. J. Clin. Pharmacol.*, 2013, **75**, 323–333.

50 R. Mechoulam, M. Peters, E. Murillo-Rodriguez and L. O. Hanuš, *Chem. Biodiversity*, 2007, **4**, 1678–1692.

51 C. M. Andre, J.-F. Hausman and G. Guerriero, *Front. Plant Sci.*, 2016, **7**, 19.

52 H. Mölleken and R. R. Theimer, *J. Ind. Hemp*, 1997, **4**, 13–17.

53 S. A. Ross, Z. Mehmedic, T. P. Murphy and M. A. ElSohly, *J. Anal. Toxicol.*, 2000, **24**, 715–717.

54 M. B. Amar, *J. Ethnopharmacol.*, 2006, **105**, 1–25.

55 D. Baker, G. Pryce, G. Giovannoni and A. J. Thompson, *Lancet Neurol*, 2003, **2**, 291–298.

56 S. P. Alexander, *Prog. Neuro-Psychopharmacol. Biol. Psychiatry*, 2016, **64**, 157–166.

57 M. Guzman, *Nat. Rev. Cancer*, 2003, **3**, 745–755.

58 M. P. Barnes, *Expert Opin. Pharmacother.*, 2006, **7**, 607–615.

59 O. Devinsky, C. Verducci, E. A. Thiele, L. C. Laux, A. D. Patel, F. Filloux, J. P. Szaflarski, A. Wilfong, G. D. Clark and Y. D. Park, *Epilepsy Behav.Epilepsy Behav.*, 2018, **86**, 131–137.

60 B. Palmieri, C. Laurino and M. Vadalà, *Int. J. Pharm. Pract.*, 2019, **27**, 264–270.

61 J. Sastre-Garriga, C. Vila, S. Clissold and X. Montalban, *Expert Rev. Neurother.*, 2011, **11**, 627–637.

62 S. Giacoppo, P. Bramanti and E. Mazzon, *Mult. Scler. Relat. Disord.*, 2017, **17**, 22–31.

63 US-Food-and-Drug-Administration, *FDA approves first drug comprised of an active ingredient derived from marijuana to treat rare, severe forms of epilepsy*, US Food and Drug Administration, 2018.

64 S. Elzinga, J. Fischedick, R. Podkolinski and J. C. Raber, *Nat. Prod. Chem. Res.*, 2015, **3**, 1–9.

65 A. Hazekamp, K. Tejkalová and S. Papadimitriou, *Cannabis Cannabinoid Res.*, 2016, **1**, 202–215.

66 E. Small and H. D. Beckstead, *Nature*, 1973, **245**, 147–148.

67 J. C. Callaway, *Euphytica*, 2004, **140**, 65–72.

68 H. Wang and Y. Wei, *Med. Plant*, 2012, **3**, 11–14.

69 C.-W. Cheng, Z.-X. Bian, L.-X. Zhu, J. C. Wu and J. J. Sung, *Am. J. Gastroenterol.*, 2011, **106**, 120–129.

70 C. Leizer, D. Ribnicky, A. Poulev, S. Dushenkov and I. Raskin, *J. Diet. Suppl.*, 2000, **2**, 35–53.

71 C. R. Vogl, H. Mölleken, G. Lissek-Wolf, A. Surböck and J. Kobert, *J. Ind. Hemp*, 2004, **9**, 51–68.

72 R. Wall, R. P. Ross, G. F. Fitzgerald and C. Stanton, *Nutr. Rev.*, 2010, **68**, 280–289.

73 J.-L. Deferne and D. W. Pate, *J. Ind. Hemp*, 1996, **3**, 1–7.

74 A. P. Simopoulos, *Biomed. Pharmacother.*, 2002, **56**, 365–379.

75 B. D. Oomah, M. Busson, D. V. Godfrey and J. C. Drover, *Food Chem.*, 2002, **76**, 33–43.

76 D. Spielmann, U. Bracco, H. Traitler, G. Crozier, R. Holman, M. Ward and R. Cotter, *J. Parenter. Enteral Nutr.*, 1988, **12**, 111S–123S.

77 D. Wirtshafter, in *Bioresource Hemp: proceedings of the symposium*, Hemptech, Frankfurt Am Main, Germany, 1995, pp. 546–555.

78 A. Rezvankhah, Z. Emam-Djomeh, M. Safari, G. Askari and M. Salami, *J. Food Process. Preserv.*, 2018, **42**, e13766.

79 A. Kamal-Eldin and L. Å. Appelqvist, *Lipids*, 1996, **31**, 671–701.

80 S. Sapino, M. E. Carlotti, E. Peira and M. Gallarate, *Int. J. Cosmet. Sci.*, 2005, **27**, 355.

81 L. L. Yu, K. K. Zhou and J. Parry, *Food Chem.*, 2005, **91**, 723–729.

82 C.-H. Tang, Z. Ten, X.-S. Wang and X.-Q. Yang, *J. Agric. Food Chem.*, 2006, **54**, 8945–8950.

83 S.-K. Park, J.-B. Seo and M.-Y. Lee, *Biochim. Biophys. Acta, Proteins Proteomics*, 2012, **1824**, 374–382.

84 E. Vonapartis, M.-P. Aubin, P. Seguin, A. F. Mustafa and J.-B. Charron, *J. Food Compos. Anal.*, 2015, **39**, 8–12.

85 E. Guenther, *Essent. Oils*, 1972, **1**, 87–226.

86 M. W. Giese, M. A. Lewis, L. Giese and K. M. Smith, *J. AOAC Int.*, 2019, **98**, 1503–1522.

714 | *Nat. Prod. Rep.*, 2023, **40**, 676–717

119

This journal is © The Royal Society of Chemistry 2023

87 H. Hendriks, T. M. Malingré, S. Batterman and R. Bos, *Phytochemistry*, 1975, **14**, 814–815.

88 E. Lemberkovics, P. Veszki, G. Verzar-Petri and A. Trka, *Sci. Pharmacol.*, 1981, **49**, 401–408.

89 L. Hood, M. Dames and G. Barry, *Nature*, 1973, **242**, 402–403.

90 V. Mediavilla and S. Steinemann, *J. Ind. Hemp*, 1997, **4**, 80–82.

91 J. Novak and C. Franz, *J. Essent. Oil Res.*, 2003, **15**, 158–160.

92 E. B. Russo, *Br. J. Pharmacol.*, 2011, **163**, 1344–1364.

93 J. M. McPartland and E. B. Russo, *J. Cannabis Ther.*, 2001, **1**, 103–132.

94 M. Hesami, A. Baiton, M. Alizadeh, M. Pepe, D. Torkamaneh and A. M. P. Jones, *Int. J. Mol. Sci.*, 2021, **22**, 5671.

95 B. Farinon, R. Molinari, L. Costantini and N. Merendino, *Nutrients*, 2020, **12**, 1935.

96 M. Kuddus, I. A. Ginawi and A. Al-Hazimi, *Emir. J. Food Agric.*, 2013, 736–745.

97 E. Small and D. Marcus, in *Trends in New Crops and New Uses*, Alexandria, VA, 2002, pp. 284–326.

98 E. Small, in *Natural fibers and composites*, Studium Press, Houston, 2014, pp. 29–64.

99 E. Kreuger, T. Prade, F. Escobar, S.-E. Svensson, J.-E. Englund and L. Björnsson, *Biomass Bioenergy*, 2011, **35**, 893–900.

100 L. Nissen, A. Zatta, I. Stefanini, S. Grandi, B. Sgorbati, B. Biavati and A. Monti, *Fitoterapia*, 2010, **81**, 413–419.

101 D. Gibb, M. Shah, P. Mir and T. McAllister, *Can. J. Anim. Sci.*, 2005, **85**, 223–230.

102 A. Mustafa, J. McKinnon and D. Christensen, *Can. J. Anim. Sci.*, 1999, **79**, 91–95.

103 A. Hessle, M. Eriksson, E. Nadeau, T. Turner and B. Johansson, *Acta Agric. Scand., Sect. A*, 2008, **58**, 136–145.

104 J. W. Roulac, *Hemp horizons: the comeback of the world's most promising plant*, Chelsea Green Publishing Company, Vermount, United States, 1st edn, 1997.

105 S.-Y. Li, J. D. Stuart, Y. Li and R. S. Parnas, *Bioresour. Technol.*, 2010, **101**, 8457–8460.

106 R. Weightman and D. Kindred, *Review and analysis of breeding and regulation of hemp and flax varieties available for growing in the UK*, ADAS Centre for Sustainable Crop Management, Boxworth, Cambridge, 2005.

107 *The science of cannabis and hemp storage*, https://bovedainc.com/the-science-of-cannabis-and-hemp-storage/, accessed October, 2020.

108 P. L. Atkins, *J. AOAC Int.*, 2019, **102**, 427–433.

109 L. Zamengo, C. Bettin, D. Badocco, V. Di Marco, G. Miolo and G. Frison, *Forensic Sci. Int.*, 2019, **298**, 131–137.

110 D. J. Harvey, *J. Ethnopharmacol.*, 1990, **28**, 117–128.

111 P. Lerner, The precise determination of tetrahydrocannabinol in marihuana and hashish, United Nations Office on Drugs and Crime, Vienna, *Bull. Narc.*, 1969, **21**, 39–42.

112 K. Grafström, K. Andersson, N. Pettersson, J. Dalgaard and S. J. Dunne, *Forensic Sci. Int.*, 2019, **301**, 331–340.

113 C. Lindholst, *Aust. J. Forensic Sci.*, 2010, **42**, 181–190.

114 R. N. Smith and C. G. Vaughan, *J. Pharm. Pharmacol.*, 1977, **29**, 286–290.

115 J. W. Fairbairn, J. A. Liebmann and M. G. Rowan, *J. Pharm. Pharmacol.*, 1976, **28**, 1–7.

116 K. D. Roth, N. A. Siegel, R. W. Johnson Jr, L. Litauszki, L. Salvati Jr, C. A. Harrington and L. K. Wray, *J. Anal. Toxicol.*, 1996, **20**, 291–300.

117 T. Moreno, F. Montanes, S. J. Tallon, T. Fenton and J. W. King, *J. Supercrit. Fluids*, 2020, **161**, 104850.

118 M. Sexton, K. Shelton, P. Haley and M. West, *Planta Med.*, 2018, **84**, 234–241.

119 D. R. Grijó, I. A. V. Osorio and L. Cardozo-Filho, *J. CO$_2$ Util.*, 2018, **28**, 174–180.

120 C. Da Porto, D. Decorti and A. Natolino, *Ind. Crops Prod.*, 2014, **58**, 99–103.

121 L. L. Romano and A. Hazekamp, *Cannabinoids*, 2013, **1**, 1–11.

122 A. Casiraghi, G. Roda, E. Casagni, C. Cristina, U. M. Musazzi, S. Franzè, P. Rocco, C. Giuliani, G. Fico and P. Minghetti, *Planta Med.*, 2018, **84**, 242–249.

123 M.-V. Morar, K. Dragan, C. Bele, C. Matea, I. Tarta, R. Suharovschi and C. Semeniuc, *Bull. Univ. Agric. Sci. Vet. Med. Cluj-Napoca, Agric.*, 2010, **67**, 2.

124 A. C. Gallo-Molina, H. I. Castro-Vargas, W. F. Garzón-Méndez, J. A. M. Ramírez, Z. J. R. Monroy, J. W. King and F. Parada-Alfonso, *J. Supercrit. Fluids*, 2019, **146**, 208–216.

125 L. J. Rovetto and N. V. Aieta, *J. Supercrit. Fluids*, 2017, **129**, 16–27.

126 C. Da Porto, D. Voinovich, D. Decorti and A. Natolino, *J. Supercrit. Fluids*, 2012, **68**, 45–51.

127 Z. Drinić, S. Vidović, J. Vladić, A. Koren, B. Kiprovski and V. Sikora, *Lek. Sirovine*, 2018, 17–21.

128 S.-S. Teh and E. J. Birch, *Ultrason. Sonochem.*, 2014, **21**, 346–353.

129 S.-S. Teh, B. E. Niven, A. E.-D. A. Bekhit, A. Carne and E. J. Birch, *Food Bioprocess Technol.*, 2014, **7**, 3064–3076.

130 J. Y. Lin, Q. X. Zeng, Q. An, Q. Z. Zeng, L. X. Jian and Z. W. Zhu, *J. Food Process Eng.*, 2012, **35**, 76–90.

131 D. R. Grijó, G. K. Piva, I. V. Osorio and L. Cardozo-Filho, *J. Supercrit. Fluids*, 2019, **143**, 268–274.

132 K. Aladić, S. Vidović, J. Vladić, D. Balić, H. Jukić and S. Jokić, *Int. J. Food Sci. Technol.*, 2016, **51**, 885–893.

133 E. Vági, M. Balázs, A. Komóczi, I. Kiss, M. Mihalovits and E. Székely, *Period. Polytech., Chem. Eng.*, 2019, **63**, 357–363.

134 D. Fiorini, S. Scortichini, G. Bonacucina, N. G. Greco, E. Mazzara, R. Petrelli, J. Torresi, F. Maggi and M. Cespi, *Ind. Crops Prod.*, 2020, **154**, 112688.

135 J. Liang, E. Zago, R. Nandasiri, R. Khattab, N. M. Eskin, P. Eck and U. Thiyam-Holländer, *J. Am. Oil Chem. Soc.*, 2018, **95**, 1319–1327.

136 Y. Nuapia, H. Tutu, L. Chimuka and E. Cukrowska, *Molecules*, 2020, **25**, 1335.

137 M. Crimaldi, S. Faugno, M. Sannino and L. Ardito, *Chem. Eng. Trans.*, 2017, **58**, 373–378.

138 S. Rochfort, A. Isbel, V. Ezernieks, A. Elkins, D. Vincent, M. A. Deseo and G. C. Spangenberg, *Sci. Rep.*, 2020, **10**, 1–7.

This journal is © The Royal Society of Chemistry 2023

120

Nat. Prod. Rep., 2023, **40**, 676–717 | **715**

139 T. Väisänen, P. Kilpeläinen, V. Kitunen, R. Lappalainen and L. Tomppo, *Ind. Crops Prod.*, 2019, **131**, 224–233.

140 K. Leiman, L. Colomo, S. Armenta, M. de la Guardia and F. A. Esteve-Turrillas, *Talanta*, 2018, **190**, 321–326.

141 J. Omar, M. Olivares, M. Alzaga and N. Etxebarria, *J. Sep. Sci.*, 2013, **36**, 1397–1404.

142 D. De Vita, V. N. Madia, V. Tudino, F. Saccoliti, A. De Leo, A. Messore, P. Roscilli, A. Botto, I. Pindinello and G. Santilli, *Nat. Prod. Res.*, 2020, **34**, 2952–2958.

143 C.-W. Chang, C.-C. Yen, M.-T. Wu, M.-C. Hsu and Y.-T. Wu, *Molecules*, 2017, **22**, 1894.

144 S. Naz, M. A. Hanif, T. M. Ansari and J. N. Al-Sabahi, *Spectrosc. Spectral Anal.*, 2017, **37**, 306–311.

145 S. Naz, M. A. Hanif, H. N. Bhatti and T. M. Ansari, *J. Essent. Oil-Bear. Plants*, 2017, **20**, 175–184.

146 M. D. Kostić, N. M. Joković, O. S. Stamenković, K. M. Rajković, P. S. Milić and V. B. Veljković, *Ind. Crops Prod.*, 2014, **52**, 679–686.

147 S. Latif and F. Anwar, *Eur. J. Lipid Sci. Technol.*, 2009, **111**, 1042–1048.

148 D. Fiorini, A. Molle, M. Nabissi, G. Santini, G. Benelli and F. Maggi, *Ind. Crops Prod.*, 2019, **128**, 581–589.

149 A. Aiello, F. Pizzolongo, G. Scognamiglio, A. Romano, P. Masi and R. Romano, *Int. J. Food Sci. Technol.*, 2020, **55**, 2472–2480.

150 L. Eöry, B. Dános and T. Veress, *Z Zagadnien Nauk Sadowych*, 2001, **47**, 322–327.

151 C. Da Porto, D. Decorti and F. Tubaro, *Ind. Crops Prod.*, 2012, **36**, 401–404.

152 C. Da Porto, A. Natolino and D. Decorti, *J. Food Sci. Technol.*, 2015, **52**, 1748–1753.

153 K. Tomita, S. Machmudah, A. T. Quitain, M. Sasaki, R. Fukuzato and M. Goto, *J. Supercrit. Fluids*, 2013, **79**, 109–113.

154 K. Aladić, K. Jarni, T. Barbir, S. Vidović, J. Vladić, M. Bilić and S. Jokić, *Ind. Crops Prod.*, 2015, **76**, 472–478.

155 V. Devi and S. Khanam, *J. Environ. Chem. Eng.*, 2019, **7**, 102818.

156 C. Kornpointner, A. Sainz Martinez, S. Marinovic, C. Haselmair-Gosch, P. Jamnik, K. Schröder, C. Löfke and H. Halbwirth, *Ind. Crops Prod.*, 2021, **165**, 113422.

157 C. Kornpointner, A. Sainz Martinez, M. Schnürch, H. Halbwirth and K. Bica-Schröder, *Green Chem.*, 2021, **23**, 10079–10089.

158 C. Cai, W. Yu, C. Wang, L. Liu, F. Li and Z. Tan, *J. Mol. Liq.*, 2019, **287**, 110957.

159 C. Cai, Y. Wang, Y. Yi, F. Li and Z. Tan, *Ind. Crops Prod.*, 2020, **155**, 112796.

160 T. M. Attard, C. Bainier, M. Reinaud, A. Lanot, S. J. McQueen-Mason and A. J. Hunt, *Ind. Crops Prod.*, 2018, **112**, 38–46.

161 E. Vági, M. Balázs, A. Komoczi, M. Mihalovits and E. Székely, *J. Supercrit. Fluids*, 2020, **164**, 104898.

162 V. Kitrytė, D. Bagdonaitė and P. R. Venskutonis, *Food Chem.*, 2018, **267**, 420–429.

163 K. Aladić, S. Jokić, T. Moslavac, S. Tomas, S. Vidović, J. Vladić and D. Šubarić, *Chem. Biochem. Eng. Q.*, 2014, **28**, 481–490.

164 T. Křížek, M. Bursová, R. Horsley, M. Kuchař, P. Tůma, R. Čabala and T. Hložek, *J. Cleaner Prod.*, 2018, **193**, 391–396.

165 M. D. Kostić, N. M. Joković, O. S. Stamenković, K. M. Rajković, P. S. Milić and V. B. Veljković, *Ind. Crops Prod.*, 2013, **48**, 133–143.

166 C. Agarwal, K. Máthé, T. Hofmann and L. Csóka, *J. Food Sci.*, 2018, **83**, 700–710.

167 A. Rezvankhah, Z. Emam-Djomeh, M. Safari, G. Askari and M. Salami, *J. Food Sci. Technol.*, 2019, **56**, 4198–4210.

168 Z. Drinić, J. Vladić, A. Koren, T. Zeremski, N. Stojanov, B. Kiprovski and S. Vidović, *J. Chem. Technol. Biotechnol.*, 2020, **95**, 831–839.

169 S. Faugno, S. Piccolella, M. Sannino, L. Principio, G. Crescente, G. M. Baldi, N. Fiorentino and S. Pacifico, *Ind. Crops Prod.*, 2019, **130**, 511–519.

170 V. Devi and S. Khanam, *J. Cleaner Prod.*, 2019, **207**, 645–657.

171 L. Candy, S. Bassil, L. Rigal, V. Simon and C. Raynaud, *Ind. Crops Prod.*, 2017, **109**, 335–345.

172 F. Potin, S. Lubbers, F. Husson and R. Saurel, *J. Food Sci.*, 2019, **84**, 3682–3690.

173 M. P. Lazarjani, O. Young, L. Kebede and A. Seyfoddin, *J. Cannabis Res*, 2021, **3**, 32.

174 World-Health-Organization, *Drugs (psychoactive)*, **https://www.who.int/health-topics/drugs-psychoactive#tab=tab_3**, accessed October 2022.

175 NHS, Psychotropic Medication, **https://www.datadictionary.nhs.uk/nhs_business_definitions/psychotropic_medication.html**, accessed October 2022.

176 F. Caraci, S. J. Enna, J. Zohar, G. Racagni, G. Zalsman, W. van den Brink, S. Kasper, G. F. Koob, C. M. Pariante, P. V. Piazza, K. Yamada, M. Spedding and F. Drago, *Br. J. Clin. Pharmacol.*, 2017, **83**, 1614–1616.

177 J. McMurry, *Organic Chemistry*, Thomson-Brooks/Cole, 2004.

178 F. Pattnaik, S. Nanda, S. Mohanty, A. K. Dalai, V. Kumar, S. K. Ponnusamy and S. Naik, *Chemosphere*, 2022, **289**, 133012.

179 H. M. S. AL Ubeed, D. J. Bhuyan, M. A. Alsherbiny, A. Basu and Q. V. Vuong, *Molecules*, 2022, **27**, 604.

180 S. Qamar, Y. J. M. Torres, H. S. Parekh and J. Robert Falconer, *J. Chromatogr. B: Anal. Technol. Biomed. Life Sci.*, 2021, **1167**, 122581.

181 J. Peach and J. Eastoe, *Beilstein J. Org. Chem.*, 2014, **10**, 1878–1895.

182 E. L. N. Escobar, T. A. Da Silva, C. L. Pirich, M. L. Corazza and L. P. Ramos, *Front. Bioeng. Biotechnol.*, 2020, **8**, 252.

183 M. Freemantle, *An introduction to ionic liquids*, RSC Publishing, Cambridge, UK, 2009.

184 M. J. Earle and K. R. Seddon, *Pure Appl. Chem.*, 2000, **72**, 1391–1398.

185 A. K. Ressmann and K. Bica, in *Ionic Liquids for Better Separation Processes*, Springer, 2016, pp. 135–165.

716 | *Nat. Prod. Rep.*, 2023, **40**, 676-717

121

This journal is © The Royal Society of Chemistry 2023

186 H. Wang, G. Gurau and R. D. Rogers, *Chem. Soc. Rev.*, 2012, **41**, 1519–1537.

187 N. Mosier, C. Wyman, B. Dale, R. Elander, Y. Y. Lee, M. Holtzapple and M. Ladisch, *Bioresour. Technol.*, 2005, **96**, 673–686.

188 E. L. Smith, A. P. Abbott and K. S. Ryder, *Chem. Rev.*, 2014, **114**, 11060–11082.

189 D. Rengstl, V. Fischer and W. Kunz, *Phys. Chem. Chem. Phys.*, 2014, **16**, 22815–22822.

190 S. A. Malomo and R. E. Aluko, *Food Hydrocolloids*, 2015, **43**, 743–752.

191 J. M. Danlami, A. Arsad, M. A. A. Zaini and H. Sulaiman, *Rev. Chem. Eng.*, 2014, **30**, 605–626.

192 F. Chemat, N. Rombaut, A.-G. Sicaire, A. Meullemiestre, A.-S. Fabiano-Tixier and M. Abert-Vian, *Ultrason. Sonochem.*, 2017, **34**, 540–560.

193 B. Maazinejad, O. Mohammadnia, G. A. M. Ali, A. S. H. Makhlouf, M. N. Nadagouda, M. Sillanpää, A. M. Asiri, S. Agarwal, V. K. Gupta and H. Sadegh, *J. Mol. Liq.*, 2020, **298**, 112001.

194 N. Flórez, E. Conde and H. Domínguez, *J. Chem. Technol. Biotechnol.*, 2015, **90**, 590–607.

195 H.-F. Zhang, X.-H. Yang and Y. Wang, *Trends Food Sci. Technol.*, 2011, **22**, 672–688.

196 S. Serna-Loaiza, J. Adamcyk, S. Beisl, C. Kornpointner, H. Halbwirth and A. Friedl, *Processes*, 2020, **8**, 1334.

197 A. Oreopoulou, D. Tsimogiannis and V. Oreopoulou, in *Polyphenols in Plants*, ed. R. R. Watson, 2nd edn, Academic Press, 2019, ch. 15, pp. 243–259.

198 V. Gunjević, G. Grillo, D. Carnaroglio, A. Binello, A. Barge and G. Cravotto, *Ind. Crops Prod.*, 2021, **162**, 113247.

199 B. Cakaloglu, V. H. Ozyurt and S. Otles, *Ukr. Food J.*, 2018, **7**, 640–654.

This journal is © The Royal Society of Chemistry 2023

122

Nat. Prod. Rep., 2023, **40**, 676–717 | **717**

Combined ionic liquid and supercritical carbon dioxide based dynamic extraction of six cannabinoids from *Cannabis sativa* L.†

Christoph Kornpointner,‡[a] Aitor Sainz Martinez, ‡[b] Michael Schnürch, [b] Heidi Halbwirth *[a] and Katharina Bica-Schröder *[b]

The potential of supercritical CO_2 and ionic liquids (ILs) as alternatives to traditional extraction of natural compounds from plant material is of increasing importance. Both techniques offer several advantages over conventional extraction methods. These two alternatives have been separately employed on numerous ocassions, however, until now, they have never been combined for the extraction of secondary metabolites from natural sources, despite properties that complement each other perfectly. Herein, we present the first application of an IL-based dynamic supercritical CO_2 extraction of six cannabinoids (CBD, CBDA, Δ^9-THC, THCA, CBG and CBGA) from industrial hemp (*Cannabis sativa* L.). Various process parameters were optimized, *i.e.*, IL-based pre-treatment time and pre-treatment temperature, as well as pressure and temperature during supercritical fluid extraction. In addition, the impact of different ILs on cannabinoid extraction yield was evaluated, namely, 1-ethyl-3-methylimidazolium acetate, choline acetate and 1-ethyl-3-methylimidazolium dimethylphosphate. This novel technique exhibits a synergistic effect that allows the solvent-free acquisition of cannabinoids from industrial hemp, avoiding further processing steps and the additional use of resources. The newly developed IL-based supercritical CO_2 extraction results in high yields of the investigated cannabinoids, thus, demonstrating an effective and reliable alternative to established extraction methods. Ultimately, the ILs can be recycled to reduce costs and to improve the sustainability of the developed extraction process.

Introduction

Cannabis sativa L. is an annual herbaceous blossoming plant that has been used throughout history in the textile industry, for recreational purposes and in medical applications. It is regarded as one of the oldest cultivated plants, and one of the most essential crops for the progress of humankind. Although native to Eastern Asia, its extensive applications led to its global spread.[1]

The medicinal properties of *Cannabis sativa* L. can be attributed to the many bioactive compounds present in the plant, such as terpenes, polyphenols, phytosterols, tocopherols, fatty acids, and, specifically, cannabinoids, which are terpenophenolic secondary metabolites.[2,3] It is important to mention that cannabinoids are not equally distributed in the plant. They are mainly found in the trichomes and in smaller to negligible amounts in the seeds, while roots contain none.[4]

Presently, over 100 cannabinoids have been identified.[5] They are primarily encountered in their carboxylated form in the plant which constitutes a structure of 22 carbon atoms. So far, cannabinoids have been categorized into 11 subclasses: (1) (−)-Δ^9-tetrahydrocannabinol (Δ^9-THC), (2) (−)-Δ^8-tetrahydrocannabinol (Δ^8-THC), (3) cannabidiol (CBD), (4) cannabigerol (CBG), (5) cannabichromene (CBC), (6) cannabinol (CBN), (7) cannabinodiol (CBND), (8) cannabicyclol (CBL), (9) cannabielsoin (CBE), (10) cannabitriol (CBT) and (11) miscellaneous. The structures of cannabinoids from hemp investigated in this study are depicted in Fig. 1.[6]

In terms of the biosynthesis of cannabinoids, CBGA is the main precursor for THCA and CBDA.[7] However, under high temperatures, both acids are prone to degrade into their respective decarboxylated analogues, Δ^9-THC and CBD.[8]

Δ^9-THC and CBD are the most abundant cannabinoids present in cannabis plants. Δ^9-THC is well-known as a psychoactive compound, which influences the central nervous and cardiovascular systems. Contrarily, CBD is non-psychoac-

[a]*Institute of Chemical, Environmental and Bioscience Engineering, TU Wien, Getreidemarkt 9/166, 1060 Vienna, Austria. E-mail: heidrun.halbwirth@tuwien.ac.at*
[b]*Institute of Applied Synthetic Chemistry, TU Wien, Getreidemarkt 9/163, 1060 Vienna, Austria. E-mail: katharina.schroeder@tuwien.ac.at*
†Electronic supplementary information (ESI) available. See DOI: 10.1039/d1gc03516a
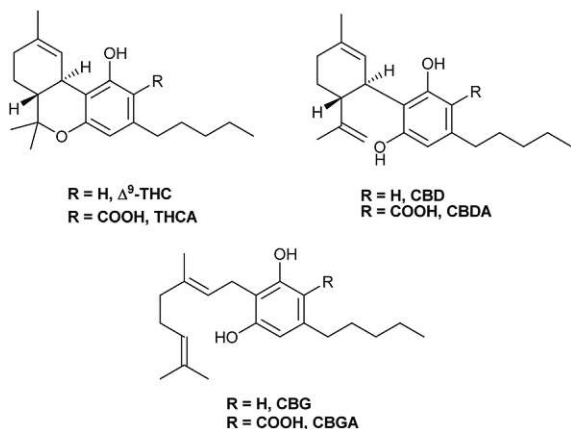‡These two authors contributed equally.

Fig. 1 Structures of the investigated cannabinoids in this study: Δ^9-THC, THCA, CBD, CBDA, CBG and CBGA.

tive, but is regarded as a compound of enormous medical interest, as it has demonstrated numerous health benefits. It has been reported to have anti-inflammatory, antiepileptic and anticonvulsive properties, among many others.[9–11] Excellent medicinal potential have been attributed to cannabinoids; thus, significant effort has been made in the past decades towards the research of the functions and mechanisms of cannabis-derived secondary metabolites in the human body.

Due to the growing medicinal interest in cannabinoids over the years, scientists have undertaken efforts in the development of extraction methods for these valuable bioactive compounds. Traditionally, Δ^9-THC and other cannabinoids have been isolated by solvent-based extractions, with hydrocarbons and alcohols delivering the highest yields.[12,13] Soxhlet extraction (SE) is also a commonly used technique,[14,15] which is characterized by shortcomings, namely, long extraction times and high temperature that may promote thermal degradation of the target compounds.[16]

Other advanced extraction techniques, such as microwave-assisted extraction (MAE) allow higher yields, shorter extraction times, less solvent and reduced energy consumption.[14,17] Nevertheless, uneven heating and/or overheating may cause thermal degradation, and thus negatively impact the extraction efficiency.[18] Alternatively, the use of ultrasound-assisted extraction (UAE) achieves high yields in short times;[19] however, the distribution of ultrasound energy lacks uniformity and over time the power decreases, which can lead to inefficient use of the ultrasound-generated energy.[20]

Supercritical fluid extraction (SFE) is an innovative separation technique, which has thus far been employed for extractions of valuable constituents from over 300 plant species.[21] Carbon dioxide is a widespread choice for SFEs due to its several advantageous properties, such as low reactivity, non-toxicity, non-flammability, affordability, availability, and recyclability. Additionally, its selectivity can be adjusted by modification of pressure and temperature, while product fractionation and recovery with high purity is feasible. Nevertheless, due to its low polarity, addition of small quantities of organic

solvents (co-solvents or modifiers) is necessary to access more polar compounds, thereby expanding its extraction range.[22] The selection of an appropriate co-solvent is key for achieving optimum solubility of the bioactive compounds present in the plant.[23] Supercritical carbon dioxide has previously been used to assess the solubility of individual cannabinoids, for example, Δ^9-THC,[24] CBD[25] and CBG.[25] Moreover, several extractions of cannabinoids from different parts of the cannabis plant, for instance, leaves, trimmings, buds, flowers and threshing residues, have been performed using ethanol as a co-solvent.[26–29]

Within the past years, ionic liquids have also emerged as alternative reaction media for the extraction of biomass that is regarded as a source of natural medicinally relevant complex compounds. Many different properties are attributed to ionic liquids, such as exceptional dissolution properties, high thermal stability and broad liquid range, to name a few. Furthermore, ILs display high tuneability, as the combination of different cations and anions leads to hydrophilicity or hydrophobicity and different polarity.[30]

The dissolution and processing of lignocellulosic biomass is a particularly interesting application of ionic liquids (ILs), as they can directly dissolve and fractionate (ligno-)cellulose in an overall less energy intensive process.[31,32] The biomass dissolution capability of ILs is impacted by both their cation and anion, however, current publications suggest that anions have a more significant impact, since they play a role in breaking the many intermolecular hydrogen bonds.[30] Regarding the cation, imidazolium-based ILs were the most successful for the direct dissolution of cellulose, followed by pyridinium- and ammonium-based ones.[33] In addition, increasing the chain length of the cation had a negative influence on the dissolving capabilities of the ILs, as the viscosity increased, and the H-bond acidity decreased. As far as the anion is concerned, dissolving efficiency seems to be determined by the H-acceptor properties of the anion. In general, anions with weak H-bond basicity, for instance, $[BF_4]^-$ and $[PF_6]^-$, could not successfully dissolve cellulose, while ionic liquids based on halide or acetate anions are typically the candidates of choice.[30,34] The growing research on ILs as solvents for lignocellulosic biorefinery also prompted innovations for the extraction of valuable ingredients from plant materials.[35] There are several aspects of ILs that are potentially advantageous for the extraction of high-value compounds: apart from their unique solvent properties and potential environmental benefits, the ability of ILs to dissolve biomass can lead to a better, and higher, yielding access to valuable ingredients embedded in the biopolymers and contribute to a value-added biorefinery.[36,37] However, the recovery of natural products from ionic liquids is often more demanding than the mere extraction: many studies require extensive back-extraction with volatile solvents to actually isolate the valuable ingredients from ILs, thereby rendering the original solvent reduction less significant or even negating it altogether.

The combination of non-volatile polar ILs with volatile non-polar $scCO_2$ has several advantages for extractions, as well as

124

for catalysis. Since $scCO_2$ is highly soluble in ILs, but ILs cannot dissolve in $scCO_2$, it can easily penetrate the IL-phase. This allows the extraction of compounds from the IL-phase into the $scCO_2$ phase, taken into account that the organic compound of interest is soluble in $scCO_2$. Ultimately they are transported into an extraction vessel in a pure, solvent-free and solid form.[38]

Furthermore, ILs in the presence of CO_2 expand their applicability, as their melting point and viscosity decrease, thus, promoting mass transportation.[39] Consequently, the combination of ionic liquids with $scCO_2$ has found application in several catalytic processes, such as hydroformylations, hydrogenations or carboxylations of alkenes in IL-$scCO_2$ biphasic reaction media.[40–43] In the IL-$scCO_2$ reaction systems, the reactants and products are carried by the $scCO_2$ and IL is used as a reaction media.[44,45] Additionally, it is demonstrated that IL-$scCO_2$ biphasic systems avoid cross-contamination of the extracted solute.[38,46]

Until now, IL-based pre-treatment and subsequent SFE (IL-SFE) for natural products has not been described, although ideal conditions arise from the unique properties of both media. Hence, by comparing IL-$scCO_2$ extraction with the utilization of both applications individually or to traditional solvent-extraction, the IL-$scCO_2$ approach is preferable. To begin with, less additional preparation, *e.g.*, filtration of the raw material and consequent evaporation of solvents or separation of IL from the organic solvent is required to obtain a solvent-free and solid extract (Fig. 2). Consequently, there is a lower chance of loss of product or impurities, due to less post processing steps. On the other hand, IL-SFE is performed without additional co-solvents, therefore it reduces further solvent consumption and leads to lower expenses. Ultimately,

if chosen appropriately, the ionic liquid can be recovered and re-used to improve the sustainability of the extraction process.

Recently, an investigation of the extraction of cannabidiol with the aid of ILs has been published; however, isolation of cannabidiol required tedious back-extraction with organic solvents or with an aqueous $AgNO_3$ solution.[47] To the best of our knowledge, no data has been reported thus far regarding a combined extraction process that takes advantage of the complementing properties.

Herein, we present the first application of IL-SFE from industrial hemp of six cannabinoids (Δ^9-THC, THCA, CBD, CBDA, CBG and CBGA). Several parameters during the IL-assisted pre-treatment, such as time, temperature and dilution with H_2O, were investigated. In addition, pressure and temperature during SFE were evaluated. Ultimately, the optimized process for 1-ethyl-3-methylimidazolium acetate ($[C_2mim][OAc]$) was additionally performed with choline acetate ($[Ch][OAc]$) and 1-ethyl-3-methylimidazolium dimethyl phosphate ($[C_2mim][DMP]$) to compare the extraction efficiency of the investigated cannabinoids. In addition, the developed extraction process is complemented by a simple ionic liquid recovering process without the usage of additional organic solvents.

Results and discussion

The focus of this research was the investigation and optimization of various parameters for the extraction of CBD, CBDA, Δ^9-THC, THCA, CBG and CBGA from partially pre-dissolved hemp in various room-temperature ILs with supercritical CO_2. The optimization was divided into three successive stages (Scheme 1).
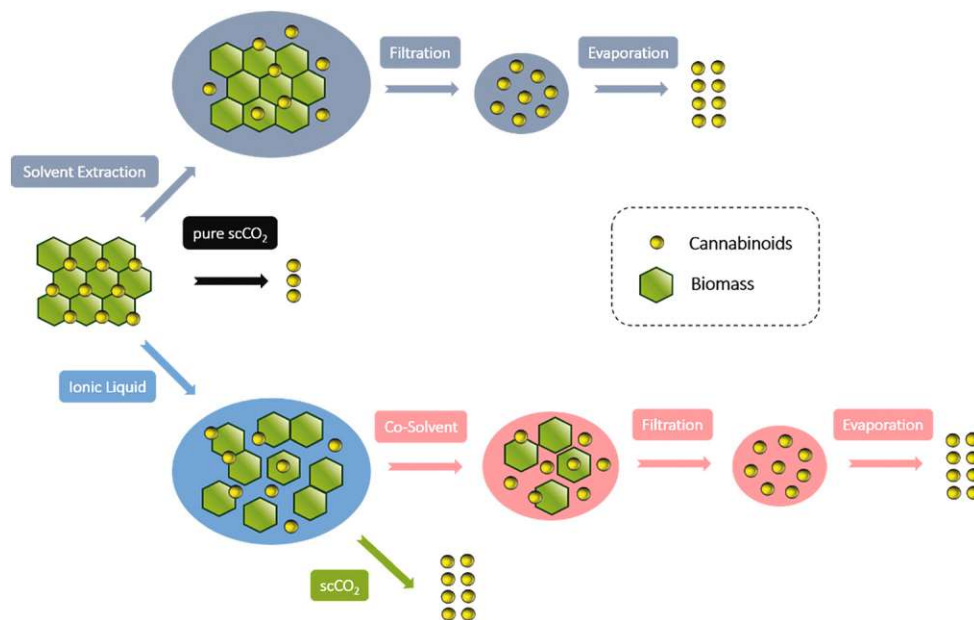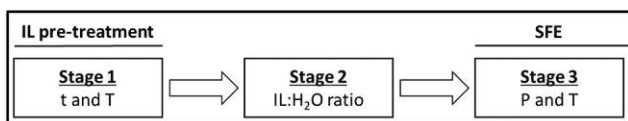

Fig. 2 Conceptualization for the comparison of work up steps and yields of cannabinoids extraction techniques.

Scheme 1 Successive optimization stages of IL-SFE.

In the first stage, the pre-treatment conditions to digest and partially dissolve hemp using $[C_2mim][OAc]$ before SFE were investigated. The lignocellulosic composition of hemp hurds is reported to contain 43.0% cellulose, 24.4% lignin and 29.0% hemicellulose.[48] ILs are known to dissolve a variety of carbohydrates, *e.g.*, cellulose, by combining strongly basic anions (*e.g.*, Cl^- or OAc^-) with various cations.[49–51] In particular, $[C_2mim][OAc]$ was selected in this study as it was used to pre-treat various lignocellulosic biomasses[52] and it is known to effectively dissolve, hemicellulose[53] and lignin.[54] Furthermore, $[C_2mim][OAc]$ is liquid at room temperature, non-halogenated and miscible with H_2O.

Subsequently, the best extraction conditions of stage 1 were employed in determining the most effective ratio of $[C_2mim][OAc]:H_2O$ during SFE. In the third stage, the previously optimized conditions from the first and second stage were utilized to investigate several combinations of pressure and temperature during SFE. Ultimately, the optimum parameters were employed with two additional ILs, namely [Ch][OAc] and $[C_2mim][DMP]$. Both ILs are liquid at room temperature, non-halogenated and hydrophilic. Moreover, both ILs have been reported for pre-treatment of biomass.[55,56] In addition, the positive rating of choline-based ILs in terms of toxicity and biodegradation renders them ideally suited for natural product extractions.[57,58]

Pre-treatment with ionic liquid (Stage 1)

Herein, the influence of temperature and time for the partial dissolution of *Cannabis sativa* L. in $[C_2mim][OAc]$ before the scCO$_2$ extraction is evaluated.

Initially, the conditions to partially dissolve industrial hemp in $[C_2mim][OAc]$ were investigated in experiments 1–4 (Table 1).

Therefore, the pre-treatments were carried out at 25 and 70 °C, each 15 and 60 min, afterwards diluted with H_2O to a ratio of 1 : 2 and subsequently subjected to SFE at 20 MPa and

70 °C. To evaluate the quality of the performed experiments during the development of IL-SFE for hemp the yields of cannabinoids are expressed as the sum of cannabinoid types *e.g.* CBD and CBDA are referred to as $\sum(CBD)$. Analogously $\sum(THC)$ and $\sum(CBG)$ are calculated. All experimental conditions and results for individual cannabinoid yields are shown in the ESI (Tables S1 and S2†).

The cannabinoids CBD and CBDA are predominantly accumulated in industrial hemp compared to THC, THCA, CBG and CBGA, which are considered minor compounds.

The pre-treatment with $[C_2mim][OAc]$ of industrial hemp at 25 °C and 70 °C indicated comparable cannabinoid yields. Increasing the time from 15 to 60 min at 70 °C in exp. 2 led to a small decrease of roughly 5% $\sum(CBD)$ and 8% $\sum(THC)$. However, similar $\sum(CBD)$, but significantly more CBD (6.58 mg g^{-1}) and less CBDA (6.3 mg g^{-1}) at 60 min, was yielded in exp. 2 compared with exp. 4 (15 min), which led to 5.29 mg g^{-1} CBD and 8.8 mg g^{-1} CBDA, respectively ($p < 0.05$, Fig. 3, Table S2†). It was reported that an extraction process including $[C_6mim][NTf_2]$ at 60 °C and 50 min leads to high amounts of CBD and that the IL preserves CBD,[47] which correlates with the observations herein. In addition, the decarboxylation of cannabinoids at higher temperatures for longer times has been described before.[8] The IL $[C_6mim][NTf_2]$ was not utilized in this study, as the anion $[NTf_2]^-$ renders it is less suit-
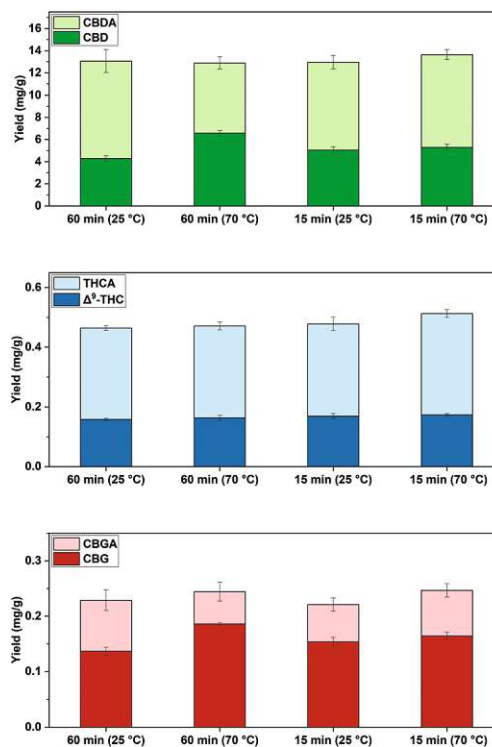

Fig. 3 Comparison of cannabinoid yields (mg g^{-1}) at different pre-treatment temperatures and pre-treatment times with $[C_2mim][OAc]:H_2O$ 1 : 2 and subsequent SFE at 20 MPa and 70 °C, ($n = 3 \pm$ SD). Experiments refer to Table 1 for Stage 1.

Table 1 Yields of cannabinoids in mg g^{-1} for the optimization of pre-treatment with $[C_2mim][OAc]$ at different temperatures and time. SFE was performed at 20 MPa and 70 °C with a ratio of $[C_2mim][OAc]:H_2O$ 1 : 2 (Stage 1)

Exp.	t_{Pre}/min	T_{Pre}/°C	$\sum(CBD)$ (mg g^{-1})	$\sum(THC)$ (mg g^{-1})	$\sum(CBG)$ (mg g^{-1})
1	60	25	13.1 ± 0.8[a]	0.464 ± 0.008[b]	0.229 ± 0.011[c]
2	60	70	12.9 ± 0.3[a]	0.471 ± 0.019[b]	0.244 ± 0.014[c]
3	15	25	13.0 ± 0.8[a]	0.48 ± 0.03[b]	0.221 ± 0.019[c]
4	15	70	13.6 ± 0.6[a]	0.513 ± 0.017[b]	0.247 ± 0.017[c]

Mean values with different letters (a, b, c, *etc.*) within the same column are statistically different ($p < 0.05$).

able to dissolve cellulose compared to the basic $[OAc]^-$ or $[DMP]^-$ and similarly, the longer alkyl side chain of the cation would be disadvantageous for this purpose.[59] Ultimately, $[NTf_2]^-$ was not considered for the extraction process, as it is hydrophobic and not mixable with H_2O and thus, not suitable for the IL recovering process shown in here.

A total time of 15 min instead of 60 min seems to be sufficient to release the investigated cannabinoids from the plant tissue with $[C_2mim][OAc]$ and hence, allows a significantly shorter pre-treatment time The highest cannabinoids yields were obtained at 70 °C for 15 min in exp. 4, namely 13.6 mg g^{-1} $\sum$(CBD), 0.513 mg g^{-1} $\sum$(THC) and 0.247 mg g^{-1} $\sum$(CBG) (Table 1).

Ratio of ionic liquid to water (Stage 2)

Optimization of temperature and time during the pre-treatment was performed with a constant ratio of 1 : 2 $[C_2mim][OAc]$: H_2O. Here, the influence of several IL : H_2O ratios was investigated and compared with the sole use of IL as well as pure H_2O in the extraction vessel (Table 2 and Fig. 4).

A decrease of water in the IL : H_2O ratio from 1 : 2 in exp. 4 to 1 : 1 in exp. 5 led to a significant reduction of $\sum$(CBD) as well as $\sum$(THC) yield (Table 2) at 20 MPa and 70 °C. However, the significantly highest yield of CBD (7.45 mg g^{-1}) of all performed IL-SFE was obtained under these conditions in exp. 5 ($p < 0.05$) and additionally, low yields of CBDA (1.09 mg g^{-1}) and no CBGA were extracted (Fig. 4, Table S2†). Therefore, a ratio of 1 : 1 $[C_2mim][OAc]$: H_2O during SFE seems to favour the extraction of neutral CBD and CBG. Recently, it has been discovered that high yields of CBD are extracted by pre-heating hemp and subsequent extraction with supercritical CO_2 combined with EtOH as a modifier.[29] Similar behaviour can be observed under the previously mentioned IL-SFE conditions, without addition of co-solvents.

On the other hand, significantly more $\sum$(CBD) and $\sum$(CBG) ($p < 0.05$) were obtained in exp. 6 by addition of more H_2O to increase the ratio of $[C_2mim][OAc]$: H_2O from 1 : 2 to 1 : 3. The $\sum$(CBD) yield increased by 15% to 15.6 mg g^{-1}, $\sum$(THC) by 6% to 0.542 mg g^{-1} and $\sum$(CBG) by 36% to (0.335 mg g^{-1}) (Table 2). Adding more than 15 wt% H_2O during $[C_2mim][OAc]$ pre-treatment does not allow complete cellulose dissolution,
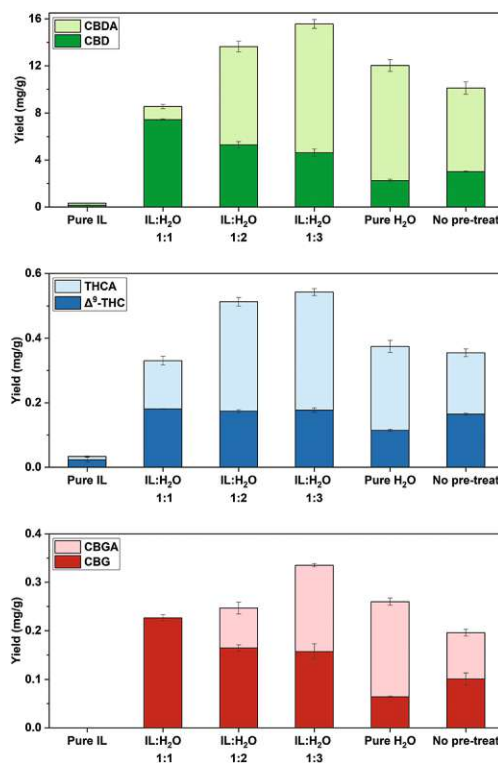

Fig. 4 Cannabinoid yields (mg g^{-1}) for IL-SFE with pure IL and different IL : H_2O ratios, using 15 min of pre-treatment time at 70 °C and for SFE with H_2O (pure H_2O) as well as for scCO$_2$ (no pre-treat). All extractions were performed at 70 °C and 20 MPa; IL = $[C_2mim][OAc]$, ($n = 3 \pm$ SD). Experiments refer to Table 2 for Stage 2.

as reported by Le *et al.* in 2012.[60] Therefore, H_2O was added to the IL after the initial pre-treatment. The addition of H_2O resulted in a reduction of the mixture's viscosity, and thus improved mass transport.[60] It is reported that the viscosity of $[C_2mim][OAc]$ is reduced by 50% when mixed with 10 wt% H_2O and that the IL is less viscous at higher temperatures.[61] Lower viscosity of the IL : H_2O mixture led to higher yields, possibly due to the higher mobility of dissolved cannabinoids and better penetration of scCO$_2$. An increase in carboxylated cannabinoids was observed by adding more water (Fig. 4). Furthermore, water is the only solvent without any negative impacts on the environment. Additionally, it is reported to have low solubility in scCO$_2$ [62] and therefore less potential contamination of the extract.

The absence of H_2O during the extraction with scCO$_2$ and $[C_2mim][OAc]$ (pure IL) led to the lowest yields of all SFE in exp. 7 (Table 2 and Fig. 4). Low yields can be a result of the high viscosity of the IL, which leads to less permeability of scCO$_2$ and subsequently lower mass transfer in the extraction. Therefore, dilution with H_2O is essential during the extraction process.

However, the sole extraction with H_2O (pure H_2O) in the absence of $[C_2mim][OAc]$ in exp. 8 compared to exp. 6, leads to a significant reduction of $\sum$(CBD) by 23% to 12.0 mg g^{-1}, $\sum$(THC) by 31% to 0.375 mg g^{-1} and $\sum$(CBG) by 22% to

Table 2 Yields of cannabinoids in mg g^{-1} by investigating the influence of H_2O and $[C_2mim][OAc]$ during SFE with a pre-treatment at 70 °C for 15 min and SFE at 20 MPa and 70 °C (Stage 2)

Exp.	m_{IL}/g	m_{H_2O}/g	$\sum$(CBD) (mg g^{-1})	$\sum$(THC) (mg g^{-1})	$\sum$(CBG) (mg g^{-1})
4	3	6	13.6 ± 0.6[b]	0.513 ± 0.017[a]	0.247 ± 0.017[b]
5	3	3	8.53 ± 0.19[e]	0.330 ± 0.014[c]	0.226 ± 0.007[bc]
6	3	9	15.6 ± 0.7[a]	0.542 ± 0.016[a]	0.335 ± 0.016[a]
7	3	—	0.322 ± 0.022[f]	0.033 ± 0.006[d]	n.d.
8	—	9	12.0 ± 0.6[c]	0.375 ± 0.022[b]	0.260 ± 0.008[b]
9	—	—	10.1 ± 0.5[d]	0.355 ± 0.009[bc]	0.196 ± 0.019[c]

Mean values with different letters (a, b, c, *etc.*) within the same column are statistically different ($p < 0.05$).

0.260 mg g^{-1} ($p < 0.05$, Table 2). In particular, the use of H$_2$O alone tends to yield fewer neutral cannabinoids (Fig. 4), which verifies what has previously been reported; ILs preserve neutral CBD.[47] When comparing exp. 8 with exp. 4, even though the same total quantity of liquid was added in the high-pressure vessel, significantly less yields of $\sum$(CBD) by 12% and $\sum$(THC) by 27% are observed ($p < 0.05$, Table 2, Fig. 4) in the sole water-based SFE extraction. Therefore, a pre-treatment with IL to liberate the cannabinoids from the plant tissue and subsequent dilution with H$_2$O positively affects the yield.

Ultimately, a reference scCO$_2$ extraction in the absence of both IL and H$_2$O in exp. 9 (no pre-treatment) yielded 10.1 mg g^{-1} $\sum$(CBD), 0.355 mg g^{-1} $\sum$(THC), 0.196 mg g^{-1} $\sum$(CBG) at 70 °C and 20 MPa (Table 2). Thus, IL-SFE with [C$_2$mim][OAc] : H$_2$O 1 : 3 in exp. 6 and 1 : 2 in exp. 4, led to significantly higher yields of $\sum$(CBD, THC, CBG) than sole SFE ($p < 0.05$). It has been reported that the cannabinoid yields during SFE can be enhanced by adding EtOH as a modifier.[26,28] In preliminary studies SFE with EtOH as a modifier at different temperatures and vol% EtOH as well as various conventional ethanolic extractions were carried out with another batch of industrial hemp. High yields of the targeted cannabinoids were obtained at 35 °C, 10 MPa and 120 min dynamic extraction with 10 and 20 vol% EtOH. In comparison to the performed conventional extraction, similar $\sum$(THC) yields, but less $\sum$(CBD) and $\sum$(CBG) were yielded ($p < 0.05$, Table S3†). All data is presented in the ESI.†

The addition of EtOH as a co-solvent to IL-SFE would lead to the extraction of both IL and cannabinoids, thus, leading to impurities in the extract. In particular, IL-SFE does not require the use of a co-solvent to obtain cannabinoids in high yields, avoiding further solvent consumption.

Hence, the highest extraction yields were obtained with a IL : H$_2$O ratio of 1 : 3 in exp. 6, which achieved 15.6 mg g^{-1} $\sum$(CBD), 0.542 mg g^{-1} $\sum$(THC) and 0.335 mg g^{-1} $\sum$(CBG) (Table 2).

SFE extraction parameters – pressure and temperature (Stage 3)

Apart from the optimization of pre-treatment conditions and the ratio of [C$_2$mim][OAc] to H$_2$O, temperature and pressure during SFE were investigated (Table 3).

Initially, the pressure was reduced from 20 MPa in exp. 6 to 15 MPa in exp. 11 at 70 °C and led to a significant reduction by 17% $\sum$(CBD) to 13.00 mg g^{-1}, 16% $\sum$(THC) to 0.457 mg g^{-1} and 23% $\sum$(CBG) to 0.245 mg g^{-1} ($p < 0.05$, Table 3). After further decreasing the pressure to 10 MPa in exp. 10, a significantly diminished yield of 3.66 mg g^{-1} $\sum$(CBD), 0.0885 mg g^{-1} $\sum$(THC), and 0.045 mg g^{-1} $\sum$(CBG) was observed (Table 3). Even though lower cannabinoid yields were obtained at 10 MPa and 70 °C in exp. 10, the extraction of neutral cannabinoids was favoured (Fig. 5). In literature, sole scCO$_2$ extractions yield neither CBD nor CBDA at 10 MPa at 70 °C for 120 min,[63] but SFE can be improved upon by adding EtOH[26] or by the pre-treatment with IL, as herein reported. In addition, the pressure was increased to 30 MPa at 70 °C in exp. 12, which resulted in comparable yields of $\sum$(CBD, THC, CBG) as IL-SFE at 20 MPa in exp. 6 (Table 3). It can be assumed that 20 MPa at 70 °C are sufficient to extract cannabinoids during IL-SFE.

Furthermore, the temperature was lowered to 35 °C at 20 MPa during SFE in exp. 13. This led to comparable yields of $\sum$(CBD) and $\sum$(CBG), but significantly lower $\sum$(THC) yields (0.493 mg g^{-1}) compared to 70 °C in exp. 6 ($p < 0.05$, Table 3). This corresponds to literature data, where similar yields of $\sum$(CBD) were extracted during SFE at 35 °C and 70 °C at 50 MPa.[63] Lower temperatures are known to reduce the viscosity of H$_2$O and additionally, have been reported to decrease the viscosity of [C$_2$mim][OAc].[61] Hence, the mixture is less pene-
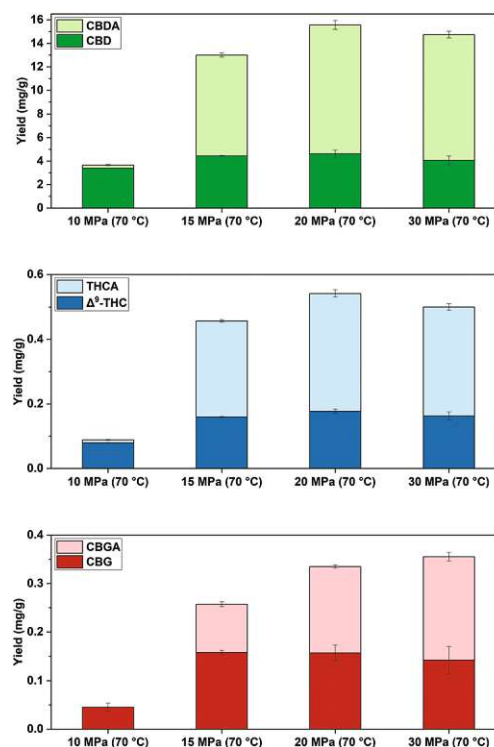
Table 3 Yields of cannabinoids (mg g^{-1}) for different temperatures and pressures during SFE. Pre-treatment with [C$_2$mim][OAc] was carried out at 70 °C for 15 min and extracted with a IL : H$_2$O ratio of 1 : 3 (Stage 3)

Exp.	P_{SFE}/ MPa	T_{SFE}/ °C	$\sum$(CBD) (mg g^{-1})	$\sum$(THC) (mg g^{-1})	$\sum$(CBG) (mg g^{-1})
6	20	70	15.6 ± 0.7[a]	0.542 ± 0.016[a]	0.335 ± 0.016[a]
10	10	70	3.66 ± 0.06[d]	0.0885 ± 0.0026[d]	0.045 ± 0.008[c]
11	15	70	13.00 ± 0.19[c]	0.457 ± 0.005[c]	0.257 ± 0.009[b]
12	30	70	14.7 ± 0.7[ab]	0.500 ± 0.024[ab]	0.36 ± 0.04[a]
13	20	35	14.9 ± 0.7[ab]	0.493 ± 0.014[bc]	0.323 ± 0.009[a]
14	10	35	13.7 ± 0.8[bc]	0.468 ± 0.019[bc]	0.248 ± 0.010[b]

Mean values with different letters (a, b, c, *etc.*) within the same column are statistically different ($p < 0.05$).

Fig. 5 Cannabinoid yields (mg g^{-1}) at 10, 15, 20 and 30 MPa at 70 °C by scCO$_2$ extraction combined with [C$_2$mim][OAc] : H$_2$O 1 : 3 and a pre-treatments at 70 °C for 15 min, ($n = 3 \pm$ SD). Experiments refer to Table 3 for Stage 3.

trable for $scCO_2$ to extract the target cannabinoids. In comparison of exp. 13 and exp. 6, the yields of decarboxylated cannabinoids decreased significantly (CBD by 28%; Δ^9-THC by 16%; CBG by 33%) and similar yields of THCA and CBDA, but significantly more CBGA by 23% was obtained in exp. 13 ($p < 0.05$, Table S3†).

A further decrease from 20 MPa at 35 °C in exp. 13 to 10 MPa in exp. 14 led to a slight reduction in $\sum$(CBD) by 8% and $\sum$(THC) by 5%, and significant reduction in $\sum$(CBG) by 23% ($p < 0.05$, Table 3). Therefore, a combination of 35 °C and 10 MPa seems to affect the total cannabinoid yield negatively, but increasing the temperature to 70 °C at the same pressure further reduces the yields. Lower CBD and CBDA yields at 10 MPa at 70 °C compared with 35 °C during SFE have been described in literature.[63] Thus, 10 MPa at 70 °C during SFE seem to be unfeasible to extract cannabinoids from industrial hemp. At 20 MPa, the temperature seems to have a minor effect on the total yields of cannabinoids.

Consequently, the optimum cannabinoid yields were obtained at 20 MPa and 70 °C in exp. 6 during supercritical CO_2 extraction.

Type of ionic liquid

Two additional ILs, namely, [Ch][OAc] and [C$_2$mim][DMP], were selected for evaluation alongside [C$_2$mim][OAc]. The optimized extraction conditions, with a pre-treatment at 70 °C for 15 min and subsequent SFE at 70 °C and 20 MPa with a IL : H$_2$O ratio of 1 : 3, were additionally applied to these two ILs to observe differences in cannabinoid yields (Table 4 and Fig. 6).

Ionic liquid assisted SFE with [Ch][OAc] in exp. 15 yielded comparable yields of $\sum$(CBD) (15.4 mg g^{-1}) and $\sum$(THC) (0.535 mg g^{-1}), but significantly more $\sum$(CBG) (0.401 mg g^{-1}) than IL-SFE with [C$_2$mim][OAc] in exp. 6 ($p < 0.05$, Table 4). The change of cation does affect the yields of cannabinoids, however, the role of the cation during the dissolution of lignocellulose structure is not yet fully understood.[64] On the other hand, anions, such as [OAc]$^-$, are described to effectively support the dissolution of cellulose by forming hydrogen bonds.[34]

Fig. 6 Cannabinoids yields (mg g^{-1}) for IL-SFE with [C$_2$mim][OAc], [Ch][OAc] as well as [C$_2$mim][DMP] (IL : H$_2$O 1 : 3), for SFE with H$_2$O (pure H$_2$O) and for scCO$_2$ (no pre-treat). All extractions were performed at 70 °C and 20 MPa, ($n = 3 \pm$ SD). Pure H$_2$O (exp. 8) and scCO$_2$ (no pre-treat) (exp. 9) refer to Table 2. [C$_2$mim][OAc] (exp. 6), [Ch][OAc] (exp. 15) and [C$_2$mim][DMP] (exp. 16) refer to Table 4.

To investigate the influence of the anion in IL-SFE of cannabinoids from industrial hemp, the imidazolium-based IL [C$_2$mim][DMP] was used in exp. 16. This resulted in a significant reduction of $\sum$(CBD) to 11.8 mg g^{-1} and total THC to 0.449 mg g^{-1} compared with the acetate-based ILs in exp. 6 and exp. 15 ($p < 0.05$, Table 4). [C$_2$mim][DMP] is described as effectively dissolving biomass, but has a high viscosity,[56,65] which could affect the extraction at supercritical conditions, due to the weaker penetration of scCO$_2$. Nonetheless, phosphate based and acetate based IL-SFE yielded higher amounts of $\sum$(CBD, THC, CBG) compared with sole supercritical CO$_2$ extraction without IL pre-treatment (Fig. 6).

The following mechanism can be proposed for IL-SFE. Firstly, the biomass is partially dissolved by breaking down the lignocellulose structure of the industrial hemp powder. This depends on the anion and cation of the ILs.[34,64] The cannabinoids are released from the plant tissues and the IL possibly stabilizes them.[47] Secondly, the water is added, which reduces the viscosity of the mixture[61] and lowers the solubility of the target cannabinoids. Due to the lower surface tension and higher mobility of cannabinoids, a higher mass transfer between the scCO$_2$ phase and the IL : H$_2$O phase is generated. As reported the scCO$_2$ dissolves in ILs, however, neither the IL nor the H$_2$O does dissolve in scCO$_2$.[38,62] Finally, these synergic

Table 4 Yields of cannabinoids (mg g^{-1}) by comparing different ILs and reference extractions in EtOH and H$_2$O. IL-SFE was performed with a pre-treatment at 70 °C for 15 min, a ratio of 1 : 3 IL : H$_2$O at 70 °C and 20 MPa during SFE

Exp.	IL or solvent	$\sum$(CBD) (mg g^{-1})	$\sum$(THC) (mg g^{-1})	$\sum$(CBG) (mg g^{-1})
6	[C$_2$mim][OAc]	15.6 ± 0.7[a]	0.542 ± 0.016[a]	0.335 ± 0.016[c]
15	[Ch][OAc]	15.4 ± 0.5[a]	0.535 ± 0.010[ab]	0.401 ± 0.024[b]
16	[C$_2$mim][DMP]	11.8 ± 0.9[b]	0.449 ± 0.025[c]	0.292 ± 0.028[c]
17[a]	EtOH for 2 h	15.4 ± 0.4[a]	0.498 ± 0.018[b]	0.452 ± 0.019[a]
18[a]	EtOH for 24 h	14.84 ± 0.15[a]	0.447 ± 0.005[c]	0.440 ± 0.004[ab]
19[a]	H$_2$O for 2 h	1.6 ± 0.3[c]	0.057 ± 0.012[d]	0.031 ± 0.007[d]

Mean values with different letters (a, b, c, *etc.*) within the same column are statistically different ($p < 0.05$). [a] At 70 °C.
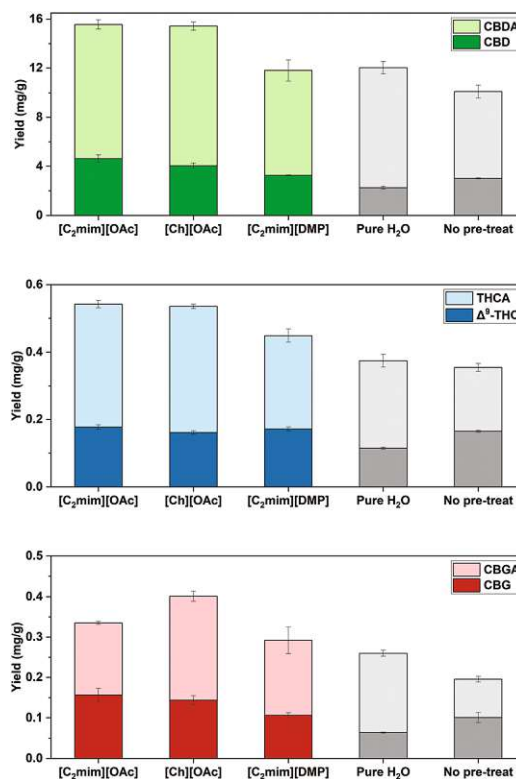
effects allow the scCO$_2$ to extract the targeted cannabinoids, due to better solubility in the supercritical phase without contaminating it with IL or H$_2$O. Thus, no further organic solvents are necessary to purify the compounds from the IL phase and consequently, no additional work up is needed to obtain a solid and solvent free product (Fig. 2).

Ultimately, IL-SFE was compared with reference solvent extraction (exp. 17–19). Ethanol is one of the most commonly used solvents to extract cannabinoids.[66] Herein, a conventional extraction for 2 h, at 70 °C, with EtOH in exp. 17, sufficiently extracted the investigated cannabinoids; however, employing H$_2$O in exp. 19 alone under the same conditions, low yields of cannabinoids were obtained (Table 4). A control extraction in EtOH for 24 h was carried out in exp. 18 to investigate the influence of longer extraction times. Longer times at high temperatures seem to degrade carboxylated cannabinoids significantly, reducing CBDA by 52%, THCA by 65% and CBGA by 53% ($p < 0.05$, Table S2†). The decarboxylation of cannabinoic acids at high temperatures for longer times is described in literature.[8] However, it can be reported that the degradation over time does not affect the overall cannabinoid yields.

By comparing the two-hour ethanolic extraction (exp. 17) with acetate based ionic liquid-SFE, several differences can be observed. Firstly, the yields of ∑(CBD) by SFE with [C$_2$mim][OAc] in exp. 6 and [Ch][OAc] in exp. 15 are slightly higher but comparable to the 2 h ethanolic extraction (Table 4). Secondly, significantly more ∑(THC) with [C$_2$mim][OAc] compared with the two-hour reference extraction with EtOH is obtained. Ultimately, the reference extraction yielded more ∑(CBG) than IL-SFE using [Ch][OAc] or [C$_2$mim][OAc] ($p < 0.05$, Table 4). Hence, the results underline the importance of appropriately selecting the IL cation and anion, as well as the optimal extraction parameters for IL-SFE to extract cannabinoids from industrial hemp. Ultimately, [Ch][OAc] based SFE yields high amounts of the investigated cannabinoids and also provides environmental and economic benefits. Not only is [Ch][OAc] biodegradable, but it is also considered relatively cheap (88 € for 25 g), easy to synthesize, as well as less toxic compared to other ionic liquids.[57,58,67,68] Furthermore, no co-solvents are applied during IL-SFE, which avoids additional solvent consumption and consequently leads to a purer, solid extract (Fig. S2†). Ultimately, all three ILs were purified without any additional use of organic solvents. Neither water nor significant impurities were detected by NMR spectroscopic analysis for the purified ILs (Table S4 and Fig. S5–S7†) and thus, can be re-used for IL-SFE.

Conclusions

Herein, we report a novel IL-based dynamic supercritical CO$_2$ extraction process for the isolation of cannabinoids from *Cannabis sativa* L. The investigation showed that 15 min at 70 °C pre-treatment of hemp with [C$_2$mim][OAc] and [Ch][OAc], dilution of IL with H$_2$O (1 : 3) and ultimately, scCO$_2$ extraction at 20 MPa and 70 °C for 2 h, led to high yields of the

investigated cannabinoids. Acetate-based ILs resulted in higher yields of cannabinoids compared to phosphate-based ILs. In addition, IL-SFE with [C$_2$mim][OAc] yielded significantly more ∑(THC) than conventional extraction with EtOH. Hence, the type of IL is of great importance and affects the cannabinoid yield significantly. However, not only the type of IL needs to be selected carefully, also the SFE parameters. In dependence of various parameters, *e.g.* IL pre-treatment temperature or the ratio of IL : H$_2$O during SFE, it is possible to adjust the proportion of carboxylated and decarboxylated cannabinoids in the extracts. In addition, IL-SFE allows extracting cannabinoids in highest yields and, therefore, it can be reported as a novel competitive alternative to traditional extraction techniques or supercritical fluid extraction with co-solvents. Ultimately, the ILs can be recycled without additional usage of further organic solvents to reduce costs and improve the sustainability of the process. IL-SFE offers the opportunity to extract secondary metabolites from different natural sources without volatile organic solvents and the presented process has great potential for future industrial applications.

Experimental

Plant material

The type III chemovar Futura 75 was cultivated in Austria, in the fields of Biobloom (Apetlon, Austria, 7°41′23.4″N 16°56′26.7″E), in September 2020. After the harvest, the plants (flowers, leaves and stems) were stored under mild conditions at 40 °C for 14 h. The samples were milled with a Fritsch Universal Pulverisette 19 mill through a 2 mm sieve (Fritsch, Oberstein, Germany). The dry matter was 94.73 ± 0.05 wt% (n = 3). A second batch of the same industrial hemp harvested in 2019 was used for the preliminary experiments, mentioned in section Results and discussion. The dry matter was 93.68 ± 0.03 wt% (n = 3). The hemp raw material was stored in the dark, at −20 °C, between experiments.

Ionic liquid-supercritical fluid extraction

For pre-treatment, a high-pressure vessel of approximately 50 mL (EV-3), produced by Jasco (Jasco Corporation, Tokyo, Japan), containing one input and one output connections on the lid, was used. The batch reactor was charged with 0.20 g milled hemp and 3 g of IL. [C$_2$mim][OAc] (≥90%) was purchased from BASF (Ludwigshafen am Rhein, Germany), [Ch][OAc] (98%) from IoLiTec (Heilbronn, Germany) and [C$_2$mim][DMP] (98%) from ABCR (Karlsruhe, Germany). Pre-treatment optimization was performed for 15 min and 60 min, at 25 °C and 70 °C, respectively, with [C$_2$mim][OAc]. Furthermore, [C$_2$mim][OAc] was diluted with different amounts of H$_2$O (filtered through a Milli-Q ion exchange system) after the pre-treatment to evaluate the effect on extraction efficiency. Therefore, 3 g of IL were mixed with 3 g, 6 g and 9 g of H$_2$O and stirred for 10 min before SFE. In addition, extraction purely with [C$_2$mim][OAc], without the addition of water, was tested.
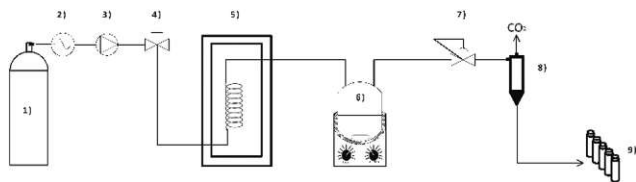
Fig. 7 General setup for the dynamic extraction of cannabinoids using IL-SFE. (1) Liquid CO_2 supply, (2) chiller/cooling system, (3) CO_2 pump, (4) manually operated valve, (5) thermostated oven with preheating coil, (6) high pressure vessel placed on a thermostated stirrer, (7) back pressure regulator (BPR), (8) gas–liquid separator, and (9) fraction collector.

The SFE setup is presented in Fig. 7. All extractions were performed with a $scCO_2$ device manufactured by Jasco (Jasco Corporation, Tokyo, Japan). Liquid CO_2 (>99.995% purity; with ascension pipe; Messer GmbH, Vienna, Austria) was pressurized by two CO_2-pumps (PU-2086, Jasco Corporation, Tokyo, Japan) with cooled heads (CF40, JULABO GmbH, Seelbach, Germany). An oven (CO-2060, Jasco Corporation, Tokyo, Japan) with a heating coil was used and was thermostated to the desired temperature. The vessel containing the IL pre-treated hemp was placed on a heating mantle set to a certain temperature and a stirring rate of 500 rpm and, subsequently, connected to the supercritical carbon dioxide ($scCO_2$) device. A back-pressure regulator (BP-2080, Jasco Corporation, Tokyo, Japan), a gas/liquid separator (HC-2086-01, Jasco Corporation, Tokyo, Japan), and a product collector (SCF-Vch-Bp, Jasco Corporation, Tokyo, Japan) were used to obtain the extracts.

The conditions employed for the SFE of cannabinoids were based on literature data[63,69] and adapted for our purposes. The CO_2 flow rate, the static extraction and the dynamic extraction were set to 5.0 mL min^{-1}, 30 min and 120 min, respectively. Different variables were evaluated during SFE, *e.g.*, oven temperature, heating mantle temperature (35 °C and 70 °C, respectively) and pressure (10 MPa, 15 MPa, 20 MPa and 30 MPa), using [C$_2$mim][OAc]. Ultimately, the optimized conditions were applied to [Ch][OAc] and [C$_2$mim][DMP]. After each extraction, the extracts were collected and diluted to a defined volume with ethanol and prepared for analysis by HPLC. EtOH was purchased from Chem-Lab (Zedelgem, Belgium, abs.).

Solvent-based extraction

For comparison, conventional solvent extractions were performed in 30 mL Teflon screw cap vials. The hemp quantity used in each extraction was 0.2 g. Two extractions were performed in triplicate using 2 mL solvent, more precisely, H_2O and EtOH, for 2 h at 70 °C and a third one, also in triplicate, using 10 mL EtOH for 24 h and 70 °C.[70]

Ionic liquid recovering

After extraction, the $scCO_2$ device was depressurized, the metallic extraction reactor was disconnected and brought to room temperature. The IL–water–hemp mixture (Fig. S3†) was

filtered to remove hemp particles, the water was evaporated *in vacuo* and the remaining ionic liquid was dried under vacuum (0.65 mbar) for 24 h. Afterwards 20 mg of purified IL (Fig. S4†) were dissolved in chloroform-d_3 (Sigma Aldrich, St Louis, USA) and a ^{1}H-NMR was recorded with a 400 MHz Bruker Advanced Ultra Shield 400 spectrometer (Bruker, Billerica, USA). Spectroscopic data and NMR spectra are given in the ESI (Table S4 and Fig. S5–7†)

Cannabinoid quantification

The determination of CBDA, CBD, CBGA, CBG, THCA, Δ^9-THC, was carried out on a High-Performance Liquid Chromatography (HPLC) in a Dionex UltiMate© RSLC System, with DAD-3000RS Photodiode Array Detector (Thermo Scientific, Germering, Germany), on a Dionex Acclaim™ RSLC 120 C18 (2.2 µm, 120 Å, 2.1 × 150 mm, Bonded Silica Products: no. 01425071, Thermo Scientific, Germering, Germany). A mobile phase flow rate of 0.2 mL min^{-1} was employed and the oven temperature was set to 25 °C. As a mobile phase, H_2O with 0.1% formic acid (A) and acetonitrile with 0.1% formic acid (B) were used. The following gradient was carried out: 2 min of pre-equilibration at 70% B, 6 min hold at 70% B, 6 min from 70% B to 77% B, 18 min hold at 77% B, 0.5 min from 77% B to 95% B, 1.5 min at 95% B, 0.5 min from 95% B to 70% B, and 5 min at 70% B.[71] Acetonitrile was purchased from VWR Chemicals (Radnor, PA, USA) and formic acid from Merck (Darmstadt, Germany). All solvents for HPLC were of analytical grade.

The cannabinoid standards CBD, CBDA, THCA, Δ^9-THC, CBG and CBGA were provided by Medical Cannabinoids Research and Analysis GmbH (Brunn am Gebirge, Austria) in the course of previous joint research. A mixed cannabinoid stock solution (1 mg mL^{-1}) in MeOH of the investigated cannabinoids diluted for calibration.

Statistical analysis

Statistical data analysis was performed with Origin 2021. One-way ANOVA for multiple groups, followed by Tukey honestly significant difference (HSD) *post hoc* test at the 0.05 significance level, was carried out.

Addendum

The authors would like to point out that the focus of this study was the extraction of cannabinoids as a class, not THC specifically. Any THC extraction is purely incidental, and bound to be negligible, given that industrial hemp was used, which in the EU must have a THC content not in excess of 0.2%.

The relevant EU law can be perused under: https://eur-lex.europa.eu/legal-content/EN/TXT/HTML/?uri=CELEX:32013R1307&from=de.

In particular, we refer to Article 32, paragraph 6.

Additionally, the authors do hold a licence to for the purposes of research, in accordance with Austrian law, available under:

https://www.ris.bka.gv.at/GeltendeFassung.wxe?Abfrage=Bundesnormen&Gesetzesnummer=10011053.

Author contributions

C.K. & A.S.M.: conceived the research, designed and performed the experiments, analysed the data, wrote the original draft, edited and reviewed the manuscript. M.S.: supervised the research, edited and reviewed the manuscript. K.S. & H.H.: conceived and supervised the research, designed the experiments, edited and reviewed the manuscript.

Conflicts of interest

The authors declare that they have no known competing financial interests or personal relationships that could have appeared to influence the work reported in this article.

Acknowledgements

References

1 J. F. Hancock, *Plant evolution and the origin of crop species*, CABI, 2012.

2 E. Small, *Cannabis: a complete guide*, CRC Press, 2016.

3 C. Kornpointner, A. Sainz Martinez, S. Marinovic, C. Haselmair-Gosch, P. Jamnik, K. Schröder, C. Löfke and H. Halbwirth, *Ind. Crops Prod.*, 2021, **165**, 113422.

4 D. J. Potter, in *Handbook of Cannabis*, ed. R. Pertwee, Oxford Scholarship Online, 2014, pp. 82–83.

5 M. ElSohly and W. Gul, in *Handbook of Cannabis*, ed. R. Pertwee, Oxford Scholarship Online, 2014, p. 1093.

6 R. Brenneisen, in *Marijuana and the Cannabinoids*, ed. M. A. ElSohly, Springer, 2007, pp. 17–49.

7 I. J. Flores-Sanchez and R. Verpoorte, *Phytochem. Rev.*, 2008, **7**, 615–639.

8 M. Wang, Y.-H. Wang, B. Avula, M. M. Radwan, A. S. Wanas, J. van Antwerp, J. F. Parcher, M. A. ElSohly and I. A. Khan, *Cannabis Cannabinoid Res.*, 2016, **1**, 262–271.

9 N. M. Kogan and R. Mechoulam, *Dialogues Clin. Neurosci.*, 2007, **9**, 413–430.

10 R. Mechoulam, L. A. Parker and R. Gallily, *J. Clin. Pharmacol.*, 2002, **42**, 11–19.

11 S. P. H. Alexander, *Prog. Neuropsychopharmacol. Biol. Psychiatry*, 2016, **64**, 157–166.

12 A. Hazekamp, R. Simons, A. Peltenburg-Looman, M. Sengers, R. van Zweden and R. Verpoorte, *J. Liq. Chromatogr. Relat. Technol.*, 2004, **27**, 2421–2439.

13 L. L. Romano and A. Hazekamp, *Cannabinoids*, 2013, **1**, 1–11.

14 C.-W. Chang, C.-C. Yen, M.-T. Wu, M.-C. Hsu and Y.-T. Wu, *Molecules*, 2017, **22**, 1894.

15 A. C. Gallo-Molina, H. I. Castro-Vargas, W. F. Garzón-Méndez, J. A. M. Ramírez, Z. J. R. Monroy, J. W. King and F. Parada-Alfonso, *J. Supercrit. Fluids*, 2019, **146**, 208–216.

16 Q. W. Zhang, L. G. Lin and W. C. Ye, *Chin. Med.*, 2018, **13**, 1–26.

17 Z. Drinić, J. Vladić, A. Koren, T. Zeremski, N. Stojanov, B. Kiprovski and S. Vidović, *J. Chem. Technol. Biotechnol.*, 2020, **95**, 831–839.

18 S. Al Jitan, S. A. Alkhoori and L. F. Yousef, in *Studies in Natural Products Chemistry*, ed. A. Rahman, Elsevier, 2018, vol. 58, pp. 389–417.

19 C. Agarwal, K. Máthé, T. Hofmann and L. Csóka, *J. Food Sci.*, 2018, **83**, 700–710.

20 C. Ajila, S. Brar, M. Verma, R. Tyagi, S. Godbout and J. Valero, *Crit. Rev. Biotechnol.*, 2011, **31**, 227–249.

21 M. De Melo, A. Silvestre and C. Silva, *J. Supercrit. Fluids*, 2014, **92**, 115–176.

22 B. A. S. Machado, C. G. Pereira, S. B. Nunes, F. F. Padilha and M. A. Umsza-Guez, *Sep. Sci. Technol.*, 2013, **48**, 2741–2760.

23 A. Sainz Martinez, C. Kornpointner, C. Haselmair-Gosch, M. Mikulic-Petkovsek, K. Schröder and H. Halbwirth, *LWT*, 2021, **138**, 110633.

24 H. Perrotin-Brunel, P. C. Perez, M. J. van Roosmalen, J. van Spronsen, G.-J. Witkamp and C. J. Peters, *J. Supercrit. Fluids*, 2010, **52**, 6–10.

25 H. Perrotin-Brunel, M. C. Kroon, M. J. Van Roosmalen, J. Van Spronsen, C. J. Peters and G.-J. Witkamp, *J. Supercrit. Fluids*, 2010, **55**, 603–608.

26 L. J. Rovetto and N. V. Aieta, *J. Supercrit. Fluids*, 2017, **129**, 16–27.

27 E. Vági, M. Balázs, A. Komoczi, M. Mihalovits and E. Székely, *J. Supercrit. Fluids*, 2020, **164**, 104898.

28 J. Omar, M. Olivares, M. Alzaga and N. Etxebarria, *J. Sep. Sci.*, 2013, **36**, 1397–1404.

29 D. R. Grijó, I. A. V. Osorio and L. Cardozo-Filho, *J. CO$_2$ Util.*, 2018, **28**, 174–180.

30 H. Wang, G. Gurau and R. D. Rogers, in *Structures and Interactions of Ionic Liquids. Structure and Bonding*, ed. S. Zhang, J. Wang, X. Lu and Q. Zhou, Springer, 2014, vol. 151, pp. 79–105.

31 H. Wang, G. Gurau and R. D. Rogers, *Chem. Soc. Rev.*, 2012, **41**, 1519–1537.

32 A. Brandt, J. Gräsvik, J. P. Hallett and T. Welton, *Green Chem.*, 2013, **15**, 550–583.

33 S. Zhu, Y. Wu, Q. Chen, Z. Yu, C. Wang, S. Jin, Y. Ding and G. Wu, *Green Chem.*, 2006, **8**, 325–327.

34 Y. Li, J. Wang, X. Liu and S. Zhang, *Chem*, 2018, **9**, 4027–4043.

35 S. P. Ventura, F. A. e Silva, M. V. Quental, D. Mondal, M. G. Freire and J. A. Coutinho, *Chem. Rev.*, 2017, **117**, 6984–7052.

36 A. K. Ressmann, K. Strassl, P. Gaertner, B. Zhao, L. Greiner and K. Bica, *Green Chem.*, 2012, **14**, 940–944.

37 E. G. García, A. K. Ressmann, P. Gaertner, R. Zirbs, R. L. Mach, R. Krska, K. Bica and K. Brunner, *Anal. Bioanal. Chem.*, 2014, **406**, 7773–7784.

38 L. A. Blanchard, Z. Gu and J. F. Brennecke, *J. Phys. Chem. B*, 2001, **105**, 2437–2444.

39 R. Liu, P. Zhang, S. Zhang, T. Yan, J. Xin and X. Zhang, *Rev. Chem. Eng.*, 2016, **32**, 587–609.

40 M. F. Sellin, P. B. Webb and D. J. Cole-Hamilton, *Chem. Commun.*, 2001, 781–782.

41 P. B. Webb, M. F. Sellin, T. E. Kunene, S. Williamson, A. M. Slawin and D. J. Cole-Hamilton, *J. Am. Chem. Soc.*, 2003, **125**, 15577–15588.

42 F. Liu, M. B. Abrams, R. T. Baker and W. Tumas, *Chem. Commun.*, 2001, 433–434.

43 A. Sainz Martinez, C. Hauzenberger, A. R. Sahoo, Z. Csendes, H. Hoffmann and K. Bica, *ACS Sustainable Chem. Eng.*, 2018, **6**, 13131–13139.

44 U. Hintermair, G. Zhao, C. C. Santini, M. J. Muldoon and D. J. Cole-Hamilton, *Chem. Commun.*, 2007, 1462–1464.

45 R. A. Brown, P. Pollet, E. McKoon, C. A. Eckert, C. L. Liotta and P. G. Jessop, *J. Am. Chem. Soc.*, 2001, **123**, 1254–1255.

46 L. A. Blanchard, D. Hancu, E. J. Beckman and J. F. Brennecke, *Nature*, 1999, **399**, 28–29.

47 C. Cai, Y. Wang, Y. Yi, F. Li and Z. Tan, *Ind. Crops Prod.*, 2020, **155**, 112796.

48 K. S. Salem, V. Naithani, H. Jameel, L. Lucia and L. Pal, *Global Challenges*, 2021, **5**, 2000065.

49 Y. Li, X. Liu, S. Zhang, Y. Yao, X. Yao, J. Xu and X. Lu, *Phys. Chem. Chem. Phys.*, 2015, **17**, 17894–17905.

50 H. Zhao, G. A. Baker, Z. Song, O. Olubajo, T. Crittle and D. Peters, *Green Chem.*, 2008, **10**, 696–705.

51 Q. Zhang, J. Hu and D.-J. Lee, *Renew. Energy*, 2017, **111**, 77–84.

52 E. Bahcegul, S. Apaydin, N. I. Haykir, E. Tatli and U. Bakir, *Green Chem.*, 2012, **14**, 1896–1903.

53 L. Hu, H. Peng, Q. Xia, Y. Zhang, R. Ruan and W. Zhou, *J. Mol. Struct.*, 2020, **1210**, 128067.

54 S. H. Lee, T. V. Doherty, R. J. Linhardt and J. S. Dordick, *Biotechnol. Bioeng.*, 2009, **102**, 1368–1376.

55 F. Cheng, H. Wang, G. Chatel, G. Gurau and R. D. Rogers, *Bioresour. Technol.*, 2014, **164**, 394–401.

56 Q. Li, X. Jiang, Y. He, L. Li, M. Xian and J. Yang, *Appl. Microbiol. Biotechnol.*, 2010, **87**, 117–126.

57 T. P. T. Pham, C.-W. Cho and Y.-S. Yun, *Water Res.*, 2010, **44**, 352–372.

58 A. Jordan and N. Gathergood, *Chem. Soc. Rev.*, 2015, **44**, 8200–8237.

59 K. C. Badgujar and B. M. Bhanage, *Bioresour. Technol.*, 2015, **178**, 2–18.

60 K. A. Le, R. Sescousse and T. Budtova, *Cellulose*, 2012, **19**, 45–54.

61 S. Fendt, S. Padmanabhan, H. W. Blanch and J. M. Prausnitz, *J. Chem. Eng. Data*, 2011, **56**, 31–34.

62 Z. Wang, Q. Zhou, H. Guo, P. Yang and W. Lu, *Fluid Ph. Equilibria*, 2018, **476**, 170–178.

63 V. Kitryte, D. Bagdonaite and P. R. Venskutonis, *Food Chem.*, 2018, **267**, 420–429.

64 B. D. Rabideau, A. Agarwal and A. E. Ismail, *J. Phys. Chem. B*, 2013, **117**, 3469–3479.

65 B. Zheng, C. Harris, S. R. Bhatia and M. F. Thomas, *Polym. Adv. Technol.*, 2019, **30**, 1751–1758.

66 F. Fathordoobady, A. Singh, D. D. Kitts and A. Pratap Singh, *Food Rev. Int.*, 2019, **35**, 664–684.

67 D. Rengstl, V. Fischer and W. Kunz, *Phys. Chem. Chem. Phys.*, 2014, **16**, 22815–22822.

68 E. L. Smith, A. P. Abbott and K. S. Ryder, *Chem. Rev.*, 2014, **114**, 11060–11082.

69 V. Brighenti, F. Pellati, M. Steinbach, D. Maran and S. Benvenuti, *J. Pharm. Biomed. Anal.*, 2017, **143**, 228–236.

70 M. Szalata and K. Wielgus, *New Biotechnol.*, 2016, S162.

71 S. Serna-Loaiza, J. Adamcyk, S. Beisl, C. Kornpointner, H. Halbwirth and A. Friedl, *Processes*, 2020, **8**, 1334.

5. Continuous production of propylene carbonate

5.1 Overview

Two centuries ago, phosgene and ethylene glycol were combined by Nemirowski for the synthesis of ethylene carbonate. However, this synthetic route has as major drawback which is the high toxicity of phosgene.[474] Later on, many alternative paths were discovered starting from C1 building blocks[475-478] and several other compounds such as halohydrins[479], propargyl alcohols[480] and alkenes.[481]

Latest research on the field has shifted away from previous synthetic routes and has come closer to the synthesis of cyclic carbonates *via* the cycloaddition reaction between carbon dioxide and epoxides, which is characterized by the major advantage of atom-economy.[482] Through this process a wide variety of valuable cyclic carbonates has been synthesized.[483],[484] A variety of processes employing homogeneous catalysts for the synthesis of cyclic carbonate has been published. For instance, metal salts, organometallics (salen complexes and non-salen complexes), metal organic frameworks and organocatalysts (deep eutectic solvents, amines and organic bases and ILs) have been reported as homogeneous catalysts.[485]

In this section, the preliminary cycloaddition reaction between propylene oxide and carbon dioxide under homogeneous conditions using ILs is presented, followed by the investigation of the reaction in heterogeneous fashion utilizing supported ILs with the final purpose of achieving the continuous production of PC in high yields and with stability (Figure 43).
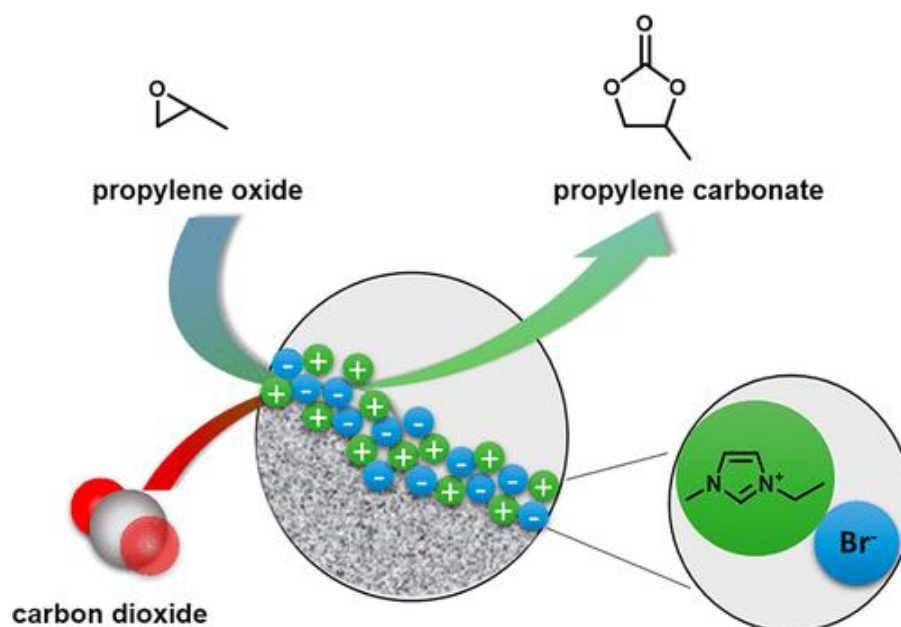

Figure 43. Conceptualization of the continuous production of PC *via* silica-supported ILs utilizing propylene oxide and supercritical carbon dioxide.[486]

The following manuscript will be presented in this chapter:

❖ Sainz Martinez, A.; Hauzenberger C.; Sahoo, A. R.; Csendes, Z.; Hoffmann, H.; Bica, K. Continuous Conversion of Carbon Dioxide to Propylene Carbonate with Supported Ionic Liquids. *ACS Sustainable Chem. Eng*. **2018**, *6*, 13131-13139.

The first and main author of the manuscript contributed by planning, designing, performing the experimental work and also drafting the manuscript.
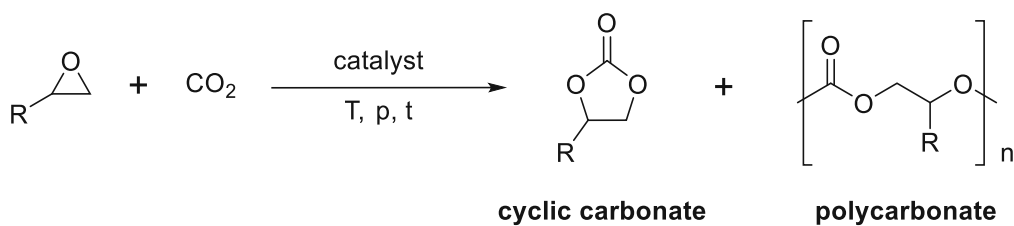
5.2 Production of cyclic carbonates in homogeneous fashion

Carbon dioxide is a greenhouse gas which is generated by the aerobic combustion of carbon-containing products.[487] Over the last two decades, CO_2 emissions have significantly increased, affecting the global climate and increasing the global temperature. Currently, more than 36 Gt (gigaton) of anthropogenic CO_2 is emitted into the atmosphere. Many efforts have been invested in finding strategies to tackle this issue and, as a consequence, carbon capture and storage (CCS) and carbon capture and utilization (CCU) were developed.[488] These developed technologies allow the utilization of CO_2 from anthropogenic origin for chemical transformations.

The CO_2 transformation to high value-added products has drawn remarkable interest within the scientific community because it is a renewable, non-toxic, non-flammable, cheap and can be used as C1 source. In the last decades, CO_2 has been utilized for the synthesis of high value-added products[489],[490] for instance, organic chemicals,[491] polymers,[492],[493] fuels[494],[495] and fine chemicals.[496] Among all potential transformation, the production of cyclic carbonates has attracted considerable interest, with an approximate annual production volume of 100000 tons worldwide in 2013.[497] They are utilized in the electrochemistry field as electrolytes for fuel cells and lithium-ion batteries. Additionally, they are employed as monomers in polymer chemistry for the synthesis of polyurethanes and synthetic building blocks.[483] Several strategies have been published aiming for the synthesis of cyclic carbonates (Scheme 8).
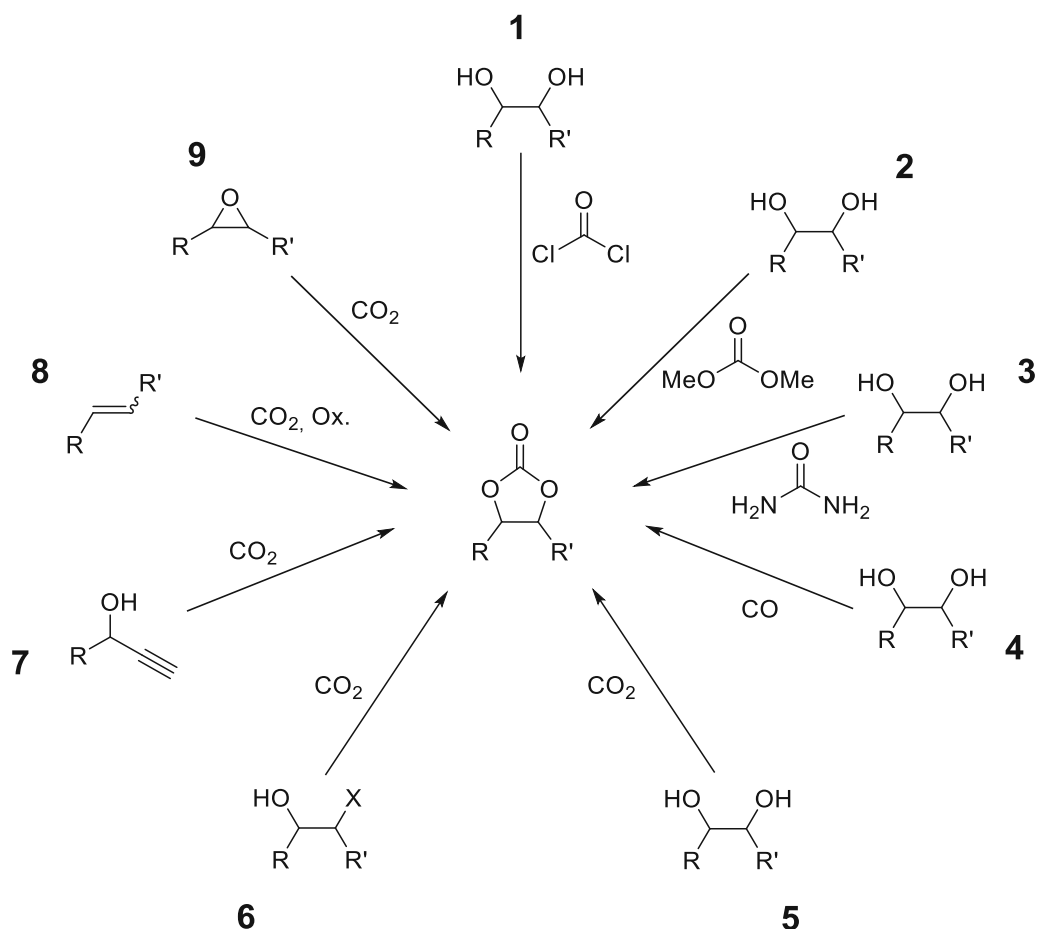
Scheme 8. Several synthetic strategies to produce cyclic carbonates.[482]

In 1883, Nemirowski published the synthetical procedure of ethylene carbonate using highly toxic phosgene and ethylene glycol (Scheme 8, pathway **1**).[474] Apart from phosgene, dimethyl carbonate,[475] urea,[476] CO (carbon monoxide)[477] and CO_2[478] can also be employed as C1 building blocks (Scheme 8, pathways **2**, **3**, **4** and **5** respectively) to obtain cyclic carbonates. Additionally, other compounds can be used as substrates, for instance halohydrins,[479] propargyl alcohols[480] and alkenes[481] (Scheme 8, pathways **6**, **7** and **8** respectively). The latter requires first the epoxidation of the alkene followed by the transformation with CO_2. All these aforementioned routes are not as advantageous as the latest route (Scheme 8, pathway **9**), i.e., the cycloaddition reaction between CO_2 and epoxides, because of its atom-economy and the already invested substantial efforts towards the progress of this synthetic route over the past decades (Scheme 9).

Scheme 9. Production of cyclic carbonates starting from epoxides and CO_2.[482]

It is employed on an industrial level to generate certain valuable cyclic carbonates (Figure 44).[483],[484]
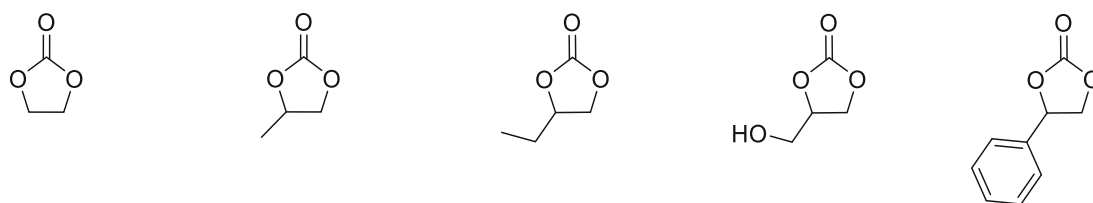
ethylene carbonate   propylene carbonate   butylene carbonate   glycerol carbonate   styrene carbonate

Figure 44. Some examples of frequently produced cyclic carbonates.[482],[484]

The classification of general catalysts employed in the cycloaddition reaction between epoxides and CO_2 in homogeneous fashion, is presented in Figure 45.[485]
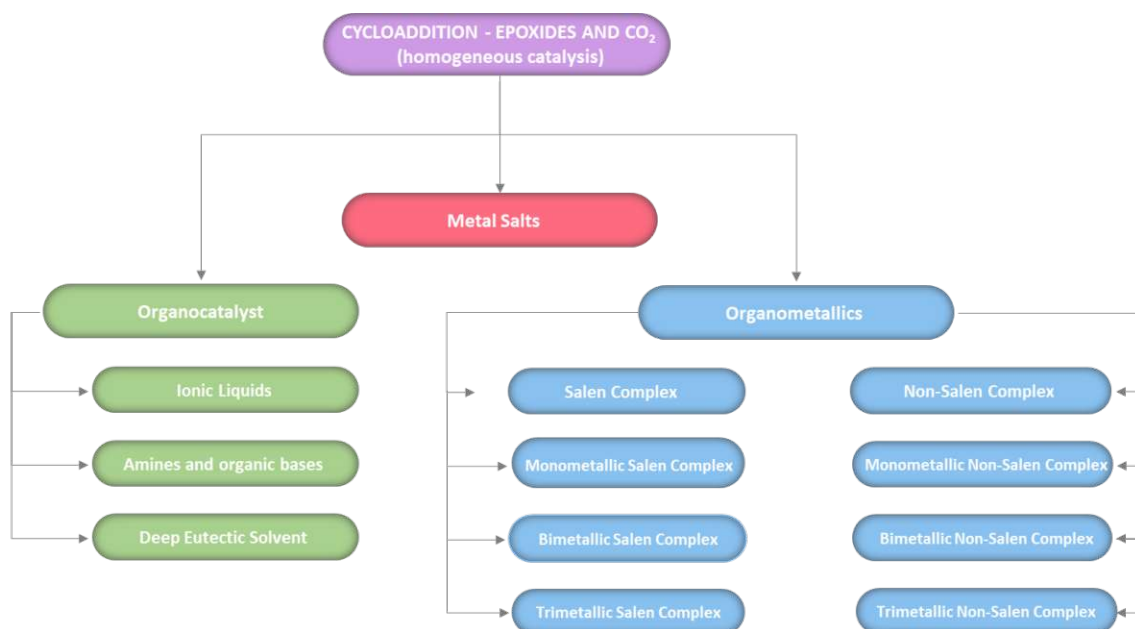

Figure 45. Catalysts for the cycloaddition reaction between epoxides and CO_2 in homogeneous fashion.[485]

Over the past years, this reaction has been studied employing a variety of different catalysts and catalytic systems. Currently, there are several comprehensive reviews published, involving organocatalysts,[498],[499] ILs,[500],[501] metal organic frameworks[502],[503] and homogeneous metal-based catalysts,[504-506] as well as various reviews with regard to general different aspects of this reaction.[507-509]

The cycloaddition reaction between epoxides and CO_2 is significantly affected by the reaction conditions and those substrates contain different polarities. All components of the reaction need to be in maximum contact, in order to enhance the efficiency of the reaction. Additionally, the CO_2 dissolution in the reaction mixture is influenced by the reaction conditions, which can vary with the density of the epoxide. By increasing the pressure of the CO_2 or by lowering the temperature of the reaction, the density of the epoxide can increase. By decreasing the reaction temperature, the CO_2 solubility can increase, and on the negative side, the catalyst or catalysts system solubility can concomitantly be reduced. The solubility of the catalyst can also be negatively influenced by high CO_2 dissolution in the reaction mixture.[488]

Concerning the influence of the reaction temperature, by increasing it, the reaction rate increases, because the catalytic activity is positively affected. Furthermore, the increase of the reaction temperature favours the formation of cyclic carbonates (thermodynamic product, higher activation energy), in contrast to polycarbonate (kinetic product, lowest activation energy).[510],[511] Nevertheless, reaction temperature above 120 °C are detrimental for the selectivity of the reaction, due to the promotion of side reactions (Scheme 10) (i.e., isomerization, hydrolysis).[512-514]
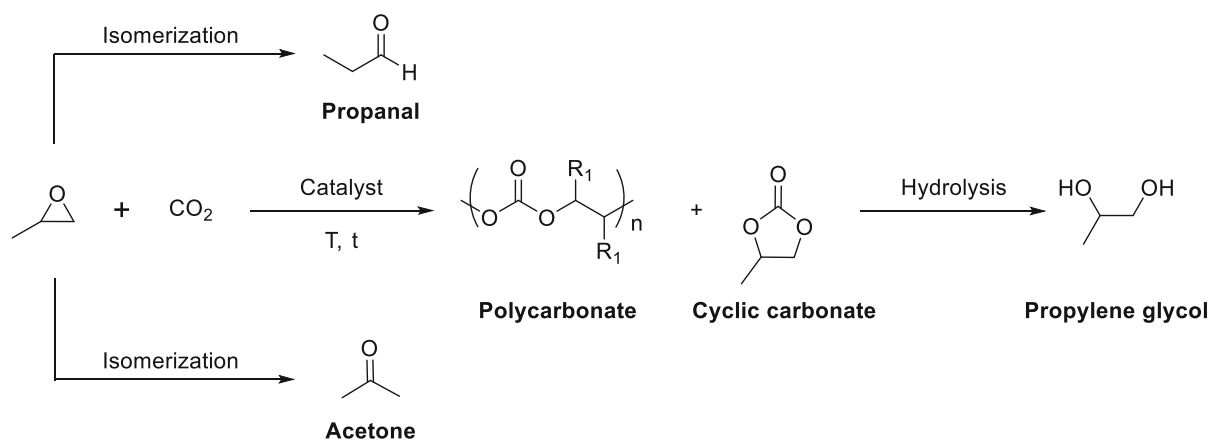
Scheme 10. Possible reaction pathways of PO to PC and side products.[512-514]

With regard to the CO_2 pressure, augmenting it up to a certain point, can improve the reaction rate. However, above that CO_2 pressure limit, the reaction rate may drastically drop, because the epoxide concentration near the catalyst is reduced, thus, decreasing the interaction possibilities between the epoxide and the catalyst.[515],[516]

The use of conventional solvent (i.e., dichloromethane, acetone, acetonitrile) for the synthesis of cyclic carbonates should be preferably avoided. Nonetheless, if there is poor solubility of the catalyst or catalysts system in the specific concentration of epoxide, the addition of solvent may be necessary, for instance dichloromethane, acetone and acetonitrile. On the downside, by adding a solvent the contact between the substrates may drastically decrease, along with the reaction rate.[488]

5.2.1 Ammonium-based ionic liquids as catalysts

Quaternary ammonium halides were utilized as catalysts by Lichtenwalter and Cooper, in 1956, to produce cyclic carbonates.[517] Ethylene oxide (EO) and CO_2 were employed as substrates in conjunction with different ammonium-based ILs catalysts, such as tetrabutylammonium bromide (TBABr) and tetraethylammonium bromide (TEABr). Ultimately, TBABr exhibited the highest activity. However, tetramethylammonium halides do not show catalytic activity in the reaction between epoxides and CO_2. The high melting point of the tetramethylammonium bromide (m.p. > 300°C) may have been the main cause of the unsuccessful catalytic activity, because the system did not become homogeneous and therefore, the catalyst was acting inefficiently.[518]

Several ammonium-based ILs have been employed for the synthesis of cyclic carbonates (Figure 46).[482],[499],[519]

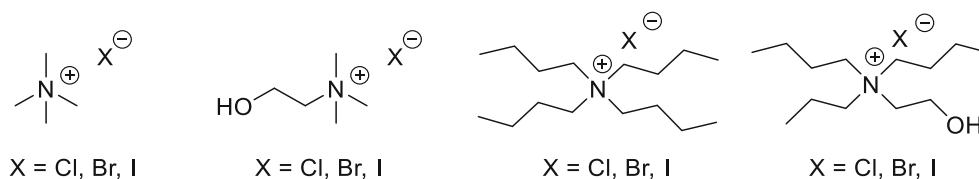| X = Cl, Br, I | X = Cl, Br, I | X = Cl, Br, I | X = Cl, Br, I |

Figure 46. Some of the employed ammonium-based ILs.

In 1993, Nishikubo et al.[520] reported a metal-free strategy to produce cyclic carbonates employing ammonium-based ILs (Scheme 11). The reaction consisted of 2-phenoxymethyloxirane (PMO) as a substrate, catalysed by 1 mol % of tetrabutylammonium chloride (TBACl) at 80°C and 24 h, obtaining a yield of 69 %.
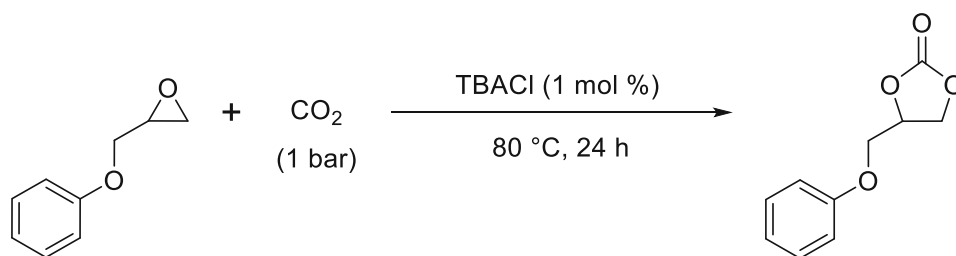
Scheme 11. Metal-free route to produce cyclic carbonates by Nishikubo et al.[520]

In another example Calo et al.[521] employed styrene oxide (SO) at 1 bar of CO_2, for 4 h, at 120 °C, with a mixture of ammonium-based ILs that were used as solvents and catalysts. The catalyst consisted of a mixture of tetrabutylammonium bromide (TBABr) and tetrabutylammonium iodide (TBAI) in a ratio of 1:1 w/w, obtaining styrene carbonate (SC) in 83% yield (Scheme 12).
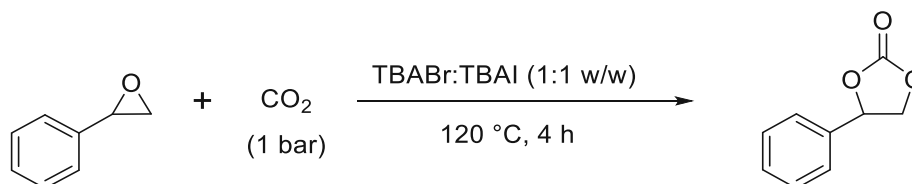
**Scheme 12.** Metal-free route to produce cyclic carbonates by Calo et al.[521]

Eventually, the mechanism for production of cyclic carbonates catalysed by ammonium-based ILs containing halides was postulated (Scheme 13). Initially, the epoxide ring is opened by nucleophilic attack of the halide (step **A**), forming an oxy-anion species (step **B**). Afterwards, the negatively charged oxygen atom reacts with the electrophilic carbon atom of the CO_2 (step **C**). Subsequently, the formed product undergoes an intramolecular nucleophilic attack (step **D**). As a consequence, the halide is removed, and the correspondent cyclic carbonate product is obtained.[521]
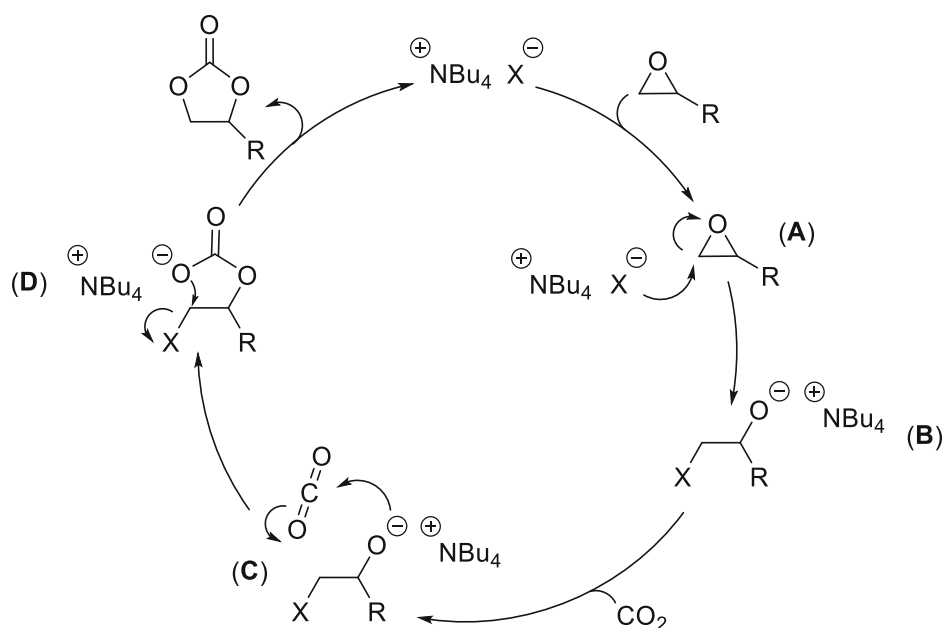
Scheme 13. Postulated mechanism for cyclic carbonate production utilizing ammonium halides.[521]

The reaction between glycidyl methacrylate and CO_2 employing toluene as solvent at 80 °C and under ambient pressure was investigated by Park et al.[522] They provided a detailed kinetic study on the influence of the alkyl chain of several ammonium-based chloride ILs. It was concluded that the rate of the reaction increased in the following order: tetrabutyl ammonium chloride (TBACl) < tetrahexylammonium chloride (THACl) < tetraoctylammonium chloride (TOACl). This led to the conclusion that bulky cations demonstrate higher activity, due to the weaker electrostatic interaction between NR_4^+/Cl^- ion pair, thus, affecting the halide anion by augmenting its nucleophilicity and reactivity.[523],[524] In addition, the catalytic activity of the halides increased in the following order: I^- (iodide anion)> Br^- > Cl^-.[524]

The activity of hydroxyl-functionalized tetraalkylammonium halide salts in the reaction between neat 1,2-epoxybutane and CO_2 was investigated by Ren et al.[525] and Werner et al.[526] It was demonstrated that the reaction rate was affected by the steric size of the *N*-alkyl substituents. As the side of the alkyl substituents increases the reactivity also increases. The separation between the hydroxyl group of the ammonium-based ILs and the nitrogen atom also proved to be a key factor; by increasing the chain length of the hydroxyl-containing alkyl group from ethyl to propyl the yield drastically decreased.[525],[526] Furthermore, the nucleophilic nature and leaving group capacity of the halide influenced the reaction rate in the following increasing order: Cl^- < Br^- < I^-. Consequently, the highest yield was obtained by the 2-(hydroxylethyl)tributylammonium iodide (Scheme 14). It was also observed that the reactivity of the hydroxyl-functionalized ILs was considerably higher than their non-hydroxyl-functionalized analogues.
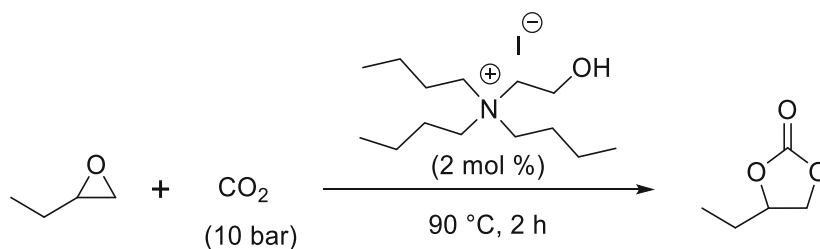
Scheme 14. Synthesis of butylene carbonate using hydroxyl-functionalized IL by Werner et al.[526]

As it can be seen from the mechanism depicted in Scheme 15, the efficiency of the reaction depends on the structure of the cation and the respective employed halide. In order to enhance the catalytic activity, functional groups containing protons were introduced, for instance OH and NH groups. These bifunctional catalysts could coordinate to the epoxide via hydrogen bonding, thereby polarizing the C-O bond. Subsequently, the rate-determining step, the ring opening of the epoxide, is promoted. Ionic liquids bearing OH and NH groups in their cation structure, assisted the nucleophilic attack of the halide anion to the least sterically prominent carbon atom of the epoxide, thus, increasing the catalytic activity.[525]
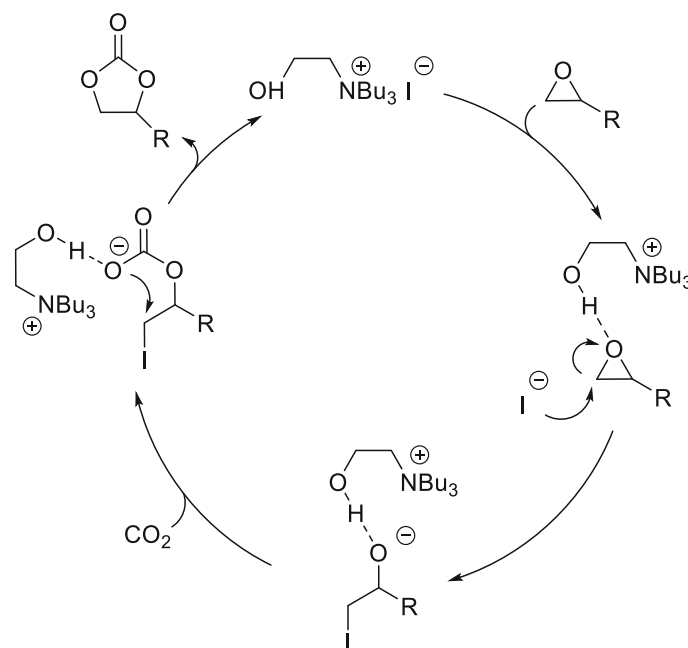
Scheme 15. Proposed mechanism for the synthesis of cyclic carbonate employing a bifunctional ammonium salt catalyst.[526]

Apart from the bifunctional catalyst hydroxyethyltributylammonium bromide,[525],[527] other OH-functionalized analogues of TBABr, betaine-/amino acid derived halides,[528],[529] betaine-derived phenoxide[530] and choline-based ILs[531] promote this reaction.

Cheng et al.[532] investigated the influence of the number of hydroxyl groups present in the alkylammonium cation backbone for the reaction between propylene oxide (PO) and CO_2 (Scheme 16). This was performed by exchanging the non-hydroxylated alkyl groups present in tetraethylammonium bromide by hydroxyl containing ethyl groups. The quantities of hydroxylated ethyl groups ranged from monosubstituted to tetrasubstituted and their reactivity increased as follows: NEt_4Br (tetraethylammonium bromide) < $NEt_3(HE)Br$ (*N,N,N*-triethyl-2-hydroxyethanamonium bromide) < $NEt_2(HE)_2Br$ (*N,N*-diethyl-2-hydroxy-*N*-(2-hydroxyethyl)ethanamonium bromide) < $NEt(HE)_3Br$ (*N*-ethyl-2-hydroxy-*N,N*-bis(2-hydroxyethyl)ethanamonium bromide). Nonetheless, the tetrasubstituted $N(HE)_4Br$ (tetrakis(2-hydroxyethyl)ammonium bromide) did not achieve the highest yield. It was supposed that the fourth hydroxyl group was interacting with the halide anion by forming a hydrogen bond and therefore, decreasing its nucleophilicity.[532]
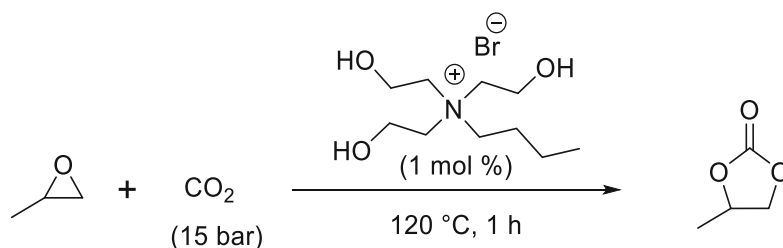
Scheme 16. Synthesis of butylene carbonate employing hydroxyl-functionalized IL by Cheng et al.[532]

5.2.2 Phosphonium-based ionic liquids as catalysts

In 1993, Nishikubo et al.[520] employed tetrabutylphosphonium bromide (PBu_4Br) as catalyst for the transformation of 2-phenoxymethyloxirane (PMO) into the correspondent cyclic carbonate, obtaining 35 % yield (Scheme 17).
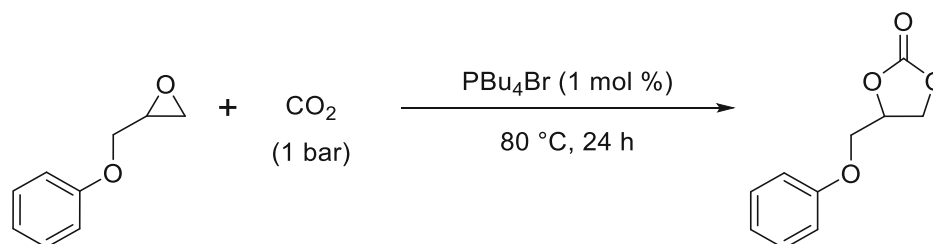
Scheme 17. Metal-free route to produce cyclic carbonates by Nishikubo et al.[520]

Several other phosphonium halide ILs have been employed as catalysts for the cycloaddition reaction between CO_2 and epoxides (Figure 47).[374, 533-536]
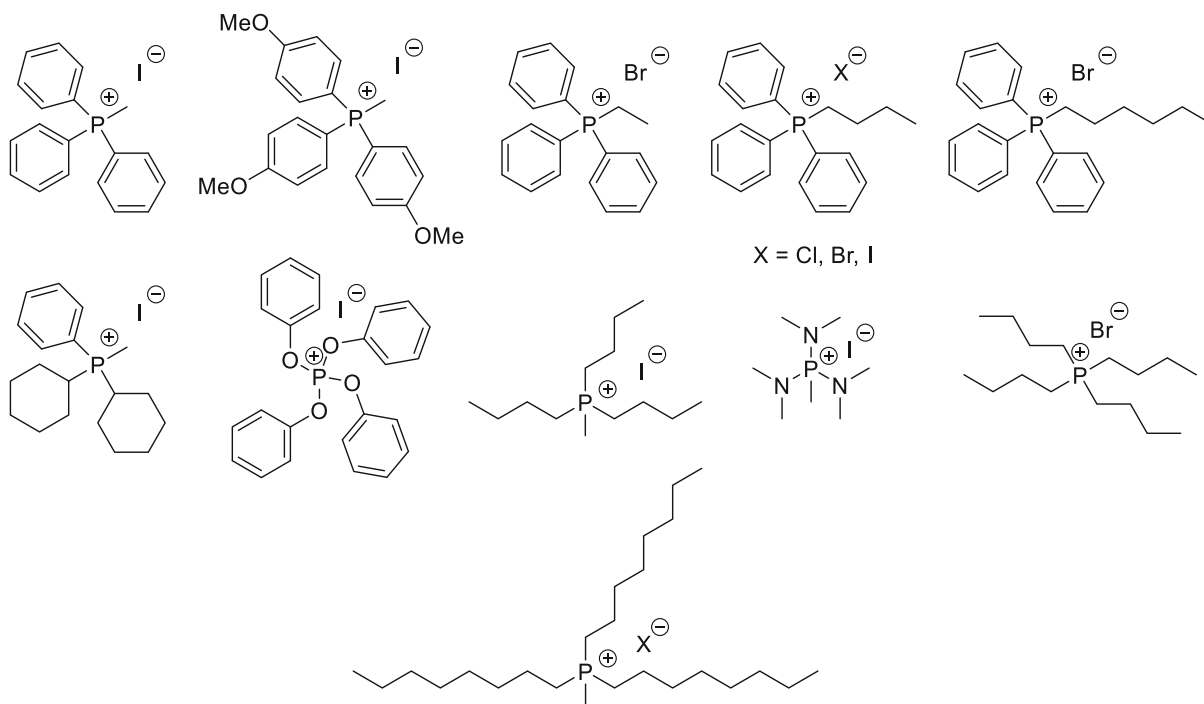
X = MeOCO₂, AcO, CF₃SO₃, PhCO₂, 4-CH₃C₆H₄CO₂; 4-NO₂C₆H₄CO₂, 2-NH₂C₆H₄CO₂, 4-CH₃C₆H₄SO₃

Figure 47. Some of the employed phosphonium-based ILs.

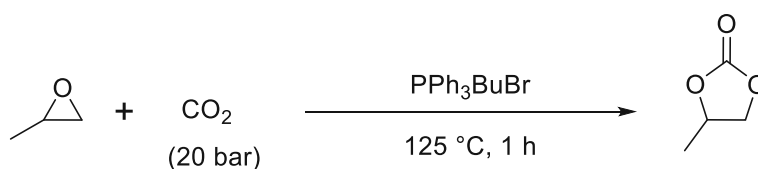In another publication, Cheng et al.[533] reported that in the reaction between CO_2 and PO among all the phosphonium halide ILs, triphenylbutylphosphonium bromide (PPh_3BuBr) exhibited the highest catalytic activity, yielding a 54 % conversion, at 125 °C, 20 bar, for 1 h (Scheme 18).

Scheme 18. Synthesis of PC with PPh_3BuBr by Cheng et al.[533]

The synthesis of PC by reacting PO and CO_2 in the presence of tetrabutylphosphonium halides (X = Cl, Br, I) ILs at 100 °C, 100 bar, for 1 h was reported by Sakakura et al.[374] obtaining very low yields, in the range of 4 – 10 % (Scheme 19).
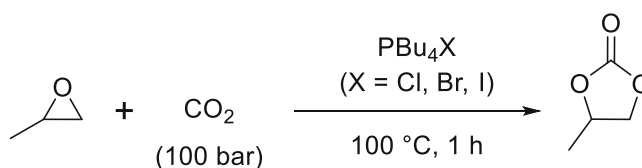
Scheme 19. Synthesis of PC with tetrabutylphosphonium halides by Sakakura et al.[374]

145

In other related publication, Cheng et al.[533] combined several organocatalysts with substoichiometric quantities of H_2O, increasing their catalytic activity (Scheme 20). The hydrogen bond donor properties of H_2O combined with triphenylbutylphosphonium iodide (PPh₃BuI) achieved >97 % yield of PC at 125 °C, 20 bars and for 1 h.
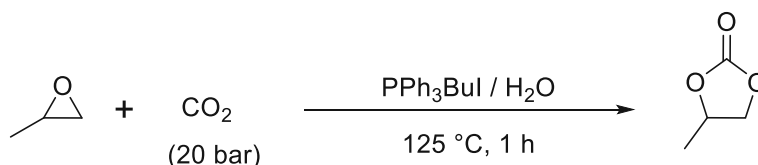

Scheme 20. Synthesis of PC, using PPh₃BuBr and H_2O by Cheng et al.[533]

Afterwards, Endo et al.[536] employed isopropanol, as solvent and hydrogen bond donor, and methyltriphenylphosphonium iodide (PPh₃MeI) as nucleophilic catalyst (Scheme 21). The reaction between 2-phenoxymethyloxirane (PMO) and CO_2 in room temperature and ambient CO_2 pressure in 24 h, obtained the correspondent cyclic carbonate in high yield (97 %).
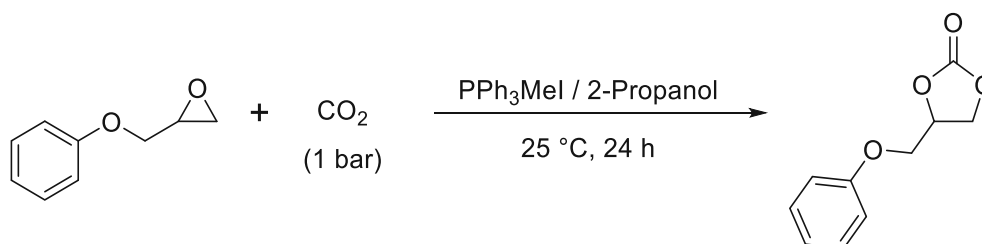
Scheme 21. The reaction between PMO and CO_2, using PPh₃BuBr as catalyst and H_2O as solvent to obtain the correspondent cyclic carbonate by Endo et al.[536]

Tailor-made phosphonium catalysts bearing bromoethylene derivatives with carboxyl (-COOH), hydroxyl (-OH) and amino (-NH₂) groups (Figure 48) were utilized by Sheng-Lian et al.[537] The reaction between PO and CO_2 using those catalysts at 130 °C, 25 bar of CO_2 for 3 h, obtained high yields in the range of 85% - 99%.
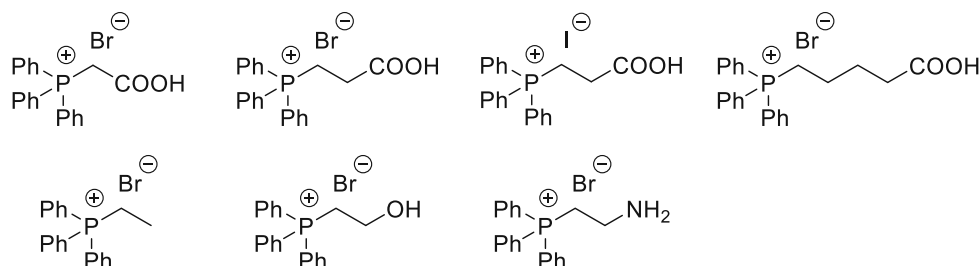
Figure 48. Tailor made phosphonium catalysts which obtained high yields by Sheng-Lian et al.[537]

146

Halide-free phosphonium ILs containing hydroxyl, acetate or carbonate anions have been also employed in the transformation of epoxides into cyclic carbonates. However, tetrabutylphosphonium hydroxide (PBu$_4$OH) achieved very low conversion (22 %) at 120 °C, 10 bar and 24 h (Scheme 22).[534]
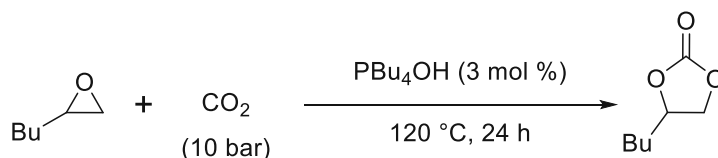
Scheme 22. Synthesis of cyclic carbonate employing PBu$_4$OH by Hasegawa et al.[534]

A mechanism for the reaction between epoxides and CO$_2$, using phosphonium-based IL bearing a carboxyl functional group in the cation structure has been proposed (Scheme 23).[537] As previously explained, in the case of the ammonium-based ILs, a similar pathway is suggested. Initially, the polarization of the epoxide C-O bond occurs via hydrogen bonding with the hydrogen of the carboxyl group present in the phosphonium IL giving the intermediate **A**. After, the nucleophilic attack of bromide ion occurs in the less substituted β-carbon atom of the epoxide, promoting the ring opening of the epoxide and generating intermediate **B**. Subsequently, the insertion of the CO$_2$ into the intermediate **B** occurs, producing the halocarbonate **C**, which then converts into the cyclic carbonate via nucleophilic intramolecular substitution reaction of the bromide anion.
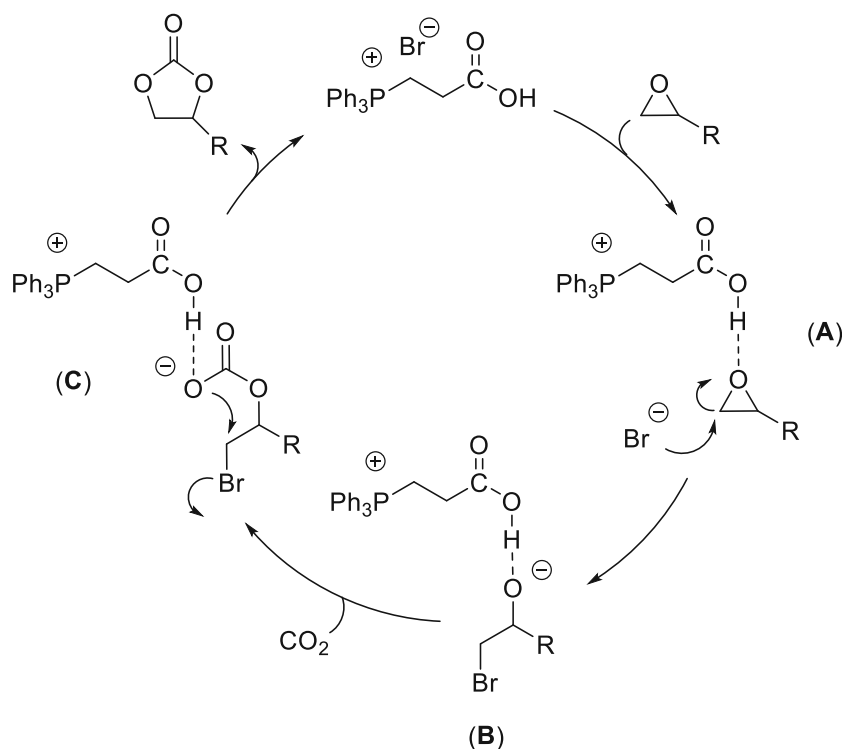
Scheme 23. Proposed mechanism for the cycloaddition reaction using phosphonium-based ILs bearing carboxyl functional group.[537]

The reaction between styrene oxide and CO_2 was investigated by Noè et al.[535] employing methyl-*n*-trioctylphosphonium methylcarbonate ([POct$_3$][MeOCO$_2$]) and the acetate analogue achieving low catalytic activity.[535] The main reason for the low catalytic activity was the deactivation of the catalyst due to the degradation of the catalyst into phosphine oxides in contact with acetate or carbonate anions and/or epoxides.

It was reported by Werner et al.[538] the reaction between 1,2-epoxybutane and CO_2 catalyzed by air-stable hydroxyl-functionalized phosphonium ILs. More precisely, not only the influence of the alkyl chain length and the bulky structure of the hydroxyl-functionalized quaternary phosphonium halide was analyzed, but also the impact of the halide anion. It was determined that the catalytic activity raised by increasing the length of the alkyl chain. At last, the activity of the halide anions increased in this order: Cl$^-$ < Br$^-$ < I$^-$. Additionally, the reaction scope was expanded by employing different epoxide-based substrates, achieving high yields (Scheme 24).[538],[539] Similar reaction conditions have been reported for the same reaction; however, a hydroxyl-functionalized ammonium catalyst was employed and similar conclusions were reached.[526]
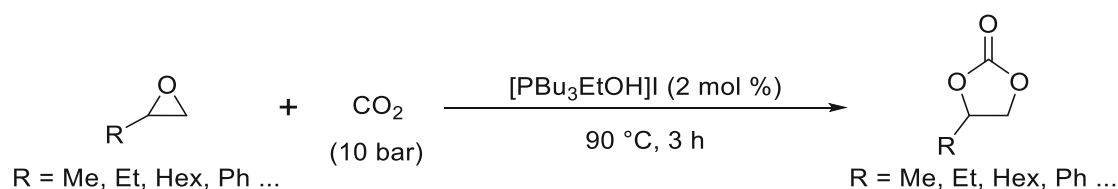
Scheme 24. Synthesis of cyclic carbonates in high yields using [PBu$_3$EtOH]I by Werner et al.[538],[539]

In another example, Shirakawa et al.[540] investigated the reaction between terminal epoxides and CO$_2$ under mild conditions, employing several biphenyl quaternary phosphonium halides bearing a phenolic hydroxyl group (Scheme 25). Two main factors played a role in the catalytic activity, such as the distance between the phosphonium and phenolic hydroxyl groups and the selection of halide anion. It was determined that the catalytic activity increased in the following positioning order: ortho > meta > para. For the halide anion, the reactivity increased as follows: Br$^-$ < I$^-$. Consequently, the highest yield (91 %) was obtained by ((2'-hydroxy-[1,1'-biphenyl]-2-yl)methyl)triphenylphosphonium iodide.
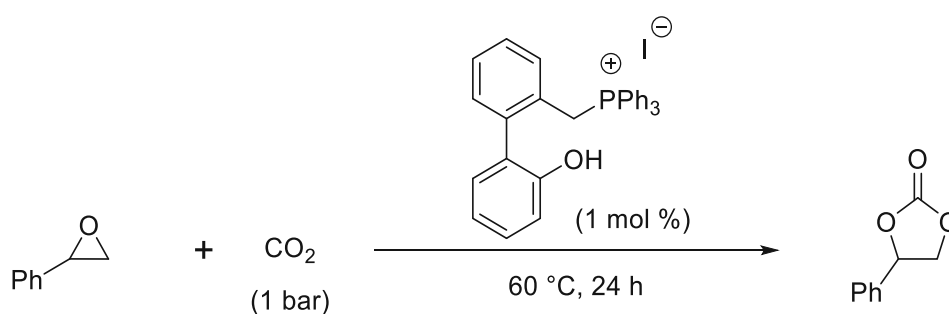
Scheme 25. Synthesis of styrene carbonates in high yields by Shirakawa.[540]

Suga et al.[541] investigated several tetraarylphosphonium halide catalysts for the reaction between styrene oxide and CO$_2$ (Scheme 26). The highest yield (90 %) were obtained with (2-hydroxyl-5-methylphenyl)triphenylphosphonium bromide.
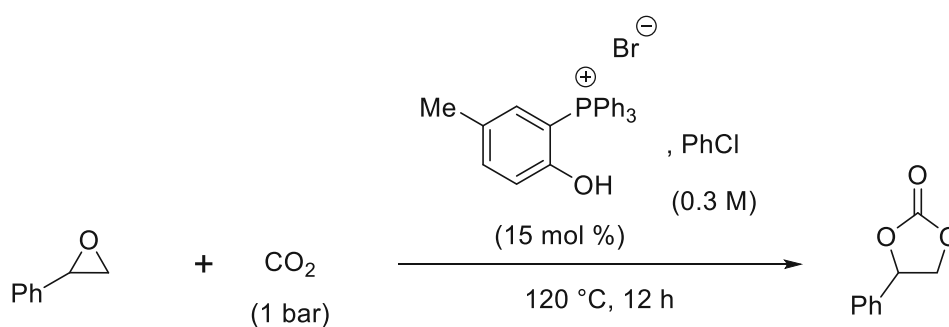
Scheme 26. Synthesis of styrene carbonates using tetraarylphosphonium halides by Suga.[541]

149

5.2.3 Imidazolium-based ionic liquids as catalysts

In the cycloaddition reaction between epoxides and CO_2 imidazolium-based catalysts are employed not only as catalysts, but also as solvents, due to their remarkable CO_2 dissolving capacity. With this type of catalysts, reactions are carried out at temperatures > 80 °C and high yields are obtained. The typically employed imidazolium-based ILs for the cycloaddition between terminal epoxides and CO_2 are illustrated in Figure 49.[500]

[C₄mim]PF₆   **[C₈mim]BF₄**   **[HC₂mim]Br**

1,3-di(3-carboxypropyl)imidazolium bromide

R = Me, Et and Bu
X = Cl, Br and I

1-carboxypropyl-3-alkylimidazolium halide
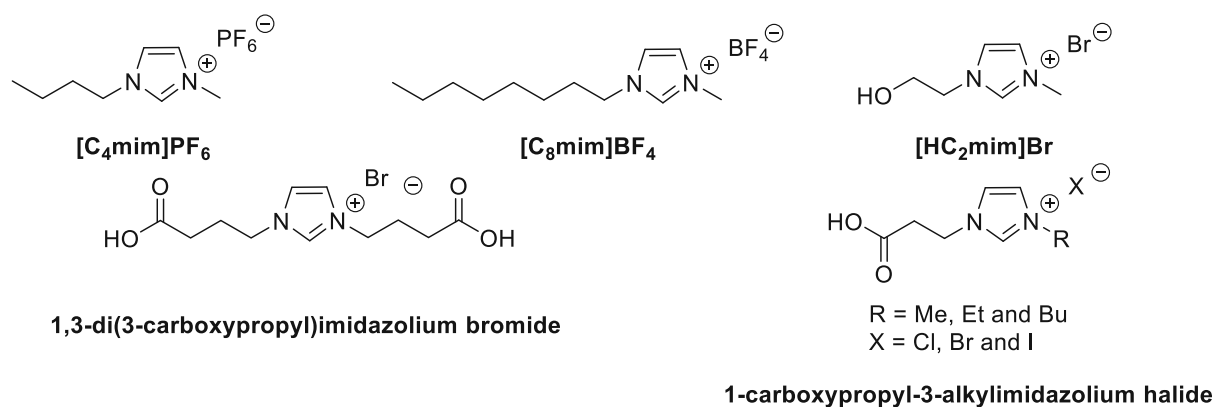
Figure 49. Some of the employed imidazolium-based ILs.[500]

Initially, imidazolium-based ILs were employed by Peng and Deng,[542] in 2001, for the transformation of epoxides and CO_2 into cyclic carbonates (Scheme 27). Specifically, 1-butyl-3-methylimidazolium salts were employed, among which, [C₄mim]BF₄ exhibited the highest catalytic activity and selectivity (both 100 %).[542] In addition, it has been demonstrated that ILs containing [C₄mim]⁺ backbone and halides as anion, achieve quantitative conversion of PO.[543]
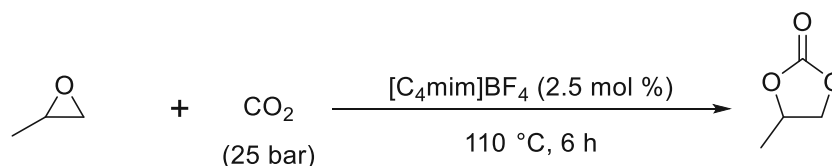
Scheme 27. Synthesis of cyclic carbonates in high yields using [C₄mim]BF₄ by Peng and Deng.[542]

Methylimidazolium ILs containing BF_4^- as an anion were employed to study the influence of the chain length of the alkyl substituent in two cycloaddition reactions, namely the cycloaddition reaction of PO and 1,2-epoxyoctane with CO_2. It was demonstrated that its impact in the catalytic activity was significant, as by increasing its length the catalytic activity was enhanced.[544],[545]

In another publication by Dupont et al.[546] the influence of the anion was investigated in C_4mim-based ILs for the reaction between styrene oxide and CO_2 to produce the correspondent carbonate (Scheme 28). It was shown that the catalytic activity followed the: $AcO^- < Cl^- < HCO_3^-$ (hydrogen carbonate anion) $< I^- \sim Br^-$. Between the halide anions, the compromise between nucleophilicity and leaving group ability gave the highest catalytic activity.
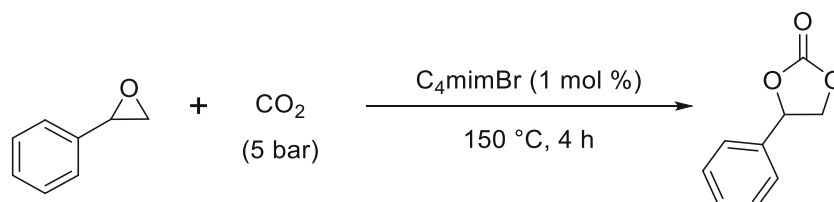
Scheme 28. Synthesis of SC using C_4mimBr (1-butyl-3-methylimidazolium bromide).[546]

In a publication by Wu et al.[547] HC_nim$^+$-based protic ILs with bromide anion with different alkyl chain length were investigated for the reaction between PO and CO_2 (Scheme 29). It was determined that by augmenting the alkyl chain length the catalytic activity decreased.[547] This trend can be attributed to the change in acidity of the imidazolium-based protic IL, as by increasing the chain length the acidity decreased. Between the tested protic ILs, [HC$_1$im]Br (1-methylimidazolium bromide) exhibited strong acidity leading to the highest catalytic activity.

Scheme 29. Synthesis of cyclic carbonates employing protic IL [HC$_1$im]Br by Wu et al.[547]

In the same publication, Wu et al.[547] postulated the mechanism related to the coupling between PO and CO_2 employing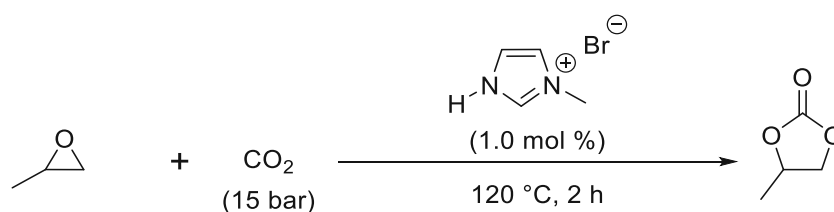 the aforementioned protic IL (Scheme 30). Initially, the hydrogen present in the nitrogen of the imidazolium ring creates a hydrogen bond with the oxygen atom of the epoxide, consequently the C-O bond of the epoxide is polarized, generating the active epoxide intermediate **A**. Thereafter, the nucleophilic attack of Br$^-$ occurs on the less-substituted or sterically hindered β-carbon atom of the epoxide, yielding the ring-opened intermediate **B**. Later, the interaction between the oxygen anion and the CO_2, results in the insertion of CO_2 into the halohydrin, generating the alkyl carbonate anion intermediate **C**. Ultimately, via intramolecular ring closing, the PC is produced. Meanwhile, the protic-IL catalyst is regenerated.
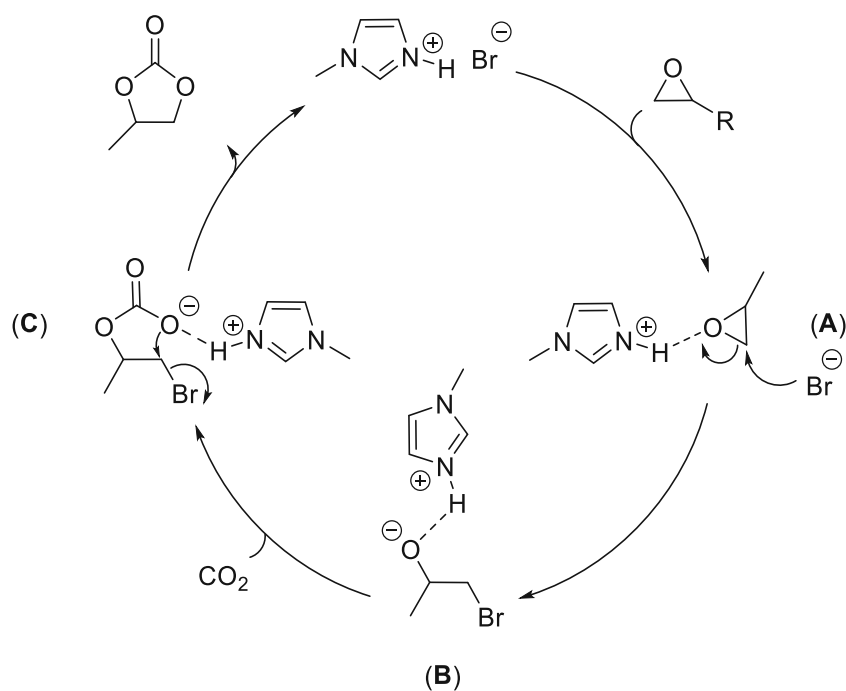
Scheme 30. Postulated mechanism for protic IL [HC$_1$Im]Br in PC synthesis.[547]

It was reported by Cokoja et al.[548] that the reaction between several epoxides and CO_2 in presence of simple imidazolium-based bromides can be carried out in milder conditions (Scheme 31).
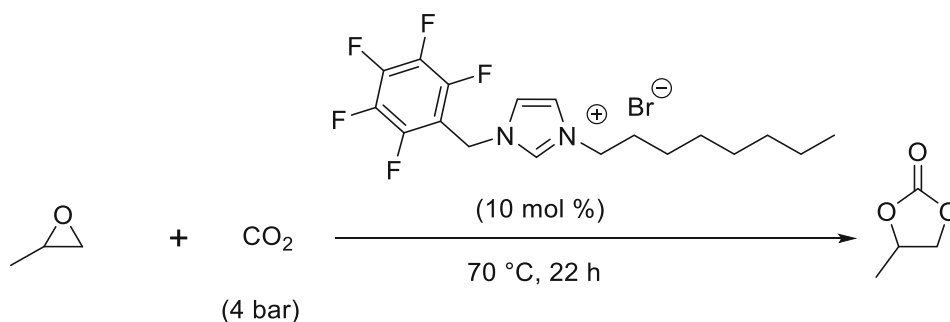
Scheme 31. Synthesis of cyclic carbonates using simple imidazolium-based bromides.[548]

Cokoja et al.[499] postulated the mechanism for imidazolium-based ILs containing halides for cyclic carbonate production. A similar mechanistic route was proposed for ILs bearing imidazolium backbone (Scheme 32), compared to ammonium- and phosphonium-based ILs. At first, the hydrogen present in the C2 position of the imidazole ring affects the polarization of the C-O bond through hydrogen bonding, generating the intermediate **A**. Subsequently, the sterically less hindered β-carbon atom of the epoxide suffers the nucleophilic attack of the bromide anion, assisting the ring opening of the epoxide generating intermediate **B**. Afterwards, the insertion of the CO_2 into the intermediate **B** takes place, producing the halocarbonate intermediate **C**. Eventually, the nucleophilic intramolecular nucleophilic attack occurs producing the correspondent cyclic carbonate and the halide is removed.
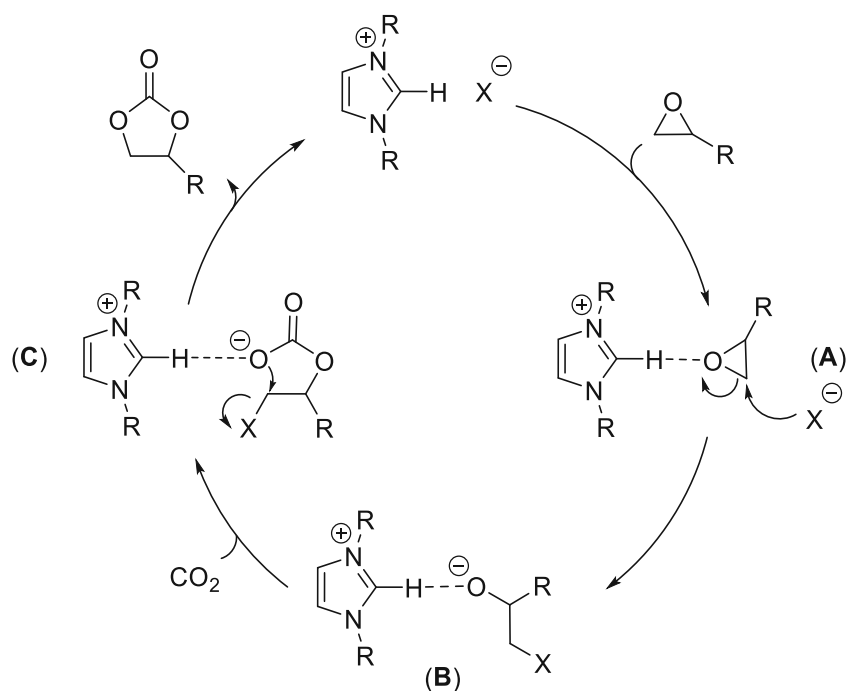
Scheme 32. Postulated mechanism for cyclic carbonate production utilizing imidazolium halides.[499]

Imidazolium-based catalysts bearing a hydroxyl group in the cation were used for this reaction by Zhang et al.[525] It was demonstrated that ILs containing hydroxyl groups had higher activity (Scheme 33).
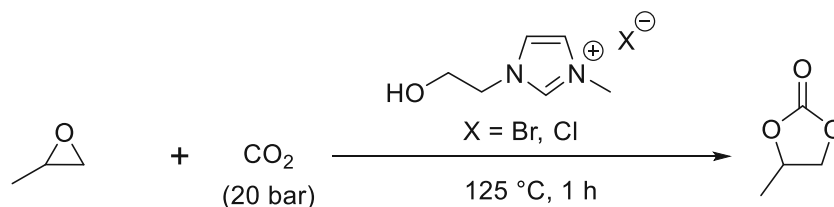
Scheme 33. Synthesis of cyclic carbonates using hydroxyl-functionalized ILs.[525]

They postulated the respective mechanism of the imidazolium-based ILs bearing hydroxyl groups in the side chain for the production of PC. The mechanism is similar to the ammonium- and phosphonium-based ILs analogues. Initially, the polarization of the epoxide C-O bond occurs via hydrogen bonding with the hydrogen of the hydroxyl group present in the imidazolium IL giving the intermediate **A**. After, the nucleophilic attack of bromide ion occurs in the less substituted β-carbon atom of the epoxide, promoting the ring opening of the epoxide and generating intermediate **B**. Subsequently, the insertion of the CO_2 into the intermediate **B** occurs, producing the halocarbonate **C**, which then converts into the cyclic carbonate via nucleophilic intramolecular substitution reaction of the bromide ion.

153

In another publication by Denizalti in 2015,[549] the reaction between PO and CO_2 was investigated employing several β-hydroxyl-functionalized imidazolium-based ILs (Scheme 34). It was found out that the C1 alkyl chain has a significant influence. The catalytic activity increased by substituting the alkyl chain from ethyl to butyl, however, the activity decreased when it was substituted by hexyl. Interestingly, by introducing branched alkyl substituents in the α-carbon atom of the C3, such as isopropyl, the catalytic activity increased. Additionally, by exchanging the isopropyl group with an isobutyl group, the catalytic activity further increased. The β-hydroxyl-functionalized imidazolium-based iodine IL containing the aforementioned substituents, exhibited high catalytic activity at milder reaction conditions, producing PC in high yields, as well as other cyclic carbonates.
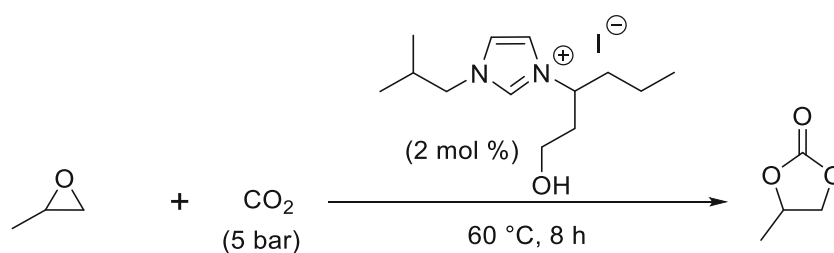
Scheme 34. Synthesis of cyclic carbonates using hydroxyl-functionalized ILs by Denizalti et al.[549]

Therefore, the catalytic activity can be further enhanced, by increasing the acidity of the proton present in the imidazolium backbone. This can be obtained by incorporating electron withdrawing groups into the nitrogen atoms.[482]

Ultimately, Cokoja et al.[550] reported the reaction between PO and CO_2 to selectively produce PC under mild conditions by employing a bis-N-alkylimidazolium ring linked by a propan-2-ol spacer (Scheme 35). The alkyl chain length had a significant impact on the catalytic activity following this order: methyl < benzyl < n-octyl. It was suggested that the longer the alkyl chain, the better the solubility in pure PO which benefitted the catalytic activity. Additionally, when comparing the hydroxyl-functionalized bis-alkylimidazolium bromide to its hydroxyl-functionalized mono-alkylimidazolium analogues, the former exhibited higher activity.
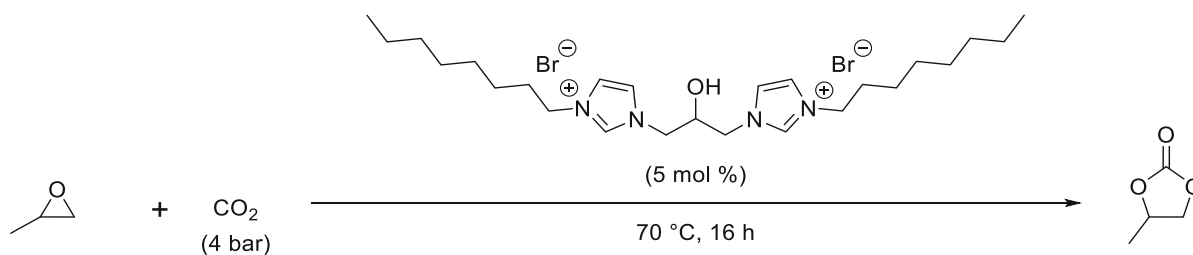
Scheme 35. Synthesis of PC employing hydroxyl-functionalized bis-N-alkylimidazolium bromide.[550]

154

5.3 Production of cyclic carbonates using silica-supported ionic liquids

For the synthesis of cyclic organic carbonates starting from epoxides and CO_2, the immobilization of ILs on solid supports provided a facile separation of product by filtration techniques together with a probable high dispersion of the catalytically active species.[286] Silica is one of the most frequently selected inorganic support materials for ILs, because of its abundance, non-toxicity and facile functionalization.[551]

Wang and co-workers employed for the first time tetrabutylammonium halides immobilized on silica, synthesized via simple adsorption technique.[375] Full conversion was reached using 150 °C, 80 bar CO_2 pressure and after 5 to 10 hours reaction time. Several ammonium ILs in combination with different halides as anions were tested. It was demonstrated that the activity increased in accordance with the nucleophilicity of the anion. Apart from that, the alkyl chain length of the cation was found out to be not significant.

At a later point in time, imidazolium-based ILs supported on silica were introduced by Wang et al.[376] broadening the variety of immobilized catalyst. Results pointed out that the highest activity was obtained with [C₄mim][BF₄] immobilized on silica. After parameter optimization, the cycloaddition was performed at 150 °C and 80 bar and after 4 h of reaction time, the conversion was almost complete. Additionally, a variety of epoxides were also tested and there was not a significant loss of activity in the catalyst after 4 cycles.

In another publication, Zhu and co-workers employed a combination of catalyst immobilized in a heterogeneous catalyst. Molecular sieves were utilized as solid support and a catalyst system consisting of [Chol]Cl together with urea (molecular ratio 1:2) was immobilized on its surface via physical impregnation.[552] Not only high yields (99%) were obtained with PC after 5 h at 110°C, but also other substrates yielded similarly high activities.

A wide array of methods to synthesize covalently immobilized ILs on several support materials have been reported. Many different support materials were employed, such as silicas[374],[377],[553-557],other oxides[553], polystyrene resins[374],[558], zeolites[559],[560] and organic polymers (chitosan).[561] Regarding the IL catalyst, ammonium-, phosphonium- and imidazolium-based cations together with halide anions are mostly utilized. In addition, a wide variety of reaction conditions and substrates have been employed, sometimes, even co-catalytic metal salts were utilized along with the catalyst.[377],[555],[556],[562]

In another publication by Lee et al.,[563] the cycloaddition reaction of allyl glycidyl ether (AGE) at low pressure (0.86 MPa) was achieved employing a silica-supported imidazolium IL obtained via the sol-gel method.

Udayakumar et al.[555] reported the cycloaddition reaction of AGE employing an imidazolium-based IL functionalized mesoporous silica synthesized via template-free conditions. The mechanism for the synthesis of cyclic carbonate, starting from an epoxide employing a RImBr_SiO_2 in a high-pressure batch reactor was proposed. A plausible mechanism was proposed (Scheme 36). In the first step, the coordination of the immobilized IL with the epoxide would occur via the attack of the anionic site of the immobilized IL on the oxirane. Subsequently, the formed intermediate would be a charged five-membered cyclic ring. In the second step, the insertion of the CO_2 into the ring (rate determining step) would take place, afterwards, the formation of a new four-membered cyclic ring allows the distribution of the charge density, yielding the final cyclic carbonate.[555]
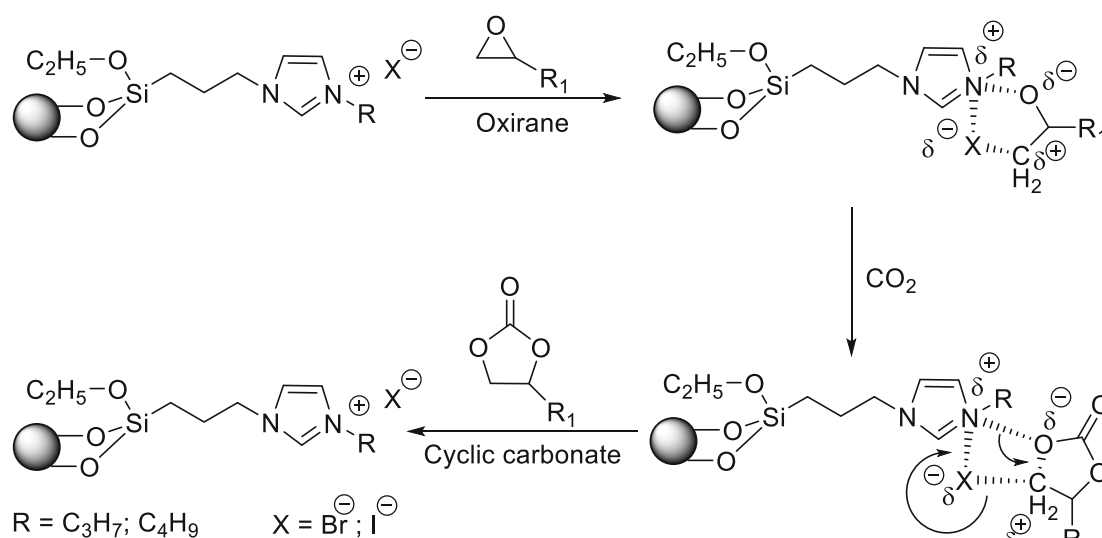
Scheme 36. Mechanism for the formation of carbonates via cyclic intermediate using immobilized ILs.[555]

In a publication by Han et al.,[377] the cycloaddition of AGE was performed employing a commercial silica (IMIS) as solid support and grafting silyl ether-containing imidazolium ILs to it via co-condensation. Numerous ILs with different alkyl chain lengths and anions were uniformly distributed over the silica surface. For the cycloaddition reaction with the IL-functionalized commercial silica (IMIS), it was beneficial to increase the applied CO_2 pressure and the catalytic activity of the anion was in accordance with its nucleophilicity: I$^-$ > Br$^-$ > Cl$^-$. Furthermore, it was observed that the bulkier alkyl group in the IL, the higher the activity.[377]

Motokura et al.[378] reported a synthesis of cyclic carbonates at atmospheric CO_2 conditions, employing SiO_2-supported aminopyridinium halides. They were selected because aminopyridinium-based ILs are easier to synthesize and are more stable in air compared to imidazolium-based ILs. The majority of the terminal epoxides exhibited 90 % yields at 100 °C and 1 atm CO_2 with a reaction time of 8-24 h.

Takahashi et al.[374] in 2005 employed hydrogen bonding groups to achieve higher catalytic activity for the CO_2-epoxide catalysis. However, carboxyl functionalized ILs were not employed until 2011. Han et al.[564] published for the first-time carboxyl-possessing imidazolium ILs (CILs) grafted onto commercial silica for the synthesis of cyclic carbonates. It was found out that the CILs had much better catalytic activity than IMIS catalysts lacking carboxyl groups, respectively TON 170 and TON 40. Additionally, the mechanism of carboxyl mediated ring opening of epoxides employing CILX-SI is depicted in Scheme 37.
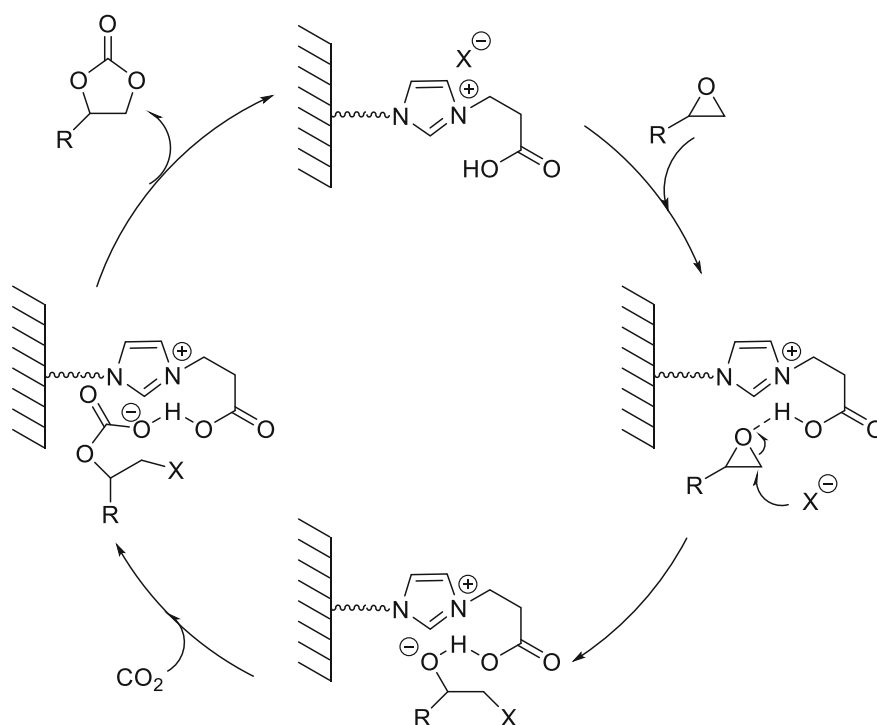
Scheme 37. Proposed reaction mechanism for cycloaddition of epoxide and CO_2 catalyzed by CILX-Si.[564]

Takahashi et al.[374] published a method, where a heterogeneous catalyst was used at 100°C, consisting of a covalently immobilized phosphonium salt on silica gel. Based on their control experiments, they proposed a synergism between the acidic silanol groups on the silica support and the basic nucleophile to yield cooperative catalysis. The ring-opened complex was stabilized via the hydrogen bonding between the epoxide and the silanol -OH (Scheme 38).
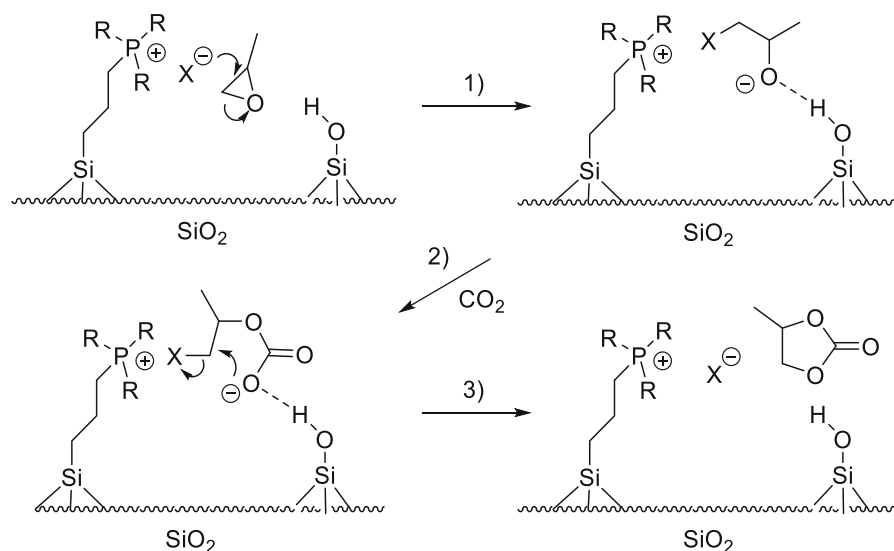
Scheme 38. Proposed CO_2-epoxide cycloaddition reaction mechanism, including the synergistic effect of silanol hydroxyl and the IL.[374]

For the case of covalently immobilized ILs, the activity is extremely affected by the selection of the support material. The most utilized solid support materials are the silicates due to their high thermal and chemical stability and wide structural versatility (mesoporous, amorphous, or zeolite-type structures). In addition, the condensation of silanol-groups allows a facile covalent anchoring of organic compounds and the surface free hydroxyls can interact advantageously with the substrate or catalyst.[286] The catalytic activity is also significantly influenced by the class of IL employed. In this regard, the cation core utilized for the ILs, are imidazolium-, phosphonium-, ammonium- and pyridinium-based.[374],[553],[560],[565] Interestingly, it seems that the anion significantly influences the catalytic activity, whereas the cation plays a less significant role. With regard to anion selection, halides are often employed and their activity is in accordance with their nucleophilicity ($I^- > Br^- > Cl^-$).[559],[561],[562] There are vast opportunities for optimization, due to the nearly limitless modifications that can be introduced into the organic cations. This modifiability is one of the greatest advantages that IL-based catalysts provide. In the case of ammonium-based ILs, it seems that long alkyl chains inhibit the catalytic activity[560], however, in the case of imidazolium-based ILs, the inhibition effect is much less significant.[559] Additionally, by modifying the IL cation and introducing hydroxyl groups, it seems that the activity can be enhanced.[561],[566]

Another important factor to consider is the addition of metal salts, which highly increase the catalytic activity. Between the metal halides available, it was reported that the addition of zinc halides, particularly $ZnBr_2$, in homogeneous systems, remarkably increased the activity.[377],[555],[562] In a publication by Xiao et al.,[556] after having optimized many parameters in their SiO2-grafted IL catalyst

system, different metal salt additives were tested. It was demonstrated that zinc yielded the highest activity compared to Al, Co, Cu, Fe and Ni alternatives.

The covalently immobilized IL-based catalysts are an appropriate alternative strategy for the cycloaddition reaction of CO_2 to epoxides. This type of catalyst has several advantages in comparison to the homogeneous systems, such as easy handling, easy product separation and reusability. However, there is also a major drawback which limits the application of the covalently immobilized ILs. To be more precise, the expensive synthetic routes related to the necessary functionalization of these catalysts limit their appeal for industrial use in the near future.[286]

# Continuous Conversion of Carbon Dioxide to Propylene Carbonate with Supported Ionic Liquids

Aitor Sainz Martinez, Christian Hauzenberger, Apurba Ranjan Sahoo, Zita Csendes, Helmuth Hoffmann, and Katharina Bica*

Institute of Applied Synthetic Chemistry, Vienna University of Technology, Getreidemarkt 9/163, 1060 Vienna, Austria

S *Supporting Information*

ABSTRACT: We present the use of silica-supported ionic liquids as catalysts for the continuous production of propylene carbonate from propylene oxide using supercritical carbon dioxide as solvent and reagent. Considerable differences in the catalytic activity of ionic liquids in homogeneous catalysis in batch mode and in continuous-flow using supported species processes were found, suggesting that a synergistic effect between ionic liquid and silica support material takes place. While supported ionic liquids prepared via physisorption of $[C_2mim]Br$ showed the highest catalytic activity, studies on long-term stability showed a rapid loss in yield due to the formation of undesired polypropylene carbonate that agglomerated in the ionic liquid layer. Improved long-term stability was found for ionic liquids covalently bound to the silica support materials, suggesting that a compromise between activity and stability is the best solution for the continuous production of propylene carbonate.

KEYWORDS: *Carbon dioxide, Ionic liquids, Continuous flow, Supported ionic liquid phases, Heterogeneous catalysis*
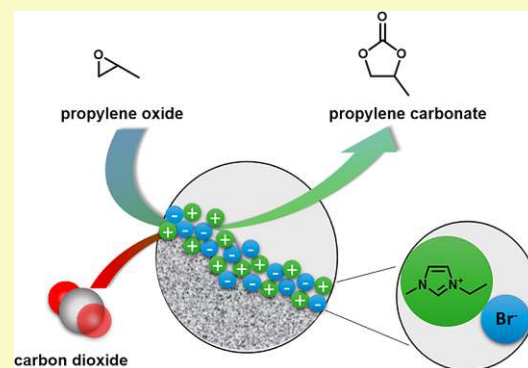
INTRODUCTION

Carbon dioxide (CO_2) from the combustion of fossil sources is regarded as the most significant greenhouse gas; hence, CO_2 capture and conversion have attracted considerable public attention in the past years.[1] The implementation of CO_2 capture from flue gases in industrial combustion processes provides an enormous stream of potential raw material for chemical production.[2] As an abundant, nontoxic, nonflammable, and renewable carbon resource, CO_2 is very attractive as a feedstock for fine chemicals and materials.[3,4] However, few industrial processes utilize CO_2 as a raw material, as CO_2 is a notoriously stable and rather unreactive molecule whose conversion represents a grand challenge for process development.[5] The recent implantation of potent catalysts and catalytic systems can overcome the thermodynamic and kinetic barriers of CO_2. Within the past years, numerous chemical reactions for synthesizing organic molecules from CO_2 have been developed.[6] Examples include C1 bulk chemicals such as methanol, formic acid, or urea, but also high-value fine chemicals with importance for the pharmaceutical industries as summarized in several recent reviews.[3,7,8] In this regard, ionic liquids have attracted considerable interest: apart from their application in carbon capture and storage (CCS) technologies, ionic liquids can be used as tailored catalysts for the conversion of carbon dioxide to chemical feedstocks.[9−13]

Among all potential products that can be obtained from CO_2, its conversion into cyclic carbonates via the reaction with epoxides probably received the most attention (Figure 1).

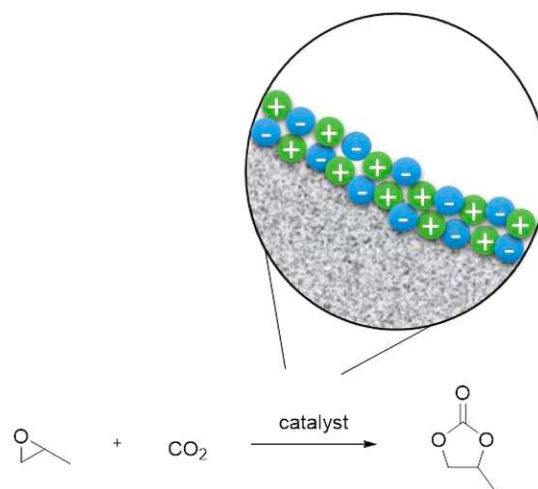**Figure 1.** Formation of propylene carbonates from propylene oxide and carbon dioxide catalyzed by supported ionic liquids.

The annual production volume worldwide of cyclic carbonates reaches 80 000 tons at present, and approximately 50% of the total production relies on carbon dioxide as feedstock.[2] Cyclic carbonates are currently used as electrolytes in fuel cells and in lithium ion batteries. Furthermore, they
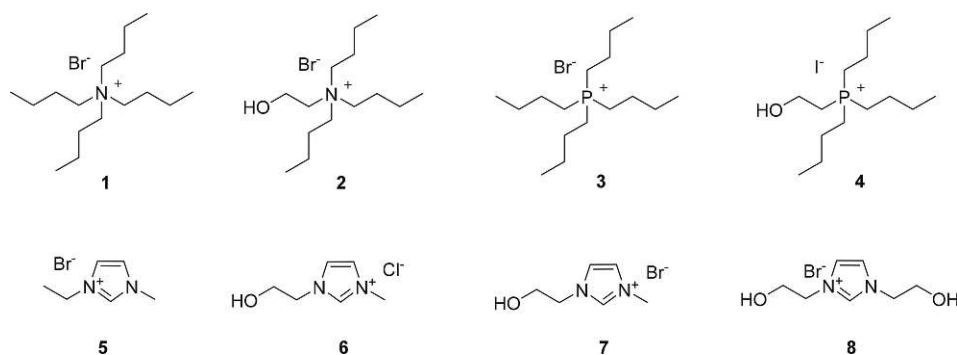
Figure 2. Selection of ammonium-, phosphonium-, and imidazolium-based ionic liquids with different halide anions and optional side chain functionalization for this study.

have found application as an aprotic polar solvent and as intermediates in the production of fine chemicals and pharmaceutical materials. Since they can undergo ring opening polymerization, cyclic carbonates are useful raw materials in polymer chemistry, e.g., for the production of polyurethanes. Consequently, considerable research interest has been dedicated to the development of catalysts for the efficient production of cyclic carbonates from epoxides and carbon dioxide.[14,15] Different systems including well-defined metal complexes,[16] alkali metal halides,[17] metal oxides,[18] organic bases,[19] or ionic liquids[14] based on imidazolium, ammonium, or phosphonium cations and their polymers[20] have been reported for this purpose. The pool of ionic liquids is not limited to simple core structures, as the structural variability inherent in these organic ions provides a simple opportunity to enhance their catalytic activity. Independent of the cation structure, the presence of an intramolecular hydrogen bond donor increases the catalytic activity for the conversion of cyclic epoxides.[21,22] A variety of protic, hydroxyl-, and carboxy-functionalized ionic liquids are known to show higher catalytic activity than the unfunctionalized systems.[23] Similarly, considerable attention has been spent on the impact of the ionic liquid anions and on the use of Lewis-acidic ionic liquids such as chlorozincate-based species, so that nowadays a large pool of potential ionic liquids is available for the conversion of CO_2 to cyclic carbonates.[24,25] The immobilization of ionic liquids on suitable support materials either via covalent or noncovalent approaches for slurry-phase batch reactions has also attracted attention, and various support types including silica, molecular sieves, or biopolymers have been reported.[12]

Despite this considerable research interest, examples for the continuous conversion of CO_2 to cyclic carbonates are rare, as the overwhelming majority of all experiments, even with supported ionic liquid phases, have been performed under batch-wise conditions.[24] While fixed-bed, bubble-bed, as well as microwave or microreactors have been described for the chemical fixation of carbon dioxide into carbonates, the results of continuous flow processes vary considerably from those obtained in batch-wise processing. In 2012, the reaction of carbon dioxide with propylene oxide was carried out under flow conditions in a microreactor setup.[26] The hydroxyl-functionalized ionic liquid catalyst was pumped through the reactor in a solution with the substrate, and high turnover frequency was found at low residence times. More recently, an example of carboxymethyl cellulose (CMC) supported imidazolium based ionic liquids was used as a heterogeneous catalyst for the cycloaddition of CO_2 to cyclic carbonates,

allowing to convert CO_2 to cyclic epoxides in continuous flow with high efficiency for the first time.[27]

This lack of ionic liquid-based continuous flow processes for the conversion of epoxides with CO_2 is surprising, as the liaison of ionic liquids with (supercritical) CO_2 provides an ideal prerequisite for this purpose. Ionic liquids can be conveniently immobilized on solid support, e.g., on mesoporous silica via physisorption or covalent anchoring, as has been demonstrated for multiple catalytic purposes.[28−30] The supported ionic liquid phase (SILP) technology combines the advantages from homogeneous and heterogeneous catalysis and provides short diffusion distances in the ionic liquid film. This is particularly attractive to overcome mass transfer limitations that are often encountered in traditional ionic liquid−liquid biphasic catalysis. The SILP catalyst concept is particularly well established for gas phase reactions such as hydroformylations[31−36] or hydrogenations;[37−39] however, there are also successful examples of SILP catalysts in combination with supercritical carbon dioxide.[40,41] The high solubility of carbon dioxide in ionic liquids is advantageous and can overcome mass transfer limitations observed in bulk ionic liquid phases. Moreover, the extremely low solubility of ionic liquids in scCO$_2$ can suppress ionic liquid leaching into the product phase, a limiting factor when conventional solvents are used.[42]

Here, we present our investigations toward the use of supported ionic liquids as sole catalysts for the conversion of supercritical carbon dioxide as solvent and reagent, aiming for the continuous production of propylene carbonate from propylene oxide.

■ RESULTS AND DISCUSSION

On the basis of recent literature data, we selected a set of eight ionic compounds based on imidazolium, ammonium, or phosphonium core structures with halide anions and optional side chain functionalization (Figure 2).

As reaction conditions in literature vary, we initially performed the reaction of propylene oxide with carbon dioxide under homogeneous conditions in batch mode to compare their catalytic properties (Figure 3). Reactions were conducted using 5 mol % ionic liquid as catalyst under subcritical conditions at 50 bar and 45 or 70 °C for 18 h. As expected, all ionic liquids with a hydroxyl group as substituent were revealed to have higher reactivity than those without. In a similar way, the influence of the anion could be confirmed as ionic liquids with bromide as anion showed higher reaction rates following the order of nucleophilicity and size.[43] The highest catalytic
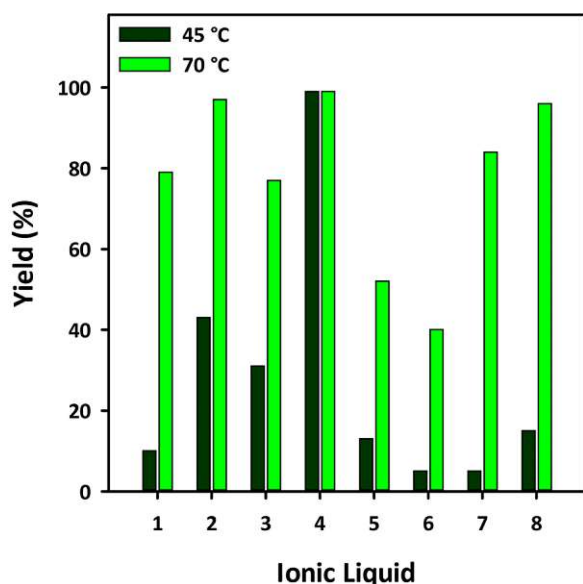
Figure 3. Catalytic activity of selected ionic liquids at 45 and 70 °C under homogeneous conditions.

activity was obtained with the phosphonium based ionic liquid **4**, which is in accordance with recent literature data.[22] Even at 45 °C, high yields were obtained, indicating that the catalyst is not at its limit and might exhibit even better performance under stressed conditions.

After the evaluation of different ionic liquids under batch conditions in an autoclave, the conversion of propylene oxide with carbon dioxide was further studied in continuous flow using supported ionic liquids on mesoporous silica. SILP catalysts were prepared according to standard procedures reported in the literature.[44] All SILP catalyst **SILP 1−8** were obtained as free-flowing powders that could be easily immobilized in a thermostated catalyst cartridge.

As leaching of physisorbed ionic liquid might become an issue, we looked in parallel at supported ionic liquid catalysts with a covalently bound layer of imidazolium cations (**SILCs**).

A monolayer of imidazolium-based ionic liquid with chloride (**SILC-1**) or bromide anion (**SILC-2**) and optional hydroxyl-ethyl side chain (**SILC-3** and **SILC-4**) was immobilized on silica-60 according to literature procedures relying on a siloxane-modified precursor (Figure 4).[45] Two different routes were followed: alkylmethylimidazolium-functionalized materials **SILC-1** and **SILC-2** were prepared via direct condensation of the siloxy functionalized ionic liquid with silica. For hydroxyl-functionalized supported ionic liquids (**SILC-3** and **SILC-4**), a two-step procedure involving the reaction of silica with the halide-precursor and consecutive alkylation with methylimidazol was followed.

For both pathways, analysis via FT-IR spectroscopy showed the disappearance of the isolated silanol stretching vibration at 3741 cm^{-1} in the corresponding spectra, confirming the successful surface modification of silica with a monolayer of imidazolium-based ionic liquid. Besides, C−H peaks belonging to the C−H vibrations in the imidazolium ring (3200−3050 cm^{-1}) and in the alkyl groups (3000−2850 cm^{-1}) became visible. The absorbance bands at approximately 1570 cm^{-1} (**SILC-1−SILC-4**) are attributed to the (CC/CN) stretching vibrations of the imidazolium ring (Figure 5).

Further analysis via BET, TGA, and elemental analyses confirmed the successful modification but also the mesoporous character of the support material (see Figure S2−5 and Table S1). Results from BET gave a type IV shape of the N$_2$-adsorption−desorption isotherm for **SILC-1** to **SILC-4** according to the IUPAC classification which is characteristic for materials with mesoporosity. Results from TGA showed that **SILC-1** to **SILC-4** are stable until 250−290 °C after an initial weight loss of water traces around 80−100 °C. Further data obtained from elemental analysis revealed a nitrogen content varying from 2.51 to 3.43 wt %, corresponding to a range from 0.90 to 1.22 mmol imidazolium per gram of **SILC** (see Table S2).

A reactor setup and system parameters as indicated in Figure 6 were chosen. A liquid carbon dioxide cylinder with an ascending pipe served as the CO$_2$ supply. Liquid carbon dioxide was further pressurized with two chilled pumps to the

Figure 4. Preparation of surface-modified silica **SILC 1−4** from 1-(3-trimethoxysilylpropyl)-3-methylimidazolium chloride and silica-60.

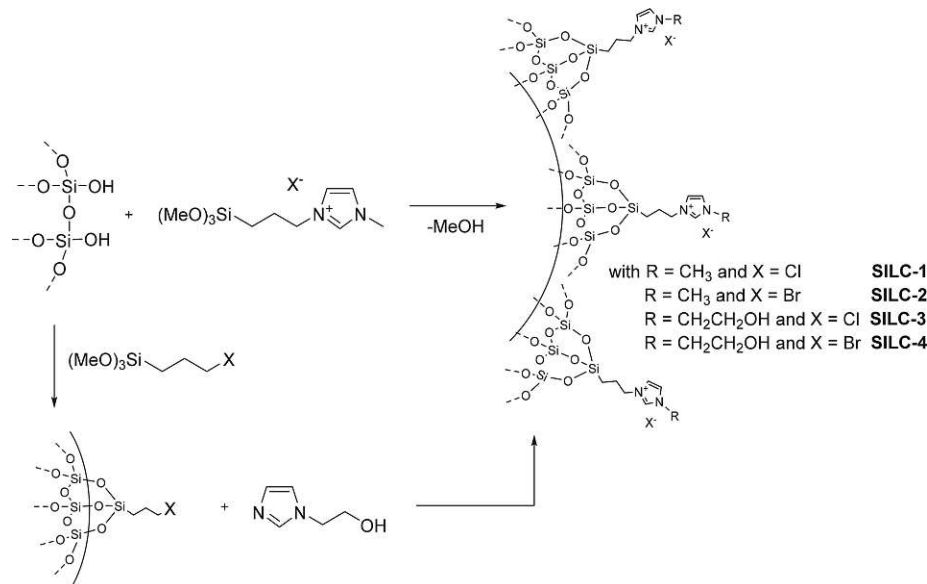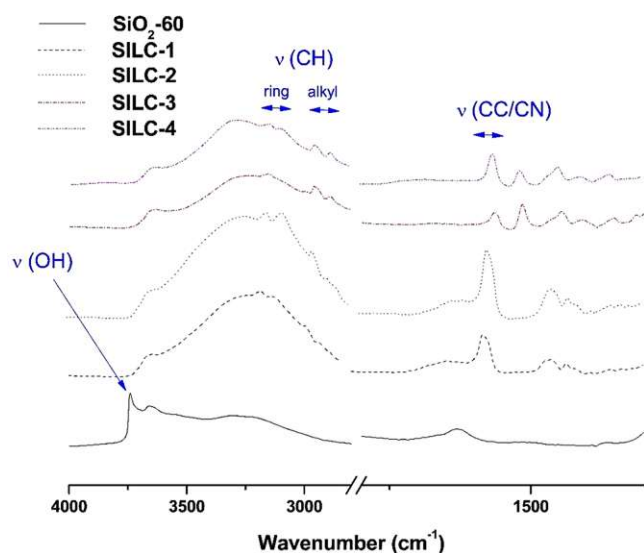**Figure 5.** FT-IR spectroscopy of surface-modified silica **SILC 1−4** in comparison with pristine SiO$_2$-60.

desired pressure before the substrate stream was added with an additional HPLC pump. After preheating in a coil, the reaction mixture in supercritical carbon dioxide was pumped through a catalyst cartridge filled with silica-supported ionic liquids. After this thermostated reaction unit, the reaction mixture in scCO$_2$ was decompressed in a back pressure regulator, followed by a gas/liquid separator and a fraction collector allowing for the continuous collection of samples over time. Some consideration regarding the boiling point of the starting materials had to be taken into account when selecting the flow rate and substrate mixture since the low boiling point of propylene oxide could cause issues with incorrect flow rates. Consequently, we worked in a 50% (v/v) mixture with n-hexane to ensure a correct substrate flow rate, although it should be noted that n-hexane is not an environmentally preferred solvent option. However, due to the low boiling point of n-hexane, the product could be collected in pure form after depressurization, as the remaining starting material and the cosolvent n-hexane were evaporated together with CO$_2$. This allowed for directly determining the yield gravimetrically, and finally calculating the yield based on the substrate input after purity control via GC and NMR. In terms of green chemistry metrics, it would be clearly advisable to avoid the use of any cosolvent, and later studies showed that comparable results are

obtained when using propylene oxide in pure form (see Figure S6 for details). However, for comparability and to maintain a correct flow rate, we used a 50% (v/v) mixture with n-hexane in all experiments.

Initially, the catalytic performance of all SILP for the continuous conversion of propylene oxide was investigated under standard conditions (Figure 7).
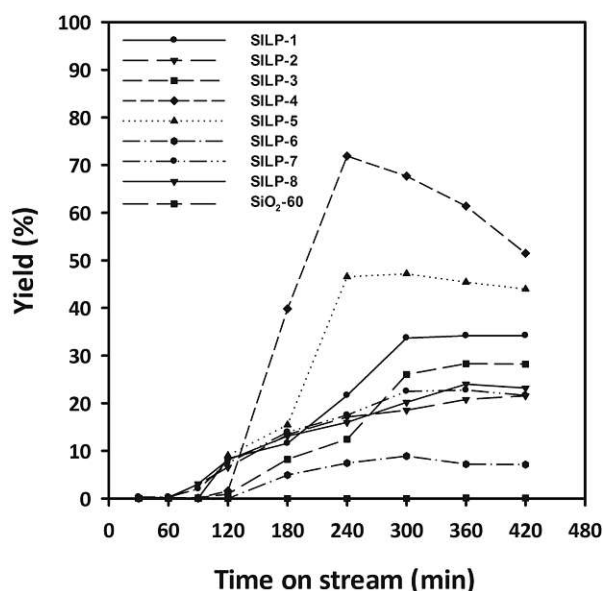
Figure 7. Comparison of the catalytic performance of supported ionic liquids **SILP-1−8** and unfunctionalized silica in the continuous conversion of propylene oxide with scCO$_2$ as reactant and solvent. Performed at 80 °C and 100 bar with a flow rate of 2 mL/min (1.98 mL/min scCO$_2$ and 0.02 mL/min propylene oxide/n-hexane 1:1).

Considerable differences in the catalytic performance of supported ionic liquids **SILP-1−8** were observed when monitoring the product output over 7 h (Figure 7). While a constant product output was observed with all imidazolium and ammonium-based SILP catalysts, the supported phosphonium-based ionic liquid **SILP-4** differed considerably. Despite showing high catalytic activity, as it would be expected from the previous experiments in the autoclave, a rapid decrease in yield to 52% yield was observed after 420 min after reaching a maximum of 72%. Surprisingly, this loss in activity could not be traced to catalyst leaching, as we did not find any traces of the ionic liquid in the product. Further investigations of the
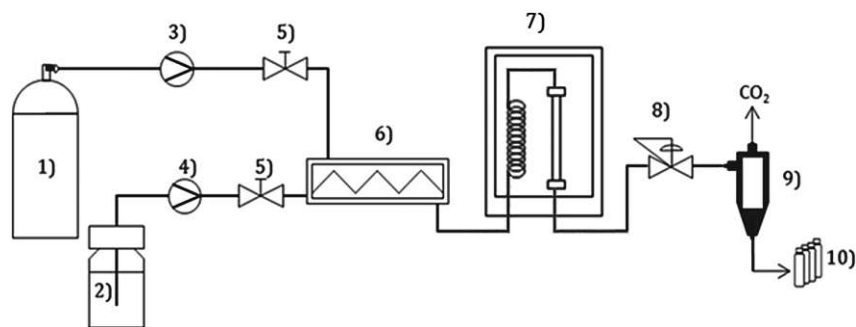
Figure 6. General setup for the continuous conversion of propylene oxide with scCO$_2$ as reactant and solvent using silica-supported ionic liquids. (1) Liquid CO$_2$ supply; (2) substrate supply; (3) CO$_2$ pump; (4) solvent pump; (5) manually operated valve; (6) inline mixer; (7) thermostated oven with preheating coil and catalyst cartridge; (8) back pressure regulator; (9) gas−liquid separator; (10) fraction collector.

recovered ionic liquid from a spent catalyst sample via NMR showed that this ionic liquid was decomposing during the reaction. ^{1}H NMR analysis indicated a degradation of the hydroxyethyl chain in the phosphonium salt as the main reason for the decrease of catalytic activity over time. This is in contrast to the unsupported material used under batch conditions, where we did not see any evidence for the decomposition of ionic liquid **4**.

In contrast, we did not observe the problem of catalyst deactivation for any other ionic liquid, and reasonably stable product output was observed over time for 420 min. Moreover, it is worth noticing that the product was obtained in pure form without any contamination, indicating that ionic liquid leaching is successfully suppressed. However, a different order of catalytic activity of all ionic liquids on silica in flow was observed compared to the use of unsupported ionic liquids batch conditions. The functionalized supported ionic liquid **SILP-5** without any intermolecular hydroxyl groups on silica seemed to be the most efficient ionic liquid on silica based on all tested ionic liquids under flow conditions. This indicates a synergistic effect of surface hydroxyl groups on the silica support material promoting the cycloaddition of epoxides that outperforms the intramolecular hydroxyl groups in ionic liquids **7** and **8**. To test this hypothesis, silica-60 was heated to 550 °C for 48 h to reduce the available surface hydroxyl groups. A decrease in yield was obtained with ionic liquid **5** supported on calcined silica (see Figure S7), which clearly supports the cocatalytic effect of surface hydroxyl groups.

A cocatalytic effect of the support material is also supported by literature data, as has been demonstrated that the catalytic activity of unfunctionalized ionic liquids can be enhanced by an intermolecular hydrogen bond donor such as alcohols or solid materials, e.g., silica.[46−48] As previously suggested by Takahasi et al., the acidic surface silanol groups interact and activate propylene oxide for nucleophilic attack. Synergistic behavior was found with a silica supported phosphonium salt in the fixed bed continuous flow conversion of propylene oxide with subcritical carbon dioxide.[49] When using the supported phosphonium salt $SiO_2-C_3H_6-P(Bu)_3Br$ as catalyst, high yields of 80−100% propylene carbonate with good long-term stability for 1000 h could be obtained, although the temperature had to be increased from 90 to 160 °C to maintain the high activity. A similar effect has been reported by Wu et al., who recently reported the application of imidazolium-based ionic liquids supported on carboxymethyl cellulose as heterogeneous catalysts for the cycloaddition of CO_2 to cyclic carbonate and described a cocatalytic effect of the support material.[27]

The absence of surface hydroxyl groups also is evident in the catalytic performance of covalently immobilized ionic liquids (**SILC-1−4**), as yields were significantly lower compared to those of the physisorbed species (Figure 8), yet the impact of anion seems to be maintained, as the highest yield was obtained with **SILC-2**. In this regard, it should be also noted that pure silica without any supported ionic liquid did not exhibit any significant catalytic effect under standard conditions, as only traces of product could be detected in the output stream (Figure 8).

On the basis of all tested systems, the combination of $[C_2mim]Br$ **5** and untreated silica as support material (**SILP-5**) was revealed to be the optimum system for the formation of propylene carbonate. Further optimization of the system
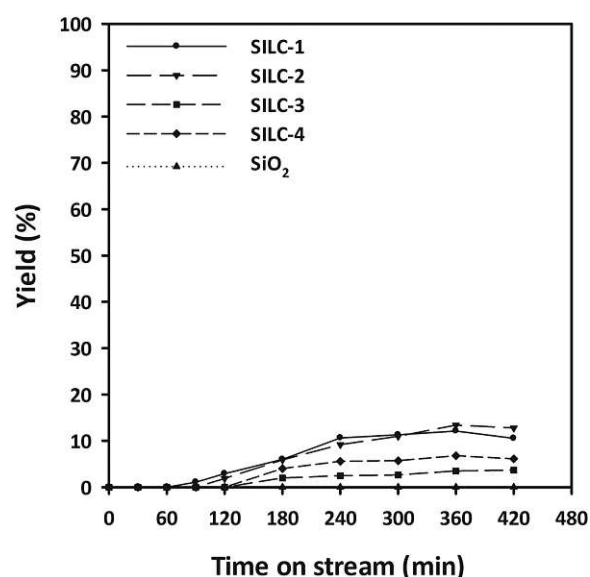

Figure 8. Comparison of the catalytic performance of covalently immobilized ionic liquids **SILC-1−4** and unfunctionalized silica in the continuous conversion of propylene oxide with $scCO_2$ as reactant and solvent. Performed at 80 °C and 100 bar with a flow rate of 2 mL/min (1.98 mL/min $scCO_2$ and 0.02 mL/min propylene oxide/n-hexane 1:1).

parameters regarding catalyst loading, temperature, pressure, and column length was done (Table 1).

Table 1. Optimization of Continuous Reaction Conditions for the Conversion of Carbon Dioxide and Propylene Oxide into Propylene Carbonate with Supported Ionic Liquid Phase SILP-5

entry[a]	temperature [°C]	pressure [bar]	IL loading [wt %]	yield at 420 min[c] [%]	TON[d]	TOF [h⁻¹][e]
1	80	100	0	0	0	0.0
2	80	100	10	44	21.6	3.1
3	100	100	10	54	30.6	4.4
4	120	100	10	65	34.0	4.9
5	120	100	5	38	57.7	8.2
6	120	100	20	78	16.5	2.4
7	120	60	10	59	19.4	2.8
8	120	160	10	79	24.6	3.5
9[b]	120	100	10	89	19.1	2.7

[a]Performed with a flow rate of 2 mL/min (1.98 mL/min $scCO_2$ and 0.02 mL/min propylene oxide/n-hexane 1:1; column: 4.5 mm ID × 150 mm). [b]Column length 4.5 mm ID × 250 mm. [c]Defined as yield obtained in the period from 360 to 420 min based on the substrate input. [d]Calculated as mmol propylene carbonate per mmol catalyst in the period from 0 to 420 min. [e]Calculated as TON per reaction time (420 min).

As expected, an increase in temperature from 80 to 100 °C or 120 °C was clearly beneficial for the reactions, and yields increased to 65%. Even at this temperature, we did not detect any leaching or decomposition of the ionic liquid, and the product propylene carbonate was collected in spectroscopically pure form. In contrast, an increase in pressure from 100 to 160 bar did not significantly affect the yield. However, when we deliberately reduced the pressure to 60 bar to run the reaction in subcritical state, a drastic decrease in the yield was observed.

Further studies on ionic liquid loading showed that an increase in ionic liquid loading to 20 wt % did not improve the yield. In fact, we observed a constant decrease of the catalytic performance and detected for the first time contamination of the product with ionic liquid **5**, indicated by ^{1}H NMR studies and a nitrogen content of 0.72 wt % in the fraction obtained between 360 and 420 min according to elemental analysis. When monitoring and quantifying catalyst leaching over time via ^{1}H NMR analysis of the collected samples, we observed that leaching reached its maximum at 300 min with almost 5% ionic liquid loss. Afterward, leaching decreased, indicating that the amount of ionic liquid **5** on silica should be reduced to less than 15 wt % to avoid leaching at 120 °C. When we further increased the column length to 250 mm, corresponding to approximately 2.3 g of SILP material, the product yield increased as well, although the cumulative yield after 420 min is lower due to a longer break-through. Under these optimized parameters, the process reached a maximum yield of 89% based on substrate input at 420 min. This corresponds to a turnover number (TON) of 25, and a production rate of propylene carbonate in high purity of 0.6 mL/h could be achieved.

Eventually, we addressed the aspect of long-term stability and ran experiments under optimized conditions in continuous flow for 48 h. However, we found that yields were drastically decreasing for the favored ionic liquids [C_2mim]Br **5** on silica support material (**SILP-5**) over time (Figure 9).

Figure 9. Stability of the continuous conversion of propylene oxide with scCO$_2$ catalyzed by supported ionic liquids over 48 h.
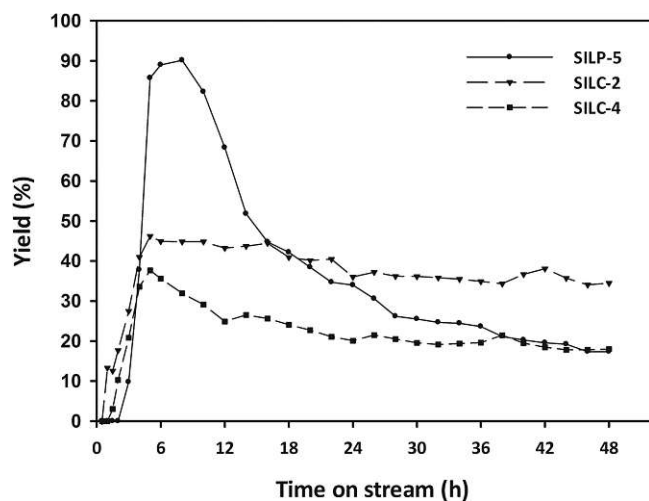
This loss of activity cannot be caused by the loss of the supported ionic liquid as previous experiments did not show any leaching at 10 wt % SILP loading. To verify this, we ran ^{1}H NMR and elemental analysis of the sample at different intervals: both N and Br content was extremely low if not below the detection limit and thus proved the absence of ionic liquid in the product stream. Further analysis of the ionic liquid recovered from the SILP catalyst did not show any decomposition of the ionic liquid either. However, when the spent catalyst material was extracted with methanol, a mixture of ionic liquid contaminated with polypropylene glycol was found, as indicated by the additional peaks at 1.6 and 3.5 ppm (Figure 10). While we did not detect this byproduct in batch reaction mode, it seems that the slow accumulation of

polypropylene glycol is responsible for the loss of catalytic activity on a longer time scale.

When running experiments on long-term stability with the supported ionic liquid catalysts prepared with covalent anchoring, a different picture was observed. Despite the lower catalytic activity, considerably improved long-term stability was found. The best results were obtained with the immobilized ionic liquid catalyst **SILC-2** and were reasonably stable. Constant product output in high purity with 38% cumulative yield was observed over a period of 48 h (see Figure S8 and Table S3). Overall, this outperforms the SILP system, which reaches only an overall yield of 36% due to the rapid loss of catalytic activity (Figure 9).

It seems that the absence of surface hydroxyl groups results in a lower catalytic activity and also in the suppression of the undesired formation of the oligomeric byproducts. This is in contrast to all physisorbed SILP catalysts with unmodified silica that rapidly lost their catalytic activity over time. In the case of hydroxyl-functionalized supported ionic liquid catalyst **SILC-3** and **SILC-4**, the product output was less stable and dropped from 37% yield to 17% after 48 h on stream, indicating again that the presence of hydroxyl groups in the catalyst is not beneficial for continuous processing.

■ CONCLUSION

Here, we showed the use of supported ionic liquids on mesoporous silica for the continuous production of propylene carbonate from propylene oxide using supercritical carbon dioxide as solvent and reagent. A number of ionic liquids based on ammonium, phosphonium, and imidazolium cations with halide-based anions and optional side chain functionalization were investigated. A fundamentally different order of catalytic activity was observed when comparing homogeneous catalysis in batch mode and a continuous process using supported ionic liquids. While high catalytic activity was observed for unfunctionalized imidazolium-based ionic liquids such as [C_2mim]Br on SiO$_2$ due to a cocatalytic effect of the surface hydroxyl groups of silica, ionic liquids covalently bound on the silica surface were less active but superior systems for the continuous production of propylene carbonate.

Eventually, this provides a sensible compromise between catalytic activity and long-term stability. Although the catalytic activity remains below the values obtained with conventional SILP catalysts prepared with unmodified silica, the constant and stable performance with supported ionic liquid catalysts (SILC) indicates that a compromise between high activity and stability is the best solution with this particular catalyst system. However, it should be noted that the absence of water is a prerequisite that must be maintained during the process, as even traces that would lead to a gradual hydrolysis and a reformation of surface hydroxyl groups.

■ MATERIALS AND METHODS

Commercially available reagents and solvents from Sigma-Aldrich were used as received without further purification, unless otherwise specified. All ionic liquids were dried for at least 24−48 h at room temperature or at 50 °C and 0.01 mbar before use and stored under argon.

^{1}H and ^{13}C NMR spectra were recorded on a Bruker Advance UltraShield 400 (400 MHz) spectrometer, using the solvent peak as reference. Infrared spectra were recorded with a Bruker Vertex 80 FTIR spectrophotometer using a narrow band MCT detector measuring diffuse reflectance. 256 scans were collected for each spectrum with 4 cm^{-1} resolution. Gas chromatography (GC) was
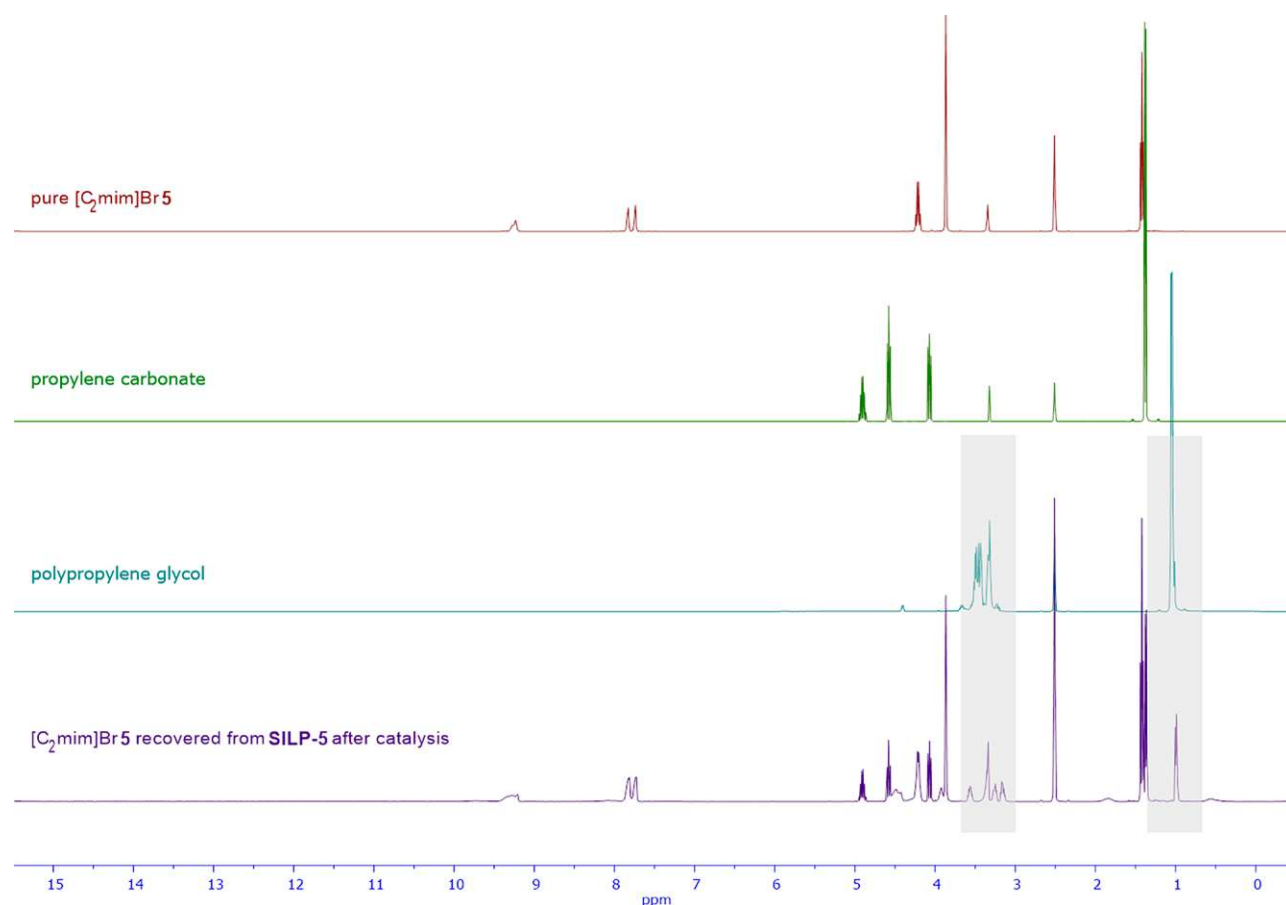
Figure 10. Evidence for the formation of polypropylene glycol accumulated in the ionic liquids layer in **SILP-5** after 48 h.

recorded by a GC Thermo Scientific Focus with a FID detector. The column used was a BGB-5 (3 m x 0.32 mm ID; 0.25 μm film) with the temperature program starting at 60 °C up to 170 °C with 15 °C/min, followed by heating from 170 °C up to 300 °C with 50 °C/min and a final hold time at 300 °C for 5 min. N-Hexadecane was used as internal standard.

Thermogravimetric analysis (TGA) was performed on a Netzsch STA 449 F1 system. The temperature was increased from 25 to 500 °C with a rate of 5 °C/min. Nitrogen gas flow was set to 40 mL/min. Textural properties were analyzed by N_2 physisorption (ASAP 2020 Micrometics GmbH) using the Brunauer−Emmet−Teller (BET) theory for determining the surface area and the Barret−Joyner−Halenda (BJH) method for obtaining the pore size distribution. Elemental analysis was performed at Vienna University, Department of Physicochemistry, Laboratory for Microanalysis, Währingerstraße 42, A-1090 Vienna.

All continuous flow experiments were carried out with a scCO$_2$ device produced by Jasco (Jasco Corporation, Tokyo, Japan), if not otherwise noted. Liquid CO$_2$ (>99.995% purity; with ascension pipe; Messer Austria GmbH) was pressurized by two CO$_2$-pumps (PU2086) with cooled heads (FL300, JULABO GmbH). An HPLC-pump (PU2082) delivered substrates and solvents. A heating coil and HPLC-columns (50 mm, 150 mm, and 250 mm × 4.5 mm ID) filled with catalyst material were equilibrated in a thermostated oven (CO-2060) to the desired temperature. A back pressure regulator (BP-2080), gas/liquid separator (HC-2086-01), and a product collector (SCF-Vch-Bp) were used.

Synthesis of Ionic Liquids. Tetrabutylammonium bromide **1** and tetrabutylphosphonium bromide **3** were purchased from commercial suppliers and used as received. All other ionic liquids **2, 4−7**, and 1-(3-trimethoxysilylpropyl)-3-methylimidazolium chloride and bromide were synthesized according to standard methodologies, and analytical

data were in accordance with the literature.[21,22,50] For ionic liquid **8**, a modified protocol was followed as indicated below.

1,3-Bis(2-hydroxyethyl)imidazolium Bromide **8**. A round-bottomed flask was charged with imidazole (2.41 g, 35.4 mmol), 1,3-dioxolan-2-one (3.18 g, 36.1 mmol), and 30 mL of anhydrous dioxane. The mixture was stirred for 2 h at 80 °C. 2-Bromoethanol (4.43 g, 35.4 mmol) was slowly added, and the reaction mixture was stirred for 24 h at 80 °C. A second viscous phase appeared. The dioxane phase was removed, and the obtained ionic liquid was washed with diethyl ether and acetone. Solvent traces were removed under vacuum (0.01 mbar, 50 °C) with stirring for 24 h to obtain the ionic liquid as a yellowish viscous liquid in 97% yield.

^{1}H NMR (400 MHz, DMSO-d_6, 25 °C): δ (ppm) = 9.15 (s, 1H); 7.78 (s, 2H,); 5.16 (br s, 2H); 4.25 (t, 4H); 3.72 (t, 4H). Analytical data correspond to the literature.[51]

Preparation of Supported Ionic Liquids. *General Procedure for the Preparation of SILP Materials on the Example of SILP-5*. A round-bottomed flask was charged with SiO$_2$-60 (22.8 g) and 1-ethyl-3-methylimidazolium bromide **5** (2.3 g, 11.67 mol). The mixture was suspended in 100 mL of CH$_2$Cl$_2$ and shaken at room temperature for 60 min. The solvent was evaporated, and remaining solvent traces were removed by vacuum (0.01 mbar) for 24 h.

Preparation of Surface-Modified Silica SILC-1 and SILC-2. A round-bottomed flask was charged with SiO$_2$-60 (10.0 g), 1-(3-trimethoxysilylpropyl)-3-methylimidazolium chloride (4.7 g, 16.74), or 1-(3-trimethoxysilylpropyl)-3-methylimidazolium bromide (5.0 g, 15.37 mmol) and a mixture of anhydrous chloroform (50 mL) and 1,4-dioxane (50 mL). The suspension was refluxed for 48 h at 90 °C with magnetic stirring. The product was removed via filtration and subsequently washed with dichloromethane. The crude material was dried under reduced pressure, and the procedure was repeated for a second time to ensure complete coating of the surface. Remaining volatile traces were removed under vacuum (0.01 mbar) to obtain

supported ionic liquid catalyst **SILC-1** or **SILC-2** as a colorless powder.

Preparation of Surface-Modified Silica **SILC-3**. SiO$_2$-60 (14.4 g) and 3-chloropropyltrimethoxysilane (5 g, 23.90 mmol) were suspended in anhydrous toluene (100 mL) and stirred at 60 °C for 24 h. The product was collected via filtration and subsequently washed with dichloromethane. Remaining volatile traces were removed under reduced pressure, and the product was dried under high vacuum to obtain surface-modified silica as colorless powder.

The intermediate surface-modified silica was further suspended in anhydrous toluene (75 mL), and 1-(2-hydroxyethyl)imidazole (1.9 g, 16.43 mmol) was added. The suspension was stirred for 24 h at 90 °C. Modified silica was collected via filtration, repeatedly washed with dichloromethane, and remaining volatile traces were removed under reduced pressure. This procedure was repeated a second time to obtain supported ionic liquid catalyst **SILC-3** as a light yellow powder.

Preparation of Surface-Modified Silica **SILC-4**. Surface-modified silica **SILC-4** was prepared according to the preparation method of **SILC-3** using silica (12.0 g), 3-bromopropyltrimethoxysilane (5 g, 19.9 mmol), and 1-(2-hydroxyethyl)imidazole (2 × 1.63 g, 14.10 mmol). Supported ionic liquid catalyst **SILC-4** was obtained as a light yellow powder.

Ionic Liquid Catalyzed Synthesis of Propylene Carbonate from Propylene Oxide and CO$_2$. *General Procedure under Batch Conditions.* A 40 cm^3 stainless steel autoclave with magnetic stirring was charged with propylene oxide (1.0 eq; 34.4 mmol; 2.0 g) and 5 mol % [C$_2$mim]Br **5** (0.3 g, 1.7 mmol). The autoclave was tightly closed and filled with approximately 40 bar of carbon dioxide. The temperature was set to 45 °C and kept for 18 h. At room temperature, carbon dioxide was released, and the product was separated from the catalyst by flash chromatography with dichloromethane as solvent. Substrate and solvent were removed under reduced pressure to obtain pure propylene carbonate as a colorless liquid.

^{1}H NMR (400 MHz, CDCl$_3$, 25 °C): δ (ppm) = 4.84 (sx, 1H) 4.49 (t, 1H); 3.97 (t, 2H,); 1.43 (d, 3H).

General Procedure under Flow Conditions. An empty HPLC column cartridge (150 mm × 4.5 mm ID) was filled with SILP catalyst (10 w% [C$_2$mim]Br **5** on silica; 1.36 g) and connected to the scCO$_2$-device in a preheated oven (80 °C). A substrate solution of *n*-hexane and propylene oxide cooled in an external ice bath was used as the substrate supply. After the pressure reached 100 bar, the process was started by adding the substrate solution with a flow rate of 0.02 mL/min. The product was collected as a colorless liquid at different fractions. The collection time for each flask was set to 30 min for 2 h and to 60 min until the process ended after 420 min. The yield in each fraction was determined gravimetrically, and ^{1}H NMR spectroscopy and GC-MS were measured for every collected fraction to verify purity.

■ ASSOCIATED CONTENT

ⓢ Supporting Information

The Supporting Information is available free of charge on the ACS Publications website at DOI: 10.1021/acssusche-meng.8b02627.

> Detailed characterization of supported ionic liquid phases **SILP-5** with different loadings and **SILC-1−4** via FT-IR, BET, TGA and elemental analysis, NMR spectra of collected product, and additional graphs on catalytic performance (PDF)

■ AUTHOR INFORMATION

Corresponding Author

*Tel: +43 1 58801 163601. Fax: +43 1 58801 16360. E-mail: katharina.schroeder@tuwien.ac.at.

ORCID ⓘ

Katharina Bica: 0000-0002-2515-9873

Notes

The authors declare no competing financial interest.

■ REFERENCES

(1) Ausfelder, F.; Bazzanella, A. *Verwertung und Speicherung von CO$_2$: Diskusionspapier*; Dechema eV, 2008.

(2) Aresta, M. *Carbon Dioxide as Chemical Feedstock*; Wiley, 2010.

(3) Peters, M.; Köhler, B.; Kuckshinrichs, W.; Leitner, W.; Markewitz, P.; Müller, T. E. Chemical technologies for exploiting and recycling carbon dioxide into the value chain. *ChemSusChem* **2011**, *4*, 1216−1240.

(4) Kuckshinrichs, W.; Markewitz, P.; Linssen, J.; Zapp, P.; Peters, M.; Köhler, B.; Müller, T. E.; Leitner, W. *Weltweite Innovationen bei der Entwicklung von CCS-Technologien und Möglichkeiten der Nutzung und des Recyclings von CO$_2$*; Schriften des Forschungszentrums; Jülich Reihe Energie & Umwelt: Jülich, Germany, 2010.

(5) Sakakura, T.; Choi, J.-C.; Yasuda, H. Transformation of Carbon Dioxide. *Chem. Rev.* **2007**, *107*, 2365−2387.

(6) Liu, Q.; Wu, L.; Jackstell, R.; Beller, M. Using carbon dioxide as a building block in organic synthesis. *Nat. Commun.* **2015**, *6*, 5933−5948.

(7) Maeda, C.; Miyazaki, Y.; Ema, T. Recent progress in catalytic conversions of carbon dioxide. *Catal. Sci. Technol.* **2014**, *4*, 1482−1497.

(8) Tsuji, Y.; Fujihara, T. Carbon dioxide as a carbon source in organic transformation: carbon-carbon bond forming reactions by transition-metal catalysts. *Chem. Commun.* **2012**, *48*, 9956−9964.

(9) Ramdin, M.; de Loos, T. W.; Vlugt, T. J. H. State-of-the-Art of CO$_2$ Capture with Ionic Liquids. *Ind. Eng. Chem. Res.* **2012**, *51*, 8149−8177.

(10) Zeng, S.; Zhang, X.; Bai, L.; Zhang, X.; Wang, H.; Wang, J.; Bao, D.; Li, M.; Liu, X.; Zhang, S. Ionic-Liquid-Based CO$_2$ Capture Systems: Structure, Interaction and Process. *Chem. Rev.* **2017**, *117*, 9625−9673.

(11) Yang, Z.-Z.; Zhao, Y.-N.; He, L.-N. CO$_2$ chemistry: task-specific ionic liquids for CO$_2$ capture/activation and subsequent conversion. *RSC Adv.* **2011**, *1*, 545−567.

(12) Zhang, J.; Sun, J.; Zhang, X.; Zhao, Y.; Zhang, S. The recent development of CO$_2$ fixation and conversion by ionic liquid. *Greenhouse Gases: Sci. Technol.* **2011**, *1*, 142−159.

(13) Weilhard, A.; Qadir, M. H.; Sans, V.; Dupont, J. Selective CO$_2$ Hydrogenation to Formic Acid with Multifunctional Ionic Liquids. *ACS Catal.* **2018**, *8*, 1628−1634.

(14) Cokoja, M.; Wilhelm, M. E.; Anthofer, M. H.; Herrmann, W. A.; Kühn, F. E. Synthesis of Cyclic Carbonates from Epoxides and Carbon Dioxide by Using Organocatalyst. *ChemSusChem* **2015**, *8*, 2436−2454.

(15) Büttner, H.; Longwitz, L.; Steinbauer, J.; Wulf, C.; Werner, T. Recent Developments in the Synthesis of Cyclic Carbonates from Epoxides and CO$_2$. *Top. Curr. Chem.* **2017**, *375*, 50.

(16) North, M.; Pasquale, R. Mechanism of cyclic carbonate synthesis from epoxides and CO$_2$. *Angew. Chem., Int. Ed.* **2009**, *48*, 2946−2948.

(17) Kihara, N.; Hara, N.; Endo, T. Catalytic activity of various salts in the reaction of 2,3-epoxypropyl phenyl ether and carbon dioxide under atmospheric pressure. *J. Org. Chem.* **1993**, *58*, 6198−6202.

(18) Yasuda, H.; He, L.-N.; Takahashi, T.; Sakakura, T. Non-halogen catalysts for propylene carbonate synthesis from CO$_2$ under supercritical conditions. *Appl. Catal., A* **2006**, *298*, 177−180.

(19) Barbarini, A.; Maggi, R.; Mazzacani, A.; Mori, G.; Sartori, G.; Sartorio, R. Cycloaddition of CO$_2$ to epoxides over both homogeneous and silica-supported guanidine catalysts. *Tetrahedron Lett.* **2003**, *44*, 2931−2934.

(20) Ghazali-Esfahani, S.; Song, H.; Pâunescu, E.; Bobbink, F. D.; Liu, H.; Fei, Z.; Laurenczy, G.; Bagherzadeh, M.; Yan, N.; Dyson, P. J. Cycloaddition of CO_2 to epoxides catalyzed by imidazolium-based polymeric ionic liquids. *Green Chem.* **2013**, *15*, 1584−1589.

(21) Sun, J.; Zhang, S.; Cheng, W.; Ren, J. Hydroxyl-functionalized ionic liquid: a novel efficient catalyst for chemical fixation of CO_2 to cyclic carbonate. *Tetrahedron Lett.* **2008**, *49*, 3588−3591.

(22) Büttner, H.; Steinbauer, J.; Werner, T. Synthesis of Cyclic Carbonates from Epoxides and Carbon Dioxide by Using Bifunctional One-Component Phosphorus-Based Organocatalysts. *ChemSusChem* **2015**, *8*, 2655−2669.

(23) Wang, T.; Zheng, D.; Zhang, J.; Fan, B.; Ma, Y.; Ren, T.; Wang, L.; Zhang, J. Protic Pyrazolium Ionic Liquids: An Efficient Catalyst for Conversion of CO_2 in the Absence of Metal and Solvent. *ACS Sustainable Chem. Eng.* **2018**, *6*, 2574−2582.

(24) He, Q.; O'Brein, J. W.; Kitselman, K. A.; Tompkins, L. E.; Curtis, G. C.T.; Kerton, F. M. Synthesis of cyclic carbonates from CO_2 and epoxides using ionic liquids and related catalysts including choline chloride−metal halide mixtures. *Catal. Sci. Technol.* **2014**, *4*, 1513−1528.

(25) Xu, B.-H.; Wang, J.-Q.; Sun, J.; Huang, Y.; Zhang, J.-P.; Zhang, X.-P.; Zhang, S.-J. Fixation of CO_2 into cyclic carbonates catalyzed by ionic liquids: a multi-scale approach. *Green Chem.* **2015**, *17*, 108−122.

(26) Zhao, Y.; Yao, C.; Chen, G.; Yuan, Q. Highly efficient synthesis of cyclic carbonate with CO_2 catalyzed by ionic liquid in a microreactor. *Green Chem.* **2013**, *15*, 446−452.

(27) Wu, X.; Wang, M.; Xie, Y.; Chen, C.; Li, K.; Yuan, M.; Zhao, X.; Hou, Z. Carboxymethyl cellulose supported ionic liquid as a heterogeneous catalyst for the cycloaddition of CO_2 to cyclic carbonate. *Appl. Catal., A* **2016**, *519*, 146−154.

(28) van Doorslaer, C.; Wahlen, J.; Mertens, P.; Binnemans, K.; De Vos, D. Immobilization of molecular catalysts in supported ionic liquid phases. *Dalton Trans.* **2010**, *39*, 8377−8390.

(29) Fehrmann, R.; Riisager, A.; Haumann, M. *Supported Ionic Liquids: Fundamentals and Applications*, 1st ed.; Wiley-VCH Verlag, 2014.

(30) García-Verdugo, E.; Altava, B.; Burguete, M. I.; Lozano, P.; Luis, S. V. Ionic liquids and continuous flow processes: a good marriage to design sustainable processes. *Green Chem.* **2015**, *17*, 2693−2713.

(31) Riisager, A.; Wasserscheid, P.; van Hal, R.; Fehrmann, R. Continuous fixed-bed gas-phase hydroformylation using supported ionic liquid-phase (SILP) Rh catalysts. *J. Catal.* **2003**, *219*, 452−455.

(32) Riisager, A.; Eriksen, K. M.; Wasserscheid, P.; Fehrmann, R. Propene and 1-Octene Hydroformylation with Silica-Supported, Ionic Liquid-Phase (SILP) Rh-Phosphine Catalysts in Continuous Fixed-Bed Mode. *Catal. Lett.* **2003**, *90*, 149−153.

(33) Haumann, M.; Dentler, K.; Joni, J.; Riisager, A.; Wasserscheid, P. Continuous Gas-Phase Hydroformylation of 1-Butene using Supported Ionic liquid Phase (SILP) Catalysts. *Adv. Synth. Catal.* **2007**, *349*, 425−431.

(34) Haumann, M.; Jakuttis, M.; Franke, R.; Schönweiz, A.; Wasserscheid, P. Continuous Gas-Phase Hydroformilation of a Highly Diluted Technical C4 Feed using Supported Ionic Liquid Phase Catalysts. *ChemCatChem* **2011**, *3*, 1822−1827.

(35) Weiß, A.; Munoz, M.; Haas, A.; Rietzler, F.; Steinrück, H.-P.; Haumann, M.; Wasserscheid, P.; Etzold, B. J. M. Boosting the Activity in Supported Ionic Liquid-Phase-Catalyzed Hydroformylation via Surface Functionalization of the Carbon Support. *ACS Catal.* **2016**, *6*, 2280−2286.

(36) Becker, M.; Nicole, B.; Christiansen, A.; Robert, F.; Fridag, D.; Haumann, M.; Jakuttis, M.; Schönweiz, A.; Peter, P. W.; Werner, S. Use of supported ionic liquid phase (silp) catalyst systems in the hydroformylation of olefin-containing mixtures to aldehyde mixtures with a high content of aldehydes unbranched in the 2 position. US 20130289313, 2012.

(37) Gelesky, M. A.; Chiaro, S. S. X.; Pavan, F. A.; dos Santos, J. H. Z.; Dupont, J. Supported ionic liquid phase rhodium nanoparticle hydrogenation catalysts. *Dalton Trans.* **2007**, 5549−5553.

(38) Ruta, M.; Yuranov, I.; Dyson, P. J.; Laurenczy, G.; KiwiMinsker, L. Structured fibre supports for ionic liquid-phase catalysis used in gas-phase continuous hydrogenation. *J. Catal.* **2007**, *247*, 269−276.

(39) Brünig, J.; Csendes, Z.; Weber, S.; Gorgas, N.; Bittner, R. W.; Limbeck, A.; Bica, K.; Hoffmann, H.; Kirchner, K. Chemoselective Supported Ionic-Liquid-Phase (SILP) Aldehyde Hydrogenation Catalyzed by an Fe(II) PNP Pincer Complex. *ACS Catal.* **2018**, *8*, 1048−1051.

(40) Hintermair, U.; Höfener, T.; Pullmann, T.; Franciò, G.; Leitner, W. Continuous Enantioselective Hydrogenation with a Molecular Catalyst in Supported Ionic Liquid Phase under Supercritical CO_2 Flow. *ChemCatChem* **2010**, *2*, 150−154.

(41) Hintermair, U.; Gong, Z.; Serbanovic, A.; Muldoon, M. J.; Santini, C. C.; Cole-Hamilton, D. J. Continuous flow hydroformylation using supported ionic liquid phase catalysts with carbon dioxide as a carrier. *Dalton Trans.* **2010**, *39*, 8501−8510.

(42) Blanchard, L. A.; Hancu, D.; Beckman, E. J.; Brennecke, J. F. Green processing using ionic liquids and CO_2. *Nature* **1999**, *399*, 28−29.

(43) Jutz, F.; Andanson, J.-M.; Baiker, A. Ionic Liquids and Dense Carbon Dioxide: A beneficial Biphasic System for Catalysis. *Chem. Rev.* **2011**, *111*, 322−353.

(44) Bica, K.; Rodriguez, H.; Gurau, G.; Cojocaru, O. A.; Riisager, A.; Fehrmann, R.; Rogers, R. D. Pharmaceutically active ionic liquids with solids handling, enhanced thermal stability, and fast release. *Chem. Commun.* **2012**, *48*, 5422−5424.

(45) Mehnert, C. P.; Cook, R. A.; Dispenziere, N. C.; Afeworki, M. Supported Ionic Liquid Catalysis − A new concept for Homogeneous Hydroformylation Catalysis. *J. Am. Chem. Soc.* **2002**, *124*, 12932−12933.

(46) Cheng, W.; Su, Q.; Wang, J.; Sun, J.; Ng, F. T. Ionic Liquids: The Synergistic Catalytic Effect in the Synthesis of Cyclic Carbonates. *Catalysts* **2013**, *3*, 878−901.

(47) Sun, J.; Ren, J.; Zhang, S.; Cheng, W. Water as an efficient medium for the synthesis of cyclic carbonate. *Tetrahedron Lett.* **2009**, *50*, 423−426.

(48) Wang, J.-Q.; Yue, X.-D.; Cai, F.; He, L.-N. Solventless synthesis of cyclic carbonates from carbon dioxide and epoxides catalyzed by silica-supported ionic liquids under supercritical conditions. *Catal. Commun.* **2007**, *8*, 167−172.

(49) Takahashi, T.; Watahiki, T.; Kitazume, S.; Yasuda, H.; Sakakura, T. Synergistic hybrid catalyst for cyclic carbonate synthesis: Remarkable acceleration caused by immobilization of homogeneous catalyst on silica. *Chem. Commun.* **2006**, 1664−1666.

(50) Bresien, J.; Ellinger, S.; Harloff, J.; Schulz, A.; Sievert, K.; Stoffers, A.; Taschler, C.; Villinger, A.; Zur Täschler, C. Tetracyanido-(difluorido)phosphates $M^+[PF_2(CN)_4]^−$. *Angew. Chem., Int. Ed.* **2015**, *54*, 4474−4477.

(51) Deng, F.; Reeder, Z. K.; Miller, K. M. 1,3-Bis(2′-hydroxyethyl)-imidazolium ionic liquids: correlating structure and properties with anion hydrogen bonding ability. *J. Phys. Org. Chem.* **2014**, *27*, 2−9.

6. Conclusion

In the first part of thesis, the behavior of certain secondary metabolites in haskap berries *(Lonicera Caerulea* L.) was investigated utilizing $scCO_2$ and ethanol as modifier. A novel dynamic streamlined extraction with the initial extraction of lipids and simultaneous extraction of iridoids (i.e., loganin and loganic acid) and anthocyanins (i.e., cyanidin, peonidin and pelargonidin) was developed using $scCO_2$ at different EtOH concentrations (Figure 50). Fatty acids were extracted from haskap berries using SFE for the first-time at 1 vol % ethanol. By increasing the co-solvent concentration from 1 vol % to 10 vol % ethanol, an initial partial separation of the aforementioned iridoids was achieved. A further increase of the ethanol concentration from 10 vol % to 50 vol %, led to the concomitant extraction of the anthocyanins. Overall, not only is this novel technique a notable contribution in terms of fractionation of important compounds from haskap berries, but also one that generates extraction yields comparable to conventional extraction techniques. This promising and eco-friendly concept provides a platform for the extraction of a wide array of source materials and high value-added natural product classes.
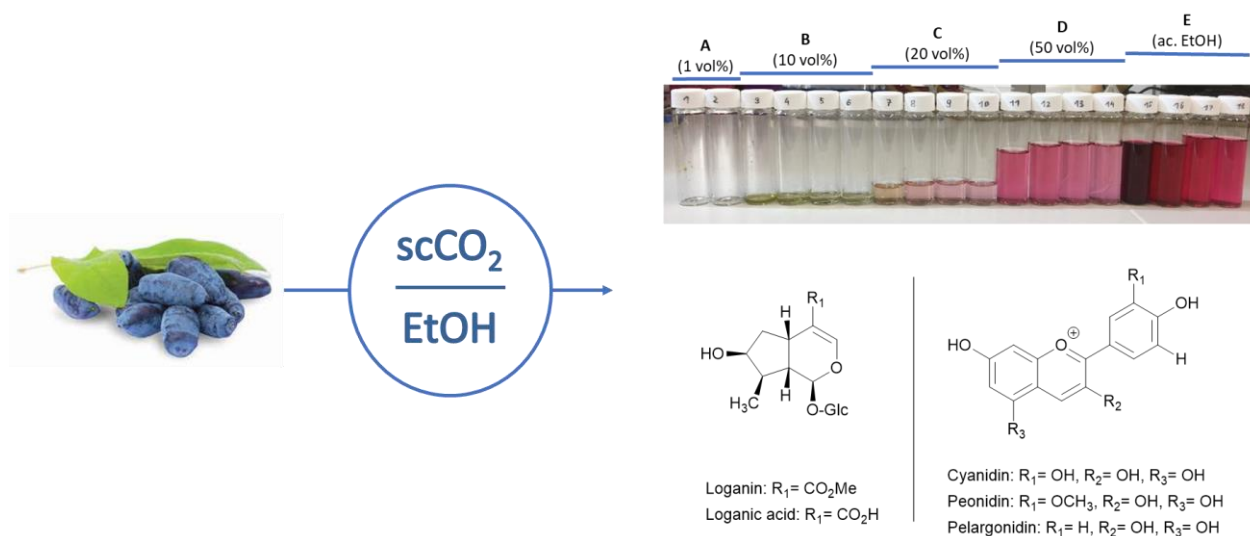
Figure 50. Dynamic streamlined extraction of secondary metabolites in haskap berries**.**

In the second part of the thesis, two different technologies, namely IL-based extraction and supercritical-fluid extraction, were combined to extract cannabinoids from hemp (*Cannabis Sativa* L.). A novel IL-based/scCO$_2$ extraction process was developed with the purpose of isolating six cannabinoids from hemp. Three steps were designed, investigated and optimized, to be more precise 1) IL-assisted pre-treatment, 2) extract dilution with water and 3) supercritical fluid extraction process. Firstly, the optimum conditions for the dissolution of hemp plant matter with [C$_2$mim][OAc] were determined as 15 min and 70 °C. Secondly, a 1:3 dilution of IL with H$_2$O was the optimum ratio for the extraction of cannabinoids and for the reduction of the mixture´s viscosity that would improve the mass transfer. Lastly, the most appropriate SFE parameters were determined to be 20 MPa and 70 °C for 2 h extraction time. This technique achieves high cannabinoid extraction efficiency and is able to compete with both sophisticated and traditional techniques (Figure 51). Additionally, this process is considered to be more sustainable, because the employed ILs can be recycled without utilizing organic solvents. It can be applied for a wide range of different source materials and high value-added natural product classes and, ultimately, is a promising approach for future industrial applications.
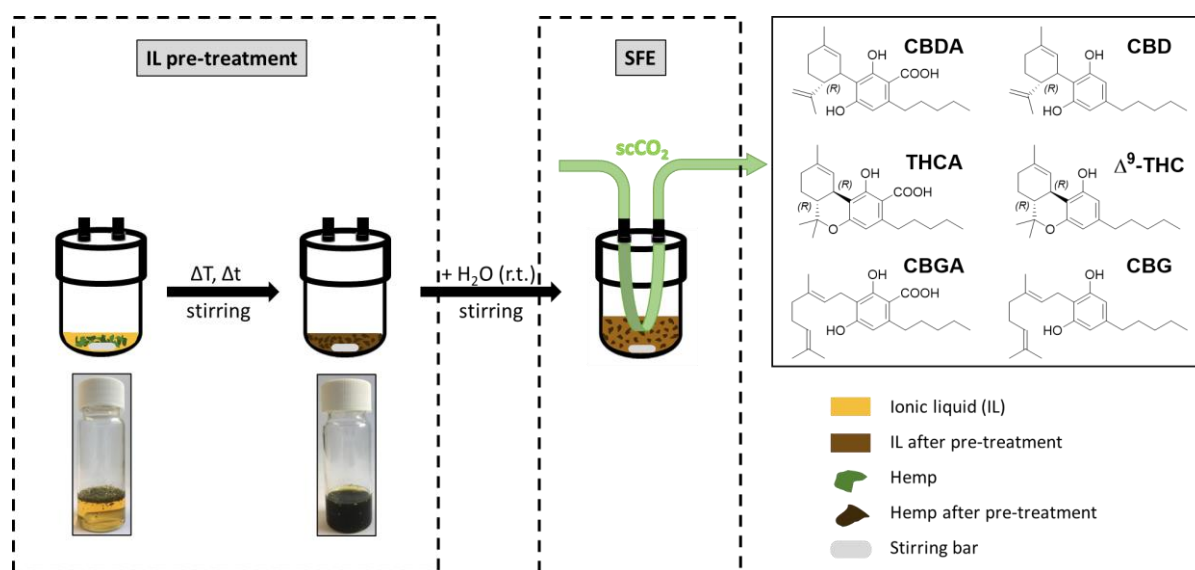
Figure 51. Ionic liquid-based dynamic scCO$_2$ extraction of cannabinoids from hemp**.**

In the third part of the thesis, the continuous production of PC was investigated, starting from PO and using supported ILs as single catalyst.

The continuous production of PC was achieved by employing $scCO_2$ as solvent and reagent, PO and supported ILs on mesoporous silica as heterogeneous catalyst. Initially, the reaction was investigated in batch mode and in a homogeneous fashion. Between the different IL cation moieties, phosphonium-based ILs containing hydroxyl groups as substituent and the anion with highest nucleophilicity, achieved the highest reactivity. Subsequently, supported ILs on mesoporous silica (SILP - physisorption) and supported IL catalyst with a covalently bound layer of IL (SILC - chemisorption) was investigated in continuous flow. Overall, SILPs exhibited higher catalytic activity than SILCs (supported ionic liquid catalysts); moreover, among the SILPs, the non-functionalized [C_2mim]Br on mesoporous silica exhibited the highest catalytic activity due to the presence of surface hydroxyl groups on silica, which induced a co-catalytic effect. Even though SILCs achieved lower yields, in the long run they demonstrated the optimum middle ground between catalytic activity and long-term stability (Scheme 39).

Yield: 38%
TON: 46
TOF: 0,95 h^{-1}
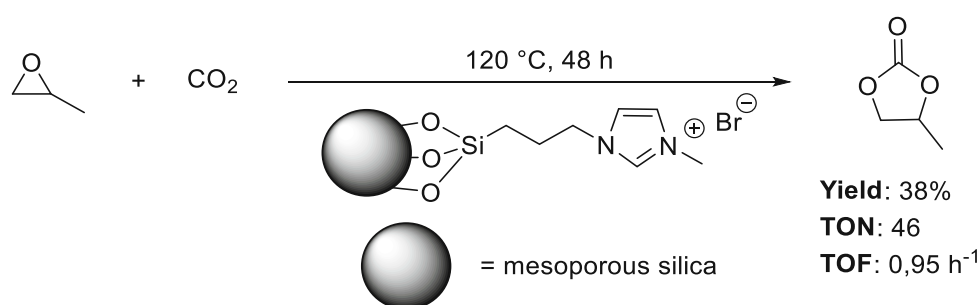
Scheme 39. Formation of propylene carbonates (PCs) from PO and CO_2 catalyzed by SILCs.

7. References

[1]   J. H. Clark, S. J. Tavener, Alternative solvents: shades of green, *Org. Process Res. Dev.* **2007**, *11*, 149-155.

[2]   J. A. Branch, P. N. Bartlett, Electrochemistry in supercritical fluids, *Philos. Trans. R. Soc. A* **2015**, *373*, 20150007.

[3]   A. P. Sánchez-Camargo, J. A. Mendiola, E. Ibáñez, M. Herrero, Supercritical Fluid Extraction, in *Reference module in chemistry, molecular sciences and chemical engineering*, Elsevier, **2014**.

[4]   A. Kate, A. Singh, N. Shahi, J. Pandey, O. Prakash, T. Singh, Novel eco-friendly techniques for extraction of food based lipophilic compounds from biological materials, *Nat. Prod. Chem. Res.* **2016**, *4*, 231.

[5]   M. Kulazynski, M. Stolarski, H. Faltynowicz, B. Narowska, L. Swiatek, M. Lukaszewicz, Supercritical fluid extraction of vegetable materials, *Chem. Chem. Technol.* **2016**, 637-644.

[6]   K. Zosel, Separation with supercritical gases: practical applications, *Angew. Chem. Int. Ed. Engl.* **1978**, *17*, 702-709.

[7]   M. Raventós, S. Duarte, R. Alarcón, Application and possibilities of supercritical CO_2 extraction in food processing industry: an overview, *Food Sci. Technol. Int.* **2002**, *8*, 269-284.

[8]   G. Sapkale, S. Patil, U. Surwase, P. Bhatbhage, Supercritical fluid extraction, *Int. J. Chem. Sci* **2010**, *8*, 729-743.

[9]   K. M. Schlosky, Supercritical phase transitions at very high pressure, *J. Chem. Educ.* **1989**, *66*, 989.

[10]   A. El-Banbi, A. Alzahabi, A. El-Maraghi, Chapter 3 - Dry gases, in *PVT property correlations* (Eds.: A. El-Banbi, A. Alzahabi, A. El-Maraghi), Gulf Professional Publishing, **2018**, pp. 29-63.

[11]   R. C. Reid, J. M. Prausnitz, B. E. Poling, The properties of gases and liquids, **1987**.

[12]   J. L. Hedrick, L. J. Mulcahey, L. T. Taylor, Supercritical fluid extraction, *Microchim. Acta* **1992**, *108*, 115-132.

[13]   B. Finney, M. Jacobs, Carbon dioxide pressure-temperature phase diagram, https://en.wikipedia.org/wiki/Supercritical_carbon_dioxide#/media/File:Carbon_dioxide_pressure-temperature_phase_diagram.svg, (accessed 11 July 2022).

[14]   Clean-Technology-Group-(The-University-of-Nottingham), Introduction to supercritical fluids, https://www.nottingham.ac.uk/supercritical/beta/introduction.html, (accessed 11 July 2022).

[15]   E. Ramsey, Q. Sun, Z. Zhang, C. Zhang, W. Gou, Mini-Review: Green sustainable processes using supercritical fluid carbon dioxide, *J. Environ. Sci.* **2009**, *21*, 720-726.

[16]   A. Baiker, Supercritical fluids in heterogeneous catalysis, *Chem. Rev.* **1999**, *99*, 453-474.

[17]   T. Greibrokk, Applications of supercritical fluid extraction in multidimensional systems, *J. Chromatogr. A* **1995**, *703*, 523-536.

[18]   M. Herrero, J. A. Mendiola, A. Cifuentes, E. Ibáñez, Supercritical fluid extraction: Recent advances and applications, *J. Chromatogr. A* **2010**, *1217*, 2495-2511.

[19]   R. P. F. F. da Silva, T. A. P. Rocha-Santos, A. C. Duarte, Supercritical fluid extraction of bioactive compounds, *TrAC, Trends Anal. Chem.* **2016**, *76*, 40-51.

[20]   E. Reverchon, I. De Marco, Supercritical fluid extraction and fractionation of natural matter, *J. Supercrit. Fluids.* **2006**, *38*, 146-166.

[21]   J. Peach, J. Eastoe, Supercritical carbon dioxide: a solvent like no other, *Beilstein J. Org. Chem.* **2014**, *10*, 1878-1895.

[22]   T. Ahmad, F. Masoodi, A. Rather, S. Wani, A. Gull, Supercritical Fluid Extraction: A review, *J. Biol. Chem. Chron* **2019**, *5*, 114-122.

[23]   B. Metz, O. Davidson, H. De Coninck, *Carbon dioxide capture and storage: special report of the intergovernmental panel on climate change*, Cambridge University Press, **2005**.

[24]   G. Brunner, *Gas extraction - An introduction to fundamentals of supercritical fluids and the application to separation processes, Vol. 4*, Springer-Verlag Berlin Heidelberg GmbH, Damrstadt : Steinkopff ; New York, **1994**.

[25]   P. G. Jessop, T. Ikariya, R. Noyori, Homogeneous catalysis in supercritical fluids, *Chem. Rev.* **1999**, *99*, 475-494.

[26]   K.-Y. Khaw, M.-O. Parat, P. N. Shaw, J. R. Falconer, Solvent supercritical fluid technologies to extract bioactive compounds from natural sources: A review, *Molecules* **2017**, *22*, 1186.

[27]   L. Wang, C. L. Weller, Recent advances in extraction of nutraceuticals from plants, *Trends Food Sci. Technol.* **2006**, *17*, 300-312.

[28]   E. Uquiche, C. Campos, C. Marillán, Assessment of the bioactive capacity of extracts from Leptocarpha rivularis stalks using ethanol-modified supercritical CO_2, *J. Supercrit. Fluids.* **2019**, *147*, 1-8.

[29]   T. Sato, Y. Ikeya, S.-i. Adachi, K. Yagasaki, K.-i. Nihei, N. Itoh, Extraction of strawberry leaves with supercritical carbon dioxide and entrainers: Antioxidant capacity, total phenolic content, and inhibitory effect on uric acid production of the extract, *Food Bioprod. Process.* **2019**, *117*, 160-169.

[30]   M. C. Bubalo, S. Vidović, I. R. Redovniković, S. Jokić, New perspective in extraction of plant biologically active compounds by green solvents, *Food Bioprod. Process.* **2018**, *109*, 52-73.

[31]   F. A. Espinosa-Pardo, V. M. Nakajima, G. A. Macedo, J. A. Macedo, J. Martínez, Extraction of phenolic compounds from dry and fermented orange pomace using supercritical CO_2 and co-solvents, *Food Bioprod. Process.* **2017**, *101*, 1-10.

[32]   S. M. Pourmortazavi, S. S. Hajimirsadeghi, Supercritical fluid extraction in plant essential and volatile oil analysis, *J. Chromatogr. A* **2007**, *1163*, 2-24.

[33]   A. Natolino, C. Da Porto, Supercritical carbon dioxide extraction of pomegranate (*Punica granatum* L.) seed oil: Kinetic modelling and solubility evaluation, *J. Supercrit. Fluids.* **2019**, *151*, 30-39.

[34]   O. Wrona, K. Rafińska, C. Możeński, B. Buszewski, Supercritical fluid extraction of bioactive compounds from plant materials, *J. AOAC Int.* **2017**, *100*, 1624-1635.

[35]   C. G. Pereira, M. A. A. Meireles, Supercritical fluid extraction of bioactive compounds: fundamentals, applications and economic perspectives, *Food Bioproc. Tech.* **2010**, *3*, 340-372.

[36]   J. J. Schuster, L. A. Bahr, L. Fehr, M. Tippelt, J. Schulmeyr, A. Wuzik, A. S. Braeuer, Online monitoring of the supercritical CO_2 extraction of hop, *J. Supercrit. Fluids.* **2018**, *133*, 139-145.

[37]   A. A. Clifford, J. R. Williams, Introduction to supercritical fluids and their application, *Supercritical Fluids Methods and Protocols* **2000**, 1-16.

[38]   D. T. Santos, M. A. d. A. Meireles, Developing novel one-step processes for obtaining food-grade O/W emulsions from pressurized fluid extracts: processes description, state of the art and perspectives, *Food Sci. Technol.* **2015**, *35*, 579-587.

[39]   S. Machmudah, K. Kitada, M. Sasaki, M. Goto, J. Munemasa, M. Yamagata, Simultaneous extraction and separation process for coffee beans with supercritical CO_2 and water, *Ind. Eng. Chem. Res.* **2011**, *50*, 2227-2235.

[40]   J. Azmir, I. S. M. Zaidul, M. Rahman, K. Sharif, A. Mohamed, F. Sahena, M. Jahurul, K. Ghafoor, N. Norulaini, A. Omar, Techniques for extraction of bioactive compounds from plant materials: A review, *J. Food Eng.* **2013**, *117*, 426-436.

[41]   S. A. Moreira, E. M. Alexandre, M. Pintado, J. A. Saraiva, Effect of emergent non-thermal extraction technologies on bioactive individual compounds profile from different plant materials, *Food Res. Int.* **2019**, *115*, 177-190.

[42]   P. A. Uwineza, A. Waśkiewicz, Recent advances in supercritical fluid extraction of natural bioactive compounds from natural plant materials, *Molecules* **2020**, *25*, 3847.

[43]   B. Díaz-Reinoso, A. Moure, H. Domínguez, J. C. Parajó, Supercritical CO_2 extraction and purification of compounds with antioxidant activity, *J. Agric. Food Chem.* **2006**, *54*, 2441-2469.

[44]   M. Zaynab, M. Fatima, S. Abbas, Y. Sharif, M. Umair, M. H. Zafar, K. Bahadar, Role of secondary metabolites in plant defense against pathogens, *Microb. Pathog.* **2018**, *124*, 198-202.

[45]   M. De Melo, A. Silvestre, C. Silva, Supercritical fluid extraction of vegetable matrices: Applications, trends and future perspectives of a convincing green technology, *J. Supercrit. Fluids.* **2014**, *92*, 115-176.

[46]   N. V. Petrović, S. S. Petrović, A. M. Džamić, A. D. Ćirić, M. S. Ristić, S. L. Milovanović, S. D. Petrović, Chemical composition, antioxidant and antimicrobial activity of Thymus praecox supercritical extracts, *J. Supercrit. Fluids.* **2016**, *110*, 117-125.

[47]   E. Arranz, L. Jaime, M. L. de la Hazas, G. Vicente, G. Reglero, S. Santoyo, Supercritical sage extracts as anti-inflammatory food ingredients, *Ind. Crops Prod.* **2014**, *54*, 159-166.

[48]   E. Rój, V. M. Tadić, D. Mišić, I. Žižović, I. Arsić, A. Dobrzyńska-Inger, D. Kostrzewa, Supercritical carbon dioxide hops extracts with antimicrobial properties, *Open Chem. J.* **2015**, *13*, 1157-1171.

[49]   L. Baldino, E. Reverchon, G. Della Porta, An optimized process for SC-CO$_2$ extraction of antimalarial compounds from *Artemisia annua* L, *J. Supercrit. Fluids.* **2017**, *128*, 89-93.

[50]   H.-H. Chung, Y.-C. Sung, L.-F. Shyur, Deciphering the biosynthetic pathways of bioactive compounds *in planta* using omics approaches, in *Medicinal Plants-Recent Advances in Research and Development*, Springer, **2016**, pp. 129-165.

[51]   S. Sasidharan, Y. Chen, D. Saravanan, K. Sundram, L. Y. Latha, Extraction, isolation and characterization of bioactive compounds from plants' extracts, *Afr. J. Tradit. Complement. Altern. Med.* **2011**, *8*, 1-10.

[52]   O. Pino, Y. Sánchez, M. M. Rojas, Plant secondary metabolites as an alternative in pest management. I: Background, research approaches and trends, *Rev. Protección Veg.* **2013**, *28*, 81-94.

[53]   E. Christaki, E. Bonos, I. Giannenas, P. Florou-Paneri, Aromatic plants as a source of bioactive compounds, *Agriculture* **2012**, *2*, 228-243.

[54]   P. J. Facchini, Alkaloid biosynthesis in plants: biochemistry, cell biology, molecular regulation, and metabolic engineering applications, *Annu. Rev. Plant Biol.* **2001**, *52*, 29-66.

[55]   P. Nawrot, S. Jordan, J. Eastwood, J. Rotstein, A. Hugenholtz, M. Feeley, Effects of caffeine on human health, *Food Addit. Contam.* **2003**, *20*, 1-30.

[56]   H. S. Park, H.-K. Choi, S. J. Lee, K. W. Park, S.-G. Choi, K. H. Kim, Effect of mass transfer on the removal of caffeine from green tea by supercritical carbon dioxide, *J. Supercrit. Fluids.* **2007**, *42*, 205-211.

[57]   V. Carrara, V. Garcia, V. Faiões, E. Cunha-Júnior, E. Torres-Santos, D. Cortez, Supercritical fluid extraction of pyrrolidine alkaloid from leaves of Piper amalago L, *Evid.-Based Complementary Altern. Med.* **2017**, *2017*.

[58]   E. Ellington, J. Bastida, F. Viladomat, C. Codina, Supercritical carbon dioxide extraction of colchicine and related alkaloids from seeds of *Colchicum autumnale* L, *Phytochem. Anal.* **2003**, *14*, 164-169.

[59]   M. A. Falcão, R. Scopel, R. N. Almeida, A. T. do Espirito Santo, G. Franceschini, J. J. Garcez, R. M. Vargas, E. Cassel, Supercritical fluid extraction of vinblastine from *Catharanthus roseus*, *J. Supercrit. Fluids.* **2017**, *129*, 9-15.

[60]   R. G. Berger, *Flavours and fragrances: chemistry, bioprocessing and sustainability*, Springer Science & Business Media, Berlin, Heidelberg, **2007**.

[61]   M. de Andrade Lima, I. Kestekoglou, D. Charalampopoulos, A. Chatzifragkou, Supercritical fluid extraction of carotenoids from vegetable waste matrices, *Molecules* **2019**, *24*, 466.

[62]   M. Durante, M. S. Lenucci, G. Mita, Supercritical carbon dioxide extraction of carotenoids from pumpkin (*Cucurbita* spp.): A review, *Int. J. Mol. Sci.* **2014**, *15*, 6725-6740.

[63]   M. de Andrade Lima, D. Charalampopoulos, A. Chatzifragkou, Optimisation and modelling of supercritical CO$_2$ extraction process of carotenoids from carrot peels, *J. Supercrit. Fluids.* **2018**, *133*, 94-102.

[64]   A. del Pilar Sanchez-Camargo, L.-F. Gutierrez, S. M. Vargas, H. A. Martinez-Correa, F. Parada-Alfonso, C.-E. Narvaez-Cuenca, Valorisation of mango peel: Proximate composition, supercritical fluid extraction of carotenoids, and application as an antioxidant additive for an edible oil, *J. Supercrit. Fluids.* **2019**, *152*, 104574.

[65] L. A. Conde-Hernández, J. R. Espinosa-Victoria, J. Á. Guerrero-Beltrán, Supercritical extraction of essential oils of *Piper auritum* and *Porophyllum ruderale*, *J. Supercrit. Fluids.* **2017**, *127*, 97-102.

[66] T. Fornari, G. Vicente, E. Vázquez, M. R. García-Risco, G. Reglero, Isolation of essential oil from different plants and herbs by supercritical fluid extraction, *J. Chromatogr. A* **2012**, *1250*, 34-48.

[67] R. G. Bitencourt, N. J. Ferreira, A. L. Oliveira, F. A. Cabral, A. J. Meirelles, High pressure phase equilibrium of the crude green coffee oil–CO_2–ethanol system and the oil bioactive compounds, *J. Supercrit. Fluids.* **2018**, *133*, 49-57.

[68] F. Montañés, O. J. Catchpole, S. Tallon, K. A. Mitchell, D. Scott, R. F. Webby, Extraction of apple seed oil by supercritical carbon dioxide at pressures up to 1300 bar, *J. Supercrit. Fluids.* **2018**, *141*, 128-136.

[69] M. Shahsavarpour, M. Lashkarbolooki, M. J. Eftekhari, F. Esmaeilzadeh, Extraction of essential oils from Mentha spicata L.(Labiatae) via optimized supercritical carbon dioxide process, *J. Supercrit. Fluids.* **2017**, *130*, 253-260.

[70] L. A. Conde-Hernández, J. R. Espinosa-Victoria, A. Trejo, J. Á. Guerrero-Beltrán, CO_2-supercritical extraction, hydrodistillation and steam distillation of essential oil of rosemary (*Rosmarinus officinalis*), *J. Food Eng.* **2017**, *200*, 81-86.

[71] V. Lattanzio, P. A. Kroon, S. Quideau, D. Treutter, Plant phenolics—secondary metabolites with diverse functions, in *Recent advances in polyphenol research, Vol. 1*, Wiley, New York, NY, USA, **2008**, pp. 1-35.

[72] M. Liza, R. A. Rahman, B. Mandana, S. Jinap, A. Rahmat, I. Zaidul, A. Hamid, Supercritical carbon dioxide extraction of bioactive flavonoid from *Strobilanthes crispus* (Pecah Kaca), *Food Bioprod. Process.* **2010**, *88*, 319-326.

[73] K. E. Heim, A. R. Tagliaferro, D. J. Bobilya, Flavonoid antioxidants: chemistry, metabolism and structure-activity relationships, *J. Nutr. Biochem.* **2002**, *13*, 572-584.

[74] S. Akay, I. Alpak, O. Yesil-Celiktas, Effects of process parameters on supercritical CO_2 extraction of total phenols from strawberry (*Arbutus unedo* L.) fruits: An optimization study, *J. Sep. Sci.* **2011**, *34*, 1925-1931.

[75] R. Vardanega, G. C. Nogueira, C. D. Nascimento, A. F. Faria-Machado, M. A. A. Meireles, Selective extraction of bioactive compounds from annatto seeds by sequential supercritical CO_2 process, *J. Supercrit. Fluids.* **2019**, *150*, 122-127.

[76] O. Benito-Román, M. Rodríguez-Perrino, M. T. Sanz, R. Melgosa, S. Beltrán, Supercritical carbon dioxide extraction of quinoa oil: Study of the influence of process parameters on the extraction yield and oil quality, *J. Supercrit. Fluids.* **2018**, *139*, 62-71.

[77] E. Boselli, M. F. Caboni, Supercritical carbon dioxide extraction of phospholipids from dried egg yolk without organic modifier, *J. Supercrit. Fluids.* **2000**, *19*, 45-50.

[78] N. Vedaraman, C. Srinivasakannan, G. Brunner, B. Ramabrahmam, P. Rao, Experimental and modeling studies on extraction of cholesterol from cow brain using supercritical carbon dioxide, *J. Supercrit. Fluids.* **2005**, *34*, 27-34.

[79] L. Fiori, M. Manfrini, D. Castello, Supercritical CO_2 fractionation of omega-3 lipids from fish by-products: Plant and process design, modeling, economic feasibility, *Food Bioprod. Process.* **2014**, *92*, 120-132.

[80] A. Erkucuk, I. Akgun, O. Yesil-Celiktas, Supercritical CO_2 extraction of glycosides from *Stevia* rebaudiana leaves: Identification and optimization, *J. Supercrit. Fluids.* **2009**, *51*, 29-35.

[81] M. Varaee, M. Honarvar, M. H. Eikani, M. R. Omidkhah, N. Moraki, Supercritical fluid extraction of free amino acids from sugar beet and sugar cane molasses, *J. Supercrit. Fluids.* **2019**, *144*, 48-55.

[82] G. Brandão, G. Rigo, A. Roque, A. Souza, M. Scopel, C. Nascimento, T. Tasca, C. Pereira, R. Giordani, Extraction of bioactive alkaloids from *Melocactus zehntneri* using supercritical fluid, *J. Supercrit. Fluids.* **2017**, *129*, 28-35.

[83]   T.-J. Yang, F.-J. Tsai, C.-Y. Chen, T. C.-C. Yang, M.-R. Lee, Determination of additives in cosmetics by supercritical fluid extraction on-line headspace solid-phase microextraction combined with gas chromatography–mass spectrometry, *Anal. Chim. Acta.* **2010**, *668*, 188-194.

[84]   O. Vogt, E. Sikora, J. Ogonowski, The effect of selected supercritical CO_2 plant extract addition on user properties of shower gels, *Pol. J. Chem. Technol.* **2014**, *16*, 51-54.

[85]   F. Van Assche, H. Clijsters, Effects of metals on enzyme activity in plants, *Plant Cell Environ.* **1990**, *13*, 195-206.

[86]   W. W. Ngah, M. M. Hanafiah, Removal of heavy metal ions from wastewater by chemically modified plant wastes as adsorbents: a review, *Bioresour. Technol.* **2008**, *99*, 3935-3948.

[87]   T. D. Luckey, B. Venugopal, *Metal toxicity in mammals, Vol. 1*, 1st ed., Plenum Press: New York and London, **1977**.

[88]   S. Lee, B. Peirano, *Biochemical effects of environmental pollutants*, Ann Arbor, Mich., Ann Arbor Science Publishers, Inc., **1977**.

[89]   P. Rivaro, A. Çullaj, R. Frache, C. Lagomarsino, S. Massolo, M. C. De Mattia, N. Ungaro, Heavy metals distribution in suspended particulate matter and sediment collected from Vlora Bay (Albania): a methodological approach for metal pollution evaluation, *J. Coast. Res.* **2011**, 54-66.

[90]   H. Harmens, I. Ilyin, G. Mills, J. Aboal, R. Alber, O. Blum, M. Coşkun, L. De Temmerman, J. Fernandez, R. Figueira, Country-specific correlations across Europe between modelled atmospheric cadmium and lead deposition and concentrations in mosses, *Environ. Pollut.* **2012**, *166*, 1-9.

[91]   M. Muchuweti, J. Birkett, E. Chinyanga, R. Zvauya, M. D. Scrimshaw, J. Lester, Heavy metal content of vegetables irrigated with mixtures of wastewater and sewage sludge in Zimbabwe: implications for human health, *Agric. Ecosyst. Environ.* **2006**, *112*, 41-48.

[92]   S. A. Amuno, Potential ecological risk of heavy metal distribution in cemetery soils, *Water Air Soil Pollut.* **2013**, *224*, 1435.

[93]   T. A. Hughes, N. Gray, O. S. Guillamón, Removal of metals and acidity from acid mine drainage using liquid and dried digested sewage sludge and cattle slurry, *Mine Water Environ.* **2013**, *32*, 108-120.

[94]   C. Blöcher, J. Dorda, V. Mavrov, H. Chmiel, N. Lazaridis, K. Matis, Hybrid flotation—membrane filtration process for the removal of heavy metal ions from wastewater, *Water Res.* **2003**, *37*, 4018-4026.

[95]   M. M. A. Khan, PVC based polyvinyl alcohol zinc oxide composite membrane: Synthesis and electrochemical characterization for heavy metal ions, *J Ind. Eng. Chem.* **2013**, *19*, 1365-1370.

[96]   R. A. Shawabkeh, D. A. Rockstraw, R. K. Bhada, Copper and strontium adsorption by a novel carbon material manufactured from pecan shells, *Carbon* **2002**, *40*, 781-786.

[97]   K. Gopal, S. S. Tripathy, J. L. Bersillon, S. P. Dubey, Chlorination byproducts, their toxicodynamics and removal from drinking water, *J. Hazard. Mater.* **2007**, *140*, 1-6.

[98]   M. Kowalczyk, Z. Hubicki, D. Kołodyńska, Removal of heavy metal ions in the presence of the biodegradable complexing agent of EDDS from waters, *Chem. Eng. J.* **2013**, *221*, 512-521.

[99]   J.-J. Yu, Removal of organophosphate pesticides from wastewater by supercritical carbon dioxide extraction, *Water Res.* **2002**, *36*, 1095-1101.

[100]   I. Fernández, J. Dachs, J. M. Bayona, Application of experimental design approach to the optimization of supercritical fluid extraction of polychlorinated biphenyls and polycyclic aromatic hydrocarbons, *J. Chromatogr. A* **1996**, *719*, 77-85.

[101]   I. J. Barnabas, J. R. Dean, W. R. Tomlinson, S. P. Owen, Experimental design approach for the extraction of polycyclic aromatic hydrocarbons from soil using supercritical carbon dioxide, *Anal. Chem.* **1995**, *67*, 2064-2069.

[102]   M. D. Burford, S. B. Hawthorne, D. J. Miller, Extraction rates of spiked versus native PAHs from heterogeneous environmental samples using supercritical fluid extraction and sonication in methylene chloride, *Anal. Chem.* **1993**, *65*, 1497-1505.

[103] S. Sarrade, G. Rios, M. Carles, Supercritical CO_2 extraction coupled with nanofiltration separation: applications to natural products, *Sep. Purif. Technol.* **1998**, *14*, 19-25.

[104] H. Cui, T. Wang, Z. Shen, Removal of trace heavy metals from a natural medicine material by supercritical CO_2 chelating extraction, *Ind. Eng. Chem. Res.* **2001**, *40*, 3659-3663.

[105] S. Babel, D. del Mundo Dacera, Heavy metal removal from contaminated sludge for land application: a review, *Waste Manag.* **2006**, *26*, 988-1004.

[106] T. A. Berger, K. Fogleman, T. Staats, P. Bente, I. Crocket, W. Farrell, M. Osonubi, The development of a semi-preparatory scale supercritical-fluid chromatograph for high-throughput purification of 'combi-chem' libraries, *J. Biochem. Biophys.* **2000**, *43*, 87-111.

[107] F. Lin, D. Liu, S. Maiti Das, N. Prempeh, Y. Hua, J. Lu, Recent progress in heavy metal extraction by supercritical CO_2 fluids, *Ind. Eng. Chem. Res.* **2014**, *53*, 1866-1877.

[108] Y. Liu, V. Lopez-Avila, M. Alcaraz, W. Beckert, E. Heithmar, Determination of metals in solid samples by complexation—supercritical fluid extraction and gas chromatography—atomic emission detection, *J. Chromatogr. Sci.* **1993**, *31*, 310-316.

[109] J. A. Darr, M. Poliakoff, New directions in inorganic and metal-organic coordination chemistry in supercritical fluids, *Chem. Rev.* **1999**, *99*, 495-542.

[110] J. Wang, W. D. Marshall, Metal speciation by supercritical fluid extraction with online detection by atomic absorption spectrometry, *Anal. Chem.* **1994**, *66*, 3900-3907.

[111] M. Ashraf-Khorassani, M. T. Combs, L. T. Taylor, Supercritical fluid extraction of metal ions and metal chelates from different environments, *J. Chromatogr. A* **1997**, *774*, 37-49.

[112] C. Kersch, M. Van Roosmalen, G. Woerlee, G. Witkamp, Extraction of heavy metals from fly ash and sand with ligands and supercritical carbon dioxide, *Ind. Eng. Chem. Res.* **2000**, *39*, 4670-4672.

[113] J. S. Wang, K.-H. Chiu, Mass balance of metal species in supercritical fluid extraction using sodium diethyldithiocarbamate and dibutylammonium dibutyldithiocarbamate, *Anal. Sci.* **2006**, *22*, 363-369.

[114] B. Wenclawiak, M. Krah, Reactive supercritical fluid extraction and chromatography of arsenic species, *Fresenius J. Anal. Chem.* **1995**, *351*, 134-138.

[115] C. Wai, Emerging separation techniques: Supercritical fluid and ionic liquid extraction techniques for nuclear fuel reprocessing and radioactive waste treatment, in *Advanced separation techniques for nuclear fuel reprocessing and radioactive waste treatment*, Elsevier, **2011**, pp. 414-435.

[116] K. Laintz, C. Wai, C. Yonker, R. Smith, Solubility of fluorinated metal diethyldithiocarbamates in supercritical carbon dioxide, *J. Supercrit. Fluids.* **1991**, *4*, 194-198.

[117] K. E. Laintz, C. M. Wai, C. R. Yonker, R. D. Smith, Extraction of metal ions from liquid and solid materials by supercritical carbon dioxide, *Anal. Chem.* **1992**, *64*, 2875-2878.

[118] Y. Lin, R. Brauer, K. Laintz, C. Wai, Supercritical fluid extraction of lanthanides and actinides from solid materials with a fluorinated *β*-diketone, *Anal. Chem.* **1993**, *65*, 2549-2551.

[119] Y. Lin, C. Wai, Supercritical fluid extraction of lanthanides with fluorinated *β*-diketones and tributyl phosphate, *Anal. Chem.* **1994**, *66*, 1971-1975.

[120] Y. Lin, C. M. Wai, F. M. Jean, R. D. Brauer, Supercritical fluid extraction of thorium and uranium ions from solid and liquid materials with fluorinated *β*-diketones and tributyl phosphate, *Environ. Sci. Technol.* **1994**, *28*, 1190-1193.

[121] C. M. Wai, B. Waller, Dissolution of metal species in supercritical fluids principles and applications, *Ind. Eng. Chem. Res.* **2000**, *39*, 4837-4841.

[122] R. V. Fox, B. J. Mincher, Supercritical fluid extraction of plutonium and americium from soil using β-diketone and tributyl phosphate complexants, in *Supercritical Carbon Dioxide, Vol. 860* (Eds.: A. S. Gopalan, C. M. Wai, H. K. Jacobs), American Chemical Society, **2003**, pp. 36-49.

[123] A. Murzin, V. Babain, A. Y. Shadrin, I. Smirnov, A. Lumpov, N. Gorshkov, A. Miroslavov, M. Muradymov, Supercritical fluid extraction of actinide complexes: II. SFE of actinide β-diketonates, *Radiochemistry* **2002**, *44*, 467-471.

[124] Y. Lin, N. G. Smart, C. M. Wai, Supercritical fluid extraction of uranium and thorium from nitric acid solutions with organophosphorus reagents, *Environ. Sci. Technol.* **1995**, *29*, 2706-2708.

[125] Y. Meguro, S. Iso, T. Sasaki, Z. Yoshida, Solubility of organophosphorus metal extractants in supercritical carbon dioxide, *Anal. Chem.* **1998**, *70*, 774-779.

[126] Y. Meguro, S. Iso, Z. Yoshida, Correlation between extraction equilibrium of uranium (VI) and density of CO_2 medium in a HNO_3/Supercritical CO_2– tributyl phosphate system, *Anal. Chem.* **1998**, *70*, 1262-1267.

[127] N. Smart, C. Wai, C. Phelps, Supercritical solutions, *Chem. Br.* **1998**, *34*, 34-36.

[128] C. M. Wai, Reprocessing spent nuclear fuel with supercritical carbon dioxide, in *Separations for the Nuclear Fuel Cycle in the 21st Century, Vol. 933* (Eds.: G. J. Lumetta, K. L. Nash, S. B. Clark, J. E. Friese), American Chemical Society, Washington, DC, **2006**, pp. 57-67.

[129] C. M. Wai, Metal processing in supercritical carbon dioxide, in *Supercritical fluid technology in materials science and engineering* (Eds.: Y. P. Sun, M. Dekker), CRC Press, New York, NY, **2002**, pp. 355-391.

[130] C. M. Wai, Supercritical fluid extraction of radionuclides: a green technology for nuclear waste management, in *Nuclear waste management, Vol. 943* (Eds.: P. W. Wang, T. Zachry), American Chemical Society, Washington, DC, **2006**, pp. 161-170.

[131] C. M. Wai, H.-K. Yak, X. Chen, S.-J. Lee, Y. Kulyako, Selective extraction of strontium with supercritical fluid carbon dioxide, *ChemComm* **1999**, 2533-2534.

[132] C. M. Wai, Y. M. Kulyako, B. F. Myasoedov, Supercritical carbon dioxide extraction of caesium from aqueous solutions in the presence of macrocyclic and fluorinated compounds, *Mendeleev Commun.* **1999**, *9*, 180-181.

[133] S. Gabriel, J. Weiner, Ueber einige abkömmlinge des propylamins, *Ber. Dtsch. Chem. Ges.* **1888**, *21*, 2669-2679.

[134] P. Walden, Über die Molekulargrösse und elektrische Leitfähigkeit einiger geschmolzenen Salze, *Bull. Acad. Imper. Sci. (St. Petersburg)* **1914**, *8*, 405-422.

[135] H. L. Chum, V. Koch, L. Miller, R. Osteryoung, An electrochemical scrutiny of organometallic iron complexes and hexamethylbenzene in a room temperature molten salt, *J. Am. Chem. Soc.* **1975**, *97*, 3264-3265.

[136] J. Robinson, R. Osteryoung, An electrochemical and spectroscopic study of some aromatic hydrocarbons in the room temperature molten salt system aluminum chloride-*n*-butylpyridinium chloride, *J. Am. Chem. Soc.* **1979**, *101*, 323-327.

[137] J. S. Wilkes, J. A. Levisky, R. A. Wilson, C. L. Hussey, Dialkylimidazolium chloroaluminate melts: a new class of room-temperature ionic liquids for electrochemistry, spectroscopy and synthesis, *Inorg. Chem.* **1982**, *21*, 1263-1264.

[138] C. L. Hussey, Room temperature haloaluminate ionic liquids. Novel solvents for transition metal solution chemistry, *Pure Appl. Chem.* **1988**, *60*, 1763-1772.

[139] J. S. Wilkes, M. J. Zaworotko, Air and water stable 1-ethyl-3-methylimidazolium based ionic liquids, *J. Chem. Soc., Chem. Commun.* **1992**, 965-967.

[140] P. Bonhote, A.-P. Dias, N. Papageorgiou, K. Kalyanasundaram, M. Grätzel, Hydrophobic, highly conductive ambient-temperature molten salts, *Inorg. Chem.* **1996**, *35*, 1168-1178.

[141] J. Sun, D. R. Macfarlane, M. Forsyth, Synthesis and properties of ambient temperature molten salts based on the quaternary ammonium ion, *Ionics* **1997**, *3*, 356-362.

[142] M. Freemantle, Designer solvents-Ionic liquids may boost clean technology development, *Chem. Eng. News* **1998**, *76*, 32-37.

[143] R. P. Swatloski, S. K. Spear, J. D. Holbrey, R. D. Rogers, Dissolution of cellose with ionic liquids, *J. Am. Chem. Soc.* **2002**, *124*, 4974-4975.

[144] I. Kilpeläinen, H. Xie, A. King, M. Granstrom, S. Heikkinen, D. S. Argyropoulos, Dissolution of wood in ionic liquids, *J. Agric. Food Chem.* **2007**, *55*, 9142-9148.

[145] A. Brandt, J. Gräsvik, J. P. Hallett, T. Welton, Deconstruction of lignocellulosic biomass with ionic liquids, *Green Chem.* **2013**, *15*, 550-583.

[146] Z. Zhang, J. Song, B. Han, Catalytic transformation of lignocellulose into chemicals and fuel products in ionic liquids, *Chem. Rev.* **2017**, *117*, 6834-6880.

[147] M. Watanabe, M. L. Thomas, S. Zhang, K. Ueno, T. Yasuda, K. Dokko, Application of ionic liquids to energy storage and conversion materials and devices, *Chem. Rev.* **2017**, *117*, 7190-7239.

[148] D. R. MacFarlane, N. Tachikawa, M. Forsyth, J. M. Pringle, P. C. Howlett, G. D. Elliott, J. H. Davis, M. Watanabe, P. Simon, C. A. Angell, Energy applications of ionic liquids, *Energy Environ. Sci.* **2014**, *7*, 232-250.

[149] M. A. Navarra, Ionic liquids as safe electrolyte components for Li-metal and Li-ion batteries, *MRS Bull.* **2013**, *38*, 548-553.

[150] A. Balducci, Ionic Liquids in Lithium-Ion Batteries, *Top. Curr. Chem.* **2017**, *375*, 20.

[151] S. P. Ventura, F. A. e Silva, M. V. Quental, D. Mondal, M. G. Freire, J. A. Coutinho, Ionic-liquid-mediated extraction and separation processes for bioactive compounds: past, present, and future trends, *Chem. Rev.* **2017**, *117*, 6984-7052.

[152] S. K. Singh, A. W. Savoy, Ionic liquids synthesis and applications: An overview, *J. Mol. Liq.* **2020**, *297*, 112038.

[153] R. D. Rogers, K. R. Seddon, Ionic liquids--solvents of the future?, *Science* **2003**, *302*, 792-793.

[154] K. N. Marsh, J. A. Boxall, R. Lichtenthaler, Room temperature ionic liquids and their mixtures—a review, *Fluid Ph. Equilibria* **2004**, *219*, 93-98.

[155] I. Krossing, J. M. Slattery, C. Daguenet, P. J. Dyson, A. Oleinikova, H. Weingärtner, Why are ionic liquids liquid? A simple explanation based on lattice and solvation energies, *J. Am. Chem. Soc.* **2006**, *128*, 13427-13434.

[156] J. N. Canongia Lopes, A. A. Pádua, Nanostructural organization in ionic liquids, *J. Phys. Chem. B* **2006**, *110*, 3330-3335.

[157] R. Hayes, G. G. Warr, R. Atkin, Structure and nanostructure in ionic liquids, *Chem. Rev.* **2015**, *115*, 6357-6426.

[158] A. I. Siriwardana, Industrial applications of ionic liquids, in *Electrochemistry in ionic liquids: Volume 2: applications* (Ed.: A. A. J. Torriero), Springer International Publishing, Cham, **2015**, pp. 563-603.

[159] Z.-Z. Yang, Y.-N. Zhao, L.-N. He, CO_2 chemistry: task-specific ionic liquids for CO_2 capture/activation and subsequent conversion, *RSC Adv.* **2011**, *1*, 545-567.

[160] Y.-S. Ye, J. Rick, B.-J. Hwang, Ionic liquid polymer electrolytes, *J. Mater. Chem. A* **2013**, *1*, 2719-2743.

[161] J. G. Huddleston, A. E. Visser, W. M. Reichert, H. D. Willauer, G. A. Broker, R. D. Rogers, Characterization and comparison of hydrophilic and hydrophobic room temperature ionic liquids incorporating the imidazolium cation, *Green Chem.* **2001**, *3*, 156-164.

[162] S. Sowmiah, V. Srinivasadesikan, M.-C. Tseng, Y.-H. Chu, On the chemical stabilities of ionic liquids, *Molecules* **2009**, *14*, 3780-3813.

[163] R. M. Moshikur, M. R. Chowdhury, M. Moniruzzaman, M. Goto, Biocompatible ionic liquids and their applications in pharmaceutics, *Green Chem.* **2020**, *22*, 8116-8139.

[164] H. Niedermeyer, J. P. Hallett, I. J. Villar-Garcia, P. A. Hunt, T. Welton, Mixtures of ionic liquids, *Chem. Soc. Rev.* **2012**, *41*, 7780-7802.

[165] H. Weingärtner, Understanding ionic liquids at the molecular level: facts, problems, and controversies, *Angew. Chem. Int. Ed.* **2008**, *47*, 654-670.

[166] S. Zhang, N. Sun, X. He, X. Lu, X. Zhang, Physical properties of ionic liquids: database and evaluation, *J. Phys. Chem. Ref. Data* **2006**, *35*, 1475-1517.

[167] H. Tokuda, K. Hayamizu, K. Ishii, M. A. B. H. Susan, M. Watanabe, Physicochemical properties and structures of room temperature ionic liquids. 1. Variation of anionic species, *J. Phys. Chem. B* **2004**, *108*, 16593-16600.

[168] A. B. McEwen, H. L. Ngo, K. LeCompte, J. L. Goldman, Electrochemical properties of imidazolium salt electrolytes for electrochemical capacitor applications, *J. Electrochem. Soc.* **1999**, *146*, 1687.

[169]   S. Tsuzuki, H. Tokuda, K. Hayamizu, M. Watanabe, Magnitude and directionality of interaction in ion pairs of ionic liquids: Relationship with ionic conductivity, *J. Phys. Chem. B* **2005**, *109*, 16474-16481.

[170]   M. J. Earle, J. M. Esperança, M. A. Gilea, J. N. C. Lopes, L. P. Rebelo, J. W. Magee, K. R. Seddon, J. A. Widegren, The distillation and volatility of ionic liquids, *Nature* **2006**, *439*, 831-834.

[171]   D. H. Zaitsau, G. J. Kabo, A. A. Strechan, Y. U. Paulechka, A. Tschersich, S. P. Verevkin, A. Heintz, Experimental vapor pressures of 1-alkyl-3-methylimidazolium bis (trifluoromethylsulfonyl) imides and a correlation scheme for estimation of vaporization enthalpies of ionic liquids, *J. Phys. Chem. A* **2006**, *110*, 7303-7306.

[172]   T. Köddermann, D. Paschek, R. Ludwig, Ionic liquids: Dissecting the enthalpies of vaporization, *ChemPhysChem* **2008**, *9*, 549-555.

[173]   L. Cammarata, S. Kazarian, P. Salter, T. Welton, Molecular states of water in room temperature ionic liquids, *Phys. Chem. Chem. Phys.* **2001**, *3*, 5192-5200.

[174]   C. M. Gordon, J. D. Holbrey, A. R. Kennedy, K. R. Seddon, Ionic liquid crystals: hexafluorophosphate salts, *J. Mater. Chem.* **1998**, *8*, 2627-2636.

[175]   D. R. Macfarlane, P. Meakin, J. Sun, N. Amini, M. Forsyth, Pyrrolidinium imides: a new family of molten salts and conductive plastic crystal phases, *J. Phys. Chem. B* **1999**, *103*, 4164-4170.

[176]   P. Lucas, N. El Mehdi, H. A. Ho, D. Belanger, L. Breau, Expedient synthesis of symmetric aryl ketones and of ambient-temperature molten salts of imidazole, *Synthesis* **2000**, *2000*, 1253-1258.

[177]   V. V. Namboodiri, R. S. Varma, Solvent-free sonochemical preparation of ionic liquids, *Org. Lett.* **2002**, *4*, 3161-3163.

[178]   M. Deetlefs, K. R. Seddon, Improved preparations of ionic liquids using microwave irradiation, *Green Chem.* **2003**, *5*, 181-186.

[179]   D. Wilms, J. Klos, A. F. Kilbinger, H. Löwe, H. Frey, Ionic liquids on demand in continuous flow, *Org. Process Res. Dev.* **2009**, *13*, 961-964.

[180]   J. Davis, C. Gordon, C. Hilgers, P. Wasserscheid, T. Welton, Synthesis of ionic liquids, in *Ionic Liquids in Synthesis, Wiley-VCH Verlag GmbH & Co. KGaA, Weinheim, 2003, pp. 7-21*.

[181]   R. Ratti, Ionic liquids: synthesis and applications in catalysis, *Adv. Chem.* **2014**, *2014*, 1-16.

[182]   S. Pitula, A. V. Mudring, Synthesis, structure, and physico-optical properties of manganate (II)-based ionic liquids, *Chem. Eur. J.* **2010**, *16*, 3355-3365.

[183]   X. Creary, E. D. Willis, M. Gagnon, Carbocation-forming reactions in ionic liquids, *J. Am. Chem. Soc.* **2005**, *127*, 18114-18120.

[184]   N. V. Ignat'ev, P. Barthen, A. Kucheryna, H. Willner, P. Sartori, A convenient synthesis of triflate anion ionic liquids and their properties, *Molecules* **2012**, *17*, 5319-5338.

[185]   B. Fan, J. Wei, X. Ma, X. Bu, N. Xing, Y. Pan, L. Zheng, W. Guan, Synthesis of lanthanide-based room temperature ionic liquids with strong luminescence and selective sensing of Fe (III) over mixed metal ions, *Ind. Eng. Chem. Res.* **2016**, *55*, 2267-2271.

[186]   A. J. Greer, J. Jacquemin, C. Hardacre, Industrial applications of ionic liquids, *Molecules* **2020**, *25*, 5207.

[187]   J. D. Holbrey, N. V. Plechkova, K. R. Seddon, Recalling COIL, in *Green Chem.*, The Royal Society of Chemistry, Salzburg (Austria), **2006**, *Vol. 8*, pp. 411-414.

[188]   G. W. Phillips, S. N. Falling, T. Kingsport, S. A. Godleski, J. R. Monnier, Continuous Process for the Manufacture of 2,5-dihydrofurans from γ,δ-epoxybutenes., U.S. Patent 5315019A, **24 May 1994.**

[189]   E. García-Verdugo, B. Altava, M. I. Burguete, P. Lozano, S. Luis, Ionic liquids and continuous flow processes: A good marriage to design sustainable processes, *Green Chem.* **2015**, *17*, 2693-2713.

[190]   M. Volland, V. Seitz, M. Maase, M. Flores, R. Papp, K. Massonne, V. Stegmann, K. Halbritter, R. Noe, M. Bartsch, W. Siegel, M. Becker, O. Huttenloch, Method for the separation of acids from chemical reaction mixtures by means of ionic fluids, World. Pat., WO 03062251,

[191] M. Maase, K. Massonne, Biphasic acid scavenging utilizing ionic liquids: the first commercial process with ionic liquids, in *Ionic liquids IIIB: fundamentals, progress, challenges, and opportunities, Vol. 902* (Eds.: R. D. Rogers, K. Seddon), ACS Publications, Washington, D. C., **2005**.

[192] A. H. Tullo, The time is now for ionic liquids, *Chem. Eng. News* **2020**, *98*, 24-27.

[193] H. K. C. Timken, S. Elomari, S. Trumbull, R. Cleverdon, Integrated alkylation process using ionic liquid catalysts, WO2006073749A2, **13 July 2006.**

[194] S. Elomari, S. Trumbull, H. K. C. Timken, R. Cleverdon, Alkylation process using chloroaluminate ionic liquid catalysts, WO2006068983A2, **29 June 2006.**

[195] S. C. Martins, D. A. Nafis, A. Bhattacharyya, Alkylation Process Using Phosphonium-Based Ionic Liquids., US9156028B2, **13 October 2013.**

[196] H. K. Timken, H. Luo, B.-K. Chang, E. Carter, M. Cole, ISOALKY™ Technology: Next-Generation Alkylate Gasoline Manufacturing Process Technology Using Ionic Liquid Catalyst, in *Commercial Applications of Ionic Liquids* (Ed.: M. B. Shiflett), Springer International Publishing, Cham, **2020**, pp. 33-47.

[197] Y. Liu, R. Hu, C. Xu, H. Su, Alkylation of isobutene with 2-butene using composite ionic liquid catalysts, *Appl. Catal. A: Gen.* **2008**, *346*, 189-193.

[198] C.-P. Huang, Z.-C. Liu, C.-M. Xu, B.-H. Chen, Y.-F. Liu, Effects of additives on the properties of chloroaluminate ionic liquids catalyst for alkylation of isobutane and butene, *Appl. Catal. A: Gen.* **2004**, *277*, 41-43.

[199] W. Chung, R. Zhang, D. Song, Safe and sustainable alkylation: Performance and update on composite ionic liquid alkylation technology, *Hydrocarb. Process* **2020**.

[200] Well-Resources., Ionikylation https://www.wellresources.ca/ionikylation, (accessed 10 July 2022).

[201] Supelco-Ionic-Liquid-GC-Column-Literature&Applications, https://www.sigmaaldrich.com/AT/en/technical-documents/protocol/analytical-chemistry/gas-chromatography/ionic-liquid-gc-capillary-columns, (accessed 10 July 2022).

[202] Hitachi-High-Tech-Corporation., Hitachi Ionic liquid HILEM© for Easy Sample Preparation Hitachi Ionic liquid HILEM© for Easy Sample Preparation, https://www.hitachi-hightech.com/global/expo/science/panel/, (accessed 10 July 2022).

[203] L.-M. Joubert, K. McDonald, SEM Visualization of Biological Samples using Hitachi Ionic Liquid HILEM® IL 1000: a Comparative Study, *Microsc. Microanal.* **2016**, *22*, 1170-1171.

[204] D. J. Tempel, P. B. Henderson, J. R. Brzozowski, Reactive Liquid Based Gas Storage and Delivery Systems, US7172646B2, **6 February 2007.**

[205] M. Freemantle, Ionic liquids make an splash in industry, *Chem. Eng. News* **2005**, *83*, 33-38.

[206] M. Abai, M. P. Atkins, A. Hassan, J. D. Holbrey, Y. Kuah, P. Nockemann, A. A. Oliferenko, N. V. Plechkova, S. Rafeen, A. A. Rahman, R. Ramli, S. M. Shariff, K. R. Seddon, G. Srinivasan, Y. Zou, An ionic liquid process for mercury removal from natural gas, *Dalton Trans.* **2015**, *44*, 8617-8624.

[207] R. Boada, G. Cibin, F. Coleman, S. Diaz-Moreno, D. Gianolio, C. Hardacre, S. Hayama, J. D. Holbrey, R. Ramli, K. R. Seddon, G. Srinivasan, M. Swadźba-Kwaśny, Mercury capture on a supported chlorocuprate(ii) ionic liquid adsorbent studied using operando synchrotron X-ray absorption spectroscopy, *Dalton Trans.* **2016**, *45*, 18946-18953.

[208] R. D. Rogers, J. Holbrey, H. Rodriguez, Process for Removing Metals from Hydrocarbons, WO2010116165A2, **14 October 2010.**

[209] M. Abai, M. P. Atkins, K. Y. Cheun, J. Holbrey, P. Nockemann, K. Seddon, G. Z. Srinivasan, Y. , Process for Removing Metals from Hydrocarbons, WO2012046057A2, **12 April 2012.**

[210] K. Y. Cheun, J. D. Holbrey, M. P. Atkins, Process for Removing Heavy Metals from Hydrocarbons, WO2016139280A1, **9 September 2016.**

[211] L. M. Haverhals, W. M. Reichert, H. C. De Long, P. C. Trulove, Natural Fiber Welding, *Macromol. Mater. Eng.* **2010**, *295*, 425-430.

[212] L. M. Haverhals, D. P. Durkin, P. C. Trulove, Natural Fiber Welding, in *Commercial Applications of Ionic Liquids* (Ed.: M. B. Shiflett), Springer International Publishing, Cham, **2020**, pp. 211-226.

[213] H. Wang, Z. Li, Y. Liu, X. Zhang, S. Zhang, Degradation of poly(ethylene terephthalate) using ionic liquids, *Green Chem.* **2009**, *11*, 1568-1575.

[214] Q. Wang, Y. Geng, X. Lu, S. Zhang, First-row transition metal-containing ionic liquids as highly active catalysts for the glycolysis of poly(ethylene terephthalate) (PET), *ACS Sustain. Chem. Eng.* **2015**, *3*, 340-348.

[215] Ioniqa, Ioniqa Takes First 10 Kiloton PET Upcycling Factory into Operation, https://ioniqa.com/ioniqa-takes-first-10-kiloton-pet-upcycling-factory-into-operation/, (accessed 12 July 2020).

[216] J. Timonen, T. Hooghoudt, M. Vilaplana Artigas, A. Philipse, C. G. Sanchez, J. C. Ribot, V. Philippi, R. De Groot, Magnetic Fluid, WO2014142661A2, **18 September 2014.**

[217] A. P. Abbott, D. L. Davies, G. Capper, R. K. Rasheed, V. Tambyrajah, Ionic liquids and their use, WO2002026381A2, **4 April 2002.**

[218] A. P. D. Abbott, D.L.; Capper, G.; Rasheed, R.K.; Tambyrajah, V, Ionic liquids and their use as solvents, WO2002026701A2, **4 April 2002.**

[219] A. P. Abbott, G. Capper, D. L. Davies, R. K. Rasheed, J. Archer, C. John, Electrodeposition of chromium black from ionic liquids, *Trans. Inst. Met. Finish.* **2004**, *82*, 14-17.

[220] A. P. Abbott, G. Capper, D. L. Davies, R. K. Rasheed, Ionic Liquid Analogues Formed from Hydrated Metal Salts, *Chem. Eur. J.* **2004**, *10*, 3769-3774.

[221] S. Iyer, A. Ramani M R S C, S. Bhandari, Ionic Liquids: Benign by design, high-tech operational windows in organic synthesis, Chemical Weekly, **10 May 2022**.

[222] NOHMs-Technologies-Inc., NOHMs Advanced Electrolyte Solutions, http://www.nohms.com/technology/, (accessed 12 July 2022).

[223] S. S. Moganty, J. Lee, Hybrid ionic liquid electrolytes, US20160164137A1, **9 June 2016.**

[224] L. Zyga, Metal-air battery could store 11 times more energy than lithium-ion, https://phys.org/news/2009-11-metal-air-battery-energy-lithium-ion.html, (accessed 13 July 2022).

[225] A. H. Tullo, Batteries that breathe air, *C&EN Global Enterprise* **2017**, *95*, 21-22.

[226] C. A. Friesen, R. Krishnan, T. Tang, D. Wolfe, Metal-air cell with tuned hydrophobicity., WO2011159391A1, **22 December 2011.**

[227] C. A. Friesen, D. Wolfe, P. B. Johnson, Metal-air cell with ion exchange material, WO2012174558A1, **20 December 2012.**

[228] R. S. Kalb, Toward industrialization of ionic liquids, in *Commercial Applications of Ionic Liquids* (Ed.: M. B. Shiflett), Springer International Publishing, Cham, Switzerland, **2020**, pp. 261-282.

[229] K. Oster, P. Goodrich, J. Jacquemin, C. Hardacre, A. P. C. Ribeiro, A. Elsinawi, A new insight into pure and water-saturated quaternary phosphonium-based carboxylate ionic liquids: Density, heat capacity, ionic conductivity, thermogravimetric analysis, thermal conductivity and viscosity, *J. Chem. Thermodyn.* **2018**, *121*, 97-111.

[230] K. Oster, C. Hardacre, J. Jacquemin, A. P. C. Ribeiro, A. Elsinawi, Ionic liquid-based nanofluids (ionanofluids) for thermal applications: an experimental thermophysical characterization, *Pure Appl. Chem.* **2019**, *91*, 1309-1340.

[231] Proionic, Ionic liquid applications — intrinsically safe high-temperature cooling, https://www.proionic.com/ionic-liquids/applications-high-temperature-cooling.php, (accessed 13 July 2022).

[232] Mettop-GmbH-(ILTEC-Technology), Ionic liquid cooling technology - description and application, https://mettop.com/api/cdn/uploads/1526032491_k7timr64.pdf, (accessed 13 July 2022).

[233] Klüber-Lubrication, Ionic liquids — innovative lightning conductor in e-mobility, https://www.klueber.com/de/en/company/newsroom/news/ionic-liquids-innovative-lightning-conductor-in-e-mobility/, (accessed 13 July 2022).

[234] R. Adler, G. Siebert, Method and devices for compressing a gaseous medium, US20070258828A1, **8 Nov 2007.**

[235] M. Kompf, Mobility under high pressure, in *In Reports on science and technology*, Linde, Pullach, Germany, **2006**, pp. 24-29.

[236] BOC, Europe's largest hydrogen vehicle refuelling station case study, BOC: Guildford, UK, Kittybrewster, Aberdeen, **2019**.

[237] Linde, The driving force. Managing hydrogen projects with Linde*,*Brochure tcm17-233488, Linde, Pullach (Germany), **2012**.

[238] 3MTM-Antistatic-Additives, Ionic liquids and solids, 3M, Saint Paul, MI, USA, **2016**.

[239] BASF, Basionics—High-Performance Antistatic Additives Brochure, BASF, Ludwigshafen, Germany, **2016**.

[240] Evonik-Industries, New Tego products increase conductivity and electrostatic charge dissipation of paints and coatings, https://www.coating-additives.com/en/new-tego-products-increase-conductivity-and-electrostatic-charge-dissipation-of-paints-and-coatings-101049.html, (accessed 13 July 2022).

[241] Koei-Chemical-Co-(Ltd), Ionic liquids-type antistatic agents for resins, https://www.koeichem.com/en/en_product/ion/antistatic.html, (accessed 13 July 2022).

[242] A. Hoff, C. Jost, A. Prodi-Schwab, F. Schmidt, B. Weyershausen, Ionic Liquids: New designer compounds for more efficient chemistry, *Elements: Degussa Science Newsletter* **2004**, *9*.

[243] B. Weyershausen, K. Lehmann, Industrial application of ionic liquids as performance additives, *Green Chem.* **2005**, *7*, 15-19.

[244] P. Wasserscheid, T. Welton, *Ionic Liquids in Synthesis*, 2nd ed., Wiley, Hoboken, NJ, USA, **2008**.

[245] V. Stegmann, K. Massonne, Method for Producing Haloalkanes from Alcohols, WO2005026089A2, **24 March 2005.**

[246] C. R. Schmid, C. A. Beck, J. S. Cronin, M. A. Staszak, Demethylation of 4-methoxyphenylbutyric acid using molten pyridinium hydrochloride on multikilogram scale, *Org. Process Res. Dev.* **2004**, *8*, 670-673.

[247] N. V. Plechkova, K. R. Seddon, Applications of ionic liquids in the chemical industry, *Chem. Soc. Rev.* **2008**, *37*, 123-150.

[248] A. Forestière, H. Olivier-Bourbigou, L. Saussine, Oligomerization of monoolefins by homogeneous catalysts, *Oil Gas Sci. Technol.* **2009**, *64*, 649-667.

[249] V. I. Pârvulescu, C. Hardacre, Catalysis in ionic liquids, *Chem. Rev.* **2007**, *107*, 2615-2665.

[250] M. Freemantle, *An introduction to ionic liquids*, RSC Publishing, Cambridge, UK, **2009**.

[251] Ionike, IFP's Difasol process based on ionic liquids, http://www.ionike.com/en/application/2014-04-24/26.html, (accessed 13 July 2022).

[252] Ioncell, Enter the new era of textile production!, https://ioncell.fi/, (accessed 13 July 2022).

[253] A. Michud, M. Tanttu, S. Asaadi, Y. Ma, E. Netti, P. Kääriainen, A. Persson, A. Berntsson, M. Hummel, H. Sixta, Ioncell-F: ionic liquid-based cellulosic textile fibers as an alternative to viscose and Lyocell, *Text. Res. J.* **2016**, *86*, 543-552.

[254] Metsä-Fibre, Shaping the new sustainable textile fibre future, https://www.metsafibre.com/en/media/Stories/Pages/Shaping-the-new-textile-fibre-future.aspx, (accessed 13 July 2022).

[255] Grete-Project, Green chemicals and technologies for the wood-to-textile value chain, https://www.greteproject.eu/, (accessed 13 July 2022).

[256] C. L. Chambon, P. Verdía, P. S. Fennell, J. P. Hallett, Process intensification of the ionoSolv pretreatment: effects of biomass loading, particle size and scale-up from 10 mL to 1 L, *Sci. Rep.* **2021**, *11*, 15383.

[257] A. George, A. Brandt, K. Tran, S. M. S. N. S. Zahari, D. Klein-Marcuschamer, N. Sun, N. Sathitsuksanoh, J. Shi, V. Stavila, R. Parthasarathi, S. Singh, B. M. Holmes, T. Welton, B. A. Simmons, J. P. Hallett, Design of low-cost ionic liquids for lignocellulosic biomass pretreatment, *Green Chem.* **2015**, *17*, 1728-1734.

[258]   A. R. Abouelela, F. V. Gschwend, F. Malaret, J. P. Hallett, Commercial aspects of biomass deconstruction with ionic liquids, in *Commercial applications of ionic liquids* (Ed.: M. B. Shiflett), Springer International Publishing, Cham, **2020**, pp. 87-127.

[259]   D. H. Bartlett, F. Azam, Chitin, cholera, and competence, *Science* **2005**, *310*, 1775-1777.

[260]   Y. Qin, X. Lu, N. Sun, R. D. Rogers, Dissolution or extraction of crustacean shells using ionic liquids to obtain high molecular weight purified chitin and direct production of chitin films and fibers, *Green Chem.* **2010**, *12*, 968-971.

[261]   J. L. Shamshina, P. Berton, R. D. Rogers, Advances in functional chitin materials: A review, *ACS Sustain. Chem. Eng.* **2019**, *7*, 6444-6457.

[262]   IoLiTec, Electrolytes for metal deposition, https://iolitec.de/node/652 (accessed 13 July 2022).

[263]   M. O'Meara, A. Alemany, M. Maase, U. Vagt, I. Malkowsky, Deposition of aluminum using ionic liquids: BASF process improves adhesion and coating density, *Met. Finish.* **2009**, *107*, 38-39.

[264]   A. Alemany, I. Malkowsky, U. Vagt, M. Maase, M. O'Meara, Recent developments in the field of aluminum deposition using ionic liquids, *Plat. Surf. Finish* **2010**, *97*, 34-37.

[265]   E. Freydina, J. G. Abbott, A. C. Lund, R. D. Hilty, S. Ruan, J. Reese, L. J. Chan, J. A. Wright, J. A. Curran, Nanostructured aluminum alloys for improved hardness, US10590558B2, **17 March 2020.**

[266]   CORDIS-European-Commission., Final report summary — SCAIL-UP (scaling-up of the aluminium plating process from ionic liquids), https://cordis.europa.eu/project/id/608698/reporting, (accessed 13 July 2022).

[267]   D. Teramoto, R. Yokoyama, H. Kagawa, T. Sada, N. Ogata, A novel ionic liquid-polymer electrolyte for the advanced lithium ion polymer battery, in *Molten salts and ionic liquids*, **2010**, pp. 367-388.

[268]   ZapGo-Ltd, Carbon-IonTM: A new, safer and faster charging category of rechargeable energy storage devices, in Brochure, ZapGo, Oxford, UK **2016**, pp. 1–16.

[269]   D. Kołodyńska, D. Fila, B. Gajda, J. Gęga, Z. Hubicki, Rare earth elements — separation methods yesterday and today, in *Applications of ion exchange materials in the environment*, Springer, Cham, Switzerland, **2019**, pp. 161-185.

[270]   P. Nockemann, R. Ritesh, Separation of rare earth metals, WO2018109483A1, **21 June 2018.**

[271]   P. Nockemann, D. Brolly, E. Bradley, E. McCourt, Countercurrent rare earth separation process, WO2019239151A1, **19 December 2019.**

[272]   P. Nockemann, D. Brolly, E. Bradley, E. McCourt, Enhanced separation of rare earth metals, WO2019239150A1, **19 December 2019.**

[273]   Seren-Technolgies-Limited, Magnet recycling, https://www.seren-ag.com/tag/magnet-recycling/, (accessed 13 July 2022).

[274]   Seren-Technolgies-Limited, Rare earth separation and recycling, https://www.seren-ag.com/rare-earth-separation-recycling/, (accessed 13 July 2022).

[275]   Managing-IP, Recycling rare earth metals, https://www.managingip.com/article/2a5bs1a5grcbk3lh77xfk/recycling-rare-earth-metals#:~:text=Seren%20Technologies%20opened%20its%20pre,required%20to%20select%20these%20rare, (accessed 13 July 2022).

[276]   R. Franke, H. Hahn, A catalyst that goes to its limits, *Evonik Ind.* **2015**, *2*, 18-23.

[277]   C. W. Kohlpaintner, R. W. Fischer, B. Cornils, Aqueous biphasic catalysis: Ruhrchemie/Rhône-Poulenc oxo process, *Appl. Catal. A: Gen.* **2001**, *221*, 219-225.

[278]   L. Magna, S. Harry, D. Proriol, L. Saussine, H. Olivier-Bourbigou, Hydroformylation of 1-hexene with a cobalt catalyst in ionic liquids: A new efficient approach for generation and recycling of the catalyst, *Oil Gas Sci. Technol.* **2007**, *62*, 775-780.

[279]   G. Hillebrand, A. Hirschauer, D. Commereuc, H. Olivier-Bourbigou, L. Saussine, Process for hydroformylation using a catalyst based on cobalt and/or rhodium employed in a two-phase medium, US20010039363A1, **8 November 2001.**

[280] T. J. Geldbach, D. Zhao, N. C. Castillo, G. Laurenczy, B. Weyershausen, P. J. Dyson, Biphasic hydrosilylation in ionic liquids: A process set for industrial implementation, *J. Am. Chem. Soc.* **2006**, *128*, 9773-9780.

[281] B. Weyershausen, K. Hell, U. Hesse, Industrial application of ionic liquids as process aid, *Green Chem.* **2005**, *7*, 283-287.

[282] T. Welton, P. Wasserscheid, *Ionic liquids in synthesis* 1st ed., Wiley-VCH, Weinheim, Germany, **2002**.

[283] House-of-Commons-Environmental-Audit-Committee, UK progress on reducing F-gas emissions: fifth report of session 2017–19, House of Commons Environmental Audit Committee, London, UK, **2018**.

[284] P. Bonnet, Catalysis in nonaqueous ionic liquids, in *Multiphase homogeneous catalysis, Vol. 2* (Eds.: B. Cornils, W. A. Herrmann, I. T. Horváth, W. Leitner, S. Mecking, H. Olivier-Bourbigou, D. Vogt), Wiley-VCH Verlag, Hoboken, NJ, USA, **2005**, pp. 405 - 604.

[285] P. Bonnet, É. Lacroix, J.-P. Schirmann, Ion liquids derived from lewis acid based on titanium, niobium, tantalum, or antimony, and uses thereof, WO2001081353A1, **1 November 2001.**

[286] F. Jutz, J.-M. Andanson, A. Baiker, Ionic liquids and dense carbon dioxide: a beneficial biphasic system for catalysis, *Chem. Rev.* **2011**, *111*, 322-353.

[287] J. L. Anthony, E. J. Maginn, J. F. Brennecke, Solubilities and thermodynamic properties of gases in the ionic liquid 1-n-butyl-3-methylimidazolium hexafluorophosphate, *J. Phys. Chem. B* **2002**, *106*, 7315-7320.

[288] S. N. Aki, B. R. Mellein, E. M. Saurer, J. F. Brennecke, High-pressure phase behavior of carbon dioxide with imidazolium-based ionic liquids, *J. Phys. Chem. B* **2004**, *108*, 20355-20365.

[289] C. Cadena, J. L. Anthony, J. K. Shah, T. I. Morrow, J. F. Brennecke, E. J. Maginn, Why is CO_2 so soluble in imidazolium-based ionic liquids?, *J. Am. Chem. Soc.* **2004**, *126*, 5300-5308.

[290] S. G. Kazarian, B. J. Briscoe, T. Welton, Combining ionic liquids and supercritical fluids: in situ ATR-IR study of CO_2 dissolved in two ionic liquids at high pressures, *ChemComm* **2000**, 2047-2048.

[291] B. R. Prasad, S. Senapati, Explaining the differential solubility of flue gas components in ionic liquids from first-principle calculations, *J. Phys. Chem. B* **2009**, *113*, 4739-4743.

[292] T. Seki, J.-D. Grunwaldt, A. Baiker, In situ attenuated total reflection infrared spectroscopy of imidazolium-based room-temperature ionic liquids under "supercritical" CO_2, *J. Phys. Chem. B* **2009**, *113*, 114-122.

[293] W. Shi, E. J. Maginn, Molecular simulation and regular solution theory modeling of pure and mixed gas absorption in the ionic liquid 1-*n*-hexyl-3-methylimidazolium bis(trifluoromethylsulfonyl)amide ([hmim][Tf$_2$N]), *J. Phys. Chem. B* **2008**, *112*, 16710-16720.

[294] A. Yokozeki, M. B. Shiflett, Separation of carbon dioxide and sulfur dioxide gases using room-temperature ionic liquid [hmim][Tf$_2$N], *Energy Fuels* **2009**, *23*, 4701-4708.

[295] P. G. Jessop, B. Subramaniam, Gas-expanded liquids, *Chem. Rev.* **2007**, *107*, 2666-2694.

[296] M. J. Muldoon, S. N. Aki, J. L. Anderson, J. K. Dixon, J. F. Brennecke, Improving carbon dioxide solubility in ionic liquids, *J. Phys. Chem. B* **2007**, *111*, 9001-9009.

[297] J. L. Anthony, J. L. Anderson, E. J. Maginn, J. F. Brennecke, Anion effects on gas solubility in ionic liquids, *J. Phys. Chem. B* **2005**, *109*, 6366-6374.

[298] S. Keskin, D. Kayrak-Talay, U. Akman, Ö. Hortaçsu, A review of ionic liquids towards supercritical fluid applications, *J. Supercrit. Fluids.* **2007**, *43*, 150-180.

[299] X. Huang, C. J. Margulis, Y. Li, B. J. Berne, Why is the partial molar volume of CO_2 so small when dissolved in a room temperature ionic liquid? Structure and dynamics of CO_2 dissolved in [Bmim$^+$][PF6$^-$], *J. Am. Chem. Soc.* **2005**, *127*, 17842-17851.

[300] L. A. Blanchard, Z. Gu, J. F. Brennecke, High-pressure phase behavior of ionic liquid/CO_2 systems, *J. Phys. Chem. B* **2001**, *105*, 2437-2444.

[301] A. M. Scurto, E. Newton, R. R. Weikel, L. Draucker, J. Hallett, C. L. Liotta, W. Leitner, C. A. Eckert, Melting point depression of ionic liquids with CO_2: Phase equilibria, *Ind. Eng. Chem. Res.* **2008**, *47*, 493-501.

[302] A. Serbanovic, Ž. Petrovski, M. Manic, C. S. Marques, G. V. Carrera, L. C. Branco, C. A. Afonso, M. N. da Ponte, Melting behaviour of ionic salts in the presence of high pressure CO_2, *Fluid Ph. Equilibria* **2010**, *294*, 121-130.

[303] A. M. Scurto, W. Leitner, Expanding the useful range of ionic liquids: melting point depression of organic salts with carbon dioxide for biphasic catalytic reactions, *ChemComm* **2006**, 3681-3683.

[304] A. Ahosseini, E. Ortega, B. Sensenich, A. M. Scurto, Viscosity of *n*-alkyl-3-methyl-imidazolium bis(trifluoromethylsulfonyl)amide ionic liquids saturated with compressed CO_2, *Fluid Ph. Equilibria* **2009**, *286*, 72-78.

[305] D. Morgan, L. Ferguson, P. Scovazzo, Diffusivities of gases in room-temperature ionic liquids: data and correlations obtained using a lag-time technique, *Ind. Eng. Chem. Res.* **2005**, *44*, 4815-4823.

[306] D. Camper, C. Becker, C. Koval, R. Noble, Diffusion and solubility measurements in room temperature ionic liquids, *Ind. Eng. Chem. Res.* **2006**, *45*, 445-450.

[307] L. Ferguson, P. Scovazzo, Solubility, diffusivity, and permeability of gases in phosphonium-based room temperature ionic liquids: data and correlations, *Ind. Eng. Chem. Res.* **2007**, *46*, 1369-1374.

[308] A. M. Scurto, S. N. Aki, J. F. Brennecke, CO_2 as a separation switch for ionic liquid/organic mixtures, *J. Am. Chem. Soc.* **2002**, *124*, 10276-10277.

[309] S. N. Aki, A. M. Scurto, J. F. Brennecke, Ternary phase behavior of ionic liquid (IL)–organic–CO_2 systems, *Ind. Eng. Chem. Res.* **2006**, *45*, 5574-5585.

[310] B. R. Mellein, J. F. Brennecke, Characterization of the ability of CO_2 to act as an antisolvent for ionic liquid/organic mixtures, *J. Phys. Chem. B* **2007**, *111*, 4837-4843.

[311] Z. Zhang, W. Wu, Z. Liu, B. Han, H. Gao, T. Jiang, A study of tri-phasic behavior of ionic liquid–methanol–CO_2 systems at elevated pressures, *Phys. Chem. Chem. Phys.* **2004**, *6*, 2352-2357.

[312] Z. Zhang, W. Wu, B. Wang, J. Chen, D. Shen, B. Han, High-pressure phase behavior of CO_2/acetone/ionic liquid system, *J. Supercrit. Fluids.* **2007**, *40*, 1-6.

[313] D. Fu, X. Sun, Y. Qiu, X. Jiang, S. Zhao, High-pressure phase behavior of the ternary system CO_2+ionic liquid [bmim][PF_6]+naphthalene, *Fluid Ph. Equilibria* **2007**, *251*, 114-120.

[314] M. C. Kroon, L. J. Florusse, E. Kühne, G.-J. Witkamp, C. J. Peters, Achievement of a homogeneous phase in ternary ionic liquid/carbon dioxide/organic systems, *Ind. Eng. Chem. Res.* **2010**, *49*, 3474-3478.

[315] M. C. Kroon, L. J. Florusse, C. J. Peters, Phase behavior of the ternary 1-hexyl-3-methylimidazolium tetrafluoroborate+ carbon dioxide+ methanol system, *Fluid Ph. Equilibria* **2010**, *294*, 84-88.

[316] K. Chobanov, D. Tuma, G. Maurer, High-pressure phase behavior of ternary systems (carbon dioxide+ alkanol+ hydrophobic ionic liquid), *Fluid Ph. Equilibria* **2010**, *294*, 54-66.

[317] J.-Y. Ahn, B.-C. Lee, J. S. Lim, K.-P. Yoo, J. W. Kang, High-pressure phase behavior of binary and ternary mixtures containing ionic liquid [C_6mim][Tf_2N], dimethyl carbonate and carbon dioxide, *Fluid Ph. Equilibria* **2010**, *290*, 75-79.

[318] E. Kühne, L. R. Alfonsín, M. T. M. Martinez, G.-J. Witkamp, C. J. Peters, Comment on "Characterization of the ability of CO_2 to act as an antisolvent for ionic liquid/organic mixtures", *J. Phys. Chem. B* **2009**, *113*, 6579-6580.

[319] A. M. Scurto, S. N. Aki, J. F. Brennecke, Carbon dioxide induced separation of ionic liquids and water, *ChemComm* **2003**, 572-573.

[320] Z. Zhang, W. Wu, H. Gao, B. Han, B. Wang, Y. Huang, Tri-phase behavior of ionic liquid–water–CO_2 system at elevated pressures, *Phys. Chem. Chem. Phys.* **2004**, *6*, 5051-5055.

[321] M. D. Bermejo, M. Montero, E. Saez, L. J. Florusse, A. J. Kotlewska, M. J. Cocero, F. van Rantwijk, C. J. Peters, Liquid–vapor equilibrium of the systems butylmethylimidazolium nitrate–CO_2 and hydroxypropylmethylimidazolium nitrate–CO_2 at high pressure: Influence of water on the phase behavior, *J. Phys. Chem. B* **2008**, *112*, 13532-13541.

[322] K. R. Seddon, N. V. Plechkova, *Ionic liquids further unCOILed: Critical expert overviews*, John Wiley & Sons, **2014**.

[323] L. A. Blanchard, D. Hancu, E. J. Beckman, J. F. Brennecke, Green processing using ionic liquids and CO_2, *Nature* **1999**, *399*, 28-29.

[324] L. F. Vega, O. Vilaseca, E. Valente, J. S. Andreu, F. Llovell, R. M. Marcos, Using molecular modelling tools to understand the thermodynamic behaviour of ionic liquids, *Ionic Liquids: Theory, Properties, New Approaches* **2011**, 303-328.

[325] R. A. Brown, P. Pollet, E. McKoon, C. A. Eckert, C. L. Liotta, P. G. Jessop, Asymmetric hydrogenation and catalyst recycling using ionic liquid and supercritical carbon dioxide, *J. Am. Chem. Soc.* **2001**, *123*, 1254-1255.

[326] M. Roth, Partitioning behaviour of organic compounds between ionic liquids and supercritical fluids, *J. Chromatogr. A* **2009**, *1216*, 1861-1880.

[327] S. Mekki, C. M. Wai, I. Billard, G. Moutiers, J. Burt, B. Yoon, J. S. Wang, C. Gaillard, A. Ouadi, P. Hesemann, Extraction of lanthanides from aqueous solution by using room-temperature ionic liquid and supercritical carbon dioxide in conjunction, *Chem. Eur. J.* **2006**, *12*, 1760-1766.

[328] K. Binnemans, Lanthanides and actinides in ionic liquids, *Chem. Rev.* **2007**, *107*, 2592-2614.

[329] S. Mekki, C. M. Wai, I. Billard, G. Moutiers, C. H. Yen, J. S. Wang, A. Ouadi, C. Gaillard, P. Hesemann, Cu(II) extraction by supercritical fluid carbon dioxide from a room temperature ionic liquid using fluorinated β-diketones, *Green Chem.* **2005**, *7*, 421-423.

[330] J. S. Wang, C. N. Sheaff, B. Yoon, R. S. Addleman, C. M. Wai, Extraction of uranium from aqueous solutions by using ionic liquid and supercritical carbon dioxide in conjunction, *Chem. Eur. J.* **2009**, *15*, 4458-4463.

[331] B. Cornils, W. A. Herrmann, *Aqueous-phase organometallic catalysis: concepts and applications*, Wiley-VCH: Weinheim, New York, **1998**.

[332] I. T. Horváth, J. Rábai, Facile catalyst separation without water: fluorous biphase hydroformylation of olefins, *Science* **1994**, *266*, 72-75.

[333] B. M. Bhanage, Y. Ikushima, M. Shirai, M. Arai, Multiphase catalysis using water-soluble metal complexes in supercritical carbon dioxide, *ChemComm* **1999**, 1277-1278.

[334] R. J. Bonilla, B. R. James, P. G. Jessop, Colloid-catalysed arene hydrogenation in aqueous/supercritical fluid biphasic media, *ChemComm* **2000**, 941-942.

[335] P. G. Jessop, Y. Hsiao, T. Ikariya, R. Noyori, Catalytic production of dimethylformamide from supercritical carbon dioxide, *J. Am. Chem. Soc.* **1994**, *116*, 8851-8852.

[336] C. M. Gordon, New developments in catalysis using ionic liquids, *Appl. Catal. A: Gen.* **2001**, *222*, 101-117.

[337] S. V. Dzyuba, R. A. Bartsch, Recent advances in applications of room-temperature ionic liquid/supercritical CO_2 systems, *Angew. Chem. Int. Ed.* **2003**, *42*, 148-150.

[338] F. Liu, M. B. Abrams, R. T. Baker, W. Tumas, Phase-separable catalysis using room temperature ionic liquids and supercritical carbon dioxide, *ChemComm* **2001**, 433-434.

[339] D. Ballivet-Tkatchenko, M. Picquet, M. Solinas, G. Franciò, P. Wasserscheid, W. Leitner, Acrylate dimerisation under ionic liquid–supercritical carbon dioxide conditions, *Green Chem.* **2003**, *5*, 232-235.

[340] P. G. Jessop, R. R. Stanley, R. A. Brown, C. A. Eckert, C. L. Liotta, T. T. Ngo, P. Pollet, Neoteric solvents for asymmetric hydrogenation: supercritical fluids, ionic liquids, and expanded ionic liquids, *Green Chem.* **2003**, *5*, 123-128.

[341] G. Zhao, T. Jiang, W. Wu, B. Han, Z. Liu, H. Gao, Electro-oxidation of benzyl alcohol in a biphasic system consisting of supercritical CO_2 and ionic liquids, *J. Phys. Chem. B* **2004**, *108*, 13052-13057.

[342] A. Bösmann, G. Franciò, E. Janssen, M. Solinas, W. Leitner, P. Wasserscheid, Activation, tuning, and immobilization of homogeneous catalysts in an ionic liquid/compressed CO_2 continuous-flow system, *Angew. Chem. Int. Ed.* **2001**, *40*, 2697-2699.

[343] C. Bueno, V. Cabral, L. Cardozo-Filho, M. Dias, O. Antunes, Cationic polymerization of styrene in $scCO_2$ and [bmim][PF_6], *J. Supercrit. Fluids.* **2009**, *48*, 183-187.

189

[344] A. Ahosseini, W. Ren, A. M. Scurto, Understanding biphasic ionic liquid/CO_2 systems for homogeneous catalysis: hydroformylation, *Ind. Eng. Chem. Res.* **2009**, *48*, 4254-4265.

[345] Z. Hou, B. Han, L. Gao, T. Jiang, Z. Liu, Y. Chang, X. Zhang, J. He, Wacker oxidation of 1-hexene in 1-*n*-butyl-3-methylimidazolium hexafluorophosphate ([bmim][PF_6]), supercritical (SC) CO_2, and SC CO_2/[bmim][PF_6] mixed solvent, *New J. Chem.* **2002**, *26*, 1246-1248.

[346] M. F. Sellin, P. B. Webb, D. J. Cole-Hamilton, Continuous flow homogeneous catalysis: hydroformylation of alkenes in supercritical fluid–ionic liquid biphasic mixtures, *ChemComm* **2001**, 781-782.

[347] P. B. Webb, M. F. Sellin, T. E. Kunene, S. Williamson, A. M. Slawin, D. J. Cole-Hamilton, Continuous flow hydroformylation of alkenes in supercritical fluid–ionic liquid biphasic systems, *J. Am. Chem. Soc.* **2003**, *125*, 15577-15588.

[348] F. Zayed, L. Greiner, P. S. Schulz, A. Lapkin, W. Leitner, Continuous catalytic Friedel–Crafts acylation in the biphasic medium of an ionic liquid and supercritical carbon dioxide, *ChemComm* **2008**, 79-81.

[349] M. North, Synthesis of cyclic carbonates from epoxides and carbon dioxide using bimetallic aluminium(salen) complexes, *Arkivoc* **2012**, *(i)*, 610-628.

[350] Y. Gu, G. Li, Ionic liquids-based catalysis with solids: state of the art, *ASC* **2009**, *351*, 817-847.

[351] A. Riisager, R. Fehrmann, M. Haumann, P. Wasserscheid, Supported Ionic Liquid Phase (SILP) systems–novel fixed bed reactor concepts for homogeneous catalisis in continuous fixed-bed reactors, *Eur. J. Inorg. Chem* **2006**, 695-706.

[352] M. Haumann, A. Riisager, Hydroformylation in room temperature ionic liquids (RTILs): catalyst and process developments, *Chem. Rev.* **2008**, *108*, 1474-1497.

[353] C. Aprile, F. Giacalone, M. Gruttadauria, A. M. Marculescu, R. Noto, J. D. Revell, H. Wennemers, New ionic liquid-modified silica gels as recyclable materials for L-proline-or H–Pro–Pro–Asp–NH_2-catalyzed aldol reaction, *Green Chem.* **2007**, *9*, 1328-1334.

[354] M. Gruttadauria, S. Riela, C. Aprile, P. L. Meo, F. D'Anna, R. Noto, Supported ionic liquids. New recyclable materials for the L-proline-catalyzed aldol reaction, *ASC* **2006**, *348*, 82-92.

[355] A. Riisager, P. Wasserscheid, R. van Hal, R. Fehrmann, Continuous fixed-bed gas-phase hydroformylation using supported ionic liquid-phase (SILP) Rh catalysts, *J. Catal.* **2003**, *219*, 452-455.

[356] U. Kernchen, B. Etzold, W. Korth, A. Jess, Solid catalyst with ionic liquid layer (SCILL) – A new concept to improve selectivity illustrated by hydrogenation of cyclooctadiene, *Chem. Eng. Technol.* **2007**, *30*, 985-994.

[357] P. Virtanen, T. O. Salmi, J.-P. Mikkola, Supported Ionic Liquid Catalysts (SILCA) for preparation of organic chemicals, *Top. Catal.* **2010**, *53*, 1096-1103.

[358] M. I. Burguete, E. García-Verdugo, I. Garcia-Villar, F. Gelat, P. Licence, S. V. Luis, V. Sans, Pd catalysts immobilized onto gel-supported ionic liquid-like phases (*g*-SILLPs): A remarkable effect of the nature of the support, *J. Catal.* **2010**, *269*, 150-160.

[359] U. Hintermair, Z. Gong, A. Serbanovic, M. J. Muldoon, C. C. Santini, D. J. Cole-Hamilton, Continuous flow hydroformylation using supported ionic liquid phase catalysts with carbon dioxide as a carrier, *Dalton Trans.* **2010**, *39*, 8501-8510.

[360] H. Hagiwara, T. Kuroda, T. Hoshi, T. Suzuki, Immobilization of MacMillan Imidazolidinone as Mac-SILC and its Catalytic Performance on Sustainable Enantioselective Diels–Alder Cycloaddition, *ASC* **2010**, *352*, 909-916.

[361] C. P. Mehnert, R. A. Cook, N. C. Dispenziere, M. Afeworki, Supported ionic liquid catalysis– A new concept for homogeneous hydroformylation catalysis, *J. Am. Chem. Soc.* **2002**, *124*, 12932-12933.

[362] C. Aprile, F. Giacalone, P. Agrigento, L. F. Liotta, J. A. Martens, P. P. Pescarmona, M. Gruttadauria, Multilayered supported ionic liquids as catalysts for chemical fixation of carbon dioxide: A high-throughput study in supercritical conditions, *ChemSusChem* **2011**, *4*, 1830-1837.

[363] B. M. Dioos, I. F. Vankelecom, P. A. Jacobs, Aspects of immobilisation of catalysts on polymeric supports, *ASC* **2006**, *348*, 1413-1446.

[364] F. Cozzi, Immobilization of organic catalysts: when, why, and how, *ASC* **2006**, *348*, 1367-1390.

[365] A. Corma, H. Garcia, Silica-bound homogenous catalysts as recoverable and reusable catalysts in organic synthesis, *ASC* **2006**, *348*, 1391-1412.

[366] P. Virtanen, J.-P. Mikkola, E. Toukoniitty, H. Karhu, K. Kordas, K. Eränen, J. Wärnå, T. Salmi, Supported ionic liquid catalysts—From batch to continuous operation in preparation of fine chemicals, *Catal. Today* **2009**, *147*, S144-S148.

[367] M. Valkenberg, C. DeCastro, W. Hölderich, Immobilisation of ionic liquids on solid supports, *Green Chem.* **2002**, *4*, 88-93.

[368] S. Breitenlechner, M. Fleck, T. E. Müller, A. Suppan, Solid catalysts on the basis of supported ionic liquids and their use in hydroamination reactions, *J Mol. Catal. A: Chem.* **2004**, *214*, 175-179.

[369] D. W. Kim, D. Y. Chi, Polymer-supported ionic liquids: imidazolium salts as catalysts for nucleophilic substitution reactions including fluorinations, *Angew. Chem. Int. Ed.* **2004**, *43*, 483-485.

[370] A. Riisager, R. Fehrmann, S. Flicker, R. van Hal, M. Haumann, P. Wasserscheid, Very stable and highly regioselective supported ionic-liquid-phase (SILP) catalysis: continuous-flow fixed-bed hydroformylation of propene, *Angew. Chem. Int. Ed.* **2005**, *44*, 815-819.

[371] F. Shi, Q. Zhang, D. Li, Y. Deng, Silica-gel-confined ionic liquids: a new attempt for the development of supported nanoliquid catalysis, *Chem. Eur. J.* **2005**, *11*, 5279-5288.

[372] R. T. Carlin, T. H. Cho, J. Fuller, Catalytic immobilized ionic liquid membranes, *Proc. Electrochem. Soc.* **1998**, *1998-11*, 180-186.

[373] P. Virtanen, H. Karhu, G. Toth, K. Kordas, J.-P. Mikkola, Towards one-pot synthesis of menthols from citral: modifying supported ionic liquid catalysts (SILCAs) with Lewis and Brønsted acids, *J. Catal.* **2009**, *263*, 209-219.

[374] T. Takahashi, T. Watahiki, S. Kitazume, H. Yasuda, T. Sakakura, Synergistic hybrid catalyst for cyclic carbonate synthesis: Remarkable acceleration caused by immobilization of homogeneous catalyst on silica, *ChemComm* **2006**, 1664-1666.

[375] J.-Q. Wang, D.-L. Kong, J.-Y. Chen, F. Cai, L.-N. He, Synthesis of cyclic carbonates from epoxides and carbon dioxide over silica-supported quaternary ammonium salts under supercritical conditions, *J Mol. Catal. A: Chem.* **2006**, *249*, 143-148.

[376] J.-Q. Wang, X.-D. Yue, F. Cai, L.-N. He, Solventless synthesis of cyclic carbonates from carbon dioxide and epoxides catalyzed by silica-supported ionic liquids under supercritical conditions, *Catal. Commun.* **2007**, *8*, 167-172.

[377] L. Han, S.-W. Park, D.-W. Park, Silica grafted imidazolium-based ionic liquids: efficient heterogeneous catalysts for chemical fixation of CO_2 to a cyclic carbonate, *Energy Environ. Sci.* **2009**, *2*, 1286-1292.

[378] K. Motokura, S. Itagaki, Y. Iwasawa, A. Miyaji, T. Baba, Silica-supported aminopyridinium halides for catalytic transformations of epoxides to cyclic carbonates under atmospheric pressure of carbon dioxide, *Green Chem.* **2009**, *11*, 1876-1880.

[379] S. Chen, C. Han, C. Tsai, J. Huang, Y. Chen-Yang, Effect of morphological properties of ionic liquid-templated mesoporous anatase TiO_2 on performance of PEMFC with Nafion/TiO_2 composite membrane at elevated temperature and low relative humidity, *J. Power Sources* **2007**, *171*, 363-372.

[380] Z. Zhang, L. Wu, J. Dong, B.-G. Li, S. Zhu, Preparation and SO_2 sorption/desorption behavior of an ionic liquid supported on porous silica particles, *Ind. Eng. Chem. Res.* **2009**, *48*, 2142-2148.

[381] O. C. Vangeli, G. E. Romanos, K. G. Beltsios, D. Fokas, E. P. Kouvelos, K. L. Stefanopoulos, N. K. Kanellopoulos, Grafting of imidazolium based ionic liquid on the pore surface of nanoporous materials-study of physicochemical and thermodynamic properties, *J. Phys. Chem. B* **2010**, *114*, 6480-6491.

[382] G. Fang, J. Chen, J. Wang, J. He, S. Wang, *N*-Methylimidazolium ionic liquid-functionalized silica as a sorbent for selective solid-phase extraction of 12 sulfonylurea herbicides in environmental water and soil samples, *J. Chromatogr. A* **2010**, *1217*, 1567-1574.

[383] C. P. Mehnert, Supported ionic liquid catalysis, *Chemistry–A European Journal* **2005**, *11*, 50-56.

[384] F. Kohler, D. Roth, E. Kuhlmann, P. Wasserscheid, M. Haumann, Continuous gas-phase desulfurisation using supported ionic liquid phase (SILP) materials, *Green Chem.* **2010**, *12*, 979-984.

[385] A. Riisager, R. Fehrmann, M. Haumann, P. Wasserscheid, Supported ionic liquid phase (SILP) catalysis: An innovative concept for homogeneous catalysis in continuous fixed-bed reactors, *Eur. J. Inorg. Chem.* **2006**, *2006*, 695-706.

[386] J. Zhang, Y. Ma, F. Shi, L. Liu, Y. Deng, Room temperature ionic liquids as templates in the synthesis of mesoporous silica via a sol–gel method, *Micropor. Mesopor. Mat.* **2009**, *119*, 97-103.

[387] J. Lemus, J. Palomar, M. A. Gilarranz, J. J. Rodriguez, Characterization of supported ionic liquid phase (SILP) materials prepared from different supports, *Adsorption* **2011**, *17*, 561-571.

[388] A. Vioux, L. Viau, S. Volland, J. Le Bideau, Use of ionic liquids in sol-gel; ionogels and applications, *C. R. Chim.* **2010**, *13*, 242-255.

[389] A. Sun, J. Zhang, C. Li, H. Meng, Gas phase conversion of carbon tetrachloride to alkyl chlorides catalyzed by supported ionic liquids, *Chinese J. Chem.* **2009**, *27*, 1741-1748.

[390] N. Fontanals, S. Ronka, F. Borrull, A. W. Trochimczuk, R. M. Marcé, Supported imidazolium ionic liquid phases: A new material for solid-phase extraction, *Talanta* **2009**, *80*, 250-256.

[391] S. Werner, N. Szesni, A. Bittermann, M. J. Schneider, P. Härter, M. Haumann, P. Wasserscheid, Screening of Supported Ionic Liquid Phase (SILP) catalysts for the very low temperature water–gas-shift reaction, *Appl. Catal. A: Gen.* **2010**, *377*, 70-75.

[392] J. Joni, M. Haumann, P. Wasserscheid, Continuous gas-phase isopropylation of toluene and cumene using highly acidic Supported Ionic Liquid Phase (SILP) catalysts, *Appl. Catal. A: Gen.* **2010**, *372*, 8-15.

[393] A. Riisager, R. Fehrmann, M. Haumann, B. S. Gorle, P. Wasserscheid, Stability and kinetic studies of supported ionic liquid phase catalysts for hydroformylation of propene, *Ind. Eng. Chem. Res.* **2005**, *44*, 9853-9859.

[394] A. Riisager, R. Fehrmann, M. Haumann, P. Wasserscheid, Supported ionic liquids: versatile reaction and separation media, *Top. Catal.* **2006**, *40*, 91-102.

[395] P. Virtanen, H. Karhu, K. Kordas, J.-P. Mikkola, The effect of ionic liquid in supported ionic liquid catalysts (SILCA) in the hydrogenation of α,β-unsaturated aldehydes, *Chem. Eng. Sci.* **2007**, *62*, 3660-3671.

[396] M. Ruta, G. Laurenczy, P. J. Dyson, L. Kiwi-Minsker, Pd nanoparticles in a supported ionic liquid phase: Highly stable catalysts for selective acetylene hydrogenation under continuous-flow conditions, *J. Phys. Chem. C* **2008**, *112*, 17814-17819.

[397] W. Wu, B. Han, H. Gao, Z. Liu, T. Jiang, J. Huang, Desulfurization of flue gas: SO_2 absorption by an ionic liquid, *Angew. Chem. Int. Ed.* **2004**, *43*, 2415-2417.

[398] J. Huang, A. Riisager, P. Wasserscheid, R. Fehrmann, Reversible physical absorption of SO_2 by ionic liquids, *ChemComm* **2006**, 4027-4029.

[399] J. Ilconich, C. Myers, H. Pennline, D. Luebke, Experimental investigation of the permeability and selectivity of supported ionic liquid membranes for CO_2/He separation at temperatures up to 125° C, *J. Membr. Sci.* **2007**, *298*, 41-47.

[400] J. E. Bara, T. K. Carlisle, C. J. Gabriel, D. Camper, A. Finotello, D. L. Gin, R. D. Noble, Guide to CO_2 separations in imidazolium-based room-temperature ionic liquids, *Ind. Eng. Chem. Res.* **2009**, *48*, 2739-2751.

[401] A. Riisager, K. M. Eriksen, P. Wasserscheid, R. Fehrmann, Propene and 1-octene hydroformylation with silica-supported, ionic liquid-phase (SILP) Rh-phosphine catalysts in continuous fixed-bed mode, *Catal. Lett.* **2003**, *90*, 149-153.

[402] R. Ciriminna, P. Hesemann, J. J. E. Moreau, M. Carraro, S. Campestrini, M. Pagliaro, Aerobic oxidation of alcohols in carbon dioxide with silica-supported ionic liquids doped with perruthenate, *Chem. Eur. J.* **2006**, *12*, 5220-5224.

[403] Y. Xie, Z. Zhang, S. Hu, J. Song, W. Li, B. Han, Aerobic oxidation of benzyl alcohol in supercritical CO_2 catalyzed by perruthenate immobilized on polymer supported ionic liquid, *Green Chem.* **2008**, *10*, 278-282.

[404] U. Hintermair, G. Zhao, C. C. Santini, M. J. Muldoon, D. J. Cole-Hamilton, Supported ionic liquid phase catalysis with supercritical flow, *ChemComm* **2007**, 1462-1464.

[405] R. Fehrmann, A. Riisager, M. Haumann, *Supported ionic liquids: fundamentals and applications*, John Wiley & Sons, **2014**.

[406] U. Hintermair, T. Höfener, T. Pullmann, G. Franciò, W. Leitner, Continuous enantioselective hydrogenation with a molecular catalyst in supported ionic liquid phase under supercritical CO_2 flow, *ChemCatChem* **2010**, *2*, 150-154.

[407] U. Hintermair, G. Franciò, W. Leitner, A fully integrated continuous-flow system for asymmetric catalysis: enantioselective hydrogenation with supported ionic liquid phase catalysts using supercritical CO_2 as the mobile phase, *Chem. Eur. J.* **2013**, *19*, 4538-4547.

[408] G. B. Celli, A. Ghanem, M. S. L. Brooks, Haskap berries (*Lonicera caerulea* L.) — A critical review of antioxidant capacity and health-related studies for potential value-added products, *Food Bioproc. Tech.* **2014**, *7*, 1541-1554.

[409] O. Jerzy, Lonicera caerulea, https://commons.wikimedia.org/wiki/File:Lonicera_coerulea_a3.jpg, (accessed 20 February 2023).

[410] A. Z. Kucharska, I. Fecka, Identification of iridoids in edible honeysuckle berries (*Lonicera caerulea* L. var. kamtschatica Sevast.) by UPLC-ESI-qTOF-MS/MS, *Molecules* **2016**, *21*, 1157.

[411] A. Z. Kucharska, A. Sokół-Łętowska, J. Oszmiański, N. Piórecki, I. Fecka, Iridoids, phenolic compounds and antioxidant activity of edible honeysuckle berries (*Lonicera caerulea* var. *kamtschatica Sevast.*), *Molecules* **2017**, *22*, 405.

[412] J. Oszmiański, A. Wojdyło, S. Lachowicz, Effect of dried powder preparation process on polyphenolic content and antioxidant activity of blue honeysuckle berries (*Lonicera caerulea* L. var. *kamtschatica*), *LWT* **2016**, *67*, 214-222.

[413] E. Kaczmarska, J. Gawronski, M. Dyduch-Sieminska, A. Najda, W. Marecki, J. Zebrowska, Genetic diversity and chemical characterization of selected Polish and Russian cultivars and clones of blue honeysuckle (*Lonicera caerulea*), *Turk. J. Agric. For.* **2015**, *39*, 394-402.

[414] K. Skupień, J. Oszmiański, I. Ochmian, J. Grajkowski, Characterization of selected physico-chemical features of blue honeysuckle fruit cultivar Zielona, *Pol. J. Nat. Sci* **2007**, *4*, 101-107.

[415] M. Gołba, A. Sokół-Łętowska, A. Z. Kucharska, Health properties and composition of honeysuckle berry *Lonicera caerulea* L. An update on recent studies, *Molecules* **2020**, *25*, 749.

[416] M. Senica, M. Bavec, F. Stampar, M. Mikulic-Petkovsek, Blue honeysuckle (*Lonicera caerulea* subsp. *edulis* (Turcz. ex Herder) Hultén.) berries and changes in their ingredients across different locations, *J. Sci. Food Agric.* **2018**, *98*, 3333-3342.

[417] T. Jurikova, O. Rop, J. Mlcek, J. Sochor, S. Balla, L. Szekeres, A. Hegedusova, J. Hubalek, V. Adam, R. Kizek, Phenolic profile of edible honeysuckle berries (genus *Lonicera*) and their biological effects, *Molecules* **2012**, *17*, 61-79.

[418] I. Svarcova, J. Heinrich, K. Valentova, Berry fruits as a source of biologically active compounds: the case of *Lonicera caerulea*, *Biomed. Pap. Med. Fac. Univ. Palacky Olomouc Czech Repub.* **2007**, *151*.

[419] J. W. Finley, F. Shahidi, The chemistry, processing, and health benefits of highly Unsaturated fatty acids: an overview, in *Omega-3 fatty acids, Vol. 788*, American Chemical Society Symposium Series, **2001**, pp. 2-11.

[420] R. Tundis, M. R. Loizzo, F. Menichini, G. A. Statti, F. Menichini, Biological and pharmacological activities of iridoids: recent developments, *Mini Rev. Med. Chem.* **2008**, *8*, 399-420.

[421] Ø. M. Andersen, M. Jordheim, Anthocyanins, in *Encyclopedia of life sciences (ELS)*, John Wiley & Sons, Ltd: Chichester, **2010**, pp. 1-12.

[422] T. Pervaiz, J. Songtao, F. Faghihi, M. S. Haider, J. Fang, Naturally occurring anthocyanin, structure, functions and biosynthetic pathway in fruit plants, *J. Plant. Biochem. Physiol.* **2017**, *5*, 1-9.

[423] A. Wojdyło, P. N. N. Jáuregui, A. n. A. Carbonell-Barrachina, J. Oszmiański, T. Golis, Variability of phytochemical properties and content of bioactive compounds in *Lonicera caerulea* L. var. *kamtschatica* berries, *J. Agric. Food Chem.* **2013**, *61*, 12072-12084.

[424] I. Palíková, J. Heinrich, P. Bednář, P. Marhol, V. r. Křen, L. Cvak, K. i. Valentová, F. Růžička, V. Holá, M. Kolář, Constituents and antimicrobial properties of blue honeysuckle: a novel source for phenolic antioxidants, *J. Agric. Food Chem.* **2008**, *56*, 11883-11889.

[425] A. Garcia, A. De Lucas, J. Rincón, A. Alvarez, I. Gracia, M. García, Supercritical carbon dioxide extraction of fatty and waxy material from rice bran, *J. Am. Oil Chem. Soc.* **1996**, *73*, 1127-1131.

[426] S. Vidović, I. Mujić, Z. Zeković, Ž. Lepojević, S. Milošević, S. Jokić, Extraction of fatty acids from *Boletus edulis* by subcritical and supercritical carbon dioxide, *J. Am. Oil Chem. Soc.* **2011**, *88*, 1189-1196.

[427] J. Suomi, H. Sirén, K. Hartonen, M.-L. Riekkola, Extraction of iridoid glycosides and their determination by micellar electrokinetic capillary chromatography, *J. Chromatogr. A* **2000**, *868*, 73-83.

[428] R. P. Metivier, F. J. Francis, F. M. Clydesdale, Solvent extraction of anthocyanins from wine pomace, *J. Food Sci.* **1980**, *45*, 1099-1100.

[429] C. Garcia-Viguera, P. Zafrilla, F. A. Tomás-Barberán, The use of acetone as an extraction solvent for anthocyanins from strawberry fruit, *Phytochem. Anal.* **1998**, *9*, 274-277.

[430] A. Kazan, C. Sevimli-Gur, O. Yesil-Celiktas, N. T. Dunford, Investigating anthocyanin contents and in vitro tumor suppression properties of blueberry extracts prepared by various processes, *Eur. Food Res. Technol.* **2016**, *242*, 693-701.

[431] L. G. Müller, L. de Andrade Salles, S. Sakamoto, A. C. Stein, S. T. Cargnin, E. Cassel, R. F. Vargas, S. M. K. Rates, G. L. von Poser, Effect of storage time and conditions on the diene valepotriates content of the extract of Valeriana glechomifolia obtained by supercritical carbon dioxide, *Phytochem. Anal.* **2012**, *23*, 222-227.

[432] Ł. Woźniak, K. Marszałek, S. Skąpska, Extraction of phenolic compounds from sour cherry pomace with supercritical carbon dioxide: Impact of process parameters on the composition and antioxidant properties of extracts, *Sep. Sci. Technol.* **2016**, *51*, 1472-1479.

[433] S. Kerbstadt, L. Eliasson, A. Mustafa, L. Ahrné, Effect of novel drying techniques on the extraction of anthocyanins from bilberry press cake using supercritical carbon dioxide, *Innov. Food Sci. Emerg. Technol.* **2015**, *29*, 209-214.

[434] J. Wang, B. Liu, Y. Chang, Optimization of supercritical fluid extraction of geniposidic acid from plantain seeds using response surface methodology, *Green Chem. Lett. Rev.* **2014**, *7*, 309-316.

[435] A. A. Patil, B. S. Sachin, D. B. Shinde, P. S. Wakte, Supercritical CO_2 assisted extraction and LC–MS identification of picroside I and picroside II from *Picrorhiza kurroa*, *Phytochem. Anal.* **2013**, *24*, 97-104.

[436] F. J. Leyva-Jiménez, J. Lozano-Sánchez, Á. Fernández-Ochoa, M. d. l. L. Cádiz-Gurrea, D. Arráez-Román, A. Segura-Carretero, Optimized extraction of phenylpropanoids and flavonoids from lemon verbena leaves by supercritical fluid system using response surface methodology, *Foods* **2020**, *9*, 931.

[437] Y. M. Monroy, R. A. Rodrigues, A. Sartoratto, F. A. Cabral, Optimization the extraction of phenolic compounds from purple corn cob (*Zea mays* L.) by sequential extraction using supercritical carbon dioxide, ethanol and water as solvents, *J. Supercrit. Fluids.* **2016**, *116*, 10-19.

[438] J. T. Paula, L. C. Paviani, M. A. Foglio, I. M. Sousa, G. H. Duarte, M. P. Jorge, M. N. Eberlin, F. A. Cabral, Extraction of anthocyanins and luteolin from *Arrabidaea chica* by sequential extraction

in fixed bed using supercritical CO$_2$, ethanol and water as solvents, *J. Supercrit. Fluids.* **2014**, *86*, 100-107.

[439] M. del-Pilar-Garcia-Mendoza, F. A. Espinosa-Pardo, A. M. Baseggio, G. F. Barbero, M. R. M. Junior, M. A. Rostagno, J. Martínez, Extraction of phenolic compounds and anthocyanins from juçara (*Euterpe edulis* Mart.) residues using pressurized liquids and supercritical fluids, *J. Supercrit. Fluids.* **2017**, *119*, 9-16.

[440] Z. Idham, A. S. Zaini, N. R. Putra, N. M. Rusli, N. S. Mahat, L. N. Yian, M. A. C. Yunus, Effect of flow rate, particle size and modifier ratio on the supercritical fluid extraction of anthocyanins from *Hibiscus sabdariffa* (L), in *IOP Conference Series: Materials Science and Engineering, Vol. 932*, IOP Publishing, **2020**, p. 012031.

[441] P. Pereira, M.-J. Cebola, M. C. Oliveira, M. G. Bernardo-Gil, Supercritical fluid extraction vs conventional extraction of myrtle leaves and berries: Comparison of antioxidant activity and identification of bioactive compounds, *J. Supercrit. Fluids.* **2016**, *113*, 1-9.

[442] C. d. C. R. Batista, M. S. de Oliveira, M. E. Araújo, A. M. Rodrigues, J. R. S. Botelho, A. P. da Silva Souza Filho, N. T. Machado, R. N. C. Junior, Supercritical CO$_2$ extraction of açaí (*Euterpe oleracea*) berry oil: Global yield, fatty acids, allelopathic activities, and determination of phenolic and anthocyanins total compounds in the residual pulp, *J. Supercrit. Fluids.* **2016**, *107*, 364-369.

[443] D. Chatterjee, N. T. Jadhav, P. Bhattacharjee, Solvent and supercritical carbon dioxide extraction of color from eggplants: Characterization and food applications, *LWT* **2013**, *51*, 319-324.

[444] Z. Ahmadian-Kouchaksaraie, R. Niazmand, Supercritical carbon dioxide extraction of antioxidants from *Crocus sativus* petals of saffron industry residues: Optimization using response surface methodology, *J. Supercrit. Fluids.* **2017**, *121*, 19-31.

[445] G. Jiao, Extraction of anthocyanins from haskap berry pulp using supercritical carbon dioxide: Influence of co-solvent composition and pretreatment, *LWT* **2018**, *98*, 237-244.

[446] H. Wang, G. Gurau, R. D. Rogers, Dissolution of biomass using ionic liquids, in *Structures and Interactions of Ionic Liquids* (Eds.: S. Zhang, J. Wang, X. Lu, Q. Zhou), Springer Verlag Berlin Heidelberg, Berlin, Heidelberg, **2014**, pp. 79-105.

[447] C. Kornpointner, A. Sainz Martinez, M. Schnürch, H. Halbwirth, K. Bica-Schröder, Combined ionic liquid and supercritical carbon dioxide based dynamic extraction of six cannabinoids from *Cannabis sativa* L, *Green Chem.* **2021**, *23*, 10079-10089.

[448] M. F. Demirbas, M. Balat, H. Balat, Potential contribution of biomass to the sustainable energy development, *Energy Convers. Manage.* **2009**, *50*, 1746-1760.

[449] J.-S. Kim, S.-C. Park, J.-W. Kim, J. C. Park, S.-M. Park, J.-S. Lee, Production of bioethanol from lignocellulose: Status and perspectives in Korea, *Bioresour. Technol.* **2010**, *101*, 4801-4805.

[450] I. Lewandowski, Lignocellulosic Energy Cropslignocellulose/lignocellulosicenergy crops, Production and Provision, in *Encyclopedia of Sustainability Science and Technology* (Ed.: R. A. Meyers), Springer New York, New York, **2012**, pp. 6019-6030.

[451] I. Hasanov, M. Raud, T. Kikas, The role of ionic liquids in the lignin separation from lignocellulosic biomass, *Energies* **2020**, *13*, 4864.

[452] T. Heinze, K. Schwikal, S. Barthel, Ionic liquids as reaction medium in cellulose functionalization, *Macromol. Biosci.* **2005**, *5*, 520-525.

[453] H. Ohno, Y. Fukaya, Task specific ionic liquids for cellulose technology, *Chem. Lett.* **2009**, *38*, 2-7.

[454] B. Kosan, C. Michels, F. Meister, Dissolution and forming of cellulose with ionic liquids, *Cellulose* **2008**, *15*, 59-66.

[455] Y. Fukaya, K. Hayashi, M. Wada, H. Ohno, Cellulose dissolution with polar ionic liquids under mild conditions: required factors for anions, *Green Chem.* **2008**, *10*, 44-46.

[456] N. Sun, H. Rodriguez, M. Rahman, R. D. Rogers, Where are ionic liquid strategies most suited in the pursuit of chemicals and energy from lignocellulosic biomass?, *ChemComm* **2011**, *47*, 1405-1421.

[457] Y. Pu, N. Jiang, A. J. Ragauskas, Ionic liquid as a green solvent for lignin, *J. Wood Chem. Technol.* **2007**, *27*, 23-33.

[458] N. Sun, M. Rahman, Y. Qin, M. L. Maxim, H. Rodríguez, R. D. Rogers, Complete dissolution and partial delignification of wood in the ionic liquid 1-ethyl-3-methylimidazolium acetate, *Green Chem.* **2009**, *11*, 646-655.

[459] B. Li, J. Asikkala, I. Filpponen, D. S. Argyropoulos, Factors affecting wood dissolution and regeneration of ionic liquids, *Ind. Eng. Chem. Res.* **2010**, *49*, 2477-2484.

[460] Y. Cao, J. Wu, J. Zhang, H. Li, Y. Zhang, J. He, Room temperature ionic liquids (RTILs): A new and versatile platform for cellulose processing and derivatization, *Chem. Eng. J.* **2009**, *147*, 13-21.

[461] C. L. McCormick, T. R. Dawsey, Preparation of cellulose derivatives via ring-opening reactions with cyclic reagents in lithium chloride/*N*,*N*-dimethylacetamide, *Macromolecules* **1990**, *23*, 3606-3610.

[462] S. Fischer, W. Voigt, K. Fischer, The behaviour of cellulose in hydrated melts of the composition LiX¢n H_2O (X= I⁻, NO_3^-, CH_3COO^-, ClO_4^-), *Cellulose* **1999**, *6*, 213-219.

[463] H. Zhang, J. Wu, J. Zhang, J. He, 1-Allyl-3-methylimidazolium chloride room temperature ionic liquid: a new and powerful nonderivatizing solvent for cellulose, *Macromolecules* **2005**, *38*, 8272-8277.

[464] H. Luo, Y. Li, C. Zhou, Study on the dissolubility of the cellulose in the functionalized ionic liquid, *Polym. Mater. Sci. Eng.* **2005**, *21*, 233-235.

[465] S. T. Handy, Greener solvents: room temperature ionic liquids from biorenewable sources, *Chem. Eur. J.* **2003**, *9*, 2938-2944.

[466] Y. Fukaya, A. Sugimoto, H. Ohno, Superior solubility of polysaccharides in low viscosity, polar, and halogen-free 1,3-dialkylimidazolium formates, *Biomacromolecules* **2006**, *7*, 3295-3297.

[467] H. Zhao, G. A. Baker, Z. Song, O. Olubajo, T. Crittle, D. Peters, Designing enzyme-compatible ionic liquids that can dissolve carbohydrates, *Green Chem.* **2008**, *10*, 696-705.

[468] H. Zhao, C. L. Jones, J. V. Cowins, Lipase dissolution and stabilization in ether-functionalized ionic liquids, *Green Chem.* **2009**, *11*, 1128-1138.

[469] J. Zakzeski, P. C. Bruijnincx, A. L. Jongerius, B. M. Weckhuysen, The catalytic valorization of lignin for the production of renewable chemicals, *Chem. Rev.* **2010**, *110*, 3552-3599.

[470] S. H. Lee, T. V. Doherty, R. J. Linhardt, J. S. Dordick, Ionic liquid-mediated selective extraction of lignin from wood leading to enhanced enzymatic cellulose hydrolysis, *Biotechnol. Bioeng.* **2009**, *102*, 1368-1376.

[471] M. Rahman, N. Sun, Y. Qin, M. L. Maxim, R. D. Rogers, Ionic liquid systems for the processing of biomass, their components and/or derivatives, and mixtures thereof, WO 2010056790 A1, **20 May 2010.**

[472] R. Sun, J. Tomkinson, P. Ma, S. Liang, Comparative study of hemicelluloses from rice straw by alkali and hydrogen peroxide treatments, *Carbohydr. Polym.* **2000**, *42*, 111-122.

[473] J. Ren, R. Sun, C. Liu, Z. Cao, W. Luo, Acetylation of wheat straw hemicelluloses in ionic liquid using iodine as a catalyst, *Carbohydr. Polym.* **2007**, *70*, 406-414.

[474] J. Nemirowsky, Ueber die Einwirkung von Chlorkohlenoxyd auf Aethylenglycol; vorläufige Mittheilung, *J. Prakt. Chem.* **1883**, *28*, 439-440.

[475] M. Selva, A. Caretto, M. Noè, A. Perosa, Carbonate phosphonium salts as catalysts for the transesterification of dialkyl carbonates with diols. The competition between cyclic carbonates and linear dicarbonate products, *Org. Biomol. Chem.* **2014**, *12*, 4143-4155.

[476] M. Pena-Lopez, H. Neumann, M. Beller, Iron-catalyzed synthesis of five-membered cyclic carbonates from vicinal diols: urea as sustainable carbonylation agent, *Eur. J. Org. Chem* **2016**, *2016*, 3721-3727.

[477] B. Gabriele, R. Mancuso, G. Salerno, L. Veltri, M. Costa, A. Dibenedetto, A general and xpedient synthesis of 5-and 6-membered cyclic carbonates by palladium-catalyzed oxidative carbonylation of 1,2-and 1,3-diols, *ChemSusChem* **2011**, *4*, 1778-1786.

[478] F. D. Bobbink, W. Gruszka, M. Hulla, S. Das, P. J. Dyson, Synthesis of cyclic carbonates from diols and CO_2 catalyzed by carbenes, *ChemComm* **2016**, *52*, 10787-10790.

[479] T. Hirose, S. Shimizu, S. Qu, H. Shitara, K. Kodama, L. Wang, Economical synthesis of cyclic carbonates from carbon dioxide and halohydrins using K_2CO_3, *RSC Adv.* **2016**, *6*, 69040-69044.

[480] K. Chen, G. Shi, R. Dao, K. Mei, X. Zhou, H. Li, C. Wang, Tuning the basicity of ionic liquids for efficient synthesis of alkylidene carbonates from CO_2 at atmospheric pressure, *ChemComm* **2016**, *52*, 7830-7833.

[481] J. Wu, J. A. Kozak, F. Simeon, T. A. Hatton, T. F. Jamison, Mechanism-guided design of flow systems for multicomponent reactions: conversion of CO_2 and olefins to cyclic carbonates, *Chem. Sci.* **2014**, *5*, 1227-1231.

[482] H. Büttner, L. Longwitz, J. Steinbauer, C. Wulf, T. Werner, Recent developments in the synthesis of cyclic carbonates from epoxides and CO_2, in *Chemical Transformations of Carbon Dioxide* (Eds.: X.-F. Wu, M. Beller), Springer International Publishing, Cham, Switzerland, **2017**, pp. 89-144.

[483] P. P. Pescarmona, Cyclic carbonates synthesised from CO_2: Applications, challenges and recent research trends, *Curr. Opin. Green Sustain. Chem.* **2021**, *29*, 100457.

[484] E. J. Lopes, A. P. Ribeiro, L. M. Martins, New trends in the conversion of CO_2 to cyclic carbonates, *Catalysts* **2020**, *10*, 479.

[485] K. Kiatkittipong, M. A. A. Mohamad Shukri, W. Kiatkittipong, J. W. Lim, P. L. Show, M. K. Lam, S. Assabumrungrat, Green pathway in utilizing CO_2 via cycloaddition reaction with epoxide — A mini review, *Processes* **2020**, *8*, 548.

[486] A. Sainz Martinez, C. Hauzenberger, A. R. Sahoo, Z. Csendes, H. Hoffmann, K. Bica, Continuous Conversion of Carbon Dioxide to Propylene Carbonate with Supported Ionic Liquids, *ACS Sustain. Chem. Eng.* **2018**, *6*, 13131-13139.

[487] C. Claver, M. B. Yeamin, M. Reguero, A. M. Masdeu-Bultó, Recent advances in the use of catalysts based on natural products for the conversion of CO_2 into cyclic carbonates, *Green Chem.* **2020**, *22*, 7665-7706.

[488] A. Rehman, F. Saleem, F. Javed, A. Ikhlaq, S. W. Ahmad, A. Harvey, Recent advances in the synthesis of cyclic carbonates via CO_2 cycloaddition to epoxides, *J. Environ. Chem. Eng.* **2021**, *9*, 105113.

[489] M. Aresta, *Carbon dioxide recovery and utilization*, Springer Science & Business Media, Netherlands, **2013**.

[490] Q. Liu, L. Wu, R. Jackstell, M. Beller, Using carbon dioxide as a building block in organic synthesis, *Nat. Commun.* **2015**, *6*, 5933.

[491] I. Omae, Recent developments in carbon dioxide utilization for the production of organic chemicals, *Coord. Chem. Rev.* **2012**, *256*, 1384-1405.

[492] R. Nakano, S. Ito, K. Nozaki, Copolymerization of carbon dioxide and butadiene via a lactone intermediate, *Nat. Chem.* **2014**, *6*, 325-331.

[493] A. P. Dove, Chaining up carbon dioxide, *Nat. Chem.* **2014**, *6*, 276-277.

[494] G. Centi, S. Perathoner, Opportunities and prospects in the chemical recycling of carbon dioxide to fuels, *Catal. Today* **2009**, *148*, 191-205.

[495] X.-M. Liu, G. Lu, Z.-F. Yan, J. Beltramini, Recent advances in catalysts for methanol synthesis via hydrogenation of CO and CO_2, *Ind. Eng. Chem. Res.* **2003**, *42*, 6518-6530.

[496] K. M. K. Yu, I. Curcic, J. Gabriel, S. C. E. Tsang, Recent advances in CO_2 capture and utilization, *ChemSusChem* **2008**, *1*, 893-899.

[497] A. J. Kamphuis, F. Picchioni, P. P. Pescarmona, CO_2-fixation into cyclic and polymeric carbonates: principles and applications, *Green Chem.* **2019**, *21*, 406-448.

[498] G. Fiorani, W. Guo, A. W. Kleij, Sustainable conversion of carbon dioxide: the advent of organocatalysis, *Green Chem.* **2015**, *17*, 1375-1389.

[499] M. Cokoja, M. E. Wilhelm, M. H. Anthofer, W. A. Herrmann, F. E. Kühn, Synthesis of cyclic carbonates from epoxides and carbon dioxide by using organocatalysts, *ChemSusChem* **2015**, *8*, 2436-2454.

[500] F. D. Bobbink, P. J. Dyson, Synthesis of carbonates and related compounds incorporating CO_2 using ionic liquid-type catalysts: State-of-the-art and beyond, *J. Catal.* **2016**, *343*, 52-61.

[501] B.-H. Xu, J.-Q. Wang, J. Sun, Y. Huang, J.-P. Zhang, X.-P. Zhang, S.-J. Zhang, Fixation of CO_2 into cyclic carbonates catalyzed by ionic liquids: a multi-scale approach, *Green Chem.* **2015**, *17*, 108-122.

[502] M. H. Beyzavi, C. J. Stephenson, Y. Liu, O. Karagiaridi, J. T. Hupp, O. K. Farha, Metal–organic framework-based catalysts: chemical fixation of CO_2 with epoxides leading to cyclic organic carbonates, *Front. Energy Res.* **2015**, *2*, 63.

[503] A. C. Kathalikkattil, R. Babu, J. Tharun, R. Roshan, D.-W. Park, Advancements in the conversion of carbon dioxide to cyclic carbonates using metal organic frameworks as catalysts, *Catal. Surv. Asia* **2015**, *19*, 223-235.

[504] A. Decortes, A. M. Castilla, A. W. Kleij, Salen-complex-mediated formation of cyclic carbonates by cycloaddition of CO_2 to epoxides, *Angew. Chem. Int. Ed.* **2010**, *49*, 9822-9837.

[505] J. W. Comerford, I. D. Ingram, M. North, X. Wu, Sustainable metal-based catalysts for the synthesis of cyclic carbonates containing five-membered rings, *Green Chem.* **2015**, *17*, 1966-1987.

[506] V. D'Elia, J. D. Pelletier, J. M. Basset, Cycloadditions to epoxides catalyzed by group III–V transition-metal complexes, *ChemCatChem* **2015**, *7*, 1906-1917.

[507] B. Schaffner, F. Schaffner, S. P. Verevkin, A. Borner, Organic carbonates as solvents in synthesis and catalysis, *Chem. Rev.* **2010**, *110*, 4554-4581.

[508] V. Besse, F. Camara, C. Voirin, R. Auvergne, S. Caillol, B. Boutevin, Synthesis and applications of unsaturated cyclocarbonates, *Polym. Chem.* **2013**, *4*, 4545-4561.

[509] M. North, R. Pasquale, C. Young, Synthesis of cyclic carbonates from epoxides and CO_2, *Green Chem.* **2010**, *12*, 1514-1539.

[510] T. Sakakura, K. Kohno, The synthesis of organic carbonates from carbon dioxide, *ChemComm* **2009**, 1312-1330.

[511] P. P. Pescarmona, M. Taherimehr, Challenges in the catalytic synthesis of cyclic and polymeric carbonates from epoxides and CO_2, *Catal. Sci. Technol.* **2012**, *2*, 2169-2187.

[512] C. Jing-Xian, J. Bi, D. Wei-Li, D. Sen-Lin, C. Liu-Ren, C. Zong-Jie, L. Sheng-Lian, L. Xu-Biao, T. Xin-Man, A. Chak-Tong, Catalytic fixation of CO_2 to cyclic carbonates over biopolymer chitosan-grafted quarternary phosphonium ionic liquid as a recylable catalyst, *Appl. Catal. A: Gen.* **2014**, *484*, 26-32.

[513] X. Jin, P. Bobba, N. Reding, Z. Song, P. S. Thapa, G. Prasad, B. Subramaniam, R. V. Chaudhari, Kinetic modeling of carboxylation of propylene oxide to propylene carbonate using ion-exchange resin catalyst in a semi-batch slurry reactor, *Chem. Eng. Sci.* **2017**, *168*, 189-203.

[514] X. Jiang, F. Gou, H. Jing, Alternating copolymerization of CO_2 and propylene oxide catalyzed by C_{2v}-porphyrin cobalt: Selectivity control and a kinetic study, *J. Catal.* **2014**, *313*, 159-167.

[515] Y. Xie, Z. Zhang, T. Jiang, J. He, B. Han, T. Wu, K. Ding, CO_2 cycloaddition reactions catalyzed by an ionic liquid grafted onto a highly cross-linked polymer matrix, *Angew. Chem. Int. Ed.* **2007**, *46*, 7255-7258.

[516] J. A. Castro-Osma, M. North, X. Wu, Development of a halide-free aluminium-based catalyst for the synthesis of cyclic carbonates from epoxides and carbon dioxide, *Chem. Eur. J.* **2014**, *20*, 15005-15008.

[517] J. F. Cooper, M. Lichtenwalter, Catalytic process for producing alkylene carbonates, US2773070A, **4 December 1956.**

[518] J.-J. Shim, D. Kim, C.-S. Ra, Carboxylation of styrene oxide catalyzed by quaternary onium salts under solvent-free conditions, *Bull. Korean Chem. Soc.* **2006**, *27*, 744-746.

[519] M. Alves, B. Grignard, R. Mereau, C. Jerome, T. Tassaing, C. Detrembleur, Organocatalyzed coupling of carbon dioxide with epoxides for the synthesis of cyclic carbonates: catalyst design and mechanistic studies, *Catal. Sci. Technol.* **2017**, *7*, 2651-2684.

[520] T. Nishikubo, A. Kameyama, J. Yamashita, M. Tomoi, W. Fukuda, Insoluble polystyrene-bound quaternary onium salt catalysts for the synthesis of cyclic carbonates by the reaction of oxiranes with carbon dioxide, *J. Polym. Sci., Part A: Polym. Chem.* **1993**, *31*, 939-947.

[521] V. Caló, A. Nacci, A. Monopoli, A. Fanizzi, Cyclic carbonate formation from carbon dioxide and oxiranes in tetrabutylammonium halides as solvents and catalysts, *Org. Lett.* **2002**, *4*, 2561-2563.

[522] D. Park, J. Moon, J. Yang, J. Lee, Catalytic conversion of carbon dioxide using phase transfer catalysts, *Energy Convers. Manage.* **1997**, *38*, S449-S454.

[523] C. M. Starks, C. L. Lliotta, M. Halpern, *Phase-transfer catalysis: fundamentals, applications, and industrial perspectives*, Springer Science & Business Media, **1994**.

[524] H.-Y. Ju, M.-D. Manju, K.-H. Kim, S.-W. Park, D.-W. Park, Catalytic performance of quaternary ammonium salts in the reaction of butyl glycidyl ether and carbon dioxide, *J Ind. Eng. Chem.* **2008**, *14*, 157-160.

[525] J. Sun, S. Zhang, W. Cheng, J. Ren, Hydroxyl-functionalized ionic liquid: a novel efficient catalyst for chemical fixation of CO_2 to cyclic carbonate, *Tetrahedron Lett.* **2008**, *49*, 3588-3591.

[526] H. Büttner, K. Lau, A. Spannenberg, T. Werner, Bifunctional one-component catalysts for the addition of carbon dioxide to epoxides, *ChemCatChem* **2015**, *7*, 459-467.

[527] Y. Zhao, C. Yao, G. Chen, Q. Yuan, Highly efficient synthesis of cyclic carbonate with CO_2 catalyzed by ionic liquid in a microreactor, *Green Chem.* **2013**, *15*, 446-452.

[528] J. Tharun, D. W. Kim, R. Roshan, Y. Hwang, D.-W. Park, Microwave assisted preparation of quaternized chitosan catalyst for the cycloaddition of CO_2 and epoxides, *Catal. Commun.* **2013**, *31*, 62-65.

[529] K. R. Roshan, T. Jose, D. Kim, K. A. Cherian, D. W. Park, Microwave-assisted one pot-synthesis of amino acid ionic liquids in water: simple catalysts for styrene carbonate synthesis under atmospheric pressure of CO_2, *Catal. Sci. Technol.* **2014**, *4*, 963-970.

[530] Y. Tsutsumi, K. Yamakawa, M. Yoshida, T. Ema, T. Sakai, Bifunctional organocatalyst for activation of carbon dioxide and epoxide to produce cyclic carbonate: betaine as a new catalytic motif, *Org. Lett.* **2010**, *12*, 5728-5731.

[531] Y. Zhou, S. Hu, X. Ma, S. Liang, T. Jiang, B. Han, Synthesis of cyclic carbonates from carbon dioxide and epoxides over betaine-based catalysts, *J Mol. Catal. A: Chem.* **2008**, *284*, 52-57.

[532] W. Cheng, B. Xiao, J. Sun, K. Dong, P. Zhang, S. Zhang, F. T. Ng, Effect of hydrogen bond of hydroxyl-functionalized ammonium ionic liquids on cycloaddition of CO_2, *Tetrahedron Lett.* **2015**, *56*, 1416-1419.

[533] J. Sun, J. Ren, S. Zhang, W. Cheng, Water as an efficient medium for the synthesis of cyclic carbonate, *Tetrahedron Lett.* **2009**, *50*, 423-426.

[534] T. Ema, K. Fukuhara, T. Sakai, M. Ohbo, F.-Q. Bai, J.-y. Hasegawa, Quaternary ammonium hydroxide as a metal-free and halogen-free catalyst for the synthesis of cyclic carbonates from epoxides and carbon dioxide, *Catal. Sci. Technol.* **2015**, *5*, 2314-2321.

[535] M. Galvan, M. Selva, A. Perosa, M. Noè, Toward the design of halide- and metal-free ionic-liquid catalysts for the cycloaddition of CO_2 to epoxides, *Asian J. Org. Chem.* **2014**, *3*, 504-513.

[536] N. Aoyagi, Y. Furusho, T. Endo, Effective synthesis of cyclic carbonates from carbon dioxide and epoxides by phosphonium iodides as catalysts in alcoholic solvents, *Tetrahedron Lett.* **2013**, *54*, 7031-7034.

[537] D. Wei-Li, J. Bi, L. Sheng-Lian, L. Xu-Biao, T. Xin-Man, A. Chak-Tong, Functionalized phosphonium-based ionic liquids as efficient catalysts for the synthesis of cyclic carbonate from expoxides and carbon dioxide, *Appl. Catal. A: Gen.* **2014**, *470*, 183-188.

[538] H. Büttner, J. Steinbauer, T. Werner, Synthesis of cyclic carbonates from epoxides and carbon dioxide by using bifunctional one-component phosphorus-based organocatalysts, *ChemSusChem* **2015**, *8*, 2655-2669.

[539] T. Werner, H. Büttner, Phosphorus-based bifunctional organocatalysts for the addition of carbon dioxide and epoxides, *ChemSusChem* **2014**, *7*, 3268-3271.

[540] S. Liu, N. Suematsu, K. Maruoka, S. Shirakawa, Design of bifunctional quaternary phosphonium salt catalysts for CO_2 fixation reaction with epoxides under mild conditions, *Green Chem.* **2016**, *18*, 4611-4615.

[541] Y. Toda, Y. Komiyama, A. Kikuchi, H. Suga, Tetraarylphosphonium salt-catalyzed carbon dioxide fixation at atmospheric pressure for the synthesis of cyclic carbonates, *ACS Catal.* **2016**, *6*, 6906-6910.

[542] J. Peng, Y. Deng, Cycloaddition of carbon dioxide to propylene oxide catalyzed by ionic liquids, *New J. Chem.* **2001**, *25*, 639-641.

[543] H. Sun, D. Zhang, Density functional theory study on the cycloaddition of carbon dioxide with propylene oxide catalyzed by alkylmethylimidazolium chlorine ionic liquids, *J. Phys. Chem. A* **2007**, *111*, 8036-8043.

[544] P. Jaiswal, M. N. Varma, Catalytic performance of imidazolium based ILs in the reaction of 1,2-epoxyoctane and carbon dioxide: Kinetic study, *J. CO2 Util.* **2016**, *14*, 93-97.

[545] H. Kawanami, A. Sasaki, K. Matsui, Y. Ikushima, A rapid and effective synthesis of propylene carbonate using a supercritical CO_2–ionic liquid system, *ChemComm* **2003**, 896-897.

[546] A.-L. Girard, N. Simon, M. Zanatta, S. Marmitt, P. Gonçalves, J. Dupont, Insights on recyclable catalytic system composed of task-specific ionic liquids for the chemical fixation of carbon dioxide, *Green Chem.* **2014**, *16*, 2815-2825.

[547] L. Xiao, D. Su, C. Yue, W. Wu, Protic ionic liquids: A highly efficient catalyst for synthesis of cyclic carbonate from carbon dioxide and epoxides, *J. CO2 Util.* **2014**, *6*, 1-6.

[548] M. H. Anthofer, M. E. Wilhelm, M. Cokoja, I. I. Markovits, A. Pöthig, J. Mink, W. A. Herrmann, F. E. Kühn, Cycloaddition of CO_2 and epoxides catalyzed by imidazolium bromides under mild conditions: influence of the cation on catalyst activity, *Catal. Sci. Technol.* **2014**, *4*, 1749-1758.

[549] S. Denizaltı, Imidazolium based ionic liquids bearing a hydroxyl group as highly efficient catalysts for the addition of CO_2 to epoxides, *RSC Adv.* **2015**, *5*, 45454-45458.

[550] M. H. Anthofer, M. E. Wilhelm, M. Cokoja, M. Drees, W. A. Herrmann, F. E. Kühn, Hydroxy-functionalized imidazolium bromides as catalysts for the cycloaddition of CO_2 and epoxides to cyclic carbonates, *ChemCatChem* **2015**, *7*, 94-98.

[551] D.-W. Kim, R. Roshan, J. Tharun, A. Cherian, D.-W. Park, Catalytic applications of immobilized ionic liquids for synthesis of cyclic carbonates from carbon dioxide and epoxides, *Korean J. Chem. Eng.* **2013**, *30*, 1973-1984.

[552] A. Zhu, T. Jiang, B. Han, J. Zhang, Y. Xie, X. Ma, Supported choline chloride/urea as a heterogeneous catalyst for chemical fixation of carbon dioxide to cyclic carbonates, *Green Chem.* **2007**, *9*, 169-172.

[553] T. Sakai, Y. Tsutsumi, T. Ema, Highly active and robust organic–inorganic hybrid catalyst for the synthesis of cyclic carbonates from carbon dioxide and epoxides, *Green Chem.* **2008**, *10*, 337-341.

[554] H.-L. Shim, S. Udayakumar, J.-I. Yu, I. Kim, D.-W. Park, Synthesis of cyclic carbonate from allyl glycidyl ether and carbon dioxide using ionic liquid-functionalized amorphous silica, *Catal. Today* **2009**, *148*, 350-354.

[555] S. Udayakumar, V. Raman, H.-L. Shim, D.-W. Park, Cycloaddition of carbon dioxide for commercially-imperative cyclic carbonates using ionic liquid-functionalized porous amorphous silica, *Appl. Catal. A: Gen.* **2009**, *368*, 97-104.

[556] L.-F. Xiao, F.-W. Li, J.-J. Peng, C.-G. Xia, Immobilized ionic liquid/zinc chloride: Heterogeneous catalyst for synthesis of cyclic carbonates from carbon dioxide and epoxides, *J Mol. Catal. A: Chem.* **2006**, *253*, 265-269.

[557] X. Zhang, D. Wang, N. Zhao, A. S. Al-Arifi, T. Aouak, Z. A. Al-Othman, W. Wei, Y. Sun, Grafted ionic liquid: Catalyst for solventless cycloaddition of carbon dioxide and propylene oxide, *Catal. Commun.* **2009**, *11*, 43-46.

[558] J. Sun, W. Cheng, W. Fan, Y. Wang, Z. Meng, S. Zhang, Reusable and efficient polymer-supported task-specific ionic liquid catalyst for cycloaddition of epoxide with CO_2, *Catal. Today* **2009**, *148*, 361-367.

[559] S. Udayakumar, M.-K. Lee, H.-L. Shim, D.-W. Park, Functionalization of organic ions on hybrid MCM-41 for cycloaddition reaction: The effective conversion of carbon dioxide, *Appl. Catal. A: Gen.* **2009**, *365*, 88-95.

[560] S. Udayakumar, S.-W. Park, D.-W. Park, B.-S. Choi, Immobilization of ionic liquid on hybrid MCM-41 system for the chemical fixation of carbon dioxide on cyclic carbonate, *Catal. Commun.* **2008**, *9*, 1563-1570.

[561] Y. Zhao, J.-S. Tian, X.-H. Qi, Z.-N. Han, Y.-Y. Zhuang, L.-N. He, Quaternary ammonium salt-functionalized chitosan: An easily recyclable catalyst for efficient synthesis of cyclic carbonates from epoxides and carbon dioxide, *J Mol. Catal. A: Chem.* **2007**, *271*, 284-289.

[562] K. Qiao, F. Ono, Q. Bao, D. Tomida, C. Yokoyama, Efficient synthesis of styrene carbonate from CO_2 and styrene oxide using zinc catalysts immobilized on soluble imidazolium–styrene copolymers, *J Mol. Catal. A: Chem.* **2009**, *303*, 30-34.

[563] M.-K. Lee, H.-L. Shim, M. M. Dharman, K.-H. Kim, S.-W. Park, D.-W. Park, Synthesis of cyclic carbonate from allyl glycidyl ether and CO_2 over silica-supported ionic liquid catalysts prepared by sol-gel method, *Korean J. Chem. Eng.* **2008**, *25*, 1004-1007.

[564] L. Han, H.-J. Choi, S.-J. Choi, B. Liu, D.-W. Park, Ionic liquids containing carboxyl acid moieties grafted onto silica: Synthesis and application as heterogeneous catalysts for cycloaddition reactions of epoxide and carbon dioxide, *Green Chem.* **2011**, *13*, 1023-1028.

[565] L.-W. Xu, M.-S. Yang, J.-X. Jiang, H.-Y. Qiu, G.-Q. Lai, Ionic liquid-functionalized SBA-15 mesoporous material: efficient heterogeneous catalyst in versatile organic reactions, *Cent. Eur. J. Chem.* **2007**, *5*, 1073-1083.

[566] W.-L. Dai, L. Chen, S.-F. Yin, S.-L. Luo, C.-T. Au, 3-(2-Hydroxyl-ethyl)-1-propylimidazolium bromide immobilized on SBA-15 as efficient catalyst for the synthesis of cyclic carbonates via the coupling of carbon dioxide with epoxides, *Catal. Lett.* **2010**, *135*, 295-304.

Appendix A

Supporting information:

Dynamic streamlined extraction of iridoids, anthocyanins and lipids from haskap berries

Supporting information

Dynamic streamlined extraction of iridoids, anthocyanins and lipids from haskap berries

Aitor Sainz Martinez[a,†], Christoph Kornpointner[b,†], Christian Haselmair-Gosch[b], Maja Mikulic-Petkovsek[c], Katharina Schröder[a*], and Heidi Halbwirth[b*]

a. *Institute of Applied Synthetic Chemistry, Technische Universität Wien, Getreidemarkt 9/163, 1060 Vienna, Austria.*

b. *Institute of Chemical, Environmental and Bioscience Engineering, Technische Universität Wien, Getreidemarkt 9/166, 1060 Vienna, Austria*

c. *Department of Agronomy, Biotechnical Faculty, University of Ljubljana, Ljubljana, Slovenia*

† These two authors contributed equally to this work.

* correspondence: heidrun.halbwirth@tuwien.ac.at, katharina.schroeder@tuwien.ac.at

Number of pages: **9**

Number of figures: **12**

Number of tables: **5**

Table S1. Chemicals and Solvents

Name	Source	Purity	Purification Protocol
Water	Millipore	-	Filtration through a Milli-Q ion exchange system
Ethanol	Chem-Lab	Abs. 100% a.r.	-
Methanol	VWR Chemicals	HPLC grade	-
Acetonitrile	VWR Chemicals	HPLC grade	-
Formic acid	Merck	98-100 %	-
Loganin	Extrasynthese	≥99%	-
Loganic acid	Extrasynthese	≥99%	-
Cyanidin chloride	Sigma Aldrich	≥98%	-
Pelargonidin chloride	Extrasynthese	≥97%	-
Peonidin chloride	Extrasynthese	≥97%	-

Figure S1. General structures of investiagted anthocyanins and iridoids.
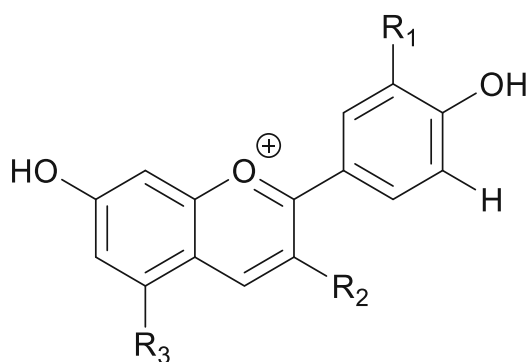
Cyanidin: R_1= OH, R_2= OH, R_3= OH

Peonidin: R_1= OCH$_3$, R_2= OH, R_3= OH

Pelargonidin: R_1= H, R_2= OH, R_3= OH
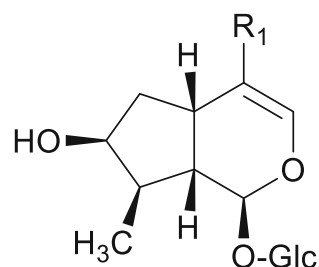
Loganin: R_1= CO$_2$Me

Loganic acid: R_1= CO$_2$H

Figure S2. Supercritical CO₂ device – General set up
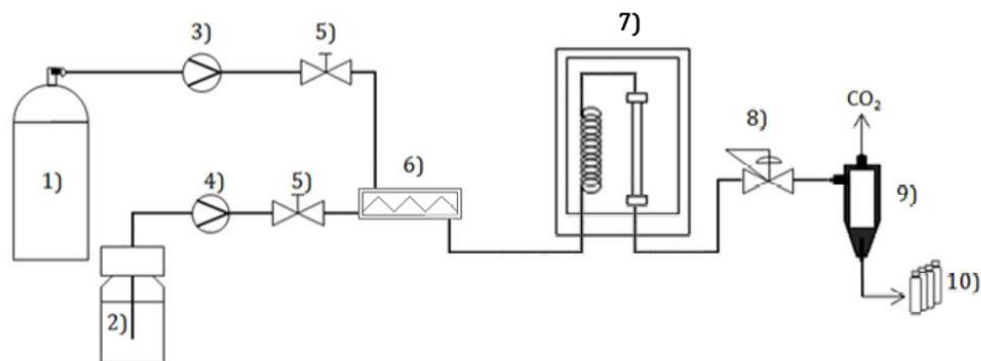
1) Liquid CO_2 supply; 2) Co-solvent or modifier supply; 3) CO_2 pump; 4) Solvent pump; 5) Manually operated valve; 6) Inline mixer; 7) Thermostated oven with preheating coil and catalyst cartridge; 8) back pressure regulator; 9) gas-liquid separator; 10) fraction collector.

Table S2. Dynamic streamlined extraction fractionation over time.

Fractionation	Specific extraction time frame / min	Fractionation	Specific extraction time frame / min
F1	0-30	F10	270-300
F2	30-60	F11	300-330
F3	60-90	F12	330-360
F4	90-120	F13	360-390
F5	120-150	F14	390-420
F6	150-180	F15	420-450
F7	180-210	F16	450-480
F8	210-240	F17	480-510
F9	240-270	F18	510-540

Figure S3. a) Dynamic streamlined extraction, modifier in increasing amounts over time, b) Dynamic streamlined extraction, CO_2 and EtOH flow rates over time and c) Dynamic streamlined extraction, pressure over time
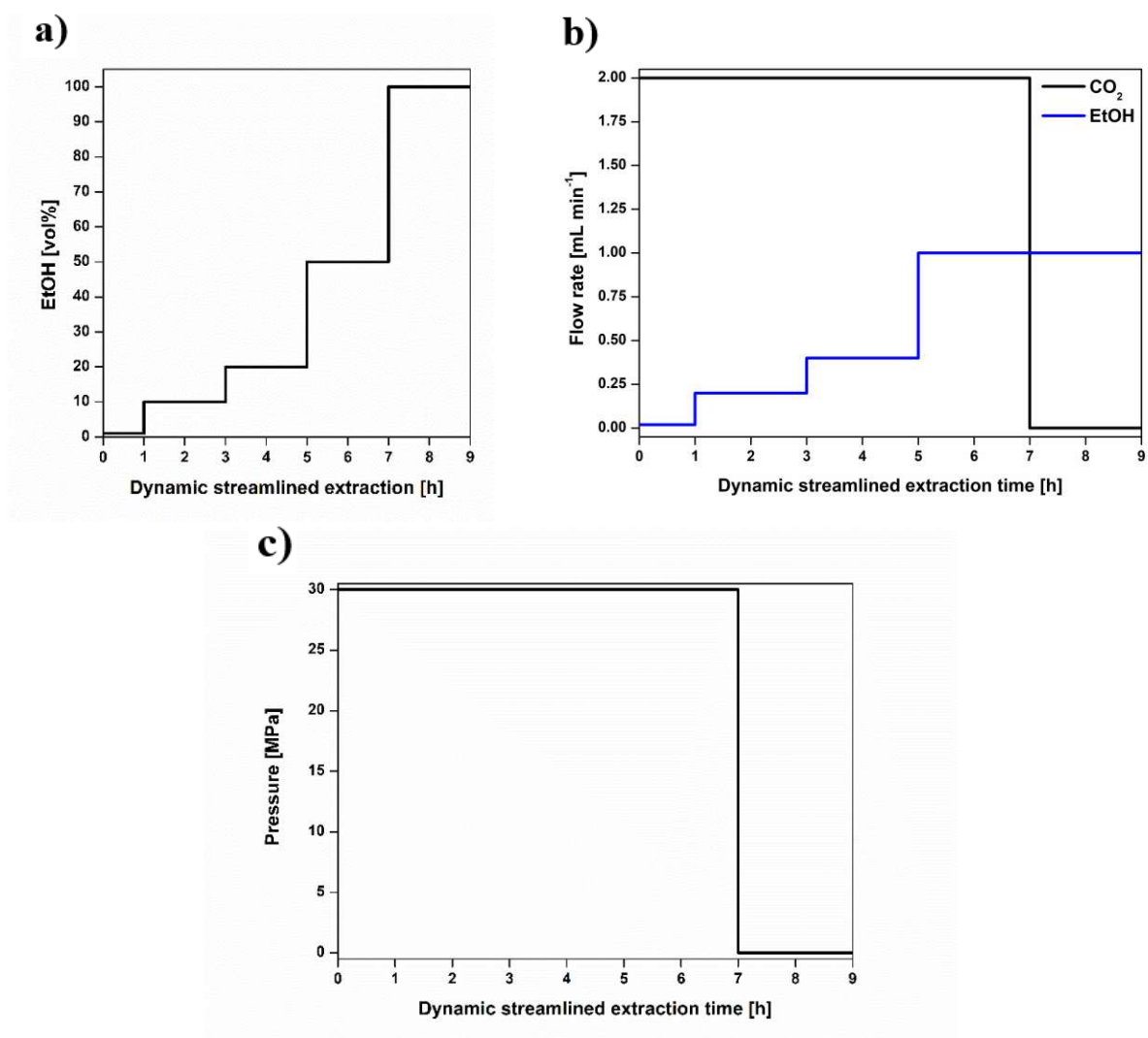
Figure S4. Calibration of loganic acid with HPLC (0.1 µg/mL to 100 µg/mL).
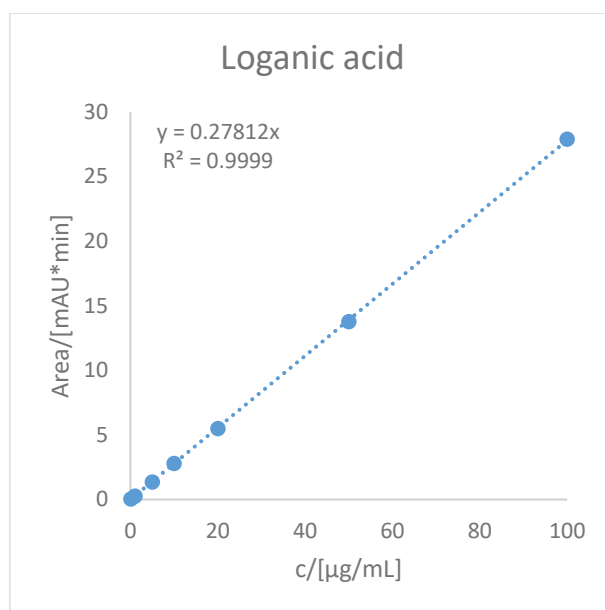
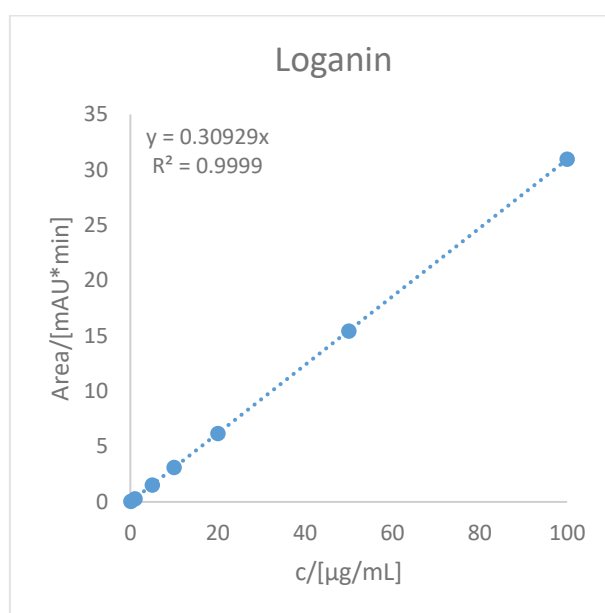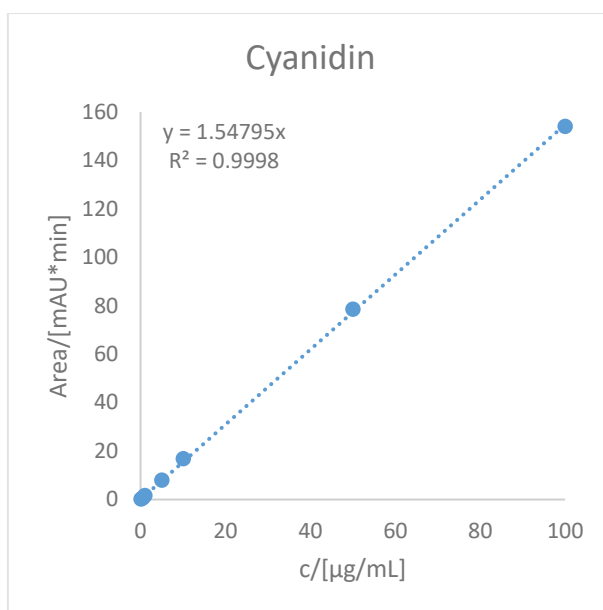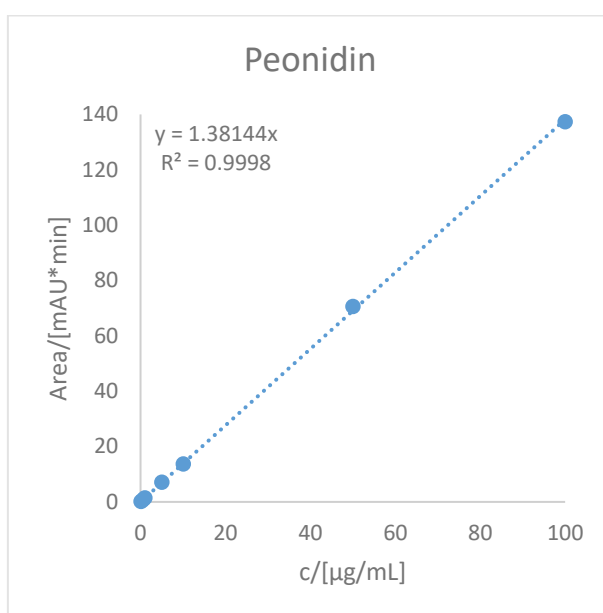**Figure S5. Calibration of loganin with HPLC (0.1 µg/mL to 100 µg/mL).**

Table S3. Additional information on loganic acid and loganin.

Compound	Retention time /min	UV absorbance /nm	Calibration function	R^2
Loganic acid	8.453	235.1	y = 0.27812x	0.9999
Loganin	9.507	236.7	y = 0.30929x	0.9999

Figure S6. Calibration of cyanidin with HPLC (0.1 μg/mL to 100 μg/mL).

Figure S7. Calibration of peonidin with HPLC (0.1 μg/mL to 100 μg/mL).

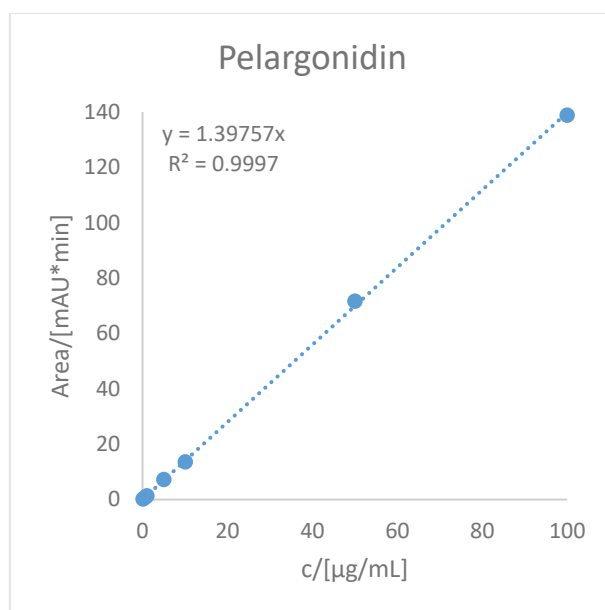**Figure S8. Calibration of pelargonidin with HPLC (0.1 µg/mL to 100 µg/mL).**

Table S4. Additional information on cyanidin, peonidin and pelargonidin.

Compound	Retention time /min	Factor for molecule without Cl-Ion	UV absorbance /nm	Calibration function	R^2
Cyanidin	17.957	0.89015	275.0/523.4	y = 1.54795x	0.9998
Pelargonidin	20.927	0.88441	267.5/422.1/512.0	y = 1.39757x	0.9997
Peonidin	22.143	0.89472	274.4/524.9	y = 1.38144x	0.9998

Table S5. Analysis of FAME´s.

FAME Compound	Retention time /min	Molecular Ion	Molecular Formula of FAME
Palmitoleic acid methyl ester	10.78	268.108	$C_{17}H_{32}O_2$
Palmitic acid methyl ester	10.94	270.088	$C_{17}H_{32}O_2$
Linoleic acid methyl ester	12.49	294.061	$C_{19}H_{34}O_2$
Oleic acid methyl ester	12.60	296.099	$C_{19}H_{36}O_2$

Figure S9. Mass spectra of palmitoleic acid methyl ester.
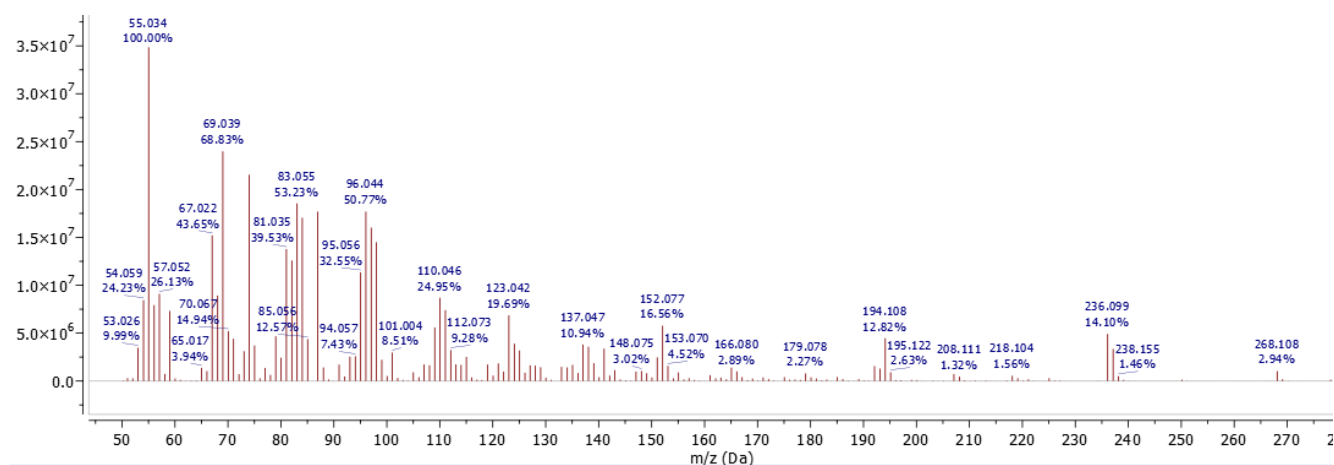
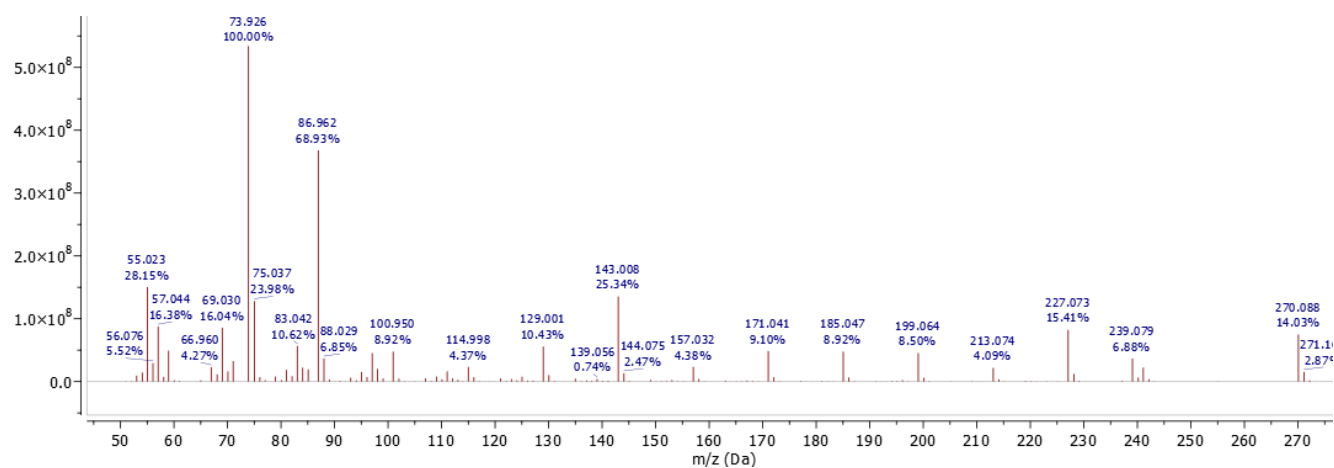**Figure S10. Mass spectra of palmitic acid methyl ester.**

212

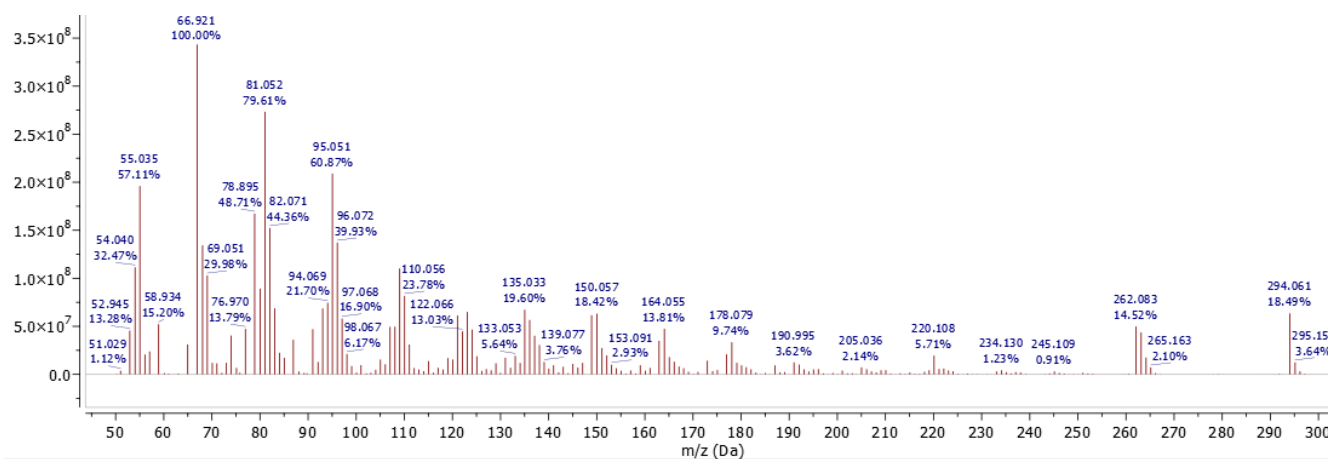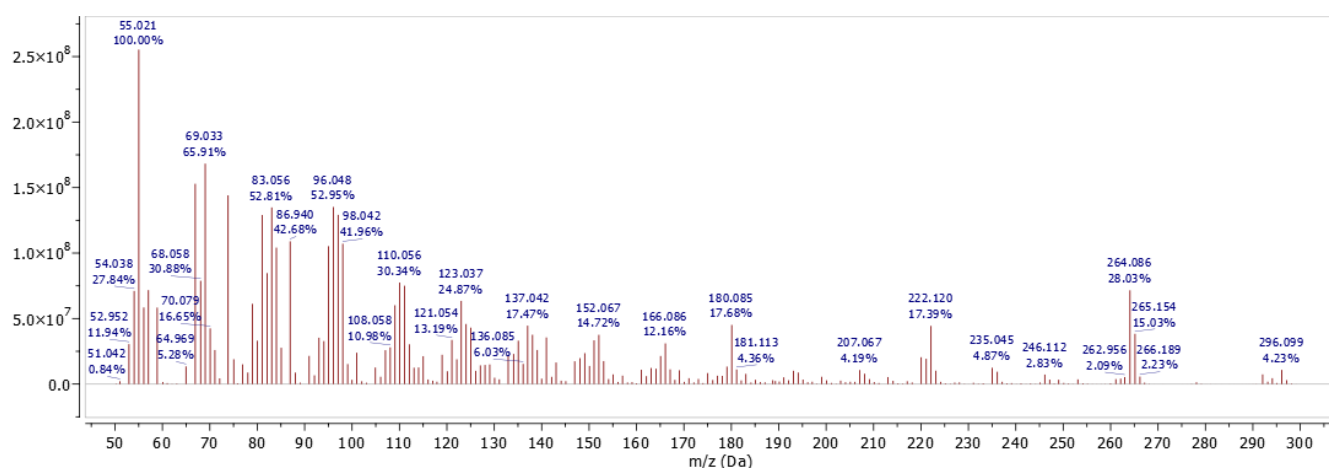**Figure S11. Mass spectra of linoleic acid methyl ester.**

Figure S12. Mass spectra of oleic acid methyl ester.

Appendix B

Supporting information:

Ionic liquid based dynamic supercritical carbon dioxide extraction of six different cannabinoids from *Cannabis sativa* L.

Supporting information

Ionic liquid based dynamic supercritical carbon dioxide extraction of six different cannabinoids from *Cannabis sativa* L.

Christoph Kornpointner[†a], Aitor Sainz Martinez[†b], Michael Schnürch[b], Heidi Halbwirth[*a] and Katharina Bica-Schröder[*b]

a. *Institute of Chemical, Environmental and Bioscience Engineering, Technische Universität Wien, Getreidemarkt 9/166, 1060, Vienna, Austria. Institute of Chemical, Environmental and Bioscience Engineering, Technische Universität Wien, Getreidemarkt 9/166, 1060 Vienna, Austria*

b. *Institute of Applied Synthetic Chemistry, Technische Universität Wien, Getreidemarkt 9/163, 1060, Vienna, Austria.*

† These two authors contributed equally to this work.

* correspondence: katharina.schroeder@tuwien.ac.at, heidrun.halbwirth@tuwien.ac.at

Number of pages: 7

Number of figures: 7

Number of tables: 4

Table S1 Extraction parameters for IL-SFE.

Exp.	IL	t_{Pre}/ min	T_{Pre}/ °C	m_{IL}/ g	m_{H2O}/ g	P_{SFE}/ MPa	T_{SFE}/ °C
1	[C$_2$mim][OAc]	60	25	3	6	20	70
2	[C$_2$mim][OAc]	60	70	3	6	20	70
3	[C$_2$mim][OAc]	15	25	3	6	20	70
4	[C$_2$mim][OAc]	15	70	3	6	20	70
5	[C$_2$mim][OAc]	15	70	3	3	20	70
6	[C$_2$mim][OAc]	15	70	3	9	20	70
7	[C$_2$mim][OAc]	15	70	3	-	20	70
8	[C$_2$mim][OAc]	15	70	-	9	20	70
9	-	-	-	-	-	20	70
10	[C$_2$mim][OAc]	15	70	3	9	10	70
11	[C$_2$mim][OAc]	15	70	3	9	15	70
12	[C$_2$mim][OAc]	15	70	3	9	30	70
13	[C$_2$mim][OAc]	15	70	3	9	20	35
14	[C$_2$mim][OAc]	15	70	3	9	10	35
15	[Ch][OAc]	15	70	3	9	20	70
16	[C$_2$mim][DMP]	15	70	3	9	20	70

Pre: IL pre-treatment before SFE
Exp. Number corresponds to the main article

Table S2. Extracted cannabinoids by IL-SFE and conventional extraction, (n = 3 ± SD).

Exp.	Yield CBD / (mg/g)	Yield CBDA / (mg/g)	Yield Δ^9-THC / (mg/g)	Yield THCA / (mg/g)	Yield CBG / (mg/g)	Yield CBGA / (mg/g)
IL-SFE						
1	4.29 ± 0.24[f]	8.8 ± 1.0[cd]	0.159 ± 0.004[de]	0.306 ± 0.008[def]	0.137 ± 0.007[d]	0.092 ± 0.019[fg]
2	6.58 ± 0.24[c]	6.3 ± 0.6[fg]	0.164 ± 0.008[cde]	0.307 ± 0.013[cdef]	0.186 ± 0.003[c]	0.058 ± 0.017[g]
3	5.0 ± 0.3[de]	7.9 ± 0.6[de]	0.169 ± 0.008[cd]	0.308 ± 0.023[cdef]	0.154 ± 0.008[d]	0.067 ± 0.012[fg]
4	5.29 ± 0.27[d]	8.3 ± 0.4[cde]	0.174 ± 0.004[cd]	0.339 ± 0.013[abcd]	0.164 ± 0.007[cd]	0.082 ± 0.012[fg]
5	7.45 ± 0.05[b]	1.09 ± 0.17[h]	0.1807 ± 0.0007[c]	0.150 ± 0.014[i]	0.226 ± 0.007[b]	n.d.
6	4.6 ± 0.3e[f]	10.9 ± 0.4[ab]	0.177 ± 0.007[cd]	0.365 ± 0.011[ab]	0.157 ± 0.016[cd]	0.178 ± 0.003[cd]
7	0.150 ± 0.021[i]	0.1727 ± 0.0025[h]	0.023 ± 0.007[i]	0.0099 ± 0.0020[k]	n.d.	n.d.
8	2.24 ± 0.12[h]	9.8 ± 0.5[bc]	0.114 ± 0.003[g]	0.260 ± 0.019[g]	0.0641 ± 0.0015[f]	0.196 ± 0.007[bc]
9	3.01 ± 0.04[g]	7.1 ± 0.5[ef]	0.165 ± 0.003[cde]	0.190 ± 0.012[h]	0.101 ± 0.012[e]	0.095 ± 0.007[fg]
10	3.388 ± 0.012[g]	0.27 ± 0.06[h]	0.0793 ± 0.0010[h]	0.0092 ± 0.0019[k]	0.045 ± 0.008[fg]	n.d.
11	4.44 ± 0.03[ef]	8.56 ± 0.18[cde]	0.1596 ± 0.0015[de]	0.297 ± 0.004[efg]	0.158 ± 0.005[cd]	0.100 ± 0.005[f]
12	4.1 ± 0.4[f]	10.68 ± 0.28[ab]	0.163 ± 0.013[cde]	0.338 ± 0.011[abcd]	0.142 ± 0.028[d]	0.213 ± 0.009[bc]
13	3.29 ± 0.20[g]	11.6 ± 0.5[a]	0.148 ± 0.006[ef]	0.345 ± 0.007[abc]	0.105 ± 0.005[e]	0.219 ± 0.013[b]
14	3.01 ± 0.17[g]	10.6 ± 0.6[ab]	0.137 ± 0.006[f]	0.330 ± 0.013[bcde]	0.103 ± 0.007[e]	0.145 ± 0.009[be]
15	4.04 ± 0.22[f]	11.4 ± 0.3[a]	0.161 ± 0.005[de]	0.374 ± 0.007[a]	0.144 ± 0.011[d]	0.258 ± 0.013[a]
16	3.255 ± 0.028[g]	8.6 ± 0.9[cde]	0.171 ± 0.006[cd]	0.278 ± 0.019[fg]	0.106 ± 0.006[e]	0.19 ± 0.03[bc]
Conventional extraction (70 °C)						
17[1]	4.24 ± 0.09[f]	11.2 ± 0.4[ab]	0.225 ± 0.006[b]	0.274 ± 0.018[fg]	0.158 ± 0.006[cd]	0.294 ± 0.018[a]
18[2]	9.50 ± 0.19[a]	5.34 ± 0.14[g]	0.351 ± 0.004[a]	0.096 ± 0.005[j]	0.300 ± 0.005[a]	0.1396 ± 0.0023[e]
19[3]	0.70 ± 0.18[i]	0.86 ± 0.15[h]	0.036 ± 0.009[i]	0.020 ± 0.004[k]	0.017 ± 0.004[g]	0.015 ± 0.003[h]

Mean values with different letters (a, b, c, etc.) within the same column are statistically different ($p < 0.05$)

[1]2 h in EtOH; [2]24 h in EtOH; [1]2 h in H_2O
Exp. Number corresponds to the main article

Figure S1. General structures of investigated ionic liquids.

[C₂mim][O   **[Ch][OAc]**   **[C₂mim][DMP]**
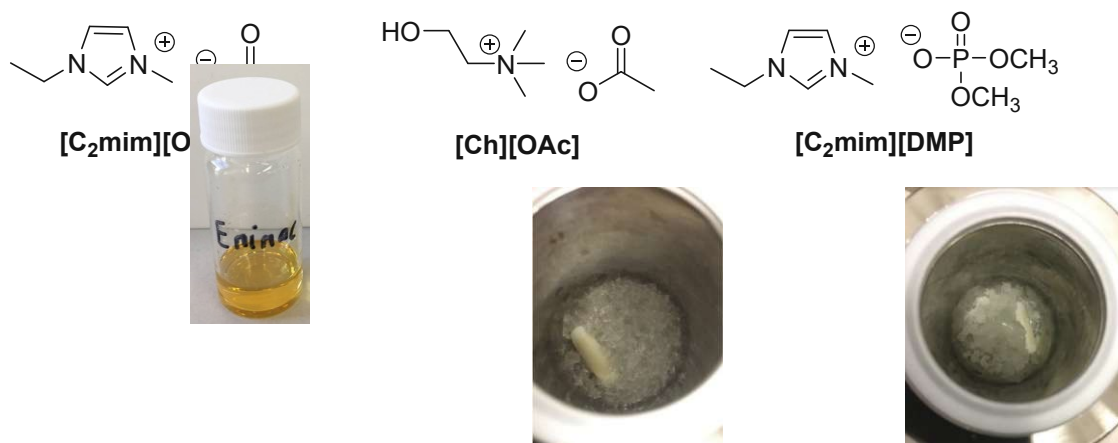

Figure S2. Extracts of different IL-SFE. Left: Extract with [C₂min][OAc]; Middle: Extract with [Ch][OAc]; Right: Extract with [C₂min][DMP].

Figure S3. Residues after extraction of different IL-SFE. Left: Extract with [C₂min][OAc]; Middle: Extract with [Ch][OAc]; Right: Extract with [C₂min][DMP].

Figure S4. ILs after purification. Left: Extract with [C$_2$min][OAc]; Middle: Extract with [Ch][OAc]; Right: Extract with [C$_2$min][DMP].
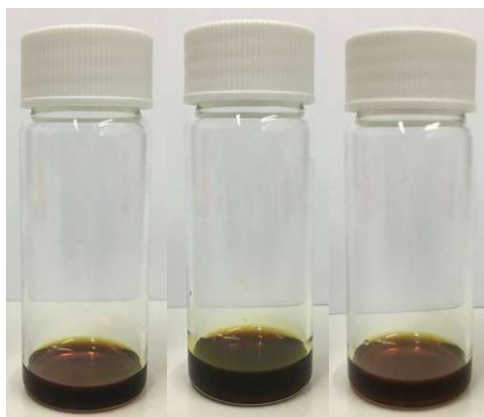
Table S3. Cannabinoid yields of supercritical CO2 extraction with EtOH as a modifier and conventional ethanolic extraction of another batch of industrial hemp, (n = 3 ± SD). SFE was performed at various temperatures, pressures and vol% EtOH. Total flow: 1 mL/min; Static extraction 30 min; Dynamic extraction 120 min. Conventional extraction was performed at various temperatures and a hemp:EtOH ratio of 1:10.

No.	EtOH/ vol%	T_{Pre}/ °C	Σ(CBD)/ (mg/g)	Σ(THC)/ (mg/g)	Σ(CBG)/ (mg/g)
SFE					
1	1	35	4.1 ± 0.4[c]	0.086 ± 0.010[b]	0.045 ± 0.006[c]
2	10	35	9.48 ± 0.18[b]	0.222 ± 0.012[a]	0.177 ± 0.003[b]
3	20	35	9.55 ± 0.20[b]	0.243 ± 0.022[a]	0.178 ± 0.005[b]
4	20	80	0.36 ± 0.10[d]	0.00492 ± 0.00021[c]	n.d.
Conventional extraction					
5	-	35	10.29 ± 0.07[a]	0.233 ± 0.006[a]	0.2173 ± 0.0017[a]
6	-	60	10.9 ± 0.4[a]	0.249 ± 0.015[a]	0.229 ± 0.010[a]
7	-	80	10.9 ± 0.3[a]	0.250 ± 0.012[a]	0.231 ± 0.009[a]

Mean values with different letters (a, b, c, etc.) within the same column are statistically different ($p < 0.05$)
n.d.: not detected

Table S4. NMR spectroscopic data of purified [C$_2$min][OAc], [Ch][OAc] and [C$_2$min][DMP] precorded in chloroform-d_4. All ^{1}H-NMR chemical shifts [ppm] are listed together with relative integral, multiplicity as well as coupling constants [Hz].

IL	δH (J in Hz)
[C$_2$min][OAc]	11.59 (s), 7.19 (d, 2.0, 1H), 7.17 (d, 2.0, 1H), 4.33 (q, 7.4, 2H), 4.02 (s, 3H), 1.96 (s, 3H), 1.52 (t, 7.4, 3H)
[Ch][OAc][b]	4.13 (m, 2H), 3.75 (m, 2H), 3.37 (s, 9H), 1.94 (s, 3H)
[C$_2$min][DMP]	10.70 (s, 1H), 7.31 (m, 1H), 7.28 (1H, m), 4.33 (q, 7.4, 2H), 4.03 (s, 3H), 3.57 (d, 10.5, 6H), 1.53 (t, 7.4, 3H)

Figure S5. ^{1}H-NMR of purified [C$_2$min][OAc] in chloroform-d_4.
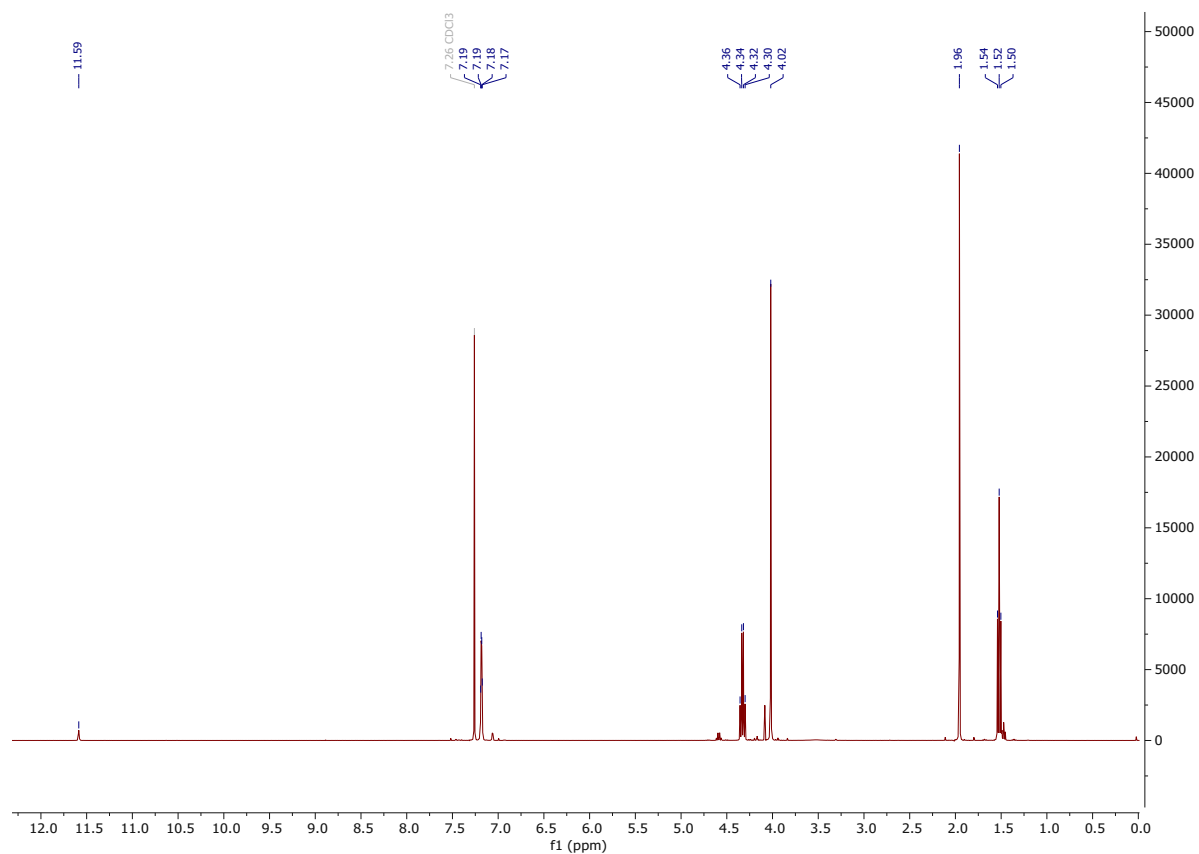
Figure S6. ^{1}H-NMR of purified [Ch][OAc] in chloroform-d_4.
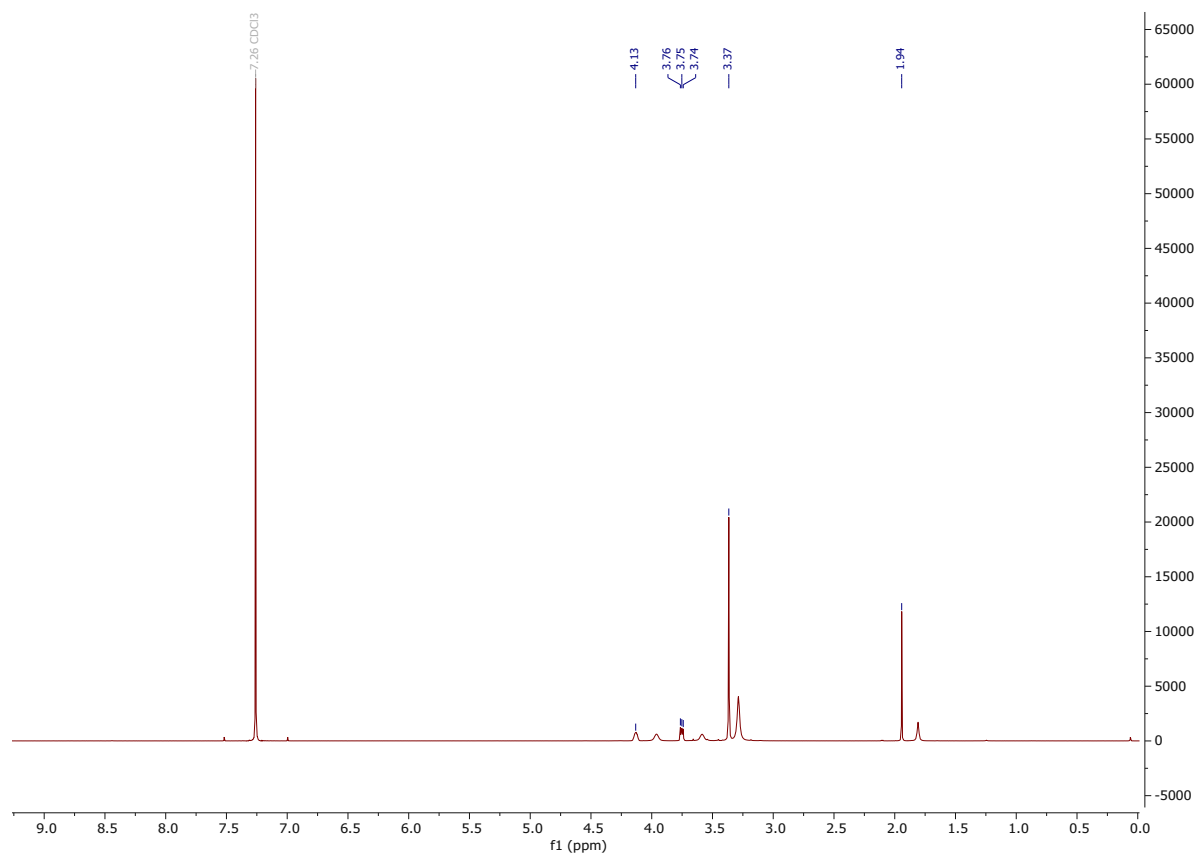
Figure S7. ^{1}H-NMR of purified [C$_2$min][DMP] in chloroform-d_4.
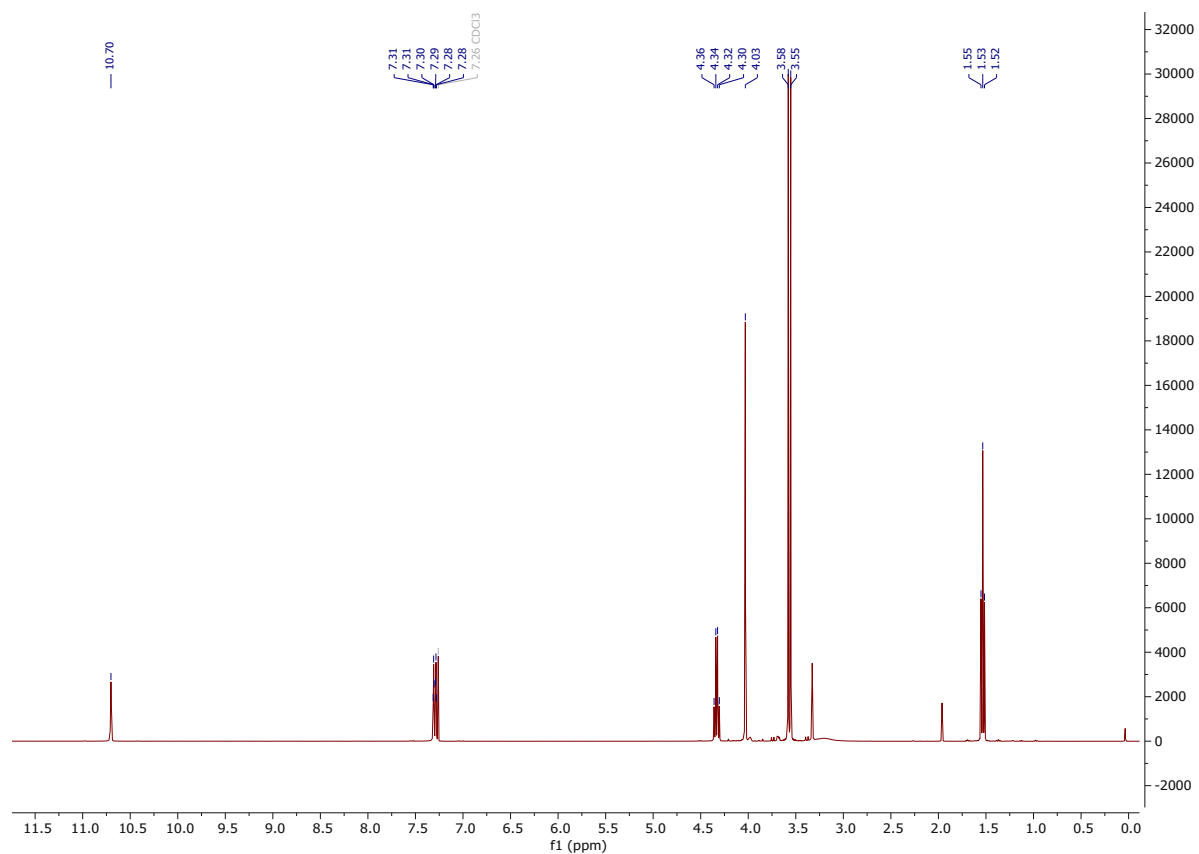
Appendix C

Supporting information:

Continuous Conversion of Carbon Dioxide to Propylene Carbonate with Supported Ionic Liquids.

Supporting information

Continuous conversion of carbon dioxide to propylene carbonate with supported ionic liquids

Aitor Sainz Martinez, Christian Hauzenberger, Apurba Ranjan Sahoo, Zita Csendes, Helmuth Hoffmann, and Katharina Bica*

Institute of Applied Synthetic Chemistry, Vienna University of Technology, Getreidemarkt 9/163, 1060 Vienna, Austria.

* Corresponding author Katharina Schröder (née Katharina Bica). Email: katharina.schroeder@tuwien.ac.at, Fax: +43 1 58801 16360; Tel: +43 1 58801 163601.

Number of pages: 11

Number of figures: 8

Number of tables: 3

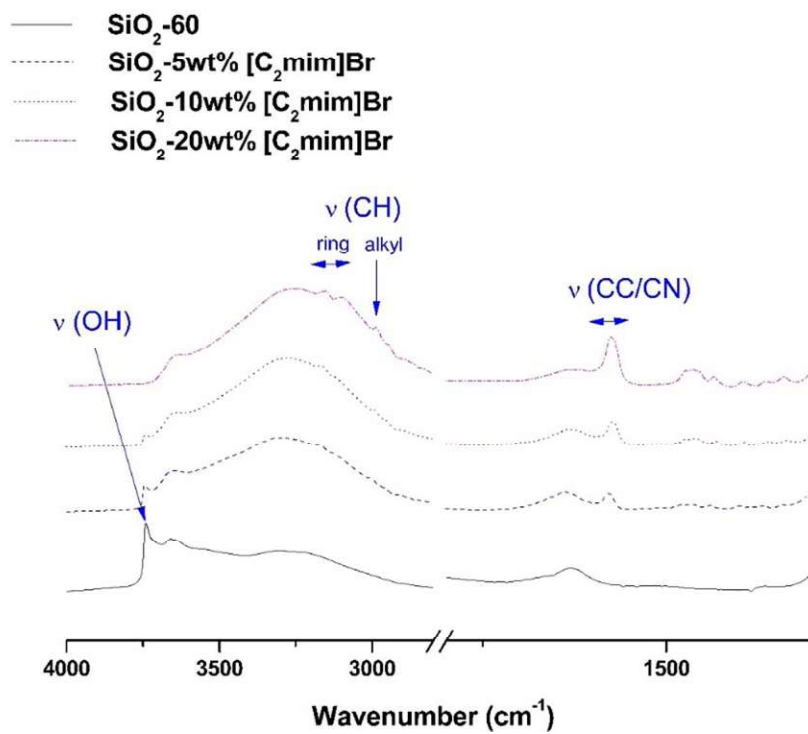**Figure S1**. FT-IR spectra of pristine SiO$_2$-60 and **SILP-5** with variable loading of 5, 10 or 20 wt% [C$_2$mim]Br, resp.

Figure S2. N$_2$ adsorption–desorption isotherms of SiO$_2$-60 and **SILP-5** with variable loading of

5, 10 or 20 wt% [C$_2$mim]Br, resp.
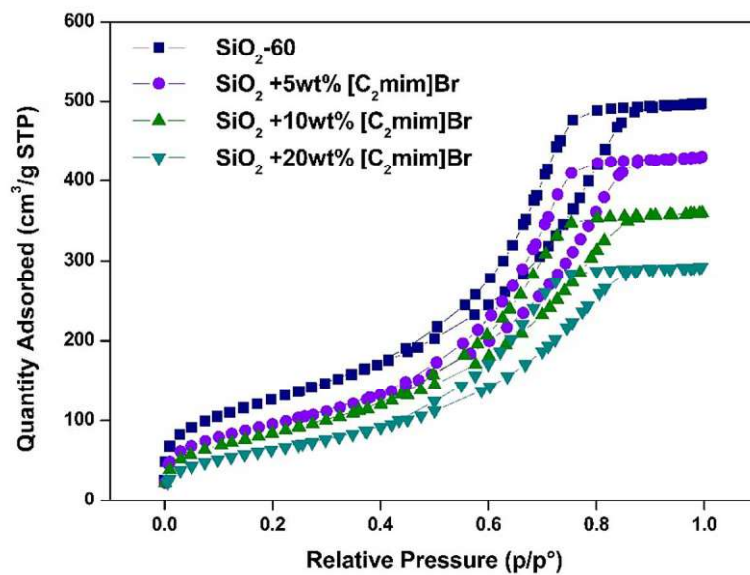

Figure S3. N$_2$ adsorption–desorption isotherms of SiO$_2$-60 and **SILC-1** to **SILC-4**.
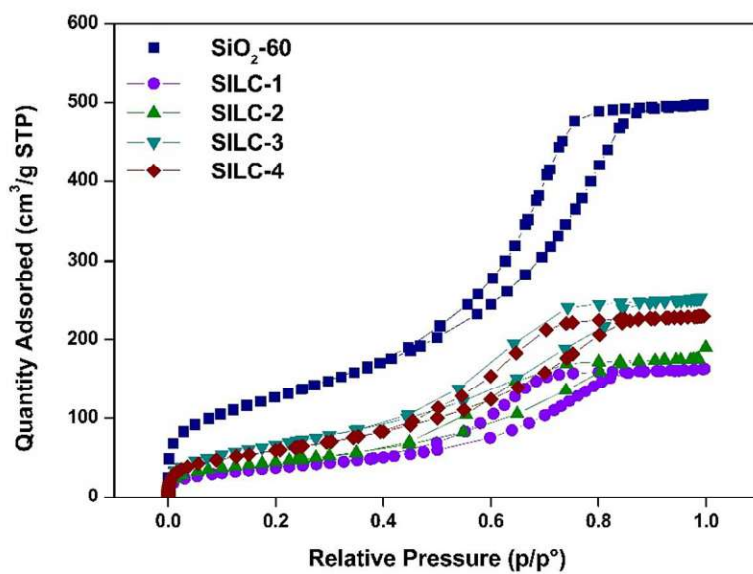
Table S1. Characterization of supported ionic liquid materials: Structural parameters calculated from the N_2 adsorption–desorption isotherms

Sample	BET surface area[a] (m^2/g)	Pore volume[b] (cm^3/g)	Average pore diameter[c] (nm)
SiO$_2$	462.35	0.79	5.68
SiO$_2$–IL5 5 wt%	349.54	0.68	5.82
SiO$_2$–IL5 10 wt%	311.68	0.57	5.45
SiO$_2$–IL5 20 wt%	237.55	0.46	5.34
SILC-1	137.06	0.26	4.98
SILC-2	164.24	0.30	4.98
SILC-3	244.79	0.40	4.78
SILC-4	218.35	0.37	4.72

[a]Calculated by the BET equation. [b]BJH pore desorption volume. [c]Desorption average pore diameter.

Figure S4. Thermogravimetric analysis (TGA) of SiO_2-60 and **SILP-5** with variable loading of 5, 10 or 20 wt% [C_2mim]Br, resp.
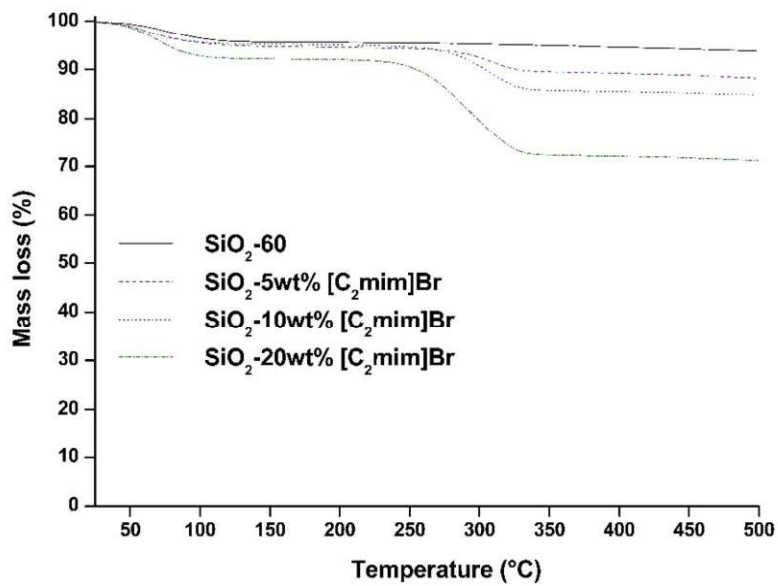
Figure S5. Thermogravimetric analysis (TGA) of **SILC-1** to **SILC-4**
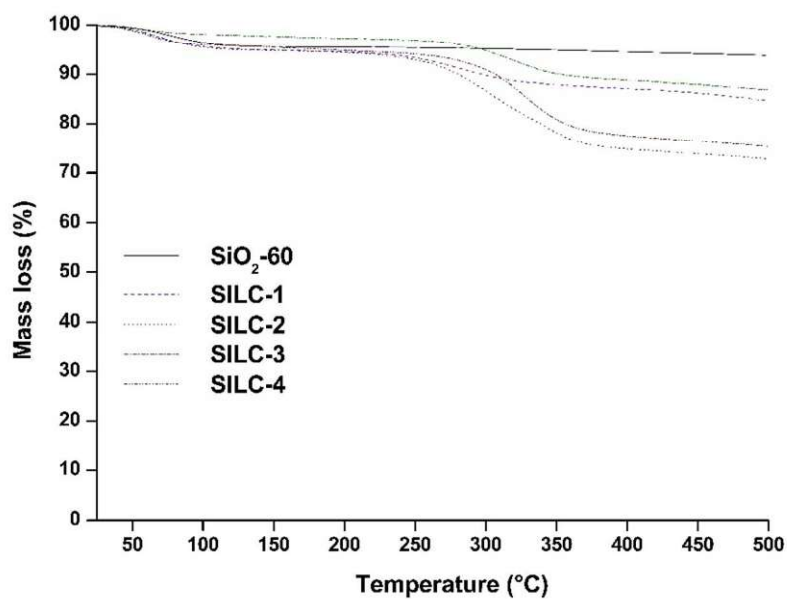
Table S2. Elemental analysis of Silica-60, SiO_2 + 10wt% [C_2mim]Br **5 (SILP-5)** and **SILC-1** to **SILC-4**

Sample	Elements		
	wt% C	wt% H	wt% N
SiO$_2$	0.026	0.75	<0.01
SILP-5 (10 wt%)	3.75	1.11	1.38
SILC-1	7.91	1.63	2.51
SILC-2	10.93	2.11	3.38
SILC-3	10.75	1.88	3.42
SILC-4	10.68	1.89	3.43

Figure S6. Comparison of the catalytic performance with supported ionic liquid [C$_2$mim]Br **5** with propylene oxide/n-hexane 1:1 at a flow rate of 0.02 ml/min and pure propylene oxide at a flow rate of 0.01 ml/min.
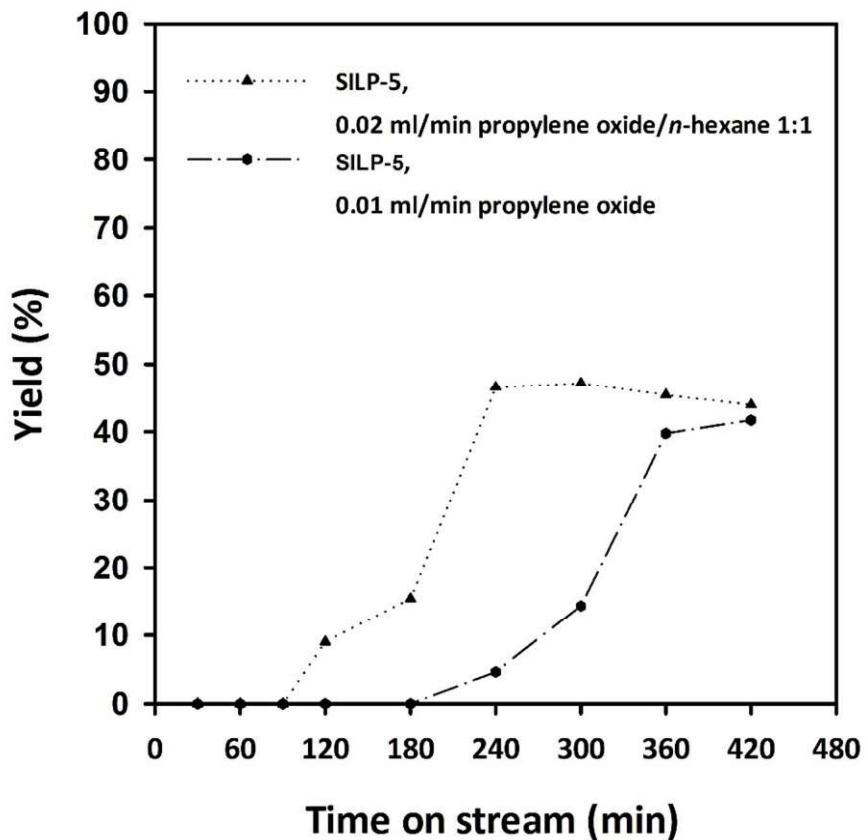
Figure S7. Comparison of the catalytic performance of supported ionic liquid [C$_2$mim]Br **5** with conventional and calcined SiO$_2$ in the continuous conversion of propylene oxide with scCO$_2$.
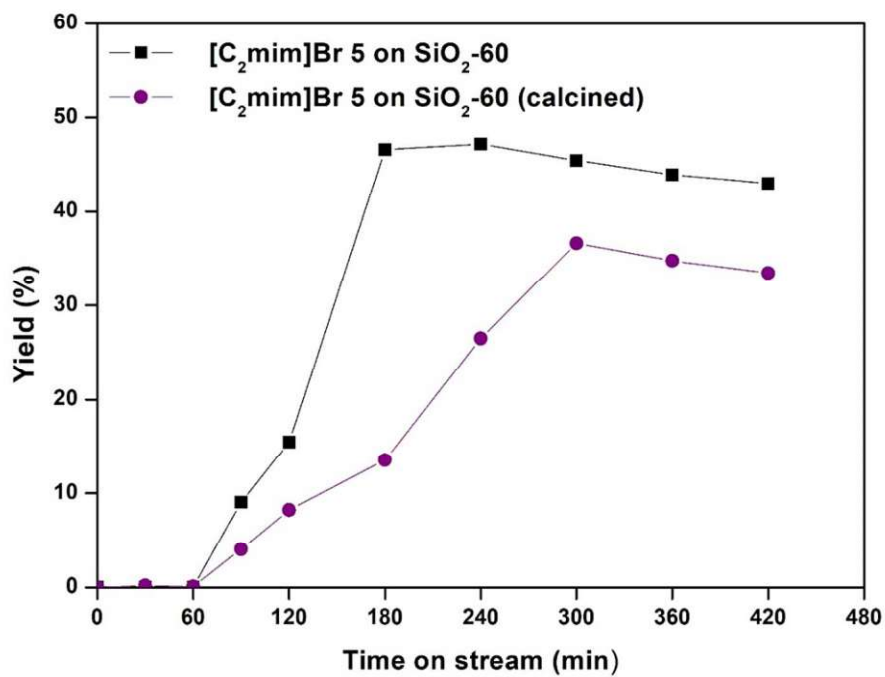
Table S3. Catalytic conversion of carbon dioxide and propylene oxide into propylene carbonate with supported ionic liquid catalysts at 120 °C for 48 h.

Entry[a]	Catalyst	Loading[b] [mmol/g]	Propylene carbonate formed [mmol]	Yield[c] [%]	TON[d]	TOF [h^{-1}][e]
1	**SILP-5**	0.52	131.7	36	110	2.28
2	**SILC-1**	1.41	91.8	26	22	0.45
3	**SILC-2**	1.21	154.9	38	46	0.95
4	**SILC-3**	1.22	44.7	11	14	0.29
5	**SILC-4**	1.22	87.1	21	27	0.55

[a] Performed with a flow rate of 2 ml/min (1.98 ml/min scCO$_2$ and 0.02 ml/min propylene oxide/n-hexane 1:1, column: 4.5 mm ID × 250 mm. [b] In case of SILC-1 to SILC-4, loading was calculated from the nitrogen content in elemental analysis. [c] Defined as yield obtained in 48 h based on the overall substrate input. [d] Calculated as mmol propylene carbonate per mmol catalyst in 48 h. [e] Calculated as TON per reaction time (48 h).

Figure S8. ^{1}H NMR of propylene carbonate (crude) obtained in the continuous conversion of propylene oxide with scCO$_2$ using supported ionic liquid catalyst **SILC-2**.
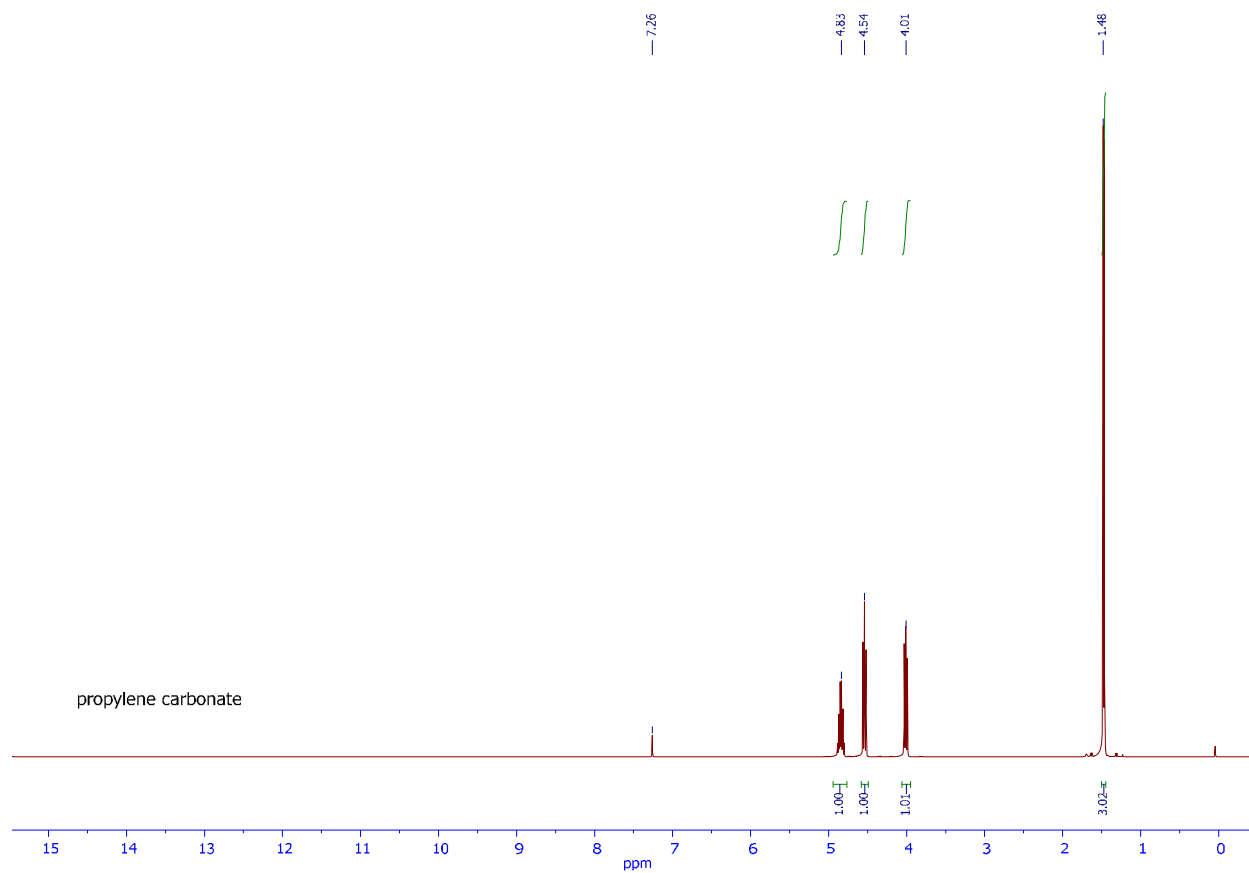
Curriculum Vitae

Curriculum Vitae

Personal Information

Name: Aitor Sainz Martinez

Date and place of birth: ▮▮▮▮▮▮▮▮▮▮▮▮)

Address: ▮▮▮▮▮▮▮▮▮▮▮

▮▮▮▮▮▮▮

Telephone: ▮▮▮▮▮▮

E-Mail: ▮▮▮▮▮▮▮

Experience

06/2021 – till date   **Associate Specialist, Project Management**

Intervet GesmbH, MSD-Tiergesundheit (Vienna, Austria)

Department: Process and Validation Implants

Project: R&D Transfer medicine (scale up & worldwide registration)

Main supervisor: Assoc. Dir, Operations Nora Kubesch

Department manager: Dir, Operations Nebojsa Nikolic

Project supervisor: Assoc. Dir, Operations Renate Franziska Oppelt

Education

10/2017 – till date   **Ph.D. in Organic Chemistry**

Vienna University of Technology, Vienna (Austria)

Research group: Stereoselective and Sustainable Synthesis

Project topic: Combined ionic liquid – supercritical CO_2 process for catalysis and separations

Supervisor: Assist. Prof. Dipl.-Ing. Dr. techn. Katharina Schröder

Substitute supervisor: Assist. Prof. Dipl.-Ing. Dr. techn. Michael Schnürch

09/2014 – 09/2015   **Master in Synthetic and Industrial Chemistry**

University of Basque Country, Leioa (Spain)

Research group: New Synthetic Methodologies

Project topic: Heteroannulation reaction between benzamides and phenylacetylene.
Synthesis of Isondolones

Supervisor: Prof. Dr. Raul San Martin

Co-supervisor: Prof. Dr. Maria Teresa Herrero Corral

10/2013 – 07/2014 ERASMUS project (Organic Chemistry) in Vienna
Vienna University of Technology, Vienna (Austria)

Research group: Stereoselective and Sustainable Synthesis

Project topic: Ionic Liquid Based Microemulsions for Catalytic Hydrogenations

Supervisor: Assist. Prof. Dipl.-Ing. Dr. techn. Katharina Schröder

Co-supervisor: Ao. Univ. Prof. Dipl.-Ing. Dr. techn. Peter Gärtner

09/2009 – 09/2014 1st and 2nd cycle (5 yrs.) Graduate in Chemistry
University of Basque Country, Leioa (Spain)

Publications - Journals

1. Sainz Martinez, A.; Hauzenberger, C.; Sahoo, A. R.; Csendes, Z.; Hoffmann, H.; Bica, K. Continuous Conversion of Carbon dioxide to Propylene carbonate with Supported Ionic Liquids, *ACS Sustain. Chem. Eng.* **2018**, *6*, 13131-13139.
DOI: 10.1021/acssuschemeng. 8b02627

2. Sainz Martinez, A.; Kornpointner, C.; Haselmair-Gosch, C.; Mikulic-Petkovsek, M.; Schröder, K.; Halbwirth, H. Dynamic streamlined of iridoids, anthocyanins and lipids from haskap berries, LWT **2021**, *138*, 110663.
DOI: https://doi.org/10.1016/j.lwt.2020.110633

3. Kornpointner, C.; Sainz Martinez, A.; Schnürch M.; Halbwirth, H.; Bica-Schröder, K. Combined ionic liquid and supercritical carbon dioxide based dynamic extraction of six cannabinoids from Cannabis sativa L, *Green Chem*., **2021**, *23*, 10079-10089.
DOI: https://doi.org/10.1039/D1GC03516A

4. Kornpointner, C.; Sainz Martinez, A.; Marinovic, S.; Haselmair-Gosch, C.; Jamnik,P.; Schröder K.; Löfke, C.; Halbwirth H. Chemical composition and antioxidant potential of Cannabis sativa L. roots, *Ind. Crops Prod*., **2021**, *165*, 113422.
DOI: https://doi.org/10.1016/j.indcrop.2021.113422

5. Sainz Martinez, A.; Lanaridi, O.; Stagel, K.; Halbwirth, H.; Schnürch M.; Bica-Schröder, K. Extraction techniques for bioactive compounds of cannabis, *Nat. Prod. Rep*., **2023**, 40, 676-717.
DOI: https://doi.org/10.1039/D2NP00059H

6. Faruck, A. A. M.; Grützmacher, P. G.; Hsu, J.-C., Dworschak, D.; Cheng, H.-W., Valtiner, M.; Stagel, K.; Mikšovsky, P.; Sahoo, A. R.; Sainz Martinez, A.; Bica-Schröder, K.; Weigand M.; Gachot, C. Applying ionic liquids as oil additives for gearboxes: Going beyond the state of the art by bridging the nano-scale and component level, *Friction,* **2023**, *11*, 1057–1078.
DOI: https://doi.org/10.1007/s40544-022-0650-5

Conference Presentations [*P* – Poster]

- (*P1*) **Sainz Martinez, A.**; Hauzenberg, C.; C.; Csendes, Z.; Bica, K. *Continuous Conversion of Carbon Dioxide with Supported Ionic Liquids* in the 2nd Advances in Green Chemistry Conference AGChem 2018, Poznań, Poland, Apr. 2018

Awards

- Best Poster Prize at 2nd Advances in Green Chemistry Conference for the poster presentation entitled: "Continuous Conversion of Carbon Dioxide to Propylene Carbonate Using Supported Ionic Liquids". (Apr. 2018)

Personal Skills

Languages:

- Spanish and Basque (native)
- English (C1, CAE)
- German (B2, ÖSD Zertifikat B2)
- Italian (B1)

Computer skills:

- Office package, Prezi, user level management of google apps
- Top Spin, MestReNova, OriginPro8, Chem BioDraw, JASCO software, Medusa, The Unscrambler, Xcalibur, Web-based chemical information (Scifinder^n, Reaxys …)

Merck applications:

- Aera, Alexx, ARIBA, Atlas Portal, MIDAS, MEDS, MUSE, MyLearning, Reliance, SAP Concur, Workday, ZeusX

Merck courses:

- Project Management course
- Process Scale-up, Validation & Technology Transfer
- 8 Steps Problem Solving

Vienna, on 09 July 2023   AITOR SAINZ MARTINEZ